50376
1989
49

UNIVERSITÉ DES SCIENCES ET TECHNIQUES
DE LILLE FLANDRES-ARTOIS

Année 1989

N° d'ordre : 337

TH ITÉ

présentée à l'Université de Lille I
pour l'obtention du grade de

DOCTEUR DES SCIENCES DE LA VIE ET DE LA SANTÉ

par

Christian BAILLY

CONCEPTION DE MOLÉCULES A HAUTE AFFINITÉ POUR L'ADN ET A ACTIVITÉ ANTICANCÉREUSE POTENTIELLE

Etudes spectroscopique, biochimique et pharmacologique

présentée le 21 Mars 1989 devant la Commission d'Examen

JURY

Président : Pr. Jean MONTREUIL
Rapporteurs : Dr. Emile BISAGNI
Dr. Bernard HECQUET
Pr. Bernard FOURNET
Membres : Pr. Claude HELENE
Dr. Jean-Pierre HENICHART

UNIVERSITE DES SCIENCES
ET TECHNIQUES DE LILLE
FLANDRES ARTOIS

DOYENS HONORAIRES DE L'ANCIENNE FACULTE DES SCIENCES

M. H. LEFEBVRE, M. PARREAU.

PROFESSEURS HONORAIRES DES ANCIENNES FACULTES DE DROIT ET SCIENCES ECONOMIQUES, DES SCIENCES ET DES LETTRES

MM. ARNOULT, BONTE, BROCHARD, CHAPPELON, CHAUDRON, CORDONNIER, DECUYPER, DEHEUVELS, DEHORS, DION, FAUVEL, FLEURY, GERMAIN, GLACET, GONTIER, KOURGANOFF, LAMOTTE, LASSERRE, LELONG, LHOMME, LIEBAERT, MARTINOT-LAGARDE, MAZET, MICHEL, PEREZ, ROIG, ROSEAU, ROUELLE, SCHILTZ, SAVARD, ZAMANSKI, Mes BEAUJEU, LELONG.

PROFESSEUR EMERITE

M. A. LEBRUN

ANCIENS PRESIDENTS DE L'UNIVERSITE DES SCIENCES ET TECHNIQUES DE LILLE

MM. M. PARREAU, J. LOMBARD, M. MIGEON, J. CORTOIS.

PRESIDENT DE L'UNIVERSITE DES SCIENCES ET TECHNIQUES DE LILLE FLANDRES ARTOIS

M. A. DUBRULLE.

PROFESSEURS - CLASSE EXCEPTIONNELLE

M. CONSTANT Eugène	Electronique
M. FOURET René	Physique du solide
M. GABILLARD Robert	Electronique
M. MONTREUIL Jean	Biochimie
M. PARREAU Michel	Analyse
M. TRIDOT Gabriel	Chimie appliquée

PROFESSEURS - 1ère CLASSE

M. BACCHUS Pierre	Astronomie
M. BIAYS Pierre	Géographie
M. BILLARD Jean	Physique du solide
M. BOILLY Bénoni	Biologie
M. BONNELLE Jean Pierre	Chimie-Physique
M. BOSCQ Denis	Probabilités
M. BOUCHON Pierre	Algèbre
M. BOURIQUET Robert	Biologie végétale
M. BREZINSKI Claude	Analyse numérique
M. BRIDOUX Michel	Chimie-Physique
M. CARREZ Christian	Informatique
M. CELET Paul	Géologie générale
M. CHAMLEY Hervé	Géotechnique
M. COEURE Gérard	Analyse
M. CORDONNIER Vincent	Informatique
M. DEBOURSE Jean Pierre	Gestion des entreprises
M. DHAINAUT André	Biologie animale
M. DOUKHAN Jean Claude	Physique du solide
M. DYMENT Arthur	Mécanique
M. ESCAIG Bertrand	Physique du solide
M. FAURE Robert	Mécanique
M. FOCT Jacques	Métallurgie
M. FRONTIER Serge	Ecologie numérique
M. GRANELLE Jean jacques	Sciences Economiques
M. GRUSON Laurent	Algèbre
M. GUILLAUME Jean	Microbiologie
M. HECTOR Joseph	Géométrie
M. LABLACHE-COMBIER Alain	Chimie organique
M. LACOSTE Louis	Biologie végétale
M. LAVEINE Jean Pierre	Paléontologie
M. LEHMANN Daniel	Géométrie
Mme LENOBLE Jacqueline	Physique atomique et moléculaire
M. LEROY Jean Marie	Spectrochimie
M. LHOMME Jean	Chimie organique biologique
M. LOMBARD Jacques	Sociologie
M. LOUCHEUX Claude	Chimie physique
M. LUCQUIN Michel	Chimie physique
M. MACKE Bruno	Physique moléculaire et rayonnements atmosphériques
M. MIGEON Michel	E.U.D.I.L.
M. PAQUET Jacques	Géologie générale
M. PETIT Francis	Chimie organique
M. POUZET Pierre	Modélisation - Calcul scientifique
M. PROUVOST Jean	Minéralogie
M. RACZY Ladislas	Electronique
M. SALMER Georges	Electronique
M. SCHAMPS Joel	Spectroscopie moléculaire
M. SEGUIER Guy	Electrotechnique
M. SIMON Michel	Sociologie
Mle SPIK Geneviève	Biochimie
M. STANKIEWICZ François	Sciences Economiques
M. TILLIEU Jacques	Physique théorique
M. TOULOTTE Jean Marc	Automatique
M. VIDAL Pierre	Automatique
M. ZEYTOUNIAN Radyadour	Mécanique

PROFESSEURS - 2ème CLASSE

M. ALLAMANDO Etienne	Composants électroniques
M. ANDRIES Jean Claude	Biologie des organismes
M. ANTOINE Philippe	Analyse
M. BART André	Biologie animale
M. BASSERY Louis	Génie des procédés et réactions chimiques
Mme BATTIAU Yvonne	Géographie
M. BEGUIN Paul	Mécanique
M. BELLET Jean	Physique atomique et moléculaire
M. BERTRAND Hugues	Sciences Economiques et Sociales
M. BERZIN Robert	Analyse
M. BKOUCHE Rudolphe	Algèbre
M. BODARD Marcel	Biologie végétale
M. BOIS Pierre	Mécanique
M. BOISSIER Daniel	Génie civil
M. BOIVIN Jean Claude	Spectrochimie
M. BOUQUELET Stéphane	Biologie appliquée aux enzymes
M. BOUQUIN Henri	Gestion
M. BRASSELET Jean Paul	Géométrie et topologie
M. BRUYELLE Pierre	Géographie
M. CAPURON Alfred	Biologie animale
M. CATTEAU Jean pierre	Chimie organique
M. CAYATTE Jean Louis	Sciences Economiques
M. CHAPOTON Alain	Electronique
M. CHARET Pierre	Biochimie structurale
M. CHIVE Maurice	Composants électroniques optiques
M. COMYN Gérard	Informatique théorique
M. COQUERY Jean Marie	Psychophysiologie
M. CORIAT Benjamin	Sciences Economiques et Sociales
Mme CORSIN Paule	Paléontologie
M. CORTOIS Jean	Physique nucléaire et corpusculaire
M. COUTURIER Daniel	Chimie organique
M. CRAMPON Norbert	Tectolique Géodynamique
M. CROSNIER Yves	Electronique
M. CURGY Jean jacques	Biologie
Mle DACHARRY Monique	Géographie
M. DAUCHET Max	Informatique
M. DEBRABANT Pierre	Géologie appliquée
M. DEGAUQUE Pierre	Electronique
M. DEJAEGER Roger	Electrochimie et Cinétique
M. DELORME Pierre	Physiologie animale
M. DELORME Robert	Sciences Economiques
M. DEMUNTER Paul	Sociologie
M. DENEL Jacques	Informatique
M. DE PARIS Jean Claude	Analyse
M. DEPREZ Gilbert	Physique du solide - Cristallographie
M. DERIEUX Jean Claude	Microbiologie
Mle DESSAUX Odile	Spectroscopie de la réactivité chimique
M. DEVRAINNE Pierre	Chimie minérale
Mme DHAINAUT Nicole	Biologie animale
M. DHAMELINCOURT Paul	Chimie physique
M. DORMARD Serge	Sciences Economiques
M. DUBOIS Henri	Spectroscopie hertzienne
M. DUBRULLE Alain	Spectroscopie hertzienne
M. DUBUS Jean Paul	Spectrométrie des solides

M. DUPONT Christophe	Vie de la firme (I.A.E.)
Mme EVRARD Micheline	Génie des procédés et réactions chimiques
M. FAKIR Sabah	Algèbre
M. FAUQUEMBERGUE Renaud	Composants électroniques
M. FONTAINE Hubert	Dynamique des cristaux
M. FOUQUART Yves	Optique atmosphérique
M. FOURNET Bernard	Biochimie structurale
M. GAMBLIN André	Géographie urbaine, industrielle et démographie
M. GLORIEUX Pierre	Physique moléculaire et rayonnements atmosphériques
M. GOBLOT Rémi	Algèbre
M. GOSSELIN Gabriel	Sociologie
M. GOUDMAND Pierre	Chimie physique
M. GOURIEROUX Christian	Probabilités et statistiques
M. GREGORY Pierre	I.A.E.
M. GREMY Jean Paul	Sociologie
M. GREVET Patrice	Sciences Economiques
M. GRIMBLOT Jean	Chimie organique
M. GUILBAULT Pierre	Physiologie animale
M. HENRY Jean Pierre	Génie mécanique
M. HERMAN Maurice	Physique spatiale
M. HOUDART René	Physique atomique
M. JACOB Gérard	Informatique
M. JACOB Pierre	Probabilités et statistiques
M. JEAN Raymond	Biologie des populations végétales
M. JOFFRE Patrick	Vie de la firme (I.A.E.)
M. JOURNEL Gérard	Spectroscopie hertzienne
M. KREMBEL Jean	Biochimie
M. LANGRAND Claude	Probabilités et statistiques
M. LATTEUX Michel	Informatique
Mme LECLERCQ Ginette	Catalyse
M. LEFEBVRE Jacques	Physique
M. LEFEVRE Christian	Pétrologie
Mle LEGRAND Denise	Algèbre
Mle LEGRAND Solange	Algèbre
M. LEGRAND Pierre	Chimie
Mme LEHMANN Josiane	Analyse
M. LEMAIRE Jean	Spectroscopie hertzienne
M. LE MAROIS Henri	Vie de la firme (I.A.E.)
M. LEROY Yves	Composants électroniques
M. LESENNE Jacques	Systèmes electroniques
M. LHENAFF René	Géographie
M. LOCQUENEUX Robert	Physique théorique
M. LOSFELD Joseph	Informatique
M. LOUAGE Francis	Electronique
M. MAHIEU Jean Marie	Optique - Physique atomique
M. MAIZIERES Christian	Automatique
M. MAURISSON Patrick	Sciences Economiques et Sociales
M. MESMACQUE Gérard	Génie Mécanique
M. MESSELYN Jean	Physique atomique et moléculaire
M. MONTEL Marc	Physique du solide
M. MORCELLET Michel	Chimie organique
M. MORTREUX André	Chimie organique
Mme MOUNIER Yvonne	Physiologie des structures contractiles
M. NICOLE Jacques	Spectrochimie
M. NOTELET Francis	Systèmes électroniques
M. PARSY Fernand	Mécanique
M. PECQUE Marcel	Chimie organique
M. PERROT Pierre	Chimie appliquée

M. PERTUZON Emile	Physiologie animale
M. PONSOLLE Louis	Chimie physique
M. PORCHET Maurice	Biologie animale
M. POSTAIRE Jack	Informatique industrielle
M. POVY Lucien	Automatique
M. RICHARD Alain	Biologie animale
M. RIETSCH François	Physique des polymères
M. ROBINET Jean CLaude	EUDIL
M. ROGALSKI Marc	Analyse
M. ROY Jean Claude	Psychophysiologie
Mme SCHWARZBACH Yvette	Géométrie
M. SLIWA Henri	Chimie organique
M. SOMME Jean	Géographie
M. STAROSWIECKI Marcel	Informatique
M. STERBOUL François	Informatique
M. TAILLIEZ Roger	Génie alimentaire
M. THERY Pierre	Systèmes électroniques
M. THIEBAULT François	Sciences de la terre
M. THUMERELLE Pierre	Démographie - Géographie Humaine
Mme TJOTTA Jacqueline	Mathématiques
M. TOURSEL Bernard	Informatique
M. TREANTON Jean rené	Sociologie du Travail
M. TURREL Georges	Spectrochimie infrarouge et Raman
M. VANDORPE Bernard	Chimie minérale
M. VASSEUR Christian	Automatique
M. VAST Pierre	Chimie inorganique
M. VERBERT André	Biochimie
M. VERNET Philippe	Génétique
M. WACRENIER Jean Marie	Electronique
M. WALLART Francis	Spectrochimie infrarouge et Raman
M. WARTEL Michel	Chimie inorganique
M. WATERLOT Michel	Géologie générale
M. WEINSTEIN Olivier	Analyse économique de la recherche et développement
M. WERNER Georges	Informatique théorique
M. WOZNIAK Michel	Spectrochimie
Mme ZINN JUSTIN Nicole	Algèbre

Ce travail a été effectué sous la direction scientifique de Monsieur Jean-Pierre HENICHART, Directeur de Recherches à l'INSERM. Vous m'avez initié avec passion à la Chimie et m'avez sans cesse apporté votre soutien amical. Je tiens à vous exprimer de tout coeur mes remerciements.

Monsieur le Professeur Jean MONTREUIL me fait l'honneur de présider ce jury. Qu'il veuille trouver ici l'expression de ma gratitude.

Monsieur Emile BISAGNI, Directeur de Recherches au CNRS, Monsieur Bernard FOURNET, Professeur à l'Université des Sciences et Techniques de Lille et Monsieur Bernard HECQUET, Directeur du Laboratoire de Pharmacodynamie Clinique du Centre Oscar Lambret, ont bien voulu juger ce travail et en être les rapporteurs. Je les en remercie très sincèrement.

Monsieur Claude HELENE, Professeur au Muséum d'Histoire Naturelle me fait l'honneur de siéger à ce Jury. Je suis très touché par votre présence et vous prie de croire en mon profond respect.

Je voudrais aussi témoigner mon amitié et toute ma reconnaissance à mes collègues de laboratoire, Raymond HOUSSIN, Jean-Luc BERNIER, Elisabeth TEISSIER, Nicole HELBECQUE et Michèle LOHEZ ainsi qu'à tous mes camarades du laboratoire.

J'associe également à ce travail toutes les personnes qui m'ont accordé leur aide et leur collaboration efficace.

Cette étude a été réalisée à l'Unité 16 de l'INSERM dirigée successivement par Monsieur le Professeur Philippe ROUSSEL puis par Monsieur le Professsseur Pierre DEGAND. Je les remercie pour l'accueil qu'ils m'ont réservé. J'ai apprécié de trouver au sein de cette formation une ambiance chaleureuse. Que tous les membres de cette Unité et des laboratoires voisins soient assurés de la sincérité de mes remerciements. Je remercie également tous ceux qui, d'une façon ou d'une autre, m'ont témoigné leur sympathie.

A Agnès, à mon garçon,

à mes parents, à mon frère, à ma famille

à tous mes amis

TABLE DES MATIERES

1) Isolement et structure

2) Liaison à l'ADN

a) Mode de liaison

b) Coupure d'ADN

3) Complexation

4) Les autres cibles de la bléomycine

a) Pénétration cellulaire de la Blm

b) La cible membrane

c) La cible proteine

5) Activité biologique

II Les modèles synthétiques

1) Les analogues de la bléomycine

2) Les modèles hybrides : bléomycine-anilinoamino-9 acridine

3) Le concept Peptide Chélateur-Intercalant : Les analogues fonctionnels de la Blm

a) Introduction

b) Le modèle Gly-His-Lys-Intercalant

Conclusion

CHAPITRE III : LE CONCEPT PEPTIDE CHELATEUR-PEPTIDE A LIAISON SPECIFIQUE-INTERCALANT

a) Liaison à l'ADN

1-Intensité de liaison

2-Mode de liaison

b) Complexation

c) Dégradation de l'ADN

d) Activité biologique

Conclusion

CONCLUSION

APPENDICE TECHNIQUE

SYNTHESES CHIMIQUES
METHODES ANALYTIQUES
METHODES BIOLOGIQUES

ABREVIATIONS

AGAGLU : ((Amino-2 éthyl)aminométhyl)-2 (((N$_\alpha$-carbonylhistidyl(amino-2 déoxy-2-D-glucosyl)-γ glutamyl-glycylamino)-4 anilino)-9 acridine)-6 pyridine

AGAMGA : ((Amino-2 éthyl)aminométhyl)-2 (((N$_\alpha$-carbonylhistidyl((N-morpholino)-3 propylamino)-γ glutamyl-glycylamino)-4 anilino)-9 acridine)-6 pyridine

AGGA : ((Amino-2 éthyl)aminométhyl)-2 ((((N$_\alpha$-carbonylhistidylamino)-4 butyrylglycylamino)-4 anilino)-9 acridine)-6 pyridine

ALGA : ((Lysyl-glycylamino)-4 anilino)-9 acridine

AMBI-A2 : ((Amino-2 éthyl)aminométhyl)-2 ((((N$_\alpha$-carbonylhistidylamino)-4 butyrylglycylamino)-2 éthyl)-2 ((iodure de carboxamido)-3 propyldiméthylsulfonium)-4' bithiazole-2':4)-6 pyridine

AMBIGLU : ((Amino-2 éthyl)aminométhyl)-2 (((N$_\alpha$-carbonylhistidyl (D-glucosamino)-γ glutamylamino)-2 éthyl)-2 (méthoxycarbonyl)-4' bithiazole-2':4)-6 pyridine

AMPHIS : ((Amino-2 éthyl)-aminométhyl)-2 (Nα-carbonylhistidinate de méthyle)-6 pyridine

AMSA : amsacrine ou (Acridinamino-9)-4 méthanesulfonyl m-anisidino

Gly-His-Lys-NETGA : Glycyl-L-histidyl-L-lysyl ((((amino-4 méthyl-1 pyrrolyl)-2 carboxamido)-4 méthyl-1 pyrrolyl)-2 carbonylglycylamino)-4 anilino)- 9 acridine

NETBI : ((((Amino-4 méthyl-1 pyrrolyl)-2 carboxamido)-4 méthyl-1 pyrrolyl)-2 carboxamido-2 éthyl)-2 (méthoxycarbonyl)-4' bithiazole-2':4

NETGA : ((((Amino-4 méthyl-1 pyrrolyl)-2 carboxamido)-4 méthyl-1 pyrrolyl)-2 carbonylglycylamino)-4 anilino))-9 acridine

PETT : Phenyl-2((éthoxycarbonyl-4')thiazolyl-2')-6 thiazolo[3,2-b] triazole-[1,2,4,]

Thia-Nt : Dibromhydrate d'((((amino-3 butyrylamino)-2' thiazolyl)-4' carboxamido)-2 amino-3 propylaminocarbonyl)-4 thiazole

ADN : acide désoxyribonucléique
Blm : bléomycine
Dst : distamycine A
Nt : Nétropsine
Gly : glycine
His : histidine
Lys : lysine
FAB : Fast Atom Bombardment
RMN : résonnance magnétique nucléaire
RPE : résonnance paramagnétique électronique
DMSO-d_6 : diméthylsulfoxyde hexadeuterié
CH_2Cl_2 : dichlorométhane
$CHCl_3$: chloroforme

Le cancer est une maladie du contrôle de la division cellulaire. Les nombreuses formes de cancers répondent à une caractéristique commune: la croissance incontrôlée de cellules anormales. Mais si le phénomène cellulaire global est commun, son évolution est différente pour chaque type de tumeur.

La thérapie du cancer n'intervient que tardivement dans le processus de cancérisation. Depuis l'événement initial d'induction de la cancérisation (que ce soit par un agent chimique, viral ou ionisant) jusqu'au moment où la prolifération néoplasique dépasse le seuil de détection clinique (approximativement 10^9 cellules soit une tumeur de un centimètre de diamètre), toute une phase du processus de tumorisation - dite phase occulte par opposition à la phase clinique - s'est déjà déroulée et conditionne très souvent le pronostic; d'où l'importance de la prévention et du dépistage précoce des cancers.

Lorsque la tumeur est implantée, celle-ci évolue dans le temps et dans l'espace. Généralement l'extension d'abord locorégionale se propage par voie lymphatique vers les ganglions. La propagation hématogène génératrice des métastases constitue le principal facteur de généralisation. La nature anarchique et imprévisible de l'évolution tumorale impose la mise en oeuvre le plus rapidement possible d'un traitement radical parfois mutilant et toujours très difficile à supporter.

La définition du meilleur traitement à proposer repose sur la connaissance du mécanisme et de l'évolution de cette maladie afin de permettre un traitement adapté à chaque type de cancer .

Les quatre thérapeutiques majeures - chirurgie, radiothérapie, chimiothérapie et immunothérapie - peuvent être utilisées isolément ou associées le plus souvent en fonction du degré de gravité, de la localisation et des données histologiques. La chimiothérapie a pris une place de plus en plus importante en raison de sa fréquente efficacité. Seul traitement possible des maladies apparaissant simultanément en plusieurs points de l' organisme ou de tumeurs déjà métastasiées, la chimiothérapie est également utilisée pour réduire le volume d'une tumeur avant une intervention chirurgicale ou pour faire disparaître les foyers métastasiques microscopiques apparaissant secondairement après le traitement d'une lésion primitive (chimiothérapie adjuvante). Cependant les cancers chimio-curables ne représentent que quelques pour cent du total des cancers et des leucémies.

L'arsenal des médicaments anticancéreux se compose d'environ 35 spécialités regroupées en quatre classes:

- Les antimétabolites : Méthotrexate, Fluoro-5 Uracile...
- Les inhibiteurs de la duplication et de la transcription de l'ADN : Cisplatine, Bléomycine, Adriamycine...
- Les antimitotiques : Vincristine, Vinblastine...
- Les hormones : Prednisone...

De plus la découverte souvent fortuite (sauf rares exceptions) de ces substances, sans une pleine connaissance de leur mécanisme d'action, conduit à une utilisation non optimale de ces produits. Pour lutter le plus efficacement possible contre les cancers , il convient donc, parallèlement à l'étude fondamentale du processus de cancérisation (qui n'a pas de but thérapeutique direct mais peut concourir à préciser et découvrir de nouvelles cibles moléculaires), de définir clairement le mécanisme d'action des substances médicamenteuses existantes afin de :

- permettre une utilisation optimale des médicaments disponibles (pharmacocinétique, chronobiologie, associations et vectorisation, élargissement du spectre d'action).
- concevoir et élaborer de nouvelles substances antitumorales plus efficaces, moins toxiques.

De la conception à la réalisation dans le domaine de la pharmacochimie du cancer, il est nécessaire d'adopter un cheminement rigoureux. Pour élaborer une substance nouvelle, la connaissance de la cible principale d'interaction est primordiale afin d'adapter au maximum la conformation du ligand à son récepteur.

L'ADN a été reconnu comme l'élément responsable du déclenchement des mécanismes moléculaires de la cancérisation. Les substances anticancéreuses conçues pour inhiber les mécanismes de transmission de l'information génétique tiennent compte de la géométrie de leur cible, l'ADN. Différents types de liaisons à l'ADN sont possibles. L'intercalation, l'alkylation et la fixation dans le petit sillon constituent les trois principaux procédés de fixation. Néanmoins si cette liaison à l'ADN est désormais reconnue comme primordiale, encore faut-il que celle-ci s'établisse en des sites oligonucléotidiques spécifiques au sein des oncogènes inducteurs du mécanisme de la prolifération cellulaire anarchique. L'activation d'un proto-oncogène en oncogène est le résultat d'une translocation, amplification ou mutation d'un gène. La

création ou la dérégulation d'une séquence nucléique inédite constitue le premier évènement initiateur du cancer.

Pour inhiber ce phénomène à sa source, il convient d'affiner l'élaboration de modèles susceptibles de se lier à l'ADN avec une forte affinité et/ou une haute spécificité.

Ces deux critères constituent le thème de ce travail. Une démarche logique est présentée, depuis la connaissance du mécanisme d'action de deux substances antitumorales d'origine naturelle - la bléomycine et la distamycine (et son analogue la nétropsine), toutes deux prises comme modèle d'un processus particulier de liaison à l'ADN - jusqu'à l'élaboration de différents modèles synthétiques. La liaison à l'ADN, élucidée au moyen de techniques physicochimiques et biochimiques très diverses et l'activité antitumorale (in vitro) de chacun de ces analogues synthétiques ont été mises en évidence.

Cette étude débouche sur la conception d'un analogue chimiquement plus complexe dont les mécanismes de liaisons multiples à l'ADN peuvent être mis à profit pour aborder sur le plan moléculaire l'étude des interactions protéines-ADN qui régissent tout le fonctionnement cellulaire.

CHAPITRE I

LES MODELES NATURELS

NETROPSINE ET DISTAMYCINE

I. Nétropsine et Distamycine : généralités.

1°) Isolement et structure.

En 1951, Finlay isole du bouillon de culture de *Streptomyces netropsis* un antibiotique riche en azote qu'il nomme nétropsine (FINLAY et al., 1951). L'analyse chimique et la synthèse totale ont permis d'en déterminer la structure (Figure 1) (VAN TAMELEN et al., 1956; NAKAMURA et al., 1964; JULIA & PREAU-JOSEPH, 1967; LOWN & KROWICKI, 1985).

La nétropsine (Nt) porte parfois différentes appellations :

-sinanomycine : isolé de *Streptomyces ambofacies* (WATANABE, 1956).

- antibiotique T 1384 ou T 1385 (WALLER et al., 1957; WEISS et al., 1957).

-congocidine : isolé de *Streptomyces chromagens* et *Streptomyces umbifaciens*, actif sur *Trypanosoma congolense* (COSAR et al., 1952). Des travaux ultérieurs ont montré que la congocidine diffère de la Nt par le remplacement du C=O par un C=NH au niveau d'un groupement acétamido (Figure 1) (BECKER et al.,1972).

La distamycine A (Dst-A ou Dst-3) est le produit majeur de fermentation de la souche *Streptomyces distacillus*, largement plus abondant que la Dst-B et la Dst-C. Sa structure chimique se rapproche de celle de la Nt (Figure 1). La synthèse totale de la Dst-A, mise au point dès 1964, a fait l'objet de fréquents remaniements (ARCAMONE et al., 1964; PENCO et al.,1967; GROKHOVSKY et al., 1975; BIALER et al., 1975; GREHN & RAGNARSSON, 1981; LOWN & KROWICKI, 1985). La Dst-A est parfois nommée stallimycine (ARCAMONE & PENCO, 1986).

Nt et Dst-A appartiennent à la classe des antibiotiques de type pyrrole-amidine, au même titre que l'anthelvencine A, la kikumycine, l'amidomycine et la noformycine (Figure 1).

Du point de vue conformationnel, Nt et Dst-A présentent la même caractéristique : la courbure du squelette de la molécule (Figure 2). Cette courbure

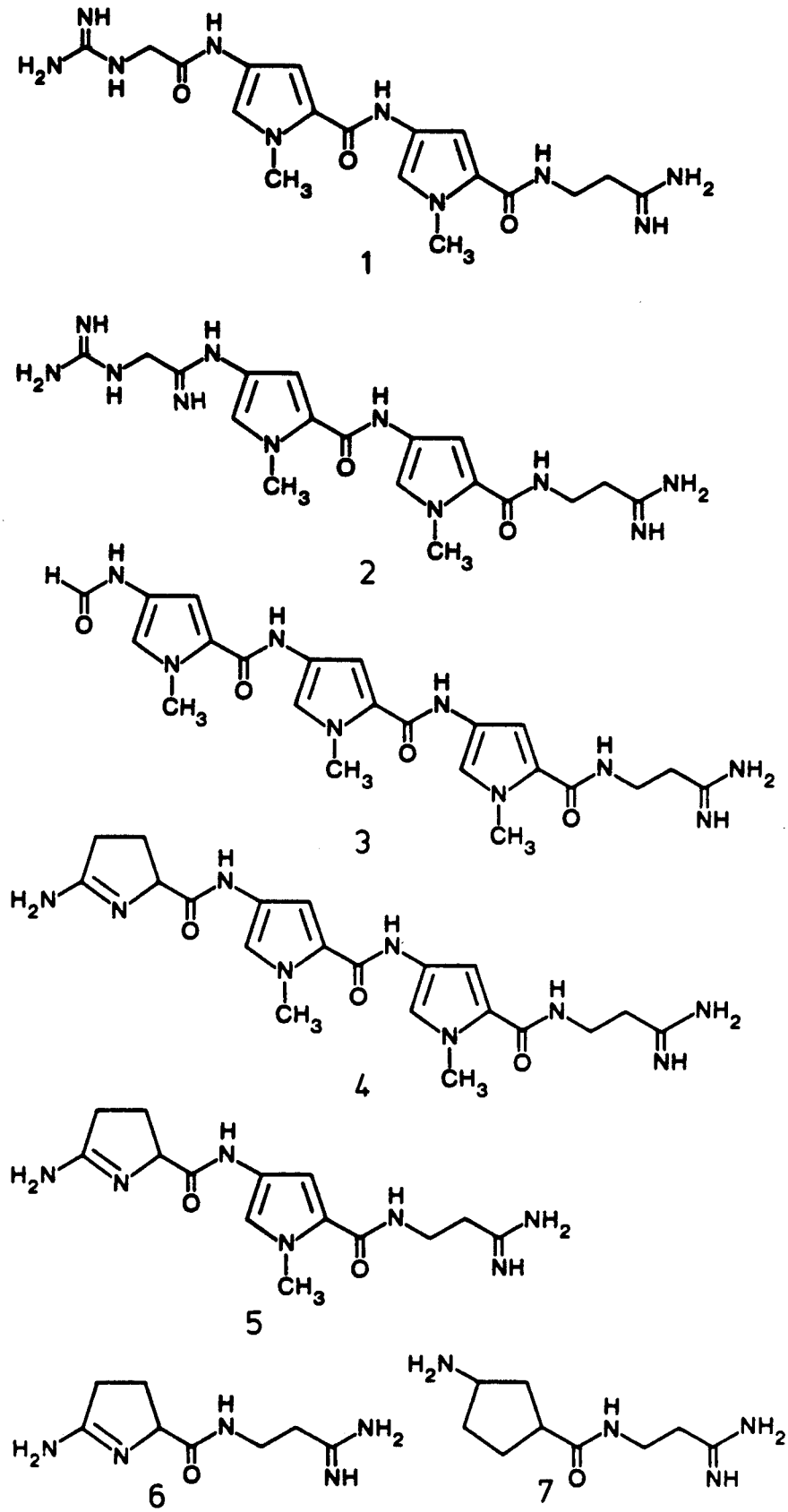

Figure 1 : Structure de la nétropsine (1), la congocidine (2), la distamycine (3), l'anthelvencine (4), la kikumycine (5), l'amidomycine (6) et la noformycine (7).

résulte de la répulsion stérique entre le groupement méthyle du pyrrole et le carbonyle de la liaison peptidique adjacente. Cette conformation particulière s'est révélée indispensable à la fixation de la molécule sur l'ADN (CHANDRA et al., 1971; MANNING & WOODY, 1986).

2°) Liaison à l'ADN.

1 Nature de l'interaction.

a) ADN natifs et polymères synthétiques.

L'interaction Nt-ADN (ou Dst-ADN) est très stable et spécifique de l'ADN double-brin en conformation B (dextrogyre, les plateaux de bases sont perpendiculaires à l'axe de l'hélice). Environ 45 paires de bases sont maintenues dans la conformation B pour 1 résidu Nt fixé. La très faible fixation sur le conformère A, où les bases sont inclinées par rapport au plan perpendiculaire à l'axe de l'hélice, s'accompagne d'une réversion de la forme A vers B (LUCK & ZIMMER, 1973; MICHENKOVA & ZIMMER, 1980; ZIMMER et al., 1982). De la même façon, on a pu noter la réversion de la forme Z (dextrogyre) vers B. Sur la base de calculs théoriques, Zimmer a émis l'hypothèse que les sites d'interactions sont virtuellement inaccessibles dans le petit sillon d'un ADN-Z (ZIMMER et al., 1983).

Cette haute sélectivité pour la forme B est mise à profit pour la détection ou l'induction d'ADN-B ou d'hybrides ADN-ARN en conformation B. Il n'y a pas de fixation sur un ADN simple-brin, ni sur les ARN (à l'exception de l'ARNt codant pour la phénylalanine, RUBIN & SUNDARALINGAM, 1984; ZAKRZEWSKA & PULLMAN, 1985).

Enfin, la fixation a toujours lieu au niveau du petit sillon d'un ADN-B (Figure 2). Différents arguments ont permis d'étayer l'hypothèse de la fixation au niveau du petit sillon :

1 - La présence de substituants encombrants dans le grand sillon d'un ADN ne modifie pas (ou peu) l'affinité de la Nt pour cet ADN.

2 - La méthylation du complexe ADN-Nt par le sulfate de diméthyle fait apparaître la présence de groupements méthyle uniquement sur les bases situées dans le grand sillon.

3 - L'utilisation d'oligonucléotides a confirmé cette hypothèse.

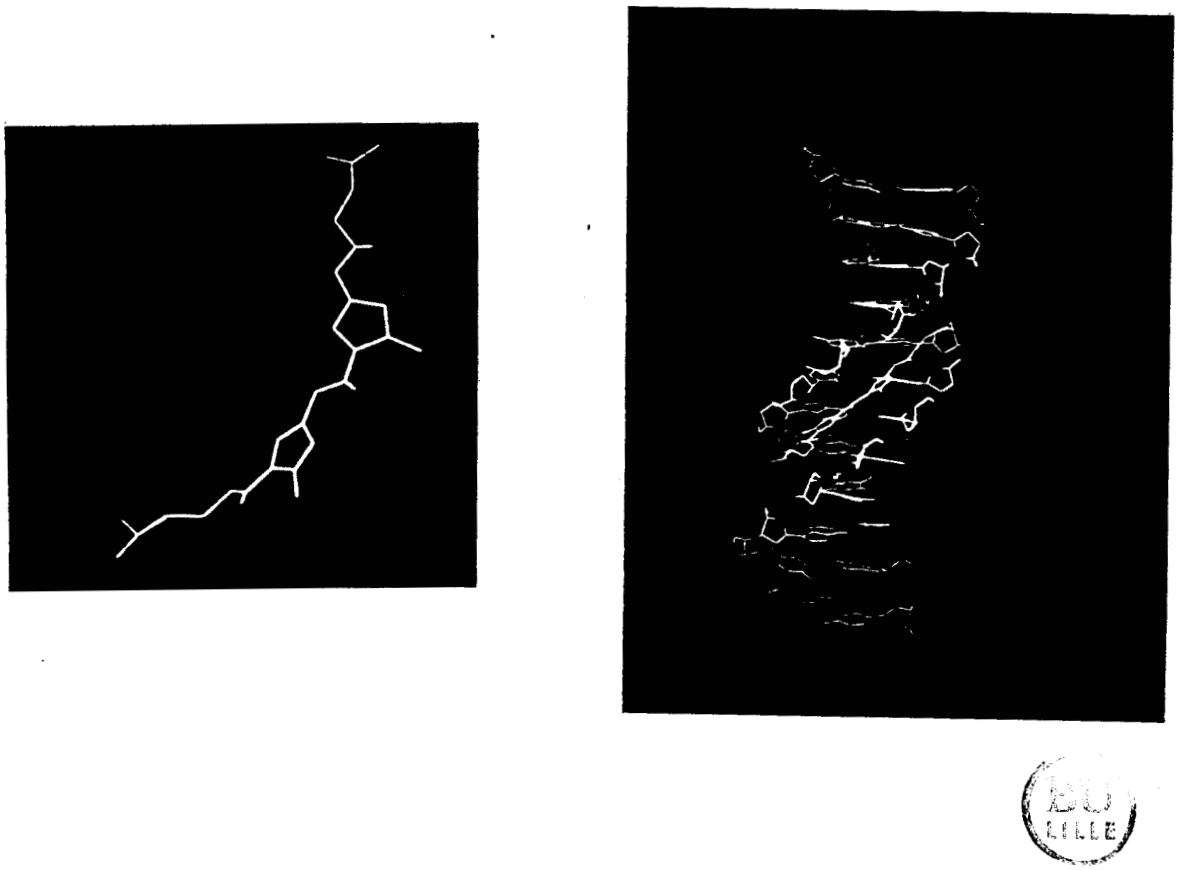

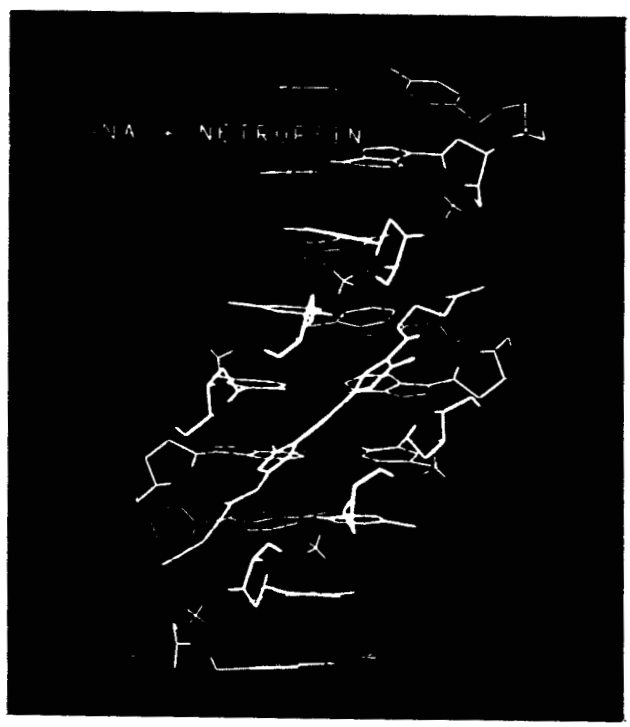

Figure 2 : Conformation et liaison de la nétropsine dans le petit sillon de l'ADN.

b) Oligonucléotides.

L'utilisation d'oligonucléotides de synthèse ou de restriction (fragments nucléotidiques issus d'un ADN natif clivé par des enzymes de restriction en des sites prédéterminés) a permis de mieux définir le type d'interaction Nt-ADN et Dst-ADN sur le plan moléculaire.

La nature moléculaire de l'interaction Nt-ADN a été étudiée par de nombreuses équipes . Le rôle exact des différents groupements chimiques dans l'interaction avec l'ADN a pu être établi.

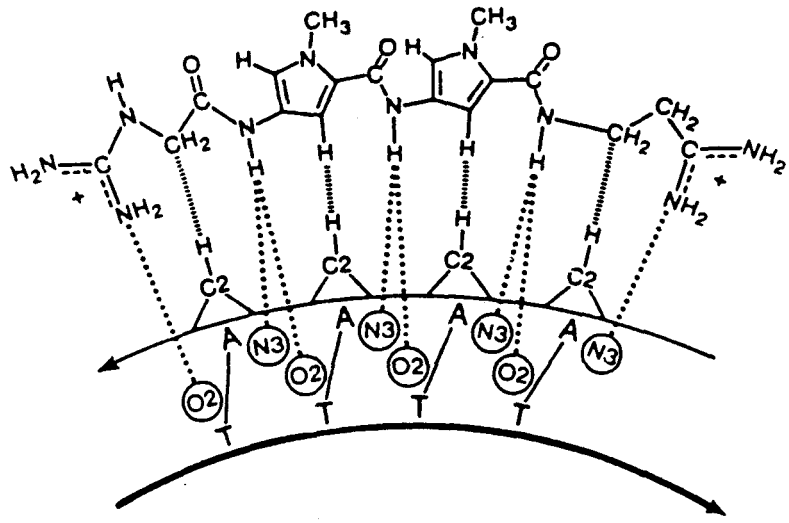

Figure 3 : Représentation des caractéristiques de la reconnaissance moléculaire de la nétropsine en vis-à-vis de la séquence 3'-AAAA-5'. (····) liaisons hydrogène, (III) contacts de Van der Waals. (LOWN et al., 1986b).

* interventions de liaisons électrostatiques

Des interactions ioniques se créent entre un résidu phosphate de l'ADN et un groupement amidine ou guanidine de la Nt (ou Dst-A). Mais la nétropsinine (Nt-D), c'est-à-dire le fragment pyrrole de la Nt dépourvu des chaînes latérales cationiques, est également capable de se lier à l'ADN avec toutefois une affinité moindre que la Nt. Les chaînes latérales ne sont donc pas indispensables à la fixation, mais permettent de consolider celle-ci et jouent un rôle dans la spécificité de liaison.

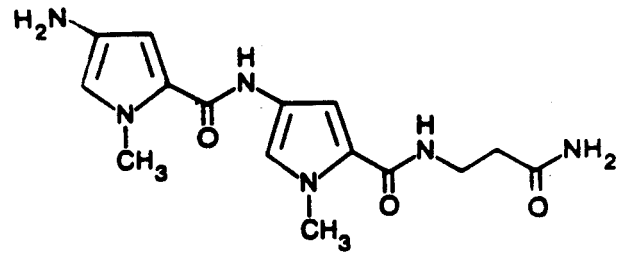

Nétropsinine (Nt-D)

*interventions de liaisons hydrogène.

Les liaisons hydrogène sont d'une grande importance pour la stabilisation des complexes Nt-ADN et Dst-ADN (LUCK et al., 1974; ZASEDATELEV et al., 1978). Elles s'établissent entre les atomes d'azote des liaisons peptidiques et des fonctions cationiques de l'antibiotique et les hétéroatomes des bases (l'azote N_3 de l'adénine ou l'oxygène O_2 de la thymine). Cependant ces liaisons hydrogènes ne semblent pas impliquées directement dans la spécificité de reconnaissance. Elles résulteraient de la formation première de liaisons de type Van der Waals (KOPKA et al., 1985a, 1985b; COLL et al., 1987).

*interventions de contacts de Van der Waals.

Ces contacts s'engagent par l'intermédiaire des protons hétérocycliques ou des résidus methylène terminaux de l'antibiotique et les protons hétérocycliques des bases (le C_2H de l'adénine). Ces liaisons de faible énergie sont considérées comme les éléments gouvernant la spécificité de liaison de la Nt et de la Dst-A (LEE et al., 1988c).

*stacking.

Des interactions de type stacking (empilement) ont lieu entre les hétérocycles pyrrole et l'atome d'oxygène $O_{1'}$ du désoxyribose de l'ADN (PELTON & WEMMER, 1988).

La multiplicité et la nature des liaisons mises en jeu assurent la formation d'un complexe très stable. Le schéma réactionnel suivant a été proposé:

ADN-12 H_2O + Nt- 5 H_2O ---> ADN-Nt + 17 H_2O

La libération de 17 molécules d'eau pour un résidu nétropsine fixé a été confirmée par les mesures de changement d'entropie du système (MARKY et al., 1983). La Nt, comme la Dst-A, se fixe à l'ADN en mimant le cortège d'eau situé dans le petit sillon. La preuve en est que l' on peut observer la formation d'un complexe Nt-ADN-B à des taux d' " hydratation " inférieurs à 23 % auxquels on observe habituellement le conformère A.

Du point de vue géométrique, l'interaction Nt-ADN provoque un changement de conformation des deux espèces (MARTIN et al., 1978; REINERT & THRUM, 1970). Il y a adaptation de la conformation de l'une pour l'autre. Les deux noyaux pyrrole de la Nt ne sont pas coplanaires mais forment un angle de 20° entre eux ; cet angle passe à 33° dans le complexe Nt-dodécamère. Sur la base de résultats de diffraction de rayons X du complexe Nt-d(CGCGAATTCGCG)$_2$, Kopka et Dickerson ont montré que la Nt ne provoque ni élongation, ni détorsion du dodécamère utilisé, mais force l'ouverture du petit sillon (passage de 0,5 à 2 Å) et impose une courbure de l'axe de l'hélice de 8° dans la région de fixation (KOPKA et al., 1985a, 1985b).

Cependant l'analyse par rayons X ne tient pas compte de l'aspect dynamique de l'interaction; l'étude en solution de la liaison Nt-oligonucléotide révèle que la Nt ne provoque pas de modifications conformationnelles importantes au niveau de la zone de fixation centrale AATT mais induit des altérations de la conformation des bases adjacentes au site de liaison (KOPKA et al., 1985a, 1985b; PATEL, 1981; PATEL et al.,1983).

Du point de vue stoechiométrique, la Nt et la Dst-A couvrent respectivement 4 et 5 paires de bases, soit une paire de bases de plus qu'il y a de liaisons peptidiques dans l'antibiotique. Ceci est également vérifié pour les homologues supérieurs de la Dst-A (Dst-4, Dst-5, Dst-6) (ZIMMER et al., 1972; LUCK et al., 1977; KRYLOV et al., 1979; YOUNGQUIST & DERVAN, 1985).

De par l'utilisation simultanée d'oligonucléotides et d'analogues structuraux de la Nt et de la Dst-A, le type d'interaction moléculaire est maintenant bien caractérisé. Mais en présence d'un ADN natif, on constate une certaine hétérogénéité du mécanisme de liaison selon la séquence nucléique visée ou selon la concentration en Nt ou Dst; on parle alors d'interaction à caractère multimodal (REINERT et al., 1979; BURCKARDT et al., 1985).

2 Spécificité de liaison à l'ADN.

A côté de la spécificité conformationnelle existe une spécificité de bases. Nt et Dst-A se fixent de façon largement préférentielle au niveau des segments d'ADN riches en paires adénine-thymine (MULLER & GAUTIER, 1975; ZIMMER et al., 1979). La spécificité dA-dT n'est pas absolue, une fixation sur les régions dG-dC est observée à forte concentration. Mais, par exemple, l'étude de l'interaction Nt-d(CGCGAATTCGCG)$_2$ par RMN-^{1}H révèle que la Nt se fixe sur la séquence centrale AATT sans induire de shift des protons des bases G ou C (PATEL, 1979, 1982; KLEVIT et al., 1986). D'une manière générale, plus la portion nucléotidique dA-dT est longue, plus la fixation est intense. L'affinité maximale est obtenue avec un polymère poly(dA)-poly(dT) (Tableau I). La très faible fixation sur les sites GC serait due à l'encombrement stérique du groupement amino-2 de la guanine rendant le petit sillon inaccessible (WARTELL et al., 1974; LUCK et al., 1974; KRYLOV et al., 1979).

Tableau I

Peptide	DNA	K_a (M^{-1})	référence
Nt	Thymus de veau	$2.9\ 10^5$	Luck et al., 1974
	Poly(dA).(dT)	$4.9\ 10^5$	Wartell et al., 1974
	Poly(dA-dT).(dT-dA)	$4.0\ 10^5$	Wartell et al., 1974
Dst-A	Thymus de veau	$1.2\ 10^6$	Luck et al., 1974

La sélectivité peut être schématisée de la manière suivante :

$$\begin{matrix} d(AAAA) \\ d(TTTT) \end{matrix} \quad , \quad \begin{matrix} d(AATT) \\ d(TTAA) \end{matrix} \quad > \quad \begin{matrix} d(ATAT) \\ d(TATA) \end{matrix} \quad \gg \quad \begin{matrix} d(ACAC) \\ d(TGTG) \end{matrix} \quad , \quad \begin{matrix} d(GCGC) \\ d(CGCG) \end{matrix}$$

Remarque : ces propriétés sont mises à profit pour la séparation de différents fragments d'ADN par centrifugation en gradient de chlorure de césium contenant de la Nt. Celle-ci est ensuite éliminée par lavages à l'isopropanol (MATTHEWS et al., 1980; TATTI et al., 1978).

Conclusion

Nt et Dst-A sont donc des marqueurs de la conformation d'un ADN (forme B, A, Z) et également de la composition en bases AT d'un ADN (WARTELL et al., 1974; REINERT et al., 1980, 1981).

3°) Activité biologique de la Nt et de la Dst-A

De par leur très haute intensité de liaison sur l'ADN, il est logique que la Nt et la Dst-A exercent leurs effets in vivo en interférant avec les fonctions de régulation de l'ADN et le mécanisme de synthèse endocellulaire de l'ADN (inactivation des systèmes enzymatiques ADN-polymérasiques) (PUSCHENDORF, 1969; CHANDRA et al., 1972; ZIMMER, 1975; HAHN,1977; KUROYEDOV et al., 1977; BRUZIK et al., 1987). Malgré leur très faible affinité pour les ARN, ces ligands sont également de bons inhibiteurs des systèmes ARN-polymérasiques (PUSCHENDORF, 1971; HAHN, 1977; PUSCHENDORF et al., 1974). Nt et Dst-A ont un spectre d'activité large. Ces composés ont essentiellement des propriétés antivirales (SCHABEL et al., 1953; WERNER et al., 1965; VERINI & GHIONE, 1965; FOURNEL et al., 1965) et antibactériennes (ZYGMUNT, 1961; HAUPT & THRUM, 1971) très marquées. La Dst-A possède également des propriétés antimitotiques et antitumorales (DIMARCO et al., 1964). Cependant la toxicité de ces deux substances n'a jamais permis leur utilisation clinique; la Dst-A induit notamment des altérations chromosomiques (SCHMID et al., 1980; OCHI et al., 1988).

L'activité biologique est fortement réduite ou parfois même supprimée lorsque le cycle pyrrole est différemment substitué (perméthylation, disubstitution en 2,5 au lieu de 2,4) (GENDLER & RAPOPORT,1981; BIALER et al., 1980a). Les analogues monopyrroliques de la Nt ou de la Dst-A sont peu actifs; par contre l'augmentation du nombre d'unités amino-4 N-méthylpyrrole carboxamide accroît l'activité antivirale (BIALER et al., 1980b).

Les protéines qui se lient à l'ADN se fixent en général sur le grand sillon (OHLENDORF et al., 1982; TAKEDA et al., 1983; FREDERICK et al., 1984; ANDERSON et al., 1985; SCHEVITZ et al., 1985; OLLIS & WHITE, 1987) alors que les non intercalants comme la Dst-A et la Nt sont spécifiques du petit sillon (MELNIKOVA et al., 1975). L'inhibition des systèmes de synthèses nucléiques n'est donc pas due au masquage direct des sites de fixation des protéines mais aux modifications de conformation

spatiale de l'ADN induites par la fixation du nonintercalant (élargissement du petit sillon, courbure de l'hélice, maintien en conformation B (NEIDLE et al., 1987; CALLADINE,1982; DICKERSON, 1983; DREW & TRAVERS, 1985).

L'ADN est la plupart du temps la cible indispensable pour que l'effet cytotoxique de ces molécules s'exerce. Cependant, dans quelques cas, l'activité biologique est totalement indépendante de la capacité de la molécule à se lier à l'ADN. Par exemple la Dst-A n'est active que sur les bactéries Gram $^{+}$ (la différence Gram $^{+}$ / Gram $^{-}$ repose sur des différences biochimiques de la paroi bactérienne). La Dst-A, en se fixant sur des récepteurs spécifiques situés en surface de la bactérie *Bacillus subtilis* (Gram $^{+}$), empêche ainsi la pénétration d'autres molécules indispensables au métabolisme bactérien. La Dst-A ne pénètre pas dans la bactérie et n'interagit pas avec l'ADN (MAZZA et al., 1973; SICCARDI et al., 1975).

Cet exemple illustre bien la difficulté à établir des relations entre la capacité de liaison à l'ADN et l'activité biologique. Les pharmacomodulations entreprises ne tiennent compte le plus souvent que de la capacité potentielle d'un composé à interagir avec l'ADN alors que de nombreuses autres cibles moléculaires (membranes, enzymes...) sont parfois mises en jeu. Malheureusement, une approche rationnelle pour la conception de nouveaux composés ne peut être entreprise en tenant compte simultanément de toutes ces cibles.

II. Les modèles synthétiques.

1°) Généralités.

L'étude des mécanismes moléculaires du cancer a clairement montré que la dérégulation de l'expression de gènes cellulaires (par exemple, le gène myc est amplifié 30 fois dans la lignée cellulaire promyélocytique HL 60) ou l'expression de gènes mutés (mutations ponctuelles, translocation) sont souvent les éléments d'induction d'une prolifération cellulaire anarchique.

Par exemple, l'induction par un agent carcinogène (la Nitroso Méthyl Urée, NMU) d'une mutation ponctuelle, identifiée comme une transition G-->A sur le second nucléotide du codon 12, suffit à transformer le proto-oncogène H-ras-1 en un oncogène NMU-H-ras actif. Cette mutation transforme le codon GGA codant pour la glycine en un codon GAA codant pour l'acide glutamique, donnant ainsi naissance à une nouvelle protéine (p21) de 189 acides aminés possédant une activité GTPasique. La cascade d'évènements résultant de cette activation conduit chez le rat à la formation d'une tumeur mammaire dans presque 100% des cas (SUKUMAR & BARBACID, 1986).

Dès lors, en masquant cette séquence par un agent exogène possédant une forte affinité et une spécificité pour cette séquence, on pourrait peut-être bloquer l'expression de cette protéine, donc arrêter la prolifération tumorale. L'élaboration de telles molécules cytostatiques agissant par le biais de ce mécanisme d'action constitue l'un des axes de la pharmacochimie du cancer auquel nous nous sommes attaché.

En prenant comme modèle les composés naturels Nt et Dst-A, une série de modifications chimiques avait été entreprise de façon à concevoir des molécules non plus A-T mais G-C spécifiques ou capables de se fixer sélectivement sur une séquence oligodésoxynucléotidique préalablement définie.

De très nombreuses molécules ont été synthétisées. Elles ont permis d'une part de mieux comprendre le mécanisme d'action des médicaments parents Nt et Dst-A et d'autre part de définir les relations structure-activité des agents non intercalants du petit sillon (BAGULEY, 1982).

Parmi tous les analogues synthétisés, la classe des lexitropsines ou "sequences reading oligopeptides" (LOWN et al., 1986a, 1986b; KISSINGER et al., 1987; LEE et al.,

1988a, 1988b, 1988c; LOWN, 1988) s'est révélée tout à fait intéressante. Les noyaux pyrrole de la Nt et de la Dst-A ont été substitués par des noyaux imidazole.

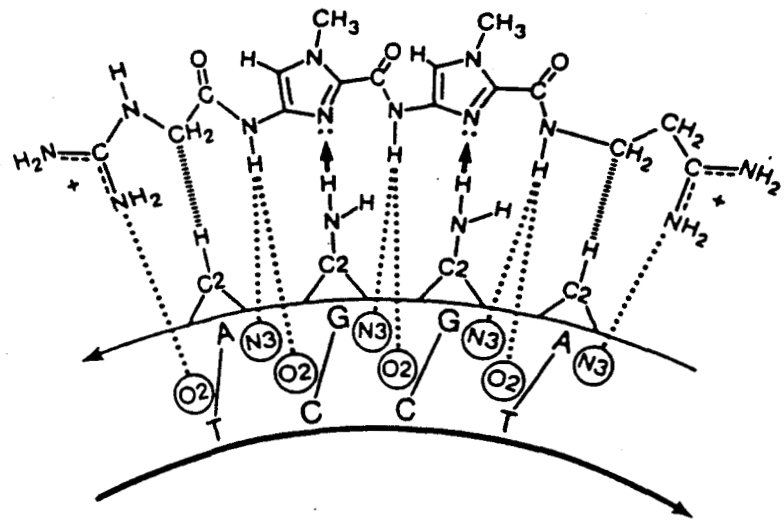

Figure 4 : Structure et représentation des caractéristiques de la reconnaissance moléculaire d'un modèle de lexitropsine en vis-à-vis de la sequence 3'-AAA-5'. (⇀↽) liaisons hydrogène, (≡) contact de Van der Waals. (LOWN et al., 1986b).

L'atome d'azote non substitué de l'imidazole permet, par son doublet libre d'électrons, l'établissement d'une liaison hydrogène avec le NH_2 d'une guanine. Les résultats expérimentaux montrent pour ces composés une diminution de la spécificité AT et une fixation possible sur un segment GC. Mais il n'y a pas de site de fixation largement préférentiel puisque la liaison a lieu en de trés nombreux sites de séquences variables.

La présence d'une liaison hydrogène $N_{hétérocycle}$-H-$N_{guanine}$ ne semble donc pas être un paramètre suffisant à l'établissement d'une spécificité GC stricte; toutefois, cette liaison est a priori nécessaire.

Sur la base des modèles synthétisés jusqu'à présent, nous avons entrepris une pharmacomodulation en tenant compte des paramètres suivants :

1 - nécessité d'un système polyaromatique.
2 - importance des chaînes latérales cationiques.
3 - importance de la courbure de la molécule.
4 - possibilités d'établissement de liaisons ioniques, hydrogène et de Van der Waals.
5 - présence d'hétéroatomes porteurs d'un doublet libre susceptible d'engager une liaison hydrogène avec le NH_2 d'une guanine.

De nombreux autres paramètres sont encore à définir pour élaborer des composés dont la conformation s'adapte au maximum à celle de l'ADN.

2°) Résultats et discussion.

1 Analogues thiazoliques de la Nétropsine et de laDistamycine-A

alStructure

Une première série de trois composés a été synthétisée. Dans ces composés le résidu commun (amino-4 carboxy-2 N-méthylpyrrole) de la Nt et de la Dst-A a été remplacé par un résidu d'acide aminé du type aminométhyl-2 carboxy-4 thiazole (une cystéine cyclisée) (Figure 5). Ces résidus possèdent deux hétéroatomes (N, S) susceptibles d'engager des liaisons hydrogène avec le NH_2 de la guanine. Toutes les caractéristiques requises citées précédemment sont réunies dans les molécules synthétisées.

Ce motif thiazolique est souvent retrouvé au sein de substances naturelles d'origine marine telles que la dolastatine, l'ulicyclamide, l'ulithiacyclamide et les patellamides, substances dotées de propriétés antitumorales trés puissantes. Par exemple une dose de 10^{-7} µg/ml de dolastatine suffit à inhiber de 50% la croissance d'une population de cellules leucémiques (P388). La trés forte activité de ces composés, au mode d'action peu ou pas connu, et l'expérience du laboratoire pour la synthèse de dérivés thiazoliques (HOUSSIN et al., 1984a,1984b, 1985a, 1985b; BERNIER et al., 1986a) nous ont incité à choisir ce motif.

Un autre modèle, **Thia-Nt** (Figure 5), analogue direct des 3 premiers composés mais pour lequel le résidu amino-4 est directement au voisinage de l'hétérocycle

a

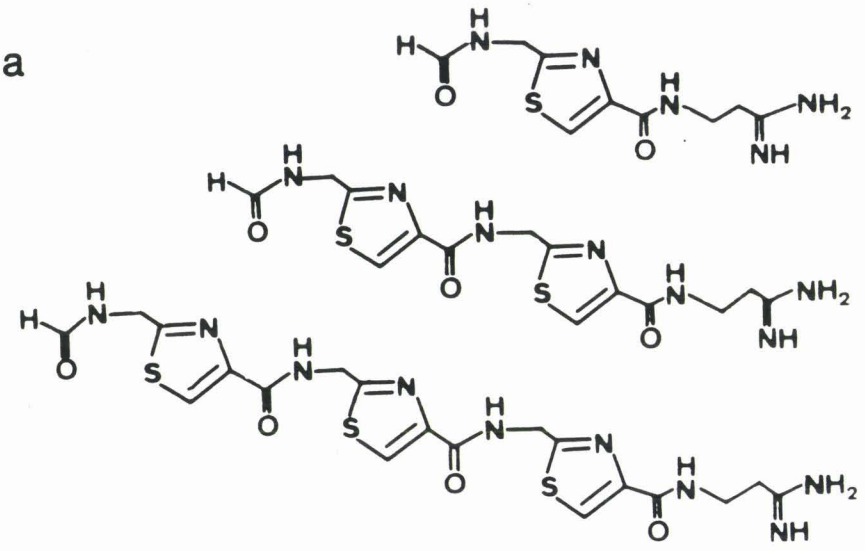

b

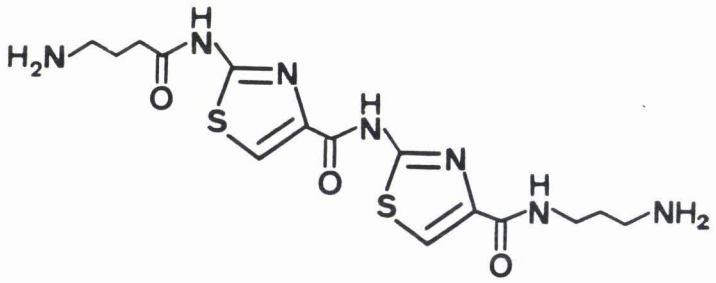

Figure 5 : Structure des analogues thiazoliques de la nétropsine. (A) composés du type poly(aminométhyl-2 carboxy-4 thiazole), (B) Thia-Nt.

thiazole (sans pontage par un résidu alkyle) a également été élaboré : l'absence de ce chaînon confère à cette molécule une plus grande rigidité.

b)Liaison à l'ADN

Les 3 premiers composés élaborés n'induisent que de trés faibles variations de la température de fusion de l'ADN. Le ΔTm maximal observé est de 3°C. L'étude par dichroisme linéaire électrique a confirmé la trés faible capacité de ces molécules à interagir dans le petit sillon de l'ADN.

L'inefficacité de ces molécules tant sur le plan physicochimique que biologique a été attribuée à leur trop grande flexibilité . La présence d'un chaînon alkyle au voisinage de l'hétérocycle induit une libre rotation à ce niveau et les composés ne peuvent plus adopter une conformation rigide en forme d'arc comme le réalise la Dst-A. Cependant une récente étude a montré que la présence d'un résidu de β-alanine entre les deux hétérocycles pyrrole de la Nt réduisait l'affinité mais n'empéchait pas la liaison dans le petit sillon de l' ADN (DASGUPTA et al., 1987). Le chaînon méthylène entre les deux thiazoles des composés 1-3 rompt la courbure de la molécule et la délocalisation électronique entre les hétérocycles. L'importance de la conformation du ligand a été confirmée pour le composé Thia-Nt plus rigide et dont la fixation à l'ADN a été bien caractérisée et a fait l'objet de la publication suivante :

article n°1:

Synthesis and DNA binding study of a thiazole-containing analog of netropsin.

PLOUVIER B., HOUSSIN R., BAILLY C., HENICHART J-P.

Soumis pour publication à Journal of Heterocyclic Chemistry.

SYNTHESIS AND DNA-BINDING STUDY OF A THIAZOLE-CONTAINING ANALOG OF NETROPSIN.

Bertrand Plouvier and Raymond Houssin

Laboratoire de Chimie de Synthèse des Médicaments
Faculté de Pharmacie, rue du Professeur Laguesse
59045 LILLE, France

Christian Bailly and Jean-Pierre Hénichart

INSERM, Unité N°16, Place de Verdun
59045 LILLE, France

DNA is the support of the genetic information; of its chemical structure depend normal or anarchic cell growth or the cell death. Differences between normal and tumor cells take origin at the gene level. Beyond the always increasing frequency of cancer, it seems particularly important to develop an efficient strategy for the design of chemotherapeutic drugs designed as gene control agents. In this way, minor groove binding compounds [1], typified by netropsin and distamycin, appear to be a promising source of active compounds because of their ability to bind to large DNA sequences.

Oligopeptide xenobiotics including antibiotic, antineoplastic and antiviral drugs interfere with the replication and transcription by the recognition and preferential binding to specific double-stranded DNA sequences. Such is the case of antiviral and antitumor distamycin-A (Dst) and of antibiotic netropsin (Nt) (Figure 1), two N-methylpyrrole drugs able to block the template function of DNA by binding to specific nucleotide sequences in the minor groove of double strand DNA [2]. On the basis of X-Ray data, it was found that the adenine-thymine base-specific binding of both drugs is due to electrostatic bonds between ends of side chains of the ligands and DNA phosphates, hydrogen-bonding interactions between amide NH and adenine N(3) and thymine O(2), and Van der Waals contacts between methylenes and heterocyclic CH of DNA bases [3,4]. In order to confirm these criteria, some structural modifications have been carried out including replacement of pyrrole ring by pyridine [5,6] and imidazole [7,8] heterocycles and/or lengthening of the chain [9,10].

In this attempt to study the influence of the nature of the heterocyclic parts and the linking groups on the curvature of the obtained compounds fitting well with DNA geometry, we proposed the design of thiazole containing Dst and Nt analogues [11]. The choice of this heterocycle was directed by chemical considerations concerning the ring size and the relative position of heterocyclic N atom in the whole peptidic chain. Moreover the thiazole carboxylic acid, a cyclized cystein, was found to play an important biological role in the cytotoxic activity of cyclopeptides isolated from marine animals [12-15] and in the DNA binding capacity of antitumor drugs such as bleomycin [16]. The chemistry of starting materials leading to the synthesis of thiazole-containing cyclopeptides [17,18] or bleomycin models [19,20] was extensively worked in our laboratory and prompted us to propose the synthesis of a new thiazole Nt analogue.

This report includes an efficient and easily reproducible synthesis of the 2-aminothiazole-4-carboxylic acid which was found to be a key compound in the strategic pathway leading to the synthesis of the Nt-analog, Thia-Nt (Figure 1), in the

structure of which the pyrrole rings of Nt were replaced by thiazole heterocycles and amidine and guanidine ends simplified in primary amines. Together with details on the optimized synthesis, the results of a preliminary study of Thia-Nt—DNA binding are also reported.

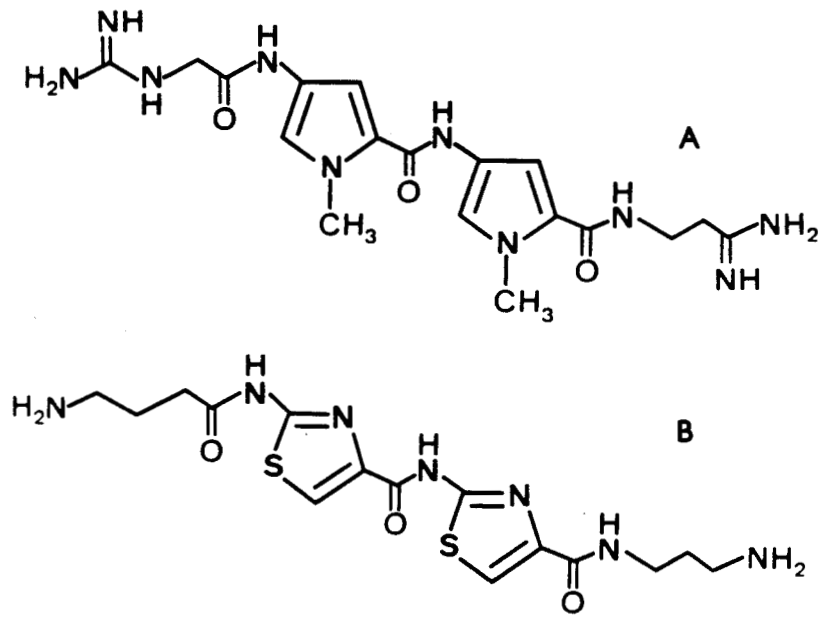

Figure 1 : Structure of netropsin (A) and Thia-Nt (B).

Chemistry

The synthetic method for the preparation of 2-amino-4-carboethoxythiazole 2 consists of the cyclising condensation of thiourea with ethyl bromopyruvate according to the Kuhn procedure [21]. Thiazole 2 was coupled with 4-tert-butyloxycarbonylaminobutyric acid [22] in the presence of dicyclohexylcarbodiimide (DCC) and 1H-hydroxy-1,2,3-benzotriazole (HOBt). After saponification of the ester group of the "dipeptide" 3, the acid 4 was coupled with 2-amino-4-carboethoxythiazole 2 in the above conditions (DCC, HOBt) to give the thiazole-containing "tripeptide" 5 which was saponified to give the acid 6.

The introduction of the second side chain was achieved by a last coupling, in the presence of DCC and HOBt, with the mono-protected diamine 7 [23] to give the protected diamine 8. The desired compound Thia-Nt (9) was obtained as a dihydrobromide by cleavage of the tert-butyloxycarbonyl (Boc) groups by dry hydrogen bromide in acetic acid (see Figure 2).

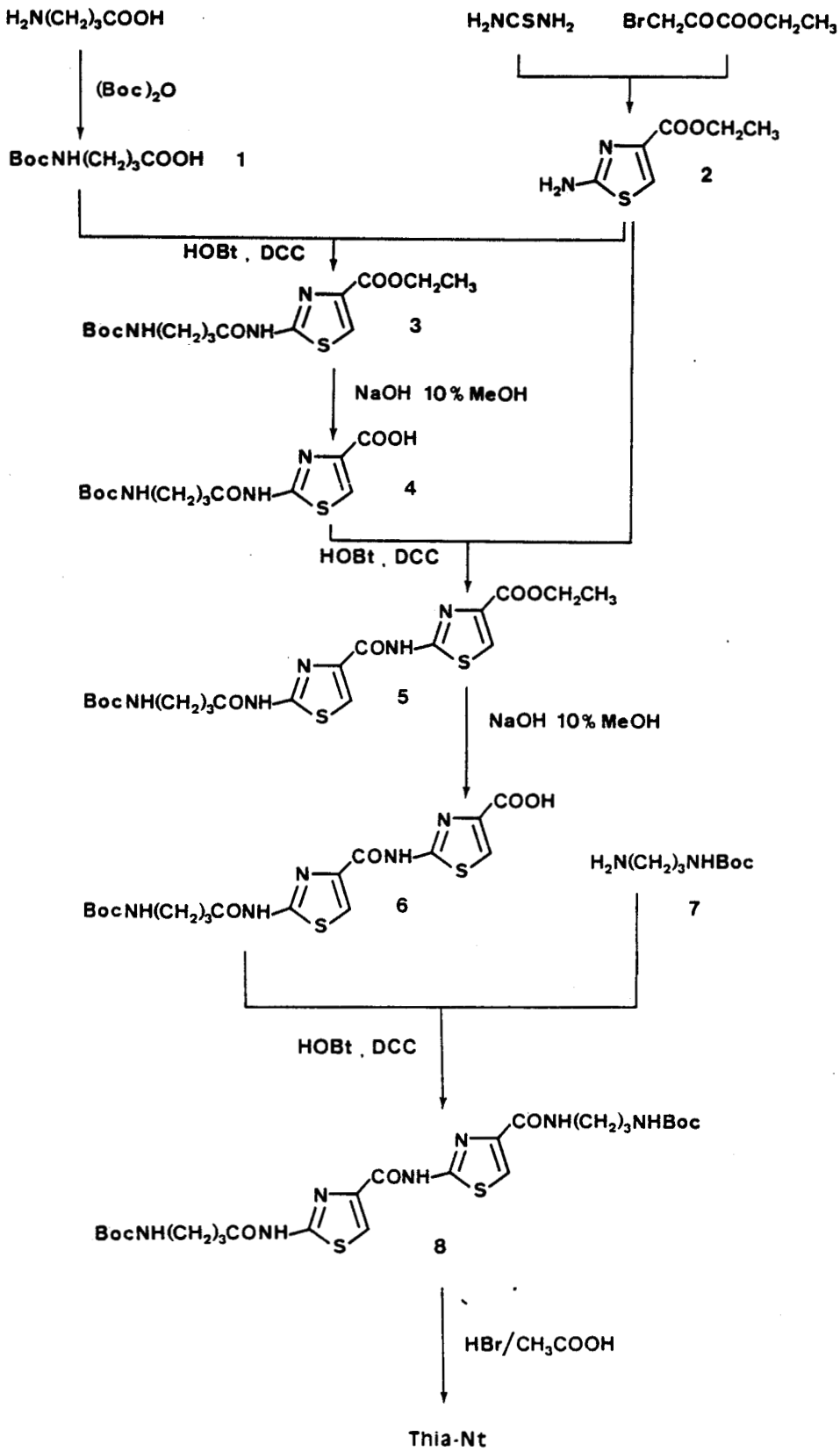

Figure 2 : Synthesis of Thia-Nt.

DNA-binding

Binding of the synthetic ligand Thia-Nt to DNA was deduced from the hypochromic effects observed in the UV absorption spectra of this ligand when DNA was added (Figure 3). A red shift (4 nm), indicative of an increased delocalization of the π-electrons in the ligand, was noted. These spectral modifications were found upon addition of coliphage T_4 DNA in which the major groove is occulted by bulky glucose residues on the 5-(hydroxymethyl)cytidine bases [24]. The results were consistent with a binding in the minor groove as established for Nt [4]. In order to verify this result, linear electric dichroism studies have been undertaken.

The Thia-Nt-calf thymus DNA complex reduced linear dichroism spectrum (Figure 4) shows a positive part (295-330 nm) reflecting the position of the bis-thiazole chromophore in the DNA complex. At these wavelengths, a significative contribution from the DNA itself was observed which certainly minimizes the measured linear dichroism values for the complex.

Nevertheless, this positive curve clearly demonstrates that the ligand is preferentially oriented parallel to the DNA axis, a geometry which excludes intercalation. Thus, replacement of the N-methylpyrrole heterocycle in Nt by a thiazole ring does not perturb the minor groove binding.

The binding affinities were calculated by means of Scatchard plots [25] (Figure 5) and allowed us to precise the binding parameters (Table I). The Scatchard plots were done at 265 nm, a wavelength at which a large DNA absorbance is observed and it was necessary to substract the DNA contribution by adding an equal concentration of DNA to the reference cell. The apparent binding constant K_a, measured with two DNAs of different base composition, indicate that Thia-Nt binds DNA with a weaker affinity than Nt does [2] (Nt-calf thymus DNA, $K_a = 2.9 \times 10^5\ M^{-1}$; Nt-poly(d(AT).d(AT)), $K_a = 4 \times 10^5\ M^{-1}$).

The ligand was found to cover 4-5 nucleotides per binding site (n) with the synthetic poly[d(A.T)-d(A.T)] DNA. This result is an argument in favor of a location of the ligand in the minor groove of DNA. The difference in the DNA binding affinity of the studied compound toward the two different DNA was also apparent considering the ΔTm values (Table I), meaning a marked preference of this drug for A-T sites as observed for Nt [2-4].

The spectroscopic measurements have provided information concerning the mode of binding of the thiazole-containing Nt analogue to DNA. Orientation of this drug in the minor groove of DNA can readily be postulated.

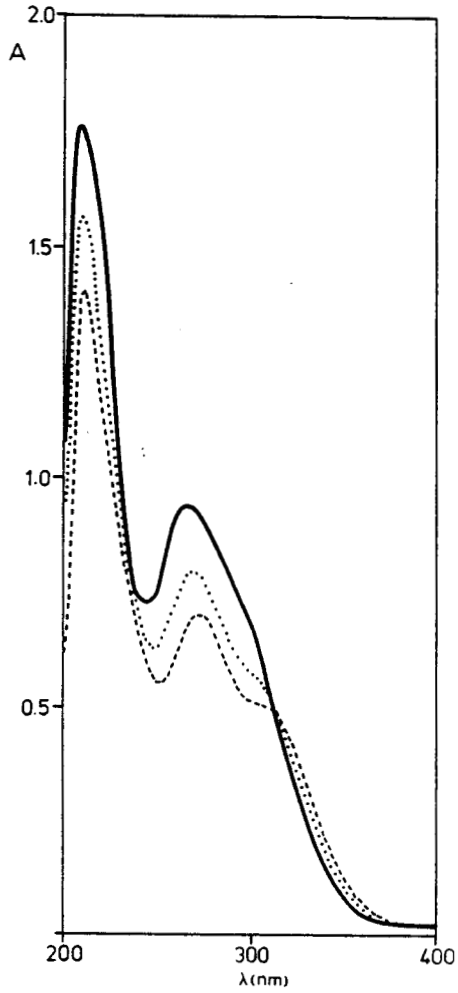

Figure 3 : UV absorption spectra of Thia-Nt at a concentration of 78 µM (—) and its complex with coliphage T_4 DNA at a DNA/Thia-Nt ratio of 0.35 (···) and 0.7 (--). The sample and reference cell contained equal concentrations of DNA [(···)27 µM and (--)55 µM].

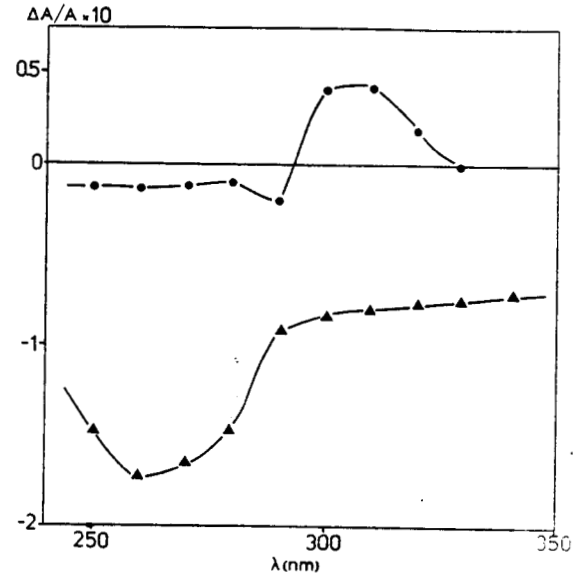

Figure 4 : Reduced linear electric dichroism (ΔA/A) spectra of the calf thymus DNA (▲) and of the Thia-Nt—DNA complex (●) at a ligand/DNA ratio of 0.1 and at 12.5 $kV.cm^{-1}$.

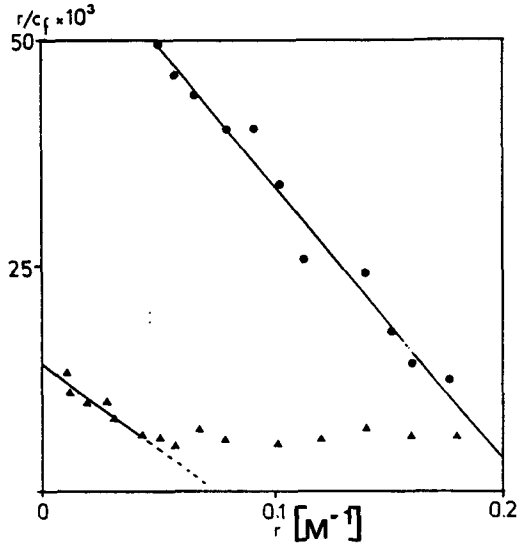

Figure 5 : Representative Scatchard plot for the evaluation of the binding parameters for the interaction of Thia-Nt with calf thymus DNA (▲) and poly[d(A.T)-d(A.T)] (●).

TABLE I : DNA-binding parameters of Thia-Net.

		ΔTm[a] (D/P)[b]		λ[c]	$K_a(M^{-1})$[d]	n[e]
Poly[d(A.T)-d(A.T)]	3°4(0.1)	9°3(0.5)	12°(1.0)	265	$6.4\ 10^4$	4.8
calf thymus DNA	0°7(0.1)	3°(0.5)	5°7(1.0)	265	$1.2\ 10^4$	....

[a] Elevation in thermal denaturation temperature (deg°C). [b] Drug to Phosphate DNA ratio.
[c] Wavelength at which the absorbance change was measured. [d] Apparent binding constant.
[e] Binding site size.

Experimental

Melting point were taken on a Tottoli Büchi 510 apparatus and are uncorrected. The ir spectra were recorded with a Perkin Elmer 297 spectrophotometer using KBr pellets. The ^{1}H-nmr spectra were recorded on a Brücker WP 80 SY spectrophotometer. Chemicals shifts are reported in ppm from tetramethylsilane as an internal standard and are given en δ units. EI mass spectra were recorded on a Ribermag R10.10 (combined with Riber 400 data system) mass spectrophotometer at 70 eV by using direct insertion. FAB mass spectra were determited on a Kratos MS-50 RF mass spectrometer. Thin layer chromatography (TLC) was carried out using silica gel 60F-254 Merck, in system solvent A(chloroform-methanol, 80/20, v:v in a saturated ammonia atmosphere). Elemental analyses were performed by the "Service Central d'Analyses", CNRS, Vernaison, France.

UV absorption spectra and melting temperature studies were recorded with a Uvikon Kontron 810/820 spectrophotometer and realised in 0.1 M SSC buffer (0.15 M sodium chloride, 0.015 M sodium citrate, pH 7.0) as previously described [26]. Linear dichroism experiment were made using a well-established procedure [27]. Scatchard analysis and determination of the binding parameters were realised using a described method [28].

Amino-2-ethoxycarbonyl-4-thiazole (2)

A mixture of thiourea (5 g, 65.8 mmoles) and ethyl 2-bromopyruvate (12.8 g, 65.8 mmoles) was heated gradually to 70° under stirring until the mixture became highly viscous. On cooling, the hydrobromide cristallized and was recristallized from ethanol-petroleum ether. The recristallized hydrobromide was solubilized in water and the base was precipitated from addition of dilute ammonia. The crude product was filtred and recristallized from methanol to give 2 in a 57.5 % yield, mp 175-177° ; Rf(A):0.8 ; ir : 1600(NH), 1680(C=O), 3100-3400 cm^{-1}(NH), ^{1}H nmr(DMSO-d_6) : δ 7.4(s,1H,CH thiazole), 7.3(s,2H,NH_2), 4.2(q,2H,CH_2), 1.2(t,3H,CH_3) ; MS-m/e (rel. intensity) : 172(M^+,44.8), 144(9.2), 73(98.8).

Anal. Calcd. for $C_6H_8N_2O_2S$: C, 41.9 ; H, 4.7 ; N, 16.3 ; O, 18.6 ; S, 18.6.

Found : C, 41.5 ; H, 4.7 ; N, 16.1 ; O, 19.0 ; S, 18.6.

Ethyl 2-(4-tert-butyloxycarbonylaminobutyryl)-amino-thiazole-4-carboxylate (3)

Cold solutions of DCC (2.64 g, 12.7 mmoles) and HOBt (1.95 g, 12.7 mmoles) in dichloromethane/dimethylformamide (1:1, 20 ml) were added to a solution of 4-tert-butyloxycarbonylaminobutyric acid 1 [22] (2.36 g, 11.6 mmoles) in 15 ml of dichloro

methane/dimethylformamide (1:1) at 0°C for 1 hour under stirring. A cold solution of 2 (2 g, 11.6 mmoles) in dichloromethane/dimethylformamide (1:1, 20 ml) was added and stirring was continued for 2 hours at 0°C and 12 hours at room temperature. The solvent was evaporated and the residue taken up with dichloromethane provided dicyclohexylurea (DCU) which was filtered. The organic solution was washed with 1 N hydrochloric acid, water and finally with 1 M sodium bicarbonate. After drying over anhydrous sodium sulfate, the solvent was removed in vacuo. The remaining DCU was discarded by precipitation with ethyl acetate, the resulting material was recristallized from acetone giving pure 3 (2.6 g, 63% yield), mp 155-157° ; Rf(A):0.95 ; ir : 1720(CO amide), 1680cm^{-1}(CO ester); ^{1}H nmr (CDCl3) : δ 11.6(m,1H,NH), 7.8(s,1H,CH thiazole), 4.9(m,1H,NHBoc), 4.4(q,2H,CH_2), 3.2(m,2H,CH_2NH), 2.6(t,2H,CH_2CO), 1.9(m,2H, CH_2), 1.4(m,12H,CH_3); MS-m/e(rel.intensity) : 357 (M^+,1.8).

Anal. Calcd. for $C_{15}H_{23}N_3O_5S$: C,50.5 ; H,6.5 ; N,11.8 ; O,22.4 ; S,9.0.

Found :C,50.5 ; H,6.6 ; H,11.5 ; O,22.0 ; S,8.6.

2-(4-tert-butyloxycarbonylaminobutyrylamino)-thiazole-4-carboxylic acid (4)

A solution of 3 (2 g, 5.6 mmoles) in methanol (11 ml) and sodium hydroxide (0.9 g in 9 ml of methanol/water, 10/1) was stirred at 65°C. The progress of the reaction was monitored by TLC and was thereby judged to be complete after 3 hours. The solvent was evaporated and the residue was taken up in water. Impurities were extracted with ethyl acetate (2x20 ml). The aqueous solution was cautiously acidified to pH 4-5 with 1 N hydrochloric acid and extracted with ethyl acetate (3x20 ml). After drying over anhydrous sodium sulfate and evaporation of the organic layer, trituration in cyclohexane and evaporation of cyclohexane yield 1.6 g of 4, (87% yield), mp 187-189° ; Rf(A):0.25 ; ir : 3000-2500 cm^{-1}(OH dimer) ; ^{1}H nmr (CDCl3) : δ 12.2(m,1H,NH), 7.8 (s,1H,CH thiazole), 5.2(m,1H,NHBoc), 3.3(m,2H, CH_2NHBoc), 2.6(t,2H,CH_2CO), 2.0(m,2H,CH_2), 1.4(s,9H,CH_3) ; MS-FAB : 330(M^+ +1).

Ethyl 2-[2'(4-tert-butyloxycarbonylaminobutyrylamino)-thiazole-4'-carboxamido]-thiazole-4-carboxylate (5)

The acid 4 (2 g, 6.08 mmoles) was coupled to the amine 2 (1.045 g, 6.08 mmoles) using DCC (1.38 g, 6.66 mmoles) and HOBt (1.023 g, 6.68 mmoles) in dichloromethane/dimethylformamide (1:1) as described for the preparation of 3. DCU was removed by precipitation with ethyl acetate and the filtrate washed with 1 N hydrochloric acid (20 ml), water (20 ml) and 1 M sodium bicarbonate (20 ml), then dried over anhydrous sodium sulfate. The solvent was removed in vacuo giving 1.17 g (38%) of 5 after

recrystallisation from a mixture of ethanol-ether, mp 131-135° ; Rf(A):0.87; ir 1720(CO amide), 1680cm^{-1}(CO ester) ; ^{1}H nmr(CDCl3) : δ 11.2(m,1H,NH), 7.9(s,1H,CH thiazole), 7.8(s,1H,CH thiazole), 5.1(m,1H,NHBoc), 4.4(q,2H,CH_2), 3.3(m,2H,CH_2NH), 2.7 (t,2H, CH_2CO), 2.0(m,2H,CH_2), 1.4(m,12H,CH_3) ; MS-FAB : 484(M^+ +1).
Anal. Calcd. for $C_{19}H_{25}N_5O_6S_2$: C,47.2 ; H,5.2 Found C,47.4 ; H,5.5.

2-[2'-(4-tert-butyloxycarbonylaminobutyrylamino)-thiazole-4'-carboxamido]-thiazole-4)-carboxylic acid (6)

The ethyl ester 5 (500 mg, 1.035 mmole) was totally converted after 3 hours to the corresponding acid 6, according to the method for preparation of 4. 6 was obtained pure after column chromatography with chloroform-methanol, 8/2, v:v, as eluent (410 mg, 87%), mp>250° ; Rf(A):0.6 ; ir : 3000-2500 cm^{-1}(OH dimer) ; ^{1}H nmr(DMSO-d_6) : δ 15.5(s,1H,OH), 7.9(s,1H,CH thiazole), 7.5(s,1H,CH thiazole), 6.8(m,1H,NHBoc), 3.2(m,2H,CH_2 NH), 2.7(m,2H,CH_2CO), 1.9(m,2H,CH_2), 1.4(s,9H,CH_3).
Anal. Calcd. for $C_{17}H_{21}N_5O_6S_2$: C,44.8 ; H,4.65 ; N,15.4 ; O,21.1 ; S,14.1.
Found : C,44.6 ; H,4.8 ; N,15.1 ; O,21.2 ; S,13.8.

tert-butyl[2-]2'-(4-tert-butyloxycarbonylaminobutyrylamino)-thiazole-4'-carboxamido]-thiazole-4-carboxamido]-propyl carbamate (8)

The acid 6 (300 mg, 0.66 mmole) was coupled to 3-tert-butyloxycarbonyl aminopropylamine 7 [23] (115 mg, 0.66 mmole) using DCC (149 mg, 0.73 mmole) and HOBt (111 mg, 0.73 mmole) in a mixture of dichloromethane-dimethylformamide (1:1, 18ml) according to the procedure described for 3. Purification of the crude material was accomplished by column chromatography with chloroform-methanol, 8/2, v:v, as eluent. Collection and evaporation of the appropriate fractions give 8 with 52% yield, mp 58-63° ; Rf(A):0.95 ; ir : 1680 cm^{-1}(CO) ; ^{1}H nmr(CDCl3) : δ 11.5(m,1H,NH), 8.3(m,1H,NHCO), 7.8(d,2H,CH thiazoles), 5.1(m,1H,NHBoc), 3.4(m,6H,CH_2NH), 2.7(m,2H,CH_2CO), 2.0(m,4H,CH_2), 1.4(s,18H,CH_3) ; MS-m/e (rel.intensity) : 612 (M^+, 30.2).
Anal. Calcd. for $C_{25}H_{37}N_7O_7S_2$: C,49.1 ; H,6.1 ; N,16.0 ; O,18.3 ; S, 10.5.
Found : C,48.9 ; H,6.0 ; N,16.1 ; O,18.1 ; S,10.2.

(2-(2'-(4-aminobutyrylamino)-thiazole-4'-carboxamido)-thiazole-4-carboxamido)-propylamine dihydrobromide (Thia-Nt) (9)

A solution of 8 (133 mg, 0.217 mmole) in acetic (30 ml) was flushed with dry bromhydric acid for 10 minutes and stirring was maintained for 20 minutes. After evaporation of the solvent under vacuum, the residue was washed with ethanol (4x30

ml) to remove acids, taken up with water, washed with chloroform and diethyl ether (15 ml). Lyophilisation of the aqueous layer yield 9 (89.5% yield), mp : 197-202° ; Rf(A):0 ; ^{1}H nmr (DMSO-d_6 ; 400MHz) : δ 12.4(s,2H,NHCO), 8.3(s,1H,CH thiazole), 8.2(t,1H,NH CH_2), 7.8(s,1H,CH thiazole), 7.75(m,6H,NH_3^+), 3.3(m,1H,CH_2NH), 2.8(m,4H,$CH_2NH_3^+$), 2.6(m,2H,CH_2CO), 1.8(m,4H,CH_2).
Anal. Calcd. for $C_{15}H_{23}N_7O_3S_7Br_2$: C,31.4 ; H,4.0 ; N,17.1 ; O,8.4 ; S,11.2. Found : C,31.2 ; H,4.2 ;N,17.5 ; O,8.1 ; S,10.9.

Acknowledgement

We thank the "Institut National de la Santé et de la Recherche Médicale" and the "Fédération Nationale des Centres de Lutte contre le Cancer" for the financial support.

References

[1] Ch. Zimmer, G. Luck, G. Burckhardt, K. Krowicki and J.W. Lown, in "Molecular Mechanism of Carcinogenic and Antitumor Activity", C. Chagas and B. Pullman, eds, 1986, pp.339-363.

[2] C. Zimmer and U. Wahnert, Prog. Biophys. Mol. Biol., 47, 31 (1986).

[3] M.L. Kopka, A.V. Fratini, H.R. Drew and R.E. Dickerson, J. Mol. Biol., 163, 129 (1983).

[4] M.L. Kopka, C. Yoon, D. Goodsell, P. Pjura and R.E. Dickerson, Proc. Natl. Acad. Sci. USA, 82, 1372 (1985).

[5] W.S. Wade and P.B. Dervan, J. Am. Chem. Soc., 109, 1574 (1987).

[6] D.H. Jones and R.H. Wooldridge, J. Chem. Soc., 550 (1968).

[7] J.W. Lown, K. Krowicki, U.G. Bhat, A. Skorobogaty, B. Ward and J.C. Dabrowiak, Biochemistry, 25, 7408 (1986).

[8] K. Kissinger, K. Krowicki, J.C. Dabrowiak and J.W. Lown, Biochemistry, 26, 5590 (1987).

[9] D. Dasgupta, P. Parrack and V. Sasisekaran, Biochemistry, 26, 6381 (1987).

[10] R.S. Youngquist and P.B. Dervan, Proc. Natl. Acad. Sci. USA, 82, 2565 (1985).

[11] C. Bailly, R. Houssin, J-L. Bernier and J-P. Hénichart, Tetrahedron, 44, 5833 (1988).

[12] G.R. Pettit, Y. Kamano, P. Brown, D. Gust, M. Inoue and C.L. Herald, J. Am. Chem. Soc., 104, 805 (1982).

[13] C.M. Ireland and P.J. Sheuer, J. Am. Chem. Soc., 102, 5688 (1980).

[14] C.M. Ireland, A.R. Durso Jr, R.A. Newman and M.P. Hacker, J. Org. Chem., 47, 1807 (1982).

[15] J.M. Wasylyk, J.E. Biskupiak, C.E. Costello and C.M. Ireland, J. Org. Chem., 48, 4445 (1983).

[16] J-P. Hénichart, J-L. Bernier, N. Helbecque and R. Houssin, Nucl. Acids Res., 13, 6703 (1985).

[17] R. Houssin, M. Lohez, J-L Bernier and J-P. Hénichart, J. Org. Chem., 50, 2787 (1985).

[18] J-L. Bernier, R. Houssin and J-P. Hénichart, Tetrahedron, 42, 2695 (1986).

[19] R. Houssin, J-L. Bernier and J-P. Hénichart, J. Heterocyclic Chem., 21, 465 (1984).

[20] R. Houssin, J-L. Bernier and J-P. Hénichart, J. Heterocyclic Chem., 21, 681 (1984).

[21] R. Kuhn and K. Dury, Liebigs Ann. Chem., 571, 44 (1951).

[22] L. Moroder, A. Hallett, E. Wunsch, O. Keller and G. Wersin, Hoppe Seyler's Z. Physiol. Chem. 357, 1651 (1976).

[23] R. Houssin, J-L. Bernier and J-P. Hénichart, Synthesis 259 (1988).

[24] R.L. Erickson and W. Szybalski, Virology 22, 11 (1964).

[25] G. Scatchard, Ann. N.Y. Acad. Sci. 51, 660 (1949).

[26] C. Bailly, J-L. Bernier, R. Houssin, N. Helbecque and J-P. Hénichart, Anti-Cancer Drug Design 1, 303 (1987).

[27] C. Houssier and C.T. O'konski, in " Molecular Electro-Optics ", series B 64, S. Krause, ed, Nato Advanced Study Institute, 1981, pp 309-339.

[28] K. Ekambareswara Rao, D. Dasgupta and V. Sasisekaran, Biochemistry 27, 3018 (1988).

Conclusion :

Ce composé Thia-Nt se fixe dans le petit sillon de l'ADN. Une affinité plus importante pour les paires de base A-T par rapport aux G-C a été montrée. Cependant aucun site de fixation spécifique n'a été mis en évidence.

De façon à obtenir des produits beaucoup plus performants sur le plan physicochimique et biologique, une autre stratégie a été envisagée.

La liaison d'une molécule intercalante et d'une molécule ligand du petit sillon peut avoir lieu simultanément sur des sites nucléiques proches malgré les changements de conformation de l'ADN induits par ces deux types de ligands (WARTELL et al., 1975; WILKINS, 1982; PATEL, 1981; PARDI et al., 1983) . Il semblait dès lors intéressant de lier de façon covalente ces deux types de molécules pour former un hybride "Intercalant-Ligand du petit sillon " qui devrait posséder une affinité pour l'ADN et peut-être une activité biologique supérieure à celle des substances modèles.

Des molécules associant un pseudopeptide de type poly(N-méthyl pyrrole carboxamide) aux extrémités 1 et 9 du chromophore phénoxazone de l'actinomycine ont ainsi été crées (KRIVTSORA et al., 1984). L'une d'entre elles, du type Dst-phénoxazone-Dst (Figure 6), peut se fixer sur un segment nucléotidique de 10 paires de bases, témoin de la fixation de la totalité de la molécule (DERVAN, 1986). Mais la fixation principale a lieu sur des sites plus courts de 4 à 6 paires de bases, témoignant de l'intercalation et de la fixation d'un seul résidu Dst-A sur l'ADN. Avec ce modèle, les importantes modifications de conformation de l'ADN induites à la fois par l'intercalation et par la fixation dans le petit sillon (soit respectivement un écartement des plateaux de paires de bases et un écartement des deux brins d'ADN) ne semblent pas permettre un recouvrement idéal de large segments nucléotidiques. De plus aucune activité antimitotique n'a été mise en évidence.

Toutefois ce modèle semblait intéressant et ouvrait la voie à une nouvelle série chimique répondant au concept " Peptide à liaison spécifique-Intercalant ".

Il est à noter que là encore, c'est à partir de substances naturelles comme la triostine et l'échinomycine appartenant à cette catégorie que ce concept a été mis en place.

La triostine et l'échinomycine sont deux antibiotiques antitumoraux capables de se lier à l'ADN à la fois par bis-intercalation de leurs chromophores quinoxaline entre deux plateaux G-C et par fixation dans le petit sillon du peptide reliant les deux

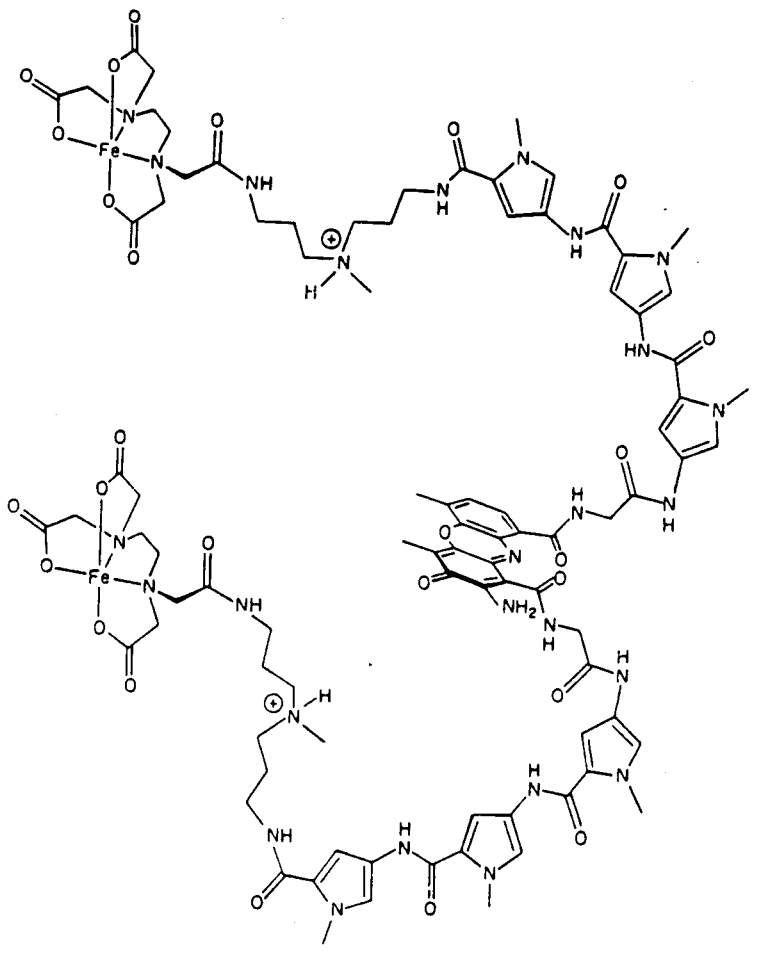

Figure 6 : Structure d'un modèle hybride Dst-phénoxazone-Dst (DERVAN, 1986). Les résidus d'EDTA en position N-terminale permettent de définir la séquence de fixation spécifique sur l'ADN par la technique de "DNA-affinity cleaving".

hétérocycles au niveau de segments AT. L'hexanucléotide GCATGC constitue la séquence spécifique de liaison de ces deux antibiotiques, spécificité directement induite par leur conformation propre en forme de pince (Figure 7) (WANG et al., 1984; WARING, 1986). Une altération de la structure de la molécule comme par exemple une déméthylation des acides aminés impliqués (une valine et deux cystéines) fournit une molécule (nommée TANDEM (Figure 8), VISWAMITRA et al., 1981; HOSSAIN et al., 1982) qui se lie préférentiellement aux séquences riches en résidus AT et non plus sur des GC (LOW et al., 1984a, 1984b). De la même façon, il avait été montré au laboratoire (HELBECQUE et al., 1985; BERNIER et al., 1981) que le remplacement des chromophores quinoxaline, individuellement non intercalants, par des chromophores acridine (Figure 8), potentiellement intercalants, conduit également à une altération de la spécificité de liaison.

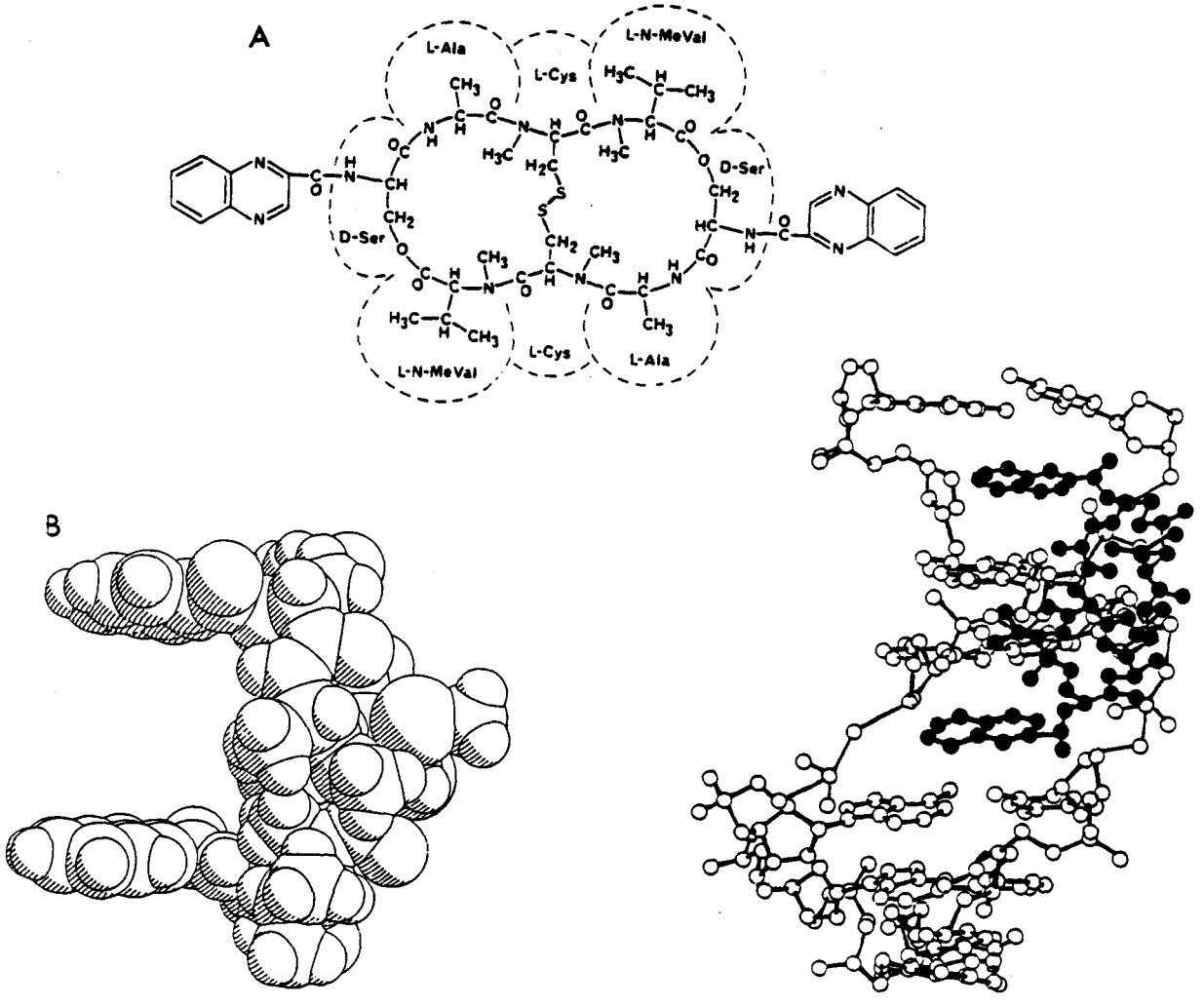

Figure 7 : Structure (A) et représentation moléculaire (B) de la triostine A. Schéma du mode d'interaction triostine A-ADN.

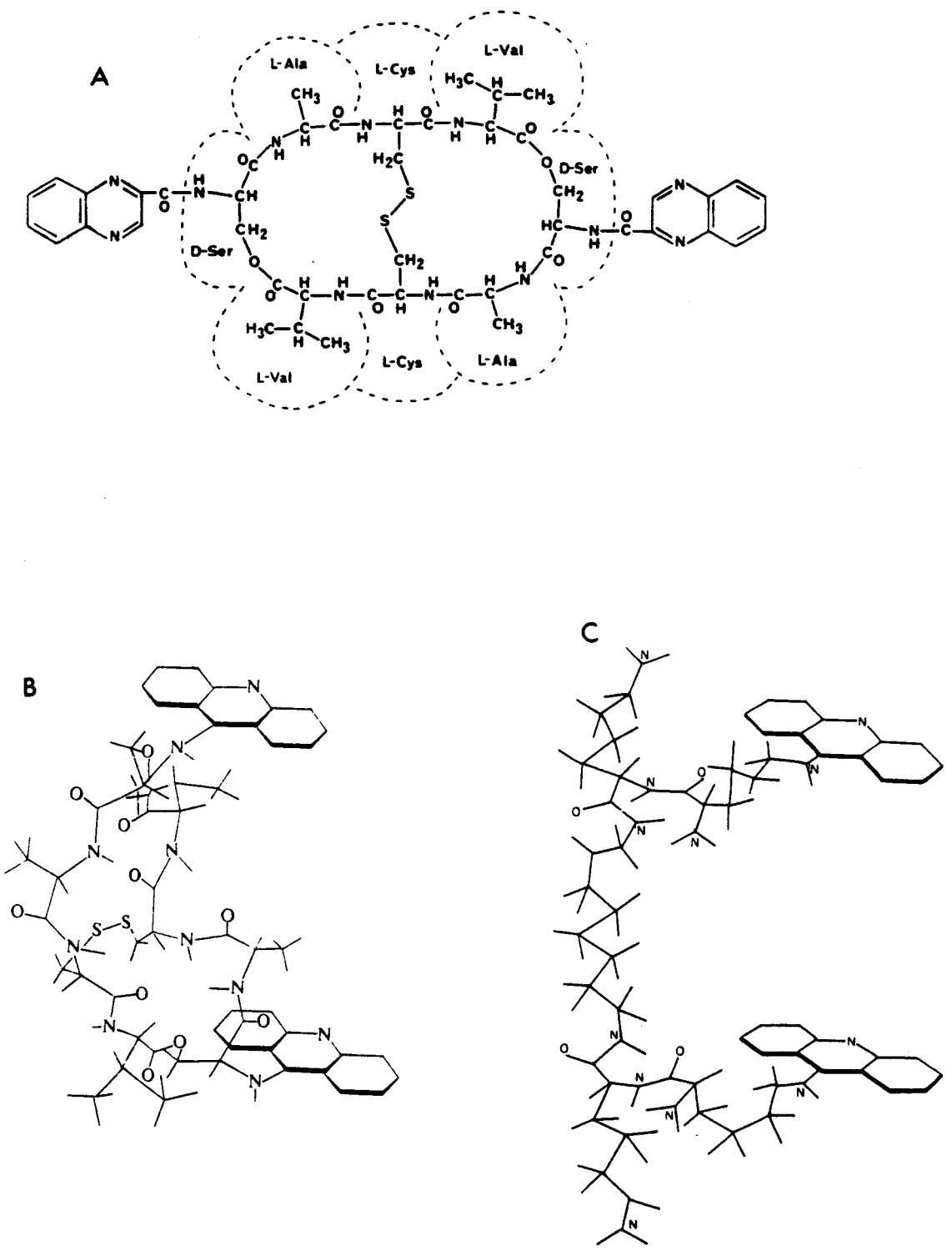

Figure 8 : Structure des analogues synthétiques de la triostine A : TANDEM (A) et les dérivés de l'acridine (B, C).

Ces exemples indiquent que, plus que la nature individuelle des fractions se liant à l'ADN, il semble très important de considérer la conformation de l'ensemble de la molécule elle-même.

Tenant compte de ces observations, du concept fixé précédemment et de l'expérience du laboratoire en matière de synthèse de dérivés hétérocycliques (BERNIER et al., 1986a; HENICHART et al., 1982a, 1982b; HOUSSIN et al., 1984a, 1984b, 1985a, 1985b, 1986), différents composés ont été synthétisés et étudiés.

2 Dérivés acridiniques de la nétropsine et la distamycine.

a) Structure.

Une série de molécules composées (I-IV) d'un chromophore anilinoamino-9 acridine lié de façon covalente à un pseudopeptide à 1, 2 ou 3 résidus (N-méthylpyrrole carboxamide) analogues à la Nt ou la Dst-A a été élaborée.

Le chromophore anilinoamino-9 acridine est intéressant à plusieurs titres :
- l'acridine est un intercalant vrai (LERMAN, 1961; WARING, 1976),
- la portion aniline se loge dans le petit sillon de l'ADN (WILSON et al., 1981),
- de plus ce chromophore est décrit comme G-C spécifique (FEIGON et al., 1984),
-il est structuralement proche de l'amsacrine, (Figure 9), médicament anticancéreux largement utilisé dans le traitement des leucémies,
- il est capable de pénétrer faiblement dans la cellule et de se concentrer au niveau nucléaire (LEMAY et al., 1983).

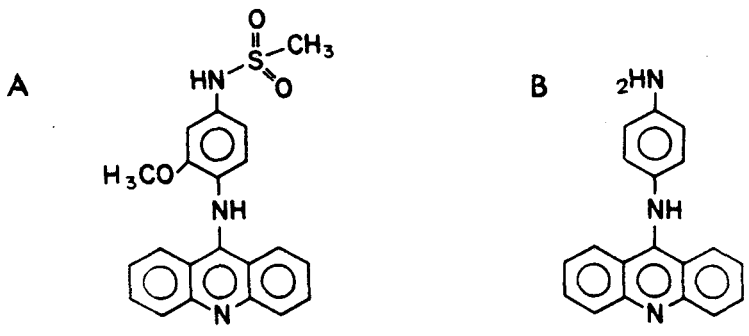

Figure 9 : Structure de l'amsacrine (A) et de l'anilinoamino-9 acridine (B).

b) Liaison à l'ADN.

Le mode d'interaction de ces quatre modèles synthétiques avec des ADN naturels ou synthétiques de différentes compositions a été étudié d'abord par spectroscopie d'absorption (détermination de la température de demi-transition de l'ADN, ΔTm) et indirectement par fluorescence en utilisant la fluorescence du complexe ADN-bromure d'éthidium. Ces résultats, ainsi que le détail de la synthèse de ces composés et l'étude préliminaire de leur activité antitumorale, font l'objet de l'article suivant :

article n°2:

Design, synthesis, DNA-binding and biological activity of a series of DNA minor groove binding intercalating drugs.

BAILLY C., POMMERY N., HOUSSIN R., HENICHART J-P.

Journal of Pharmaceutical Sciences, 1989 (sous presse).

DESIGN, SYNTHESIS, DNA-BINDING AND BIOLOGICAL ACTIVITY OF A SERIES OF DNA MINOR GROOVE BINDING INTERCALATING DRUGS

Christian BAILLY,* Nicole POMMERY,** Raymond HOUSSIN,**
Jean-Pierre HENICHART*[X]

*INSERM U. 16, Place de Verdun 59045 Lille, France.
**Faculté de Pharmacie, rue Laguesse 59045 Lille, France.

SUMMARY

A group of pseudopeptides, molecular combination of the natural and antitumor agents distamycin or netropsin and the anilinoacridine chromophore, related to the synthetic antileukemic drug m-AMSA, has been synthesized. Their DNA-binding properties were determined and discussed in terms of their structural differences and in relation with their observed base-dependent binding. Binding data are consistent with a model in which the acridine nucleus occupies an intercalation site and the netropsin or distamycin residue resides in the DNA minor groove. Cytostatic and cytotoxic activities against murine cell line are reported as well as significative differences in the inhibition of DNA synthesis.

The majority of antitumor agents in current clinical use are thought to exert their cytotoxic action by interferring with DNA metabolism[1]. Most of them bind to DNA by a non-covalently binding process and act either by inhibition of nucleic acid synthesis or by initiation of DNA breakage. This group of compounds is subdivided into agents which bind by a classical intercalative process[2] and agents which form with DNA a non-covalent non-intercalative complex[3].

Among intercalating compounds[4] used, acridine derivatives stand as the archetypes. Amsacrine[5] (m-Amsa), a synthetic antitumor drug used in the treatment of acute leukemia[6], is the leader of this group and has attracted attention with the aim of developping analogs with an improved broad spectrum activity[4]. The second class is represented by netropsin (Nt) and distamycin (Dst-A), naturally occurring non-intercalative binding compounds forming highly ordered complexes with DNA[7]. Both drugs were shown to lie across the minor groove of DNA and recognize specific DNA nucleotides sequences[7]. These natural compounds constitute models for the design of sequence-reading oligopeptides[8]. This approach is very attractive from a fundamental point of view and now permit the synthesis of peptides which bind to predetermined sequence specifically[9].

For that purpose, we decided to introduce intercalating moieties into the structure of groove selective binding agents. Nt and Dst-A demand binding sites consisting of $(AT)_4$ and $(AT)_5$ respectively[10], while the anilinoacridine moiety intercalates between GC bases pairs[11]. The linkage of peptides with strict sequence specificity to an intercalating ring with a different base specificity can lead to a new class of sequence-reading oligopeptides with enhanced antitumor activity.

In this study, we report the design, synthesis, characterization, DNA-binding properties and biological evaluation of a series of hybrid molecules in the structure of which a minor groove binding peptide (poly-aminopyrrole carboxylic acid) is linked to a classical intercalating moiety, the anilinoacridine ring (Figure 1). These studies have been carried out in order to develop more effective anticancer agents and contribute to the general preoccupation of pharmacologist and chemist which is to explore more systematically the structure-biological activity relationship of sequence directed DNA effectors.

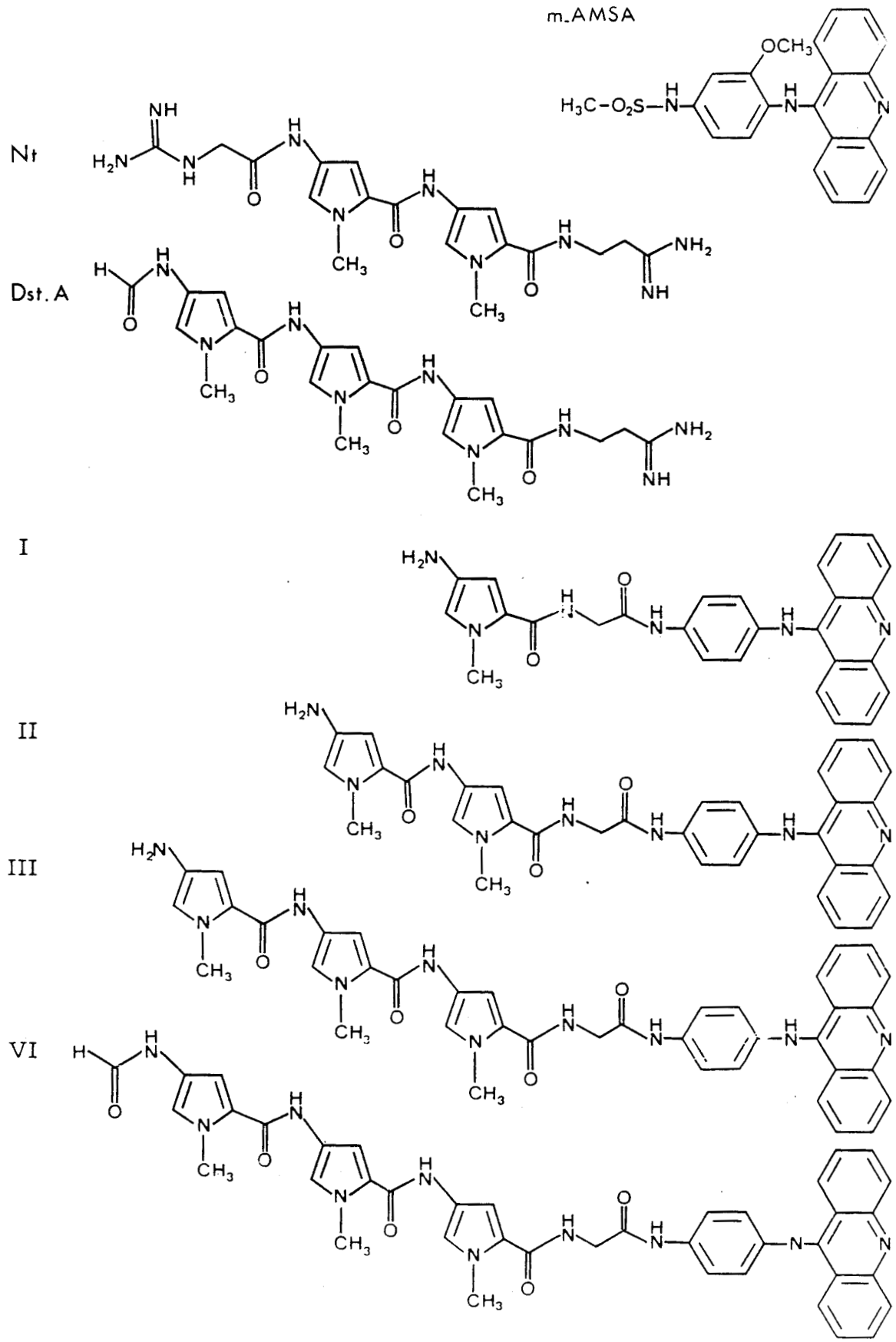

Figure 1. Structure of amsacrine (m-Amsa) netropsin (Nt), distamycin (Dst-A), and related synthetic hybrid compounds I, II, III and IV.

CHEMISTRY

N-methyl-2-pyrrole carboxylic acid was esterified with methyl iodide, then nitrated with nitric acid in acetic anhydride. Separation by column chromatography gave the methyl N-methyl-4-nitro-2-pyrrole carboxylate (2), the 5-nitro isomer and the dinitro derivative. The nitro ester 2 was reduced to the amine 3 which was condensed with ditertbutyldicarbonate to give the BOC-protected ester 4. However, it should be pointed out here that the unstable air-sensitive amino acid 3 could be easily stored as the stable trifluoroacetate salt in a high yield, making it a convenient precursor for synthesis of different oligomers. Alkaline hydrolysis of 4 afforded the acid 5 after acidification. This acid was used for the synthesis of I (see below). Coupling of 5 with the amine 3 was readily achieved with dicyclohexylcarbodiimide (DCC) in the presence of catalytic amounts of dimethylaminopyridine (DMAP). Alternatively, the amide linkage could be realised via an HOBt-active ester but the presence of unreacted products needed also a chromatographic purification.

The dimeric compound 6 was classically saponified with an hydro-methanolic sodium hydroxide solution to give the corresponding acid 7. This acid was used in the final synthesis of II.

The protecting BOC group in 6 was classically cleaved-off with trifluoroacetic acid (TFA). Due to the light decomposition observed during the extraction, the aqueous solution of the salt 8 was immediately lyophilisated. The building of the trimeric block 9 was effected by coupling the acid 5 with the appropriate amine 8 using DCC-DMAP as condensing agent. In this case, the procedure with DMAP was found to be better than with HOBt (80 % vs 45 %). Compound 9 has also been synthesised starting from the acid 7 and the amine 3 in a lower yield. In this series, the sensivity of the coupling reaction as well as the saponification and the BOC cleavage procedures are decreasing from the monomer to the trimer. Conventional conversion of the methyl ester 9 into its corresponding acid 10 preceeded the coupling with the glycylanilinoacridine moiety to give III.

The synthesis of the formylated trimeric compound IV, mimicking more precisely the distamycin antibiotic, presented a lot of difficulties and needed another strategy. The N-terminal group of 3 could be easily formylated in a satisfactory yield using formic acid, DCC and HOBt but the so-obtained N-formyl moiety was cleaved-off during the saponification of the methyl ester. The degradation of the N-formyl derivative in alcaline saponification conditions led us to prepare the benzyl ester 11 (Cs salt of 5, then benzyl bromide in DMF, as described[11]). After deprotection with TFA, aqueous extraction gave essentially pure 12. The subsequent N-formylation (formic acid, DCC-HOBt) was proved to be easier than with formic anhydride[12]. The coupling of the acid 5

Scheme I

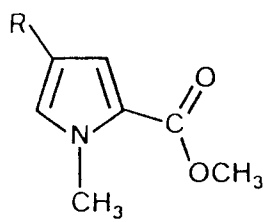

1. R=H
2. R=NO_2
3. R=NH_2

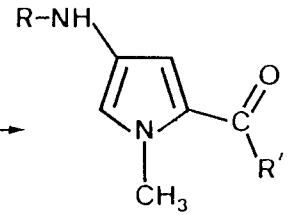

4. R=BOC, R′=OCH_3
5. R=BOC, R′=OH
11. R=BOC, R′=OBzl
12. R=H , R′=OBzl
13. R=CHO, R′=OBzl
14. R=CHO, R′=OH

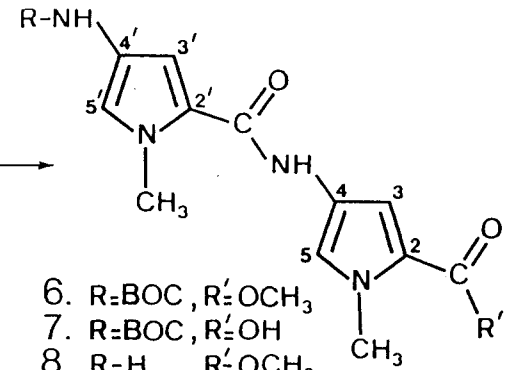

6. R=BOC, R′=OCH_3
7. R=BOC, R′=OH
8. R=H , R′=OCH_3
15. R=BOC, R′=OBzl
16. R=H , R′=OBzl

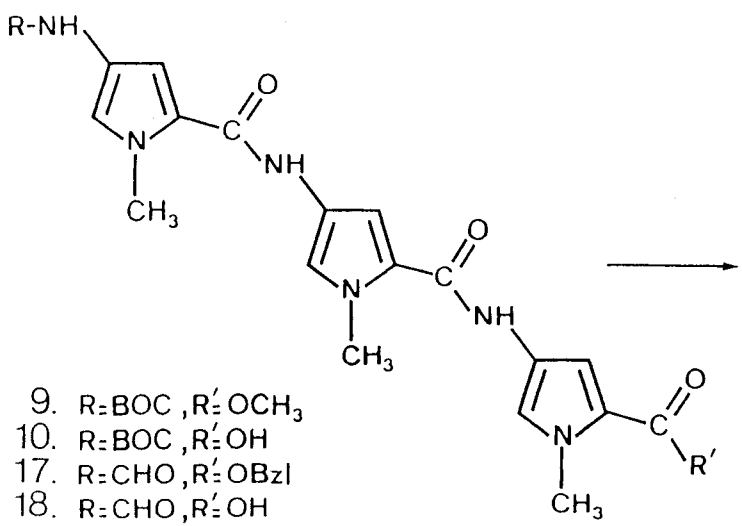

9. R=BOC, R′=OCH_3
10. R=BOC, R′=OH
17. R=CHO, R′=OBzl
18. R=CHO, R′=OH

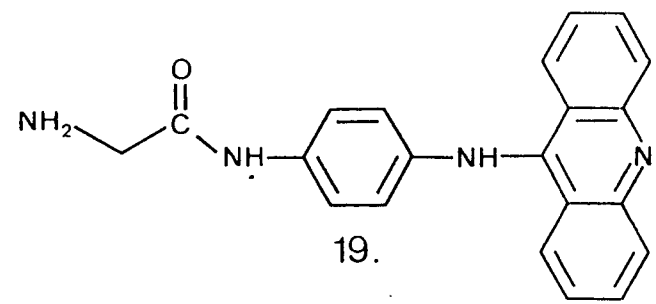

19.

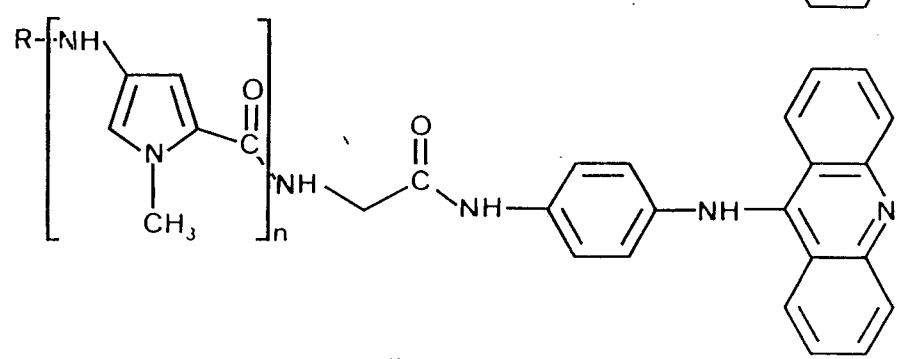

20. R=BOC, n=1
21. R=BOC, n=2
22. R=BOC, n=3

I. R=H, n=1
II. R=H, n=2
III. R=H, n=3
IV. R=CHO, n=3

Compound	m.p. (°C)	Rf (solvent)[a]	Yield %	IR ν(cm^{-1})	MS M$^+$ (rel. int.)
1	oil	0.93 (A)	90	1710 ($COOCH_3$)	e
2	112	0.97 (A) 0.53 (B)	35	3120 (CH), 1700 ($COOCH_3$), 1480 (NO_2)	184 (100)[f]
3[b]	185	0.72 (A)	92	2900-3100 (NH_3^+) 1730 ($COOCH_3$)	155 (100)[f]
4	109	0.95 (A) 0.56 (B)	84	3360 (NH), 1725 ($COOCH_3$), 1685 (OCO)	254 (58)[f]
5	146	0 (A) 0.71 (C)	93	3330 (NH), 3000 (CH), 1725 (COOH), 1620 (OCO)	240 (25)[f]
6	125	0.92 (A)	80	3340 (NH), 1770 ($COOCH_3$), 1715 (OCO), 1680 (CONH)	376 (7)[f]
7	100	0 (A) 0.84 (C)	86	1705 (COOH), 1690 (OCO), 1655 (CONH)	e
8[b]	111	0.65 (A)	93	2900-3100 (NH_3^+), 1730 ($COOCH_3$), 1670 (CONH)	276 (35)[f]
9	d	0.86 (A)	96	3340 (NH), 1720 ($COOCH_3$), 1695 (OCO), 1650 (CONH)	498 (66)[f]
10	170	0.41 (A) 0.82 (C)	72	3200 (NH), 1700 (OCO), 1650,1665 (CONH)	483 (48)[g]
11	139	0.90 (A) 0.54 (B)	86	3380 (NH), 1720 (COOBzl), 1680 (OCO)	330 (12)[f]
12[b]	d	0.78 (A) 0.29 (B)	87	3050-3150 (NH_3^+), 1720 (COOBzl)	230 (58)[f]
13	206	0.83 (A)	78	1715 (COOBzl), 1655 (CHO)	258 (100)[f]
14	186	0.1 (A) 0.72 (C)	95	3150 (NH), 1700 (COOH), 1660 (CHO)	168 (100)[f]
15	158	0.8 (A)	87	3340 (NH), 2980 (CH_3) 1700 (OCO), 1660 (CONH)	452 (4)[f]
16[b]	187	0.8 (A)	83	3200-3600 (NH), 1720 (COOBzl), 1670 (CONH)	353 (36)[h]
17	261	0.63 (A)	59	1720 (COOBzl), 1700 (CHO), 1640, 1650, 1670 (CONH)	503 (43)[h]
18	210-212	0 (A) 0.82 (C)	77	1710-1700 (CHO,COOH) 1640-1660 (CONH)	413 (17)[h]
20	247	0.77 (A)	65	2920, 2850 (NH), 1700 (OCO), 1645, 1635 (CONH)	565 (100)[h]
21	195	0.61 (A)	52	3340 (NH), 2920 (CH), 1700 (OCO), 1630-1650 (CONH)	687 (45)[h]
22	260	0.75 (A)	72	3400-3000 (NH,CH) 1690 (OCO), 1650 (CONH)	809 (52)[h]
I[c]	220-223	0 (A) 0.15 (C)	67	3600-3200 (NH_3^+,NH), 2900-3000 (CH)	466 (28)[h]
II[c]	242	0 (A) 0.22 (C)	43	3600-3200 (NH_3^+,NH), 1630, 1640 (CONH)	587 (63)[h]
III[c]	210-213	0 (A) 0.18 (C)	29	3600-3200 (NH_3^+,NH), 1625-1650 (CONH)	709 (42)[h]
IV[c]	235-239	0 (A) 0.18 (C)	43	3600-3200 (NH_3^+,NH), 1700 (CHO), 1650 (CONH)	737 (6)[h]

[a]Solvent : A : $CHCl_3$-MeOH, 80/20 (v/v) in a satured NH_3 atmosphere; B : CH_2Cl_2;
C : CH_2Cl_2-MeOH, 20/80 (v/v). [b]TFA salt. [c]Hydrochloride. [d]Decompose upon heating.
[e]No molecular ion peak in the 70-eV mass spectrum. [f]Determined by Electronic Impact (EI).
[g]M$^+$-1. [h]M$^+$+1, determined by Fast Atom Bombardment (FAB).

Compound	^{1}H NMR (δ, ppm/TMS)	^{13}C NMR (δ, ppm/TMS)
1	3.72 (s,3,OCH_3), 3.84 (s,3,NCH_3), 6.07, 6.82 and 7.0 (3m,3,3CH)[a]	37.78 (NCH_3), 51.25 (OCH_3), 110.83 (C_4), 116.71 (C_3), 124.0 (C_2), 125.52 (C_5),160.86 (CO)[b]
2	3.78 (s,3,OCH_3), 3.92 (s,3,NCH_3), 7.27 and 8.17 (2d,2,2CH,J=4.7Hz)[a]	37.73 (NCH_3), 51.63 (OCH_3), 112.42 (C_3), 122.71 (C_2), 127.51 (C_5), 135.01 (C_4),160.35 (CO)[b]
3[e]	3.55 (s,3,OCH_3), 3.60 (s,3,NCH_3), 6.71 and 6.89 (2d,2,2CH)[c]	37.89 (NCH_3), 53.0 (OCH_3), 113.46 (C_3), 122.97 (C_5), 124.83 (C_4), 125.19 (C_2), 163.21 (CO), 113.05 (CF_3), 163.63 (COO^-)[c]
4	1.42 (s,9,$(CH_3)_3$), 3.68 (s,3,OCH_3), 3.76 (s,3,NCH_3), 6.64 and 7.0 (2d,2,2CH), 8.85 (s,1,NH)[a]	28.26 (CH_3,BOC), 36.54 (NCH_3), 50.93 (OCH_3), 80.08 (C,BOC), 108.0 (C_3), 119.81 (C_5,C_4), 122.12 (C_2), 153.21 (CO,BOC), 161.45 (COO)[b]
5	1.41 (s,9,$(CH_3)_3$), 3.76 (s,3,NCH_3), 6.58 and 7.0 (2d,2,2CH), 8.87 (s,1,NH)[a]	28.22 (CH_3,BOC), 36.50 (NCH_3), 80.0 (C,BOC), 107.91 (C_3), 119.72 (C_5), 120.17 (C_4), 122.35 (C_2), 153.20 (CO.BOC), 164.81 (COOH)[b]
6	1.44 (s,9,$(CH_3)_3$), 3.67 (s,3,OCH_3), 3.74 and 3.79 (2s,6,2NCH_3), 6.80, 6.81, 6.88 and 7.4 (4d,4,4CH), 8.88 and 9.70 (2s,2,2NH)[a]	28.31 (CH_3,BOC), 36.51, 36.63 (2NCH_3), 51.02 (OCH_3), 79.56 (C,BOC), 103.63, 108.26 (C_3,C_3'), 118.43, 118.73 (C_5,C_5'), 120.88, 121.05 (C_4,C_4'), 121.74, 121.93 (C_2,C_2'), 153.51 (CO,BOC), 160.94 (CONH), 161.47 (COO)[b]
7	1.50 (s,9,$(CH_3)_3$), 3.83 (s,6,2NCH_3), 6.85, (m,3,3CH), 7.37 (d,1,CH), 8.89 and 9.68 (2s,2,2NH)[a]	28.32 (CH_3,BOC), 36.54, 36.92 (2NCH_3), 80.92 (C,BOC), 103.94, 110.04 (C_3,C_3'), 118.19, 122.10 (C_5,C_5'), 119.26, 121.74 (C_4,C_4'), 121.96, 123.20 (C_2,C_2'), 153.56 (CO,BOC), 158.90 (CONH), 164.73 (COOH)[b]
8[e]	3.72 (s,3,OCH_3), 3.79 and 3.85 (2s,6,2NCH_3), 6.88 (m,2,2CH), 7.05 and 7.40 (2d,2,2CH,J=4.7Hz), 9.90 (s,1,NH)[a]	37.13, 37.25 (2NCH_3), 52.79 (OCH_3), 113.40, 113.57 (C_3,C_3'), 123.06, 125.92 (C_5,C_5'), 124.83, 126.35 (C_4,C_4'), 125.11, 125.60 (C_2,C_2'), 161.13 (CONH), 163.30 (CO), 113.20 (CF_3), 163.50 (COO^-)[c]
9	1.48 (s,9,$(CH_3)_3$), 3.76 (s,3,OCH_3), 3.83 (s,9,3NCH_3), 4.96 (m,1,NH), 6.53, 6.64, 6.72, 6.79, 7.12 and 7.38 (6d,6,6CH), 7.79 and 8.17 (2s,2,2NH)[a]	28.34 (CH_3,BOC), 33.87 (NCH_3), 36.58 (2NCH_3), 50.71 (OCH_3), 80.34 (C,BOC), 103.73, 103.91, 108.39 (C_3,C_3',C_3''), 115.43, 116.32, 118.53, 119.33, 119.77, 119.97, 121.42, 121.78, 123.10 (C_2,C_2',C_2'', C_4,C_4',C_4'', C_5,C_5',C_5''), 153.64(CO,BOC), 158.01, 159.01 (2CONH), 161.53 (COO)[b]
10	1.50 (s,9,$(CH_3)_3$), 3.88, 3.89 and 3.92 (3s,9,3NCH_3), 6.85, 6.90, 7.01, 7.10 and 7.17 (5s,6,6CH), 7.62 (m,1,NH)[a]	26.50 (CH_3,BOC), 34.35, 34.39, 34.47 (3NCH_3), 76.54 (C,BOC), 102.18, 103.08, 106.63 (C_3,C_3',C_3''), 115.19, 116.58, 118.11, 118.37, 120.60, 120.77, 120.91, 120.98, 121.15 (C_2,C_2',C_2'', C_4,C_4',C_4'', C_5,C_5',C_5''), 151.17 (CO,BOC), 156.85 (2CONH), 160.50 (COOH)[a]
11	1.42 (s,9,$(CH_3)_3$), 3.83 (s,3,NCH_3), 5.22 (s,2,CH_2), 6.83 and 7.11 (2s,2,2CH), 7.37 (s,5,5CH), 7.45 (m,1,NH)[a]	28.25 (CH_3,BOC), 36.58 (NCH_3), 65.37 (CH_2), 79.98 (C,BOC), 108.15 (C_3) 119.30 (C_4), 121.52 (C_5), 127.32, 128.90 (CH,arom.), 136.26 (C_2), 153.11 (CO,BOC), 160.66 (CO,Bzl)[b]
12[e]	3.87 (s,3,NCH_3), 5.25 (s,2,CH_2), 6.83 and 7.06 (2d,2,2CH), 7.35 (s,5,5CH), 8.31 (m,3,NH_3^+)[a]	37.58 (NCH_3), 52.72 (CH_2), 108.56 (C_3), 120.62 (C_5), 122.0 (C_4), 123.38 (C_2), 126.0 (CH,arom), 163.35 (CO), 113.15 (CF_3), 163.50 (COO^-)[c]
13	3.88 (s,3,NCH_3), 5.24 (s,2,CH_2), 6.65 and 6.75 (2d,2,2CH), 7.32 (s,5,5CH), 7.57 (m,1,NH), 8.2 (d,1,CHO)[b]	36.62 (NCH_3), 65.46 (CH_2), 108.15 (C_3), 119.32 (C_4), 121.52 (C_5), 127.48, 129.05 (CH,arom.), 135.95 (C_2), 160.80 (CO,Bzl), 162.50 (CHO)[a]

14	3.78 (s,3,NCH_3), 5.52 (d,1,NH), 6.67 and 7.24 (2d,2,2CH), 8.1 (s,1,CHO), 9.87 (s,1,COOH)[a]	36.68 (NCH_3), 107.95 (C_3), 119.40 (C_4), 122.35 (C_5), 133.56 (C_2), 162.55 (CHO), 162.90 (COOH)[a]
15	1.50 (s,9,$(CH_3)_3$), 3.91 (s,6,2NCH_3), 5.25 (s,2,CH_2), 6.32 and 6.50 (2d,2,2CH), 6.82 (m,2,2CH), 7.30 (s,5,5CH), 7.55 and 7.64 (2s,2,2NH)[b]	28.23 (CH_3,BOC), 36.41, 36.56 (2NCH_3), 65.44 (CH_2), 80.15 (C,BOC), 103.86, 108.61 (C_3,$C_{3'}$), 118.60, 119.55 (C_5,$C_{5'}$), 121.07, 121.53 (C_4,$C_{4'}$), 121.81, 122.99 (C_2,$C_{2'}$), 127.81, 128.39 (CH,arom.), 136.27 (C,arom.), 153.51 (CO,BOC), 158.82 (CONH), 160.71 (COO)[b]
16[e]	3.90 (2s,6,2NCH_3), 5.28 (s,2,CH_2), 6.79, 6.82, 6.90 and 6.33 (4d,4,4CH), 7.35 (s,5,5CH), 7.40 (m,1,NH), 8.35 (m,3,NH_3^+)[c]	37.58 (2NCH_3), 52.75 (CH_2), 108.47, 110.83 (C_3,$C_{3'}$), 120.65 (C_5,$C_{5'}$), 122.17 (C_4,$C_{4'}$), 123.27 (C_2,$C_{2'}$), 125.98 (CH,arom.), 160.95 (CONH), 113.15 (CF_3), 163.95 (COO^-)[c]
17	3.89, 3.91 and 3.92 (3s,9,3NCH_3), 5.24 (s,2,CH_2), 6.92, 7.00, 7.08, 7.13, 7.20 and 7.33 (6s,6,6CH), 7.4 (m,2,2NH), 7.82 (s,5,5CH), 8.16 (s,1,CHO), 9.75 (m,1,NH)[a]	d
18	3.89 (m,9,3NCH_3), 6.91, 6.93 and 6.97 (3d,3,3CH), 7.12 (m,2,2CH), 7.18 (d,1,CH), 7.55 and 7.6 (m,2,2NH), 8.09 (m,1,CHO)[a]	d
20	1.45 (s,9,$(CH_3)_3$), 3.76 (s,3,NCH_3), 3.95 (d,2,CH_2, J=7.6Hz), 6.86 (d,1,NH), 7.10 (d,1,CH), 6.60-8.20 (m,14,NH,13CH), 8.90 and 9.76 (2s,2,2NH)	d
21	1.45 (s,9,$(CH_3)_3$), 3.81 and 3.82 (2s,6,2NCH_3), 3.96 (d,2,CH_2,J=5.7Hz), 6.71-7.63 (m,16,16CH), 8.28 (m,1,NH), 9.08 (m,1,NH), 9.75, 9.86 and 9.95 (3s,3,3NH)[a]	d
22	1.42 (s,9,$(CH_3)_3$), 3.70 (d,2,CH_2), 3.79 (m,12,3NCH_3, OCH_3), 6.66-8.11 (m,23,18CH,5NH), 9.70 (m,1,NH)[a]	d
I[f]	3.80 (s,3,NCH_3), 4.05 (d,2,CH_2), 6.94-8.33 (m,16, 14CH,2NH), 8.56 (m,1,NH), 10.42 (s,3,NH_3^+)[a]	d
II[f]	3.68 and 3.79 (2s,6,2NCH_3), 4.0 (d,2,CH_2,J=7.7Hz), 6.23 (s,1,NH), 6.37-7.95 (m,18,16CH,2NH), 9.37 (s,1,NH), 9.79 (s,1,NH), 10.35 (s,3,NH_3^+)[a]	d
III[f]	3.70, 3.75 and 3.77 (3s,9,3NCH_3), 4.10 (d,2,CH_2,J=7.7Hz), 6.50 (m,1,NH), 6.32-8.05 (m,21,18CH,3NH), 9.45 (s,1,NH), 9.65 (s,1,NH), 10.42 (s,3,NH_3^+)[a]	d
IV[f]	3.86, 3.87 and 3.88 (3s,9,3NCH_3), 4.10 (d,2,CH_2), 6.40-7.88 (m,CH,arom,CHO)[c]	d

[a]Solvent : Me_2SO-d_6. [b]Solvent : $CDCl_3$. [c]Solvent : D_2O. [d]Not determined. [e]TFA salt. [f]Hydrochloride.

with the amine 12 (DCC-DMAP) yielded the protected dimer 15. After removal of the BOC-group, the creation of the trimeric building block 17 was effected by condensing the amine 16 with the appropriate acid 14 using EDC as condensing agent[12]. The conversion of the benzyl ester into acids 13 and 17 was effected in a straightforward way by catalytic hydrogenation (Pd on C) in ethanol. The final incorporation of the anilinoacridine moiety into one, two or three pyrrole residues was a crucial step. The DCC-HOBt coupling procedure was used and gave, after chromatography, the corresponding N-protected compounds 20, 21, 22 and IV. Final deprotection of 20, 21 and 22 by acid hydrolysis was accomplished with dry HCl in acetic acid medium. The four hybrid compounds I, II, III and IV were used as hydrochloride salts. The analytical data and NMR characteristics of all described compounds are reported in Tables I and II.

RESULTS AND DISCUSSION

DNA-binding

Dst-A and Nt bind specifically to the minor groove of DNA[13] while amsacrine intercalates between adjacent base pairs[14]. The intercalative process for amsacrine concerns only the acridine chromophore whereas the anilino ring lodges in the minor groove with a nearly orthogonal orientation in respect to the mean plane of the acridine ring[15]. Thus, the linkage of a minor groove binding residue to the anilino ring via a short spacer should lead to compounds which bind strongly to DNA by two well distinct processes, i.e. intercalation and minor groove binding.

As shown in Table III, there is apparently no significative difference in the ΔTm and Q values observed for the compounds I, II and III. All of the compounds produce positive ΔTm increase in nucleic acids melting temperatures. These compounds also stabilized GC-containing synthetic polynucleotide against thermal denaturation even at high temperatures (up to 100°C). If the extent to which ligands stabilize the helix coil thermal transition of double stranded DNA is representative of the strength and extent of binding, it does not presume of the mode of interaction. For example, polyamines, which bind to DNA by bridging the minor groove and by inter or intramolecular cross-linking,[16] stabilize double-helical DNA against thermal melting by neutralization of the phosphate; such an interaction could not be taken into account in view of fluorescence experiments. However, in quenching assays employing an excess of poly[d(AT).d(AT)], non-intercalative binding agents can be distinguished from intercalating agents[17]. Because of their different site size for DNA, intercalating agents have much smaller effects than non-intercalative binding agents (m-AMSA, Q=25 μM; Dst-A, Q=1.6 μM). The Q values observed for the compounds I - IV with poly[d(AT).d(AT)] are in the range 3.3-6.7 μM, just greater than those observed for a minor groove binding.

Table I : DNA-binding parameters of the hybrid compounds and their parent molecules.

	Duplex native and synthetic DNAs													
	poly[d(AT):d(AT)]				Clostridium perfringens (26.5% GC)				Calf thymus (42% GC)				poly[d(GC):d(GC)]	
	ΔTm[a] (D/P)[b]			Q[c]	ΔTm (D/P)			Q	ΔTm(D/P)			Q	ΔTm[d]	Q
	0.1	0.5	1		0.1	0.5	1		0.1	0.5	1			
I	4	14	17	5.3	3	6	9	4.7	7	13	16	5	—	9
II	5	18	19	5.5	2	4	6	6	3	7	8	7	—	12
III	1	6	11	6.7	1	4	7	10.8	1	5	8	71	_	12.5
IV	6	19	23	3.3	5	12	15	2.7	9	18	20	2.7	—	3.6
Dst-A	18	34	38	1.6	15	19	29	22.2	14	22	24	39.5	—	130
m-AMSA	4	10	14	25	2	5	10	2.8	1	5	8	3.8	—	4.5

[a] ΔTm : elevation in thermal denaturation temperature (deg °C).

[b] D/P : drug to phosphate residue ratio.

[c] Q : the concentration, μM of drug to give 50% of quenching of fluorescence of bound ethidium at an added D/P ratio of 0.1; see text.

[d] Temperature elevation too high to measure because of intrumental limitations.

Moreover, the high ΔTm values are not in favor of a strict intercalative process. Thus, it seems obvious that both binding modes are involded. One can conclude to the stronger binding of IV relative to its deformylated analog III, considering the Q and ΔTm : the Q value with calf thymus DNA for IV is more than 25-fold lower than with III. With the synthetic poly[d(GC).d(GC)], the difference is lower but significative.

Previous studies[18] have shown similar differences in the binding of Dst-A and its deformylated analog. This result demonstrates the crucial role played by hydrogen acceptor (or donor) sites in the binding to DNA. This property was not observed for the potential hydrogen acceptors and donors carboxamide groups in pyrrole residues since no binding potency increase was detected when going from one (I) to three (III) methylpyrrole units. The Q values and the effects of the studied compounds on ΔTm of native or synthetic DNAs of different base composition give information on their base preferential binding. The corresponding results indicate that compounds I, III and IV do not exhibit any base selectivity. On the other hand, values observed with II could be ascribed to its enhanced affinity for poly(AT) sequence, as observed for Dst-A. These results could indicate the dominating role of the structure portion closely related to Nt, which exhibits an AT specificity[10], versus the anilino-9-aminoacridine ring which was described to have a GC specificity[11]. However, recent results[19] obtained by computation on the intercalative interaction energy of m-AMSA with B-DNA have releaved AT binding site preference.

Biological activity

The cytotoxicity, the growth inhibition and DNA synthesis inhibition abilities of the four hybrid molecules were determined on L1210 murine leukemia cells (Table IV). Increasing the length of the pseudopeptidic moiety with one, two or three N-methylpyrrole residues does not induce large changes in their antitumor activities. Among the pseudopeptide derivatives tested for their inhibitory effects on the proliferation of murine L1210, after only 24h incubation, III proved to be the most active (ID_{50}=0.5 μM or 0.39 μg/mL). Surprisingly, its formylated analog IV was 4-fold less active. On the other hand their DNA synthesis inhibitory effects reflect the stronger binding of IV to DNA than for III. This would suggest that DNA is not the only target of III and of the other drugs. The two other simpler molecules I and II are less active (ID_{50}=3 and 3.8 μM or 1.6 and 2.5 μg/mL respectively) but remain in the range of the clinically used drugs except for the highly toxic antileukemic agent m-AMSA (ID_{50}=0.05 μM or 0.02 μg/mL). The compound II seems to be interesting in another way. As shown in Figure 2, a 10 μM concentration completely inhibited the proliferation of the tumor cells, without

Table IV : Biological activities of the hybrid compounds and of their parent molecules.

Leukemia Murine L 1210 cells			
	ID_{50}[a]	LD_{50}[b]	I_{DNA50}[c]
I	3	13.5	13.5
II	8	31	12.5
III	0.5	9	26
IV	2	7	15
m-AMSA	0.05	0.5	2.7

[a] ID_{50} : µM concentration to inhibit cell growth by 50% following a 24h exposure.
[b] LD_{50} : µM concentration to kill 50% of cells following a 24h exposure.
[c] I_{DNA50} : µM concentration to inhibit DNA synthesis by 50%.

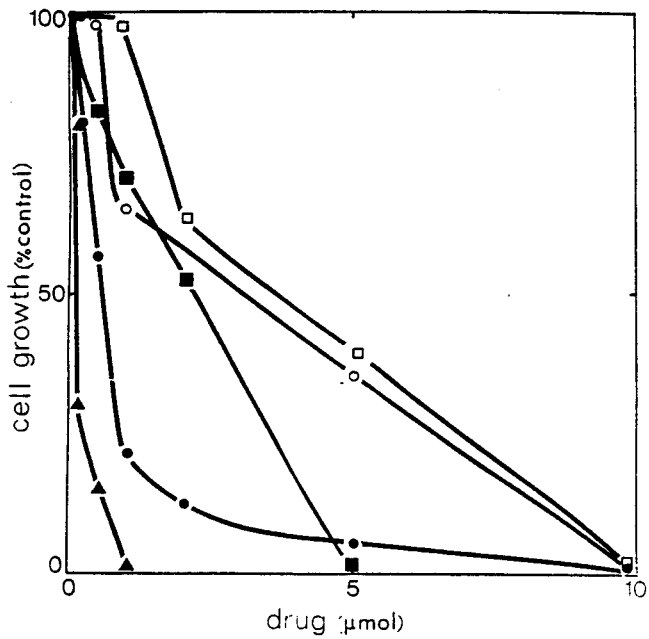

Figure 2 : Effects of m-AMSA (▲) and the synthetic hybrid compounds I (○), II (□), III (●), IV (■) on the proliferation of Murine Leukemia(L 1210) cells after 24-h exposure.

killing most than 15 % of them (LD_{50}=31 µM). Its poor cytotoxic capacity, coupled with its relative cytostatic power, could make it a convenient compound for reiterative treatments.

Thus this series of compounds shows interesting biological activities. However no correlation has emerged in attempts to relate their pharmacological activity to their nucleic acid binding ability.

Experimental section

Melting points were determined in capillary tubes and are uncorrected. The IR spectra were obtained on a Perkin-Elmer 177 spectrophotometer, in KBr pellets. ^{13}C and ^{1}H-NMR spectra were recorded on a Brücker WP 80 SY or AM 400 WB spectrophotometer. EI mass spectra were recorded on a Ribermag R10.10 (combined with Riber 400 data system) mass spectrophotometer at 70 eV by using direct insertion. FAB mass spectra were determined on a Kratos MS-50 RF mass spectrometer arranged in an EBE geometry. The sample was bombarded using a beam of xenon with a kinetic energy of 7 keV. The mass spectrometer was operated at 8 KV accelerating voltage with a mass resolution of 3000. Thin layer chromatography (TLC) was carried out using silica gel 60F-254 Merck (0,25mm thick) precoated UV-sensitive plates. Spots were visualized by inspection under UV light at 254nm and after exposure to vaporized I_2 and/or ninhydrin. Kieselgel 60 Merck (230-400 mesh) was used for flash chromatography according to the procedure of Still[20].

Methyl 1-methyl-pyrrole-2-carboxylate (1) : 1-methyl-pyrrole-2-carboxylic acid (Aldrich, 5g, 0.04 mol), sodium carbonate (21.2 g) and 99% methyl iodide (10 mL) were refluxed in dry acetone (400 mL) for 18h. The insoluble material was discarded and the filtrate evaporated. The resulting mixture was taken in ether before being filtered to remove the remaining NaI. Removal of ether under vacuum afforded a yellow oil. Distillation gave pure 1 ; b.p. : 62°/1 mm.

Methyl 1-methyl-4-nitro-pyrrole-2-carboxylate (2) : The ester 1 (5 g, 36 mmol) was dissolved in acetic anhydride (30 mL). The solution was cooled to -20° and cold nitric acid (65%, 7 mL) was added very slowly to avoid rapid elevation of temperature. Strict temperature control was essential to obtain a pure product in an acceptable yield. Slightly elevated reaction temperature increased the formation of side products and the total yield fell significantly.

The mixture was stirred at -20°C for 6h, then at room temperature for 4h. Removal of the solvent from the red mixture gave a solid. The nitro derivatives were separated by chromatography in the system solvent : CH_2Cl_2/petroleum ether, 7/3,v:v). The 5-nitro

isomer was first eluted : 1.4 g, 21.1% yield, mp : 109°C, Rf(CH_2Cl_2) : 0.70, Rf(CH_2Cl_2/petroleum ether,7/3,v:v) : 0.58. ^{1}H-NMR ($CDCl_3$) δ 3.89 (s, 3H, $COOCH_3$), 4.31 (s, 3H, NCH_3), 6.89 (d, 1H, CH, J=4.5Hz), 7.13 (d, 1H, CH, J=4.5Hz). ^{13}C-NMR ($CDCl_3$) δ 34.96 (NCH_3), 51.96 (OCH_3), 111.80 (C_4), 115.47 (C_3), 126.78 (C_2), 141.04 (C_5), 160.39 (CO). MS-m/e (rel. intensity) : 184 (100), 153 (52) , 122 (67), 107 (47), 79 (84).

Further elution with the same system solvent gave the 4,5 dinitro derivative : 150 mg, 1.8% yield, Rf(CH_2Cl_2) : 0.67, Rf(CH_2Cl_2/petroleum ether, 7/3, v:v) : 0.49. MS-m/e (rel. intensity) : 229 (3.3), 212 (1.0), 199 (1.0), 167 (31.6).

The final elution with CH_2Cl_2 gave the 4-nitro isomer (2) : 2.3 g, Rf(CH_2Cl_2) : 0.53, Rf(CH_2Cl_2/petroleum ether,7/3,v:v) : 0.36.

Methyl 4-amino-1-methyl-pyrrole-2-carboxylate (3) : The 4-nitro derivative 2 (2 g, 0.01 mol) in absolute ethanol (50 mL) was poured in a stainless steel bomb and allowed to be hydrogenated under 50 kg pressure for 12h at 50°C over Ni Raney catalyst. The catalyst was filtered off, the colorless filtrate containing the very unstable amino ester 3 was evaporated under vacuo in the dark. The resulting residue was not isolated due to its air sensitivity (light exposure provide a rapid decomposition into a purple mixture) and was immediately used for the next step.

TFA salt : To prevent degradation, this amine was dissolved in CH_2Cl_2 (5 mL) and trifluoroacetic acid (1 mL) was added dropwise under rapid stirring for 15 min. After evaporation of the solution, the residue was washed with CH_2Cl_2 (5x30 mL), precipitated with ether/petroleum ether (1/4) and collected..

Methyl 4-[[(tert-butyloxy)carbonyl]amino]-1-methyl-pyrrole-2-carboxylate (4) : A solution of ditertbutyldicarbonate (3.27 g, 0.015 mmol) in CH_2Cl_2 (150 mL) was added to 3 (1.54 g, 0.01 mmol) in CH_2Cl_2 (100 mL) for 12h under reflux. The solution was then extracted with water (3x30 mL), dried over Na_2SO_4, evaporated, washed with cold petroleum ether and finally afforded the desired compound 4. Recrystallisation from CH_2Cl_2/petroleum ether (1/25) gave a white microcrystalline product. Rf(CH_2Cl_2) : 0.56.

4-[[(tert-butyloxy)carbonyl]amino]-1-methyl-pyrrole-2-carboxylic acid (5) : A solution of 4 (2.54 g, 0.01 mol) in MeOH (50 mL) and 1.6 g (0.04 mol) of sodium hydroxide in water (5 mL) was boiled under reflux with stirring. The progress of the reaction was monitored by TLC and was thereby judged to be complete after 18h. The resulting solution was cautiously acidified to pH 3.0 with a few drops of dilute HCl. Evaporation of the solvent, trituration in absolute ethanol, elimination of sodium chloride by filtration and evaporation of ethanol, yielded 2.23 g of a white solid . The product was isolated by

precipitation with a mixture of ether-petroleum ether. Rf(MeOH/CH_2Cl_2, 80/20, v:v) : 0.71.

Methyl 4-[[[4-[[(tert-butyloxy)carbonyl]amino]-1-methyl-pyrrole-2-yl] carbonyl] amino] -1-methyl-pyrrole-2-carboxylate (6) :

DCC-DMAP coupling procedure : The acid 5 (0.61 g, 2.54 mmol) in 20 mL CH_2Cl_2 reacted with the amine 3 (0.4 g, 2.54 mmol). After evolution of the reaction (2 to 4h), the solution was filtered off and polar compounds were successively removed by extraction with 1N HCl, H_2O, 1M $NaHCO_3$ (30 mL). After drying and evaporation of the CH_2Cl_2 , the crude residue was purified by chromatography with CH_2Cl_2/acetone (20/1, v:v) as eluent.

DCC-HOBt coupling procedure : 5 (0.76 g, 3.16 mmol) in cold dry CH_2Cl_2 (50 mL) was stirred with DCC (0.72 g, 3.5 mmol) and HOBt (0.54 g, 3.5 mmol) for 1h; a cold solution of 3 (0.49 g, 3.16 mmol), plus TEA for the TFA salt, in CH_2Cl_2 (50 mL) was added. Stirring was continued for 2h at 0°C and at least 20h at 20°C. The precipitated dicyclohexylurea (DCU) was filtered off and the CH_2Cl_2 solution was washed with 30 mL 1N HCl, H_2O, 1M $NaHCO_3$. After drying over Na_2SO_4, the solvent was removed in vacuo. The remaining DCU was discarded by precipitation with acetone. Trituration with ether/petroleum ether gave a crude product containing approximately 80% of the desired dimeric compound 6 and 20% of a side copmpound : Rf(A) : 0.92; Rf[MeOH/CH_2Cl_2, 0.5/9.5, v:v) : 0.74). ^{1}H-NMR and MS (337, M^+) allowed to identify it as 1,2,3-benzotriazol-1-yl 4-[[(tert-butyloxyl)carbonyl]amino]-1-methylpyrrole-2-carboxylate[12]. This active ester of HOBt was obtained even with longer reaction times and had to be separated from 6 by flash chromatography with MeOH/CH_2Cl_2 (0.5/9.5, v:v) as eluent before the next step. Rf[MeOH/CH_2Cl_2, 0.5/9.5, v:v) : 0.45.

4-[[[4-[[(tert-butyloxy)carbonyl]amino]-1-methyl-pyrrole-2-yl] carbonyl] amino]-1-methyl-pyrrole-2-carboxylic acid (7) : The methyl ester 6 (1.2 g, 3.2 mmol) was converted to the corresponding acid 7 according to the method of preparation of 5. The saponification was stopped after 72h (longer reaction times did not afford higher yields). Evaporation of the solvent gave a white powder which was partitioned between H_2O and CH_2Cl_2 to remove the remaining ester 6. Acidification of the aqueous layer to pH 3 with dilute HCl and extraction with ethyl acetate (3x25 mL) afforded 0.88 g of the chromatographically pure acid 7. Rf[MeOH/$CHCl_3$, 8.0/2.0, v:v) : 0.84.

Methyl 4-[[[4-[[[4-(tert-butyloxy)carbonyl]amino]-1-methyl-pyrrole-2-yl] carbonyl]amino]-1-methyl-pyrrole-2-yl]carbonyl]amino]-1-methyl-pyrrole-2-carboxylate (9) :

Amine component 8 : 30 mL of CH_2Cl_2/TFA (2/1, v:v) were slowly added to 6 (0.83 g, 2.2 mmol); the brownish solution was left at ambient temperature for 1h and then evaporated. The resulting hygroscopic residue was washed several times with ether or CH_2Cl_2 (acetone or methanol were not used to avoid a rapid decomposition). The dry residue was then partitioned between H_2O (20 mL) and CH_2Cl_2 (20 mL). After centrifugation, the clear aqueous layer was collected and lyophilized. The amine 8 was obtained pure in a good yield.

The trimeric compound 9 was synthesized using DCC-DMAP as coupling agents as described for 6. The crude product obtained after the washing steps was directly used for the next step without chromatography. However, an anlytical sample could be obtained by dissolution of the crude material in a minimum volume of acetone followed by addition of sufficient cold dry ether under rapid stirring.

4-[[[4-[[[4-(tert-butyloxy)carbonyl]amino]-1-methyl-pyrrole-2-yl] carbonyl] amino]-1-methyl-pyrrole-2-yl]carbonyl]amino]-1-methyl-pyrrole-2-carboxylic acid (10) : The methyl ester 9 was saponified to give the acid 10 as described for the preparation of 7. Rf[MeOH/CH_2Cl_2, 80/20, v:v) : 0.82.

Benzyl 4-[[(tert-butyloxy)carbonyl]amino]-1-methyl-pyrrole-2-carboxylate (11) : This compound was prepared from 5 by modification of a previous procedure[12] : 1 g of 5 (4.16 mmol) in EtOH-H_2O (3/1, v:v, 50 mL) was treated dropwise with a solution of Cs_2CO_3 (0.68 g, 2.08 mmol) in H_2O (10 mL). After complete addition, the solution was evaporated to dryness. The resulting semi-solid residue was dissolved in absolute EtOH (3x40 mL) and evaporation of the solvent gave the cesium salt of 5. Benzyl bromide (0.5 mL, 4.17 mmol) was slowly added to the solution of the cesium salt in DMF (20 mL) and stirring was maintained overnight at 40°C. The DMF was evaporated and the residue was dissolved with water (10 mL). After three extractions with CH_2Cl_2 (3x30 mL), the combined organic layers were concentrated and ten-fold diluted with cold petroleum ether. The precipitated material was filtered, rinced with petroleum ether and dried. Rf(CH_2Cl_2) : 0.54.

Benzyl 4-(formylamino)-1-methyl-pyrrole-2-carboxylate (13) :

Amine component 12 : To 0.75 g (2.27 mmol) of 11 in 50 mL CH_2Cl_2, 10 mL of pure TFA were added. After 1h stirring, the solution was evaporated. Careful elimination of the TFA gave a crude residue which was dissolved in acetone (3 mL), ether (20 mL) and petroleum ether (100 mL), giving a white precipitate. This product was filtered, washed

and dried, and 12 was obtained without further purification. An analytically pure sample was obtained after two successive precipitations in CH_2Cl_2/petroleum ether (1/15) in the cold. Rf(CH_2Cl_2) : 0.29.

Formylation : Formic acid (83 µl, 2.56 mmol) in cold CH_2Cl_2 was stirred with DCC (0.53 g, 2.56 mmol) and HOBt (0.4 g, 2.56 mmol) for 1h; a cold solution of 12 (0.8 g, 2.32 mmol) and TEA (0.32 mL, 2.32 mmol) in CH_2Cl_2 was added; stirring was maintained for 2h at 0°C and 15h at 20°C. The DCU was discarded by precipitation with acetone. The remaining powder was dissolved in ether (insoluble material discarded) and addition of petroleum ether led to precipitation. Pure 13 precipitated as a microcrystalline solid after one day in the cold.

4-(formylamino)-1-methyl-pyrrole-2-carboxylic acid (14) : 13 (0.4 g, 1.55 mmol) dissolved in absolute ethanol (40 mL) was reduced by hydrogen (atmospheric pressure) for 12h in the presence of Pd catalyst (5% on C). The mixture was filtered and the clear solution concentrated to less than 4 mL. Addition of cold ether under rapid stirring give the desired acid 14. Rf(MeOH/CH_2Cl_2, 80/20, v:v) : 0.72.

Benzyl 4-[[[4-[[(tert-butyloxy)carbonyl]amino]-1-methyl-pyrrol-yl]carbonyl] amino]-1-methyl-pyrrole-2-carboxylate (15) : The acid 5 was coupled to the amine 12 in the presence of DCC and DMAP according to a well established procedure[12]. 15 was obtained pure as judged by TLC after purification by chromatography with CH_2Cl_2/acetone (20/1, v:v) as eluent. Rf(solvent of chromatography) : 0.33.

Benzyl 4-[[[4-[[[4-(formylamino)-1-methyl-pyrrol-2-yl]carbonyl]amino]-1-methyl-pyrrole-2-carboxylate (17) :

Amine 16 : The t-BOC protected amine 15 (0.3 g, 0.66 mmol) was deprotected with TFA to give the corresponding free amine 16. Purification was accomplished according to the method of preparation of 8.

A solution of 14 (57 mg, 0.34 mmol), 16 (142 mg, 0.31 ;mmol) and TFA (43 µl, 0.31 mmol) in DMF (20 mL) was immediately treated with EDC (65 mg, 0.34 mmol). The resulting solution was stirred at ambient temperature overnight and then evaporated. The brownish residue was washed with 1M $KHSO_4$, 1M $NaHCO_3$, H_2O and absolute ethanol. The remaining insoluble material was dissolved in CH_2Cl_2 (2 mL) and precipitated with ether and petroleum ether. The crude product was suitable for the preparation of 18. An analytical specimen could be obtained as white crystals by recristallization from CH_2Cl_2/ether/petroleum ether (1/10/100).

4-[[[4-[[[4-(formylamino)-1-methyl-pyrrol-2-yl]carbonyl]amino]-1-methyl-pyrrole-2-yl]carbonyl]amino]-1-methyl-pyrrole-2-carboxylic acid (18) : Crude 17 (140 mg, 0.28 mmol) in DMF (10 mL) was totally converted into the corresponding acid by catalytic hydrogenation (H_2, atmospheric pressure, Pd on C) at room temperature for 6h. After filtration of the catalyst, the solution was evaporated, the residue was dissolved in EtOH, clarified with decolorizing carbon and finally taken to dryness. Rf[MeOH/CH_2Cl_2, 80/20, v:v) : 0.82.

4-(9-acridinylamino)-N-[[4-(tert-butyloxy)carbonyl]amino]-1-methyl-pyrrol-2-carbonyl]-glycylaniline (20) :

Amine 19 : 4-(9-acridinylamino)-N-glycylaniline hydrochloride trifluoro acetate, synthesized as previously described[21] was dissolved in water; dilute $NaHCO_3$ was added to pH 8-8.5 and the amine 19 was extracted with ethyl acetate. Drying over Na_2SO_4 and evaporation of the organic layer afforded 19.

A solution of 5 (95 mg, 0.39 mmol), DCC (89 mg, 0.43 mmol) and HOBt (66 mg, 0.43 mmol) in 40 mL of CH_2Cl_2/DMF (1/1, v:v) was added at 0°C to a solution of 19 (134 mg, 0.39 mmol) in 10 mL of DMF. After 18h stirring, the solution was evaporated, the DCU was discarded by precipitation with acetone and the concentrated filtrate was precipitated with ether. Filtration gave 20 suitable for the next last step. An analytical sample was obtained by chromatography with CH_2Cl_2/MeOH, (80/20, v:v) as solvent. Rf[CH_2Cl_2/MeOH, 80/20, v:v) : 0.66.

4-(9-acridinylamino)-N-[4-[[4-[[(tert-butyloxy)carbonyl]amino]-1-methyl-pyrrol-2-yl]carbonyl]amino]-1-methyl-pyrrol-2-carbonyl]-glycylaniline (21) : 7 (105 mg, 0.29 mmol) was coupled to 19 (100 mg, 0.29 mmol) by DCC-HOBt procedure, as described for 20. The reaction mixture was stirred at 0°C for 4h and at room temperature overnight. The solution was evaporated and washed with CH_2Cl_2 to eliminate the DMF. The crude red residue was triturated with CH_2Cl_2 (10 mL), filtered, washed with CH_2Cl_2 (4x20 mL). 21 was then purified by flash chromatography with CH_2Cl_2/MeOH (80/20, v:v) as eluent. Rf[CH_2Cl_2/MeOH, 80/20, v:v) : 0.63.

4-(9-acridinylamino)-N-[4-[[4-[[[(tert-butyloxy)carbonyl]amino]-1-methyl-pyrrol-2-yl]-carbonyl]amino]-1-methyl-pyrrol-2-yl]-carbonyl]amino]-1-methyl-pyrrol-2-carbonyl]-glycylaniline (22) : 22 was obtained by coupling the acid 10 (0.4 g, 0.83 mmol) with the amine 19 (0.26 g, 0.76 mmol) using DCC-HOBt as described for 20. The purification was accomplished by the same technique used for 21.

4-(9-acridinylamino)-N-[4-amino-1-methyl-pyrrol-2-carbonyl]-glycylaniline Hydrochloride (I) : The BOC-protected amine 20 (100 mg, 0.17 mmol) in acetic acid (30 mL) was flushed with dry HCl for 10 min and stirring was maintained for 50 min. The acid solution was evaporated (below 45°C), washed with acetone and ether. The resulting residue was dissolved in water, extracted with CH_2Cl_2 (2x20 mL) and ethyl acetate (2x20 mL). Final chromatography in EtOH/$CHCl_3$ (80/20, v:v) give I. Rf(solvent of chromatography) : 0.15.

4-(9-acridinylamino)-N-[4-[[-4-amino-1-methyl-pyrrol-2-yl]carbonyl]aminol-1-methyl-pyrrol-2-carbonyl]-glycylaniline Hydrochloride (II) : The BOC-protecting group in 21 (160 mg, 0.24 mmol) was cleaved-off with dry HCl in acetic acid medium for 1h and then purified as described for I.

4-(9-acridinylamino)-N-[4-[[[-4-amino-1-methyl-pyrrol-2-yl]carbonyl]aminol-1-methyl-pyrrol-2-yl]carbonyl]aminol-1-methyl-pyrrol-2-carbonyl]-glycyl aniline Hydrochloride (III) : Cleavage of the BOC group and final purification were accomplished as described for I.

4-(9-acridinylamino)-N-[4-[[[-4-[[[4-(formylamino)-1-methyl-pyrrol-2-yl]carbonyl]aminol-1-methyl--pyrrol-2-yl]carbonyl]aminol-1-methyl-pyrrol-2-carbonyl]-glycylaniline Hydrochloride (IV) : 60 mg of the acid 18 (0.145 mmol) were coupled to 580 mg of the amine 19 (0.145 mmol) via a DCC-HOBt (0.16 mmol) procedure as adopted for 20. The compound obtained after chromatography was acidified with diluted HCl. The acid aqueous layer was lyophilized. The lyophilized material was dissolved in water (50 mL). This procedure was repeated five times to assure a complete elimination of HCl in excess.

Drug-DNA binding

Poly[d(AT).d(AT)], poly[d(GC).d(GC)], calf thymus DNA and *Clostridium perfringens* DNA were purchased from SIGMA Chemical Co. and used without purification. Concentrations of the DNAs were determined spectroscopically from their extinction coefficients (in M^{-1} cm^{-1}) ε_{260} = 6700, ε_{254} = 8400, ε_{260} = 6600, ε_{260} = 6500, respectively.

Q values for quenching were determined employing 20 µM DNA in 0.01 M ionic strength buffer (9.3 mM NaCl, 2 mM NaOAc buffer, pH 5, plus 0.1 mM EDTA) containing 2 µM ethidium in such a way that there was minimal ethidium displacement and maximum drug-induced quenching[22]. All measurements were made in 4 mL, 10 mm

pathlength quartz cuvettes, at 20°C on a Jobin-Yvon J-Y-3 spectrofluorometer equipped with an X-Y recorder (excitation at 546 nm and measurement at 595 nm). The Q value is defined as the drug concentration which reduces the fluorescence of initially DNA-bound ethidium by 50%.

Melting temperature studies were made in 0.1 SSC buffer (0.15 NaCl, 0.015 M sodium citrate, pH 7.0) as previously described[23].

Biological testing

Cell Culture : Murine L 1210 leukemia cells were maintained in logarithmic growth as suspension cultures in RPMI-1640 medium (GIBCO) containing 10% fetal calf serum. Cells were grown in 25 cm^2 tissue culture flash (Corning) in a total volume of 10 mL in a water-saturated atmosphere containing 5% CO_2 at 37°C.

Growth and viability assays (ID_{50} and LD_{50} determinations) : The cells were treated, while in logarithmic growth (10^6 cells/mL), with the hybrid derivatives diluted in sterile water and filtered through a 0.2 µm filter immediately prior to use. Following a 24h incubation, cells samples were removed for counting. Cell growth and viability were estimated by counting the cells after dilution with trypan blue solution at 0h and 24h. The cytotoxic effects on cellular growth were expressed as a function of drug concentration. For each compound, we determined a) the inhibitory dose (ID_{50}) reducing cell growth to 50% of control growth, b) the letal dose (LD_{50}) producing 50% of death cells in the culture.

DNA-synthesis inhibition assays : L1210 cells in exponential growth were incubated for 1h at 37°C in growth medium containing various doses of the hybrid compounds. The cells were incubated for 15h at 37°C in growth medium containing 10 µCi/mL [^{3}H]-thymidine (43 Ci/mM, CEA). The radioactive medium was removed, the cells washed twice in saline buffer and allowed to swell for 10 min in ice in 1 mL of hypotonic buffer (TNE : 0.01 M Tris-HCl, pH 8.1; 0.05 M NaCl; 0.001 M EDTA). The cells were then disrupted by congelation-decongelation (3 times), digested by proteinase K (100 µg/mL, 4h at 37°C). The TCA precipitable was collected on filter and counted in a liquid scintillation counter. For each compound, we determined the *in vitro* inhibitory dose (I_{DNA50}) reducing DNA synthesis by 50%.

Acknowledgement

This research was supported by grants from the "Institut National de la Santé et de la Recherche Médicale" and the "Fédération Nationale des Centres de Lutte contre le Cancer".

REFERENCES

[1] Gale, E.F., Çundliffe, E., Reynolds, P.E., Richmond, M.H., Waring, M.J. "The Molecular Basis of Antibiotic Ation" 2nd ed., Wiley : New York, 1981; pp. 258-401.

[2] Neidle, S., Abraham, Z. CRC Crit. Rev. Biochem., 1984, 17, 73-121.

[3] a-Braithwaite, A.W., Baguley, B.C. Biochemistry 1980, 19, 1101-1106.
b-Zimmer, Ch., Luck, G., Burckardt, G. In "Molecular Mechanism of Carcinogenic and Antitumor Activity", Chagas, C., Pullman, B., Eds., Adenine Press : New York, 1986, pp. 339-363.

[4] Denny; W.A., Baguley, B.C., Cain, B.F., Waring, M.J. In "Molecular Mode of Action of Antitumor Drugs", Neidle, S., Waring, M.J., Eds : MacMillan : London, 1983; pp. 1-34.

[5] Cain, B.F., Atwell, G.J. Eur. J. Cancer 1974, 10, 539-549.

[6] Cassileth, P.A., Gale, R.P., Leukemia Res. 1986, 10, 1257-1265.

[7] Zimmer, Ch., Wahnert, U. Prog. Biophys. Mol. Biol. 1986, 47, 31-112.

[8] Lown, J.W. Anti-Cancer Drug Design 1988, 3, 25-40.

[9] Dervan, P.B. Science 1986, 232, 464-471.

[10] a-Zimmer, Ch., Marck, C., Schneider, C., Guschlbauer, W. Nucl. Acids Res. 1979, 6, 2831-2837.
b-Hahn, F.E. In "Antibiotics III. Mechanism of Action of Antimicrobial and Antitumor Agents", Corcoran, J.W., Hahn, F.E., Eds, Springer-Verlag : New York, 1975, pp.79-100.

[11] Feigon, J., Denny, W.A., Leupin, W., Kearns, D.R. J. Med. Chem. 1984, 27, 450-465.

[12] Grehn, L., Ragnarsson, U. J. Org. Chem. 1981, 46, 3492-3497.

[13] a-Kopka, M.L., Yoon, C., Goodsell, D., Pjura, P., Dickerson, R.E. Proc. Natl. Acad. Sci. USA 1985, 82, 1376-1380.
b-Kopka, M.L., Yoon, C., Goodsell, D., Pjura, P., Dickerson, R.E. J. Mol. Biol. 1985, 183, 553-563.

[14] Waring, M.J. Europ. J. Cancer 1976, 12, 995-1001.

[15] Denny, W.A., Atwell, G.J., Baguley, B.C. J. Med. Chem. 1983, 26, 1625-1630.

[16] Osland, A., Kleppe, K. Nucl. Acids Res. 1977, 4, 685-695.

[17] Baguley, B.C. Molec. Cell. Biochem. 1982, 43, 167-181.

[18] Luck, G., Zimmer, Ch., Reinert, K.E., Arcamone, F. Nucl. Acids Res. 1977, 4, 2655-2670.

[19] Chen, K.X., Gresh, N., Pullman, B. Nucl. Acids Res. 1988, 16, 3061-3073.

[20] Still, W.C., Kahn, M., Mitra, A. J. Org. Chem. 1978, 43, 2923-2925.

[21] Hénichart, J-P., Bernier, J-L. Hoppe-Seyler's Z. Physiol. Chem. 1982, 363, 835-841.

[22] Baguley, B.C., Denny, W.A., Atwell, G.J., Cain, B.F. J. Med. Chem. 1981, 24, 170-177.

[23] Bailly, C., Bernier, J-L., Houssin, R., Helbecque, N., Hénichart, J-P. Anti-Cancer Drug Design 1987, 1, 303-312.

Conclusion :

Concernant le mode de liaison à l'ADN, ces résultats tendent à démontrer la présence simultanée de deux mécanismes de liaison : l'intercalation de l'acridine et l'insertion du peptide de type Dst-A dans le petit sillon. Toutefois ils ne constituent pas une preuve formelle ; aussi des techniques physicochimiques plus adaptées ont été mises en oeuvre pour établir définitivement le mode de liaison. Le composé II (encore appelé **NETGA** pour **Né**tropsine-**G**lycyl-**A**nilinoamino-9 acridine) de cette série a été choisi comme modèle (Figure 10). Devant l'éventail des techniques envisagées (spectroscopie d'absorption UV, fluorescence, polarisation de fluorescence, dichroïsme linéaire, foot-printing, RPE) seul ce composé a pu être étudié en détail. Cette étude a fait l'objet d'une publication :

article n°3:

Molecular recognition between oligopeptides and nucleic acids:
DNA sequence specificity and binding properties of bithiazole-
and acridine-linked netropsin hybrid ligands.

BAILLY C., HELBECQUE N., COLSON P., HOUSSIER C., RAO K.E., SHEA R.G.,
LOWN J.W., HENICHART J-P.

Soumis pour publication à Biochemistry

Remarque : Les études par dichroïsme linéaire et par foot-printing ont été réalisées en étroite collaboration avec respectivement le Pr. C. HOUSSIER, Université de Liège (Belgique) et le Pr. J. W. LOWN, Université d'Edmonton (Canada).

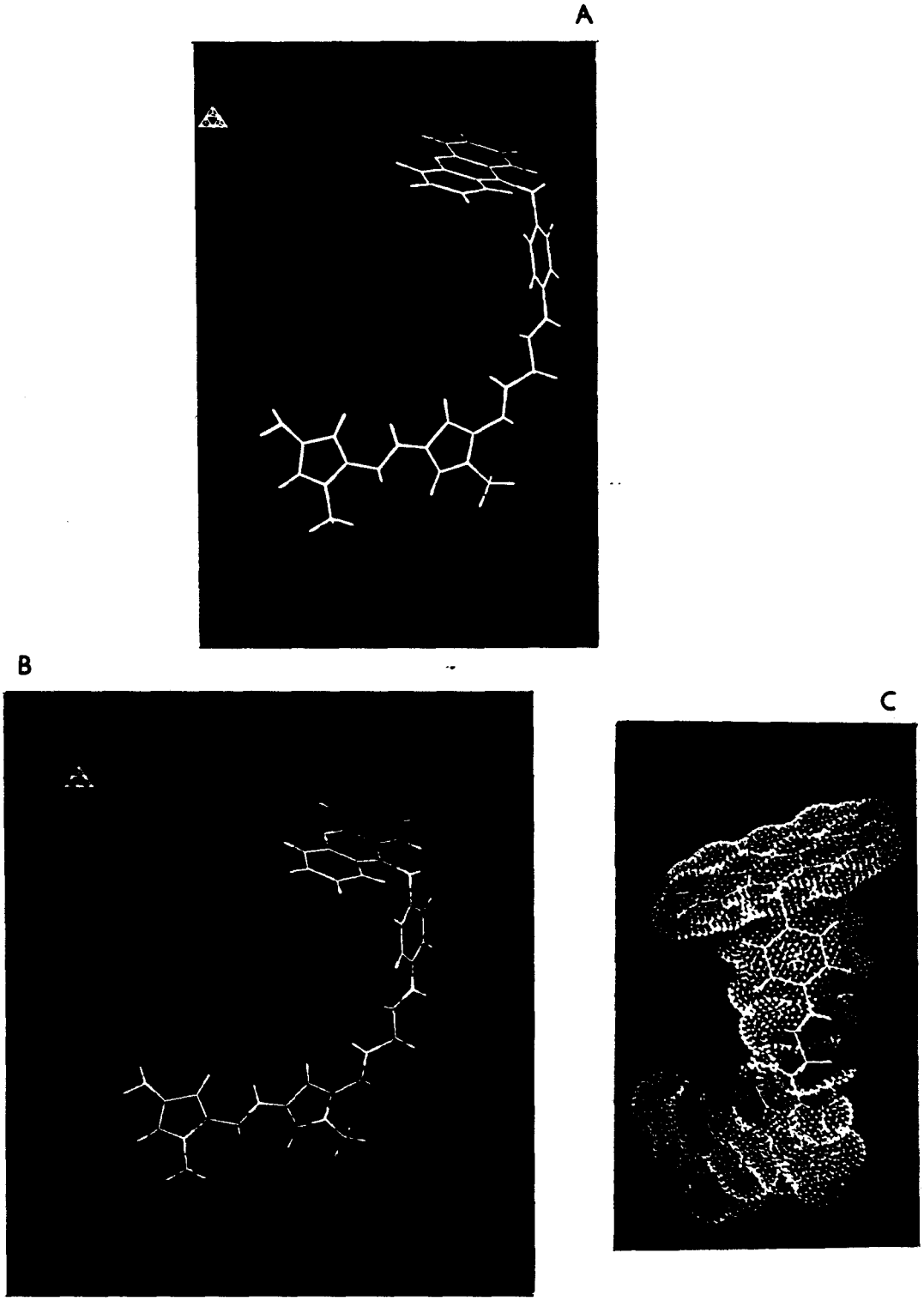

Figure 10 : Modélisation moléculaire de NETGA. (A) conformation minimisée, (B) volume moléculaire et (C) représentation des potentiels électrostatiques.

Remarque : La modélisation moléculaire par ordinateur a été réalisée par Monsieur le Professeur G. VERGOTEN (Faculté de Médecine).

Molecular Recognition between Oligopeptides and Nucleic Acids : DNA Sequence Specificity and Binding Properties of Bithiazole- and Acridine-linked Netropsin Hybrid Ligands. †

Christian Bailly,[#] Nicole Helbecque,[#] Pierre Colson,[⊥] Claude Houssier,[⊥] K. Ekambareswara Rao,[§] Regan G. Shea,[§ °] J. William Lown [§*] and Jean-Pierre Hénichart [#*]

[#] INSERM U 16, Place de Verdun, 59045, Lille, France.

[⊥] Laboratoire de Chimie Macromoléculaire et Chimie Physique , Université de Liège, Sart-Tilman, 4000 Liège, Belgique.

[§] Department of Chemistry, University of Alberta, Edmonton,Alberta, Canada, T6G 2G2.

[°] Present address, Department of Molecular Biology, Genentech Inc., South San Francisco, CA, 94080.

† This investigation was supported by grants (to J-P. H.) from the Institut National de la Santé et de la Recherche Médicale and the Fédération Nationale des Centres de Lutte contre le Cancer, France, and by grants (to J.W. L.) from the National Cancer Institute of Canada and the Biotechnology Strategic Programme of the National Sciences and Engineering Council of Canada.

Running title : DNA Molecular Recognition of Mixed Function Ligands.

* Address correspondence to either of these authors.

ABSTRACT

The design and synthesis is described of two mixed function ligands (NETBI and NETGA) in which potential intercalating groups, bithiazole and acridine, are respectively incorporated at the carboxyl terminus of the minor groove binding oligopeptide netropsin skeleton. Scatchard analysis of absorption data provided evidence of two modes of binding to DNA in each case with Ka = 6.3 x 10^5 M^{-1} for NETGA at low r_t values (0.003 to 0.1), and a binding site size n = 6, indicative of binding of both moieties. At higher r_t values (> 0.1) Ka = 3 x 10^5 M^{-1} and n = 4 for NETGA indicating only binding of the oligopeptide moiety under these conditions; Ka = 1.3 x 10^4 M^{-1} for NETBI with n = 8 at r_t (0.003 to 0.1) indicating binding of both moieties. Complementary strand MPE footprinting on a pBR322 restriction fragment showed NETBI recognizes 5'-AAATCT in accord with minor groove binding of both moieties, whereas NETGA binds to 5'-AAAT like netropsin at r = 0.78. Both ligands cause enhanced cleavage by MPE, particularly at GC rich sequences, and remote from the preferred binding sites. Viscometry measurements provided evidence for minor groove binding of both portions of NETBI. Fluorescence polarization and linear dichroism measurements were in accord with distinct modes of interaction of the acridine (intercalation) and oligopeptide (minor groove binding) portions of NETGA. Linear dichroism (LD), studies on NETBI bound to DNA are consistent with minor groove binding with an orientation angle relative to the DNA helix of β_L = 48° (β = 52°). LD measurements on NETGA indicate that the oligopeptide moiety has an orientation angle of β_L = 52°, i.e. typical of minor groove binders, whereas the acridine group has an orientation angle β_L = 60°, more characteristic of intercalation for this moiety.

The recognition of, and the preferential binding to, specific DNA sequences by proteins are responsible for selective gene expression in transcription and for the regulation of many biological processes (Berg and Von Hippel, 1988; Frederick et al., 1984; Takeda et al., 1983). When reading specific sequences promoters and repressors utilize primarily the major groove of double helical DNA where individual base pairs expose patterns of hydrogen-bond donors and acceptors, the major recognition elements in DNA-protein interactions.

On the other hand, certain oligopeptide xenobiotics, including antibiotic, antineoplastic and antiviral drugs, interfere with replication and transcription by a specific binding to double-stranded DNA within the minor groove. Such is the case for distamycin (Dst) and netropsin (Nt) (Figure 1) which act by blocking the template function of DNA by binding to specific sequences in the minor groove (Hahn, 1975). Detailed information provided by X-ray cristallographic studies and physicochemical investigations in solution (Kopka et al., 1983, 1985; Zimmer and Wahnert, 1986) indicated that the A-T base specific binding of both drugs is due to four kinds of interactions : (i) electrostatic attraction between ends of side chains of the ligands and DNA phosphates which induces the initial binding; (ii) hydrogen-bonding interactions are then formed between amide NH and adenine N(3) and thymine O(2); (iii) Van der Waals contacts between methylenes and heterocyclic CH groups of DNA bases (iv) and, finally, stacking interactions between DNA sugar O1' atoms and the drug pyrrole rings (Kopka et al., 1985; Zimmer and Wahnert, 1986; Pelton and Wemmer, 1988).

In order to understand the conformational and chemical basis of DNA binding, and to delineate the role of the heterocycle part of the base specificity, rational structural modifications of the parent molecules Dst and Nt have been carried out allowing the examination of alternative hydrogen bond accepting atoms, namely oxygen or sulfur atoms as nitrogen. In particular the pyrrole ring has been replaced by phenyl (Dasgupta et al., 1986), pyridine (Wade and Dervan, 1987), thiophene (Jones and Woodridge, 1968), thiazole (Plouvier, 1988), and imidazole (Lown, 1988, Lown et al., 1986a, 1986b; Kissinger et al., 1987). On the basis of studies on Nt and Dst analogs, in the structure of which one or more pyrrole groups have been replaced by imidazole rings, evidence for rational changes in base-specificity were obtained by DNase I footprinting. These "lexitropsins", or information-reading oligopeptides, were observed to recognize and bind to G-C rich sites (Krowicki et al., 1987, Lown, 1988).

In a second class of Nt analogs, modifications involving the number of pyrrole units (Youngquist and Dervan, 1985) and other rings (Ekambareswara et al., 1988) or the length of linking chains between the heterocyclic rings (Dasgupta et al., 1987;

Bailly et al., 1988) have been undertaken in order to delineate the role of the backbone curvature of the ligands in favoring the noncovalent interactions. From these studies it was deduced that the Van der Waals interactions between the methylenes at the carboxyl terminus of lexitropsins and DNA play a crucial role in determining the reading of base sequences. These methylene groups enter into steric contact with the guanine 2-NH_2 group of G-C base pair (Lown, 1988). It has been demonstrated that excision of one terminal methylene of oligopeptide permits the recognition of, and binding to, 3'-G-C. site (Lee et al., 1988a, 1988b).

In addition, chemical modifications involving cationic site chains have been proposed (Lown, 1988; Zakrzewska et al., 1988). For example, lexitropsins bearing only one positively charged group at the C terminus were synthesized (Krowicki and Lown, 1987; Kissinger et al., 1987). Taking into consideration the ability of Nt derivatives to concentrate in the cell nucleus (Bailly et al., in press), more sophisticated molecules were designed including those bearing alkylating moieties and these prototype hybrid drugs were found to exhibit significant cytostatic activities against murine or human tumor cell lines (Lown et al., 1986b; Krowicki et al., 1988).

To date, only two studies concerning the use of netropsin derivatives bearing intercalating moieties have been reported (Dervan, 1986; Eliadis et al., 1988). Nature provides us with examples of antibiotics whose structure, containing planar rings attached to cyclic peptides, exhibits sequence preferences in binding to DNA. For example, actinomycin-D was found to display a sequence specificity of binding around one or more G-C base pairs (Van Dyke et al., 1982a). A preference for binding DNAs rich in guanine and cytosine residues was also shown for the quinoxaline antibiotic echinomycin and its analog triostin-A (Wakelin and Waring, 1976; Lee and Waring, 1978a, 1978b). It has been demonstrated that the specific binding involved, more particularly, sites containing the dinucleotide CpG (Low et al., 1984a, 1984b; Van Dyke and Dervan, 1984). By contrast, the synthetic quinoxaline depsipeptide des-N-tetramethyltriostin A (TANDEM) binds preferentially to sequences containing adenine and thymine residues (Lee and Waring, 1978a; Fox et al., 1982; Low et al., 1984b). It has been proved that chemical changes in the nature of the intercalating chromophore (Lee and Waring, 1978a, 1978b; Fox et al., 1980; Helbecque et al., 1985) induced dramatic alterations of the base specificity or a decrease in the stability of complex with DNA.

To study the influence on DNA binding of the linkage of intercalating rings on the peptide portion of Nt we proposed here the design of hybrid molecules containing a bis-pyrrole chain and planar intercalating residues, 9-anilinoacridine (NETGA) or bithiazole (NETBI) (Figure 1).

The choice of 9-anilinoacridine was made on the basis of previous studies (Feigon et al., 1984) which described this chromophore as a GC-specific intercalating ring even though recent results (Chen et al., 1988) have revealed AT-binding site preference for the anilino-9-aminoacridine drug m-AMSA.

The bithiazole ring is known to contribute to the binding to DNA of the DNA-cleaving antibiotic antitumor bleomycin (Blm). The mode of binding to DNA was clearly established (Hénichart et al., 1985) and, moreover, studies with synthetic polynucleotides indicate that bleomycin interacts most strongly with guanine-containing nucleic acids and that alternating purine-pyrimidine sequences are preferred (Kasai et al., 1978). More precisely, the DNA sequence specific damage induced by bleomycin was studied (Murray and Martin, 1985) and it was found that the dinucleotides GT and GC were invariably cleaved.

Both drugs NETGA and NETBI (Figure 1) were studied for their mode of binding in the minor groove of DNA by conventional techniques, including electric dichroism, and the sequence recognition was determined by foot-printing experiments. The contribution of the structural components of the molecular recognition processes of DNA binding of these novel agents is discussed.

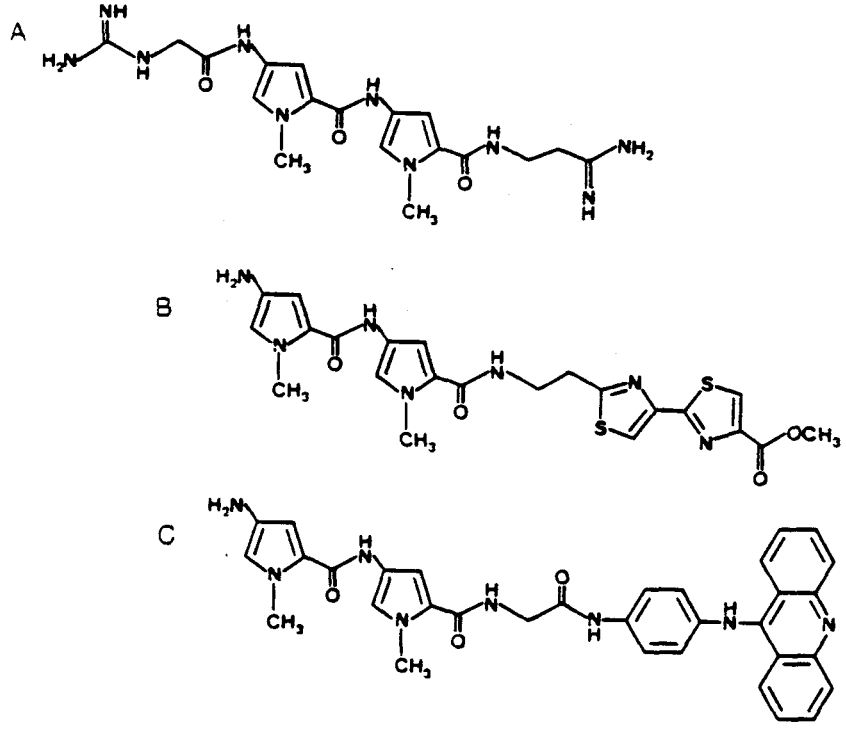

FIGURE 1 : Structure of Netropsin (A), NETBI (B) and NETGA (C).

MATERIALS AND METHODS

Chemicals

Distamycin-A hydrochloride was purchased commercially (Boehringer) and was used without purification. Full details of synthesis of NETGA together with complete spectral and analytical characterization will be reported elsewhere (Bailly et al., submitted). NETBI was obtained by coupling the bis-pyrrole moiety (described in the synthesis of NETGA) with the bithiazole moiety (Houssin et al., 1984) via an hydroxybenzotriazole active ester.

Methyl4-[[[4-[[(tert-butyloxy)carbonyl]amino]-1-methylpyrrol-2-yl]carbonyl]amino]-1-methyl pyrrole-2-carboxamido-2'-ethyl-bithiazole-4-carboxylate : A solution of 145 mg (0.4 mmol) of 4-[[[4-[[(tert-butyloxy)carbonyl]amino]-1-methylpyrrol-2-yl]carbonyl]amino]-1-methyl

pyrrole-2-carboxylic acid (Bailly et al., submitted) in CH_2Cl_2 was treated with dicyclohexyl carbodiimide (91 mg, 0.44 mmol) and 1H-hydroxy-1,2,3 benzotriazole (68 mg, 0.44 mmol) in CH_2Cl_2 for 1 h at 0°C. A cold solution of 2'-(2-aminoethyl)-4-methoxycarbonyl-2',4-bithiazole hydrobromide (140 mg, 0.4 mmol) (Houssin et al., 1984) and triethylamine (60 µl, 0.4 mmol) in CH_2Cl_2 was then added, and stirring was continued for 2 h at 0°C then overnight at ambient temperature. After removal of the dicyclohexylurea by filtration, the solution was washed with 1N HCl, H_2O and 1M $NaHCO_3$. The N-protected compound was obtained as pure crystals after chromatography with CH_2Cl_2/MeOH, 95/5, v:v as eluent (Rf: 0.31), white powder; Rf(MeOH/$CHCl_3$ 20/80, v:v, ammonia):0.83; mp.: 136°C; IR ν max 3320-3380 (NH), 3220(CH_2), 2960(CH_3), 1735($COOCH_3$), 1700(OCO), 1650(CONH) cm^{-1}; ^{1}H-NMR (400MHz, Me_2SO-d6) δ 1.45 (s, 9H, $(CH_3)_3$), 3.28 (t, 2H, CH_2, J = 7 Hz), 3.58 (m, 2H, CH_2, J = 6.25 Hz), 3.75 (s, 3H, $COOCH_3$), 3.79, 3.86 (2s, 6H, 2N-CH_3), 6.81 (s, 1H, CH), 6.86 (d, 1H, CH, J = 2.2 Hz), 6.87 (s, 1H, CH), 7.17 (d, 1H, CH, J = 2.2 Hz), 8.19 (t, 1H, NH-CH_2, J = 5.9 Hz), 8.26, 8.55 (2s, 2H, 2CH thiazolyl), 9.06, 9.80 (2s, 2H, 2NH); MS-FAB, m/z: 614 (M^++1).

Methyl 4-[[[(4-amino)-1-methylpyrrol-2-yl]carbonyl]amino]-1-methyl pyrrole -2-carboxamido -2'-ethyl-bithiazole-4-carboxylate (NETBI) : Cleavage of the BOC-protecting group was accomplished with dry HCl in acetic acid for 15 min. After careful neutralization of the acids, the crude product was dissolved in water and

impurities were extracted with ethyl acetate, giving a colorless aqueous layer which was lyophilized. NETBI was obtained as a white foam powder. Rf[MeOH/$CHCl_3$, 20/80 v:v, ammonia) : 0.60; mp. : 197°C; ^{1}H-NMR (400 MHz, Me_2SO-d6) δ 3.29 (t, 2H, CH_2, J=7 Hz), 3.59 (m, 2H, CH_2, J=6.25 Hz), 3.80 (s, 3H, $COOCH_3$), 3.88, 3.89 (2s, 6H, $2CH_3$), 6.87 (d, 1H, CH, J=1.85 Hz), 6.97 (d, 1H, CH, J=2.2 Hz), 7.09 (d, 1H, CH, J=2.2 Hz), 7.20 (d, 1H, CH, J=1.85 Hz), 8.20 (t, 1H, NH-CH_2); MS-FAB, m/z : 514 (M^++1).

Biochemicals

The polynucleotides poly [d(AT). d(AT)], poly[d(GC). d(GC)] and DNA from calf thymus and coliphage T_4 were from Sigma Chemical Co. For viscometry and electric dichroism studies, the calf thymus DNA was cut to short rod-like fragments with a French press (12600 PSIG). The DNA produced by this procedure was 300-450 base pairs in length as confirmed by gels calibrated against a Hae III digest of pBR 322 as size marker (Boehringer).

pBR 322 and sonicated calf thymus DNAs and restriction enzymes Hind III and EcoRI were obtained from Pharmacia P. L. Biochemicals. T_4 polynucleotide kinase, AMV reverse transcriptase and urea were from Bethesda Research Labs. Dithiothreitol and calf intestine alkaline phosphatase (CAP) were obtained from Calbiochem. Acrylamide, bromophenol blue and xylene cyanol were from Serva. Ferrous ammonium sulfate was from BDH. γ-^{32}P-ATP and α-^{32}P-dATP were purchased from New England Nuclear. Methidiumpropyl-EDTA (MPE) was a gift from Professor Dervan (Cal. Tech.).

Methods

Footprinting Procedure. Hind III digested pBR 322 DNA was either 5'-^{32}P-labeled (using γ-^{32}P-ATP, CAP and T_4 kinase) or 3'-^{32}P-labeled (using α-^{32}P-dATP and AMV reverse transcriptase) and then digested with EcoRI. The resulting 4332 and 31 base pair fragments (Sutcliff, 1979; Peden, 1983) were not separated prior to the cleavage reactions. The footprinting reactions were done in the presence of sonicated calf thymus DNA, labeled DNA and ligand (not added to control) in 10 mM tris, 20 mM NaCl buffer, pH 7.4. After equilibrating the ligand - DNA mixtures for 20 min at 37°C, MPE-Fe(II) (made freshly) and DTT were added to each reaction tube. The final solutions contained 100 μM DNA, 10 mM tris, 20 mM NaCl, 10 μM MPE-Fe(II), 2.5 mM DTT and 8, 16 or 78 μM of ligand. Reactions were run at room temperature for 15 min and then stopped by freezing at -70°C. The solutions were then lyophilized and resuspended in formamide loading buffer (Maniatis et al., 1982) for gel electrophoresis. After electrophoresis (0.4 mm thick, 55 cm long, 6% polyacrylamide,

7M urea, 1900 V, 55°C), the gels were dried (Bio-Rad model 483 slab dryer) and autoradiographed at -70°C using Kodak X-Omat AR film. The resulting autoradiograms were scanned using a LKB Ultroscan XL laser densitometer.

The original densitometric data were corrected for the background absorbance of the exposed film (0.4-0.5 OD). In order to compensate for possible variations in extent of reaction, all band intensities within a given lane were normalized to a particular band within that lane which did not exhibit intensity dependence on input ligand concentration. At r > 10, the intensity of all bands was diminished and normalization was not possible. The extent of protection from cleavage for each base was determined by:

$$\text{percent protection} = [1 - (OD_{\text{ligand-DNA}}/OD_{DNA})] \times 100$$

where $OD_{\text{ligand-DNA}}$ is the optical density of a band obtained from cleavage in the presence of added ligand and OD_{DNA} is the optical density of the same band produced in the absence of ligand. Negative values for protection correspond to enhancement of cleavage in the presence of the ligand.

Analysis of binding data. The binding parameters, the intrinsic binding constant K_o, and the binding stoichiometry r_b (number of ligand molecules bound per nucleotide base), were determined from the Scatchard equation on the basis of the assumption of an independent noncooperative type of binding (Scatchard, 1949): $r/c_f = K_a(r_b - r)$ where $r = c_b/c_p$,c_b and c_p are the concentrations of the bound ligand and the polynucleotide respectively (in mononucleotide residues molar concentration), and c_f is the concentration of free ligand. A plot of r/c_f against r gives a straight line with the intercept r_b on the r axis and slope $-K_a$. The experimental points were fitted by the linear least squares method.

For the determination of c_b, the concentration of the bound ligand, a small aliquot (between 4 and 10 μL of a 10^{-2} stock solution) of the ligand was added to the sample cell containing a fixed concentration of the polynucleotide (200-250 μM). The reference cell also contained the same concentration of the polynucleotide to take care of any possible contribution to absorbance from the polynucleotide at the monitoring wavelength. However, the latter was so chosen that at this wavelength there was maximum change in absorbance of the ligand due to its binding to the polynucleotide and there was no (or very little) contribution from the absorbance by the polynucleotide. The concentration of the bound ligand, c_b, corresponding to each point of the titration was calculated from the relation: $c_b = (A_f - A_b)/(\varepsilon_f - \varepsilon_b)$ were A_f = absorbance of the free ligand, A_b = absorbance of the same concentration of the ligand in the presence of the polynucleotide, ε_f = molar extinction coefficient for the free ligand, and ε_b = molar extinction coefficient for the bound ligand (determined from

the extinction coefficient of the ligand in the presence of a 100-fold excess of polynucleotide).

Absorption coefficients and "melting" curves were measured on a Uvikon Kontron 810/820 spectrophotometer coupled to a Uvikon Recorder 21 and a Uvikon Thermoprinter 48. Samples were placed in a thermostatically controlled cell-holder (10 mm pathlength). The cell was heated by circulating water from a Haake unit. The temperature inside the cell was monitored by using a thermocouple in contact with the solution. The absorbance at 260 nm was measured over the range 20-95°C at an heating rate of 1°C/min. The "melting" temperature Tm was taken to be the mid-point of the hyperchromic transition, as the melting profile is monophasic.

Helical lengthening measurements were made by using a Ubbelohde semi-micro dilution viscometer. The temperature was maintened at 28 +- 0.01°C in a thermostatically controlled water bath. Flow times were electronically measured to an accuracy of 0.1 s (Schott ABS/G type detector). Experiments were done in 0.01 SHE buffer, (9.4 mM NaCl/2 mM HEPES (N-(2-hydroxyethyl)piperazine-N'-2-ethane sulfonic acid)/10 μM EDTA (ethylenediamine tetraacetic acid) buffer, pH 7.0) as described by Wakelin and Waring (1976). Solutions were filtered through 0.45 μM Millipore filters before measurements.

Fluorescence and fluorescence polarization. Fluorescence experiments were made employing 20 μM calf thymus DNA in a 0.01M ionic strength buffer (9.3 mM NaCl, 2 mM NaOAc, 0.1 mM EDTA, pH 5) containing 2 μM ethidium bromide in such a way that there was minimal ethidium displacement and high drug-induced quenching (Baguley et al., 1981). The DNA-ethidium complex was excited at 525 nm and the fluorescence measured at 595 nm using a Jobin-Yvon J-Y-3 spectro-fluorometer equipped with an X-Y recorder and a SLM 4048 polarization spectro-fluorometer. The anisotropy parameter, μ, was calculated using the relation: $\mu=(I_{//} - I_{\perp})/(I_{//} + 2I_{\perp})$, where $I_{//}$ and $I_{\perp}$ are the emission intensities for emission polarization directions parallel and perpendicular to the plane of polarization of the exciting light respectively.

Linear dichroism. The electric dichroism measurements were performed with computerized instrumentation using the procedures previously outlined (Fredericq and Houssier, 1973, Houssier aud O'Konski, 1981). The optical set-up of a high sensitivity T-jump instrumentation equipped with a Glan polarizer was used under the following conditions: bandwidth 3 nm; sensitivity limit 0.001 in $\Delta A/A$; response time 3 μs. The rectangular electric pulses applied to the vertical platinum electrodes

(1.5 mm separation) were delivered by a Cober 606 P generator (0-2, 500 V, 12.5 A; Cober Electronics, Stamford, Conn. 06902). The field strength range covered is from 1 to 14 kV/cm; the pulse duration was carefully adjusted to reach the steady state orientation of the molecule (50-100 μs, depending on the electric field strength). The dichroism results are expressed in terms of the reduced dichroism $\Delta A/A = (A_{//} - A_{\perp})/A$ (ΔA is obtained from the measurements of $\Delta A_{//} = A_{//} - A$ using the relation $\Delta A = 1.5\,(A_{//} - A)$ where A is the absorbance in the absence of field, measured under the same pathlength (10 mm) with a Perkin-Elmer Lambda 5 spectrophotometer. The reduced dichroism values ($\Delta A/A$) for the DNA and for the ligand at low binding ratio D/P (molar drug concentration over molar mononucleotide concentration) are related to the orientation of the DNA and the ligand by the relations:

$$(\Delta A/A)_{DNA} = 3/2\ \phi\ (3\cos^2 \alpha - 1) \qquad (1)$$

$$(\Delta A/A)_{ligand} = 3/2\ \phi\ (3\cos^2 \beta - 1) \qquad (2)$$

where α and β are the local angles between the transition moments (of the bases and the dye chromophore, respectively) and the electric field direction. ϕ is the fractional orientation (O'Konski et al., 1959), which is equal to the ratio $(\Delta A/A) / (\Delta A/A)_{1/E \to 0}$ of the measured dichroism to the dichroism at perfect orientation, achieved in the limit of infinite field.

The angle β between the chromophore and the helix axis was determined according to a previously described procedure (Houssier, 1981),based on a comparison of the reduced dichroism at a given field for the bases and for the ligand in their respective absorption bands and using the ratios of the two reduced dichroisms:

$$\frac{(\Delta A/A)_{ligand}}{(\Delta A/A)_{DNA}} = \frac{3\cos^2\beta - 1}{3\cos^2\alpha - 1} \qquad (3)$$

This implies that the degree of orientation in the electric field and the macromolecular structure are not affected by the binding (a reasonable assumption at low amounts of binding). β was determined using either $\alpha_L = 90°$ (the Watson-Crick structure) or $\alpha = 72°$ (the experimental angle) giving β_L and β respectively.

This method is more adequate than the one proposed by Hogan et al. (1978) consisting in an extrapolation of $\Delta A/A$ to infinite field. In our case $\Delta A/A$ decreases exponentially with increasing 1/E ratio, leading the determination of the extrapolated dichroism hazardous.

RESULTS

Absorption spectra of ligands and their complexes with calf thymus DNA. Binding of the synthetic ligands NETGA and NETBI to DNA are evident from the changes in the UV absorption spectra (Figure 2) of the ligands when calf thymus DNA was added. The two ligands undergo red shifts of their absorption maxima due to complex formation with DNA. The red shiftis indicative of an increased delocalization of the π-electrons in the ligands as a consequence of their binding to DNA. The absence of a clear isosbestic point in these UV spectra suggests that different types of binding sites are involved.

Binding constants for ligand-calf thymus DNA interactions. The binding affinities were calculated by means of Scatchard plots (Scatchard, 1949) as shown in Figure 3. The binding parameters are summarized in Table I. The determination of c_b for the construction of the Scatchard plot was done at 266 nm for NETGA and 288 nm for NETBI, wavelengths at which there are contributions in absorbance from DNA. This was taken into account by adding an equal concentration of DNA to the reference cell.

With both drugs, the biphasic plots indicate the presence of at least two types of binding on the calf thymus DNA. For NETGA, at low r ratios (ranging from 0.003 to 0.1), the apparent binding constant K_a is 6.3×10^5 M^{-1}, i.e., similar to the one observed for the binding of Nt to calf thymus DNA, $K_a = 2.9 \times 10^5$ M^{-1} (Luck et al., 1977). The number of available binding sites per nucleotide (r_b) is 0.17, which is equivalent to 6 nucleotides/site (n). This suggests that at such low r ratios both the netrosin-like moiety (which covers 4 base pairs) and the anilino aminoacridine moiety (2 base pairs are required for intercalation) are bound to DNA.

At higher r values (up to 0.1), the apparent binding constant ($K_a = 3 \times 10^5$ M^{-1}) and the binding site size (n=4) strongly suggests that under these conditions only the bis-pyrrole moiety is involved in the binding without any contribution from the acridine chromophore. NETBI binds to DNA with a very weak affinity ($K_a=1 \times 10^3$ M^{-1}). This is confirmed by the footprinting results (see below).

Base preferential binding. Figure 4 shows the effects of binding of the two bifunctional ligands on the ΔTm of two DNAs of different base composition, implying a marked preference of these compounds for A.T sites as observed for Dst-A. In addition, the greater effect of NETGA on the quenching of the ethidium-poly[d(AT).d(AT)] complex than on the ethidium-calf thymus DNA complex (Figure 5)

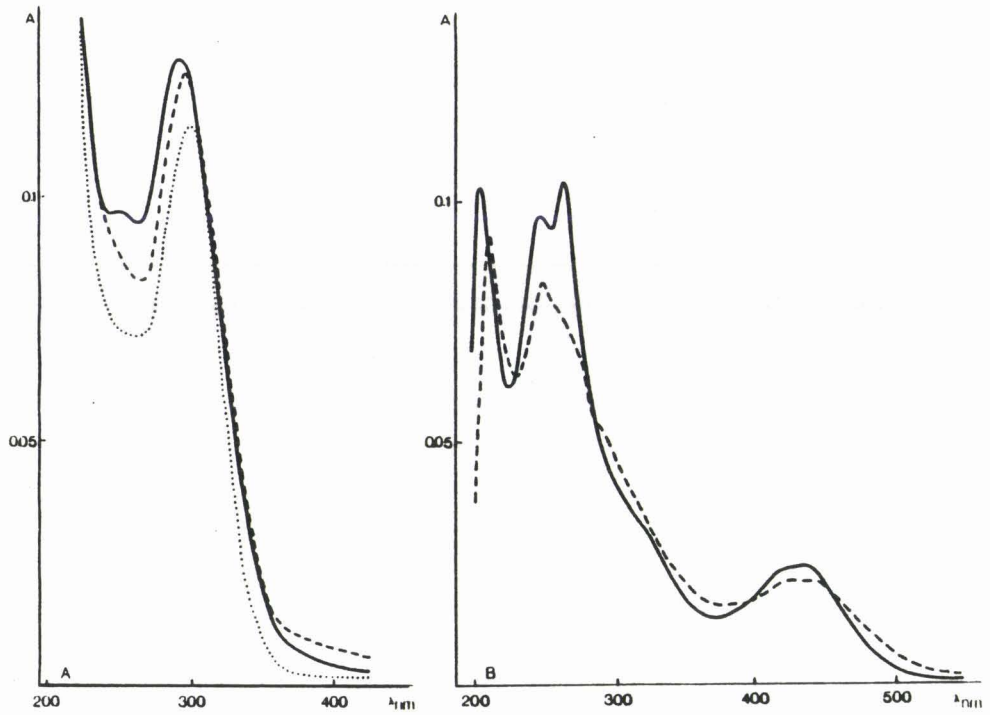

FIGURE 2 : UV absorption spectra of the ligands NETBI (A) and NETGA (B) and their complexes with calf thymus DNA. Solid lines represent the spectra of the free ligands (at a concentration of 5 μM); broken lines represent the spectra of their complexes at a ligand/DNA ratio of 0.05 (---) and 0.025 (...). The sample and reference cells contained equal concentrations of DNA [100 μM (---); 200 μM (...)].

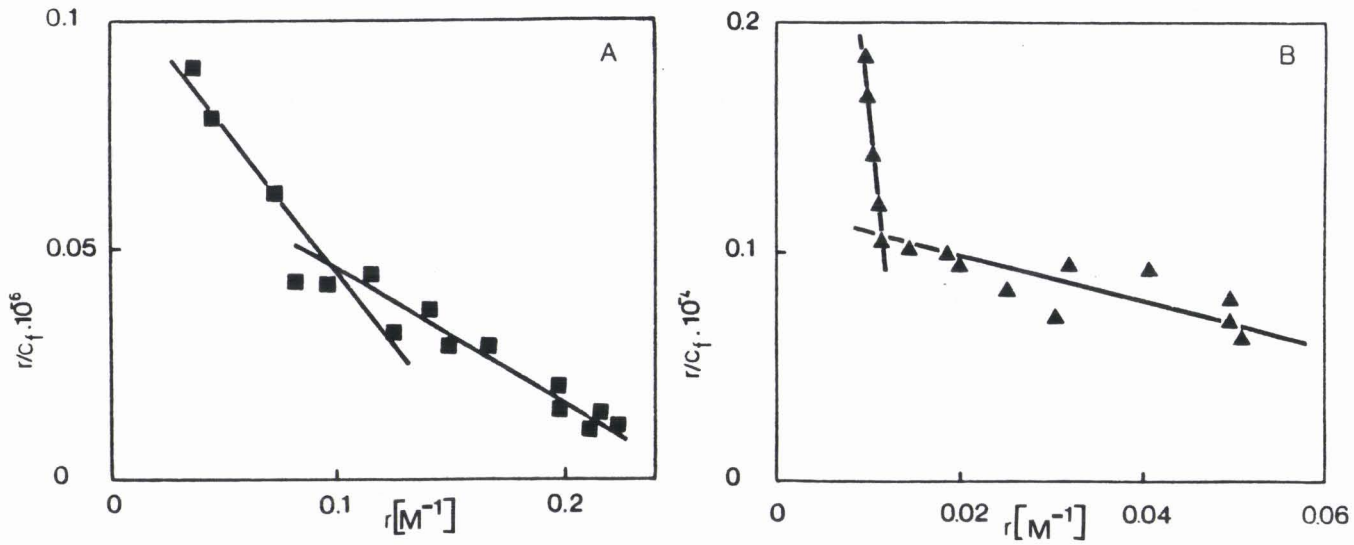

FIGURE 3 : Representative Scatchard plots (r/cf against r) for the evaluation of apparent binding constants for the interaction of NETGA (A) and NETBI (B) with calf thymus DNA.

TABLE I : Binding parameters for ligand- calf thymus DNA interaction. [a]

		First mode of binding					Second mode of binding				
Ligand	λ(nm)[b]	$K_a(M^{-1})$[c]	$K_O(M^{-1})$[d]	r_b[e]	n[f]	ΔG(Kcal/mol)[g]	$K_a(M^{-1})$	$K_O(M^{-1})$	r_b	n	ΔG(Kcal/mol)
NETBI	288	$9.0\ 10^5$	$1.3\ 10^4$	0.014	71.4	-5.5	$1\ 10^3$	$1.2\ 10^3$	0.12	8.3	-4.13
NETGA	266	$6.3\ 10^5$	$1.1\ 10^5$	0.17	5.9	-6.75	$3\ 10^5$	$0.75\ 10^5$	0.25	4	-6.54

a. Determined from Scatchard plots as shown in Figure 2 - b. Wavelength at which the absorbance change was measured to determine c_b. - c. Intrinsic binding constant. - d. Apparent binding constant , $K_a=K_O/r_b$. - e. Stoichiometry of binding of the ligand to DNA. - f. Binding site size, $n=1/r_b$. - g. Free energy for interaction, $\Delta G= -RT \ln K_a$, T=293°K.

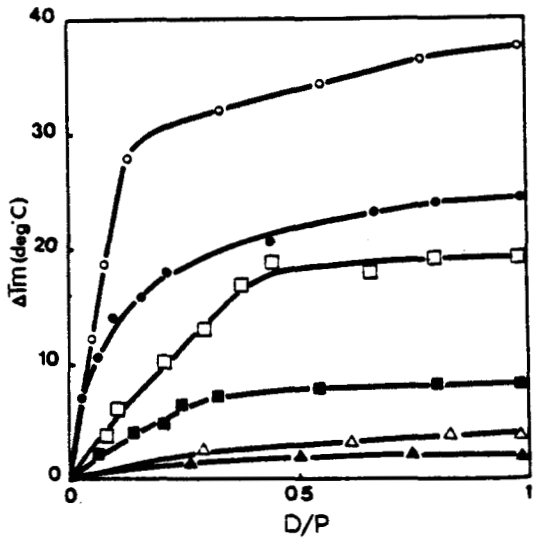

FIGURE 4 : Variation in thermal denaturation (ΔTm) of poly[d(AT).d(AT)] (open symbols) and calf thymus DNA (filled symbols) induced by the binding of Dst-A (○,●), NETBI (△,▲) and NETGA (□,■). (D/P = drug/phosphate DNA ratio).

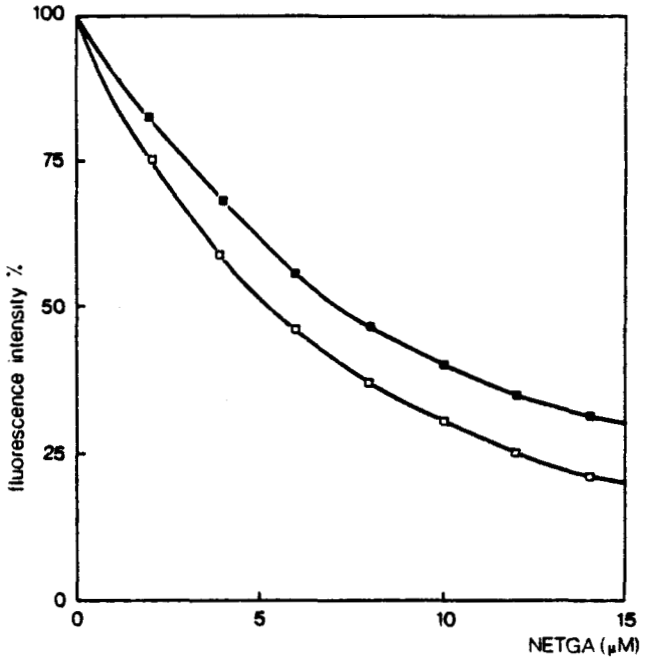

FIGURE 5 : Reduction of fluorescence intensity of ethidium-DNA complexes by addition of NETGA. (□) poly[d(AT).d(AT)] ; (■) calf thymus DNA. [20 μM DNA, 2 μM ethidium, 0.01 M ionic strength buffer (9.3 mM NaCl, 2 mM NaOAc, 0.1 mM EDTA, pH. 5)].

confirms this A.T preferential binding. More detailed information on actual preferred sequences is obtained from the footprinting experiments.

DNA Sequence Preferential Binding from Footprinting. Autoradiograms of the MPE-Fe(II) footprinting gels are shown in Figure 6. Areas of decreased intensity in ligand containing lanes compared to no ligand containing (control) lane are due to cleavage inhibition due to ligands bound to DNA. Densitometric analysis of the patterns of each lane permits estimation of the location, size and relative strength of binding sites on bases 63 to 142 of pBR 322 DNA. Binding site location and sizes for the new compounds have been determined on the basis of an earlier model proposed by Dervan (Harshman and Dervan, 1985).

The MPE-Fe (II) footprinting revealed cleavage inhibition and enhancement sites for the two mixed function ligands as well as netropsin on the Hind III, EcoRI restriction fragment of pBR 322 and are shown in the form of histograms in Figure 7. The new ligands give a smaller number and weaker footprinting than netropsin at a given r values. At low r values (<0.16) no footprinting are observed for either NETBI or NETGA. At r = 0.78 the footprints due to Nt over the analyzed portion of the DNA are at positions (all 5'-3'), 64-67 (CTAA); 84-98 (GTATGAAATCTAACA); 107-110 (ATCG). Complementary strand analysis of the MPE-footprinting gels shows the typical asymmetric shift of the footprints towards 3'-end (Van Dyke and Dervan, 1982b) indicating the minor groove is the probable site of interaction for these ligands (vide infra). Such complementary strand analysis of MPE-Fe (II) footprinting for a variety of ligands has indicated that the apparent binding sites on each strand are shifted 1 or 2 base pairs to the 3' site and are underprotected by 1 base pair on the 5' side (Harshman and Dervan, 1985; Youngquist and Dervan, 1985). It is reasonable to assume that a similar asymmetry is obtained in the complementary strand data presented here, based on extensive experience with other classes of lexitropsins. Therefore the proposed binding sites for Nt (at r=0.78) on this DNA sequence, when allowance is made for overlapping of four base binding sites, are (all 5'->3'): CTAA, GTAT, AAAT, AACA.

NETGA under comparable conditions, and by the same principles, shows an actual binding site of AAAT i.e., a four base site like netropsin, in accord with the results of the Scatchard analysis at comparable r values. The bithiazole bearing ligand NETBI under similar conditions shows protection from cleavage at 90-94 (AATCT) on the 5' labeled strand, 87-95 (ACTTTAGAT) on the 3' labeled strand. The complementary strand analysis suggests an actual binding site of AAATCT, i.e. a six base pair site for this ligand. This region of protection cannot be attributed to two


1 2 3 4 5 6 7 8 9 10 11 12 13 14 15 16 17
T
T
A
G
A
T
T
T
C
A
T
A
C
74
T
T
A
G
A
T
T
T
C
A
T
A
C
74

FIGURE 6 : A portion of footprinting autoradiogram from MPE-Fe(II) digestion of 3'-^{32}P end labeled 4332 base pair DNA fragment. Lane 1 contains intact DNA, lane 2 is control MPE-Fe(II) cleavage (no ligand present), lanes 9,11 and 15 contain ligands at 0.78 ratio. lanes 10, 12 and 16 contain ligands at 0.16 ratio. Lane 17 is Maxam-Gilbert sequencing 'G' reaction. NETBI is present in lanes 9 and 10, NETGA is present in lanes 11 and 12 and netropsin is present in lanes 15 and 16. Disregard all other lanes.

FIGURE 7 : Footprinting and cleavage enhancement of a) NETBI, b) NETGA and c) netropsin on bases 63-142 of Hind III/EcoR I cut 4332 base pair restriction fragment of pBR 322 DNA. Histogram height is proportional to the protection from the cleavage due to binding of ligands to DNA (r=0.78) at each base pair relative to unprotected DNA (in absence of ligand). Upper and lower footprints are from 5'- and 3'- end labeled DNA respectively.···· Indicate enhanced cleavage. Boxes indicate proposed binding sites.

overlapping four base sites since in that case one would expect two maxima on the histogram.

Enhancement in the MPE-Fe(II) cleavage rate occurred at the following positions on the 5'-labeled strand 85, 102,104-106, 109, 111-142 when NETBI is bound, and on the 3'-labeled strand at 108, 109, 110, and 114-130. Comparable enhancement of MPE-Fe(II) cleavage rate is seen especially at GC rich regions remote from the actual binding sites of NETGA and Nt except that, in the case of Nt, enhanced cleavage is also observed adjacent to the binding sites. The criterion used for acceptance of changes in the density of the bands from the Maxam-Gilbert sequencing as evidence for a footprint or enhanced cleavage was the same in either case, i.e. a change of > +-15% in the normalized densitometric trace.

Binding to DNA via minor groove. Figure 8 shows that addition of coliphage T_4 DNA to a solution of NETGA or NETBI induced changes in their respective UV spectra. Thus the blockage of the major groove by bulky glucose residues (on the 5' (hydroxymethyl)cytidine residues) in the T_4 DNA (Erickson and Szybalski, 1964) did not inhibit their binding. Elevation in thermal denaturation temperatures (ΔTm) was obtained with NETGA and NETBI upon interaction with T_4 DNA. NETGA and NETBI gave, at a D/P ratio of 1, the following ΔTm's respectively: 10 and 1 deg. The very small ΔTm value measured with NETBI is probably due to its weak affinity of binding to DNA. Nevertheless the observed binding is consistent with the results of the complementary strand footprinting analysis given above and with attachment in the minor groove as established for netropsin (Kopka et al., 1985; Zimmer et al., 1979).

Steady state fluorescence and fluorescence polarization measurements. As shown in Figures 5 and 9, NETGA, when bound to double stranded DNA, caused both a decrease in the observed fluorescence intensity and an increase in the fluorescence polarization (anisotropy parameter) of ethidium-DNA complexes. Similar results have been previously reported with amsacrine (Baguley and Le Bret, 1984). As shown in Figure 9, at a DNA/ethidium ratio P/D=10 the fluorescence anisotropy values are low (μ=0.12-0.14). This result could be attributed to energy transfers between molecules of ethidium (Genest and Wahl, 1972; Genest et al., 1974). Addition of NETGA to the ethidium/DNA complex induces a moving of the ethidium molecules from their intercalation sites as judged by the quenching of fluorescence (Figure 5) and the energy migration between the ethidium dyes is smaller.

Increase in the fluorescence anisotropy (μ) values uppon addition of NETGA to the ethidium/DNA complex could be ascribed to intercalation of NETGA. In such

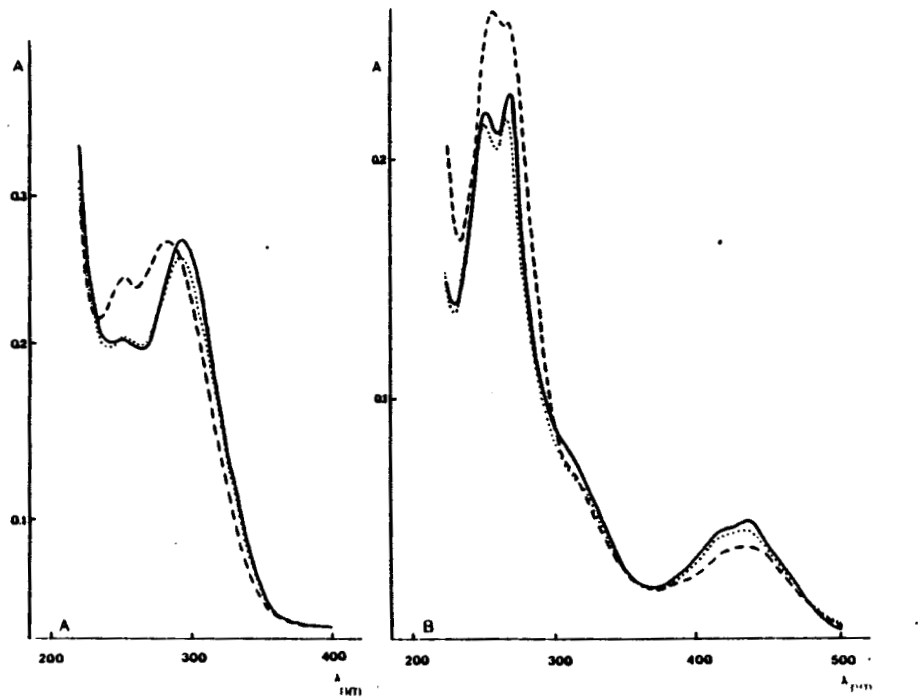

FIGURE 8 : UV absorption spectra of the ligands NETBI (A) and NETGA (B) and their complexes with Coliphage T_4 DNA. Solid lines represent the spectra of the free ligands (at a concentration of 10 μM); broken lines represent the spectra of their complexes at a ligand/DNA ratio of (A) (···) 0.3 and (---) 0.04 and (B) (···) 1 and (---) 3.

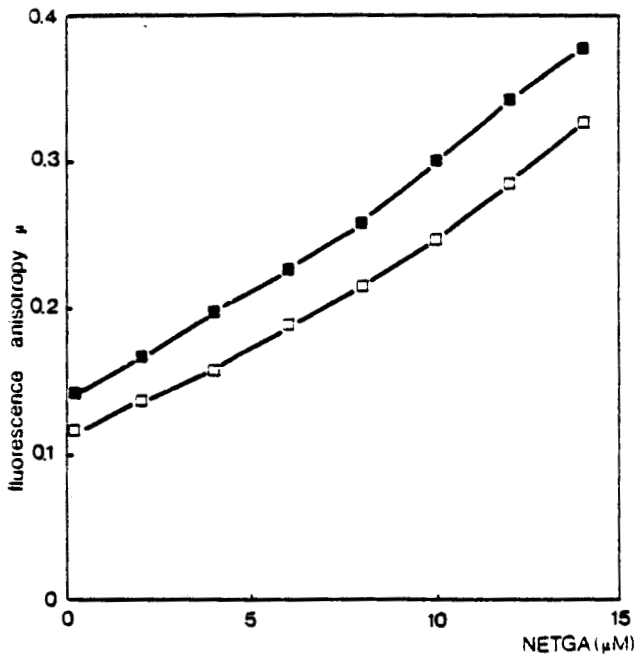

FIGURE 9 : Fluorescence anisotropy (μ) measurements of ethidium-DNA complexes in the presence of various concentration of NETGA; (□) poly[d(AT).d(AT)]; (■) calf thymus DNA. (20 μM DNA, 2 μM ethidium, 0.01M ionic strength buffer [9.3 mM NaCl, 2 mM NaOAc, 0.1 mM EDTA, pH. 5]).

assays employing an excess of DNA (ethidium-DNA ratio of 2/20), only high doses of NETBI (50 μM) were able to induce quenching of DNA-bound ethidium.

Viscometry measurements. NETBI induces a consistent length decrease (Figure 10) on adding to low molecular weight DNA. After reaching a total D/P ratio (drug to phosphate DNA ratio) of 0.05, the length is stabilized. In contrast NETGA shows an initial viscosity enhancement until a D/P valued = 0.03 is reached followed by a significant decrease and then a rapid increase beyond D/P = 0.15. The curve obtained with NETBI, where no increase in the length of DNA occurs, is similar to those previously reported by Luck et al., (1977) with two distamycin-analogues containing four (Dst-4) or five (Dst-5) N-methylpyrrole carboxamide units. This result is consistent with minor groove binding of the two parts of NETBI (i.e., the bis-pyrrole moiety and the bithiazole moiety) which could be analogous to Dst-4 in its binding properties. In contrast, the curve obtained with NETGA is in agreement with those obtained with the deformylated-distamycin analogue (Luck et al., 1977). Such a curve probably reflects a complex mechanism of interaction in which the two binding mode processes (intercalation and minor groove binding) are involved. After an initial increase at D/P<0.03, the curve drops in a manner which is typical of a local-bending mechanism (Reinert, 1981); afterwards a significant increase of DNA length is observed, corresponding to a binding region characterized by a lower association constant and reported to reflect a minor groove DNA binding mode. Such a length increase has already been shown to exist in the case of minor groove binders, both theoretically and experimentally (Reinert, 1972). It was reported as reflecting a broadening of the minor groove probably due to side-to-side binding of NETGA molecules inside the small groove of DNA. In order to verify this hypothesis, linear electric dichroism studies have been undertaken.

Electric dichroism measurements. Reduced linear dichroism (LD) ($\Delta A/A$) spectra are shown in Figure 11 for both drugs. The NETGA-DNA complex LD spectrum shows a negative region (380-460 nm) reflecting the position of the acridine chromophore in the DNA complex in an absorption range where there is no contribution of the bis-pyrrole moiety. The positive dichroism in the 300-370 nm region is attributed to the bis-pyrrole moiety. Thus for NETGA, two cleary-distinct wavelengths (310 nm and 440 nm) allowed a distinction of the binding configurations adopted by the two parts of the molecule, i.e., the bis-pyrrole moiety (potentially minor groove binding) and the anilinoacridine chromophore (potentially intercalating).

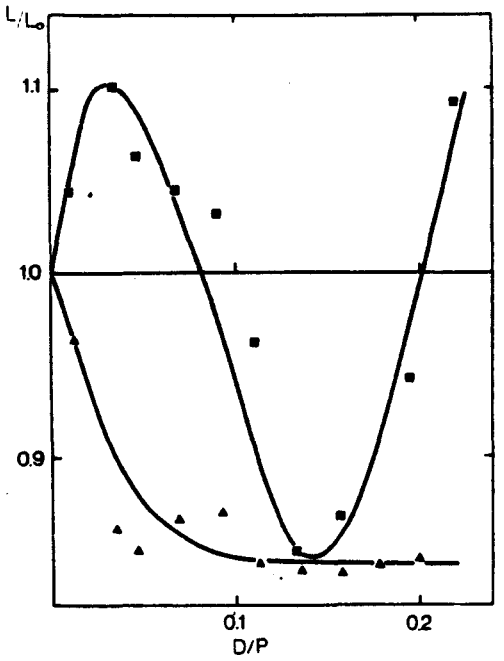

FIGURE 10 : Changes in calf thymus DNA length induced by the binding of NETBI (▲) and NETGA (■). The length L of the drug-DNA complex was measured as a function of D/P (drug to phosphate DNA ratio). Lengths were normalized to DNA length L_0 in the absence of drug.

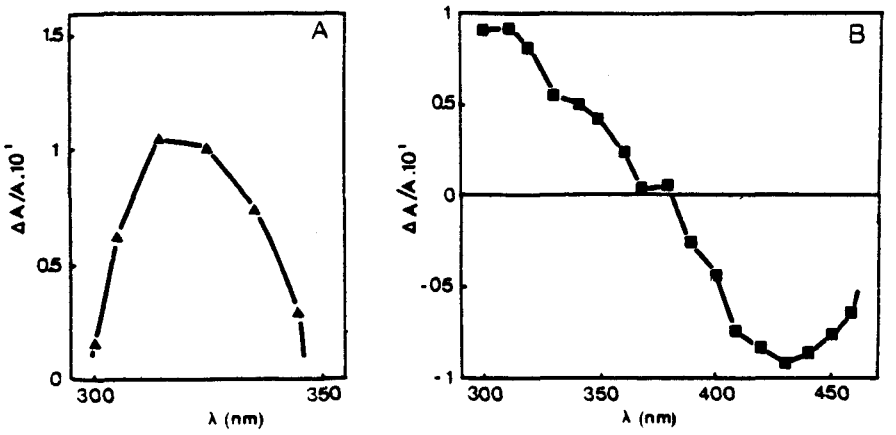

FIGURE 11 : Reduced linear dichroism (ΔA/A) spectra of NETBI-DNA (A) (D/P = 0.14) and NETGA-DNA (B) (D/P = 0.10) complexes at 12.5 $kV.cm^{-1}$.

In contrast, the NETBI-DNA complex absorption and LD spectra did not allow a distinction between the bis-pyrrole moiety and the bithiazole moiety since both chromophores absorb in the same region of the spectrum.

The variation of the reduced dichroism with the binding ratio (D/P) for NETGA (Figure 12a and b), NETBI (Figure 12c) and for the glycylanilinoaminoacridine (Figure 12b) and the bithiazole (Figure 12d) derivatives shows similar behaviors. At low D/P ratios, the slightly lower dichroism values measured for both ligands are due to the higher DNA concentration required to reach D/P values of 0.01-0.02, namely 3 to 15 times longer than the DNA concentration used for the measurements in the 260 nm band. In each case, the decrease of LD above D/P ratio up to 0.1 or 0.2 is due to the appearance (at this ratio) of free ligand molecules in the solution. These observations are in agreement with the measured K_a values and confirm the moderate affinity of these molecules for DNA. The modes of binding of NETGA and NETBI to DNA have been analyzed only on the basis of the highest LD values, obtained when the ligands are fully bound to DNA (D/P = 0.05 to 0.1 sometimes 0.2).

Orientation of NETGA and NETBI on DNA. The LD for NETBI absorption is positive demonstrating that NETBI is oriented closely parallel to the DNA groove inclination, a geometry which excludes intercalation. In contrast, the bithiazole part of Blm, studied alone (Figure 12d), shows a negative spectrum, thus excluding minor groove binding. The positive LD value measured at 320 nm for NETBI (Figure 12c) reflects the contribution of both bis-pyrrole and bithiazole parts but, on the basis of this positive LD value and of the viscometry data (Figure 10) which do not indicate any increasing intrinsic viscosity of DNA (a characteristic of intercalation), we can conclude that if the bithiazole ring alone wedges in between the base pairs of DNA (Hénichart et al., 1985), such a process does not occur for NETBI. Both parts of NETBI seem to be located at the periphery of DNA, certainly in the minor groove as described for Nt and Dst-A (Hahn, 1975; Zimmer et al., 1986). However the field strength dependence of the electric dichroism for DNA and its complexes with Dst-A or NETBI (Figure 13A,B) indicated that NETBI does not adopt the same orientation as Dst-A does when bound to DNA. The orientation angle β relative to the DNA helix is β_L=47° (β=52°), i.e. close to those observed for other non-intercalating compounds such as Hoechst 33258 β_L=44° (β=47°), dibutylproflavine β_L=52.5° (β=53°) or the stilbene derivative OHSA β_L=β=54° (Houssier, 1981).

It should be pointed out that the negative dichroism of the bithiazole alone is much lower than the amplitude observed for the 260 nm band of the DNA heterocyclic bases (Figure 13). This confirms our finding (Hénichart et al., 1985) that the bithiazole

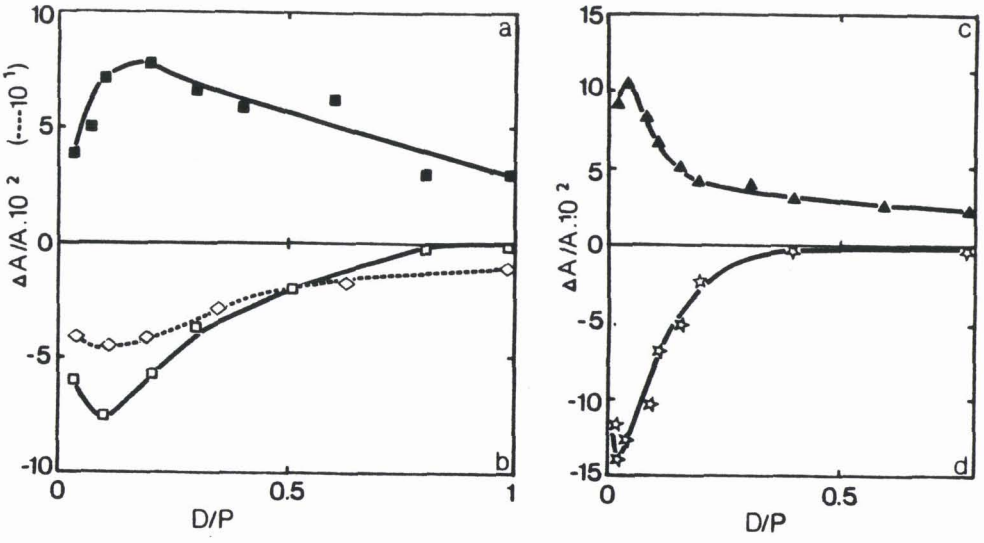

FIGURE 12 : Dependence of the reduced dichroism at 12.5 kV. cm^{-1} on drug to phosphate DNA binding ratio (D/P) for (a) NETGA at 310 nm (■) and (b) 440 nm (□) compared to the glycyl-anilino-9- amino-acridine at 440 nm (◇) and for (c) NETBI at 320 nm (▲) compared to (d) the bithiazole moiety at 310 nm (☆).

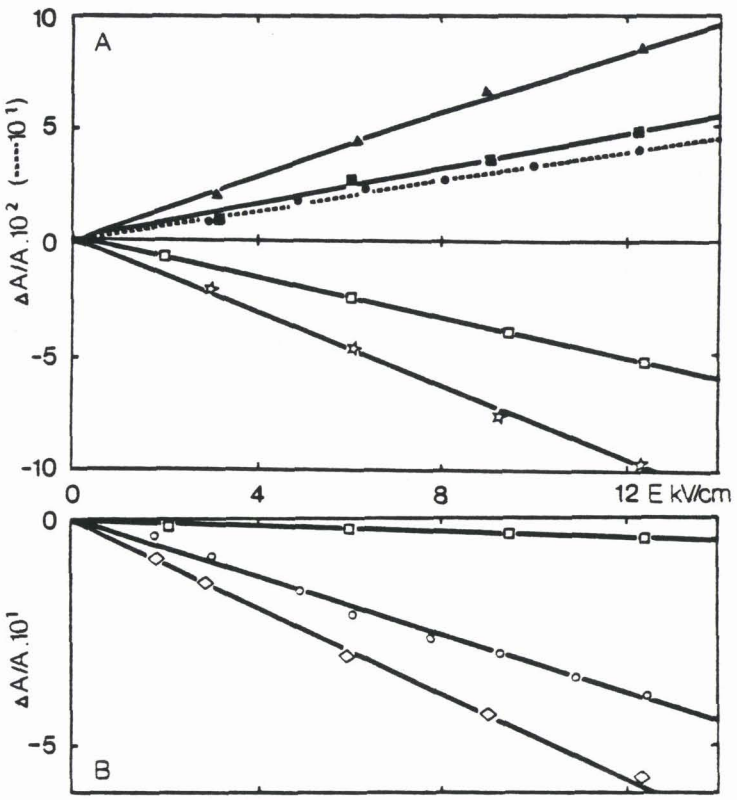

FIGURE 13 : Field strength dependence of the electric dichroism for :
(A) the DNA complexes with NETBI at 320 nm (▲), the bithiazole at 310 nm (☆), Dst-A at 318 nm (●), NETGA at 310 nm (■) and NETGA at 440 nm (□) at D/P = 0.07.
(B) DNA at 260 nm (o) and its complexes with NETGA at 440 nm (□), glycyl-anilino-9-amino-acridine at 440 nm (◇).

is not a classical intercalating agent as previously described by Povirk et al., (1979) who nevertheless found the same orientation angles (α=68° , β=58°-61°), but a pseudo-intercalative moiety as shown on the basis of EPR measurements. The LD spectrum exhibited by NETGA (Figure 11B) indicates that two binding processes are involved in the binding of NETGA to DNA. The bis-pyrrole moiety exhibits a weak positive dichroism at 310 nm which corresponds to an orientation angle of about 54° (β_L=52°) close to the observed angle for NETBI (Table II). It seems reasonable to conclude that the non-intercalating parts of these molecules have the same orientation.

At 440 nm, the measurements of LD displayed the orientation of the acridine chromophore and more particularly the orientation of the transition moment oriented along the short axis of the acridine. The glycylanilinoaminoacridine moiety of NETGA studied alone exhibits a negative LD close to that of the DNA bases (Figure 12b) favoring a binding mode in which the acridine is stacked parallel to the bases, corresponding to a classical intercalation. But when this intercalating moiety is linked to the non-intercalating bis-pyrrole, the intensity of the LD values at 440 nm falls significantly, indicating that the parallelism between the acridine and the base is disrupted. Under these conditions, complete overlap of the base pairs is not obtained and a partial intercalation is inferred. Thus it has been shown that the two parts of NETGA bind to DNA and determination of the orientation angles ($\beta_L{}^{310}$=52°, $\beta_L{}^{440}$=60°) show that the respective observed transition moment directions are aligned at approximately 8 degrees.

The measured orientation angle must be considered only as an average angle and not as reflecting the exact position of the transition moment relative to the DNA axis. It has to be noted that relatively weak dichroism values for DNA [($\Delta A/A$)=-0.495] compared to the usual values [($\Delta A/A$)=-1.0 to -1.2] (Hogan et al., 1978) were observed in this study. This may be due to the degree of orientation which is not high enough. Therefore the presence of a bending in NETGA can only be taken as indicative caution.

The LD technique directly yields information about the binding geometry of the DNA-associated ligand; but it should be pointed out that this technique does not take into account the possibility of a local DNA-bending induced by the binding. If such an effect occurs, the result might still be compatible with a classical intercalation of the acridine ring of NETGA (for example). This necessitates extreme caution in the interpretation of results and, in particular, of the validity of the orientation angles which may not reflect the exact position.

TABLE II : Linear dichroism parameters for ligand-calf thymus DNA interactions.

Ligand	a D/P	b λ	c ΔA/A	orientation angle[d] ß	ßL	e $\frac{(\Delta A/A)^{Ligand}}{(\Delta A/A)^{DNA}}$
NETGA	0.02	440	-0.060	56	60	+0.23
	0.08	440	-0.050	56	59	+0.20
	0.02	310	+0.037	54	52	-0.14
	0.08	310	+0.045	54	51	-0.18
NETBI	0.02	320	+0.094	52	47	-0.37
	0.04	320	+0.105	52	47	-0.41
	0.08	320	+0.085	52	48	-0.33
Glycyl-anilino	0.03	440	-0.218	55	77	+0.85
-9-amino	0.09	440	-0.296	63	>90	+1.15
acridine	0.12	440	-0.284	63	>90	+1.10
Bithiazole	0.01	310	-0.111	58	64	+0.43
	0.08	310	-0.097	57	63	+0.39
Dst-A	0.07	318	+0.405	44	22	-1.58
DNA	-----	260	-0.256	72(α)	90(α_L)	-----

a- Drug to phosphate DNA ratio. b- Monitoring wavelength (nm). c- LD values at 12.5 kV. cm^{-1}. d- Orientation angle (deg) between the transition moment of the ligand and the DNA helix axis. ß and ß' are determined from equation (3) using respectively $\alpha=72°$ and $\alpha_L=90°$. α and α_L denote respectively the measured and theoretical angles between the transition moment of the bases and the DNA helix axis. e- Ratio of the LD values at 12.5 kV. cm^{-1}.

DISCUSSION

The results from several different complementary techniques have provided detailed information concerning the mechanisms of binding of the two hybrid ligands NETBI and NETGA to DNA. The two compounds, which both incorporate a potential minor groove binding moiety and a potential intercalating moiety, evidently bind to DNA by quite different processes. In both cases, minor groove binding of the oligopeptide portion does not seem to be affected by the proximity of planar heterocyclic moieties and appears to dominate the binding.

The relatively low affinity of NETBI for calf thymus DNA may be, in part, due to the presence of the intervening flexible spacer between the N-methylpyrrole unit and the bithiazole unit. Previous studies (Dasgupta et al., 1987) have shown that the presence of two such methylene units between N-methylpyrrole rings does not prevent minor groove binding but substantially reduces the DNA binding affinity.

The measured binding site size for NETBI from the Scatchard analysis at low r values (0.003 to 0.1) is n=8. Owing to the low DNA affinity of this drug, measurable footprints were only obtained at higher r values (0.78) and the binding site size estimate was n=6. These complementary results suggest that each binding unit of NETBI covers 4 base pairs (if we consider Nt covers 4 base pairs) at least at low r values. The results favor location of NETBI within the minor groove of DNA without intercalation of the bithiazole. This minor groove binding is substantiated by the complementary strand analysis of the footprinting and by the ΔTm measurements with T_4 DNA. The estimate of binding site size for NETBI at very low r values (ranging from 0.008 to 0.013) cannot be considered to reflect a particular binding process. A likely explanation for the unusually large binding site size (n) of NETBI on calf thymus DNA at such r ratios may be a destabilizing effect of this ligand on the double helical structure of the nucleic acid leading to a decrease in the number of potential binding sites, seen as an increase in apparent binding site size calculated from Scatchard plots. Such unusual properties were noted with the acridine orange-poly (dA).(dT) complex (n=19.3; Kapuscinski and Darzynkiewicz, 1987) and with the Blm-calf thymus DNA complex (n=22-29, Huang et al., 1980). The difference in the DNA-binding affinity of the two compounds was also apparent considering the ΔTm values. Evidence in support of this destabilizing influence on the DNA by binding of NETBI may come from the footprinting where regions of enhanced cleavage, particularly in GC rich sequences are observed adjacent to, and even remote from, the achiral binding site. This phenomenon which has been observed by others (Fox and Waring, 1984) may be significant for the biological properties of these agents. On the other hand an

alternative explanation has recently been offered for enhanced cleavage in terms of a redistribution of the cleaving agent as a result of drug binding (Ward et al., 1988).

The complementary strand footprinting experiments with NETBI provide more direct evidence for binding location and binding site size which, as we have seen, is AAATCT, i.e. six base pairs. The AAAT section, which is held in common with NETGA and Nt, is assigned to the oligopeptide moiety of NETBI. This implies that the bithiazole moiety recognizes the CT section of the binding site which is in accord with the (G,C)T recognition and preferred cleavage site of bleomycin (Murray and Martin, 1985).

It may also be concluded that a pseudo-intercalative process of the bithiazole as described for Blm (Hénichart et al., 1985) does not occur. On the basis of the measured site size, and of viscometry and LD data, it can be postulated that the bithiazole part of NETBI is the minor groove. Such an orientation is highly probable taking into account the crescent shape of the two syn-orientated thiazole rings and the ability of the heterocyclic nitrogens to form hydrogen bonds with the amine hydrogens of bases.

NETGA shows a strict preference for AAAT dominated by the oligopeptide moiety at r=0.78 but reveals evidence for the intercalation of the acridine moiety at lower r values. The first property is in accord with results on oligopeptides analogous to netropsin and distamycin bearing acridine at the amino terminus (Eliadis et al., 1988). Such compounds also exhibit a strict AT preference but no evidence was obtained in these cases for intercalation of the acridine under any conditions.

The intercalation of the acridine nucleus of NETGA is less perturbed by the netropsin moiety. LD measurements revealed an insertion of the acridine into the DNA but no coplanarity exists between the base pairs and the acridine chromophore. An inclination of approximately 20° relative to the base planes has been previously reported (Hogan et al., 1979; Wirth et al., 1988). In the present case, the acridine chromophore is more tilted (β_L=60°, α=90°), reflecting the influence of the netropsin moiety on the binding of the acridine to DNA. The short spacer glycyl, in spite of its relative inflexibility, is apparently not an obstacle to the binding. This glycine tether, as judged from distance and steric considerations from model building studies, has been used (Dervan, 1986) to connect the distamycin tripeptide directly to the phenoxazone chromophore of actinomycin but, in that case, the local distortion on both sides of the intercalation site perturbs the binding of the distamycin moiety.

Taking into account this observation for the design of a new drug, whose binding is consistent with the groove binder-intercalation mode, we connected the netropsin moiety to the acridine nucleus via a glycyl-anilino spacer. As reported for

the antitumor drug amsacrine (Denny et al., 1983), the intercalation of the acridine is accompanied by a minor groove binding of the netropsin moiety.

The incorporation of these novel design features in the development of longer ligands capable of targeting sequences of direct biological interest will be reported in due course.

REFERENCES

Baguley, B.C., Denny, W.A., Atwell, G.J., Cain, B.F. (1981) J. Med. Chem. 24, 170-177.

Baguley,B.C. and Le Bret, M. (1984) Biochemistry 23, 937-943.

Bailly, C., Houssin, R., Bernier, J-L., Hénichart, J-P. (1988) Tetrahedron 44, 5833-5843.

Bailly, C., Catteau, J-P., Hénichart, J-P., Krowicki, K., Lown, J.W. (1989) Biochem. Pharmacol. (in press).

Berg, O.G. and von Hippel, P.H. (1988) Trends Biochem. Sci. 13, 207-211.

Chen, K.X., Gresh, N., Pullman, B. (1988) Nucl. Acids Res. 16, 3061-3073.

Dasgupta, D., Rajagopalan, M., Sasisekharan, V. (1986) Biochem. Biophys. Res. Comm. 140, 626-631.

Dasgupta, D., Parrack, P., Sasisekharan, J. (1987) Biochemistry 26, 6381-6386.

Denny, W.A., Atwell, G.J., Baguley, B.C. (1983) J. Med. Chem. 26, 1625-1630.

Dervan, P.B. (1986) Science 232, 464-471.

Ekambareswara Rao, K., Dasgupta, D., Sasisekharan, V. (1988) Biochemistry 27, 3018-3024.

Eliadis, A., Philips, D.R., Reiss, J.A., Skorobogaty, A. (1988) J. Chem. Soc., Chem. Commun. 1049-1052.

Erickson, R.L., Szybalski, W. (1964) Virology 22, 11.

Feigon, J., Denny, W.A., Leupin, W., Kearns, D.R. (1984) J. Med. Chem. 27, 450-465.

Fox, K.R., Gauvreau, D., Goodwin, D.C., Waring, M.J. (1980) Biochem. J. 191, 729-742.

Fox, K.R., Olsen, R.K., Waring, M.J. (1982) Biochim. Biophys. Acta 696, 315-322.

Fox, K.R., Waring, M.J. (1984) Nucl. Acids Res. 12, 9271-9277.

Frederick, C.A., Grable, J., Melia, M., Samudzi, C., Jen-Jacobson, L., Wang, B.C., Greene, P., Boyer, H.W., Rosenberg, J.M. (1984) Nature (London) 309, 327-331.

Fredericq, E., Houssier, C. (1973) Electric Dichroism and Electric Birefringence, Clarendon Press, Oxford.

Genest, D. and Wahl, Ph. (1973) in Dynamic aspects of conformation changes in biological macromolecules. Sadron, C., Ed. pp 367-379, Reidel, Dorderecht.

Genest, D., Wahl, Ph., Auchet, J.C. (1974) Biophys. Chem. 1, 266-278.

Hahn,F.E. (1975) in Antibiotics III. Mechanism of action of antimicrobial and antitumor agents. Corcoran, J.W. and Hahn, F.E., Eds., p 79, Springer-Verlag,

New-York.

Harshman, K.D. and Dervan, P.B. (1985) Nucl. Acids Res. 13, 4825- 4835.

Helbecque, N., Bernier, J-L., Hénichart, J-P. (1985) Biochem. J. 225, 829-832.

Hénichart, J-P., Bernier, J-L., Helbecque, N., Houssin, R. (1985) Nucl. Acids Res. 13, 6703-6717.

Hogan, M., Dattagupta, N., Crothers, D.M. (1978) Proc. Natl. Acad. Sci. USA, 75, 195-199.

Hogan, M., Dattagupta, N., Crothers, D.M. (1979) Biochemistry 18, 280-288.

Houssier, C., O'Konski, C.T. (1981) in Molecular Electro-Optics. Krause, S., Ed., Series B64, pp. 309-339, Nato Advanced Study Institute.

Houssier, C., (1981) in Molecular Electro-Optics. Krause, S., Ed., Series B64, pp.363-398, Nato Advanced Study Institute.

Houssin, R., Bernier, J-L., Hénichart, J-P. (1984) J. Heterocycl. Chem. 21, 681-683.

Huang, C.H., Galvan, L., Crooke, S.T. (1980) Biochemistry 19, 1761-1767.

Jones, D.H., Woodridge, R.H. (1968) J. Chem. Soc. 550-554.

Kapuscinski, J., Darzynkiewicz, Z. (1987) J. Biomol. Struct. Dyn. 5, 127-143.

Kasai, H., Naganawa, H., Takita, T., Umezawa, H. (1978) J. Antibiot. (Tokyo) 32, 1316-1320.

Kissinger, K., Krowicki, K., Dabrowiak, J.C., Lown, J.W. (1987) Biochemistry 26, 5590-5595.

Kopka, M.L., Fratini, A.V., Drew, H.R., Dickerson, R.E. (1983) J. Mol. Biol. 163, 129-146.

Kopka, M.L., Yoon, C., Goodsell, D., Pjura, P., Dickerson, R.E. (1985) Proc. Natl. Acad. Sci. USA 82, 1372-1380.

Krowicki, K., Lown, J.W. (1987) J. Org. Chem. 52, 3493-3501.

Krowicki, K., Balzarini, J., De Clercq, E., Newman, R.A., Lown, J.W. (1988) J. Med. Chem. 31, 341-345.

Lee, J.S., Waring, M.J. (1978a) Biochem. J. 173, 115-128.

Lee, J.S., Waring, M.J. (1978B) Biochem. J. 173,129-144.

Lee, M., Krowicki, K., Hartley, J.A., Pon, R.T., Lown, J.W. (1988a) J. Am. Chem. Soc.110, 3641-3649.

Lee, M., Krowicki, K., Shea, R.G., Pon, R.T., Lown, J.W. (1988b) J. Molec. Recogn. submitted.

Low, C.M.L., Drew, H.R., Waring, M.J. (1984a) Nucl. Acids Res. 12,4865-4879.

Low, C.M.L., Olesen, R.K., Waring, M.J. (1984b) FEBS Lett. 176, 414-420.

Lown, J.W. (1988) Anti-Cancer Drug Design 3,15-40.

Lown, J.W., Krowicki, K., Bhat, U.G., Skorobogaty, A., Ward, B., Dabrowiak; J.C. (1986a) Biochemistry 25,7408-7416.

Lown, J.W., Krowicki, K., Balzarini, J., De Clercq, E. (1986b) J. Med. Chem. 29,

1210-1214.

Luck, G., Zimmer, C., Reinhart, K.E., Arcamone, F. (1977) Nucl. Acids Res. 4, 2655-2670.

Maniatis, T., Fritsch, E.F., Sambrook, J. (1982) Molecular Cloning (A Laboratory Manual), Cold Spring Harbor Laboratory, Cold Spring Arbor, New York.

Murray, V., Martin, R.F. (1985) Nucl. Acids Res. 13,1467-1481.

O'Konski, C.T., Yoshioka, K., Orttung, W. (1959) J. Chem. Phys. 63,1558-1565.

Peden, K.W.C. (1983) Gene 22, 277-280.

Pelton, J.G., Wemmer, D.E. (1988) Biochemistry 27, 8088-8096.

Plouvier, B. (1988) Diplôme d'Etudes Approfondies, Lille.

Povirk, L.F., Hogan, M., Dattagupta, N. (1979) Biochemistry 18, 96-101.

Reinert, K.E. (1972) J. Mol. Biol. 72, 593-607.

Reinert, K.E. (1981) Biophys. Chem. 13, 1-14.

Scatchard, G. (1949) Ann. N.Y. Acad. Sci. 51, 660-663.

Sutcliff, J.G. (1979) Cold Spring Harbor Symp. Quant. Biol. 43, 77-90.

Takeda, Y., Ohlendorf, D.H., Anderson, W.F., Matthews, B.W. (1983) Science 221, 1020-1026.

Van Dyke, M.W., Hertzberg, R.P., Dervan, P.B. (1982a) Proc. Natl. Acad. Sci. USA 79, 5470-5474.

Van Dyke, M.W., Dervan, P.B. (1982b) Cold Spring Harbor Symp. Quant. Biol. 47, 347-353.

Van Dyke, M.W., Dervan, P.B. (1984) Science 225,1122-1127.

Wade, W.S., Dervan, P.B. (1987) J. Am. Chem. Soc. 109, 1574-1575.

Wakelin, L.P.G., Waring, M.J. (1976) Biochem. J. 157, 721-740.

Ward, B., Rehfuss, R., Goodisman, J., Dabrowiak, J.C. (1988) Nucl. Acids Res. 16, 1359-1369.

Wirth, M., Buckhardt, O., Koch, T., Nielsen, P.E., Norden, B. (1988) J. Am.Chem. Soc. 110, 932-939.

Youngquist, R.S., Dervan, P.B. (1985) Proc. Natl. Acad. Sci. USA 82, 2565 -2569.

Zakrzewska, K., Randrianarivelo, M., Pullman, B. (1988) J. Biomol. Struct. Dyn. 6, 331-344.

Zimmer, C., Marck, C., Scheider, C., Guschlbauer, W. (1979) Nucl. Acids Res. 6, 2831-2837.

Zimmer, C., Luck, G., Burckardt, G., Krowicki, K., Lown, J.W. (1986) in Molecular Mechanism of Carcinogenic and Antitumor Activity, Chagas, C. and Pullman, B., Eds., pp. 339-363, Adenine Press, New York.

Zimmer, C., Wahnert, U. (1986) Prog. Biophys. Mol. Biol. 47, 31-112.

Conclusion :

La mise en oeuvre de multiples techniques physicochimiques a permis de caractériser parfaitement le mode d'interaction de ce type de composé avec l'ADN. Les résultats acquis avec le composé II (NETGA), c'est-à-dire l'intercalation de l'acridine et la liaison dans le petit sillon de la fraction bis-pyrrole, sont en parfait accord avec l'hypothèse initiale. Il semble trés probable que les composés I, III et IV puissent se comporter de façon similaire.

c) Spécificité de liaison.

L'étude préliminaire menée par spectroscopie UV et quenching de fluorescence avait révélé une fixation préférentielle de ces composés I à IV sur des ADN riches en paires de bases AT (article n°2). La présence d'un motif de type Dst-A au sein de ces dérivés est certainement à l'origine de ces résultats. Une étude plus précise menée sur le composé II (NETGA) par la technique de foot-printing a permis de dégager un site de fixation plus spécifique : AAAT (article n°3).

d) Activité biologique.

1 Pénétration cellulaire.

Les composés hybrides I à IV pénètrent trés facilement dans la cellule. La grande aptitude de ces composés à pénétrer dans la cellule s'explique logiquement si l'on considère la facilité des molécules modèles (Nt et amsacrine) à se concentrer au niveau du noyau. En effet une étude menée par RPE a permis aussi bien pour l'aminoacridine (LEMAY et al., 1983) que pour la nétropsine de caractériser cette pénétration cellulaire. Ce dernier point a fait l'objet d'une publication :

article n°4:

Subcellular distribution of a nitroxyde spin-labeled netropsin in living KB cells : EPR and sequence specificity studies.

BAILLY C., CATTEAU J-P., HENICHART J-P.,
KROWICKI K., LOWN J.W.

Biochemichal Pharmacology, 1989, sous presse.

Biochemical Pharmacology, Vol. 38, No. 10, pp. 1625–1630, 1989.
Printed in Great Britain.

0006-2952/89 $3.00 + 0.00

SUBCELLULAR DISTRIBUTION OF A NITROXIDE SPIN-LABELED NETROPSIN IN LIVING KB CELLS

ELECTRON PARAMAGNETIC RESONANCE AND SEQUENCE SPECIFICITY STUDIES

CHRISTIAN BAILLY,* JEAN-PIERRE CATTEAU,† JEAN-PIERRE HÉNICHART,* KRZYSZTOF RESZKA,‡ REGAN G. SHEA,‡ KRZYSZTOF KROWICKI‡ and J. WILLIAM LOWN‡§

* INSERM, U 16, 59045, Lille Cedex, France; ‡ Department of Chemistry, University of Alberta, Edmonton, Alberta, Canada T6G 2G2; and † Laboratoire de Chimie Organique Physique, USTL, 59655 Villeneuve d'Ascq, France

(*Received* 18 *April* 1988; *accepted* 22 *September* 1988)

Abstract—A nitroxide spin-labeled netropsin was studied by EPR spectroscopy with respect to its uptake and localization in living KB cells. Whereas the drug was taken up readily, there was relatively little drug in the cytoplasm, but a significant concentration of the drug in the cell nucleus. The EPR signal in the latter site corresponded to a relatively freely rotating radical. The drug exhibited good intracellular stability up to 25 hr. While a ΔT_m of 24° between the spin-labeled netropsin and calf thymus DNA confirmed strong binding, the absence of any DNA elongation by viscometry was consistent with non-intercalative exterior binding which was confirmed to be minor groove specific by binding of the agent to T4 DNA with a ΔT_m of 17.5°. The sequence specificity of the DNA binding of the spin-labeled drug was confirmed by methidiumpropyl-EDTA (MPE) footprinting on a fragment of pBR322 DNA to be very similar to that of the parent netropsin, i.e. selective for AT-rich sites, with minor differences of protection afforded by introduction of the nitroxide label.

There is considerable interest currently in the development of sequence specific DNA binding agents for application as anti-sense cell regulatory agents in diagnosis and therapy [1–5]. Promising results have been obtained with anti-sense probes based on β-oligodeoxyribonucleotides [1, 2, 4] or modifications thereof [6] and, more recently, with the unnatural α-oligodeoxyribonucleotides [7]. While these oligonucleotide-based agents meet some of the criteria for viable anti-sense probes, i.e. high binding specificity, and resistance to intracellular nucleases in the case of β-oligomer methylphosphonates [5] and α-oligomers [7], they suffer the serious disadvantage of difficulty of penetration of the cellular membrane [4]. The methyl phosphonate β-oligomers, prepared in response to this problem, present additional difficulties in that a sequence containing n phosphate residues represents 2^n diastereomers [8]. In an alternative approach we are developing lexitropsins, or information-reading oligopeptides, for the sequence specific delivery of DNA effectors [9–12]. We report an examination of the uptake of a nitroxide spin-labeled netropsin (Fig. 1) into living KB cells and their preferential concentration in the cell nucleus by EPR spectroscopy. Additional experiments with purified DNAs provided detailed information on the sequence specificity and mode of binding of the spin-labeled agent.

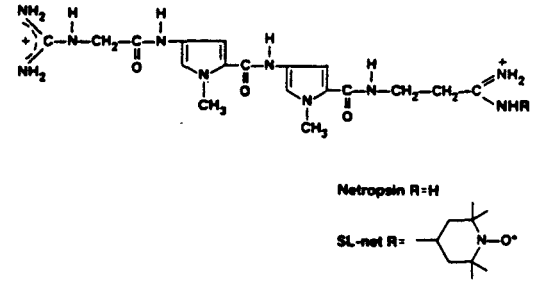

Fig. 1. Structural formulae of netropsin and spin-labeled netropsin.

MATERIALS AND METHODS

Chemicals

IR spectra were recorded on a Nicolet 7199 FT spectrophotometer and only the principal sharply defined peaks are given. FAB mass spectra were determined on an Associated Electrical Industries (AEI) MS-9 mass spectrometer. Melting points were determined on a Fisher–Johns apparatus and are uncorrected.

1 - *Methyl* - 4 - (4 - *guanidineacetylamino* - 1 - *methylpyrrole* - 2 - *carboxamido)pyrrole* - 2 - *carboxamido*-N - *(2,2,6,6-tetramethylpiperidinyl* - N - *oxide)propionamidine hydrochloride (SL-net*)*.

1 - Methyl - 4 - (4 - guanidineacetylamino - 1 - methylpyrrole - 2 - carboxamido)pyrrole - 2 - carbo-

§ To whom correspondence should be addressed.

* Abbreviations: SL-net, spin-labeled netropsin; net, netropsin; MPE, methidiumpropyl-EDTA; bp, base pairs; and ct DNA, calf thymus DNA.

xamidopropionitrile [13] (140 mg, 0.3 mmol) was dissolved in 5 ml of dry ethanol and the solution was saturated with dry HCl gas with cooling. After 1.5 hr the solvent was removed *in vacuo* and the residue was washed with dry ether. The residual solid was redissolved in dry ethanol and the solution concentrated to dryness and washed with dry ether. The residual solid was dissolved in 5 ml of dry ethanol, and 4-amino-2,2,6,6-tetramethylpiperidinyl-*N*-oxide (104 mg, 0.6 mmol) was added. After 2 hr the mixture was concentrated to dryness *in vacuo* and the excess of the free radical reagent was extracted with acetone. The residue was dissolved in a small volume of methanol and precipitated by addition of acetone. This operation was repeated twice to afford 137 mg (69% yield) of SL-net of no distinct m.p. (softens at 195° with dec.); IR ν_{max} (Nujol) 1375, 1405, 1460, 1530, 1580, 1645, 3120, 3260 cm^{-1}; MS-FAB, m/z 585(M-HCl-Cl)$^+$; Anal. Calcd. for $C_{27}H_{44}Cl_2N_{11}O_4$: C, 49.3; H, 6.7; Cl, 10.8; N, 23.4. Found: C, 49.6; H, 7.0; Cl, 11.0; N, 23.8.

Biochemicals

T4 viral DNA was from Miles Laboratories, Inc. (Elkhart, IN). Restriction enzymes Hind III and Eco RI; pBR322 DNA and sonicated calf thymus DNA (ct DNA) were from Pharmacia Inc. Dithiothreitol (DTT) was from Calbiochem. Netropsin, acrylamide, bromophenol blue, and xylene cyanol were from Serva. Ultra pure urea was from Bethesda Research Laboratories. MPE was a gift from Professor P. B. Dervan. Ferrous ammonium sulfate was from BDH Chemicals, Ltd. [γ^{32}P]ATP was from New England Nuclear.

Methods for cell studies

Cell cultures. KB cells were grown as suspension cultures in Joklik modified Eagle's medium (Seromed, Munich, F.R.G.) supplemented with 5% heat-inactivated Colt serum at 4×10^5 cells/ml.

Spin-labeling. Nitroxide-labeled netropsin (SL-net) was added to cell cultures at 3.5×10^{-5} M (initial concentration) for various incubation periods.

Cell fractionation: Nuclear and cytoplasmic fractions. Spin-labeled cells (i.e. 40×10^6 cells) were collected by low-speed centrifugation, washed once in saline, and allowed to swell for 10 min in ice in 1 ml of hypotonic buffer (0.01 M Tris–HCl, pH 8.1, 0.05 M NaCl 0.001 M EDTA) [14, 15]. The cells were then disrupted by ten strokes of a tight-fitting Dounce homogenizer. The nuclei were pelleted at 600 *g* for 10 min and stored at −80° in 400 μl of hypotonic buffer; the resulting supernatant, referred to as the cytoplasmic fraction, was kept at −80°.

EPR spectra. Prior to EPR examination the cellular fractions were defrosted and sonicated (two 5-sec bursts with the microtip probe of a Bransen sonicator (Danbury, CT, maximum power). Each sample was treated with H_2O_2 and sodium phosphotungstate [16] to reoxidize all the reduced forms of the nitroxide prior to EPR examination. EPR measurements were recorded on a Varian E 109 X-band spectrometer equipped with an E 238 cavity operating in the TM_{110} mode. A 100 kHz high frequency modulation was used with a 20 mW microwave power. The sample solutions were examined in a flat quartz cell.

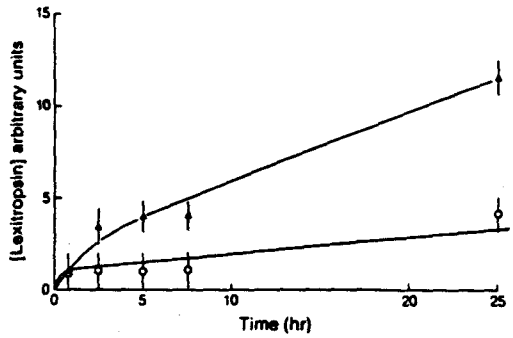

Fig. 2. Time course showing selective uptake of the nitroxide spin-labeled netropsin preferentially into the nucleus of living KB human tumor nasopharengal cells. Key: (-▲-▲-) nuclear fraction; and (-O-O-) cytoplasmic fraction.

Methods for studies with purified DNAs

Footprinting. Hind III digested pBR322 DNA was 5′-^{32}P-labeled and then digested with Eco RI. The resulting fragments (31 and 4332 bp) were not separated prior to footprinting. Solutions for footprinting experiments were prepared by mixing calf thymus DNA, radiolabeled DNA (approximately 10,000 dpm/sample) and ligand (omitted in the control) in Tris buffer, pH 7.4. The stock ligand concentration was determined by weight; ligand quantities are reported as r_t (ratio of ligand to DNA base pairs). After equilibration of the ligand–DNA mixtures for 30 min at 37°, MPE-Fe(II) [from a freshly prepared mixture of $Fe(NH_4)_2(SO_4)_2$ plus MPE] was added to each, followed by DTT. The final reaction mixtures contained 100 μM DNA base pairs, 7.5 mM Tris-HCl, 15 mM NaCl, 2 μM EDTA, 10 μM MPE-Fe(II), and 2.5 mM DTT. Reactions were run for 5 min at room temperature and were then stopped by freezing at −78°. The mixtures were lyophilized, resuspended in formamide loading buffer [17], heated at 90° for 1 min, chilled on ice, and loaded onto a polyacrylamide sequencing gel (0.4 mm thick, 55 cm long, 6% acrylamide, 7 M urea) which was run at 2500 V, 55°, on an LKB Macraphor Electrophoresis unit. After the gel was dried (Bio-Rad model 483 slab dryer) onto filter paper, autoradiography was conducted using Kodak X-Omat AR film at −70° without an intensifying screen. The resulting autoradiographs were scanned using an LKB Ultroscan XL laser densitometer.

EPR studies of DNA binding of spin-labeled netropsin. For the EPR measurements, sonicated ct DNA was dissolved in 0.1 × SSC buffer (15 mM NaCl, 1.5 mM sodium citrate), pH 7.0, to a final concentration of 553 μM in base pairs. The actual DNA base pair concentrations was estimated measuring absorbance at 260 nm of the relevant DNA solution and using the relationship: OD(260) = 1 corresponds to a base pair concentration of 150 μM. The effect of a salt concentration on the drug binding was evaluated from measurements in the presence of 150 mM, 15 mM and 6 mM NaCl in the buffer solutions.

Fig. 3. Typical EPR spectra after 25 hr of incubation of nitroxide-labeled netropsin with KB cells. Key: (a) nuclear fraction; and (b) cytoplasmic fraction.

Measurements of binding of SL-net to ct DNA were performed using a Bruker ER-400 EPR spectrometer operating at 9.5 GHz with 100 kHz field modulation. Samples of a total volume 0.5 to 0.6 ml were introduced into the quartz flat EPR cuvette and experiments were performed at room temperature. Spectra were recorded at the following instrumental settings: microwave power, 20 mW; modulation amplitude, 1.0 G; time constant, 0.5 sec; scan rate, 1000 sec; and the appropriate gain level. To determine the fraction of free (F) and DNA-bound (B) drug (SL-net) and to construct the Scatchard plot, the procedure described earlier by Bernier *et al.* [18] was adopted.

DNA thermal denaturation determinations. "Melting" curves were measured by using a Uvikon Kontron 810/820 spectrophotometer coupled to a Uvikon Recorder 21 and a Uvikon Thermoprinter 48. Samples were placed in a thermostatically controlled cell-holder (10 mm path length). The cuvette was heated by circulating water from a Haake unit set. The temperature inside the cuvette was monitored by using a thermocouple in contact with the solution. The absorbance at 260 nm was measured over the range 20–95° with a heating rate of 1°/min. The "melting" temperature (T_m) was taken to be the midpoint of the hyperchromic transition.

DNA viscometric determinations. Helical lengthening measurements were made by using an Ubbelohde semimicro dilution viscometer. Temperature was maintained at 20 ± 0.01° in a thermostatically controlled water bath. Flow times were electronically measured to an accuracy of 0.1 sec (Schott ABS/G type detector). Calf thymus DNA was sonicated as described by Wakelin and Waring [19]. Solutions were filtered through 0.45 μm Millipore filters before measurements. The viscometer contained 2.0 ml of a 150 μM solution of DNA. Drugs were added in increments of 5–10 μl from a stock solution (concn = 150 μM). Flow times were measured with an accuracy of 0.1 sec.

RESULTS

Penetration of spin-labeled netropsin into living KB cells

KB cells were incubated with the nitroxide-labeled lexitropsin (Fig. 2) at a concentration of 3.5×10^{-5} M for various times (45 min, 5 hr, 7.5 hr, 25 hr). Penetration of the drug into the cells proved to be smooth and progressive since a significant EPR signal was observed in the nuclear fraction after 45 min. Subsequently, EPR signals were detected in both the nuclear and cytoplasmic fractions up to 25 hr (Fig. 2). The EPR technique has proven to be an extremely sensitive and direct tool to study such small molecule–macromolecule interactions [14, 15, 18, 20].

Localization and environment

At low concentration of the drug (3.5×10^{-5} M) and after 45 min of incubation no detectable EPR signal resulted in either the cytoplasmic fraction or the cell membrane, whereas a significant signal was observed in the nuclear fraction. This indicated a fairly rapid passage through the cell membrane and cytoplasm and relatively high affinity of the drug for the nucleus. Subsequently, some binding was observed in the cytoplasm but the preferential binding in the nucleus expressed by the ratio $[\text{SL-net}]_{nucl} : [\text{SL-net}]_{cyt} \approx 3.0$ was maintained up to 25 hr. A somewhat broadened triplet EPR signal characteristic of a slightly restricted but essentially freely rotating nitroxide label [14, 15] was observed in both nuclear and cytoplasmic fractions (Fig. 3).

To determine if any reduction of the nitroxide-labeled portion of the drug had occurred in the cytoplasm, treatment with H_2O_2 and sodium phosphotungstate was performed. No additional EPR signals resulted. The rotational correlation time of the nucleus bound label, calculated as described by Ortner *et al.* [21], was determined to be $\tau = 0.15$ to 0.17 nsec. Under comparable conditions a control experiment with a spin-label alone, i.e. the ATEMPO probe, was found in equal concentrations either in the cytoplasm or in the nucleus, exhibiting a sharp triplet [14]. The results suggest a passive diffusion of the spin-label in the whole cell but, in contrast, ready uptake of the spin-labeled netropsin with preferential binding in the nuclear receptor. In addition, the survival of the nuclear-bound drug for 25 hr suggests substantial resistance to intracellular degradation.

Fig. 4. Summary histogram of the results of MPE footprinting experiments showing inhibition of DNA cleavage. Key: upper trace, SL-netropsin; and lower trace, netropsin.

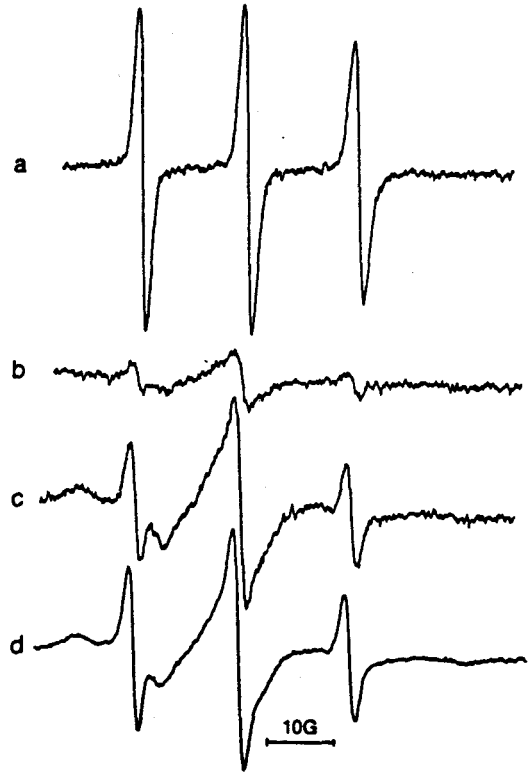

Fig. 5. EPR spectra from samples in 0.1 × SSC buffer, pH 7, containing (a) SL-net (9.8 μM); (b) SL-net (9.8 μM) and ct DNA, DNA/drug = 119; (c) SL-net (37 μM) and ct DNA, DNA/drug = 32; (d) SL-net (65 μM) and ct DNA, DNA/drug = 18. Instrumental gain conditions: (a), (b) and (c), 3.2×10^5; (d) 1.6×10^5.

Interaction of spin-labeled netropsin with purified DNAs

MPE footprinting. The protection afforded the DNA by SL-net compared with the parent netropsin was determined by MPE footprinting. The results are summarized in Fig. 4. Analysis of bases 65–165 revealed that both the degree and the location of cleavage protection by the SL-net were nearly identical to those of netropsin (Fig. 4). Both compounds yielded strong footprints (r_t 0.2) at positions 85–100 and 158–160. These bases are within the four highest affinity netropsin binding locations present in the 100 bp region studied [22].

Thermal denaturation. Thermal denaturation experiments of the spin-labeled agent with calf thymus DNA showed a $\Delta T_m = 16.5°$, indicative of a strong interaction with double helical DNA. Netropsin under comparable conditions showed a $\Delta T_m = 20.0°$. However, viscometric studies revealed no significant elongation of calf thymus DNA with the drug. This result rules out intercalative binding. Thermal denaturation of T4 DNA (in which the major groove is occluded with glucosyl moieties [23]) in the presence of the drug showed a $\Delta T_m = 17.5°$. This result confirms that the minor groove specificity of the parent netropsin (which under comparable conditions gives $\Delta T_m = 20.5°$) is maintained in the spin-labeled derivative.

Determination of binding constants of spin-labeled netropsin. EPR measurements with ct DNA were performed for DNA bp/drug ratios ranging from 5.6 to 122. Recorded EPR spectra consisted of a sharp triplet, $a_N \approx 16$ G, originating from free SL-net in solution, superimposed on a broad spectrum from DNA-bound drug molecules. Figure 5 shows examples of such spectra recorded at some selected DNA bp/drug ratios (a–0; b–119; c–32; d–18). The spectra are similar to those obtained from systems containing DNA and spin-labeled acridines [18, 24, 25]. Fractions of DNA-bound (B) and free (F) drug were estimated from EPR spectra recorded at various DNA base pair/drug ratios. Binding constant K, and number of base pairs per binding site n, were obtained from the non-linear least square best fit of the experimental data to Equation 1 (McGhee and von Hippel [26]);

$$\frac{r}{F} = K[1 - nr]\left[\frac{1 - nr}{1 - (n-1)r}\right]^{n-1} \qquad (1)$$

where r is the number of moles of compound bound per mole of DNA base pairs. The relevant Scatchard plot is shown in Fig. 6. The best fit gave $K = 3.6 \times 10^4\ M^{-1}$ and $n = 5$. These values may be compared with those reported earlier for netropsin [27] $K = 2.9 \times 10^5\ M^{-1}$ and $n = 3$.

The effects of salt concentration on the SL-net binding to ct DNA were also studied. Table 1 shows

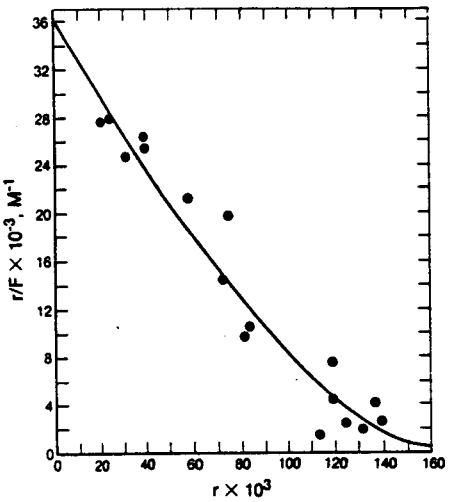

Fig. 6. Scatchard plot for binding of SL-net to sonicated ct DNA in 0.1 × SSC buffer, pH 7. Points shown are from titrations and the curve is the non-linear best fit line according to Equation 1. r is the number of moles of compound bound per mole of DNA base pair; F is the molarity of free compound.

Table 1. Effect of salt concentrations on the binding of nitroxide-labeled netropsin to calf thymus DNA

[NaCl], mM	$[B]/[F]$
6	34.6
15	23.9
150	13.1

B = bound drug; F = free drug. [SL-net] = 19 μM; DNA bp/drug = 23.

the results obtained from the EPR measurements at the DNA bp/drug ratio of 23 ([SL-net] = 19.0 μM) and at three concentrations of NaCl. It is apparent that the fraction of the DNA-bound SL-net increases as the salt concentration decreases. A similar influence of changes in ionic strength on the binding of netropsin to various DNAs was reported earlier by Luck *et al.* [27] and Wartell *et al.* [28].

DISCUSSION

The results of this study with a nitroxide spin-labeled netropsin suggest that the drug has relatively free access into living KB cells. Concentration occurs in the cell nucleus, relative to the cytoplasm. In contrast, a control nitroxide, which does not bear a DNA interactive group, diffuses to all parts of the cell equally [14]. It is reasonable to expect a higher initial concentration of SL-net in the cytoplasm than in the nucleus at some point in the uptake process. However, this was not proven because of the difficulty in obtaining early time points. The results suggest a fairly rapid passage through the cell membrane and cytoplasm. There is no evidence that the drug binds to other cellular macromolecules, e.g. a carrier protein. The results also show that the drug, whether in the cell nucleus or the cytoplasm, is relatively long-lived (i.e. up to 25 hr) and, therefore, apparently not subject to rapid intracellular degradation.

The thermal denaturation and viscosity experiments with the drug and purified calf thymus DNA confirmed strong binding, which is non-intercalative in nature, to double helical DNA. The complementary thermal denaturation experiments with T4 DNA and the labeled lexitropsin confirmed minor groove specificity as in the case of the parent antibiotic netropsin. The influence of selective groove binding to the cellular DNA was corroborated by the EPR linewidths, which were characteristic of a relatively freely-rotating, i.e. non-intercalative, interaction. It may be noted that the broad spectral components seen when the SL-net binds to purified DNA were not evident when the drug accumulated in the nucleus. This may be due to binding of the drug to other components besides DNA in the nucleus or, because of the presence of DNA proteins of chromatin, the minor groove of DNA is less accessible so that no anisotropic effect can be observed. The results of the footprinting studies confirmed that introduction of the bulky tetramethylpiperidinyloxy moiety does not alter significantly the DNA sequence specificity of SL-net compared with the parent antibiotic. This is in keeping with the view that the AAAT sequence specificity is determined principally by a combination of electrostatic interactions, bifurcated amide hydrogen bonds to the DNA bases, and van der Waals contacts with the floor of the minor groove, none of which was apparently affected by introduction of the spin-label. Similarly, the independent binding studies of SL-net to DNA, together with the salt effects, were in accord with non-intercalative binding with a significant electrostatic component. Binding of SL-net to DNA was analyzed in terms of the site exclusion method of McGhee and von Hippel [26]. The EPR study did not provide any information as to the existence of another class of binding sites, with very high binding constant ($K \sim 10^8\ M^{-1}$) as suggested earlier [27, 29]. It should be noted, however, that the strong, specific binding of netropsin to DNA occurs only at very low total drug/nucleotide ratios and could not be measured using the EPR technique employed in this study.

These results represent the first direct evidence, of which we are aware, of preferential minor groove binding of such oligopeptide antitumor antibiotics to the nucleus of living tumor cells. The results also demonstrate that lexitropsins meet many of the criteria for viable anti-sense cell regulatory probes, i.e. relative ease of access into the cell, preferential binding in the cell nucleus and acceptable intracellular stability in contrast to oligonucleotide-based probes. The implications of these results for the development of sequence specific gene probes will be reported in due course.

Acknowledgements—This research was supported by grants (to J. W. L.) from the Biotechnology Strategic Grants programme of the Natural Sciences and Engineering Research Council of Canada, the National Cancer Institute

of Canada, and Grant 1-R01CA21488-11 awarded by the National Cancer Institute, DHHS, and (to J-P. H.) from the Institut National de la Santé et de la Recherche Médicale and from the Fédération Nationale des Centres de Lutte contre le Cancer.

REFERENCES

1. Stephenson ML and Zamecnik PF, Inhibition of Rous sarcoma viral RNA translation by a specific oligodeoxyribonucleotide. *Proc Natl Acad Sci USA* **75**: 285–288, 1978.
2. Izant JG and Weintraub H, Inhibition of thymidine kinase gene expression by anti-sense RNA: A molecular approach to genetic analysis. *Cell* **36**: 1007–1015, 1984.
3. Holt, JT, Gopal TV, Moulton AD and Nieuhuis AW, Inducible production of c-fos anti-sense RNA inhibits 3T3 cell proliferation. *Proc Natl Acad Sci USA* **83**,4794–4798, 1986.
4. Helene C, Monteray-Garestier T, Saison T, Takosagi M, Toulme JJ, Asseline V, Lancelot G, Maurizot JC, Toulme F and Thuong NT, Oligodeoxynucleotides covalently linked to intercalating agents: A new class of gene regulatory substances. *Biochimie* **67**: 777–783, 1985.
5. Ts'O POP, Miller PS and Greene JJ, Nucleic acid analogs with targeted delivery as chemotherapeutic agents. In: *Development of Target-Oriented Anticancer Drugs* (Ed. Chang YC), pp. 189–206. Raven Press, New York, 1983.
6. Moser HE and Dervan PB, Sequence specific cleavage of double helical DNA by triple helix formation. *Science* **238**: 645–650, 1987.
7. Imbach J-L, Paoletti C and Lown JW, Structural conformational and biophysical properties of novel α-oligonucleotides: Potential gene control agents. *Structure and Expression*, Vol. 2, DNA and its Drug Complexes (Eds. Sarma MH and Sarma RH), pp. 181–204. Schnectady, New York, 1988.
8. Miller PS, Agris CH, Aurelian L, Blake KR, Murakami A, Reddy MP, Spitz SA and Ts'O POP, Control of ribonucleic acid function by oligonucleoside methylphosphonates. *Biochimie* **67**: 769–776, 1986.
9. Lown JW, Krowicki K, Bhat UG, Skorobogaty A, Ward B and Dabrowiak JC, Molecular recognition between oligopeptides and nucleic acids: Novel imidazole containing oligopeptides related to netropsin that exhibit altered sequence specificity. *Biochemistry* **25**: 7408–7416, 1986.
10. Kissinger K, Krowicki K, Dabrowiak JC and Lown JW, Molecular recognition between oligopeptides and nucleic acids; Monocationic imidazole lexitropsins that display enhanced GC sequence dependent DNA binding. *Biochemistry* **26**: 5590–5595, 1987.
11. Lown JW, Lexitropsins: Rational design of DNA sequence reading agents as novel anticancer agents and potential cellular probes. *Anti-Cancer Drug Design* **3**: 25–40, 1988.
12. Lee M, Krowicki K, Hartley JA, Pon RT and Lown JW, Molecular recognition between oligopeptides and nucleic acids: Influence of van der Waals contacts in determining the 3'-terminus of DNA sequences read by monocationic lexitropsins. *J Am Chem Soc* **110**: 3641–3649, 1988.
13. Lown JW and Krowicki K, Efficient total syntheses of the oligopeptide antibiotics netropsin and distamycin. *J Org Chem* **50**: 3774–3779, 1985.
14. Lemay P, Bernier J-L, Henichart J-P and Catteau J-P, subcellular distribution of nitroxide spin-labeled 9-aminoacridine in living KB cells. *Biochem Biophys Res Commun* **111**: 1074–1081, 1983.
15. Henichart J-P, Bernier J-L, Lemay P, Houssin R and Catteau J-P, Subcellular distribution of spin-labeled bithiazoles and bleomycin in living KB cells: An ESR study. *Cancer Biochem Biophys* **7**: 239–244, 1984.
16. Briere, R, Lemaire H and Rassat A, Nitroxydes XV: Synthese et etude de radicaux libres stables piperidiniques et pyrrolidinique. *Bull Soc Chim Fr* 3273–3283, 1965.
17. Maniatis T, Fritsch EF and Sambrook J, *Molecular Cloning: A Laboratory Manual*. Cold Spring Harbor Laboratory, Cold Spring Harbor, New York, 1982.
18. Bernier JL, Henichart J-P and Catteau J-P, ESR study of intercalation: Quantitative evaluation of drug-DNA binding through competition with a spin-labeled 9-aminoacridine. *Anal Biochem* **117**: 12–17, 1981.
19. Wakelin LPG and Waring MJ, The binding of echinomycin to DNA. *Biochem J* **157**: 721–740, 1976.
20. Houssin R, Bernier J-L and Henichart J-P, Synthesis of some spin-labeled bithiazoles, useful probes for studying bleomycin-DNA binding. *J Heterocyclic Chem* **21**: 465–469, 1984.
21. Ortner MJ, Turek N and Chignell, CF, Spectroscopic studies of rat mast cells, mouse mastocytoma cells, and compound 48/80-I. *Biochem Pharmacol* **30**: 277–282, 1981.
22. Ward B, Rehfuss R and Dabrowiak JC, Quantitative footprinting analysis of the netrospin–DNA interaction. *J Biomol Struct Dyn* **4**: 685–695, 1987.
23. Erikson RL and Szybalski W, The Cs_2SO_4 equilibrium density gradient and its application for the study of T-even phage DNA: Glucosylation and replication. *Virology* **22**: 111–124, 1964.
24. Henichart JP, Bernier JL and Catteau JP, Interaction of 4(9-acridinylamino)aniline and derivatives with DNA. *Hoppe-Seylers Z Physiol Chem* **363**: 835–841, 1982.
25. Sinha BK and Chignel CF, Acridine spin labels as probes for nucleic acids. *Life Sci* **17**: 1829–1836, 1975.
26. McGhee JD and von Hippel PH, Theoretical aspects of DNA-protein interactions: Cooperative and non-cooperative binding of large ligands to a one-dimensional homogeneous lattice. *J Mol Biol* **86**: 469–489, 1974.
27. Luck G, Triebel H, Warring M and Zimmer Ch, Conformation dependent binding of netropsin and distamycin to DNA and DNA model polymers. *Nucleic Acids Res* **1**: 503–530, 1974.
28. Wartell RM, Larson JE and Wells RD, Netropsin, specific probe for A-T regions of duplex deoxyribonucleic acids. *J Biol Chem* **249**: 6719–6731, 1974.
29. Zimmer Ch, Reinert KE, Luck G, Wähnert V, Löber G and Thrum H, Interaction of the oligopeptide antibiotics netropsin and distamycin A with nucleic acids. *J Mol Biol* **58**: 329–348, 1971.

Compte tenu de la facilité de l'acridine, d'une part, et de la nétropsine, d'autre part, à pénétrer dans la cellule et à se concentrer dans le compartiment nucléaire, il semblait dès lors tout à fait intéressant de poursuivre une étude semblable avec les hybrides. Là encore, le composé II (NETGA) a été pris en référence.

Afin de suivre le cheminement de ce composé dans la cellule, un marqueur de spin a été greffé sur l'extrémité amino-terminale de NETGA. Le composé synthétisé (**SL-NETGA**, SL pour "Spin Label") constitue un traceur stable (sauf en présence d'un réducteur).

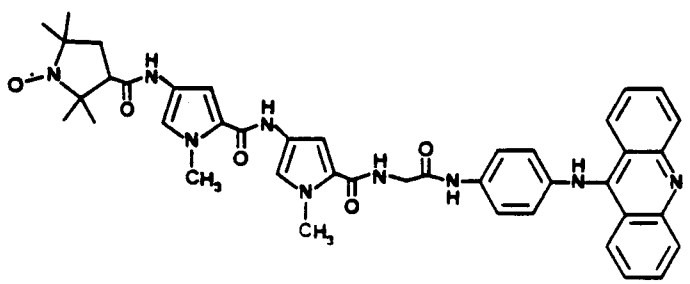

SL-NETGA

A partir d'une culture de cellules KB3 en suspension, incubées en présence du composé SL-NETGA (concentration finale 100 µM), des prélèvements réguliers sont effectués. Les cellules sont soumises à un fractionnement noyau-cytoplasme (protocole détaillé dans l'article n°4). L'intensité du signal de RPE retrouvé sur chacune des deux fractions est comparée à celle du signal initial (au temps "zéro"). Les spectres obtenus sont représentés Figure 11. Pour chacun de ces spectres, deux paramètres sont à considérer :

1. la surface des pics, proportionnelle à la quantité de produits. Cette analyse nous renseigne sur l'abondance relative en SL-NETGA sur l'une ou l'autre des fractions (Figure 11).

2. l'allure du spectre, témoin des contraintes subies par le nitroxyde dans son environnement immédiat donc de la position du marqueur.

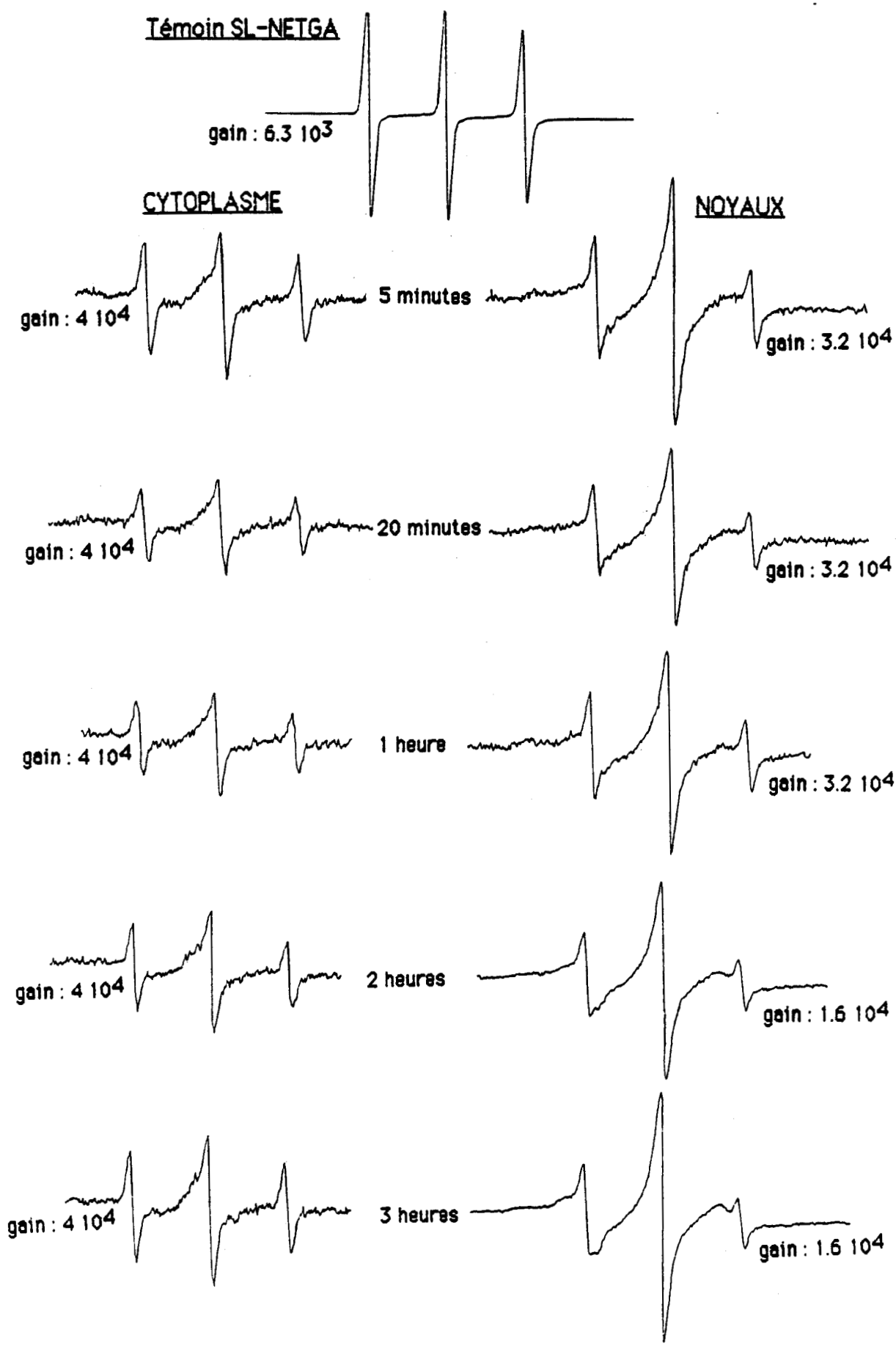

Figure 11 : Spectres de RPE du composé SL-NETGA. Cinétique d'incorporation nucléaire et cytoplasmique.

Lorsque la libre rotation du nitroxyde n'est pas perturbée, le spectre obtenu a l'allure d'un triplet constitué de raies fines d'intensité égale avec une constante de couplage de 16 Gauss (spectre isotrope). Au contraire lorsque le nitroxyde est enchâssé dans une structure moléculaire (ADN, membrane, protéine...), la vitesse de rotation du groupement portant le nitroxyde diminue, ceci se traduit par un spectre d'allure anisotrope. La mesure du temps de corrélation rotationnelle (τ) permet d'apprécier le degré de liberté (ou d'encombrement) du nitroxyde.

Sur chacun des spectres de la Figure 11 le facteur τ a été mesuré selon deux méthodes :

$$\tau_1 = 5{,}47\ 10^{-10}\ W_0\ [(h_0/h_{-1})^{1/2} + (h_0/h_{+1})^{1/2} - 2] \qquad \text{(sec)} \quad \text{(BOBST, 1979)}$$

$$\tau_2 = 6{,}5\ 10^{-10}\ \Delta H_0 [(h_0/h_{+1})^{1/2} - 1] \qquad \text{(sec)} \quad \text{(ORTNER, 1981)}$$

h_{-1}, h_0 et h_{+1} (en unité arbitraire) correspondent à l'intensité relative de chacun des pics du spectre de RPE. W_0 et ΔH_0 (en Gauss) correspondent respectivement à la largeur du pic médian à mi-hauteur et à la séparation pic-à-pic du pic central (constante de couplage).

Les mesures sont regroupées dans le tableau II.

Remarque : Ces deux modes d'évaluation du paramètre τ sont des simplifications d'une équation complexe faisant intervenir des termes linéaires et quadratiques (STONE et al., 1965).

Ces différents résultats amènent aux conclusions suivantes :

1_ Le composé NETGA possède un tropisme nucléaire trés marqué. Après 3 heures d'incubation, 35% du signal de départ est retrouvé dans la fraction nucléaire alors que le cytoplasme ne renferme que 8% du signal initial. (Remarque : ces proportions ne sont absolument pas extrapolables en terme de concentration). La pénétration cellulaire est trés rapide. L'allure de la courbe obtenue diffère de celle observée pour les deux substances modèles Nt et acridine (Figure 12).

Si l'accumulation nucléaire de l'acridine semblait répondre à un phénomène atteignant trés rapidement un maximum, celle de NETGA semble moins rapide. En

SL-NETGA : Temps de Corrélation (τ nsec.)

	Temps	τ_1	$\Delta\tau_1$	τ_2	$\Delta\tau_2$
Témoin	—	0,20	—	0,15	—
Cytoplasme	5 min.	0,39	0,19	0,30	0,15
	20 min.	0,44	0,24	0,39	0,24
	1 h.	0,47	0,27	0,35	0,20
	2 h.	0,49	0,29	0,40	0,25
	3 h.	0,42	0,22	0,34	0,19
Noyaux	5 min.	1,38	1,18	1,06	0,91
	20 min.	1,26	1,06	1,04	0,89
	1 h.	1,17	0,97	0,90	0,75
	2 h.	1,67	1,47	1,36	1,21
	3 h.	2,29	2,09	1,67	1,52

$\Delta\tau_1 = \tau_1 - 0.20$ $\Delta\tau_2 = \tau_2 - 0.15$

A

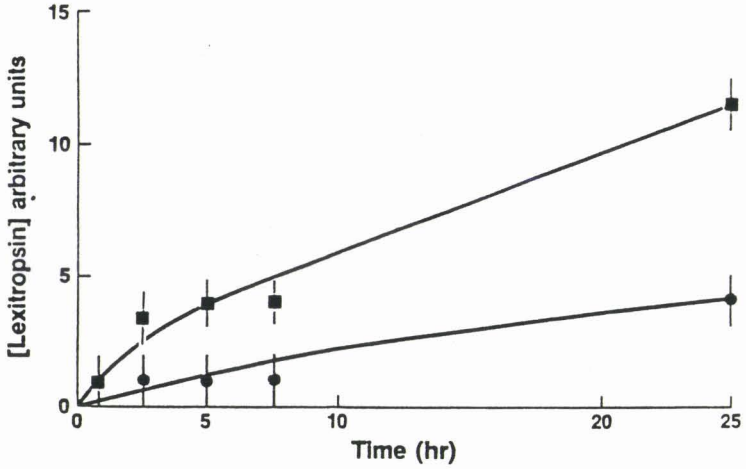

B

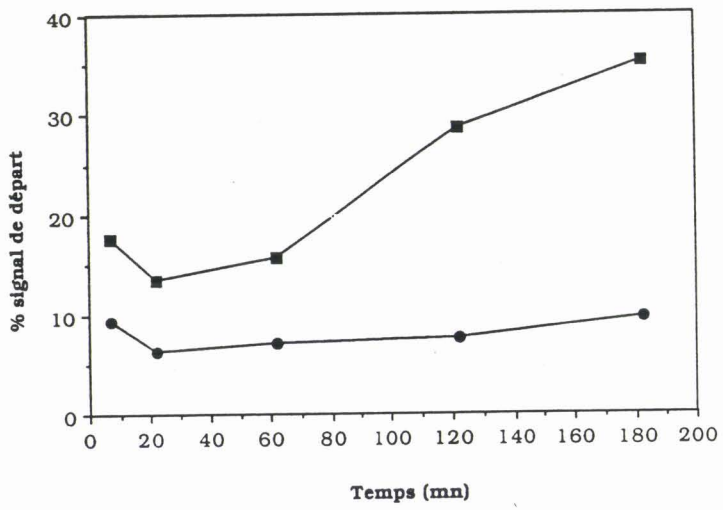

C

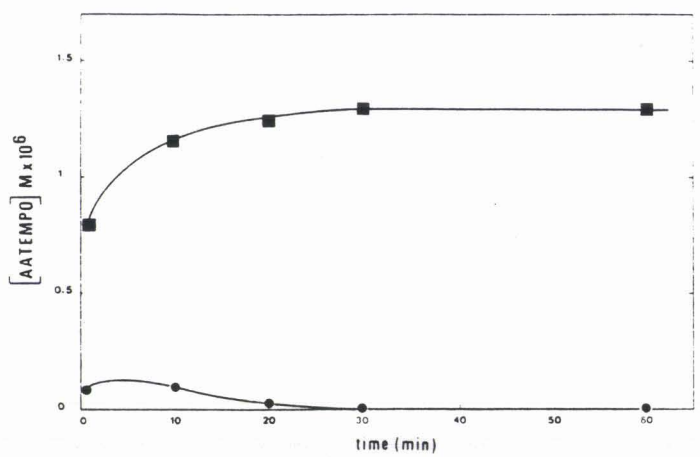

Figure 12 : Cinétique d'incorporation de la nétropsine (A), de NETGA (B) et de l'aminoacridine (C), (■) noyaux, (●) cytoplasmes.

fait, le mode de pénétration semble obéir à une cinétique intermédiaire entre celle de l'amino-9 acridine et le processus lentement évolutif observé avec la Nt (Figure 12).

2_ Sans être catégorique, on peut toutefois avancer l'hypothèse d'une fixation du composé SL-NETGA sur l'ADN (en culture). En effet au fur et à mesure de la cinétique, le spectre de la fraction nucléaire apparaît de plus en plus "bloqué" (anisotrope) comme l'indiquent les temps de corrélation τ_1 et τ_2 (ou $\Delta\tau_1$ et $\Delta\tau_2$). La libre rotation du nitroxyde dans le noyau est sévèrement ralentie ; la fixation sur l'ADN en est très probablement la cause.

Le coefficient τ mesuré au niveau cytoplasmique est légèrement plus important que celui du témoin. Une adsorption membranaire de NETGA n'est donc pas à exclure (la fraction cytoplasmique renferme le système membranaire réticulo-endothélial).

Cette étude préliminaire fournit des renseignements très intéressants, en parfait accord avec les propriétés d'inhibition de synthèse d'ADN et d'inhibition de la prolifération cellulaire observée avec le composé II(NETGA) (article n°2).

Néanmoins, ce premier essai demande à être réexaminé d'une façon légèrement différente :

- en augmentant les temps d'incubation de façon à observer la saturation du transport cellulaire de NETGA.
- en ajoutant avant chaque mesure par RPE un mélange oxydant (H_2O_2-tungstate de sodium) afin de tenir compte de la fraction de marqueur ayant pu être réduite dans le milieu intracellulaire.
- en isolant l'ADN pour vérifier qu'il constitue bien la cible du composé.

Comme il a été décrit dans l'article n°2, les quatre composés hybrides présentent une activité antitumorale "in vitro" non négligeable puisque voisine de celle observée pour le témoin amsacrine, médicament antileucémique de référence. Des doses de 0.5 à 8 µM de ces composés suffisent à inhiber la croissance de 50% des cellules leucémiques en culture (souche L 1210) après 24 heures d'incubation seulement. Ce test rapide, bien que révélateur de l'efficacité des produits, ne peut toutefois constituer à lui seul la preuve d'une activité anticancéreuse.

Une étude cellulaire plus précise a été réalisée sur le composé NETGA .

2 Mesure de l'activité inhibitrice de la prolifération des cellules cancéreuses MCF7.

*courbe de croissance.

Les cellules MCF 7 sont des effusions pleurales (métastases) de tumeur mammaire. L'incubation de ces cellules en présence de doses variables de NETGA (Figure 13) permet de confirmer le pouvoir cytostatique de ce composé.

Il est intéressant de noter qu'aux doses de 20 µM et surtout 40 µM, les cellules traitées présentent une hyperplasie très marquée, signe d'une souffrance cellulaire. La taille des cellules traitées (50 à 55 µm) est deux fois supérieure à celle des cellules témoin (25 à 30 µm) (Figure 14). Certaines de ces cellules sont bi- voir tri-nucléées. L'apparition de telles cellules géantes peut être due à la fusion de deux cellules d'une part, ou plus certainement, d'autre part, à des endomitoses c'est-à-dire à une multiplication cellulaire sans division de la membrane externe (l'étude cinématique de ce phénomène devrait nous permettre de mettre en évidence l'un ou l'autre des deux processus). Un tel phénomène a également été observé avec les composés I, III et IV aussi bien sur des cellules MCF 7 que sur des cellules leucémiques L 1210.

* courbe de survie.

La Figure 15 résume les résultats obtenus avec le dérivé NETGA (composé II) et son homologue : le composé I qui ne comporte qu'un seul cycle pyrrole au lieu de deux dans NETGA. Pour le composé I la LD_{50} est de 10 µM, légèrement supérieure à celle de l'amsacrine (LD_{50} = 3-4 µM) qui sert de référence. Par contre pour NETGA, le premier essai effectué est très positif puisque la LD_{50} est de 5 µM, donc comparable à celle de l'amsacrine. De plus l'activité antitumorale de NETGA se révèle très importante à des concentrations de l'ordre de 10 à 20 µM où le pourcentage de clonage des cellules MCF 7 est réduit à moins de 1 %. NETGA semble donc doué de propriétés cytotoxiques très marquées. Ce premier test positif nécessite toutefois une confirmation (en cours) mais d'ores et déjà l'étude de l'activité antitumorale de ce composé sur un modèle animal (la souris) a débuté en collaboration avec Monsieur le Docteur B. HECQUET (Centre Anticancéreux Oscar Lambret, Lille).

Remarque : La mesure de cette activité pharmacologique in vitro a été réalisée par Madame le Docteur M. Collyn-d'Hooghe, INSERM Unité 124, Lille.

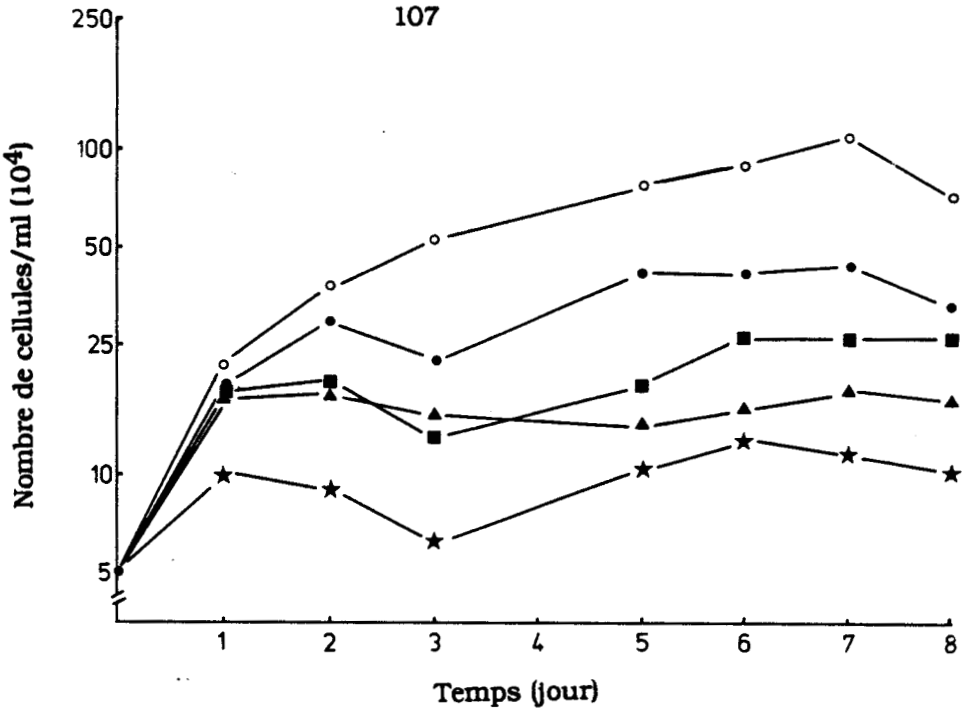

Figure 13 : Courbes d'inhibition de croissance des cellules MCF 7 en présence de concentrations variables de NETGA. (○) témoin, (●) 5µM, (■) 10µM, (▲) 20µM, (★) 40µM.

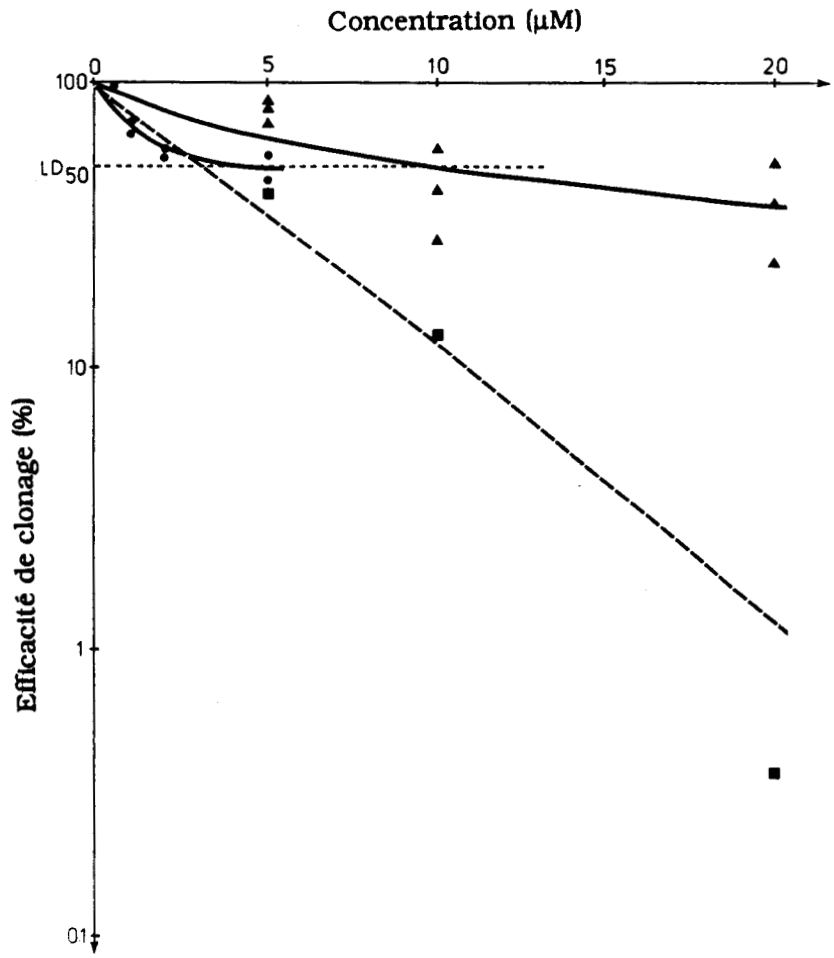

Figure 15 : Courbes dose-survie des cellules MCF 7 traitées par des concentrations variables d'amsacrine (●), du composé I (▲) et de NETGA (■). (--- essai effectué une seule fois, à confirmer).

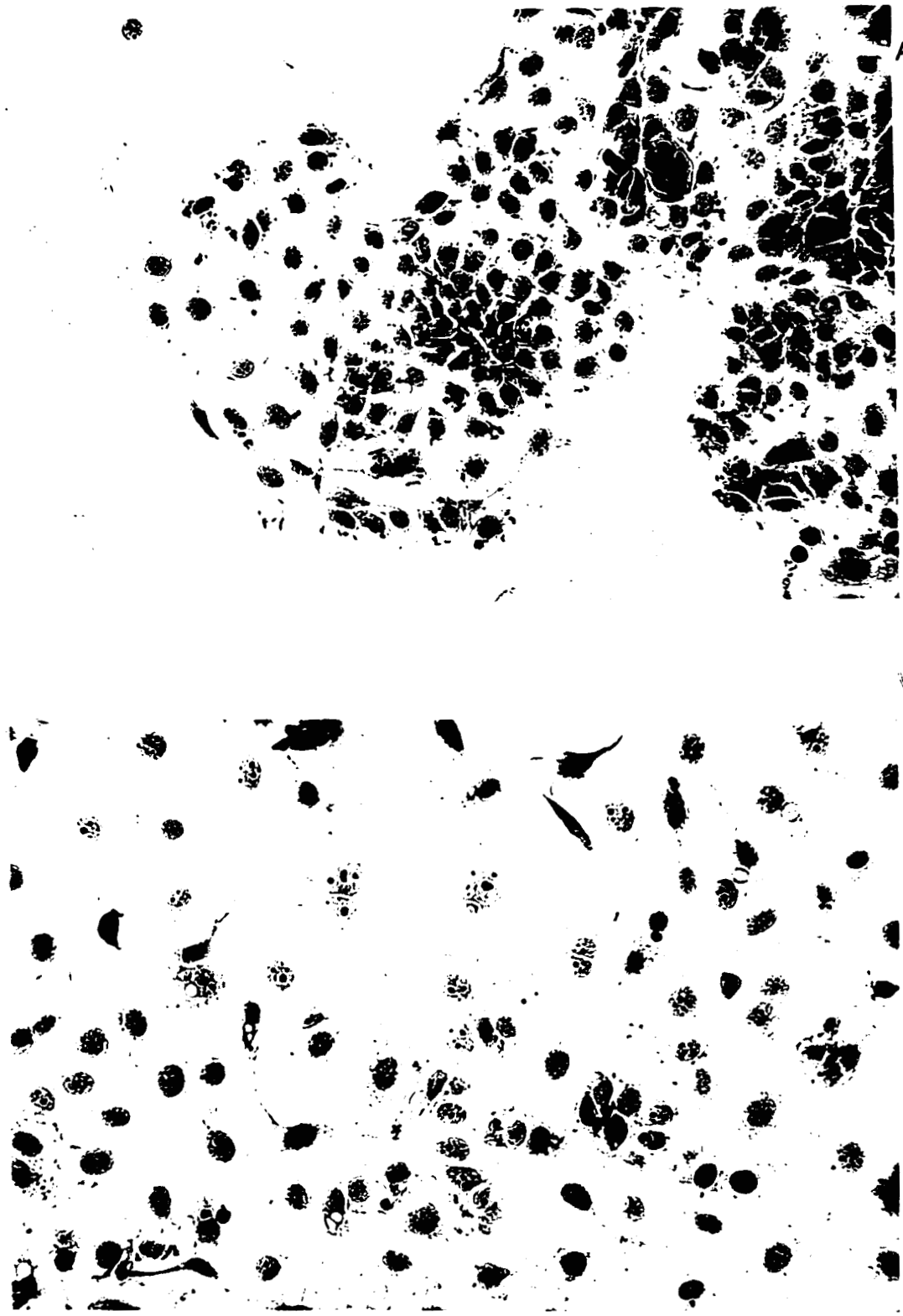

Figure 14 : Cellules MCF 7 saines (A) et traitées par 20 µM de NETGA (B). Hyperplasie cellulaire (⟶) cellules binucléées.

3°) Dérivé bithiazolique de la nétropsine.

Sur le même principe que précédemment, un autre type de système hétérocyclique intercalant a été considéré : le noyau bithiazolique. Ce chromophore constitue le point d'ancrage sur l'ADN d'une autre substance anticancéreuse, la bléomycine (chapitre II). Une étude réalisée au laboratoire (HENICHART et al., 1985b) a montré que le bithiazole n'est pas un intercalant vrai comme l'acridine.

Différents critères physicochimiques ont permis de conclure à une insertion d'un des cycles thiazole entre les paires de bases de l'ADN sans un recouvrement total de ces bases par ce chromophore (Figure 16).

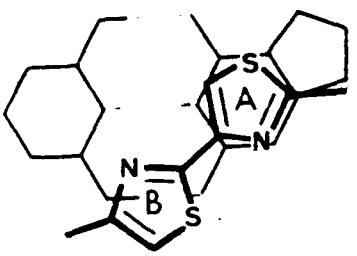

Figure 16 : Mode de recouvrement d'une paire de base de l'ADN par la fraction bithiazolique de la bléomycine.

Ce mode particulier d'insertion du bithiazole dans un kink (une cassure) de l'ADN nous a incité à concevoir un autre modèle (**NETBI** pour **Né**tropsine-**Bi**thiazole, Figure 17) hybride répondant au concept "Ligand du petit sillon-Intercalant" fixé initialement. La synthèse et l'étude complète du mode de liaison de ce composé à l'ADN ont fait l'objet d'une publication précédemment citée (article n°3).

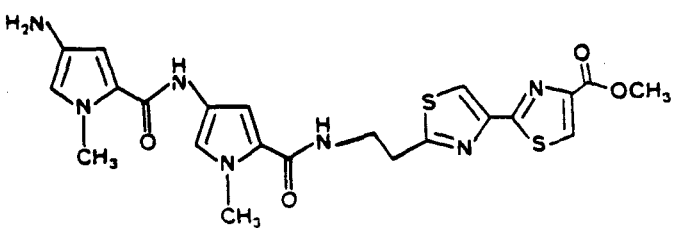

NETBI

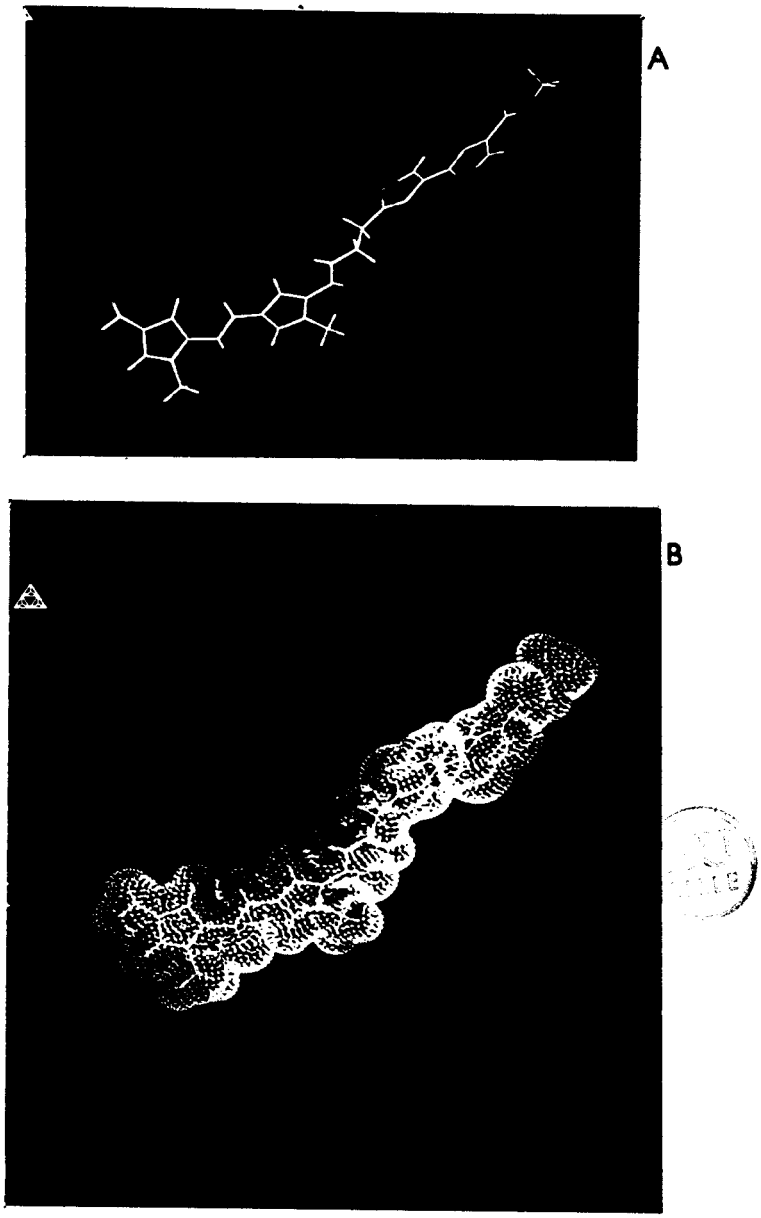

Les différentes couleurs de la surface moléculaire représentent les potentiels électrostatiques (V en kcal/mol) en un point de l'espace. Le code des couleurs est le suivant (WEINER et al., 1982) :

Blanc	V < -24.90	Vert	0.00 < V < 3.32
Pourpre	-24.90 < V < -9.96	Jaune	3.32 < V < 9.96
Bleu ciel	-9.96 < V < -3.32	Orange	9.96 < V < 24.90
Bleu marine	-3.32 < V < 0.00	Rouge	24.90 < V

Figure 17 : (A) conformation et (B) représentation du volume moléculaire et des potentiels électrostatiques de NETBI.

Ce ligand se fixe dans le petit sillon de l'ADN par sa fraction Nt et sa fraction bithiazolique sans aucune intercalation. Le mode de liaison de NETBI à l'ADN semble identique à celui de la Nt; d'ailleurs NETBI induit, comme la Nt, une réversion du conformère Z vers la forme B lors de sa fixation à l'ADN (poly(dGC)-(dGC)). Ce résultat ressort d'une étude par dichroïsme circulaire actuellement en cours. La mise en évidence d'un site de fixation de taille relativement importante (6-8 bases) d'une part, et spécifique d'autre part (séquence AAATCT), ouvre la voie vers la conception d'une nouvelle série chimique de composés analogues à NETBI (étude en cours en collaboration avec le Professeur J-L. Imbach, Université de Montpellier). A ce stade, l'approche rationnelle entreprise pour la conception de molécules capables de se lier sélectivement à l'ADN est positive.

Toutefois si ce composé s'est révélé tout à fait intéressant sur le plan physicochimique, aucune activité antitumorale n'a pu être mise en évidence d'où la nécessité d'élaborer de nouveaux composés plus actifs.

L'inactivité de ce dérivé s'explique en terme d'inaptitude à pénétrer dans la cellule et plus particulièrement à atteindre sa cible, l'ADN. En effet l'étude en RPE de la distribution cellulaire du composé SL-NETBI c'est-à-dire l'analogue marqué par un nitroxyde du composé NETBI (Figure 18a), indique qu'après 3 heures d'incubation cellulaire seulement 3 à 4% du signal initial sont retrouvés dans le cytoplasme et 2% dans les noyaux (Figure 18b). De plus les signaux observés sont du type isotrope laissant suggérer une trés faible fixation sur l'ADN (Figure 18c).

Des modifications chimiques permettant à ce produit d'atteindre plus rapidement et plus facilement l'ADN sont certainement à envisager.

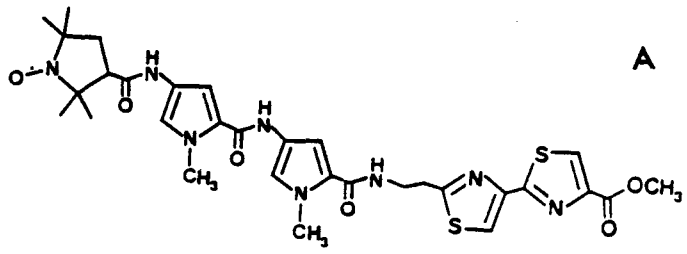

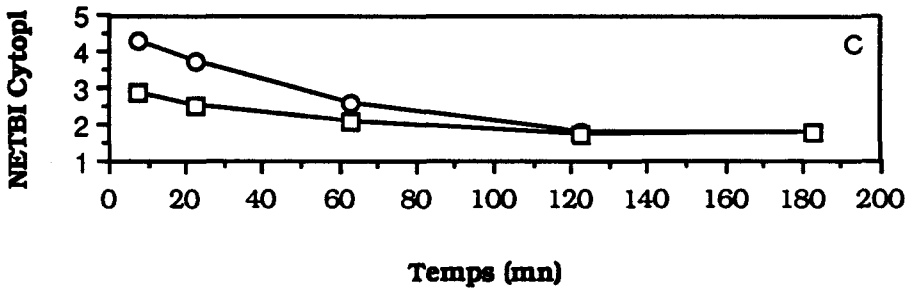

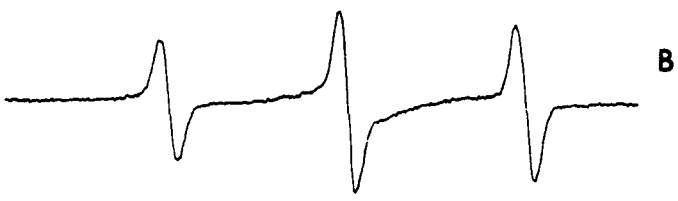

Figure 18 : Structure du composé SL-NETBI (A), spectre de RPE de SL-NETBI (B) : fraction nucléaire aprés 3 heures d'incubation, cinétique d'incorporation de SL-NETBI dans les cellules KB (C), (□) noyaux, (○) cytoplasmes.

Conclusion

L'élaboration de composés antitumoraux telle qu'elle a été entreprise en visant une fixation puissante et spécifique sur l'ADN s'est avérée intéressante et prometteuse. Concernant l'ADN, le but recherché est parfois atteint (à l'exception des dérivés aminoalkylthiazoliques de la Nt). Le concept "Peptide à liaison spécifique-Intercalant" a été clairement défini et peut déboucher sur des composés actifs. Le composé II (NETGA) en est un exemple attrayant. De l'étude physicochimique et pharmacologique de ce composé, deux résultats essentiels émergent :

-la fraction nétropsine impose à l'ensemble de la molécule sa fixation primaire dans le petit sillon de l'ADN.

-la fraction acridine permet une meilleure entrée dans la cellule et une concentration du produit au niveau nucléaire.

Les deux fractions de ce modèle sont donc parfaitement complémentaires.

La stratégie "Ligand à liaison spécifique-Intercalant" fait l'objet de nombreux travaux. Outre ces ligands et les composés naturels du type actinomycine ou triostine-échinomycine, une large classe de composés synthétiques, les oligonucléotides liés à un intercalant, entre dans ce concept. Beaucoup plus affines pour l'ARN principalement ou l'ADN (il y a alors formation d'une triple hélice), du fait même de leur nature pseudo-oligo(désoxy)nucléotidique que les dérivés cités, ces composés, stériquement trés encombrants, pénètrent mal dans la cellule. De nombreuses pharmacomodulations ont été envisagées pour améliorer leur stabilité, leur pénétration et leur distribution cellulaires (HELENE & THUONG, 1986).

Il est intéressant de constater que plusieurs stratégies sont mises en oeuvre dans un même but. La diversité chimique des moyens utilisés devrait permettre dans un proche avenir d'aboutir à des substances antimitotiques, antivirales ou antiparasitaires.

Cependant de telles molécules hautement sélectives n'ont pas de potentialités "ADN-toxiques" ; leur liaison à l'ADN est, bien que puissante, réversible, donc susceptible d'être détruite in vivo. Aussi s'oriente t-on vers la conception de substances susceptibles de dégrader physiquement l'ADN suite à une liaison spécifique. Là encore plusieurs stratégies sont employées dans différents groupes. Les modifications de la structure primaire de l'ADN peuvent être apportées par différents systèmes : alkylant,

un groupement photoactivable ou encore par un système de production de radicaux libres oxygénés, généralement un système chélateur de métaux.

Nous nous sommes plus particulièrement intéressés aux systèmes chélateurs. Dans cette catégorie, différents agents sont disponibles : l'EDTA, la phénanthroline ou des dérivés porphyriniques par exemple. Partant toujours d'un modèle naturel, notre attention s'est focalisée sur la bléomycine, médicament antitumoral largement utilisé en clinique.

CHAPITRE II.

LE MODELE NATUREL BLEOMYCINE.

I. Bléomycine : généralités.

1°) Isolement et structure.

La bléomycine (Blm) est un antibiotique anticancéreux isolé de *Streptomyces verticillus*. Près d'une dizaine de composés de structure très voisine (différents selon la nature d'une chaîne latérale) (Figure 19) sont en fait regroupés sous l'appellation bléomycine. Si tous possèdent la propriété de complexer les métaux, leur activité et leur toxicité varient. La bléomycine A_2 représente la forme la plus active, mais c'est un mélange reconstitué et bien défini (60 à 70% de Blm-A_2, 25 à 30 % de Blm-B_2 et 5 à 10 % des autres bléomycines A_5, B_4, B_6 dont la toxicité rénale est plus forte mais permettant d'obtenir une synergie d'action) qui est utilisé couramment en clinique en Europe et aux Etats Unis (Blénoxane®). En Union Soviétique et en Chine, le mélange utilisé contient majoritairement la Blm-A_5 (SEBTI & LAZO, 1988).

La structure de la bléomycine peut être décomposée en quatre fragments :

_ un fragment pseudopeptidique : responsable de la complexation d'ions métalliques. Les ions Fe(II et III), Co(II et III) et Cu(I et II) donnent les complexes les plus actifs biologiquement. La complexation d'autres métaux de transition (Mn(II), Ni(II), Zn(II)) ou émetteurs de rayons γ (^{193}Hg, ^{203}Pb, ^{99}Tc, ^{57}Co) utilisés pour le radiodiagnostic des tumeurs est également possible (RASKER et al., 1975).

_ un fragment disaccharidique : ((O-carbamoyl-3-α-D-mannopyrannosyl)-0-2-L-gulopyrannose). Son implication dans la stabilisation du complexe et l'activation de l'oxygène moléculaire a fait l'objet d'une étude très poussée au laboratoire (KENANI et al., 1988a, 1988b); ces résultats seront considérés ultérieurement.

_ un noyau bithiazolique : assure l'ancrage de l'antibiotique à l'ADN. La fixation à l'ADN de la Blm par l'intermédiaire de ce bithiazole a fait l'objet de nombreux travaux qui seront discutés plus loin.

_ une amine terminale : de nature variable selon les différentes Blm. Les différences concernant l'intensité de liaison à l'ADN, la toxicité, l'activité antitumorale et la pharmacocinétique des diverses Blm reposent uniquement sur la structure de cette fraction terminale.

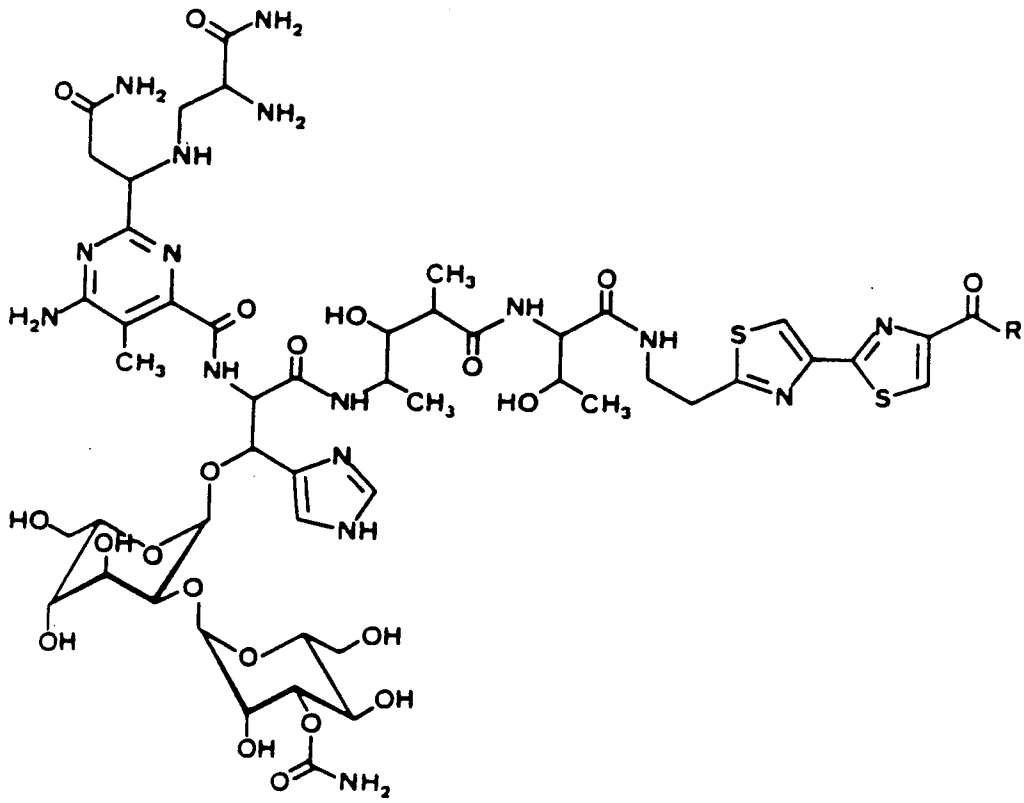

R	Blm
OH	acide blèomycinique
$NH(CH_2)_3S^+(CH_3)_2$	A_2
$NH(CH_2)_3NH(CH_2)_4NH_2$	A_5
$NH(CH_2)_3NH(CH_2)_4NH(CH_2)_3NH_2$	A_6
NH_2	B'_1
$NH(CH_2)_4NH\,C(=NH)NH_2$	B_2
$NH(CH_2)_4NH\,C(=NH)NH(CH_2)_4NH\,C(=NH)NH_2$	B_4

Figure 19 : Structure de la bléomycine.

2°) Liaison à l'ADN.

L'interaction Blm-ADN a initialement été analysée par différentes techniques incluant la RMN et le quenching de fluorescence (CHIEN et al., 1977), la dialyse à l'équilibre (POVIRK et al., 1979) et le dichroïsme circulaire (KRUEGER et al., 1973). De ces travaux, il est ressorti que le bithiazole et l'amine terminale étaient directement impliqués dans cette liaison. D'ailleurs le tripeptide S, fragment d'hydrolyse contenant la structure bithiazolique, se fixe à l'ADN dans les conditions et avec une affinité identiques à celles observées lors de l'interaction Blm-ADN (CHIEN et al., 1977; TAKESHITA et al., 1978; LIN & GROLLMAN, 1981).

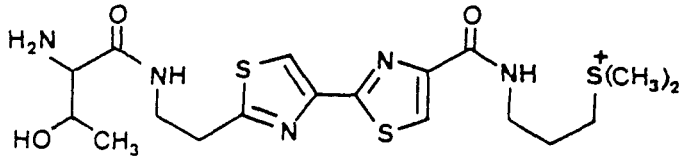

Structure du tripeptide S

Dès lors, la mise en cause de tout autre fragment : pseudopeptide ou glycanne a été exclue. Cependant l'intervention de la partie complexante, en particulier le résidu β-aminoalanine, dans la liaison à l'ADN avait été avancée en 1984 (ALBERTINI & GARNIER-SUILLEROT, 1984). De plus une étude récente tend à prouver que le centre métallique du complexe Blm-Cu(II) joue un rôle direct dans la détermination de la nature de l'interaction Blm-ADN (LEVY & HECHT, 1988).

a) Mode de liaison.

L'établissement d'une liaison électrostatique entre le groupement cationique terminal de la Blm et les groupements phosphate de l'ADN est nécessaire à la formation rapide du complexe et à sa stabilisation (KASAI et al., 1978). Malgré

l'inactivité de l'acide bléomycinique (R=OH), la capacité de la bléomycine B_1' (R=NH_2) (Figure 19) à dégrader l'ADN prouve que cette liaison saline n'est pas absolument indispensable à la liaison. La structure de cette amine terminale (plus que sa charge électrique) conditionne aussi bien la vitesse et la nature des coupures de l'ADN observées (HUANG et al., 1981) que l'intensité de l'activité antitumorale de la Blm ou même sa toxicité en particulier l'"indice de fibrose pulmonaire" (RAISFELD, 1981)

L'étude du mécanisme de liaison de l'enchaînement bithiazolique à l'ADN a fait l'objet de nombreux travaux parfois contradictoires. Divers mécanismes ont été proposés :

_ L'intercalation du bithiazole entre deux plateaux de paires de bases fut initialement proposée compte tenu de la coplanéité du système (KOYAMA et al., 1968). Ultérieurement des calculs théoriques (MURAKAMI et al., 1976) et des expériences physicochimiques (TAKESHITA et al., 1978) ont supporté cette hypothèse. Cependant certains critères physicochimiques requis pour conclure à l'intercalation n'étaient pas observés. Par exemple si la Blm est capable de relâcher les superhélices d'un ADN superenroulé, à forte concentration un superenroulement dans le sens opposé n'est pas observé. De la même façon, l'étude par RMN de l'interaction Blm-poly(dA-dT)$_2$ est en défaveur de l'intercalation (CHEN et al., 1980; GLICKSON et al., 1981).

Enfin, l'emploi d'analogues synthétiques de la partie bithiazolique a montré que le recouvrement des deux bases appariées n'a lieu qu'avec un analogue trithiazolique (SAKAI et al., 1982) ou un dérivé de structure triazolothiazolylthiazole (PETT, HOUSSIN et al., 1986) pour lequel le nuage d'électrons π du bithiazole est étendu permettant ainsi un meilleur recouvrement des paires de bases.

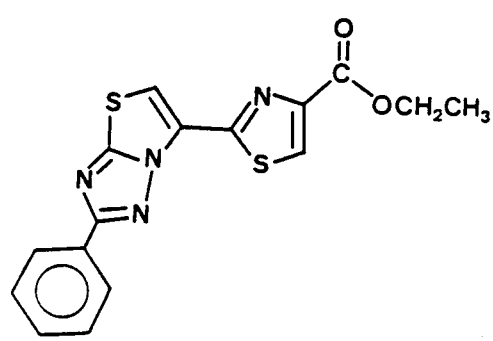

Structure du composé PETT

L'intercalation ne semble donc pas correspondre au mécanisme exact d'interaction.

_ La fixation du bithiazole dans le petit sillon de l'ADN comme pour la nétropsine fut ensuite proposée par KROSS et al. (1982). Là encore l'hypothèse fut contestée, notamment du fait de la faible aptitude de la Blm à stabiliser un duplex d'ADN (la Blm et la Nt donnent respectivement un ΔTm de 4°C et de 15°C avec l'ADN de thymus de veau).
_ En 1983, une intercalation partielle d'un seul thiazole fut avancée (BOOTH et al., 1983 ; SAKAI et al., 1983). Ce problème fut réexaminé au laboratoire en utilisant des analogues du bithiazole (HOUSSIN et al., 1984a, 1984b). Un mode de liaison à l'ADN original fut proposé : l'insertion d'un seul thiazole dans un kink (un plissement, une pliure) de l'ADN. Seul ce mécanisme permet d'expliquer le raccourcissement de bâtonnets d'ADN observé par viscosimétrie en présence de Blm (HENICHART et al., 1985b). Un tel phénomène est également observé avec des peptides contenant des hétérocycles (GABBAY et al., 1976a, 1976b). Dernièrement le mécanisme d'intercalation classique du bithiazole a été néanmoins avancé de nouveau (FISHER et al., 1985; MILLER et al., 1985).

Seule l'étude par diffraction de rayons X du complexe Blm-ADN permettra de lever l'ambigüité quant au mode de liaison. Des cristaux de ce complexe utilisables en radiocristallographie n'ont jusqu'à présent jamais été obtenus. L'aptitude de la Blm à dégrader l'ADN est sans doute la cause de cet échec.

b) Coupure d'ADN.

La présence au sein d'une même molécule d'un fragment apte à se fixer à l'ADN et d'un fragment capable de chélater des métaux et produire des radicaux libres oxygénés permet d'expliquer la capacité de la Blm à induire des coupures d'ADN. Du fait de l'ancrage de la Blm à l'ADN par le bithiazole et l'amine terminale, les espèces réactives (O_2^{-} et OH·) générées par le complexe métallique (SUGIURA & KIKUCHI, 1978) se trouvent à proximité du désoxyribose.

Le complexe ferreux est de loin le plus actif. Le complexe ferrique peut, également après réduction enzymatique in vivo, dégrader l'ADN (MAHMUTOGLU et al., 1987; STREKOWSKI et al., 1988b).Les complexes cuivrique et cuivreux, considérés comme les formes de transport sanguin et de résistance aux enzymes protéolytiques (SUGIURA et al., 1979), sont peu actifs (EHRENFELD et al., 1985, 1987), voire inactifs (SUZUKI et al., 1985).

Le mécanisme de coupure oxydative de l'ADN par le complexe ferreux fait intervenir l'oxygène (SAUSVILLE et al., 1978a, 1978b). Le complexe ternaire O_2-Fe(II)-Blm, encore appelé Blm-activée (BURGER et al., 1981, 1982; KURAMOCHI et al., 1981), dégrade totalement l'ADN en un mélange de bases libres, de bases-propénal et d'oligonucléotides possédant une extrémité phosphate glycolique en 3' (WU et al., 1983, WU & KOZARICH, 1985). Le mécanisme moléculaire et les produits de dégradation ont fait l'objet de nombreux travaux (HAIDLE, 1971; GILONI et al., 1981; BURGER et al., 1982;WU et al., 1983; AJMERA et al., 1986; BURGER et al., 1986; STUBBE & KOZARICH, 1987; SUGIYAMA et al., 1986). Les produits de dégradation du désoxyribose porteur du groupe propénal sont utilisés pour la détection et le dosage par colorimétrie de la dégradation de l'ADN, spécifique de la Blm (BURGER et al., 1980; SAUSVILLE et al., 1978b).

Les bases-propénal libérées in vivo sont hautement toxiques et laissent supposer qu'elles sont les éléments responsables des propriétés cytotoxiques de la Blm (GROLLMAN et al., 1985).

La photooxydation du complexe cobaltique de la Blm en absence d'oxygène induit également des coupures d'ADN avec libération d'oligonucléotides possédant une extrémité phosphoglycolate-3' mais sans formation de "bases propénal" (CHANG & MEARES, 1982, 1984). Le complexe manganique peut également dégrader l'ADN (BURGER et al., 1984).

Il est à noter que le désoxyribose est une cible spécifique de la Blm. En effet en présence d'un hybride ADN-ARN, seul le brin d'ADN est clivé, laissant intact le brin d'ARN (HAIDLE & BEARDEN, 1975). La nature duplex du polymère est également indispensable puisque les ARN ou les ADN monocaténaires ne sont pas dégradés (KUO et al., 1977).

La dégradation est également base-spécifique. Les coupures sont toujours observées au niveau des résidus désoxyguanosine (en 3'). Les séquences GpT et GpC sont clivées plus fréquemment que les sites GpA alors que les sites GpG le sont rarement (D'ANDREA & HASELTINE, 1978; FOX et al., 1987; TAKESHITA et al., 1978; SUGIURA & SUZUKI, 1982; MURRAY & MARTIN, 1985; MURRAY et al., 1988).

La topologie de l'ADN et son degré de méthylation déterminent la spécificité et l'intensité de la dégradation par la Blm (MIRABELLI et al., 1983; HERTZBERG et al., 1985).

Remarque : le complexe Blm-vanadium(IV) coupe également l'ADN en présence d'eau oxygénée (KUWAHARA et al., 1985).

3°) Complexation.

La nécessité d'un métal aussi bien pour la biosynthèse que pour l'activité biologique de la Blm a définitivement été établie. L'étude de la coordination des métaux de transition par la Blm a fait l'objet de très nombreux travaux (revues : DABROWIAK et al., 1979a, 1979b; DABROWIAK, 1980b; ALBERTINI, 1984).

*Structure des complexes.

Il semble désormais admis que les complexes Blm-Cu et Blm-Fe aient une structure pyramidale à base carrée. Les cinq ligands impliqués sont d'une part l'azote N_1 de l'imidazole, l'azote N_1 de la pyrimidine, l'azote de l'amine secondaire et l'azote peptidique déprotoné du résidu histidyle en tant que ligands dans le plan carré et d'autre part l'azote de l'amine primaire du résidu de β-aminoalanine comme ligand axial. L'azote ou l'oxygène de la fonction carbamate portée par le mannose ont également été proposés comme sixième ligand en position axiale aussi bien avec le cuivre (UMEZAWA, 1974a; DABROWIAK et al., 1978a, 1978b; BEREMAN & WINKLER, 1980) qu'avec le fer (DABROWIAK et al., 1979b) ou le zinc (AKKERMAN et al., 1988).

Cependant l'implication du carbamate comme sixième ligand permettant la formation d'une double pyramide n'est pas en accord avec les résultats de radiocristallographie du complexe Cu-P3A (un intermédiaire biosynthétique de la Blm) (IITAKA et al., 1978).

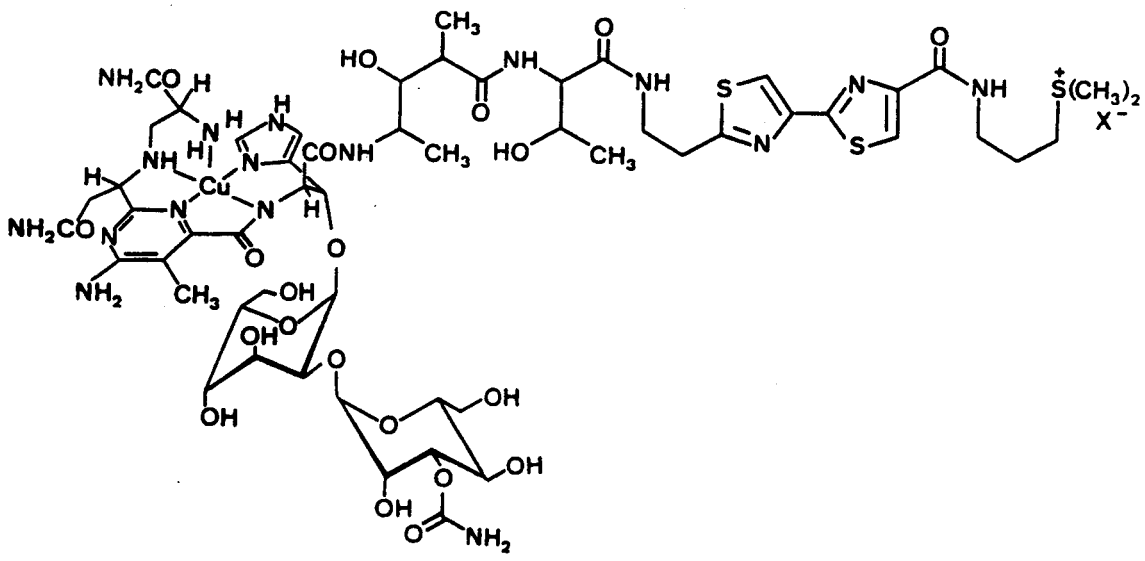

Structure du complexe Blm-A_2-Cu(II)

Une étude menée au laboratoire a définitivement écarté l'hypothèse de l'intervention du carbamate :

-Un analogue synthétique de la partie complexante de la Blm a été conçu (HENICHART et al., 1982a). L'étude par RPE n'a pas montré de différences de complexation entre cet analogue non glycosylé et la Blm (HENICHART et al., 1985a). Cet analogue nommé AMPHIS possède les 4 atomes d'azote précédemment cités et complexe le Cu de la même façon que la Blm.

-La comparaison des complexes cuivrique et ferrique de la Blm et de la déglycobléomycine (déglycosylation par l'acide fluorhydrique, KENANI et al., 1988b) n'a pas montré de différences quant à la structure des complexes. Toutefois, la partie glycannique joue un rôle important dans la stabilisation du complexe Blm-Fe-O_2 et la production de radicaux libres oxygénés (KENANI, 1988; KENANI et al., 1988a).

Remarque : le complexe manganique de la Blm, d'après les travaux de SHERIDAN, serait différemment coordiné et impliquerait les atomes d'azote des deux cycles thiazoles et de l'amine terminale. (SHERIDAN & GUPTA, 1981).

*Complexation et production de radicaux libres.

La Blm en présence de Fe(II) forme un complexe Blm-Fe(II) stable et visible en UV. Par contre, le complexe ternaire Blm-Fe(II)-O_2 a une durée de vie très brève (BURGER et al., 1979, 1981).

L'oxydation du complexe Blm-Fe(II) par l'oxygène moléculaire génère des radicaux superoxyde O_2^{-} relativement inoffensifs (SAWYER & VALENTINE, 1981) et inaptes à dégrader l'ADN directement. Mais la dismutation des radicaux superoxyde par le complexe Blm-Fe(II) en présence de peroxyde d'hydrogène produit des radicaux hydroxyle beaucoup plus réactifs (Réaction d'Haber-Weiss) (OBERLEY & BUETTNER, 1979).

L'eau oxygénée en présence de Fe(II) est également en mesure de produire des radicaux OH° et donc de dégrader l'ADN (Réaction de Fenton). De plus la présence d'ADN accroît l'intensité de la production des radicaux OH• par le Fe(II) et l'eau oxygénée (FLOYD, 1981).

L'eau oxygénée est formée en présence d'un réducteur (ascorbate de sodium, β-mercaptoéthanol, dithiothréitol) selon le schéma réactionnel suivant (CHIOU, 1983)

Ascorbate de sodium + 2Fe(III) ———> Déhydroascorbate de sodium + 2Fe(II) + $2H^+$

$2e^- + 2H^+ + O_2$ ———> H_2O_2

En présence d'un réducteur, le système peut donc fonctionner de façon cyclique :

Blm-Fe(II)-O_2 ———> Blm-Fe(III) + O_2^{-}

Ascorbate de sodium + 2Fe(III) ———> Déhydroascorbate de sodium + 2Fe(II) + $2H^+$

$2e^- + 2H^+ + O_2$ ———> H_2O_2

$H_2O_2 + O_2^{-}$ ———> $O_2 + OH^- + OH^•$ (réaction d'Haber-Weiss)
(HABER & WEISS, 1934)

H_2O_2 + Fe(II) ———> Fe(III) + OH^- + $OH^•$ (réaction de Fenton)
(FENTON, 1894)

Le mécanisme d'oxydo-réduction du système Blm-Fe-O_2 s'apparente à celui des hémoprotéines (peroxydases) in vivo (KANOFSKY, 1986) et à celui des enzymes à cytochrome P450 (WHITE & COON, 1980).

La production de radicaux libres par la Blm est donc le résultat d'un processus d'oxydo-réduction : oxydation du Fe(II) et réduction de l'oxygène.
Mais les espèces radicalaires générées, en particulier les radicaux hydroxyle, sont-elles les éléments responsables de la dégradation de l'ADN?

De nombreux travaux tendent à corroborer cette hypothèse (LOWN & SIM, 1977; SAUSVILLE et al., 1978a; LOWN, 1985)

D'autres travaux sont en désaccord avec cette théorie. Dans cette cascade d'oxydo-réductions, les radicaux O_2^{-} sont formés par l'oxydation du complexe Blm-Fe(II). Or en comparant les potentiels redox des complexes O_2/O_2^{-} ($\Delta E°$= -0.35V; WOOD, 1974) et Blm-Fe(II)/Blm-Fe(III) ($\Delta E°$= +0.129V; MELNYK et al.,1981), les radicaux O_2^{-} apparaissent comme des réducteurs potentiels du complexe Blm-Fe(III). L'intervention des radicaux libres oxygénés comme agents responsables de la dégradation de l'ADN par la Blm n'est donc pas définitivement adoptée.

La Blm-activée (c'est en fait le nom de la forme observée en RPE du complexe Blm-Fe(II)-O_2) (BURGER et al., 1981, 1985) a donc la capacité de dégrader l'ADN. Mais si ce dernier est absent du milieu, le complexe Blm-Fe(II) s'autoinactive. La forme inactivée de la Blm peut complexer le Cu(II) et peut former un complexe ternaire Blm inactivée-Fe(II)-O_2 mais ne peut plus dégrader l'ADN si celui-ci est alors ajouté. L'inactivation semble correspondre à une altération de la structure du bithiazole (NAKAMURA & PEISACH, 1988).

Si la nature exacte de l'espèce réactive responsable de la dégradation de l'ADN par la Blm-activée reste à déterminer, il est acquis que la coupure requiert la présence simultanée d'oxygène, de fer ferreux (ou fer ferrique et d'un réducteur) et de Blm.

Les autres complexes de la Blm capables d'induire des coupures (Blm-Co + illumination; Blm-Vn + H_2O_2; Blm-Mn + H_2O_2) ne sont que très peu représentés in vivo.

4°) Les autres cibles de la bléomycine.

a) Pénétration cellulaire de la Blm.

Initialement utilisée en clinique sous forme de complexe cuivrique (forme sous laquelle elle est isolée), la Blm est maintenant toujours administrée sous forme libre non complexée (UMEZAWA, 1979). Le devenir in vivo de la Blm est relativement mal connu. Du fait de son extrême hydrophilie, une très faible fraction seulement de la dose administrée pénètre dans les cellules (0,1%) (ROY & HORWITZ, 1984; MIYOKA et al., 1975). La Blm complexerait le Cu(II) dans le flux sanguin (KANAO et al., 1973) et c'est sous cette forme qu'elle pénètrerait dans la cellule avant d'être réduite en Blm-Cu(I) (UMEZAWA, 1979; FREEDMAN et al., 1982a).

L'existence d'un site spécifique de transport du complexe Blm-métal a été proposée (BARRANCO et al., 1980; UEHARA et al., 1982). L'ion cuivreux résultant de la réduction est ensuite chélaté par des composés à thiol libre (TAKAHASHI et al., 1987) ou par une protéine (TAKAHASHI et al., 1977). La Blm libre ainsi libérée est susceptible d'être dégradée par l'action de la bléomycine hydrolase. De plus, en l'absence d'ADN, la Blm s'autoinactive (NAKAMURA & PEISACH, 1988); il est donc indispensable qu'elle puisse atteindre rapidement le noyau des cellules cibles.

Les cellules disposent d'un "pool" de fer nécessaire à leur métabolisme, stocké sous forme Fe(III) par une protéine : la ferritine. La Blm peut piéger le fer ferrique des ferritines (NORSKOV-LAURITSEN et al., 1987) pour former le complexe Blm-Fe(III) stable ($K_{ass}=10^{15}$). Après réduction du complexe ferrique in vivo (MAHMUTOGLU et al., 1987), le complexe ferreux excerce son activité létale en dégradant les chromosomes en nucléosomes avant la coupure totale de l'ADN (MOORE, 1988). Le passage du cytoplasme au noyau n'est pas défini.

Si la dégradation de l'ADN nucléaire et mitochondrial (LIM & NEIMS, 1987) apparaît comme l'élément responsable de l'activité de la Blm, une relation étroite entre ces deux phénomènes n'est pas toujours observée (BERRY et al., 1985; LYMAN et al., 1986; SMITH, 1987). De plus la relative cytosélectivité de la Blm pour les cellules cancéreuses (CHEN et al., 1977) ne peut s'expliquer en tenant compte uniquement de la cible ADN.

b) La cible membrane.

Avant d'atteindre sa cible privilégiée (l'ADN), la Blm doit traverser les membranes cellulaires (plasmatique et nucléaire). La Blm se fixe sur la membrane plasmique (FUJIMOTO, 1974) et affecte certaines fonctions cellulaires de cette membrane (SUN & CRANE, 1985). L'effet majeur de la Blm au niveau membranaire concerne la peroxydation des lipides par les radicaux libres générés par le complexe Blm-Fe(II)-O_2. (EKIMOTO et al., 1985; KAPPUS et al., 1982). Parallélement à cette production de radicaux, le complexe Blm-Fer induit des modifications transitoires mais importantes de la fluidité de la membrane cytoplasmique des cellules. Cette constatation ressort d'une étude menée au laboratoire et qui fait l'objet de la publication suivante :

article n°5.

Plasma membrane perturbations induced by
the bleomycin-iron complex.

BAILLY C., BEAUVILLAIN J-C., BERNIER J-L., HENICHART J-P.

Accepté à Cancer Research.

PLASMA MEMBRANE PERTURBATIONS INDUCED BY BLEOMYCIN-IRON COMPLEX

C. BAILLY, J-C. BEAUVILLAIN, J-L. BERNIER, J-P. HENICHART.

INSERM U 16 [C. B., J-L. B., J-P. H.], INSERM U 156 [J-C. B.],
Place de Verdun, 59045 Lille Cédex, France.

SUMMARY

The effect of the anticancer drug bleomycin on acyl chain order of KB cell membranes was examined by EPR and fluorescence polarization spectroscopies using respectively the 5-doxyl stearic acid spin probe and the 1,6-diphenyl-1,3,5-hexatriene (DPH) fluorescent probe. Measurements of the order parameter, S, by the two techniques showed a transient perturbation of the plasma membrane fluidity during the 10 first minutes of incubation with Blm-Fe while no effect was observed with Blm or Fe alone. A kinetic study of the location of the fluorescent probe into the cell was followed by fluorescence microscopy. Lipid peroxidation measurements were also performed using intact cells or isolated plasma membranes whose purity was checked by electronic microscopy. These membrane perturbation effects were correlated with the ability of the complex to generate highly reactive oxygen species.

It has been demonstrated that membranes serve as a target site for a lot of drugs including antineoplastic drugs (1) and it was reported that doxorubicin could be cytotoxic without entering the cell (2). Nevertheless, it is not classical to think that cell membrane may be the main target for cytotoxic anticancer drugs which were shown to exert their effects in nucleus, interfering with DNA synthesis or directly damaging DNA. Such is the case for Bleomycin (Blm), the generic name for a group of glycopeptide antibiotics currently used in the treatment of human neoplastic diseases, particularly squamous cell carcinomas and lymphomas (3,4). This antitumor agent (Blm) is assumed to act mainly by modification of the DNA structure and functions through a pseudo-intercalative binding process (5).

However cell membrane cannot be considered as a main target for Blm. It is reasonable to suppose that the relative selective cytotoxicity for tumor cells can be explained in terms of differences in the structure and biochemistry between normal and neoplastic cell membranes. These elements might play a vital role in the control of the drug flux across the plasma membrane.

Evidence for a membrane action of an anticancer agent can be established on the basis of biochemical tests which prove that the drug alters aspects of membrane functions or on the basis of physicochemical experiments which prove the direct action of the drug with membrane components. The mechanism of transport of Blm through the cell membrane has not been established. The involvement of trypsin-sensitive components of the cell membrane in the toxicity of Blm has been reported by Barranco et al. (6) suggesting the possible presence of a transport carrier. It has been suggested (7) that Blm penetrates through the membrane as a metal chelate form and it has been postulated that the presence of a carrier mediated transport system may be one of the physical bases for why very low bleomycin doses are effective in vitro (8) and in vivo (9).

The fluidity of the lipid bilayer component of biological membranes can be defined by a variety of techniques (10, 11). In the present study, we have used electron paramagnetic resonance (EPR) spectroscopy and spin-labeled stearic acid probe as well as fluorescence polarization (FP) measurements, using 1,6-diphenyl-1,3,5-hexatriene (DPH) as a reporter molecule, to examine the modifications of structural order of the lipid domains of plasma membranes of KB_3 cells (nasopharingal cells) treated with Blm. These two techniques afford a lot of information on the lipid structure of biological membranes. The results of the experimentation have been analysed in term of "membrane fluidity" (12) which expresses the relative motional freedom of the lipid molecules.

Accumulated evidence indicates the involvement of oxygen-derived free radicals as well as transition metals, in particular Fe, in Blm toxicity (13). This, together with the high affinity of Blm for transition metal ions (14), the ubiquitous presence of adventitious metals in vivo and the first proposed clinical use of Blm (Blm-Cu) (15) prompted us to compare the nature and kinetics of interaction of Blm and metal-Blm complex with spin-labeled or fluorescent-labeled cells. Moreover, to demonstrate that the observed phenomenon is confined to the external membrane of the cell and that endogenous membranes are not involved, we present a DPH-microphotography study showing that we solely labeled the plasma membranes. Lipid peroxidation catalysed by Blm-+ Fe(II) was also studied using intact culture cells and their corresponding plasma membranes as substrate.

MATERIALS AND METHODS

Chemicals : Blm was obtained from Roger Bellon Laboratories ; it contains approximately 60 % Blm-A_2, 30 % Blm-B_2, and 10 % other Bleomycins. Fe $(NH_4)(SO_4)_2$. 12 H_2O and $CuSO_4$ were obtained from Merck (Darmstadt). The spin label, 2-(3-carboxy-propyl)-4,4-dimethyl-2-tridecyl-3-oxazolidinyl oxyl, referred to commonly as 5-doxylstearic acid, was obtained from Syva (Palo Alto, CA) and stored in the dark under refrigeration. Stock solutions of 5 mg/ml in ethanol were prepared. The fluorescent probe, 1,6-diphenyl-1,3,5-hexatriene, DPH, was obtained from Molecular Probes Inc. (Oregon) and used without further purification. A 1mM stock solution was prepared in tetrahydrofuran and stored in the dark at -20°C.

Cell cultures : KB cells were grown as suspension cultures in Joklik modified Eagle's medium (Seromed, Munich, FRG) supplemented with 5 % heat-inactived Colt serum at a 4 x 10^5 cells/ml concentration.

Plasma membrane preparation : Cytoplasmic membranes were isolated according to a previously described method (16). The purity of the preparation was assessed by appropriate marker enzyme activities and by morphological examination at the electron microscopic level. The plasma membrane preparation was tested for the specific 5'-nucleotidase (17), glucose-6-phosphatase (17) and catalase (18) activities (respectively markers for the plasma membrane, endoplasmic reticulum and peroxisomes-lysosomes).

For electron microscopy studies, the membrane pellets have been fixed in glutaraldehyde (1.5 % in 0.1 M phosphate buffer pH 7.4) for 2 h and post fixed in

osmium tetraoxide (1 % in the same phosphate buffer) for 1 h. After dehydration, the embedding was performed in Araldite. The ultrathin sections were counterstained with uranyl acetate and lead citrate before observation. Specimens were examined with an electron microscope Zeiss 902.

Lipid peroxidation analysis : peroxidation of unsaturated lipids was measured by thiobarbituric acid (TBA) assay using the procedure of Ohkawa et al. (19) in which malondialdehyde and other by-products of peroxide decomposition react with TBA to produce adducts fluorometrically detectable (λ_{exc} : 515 nm, λ_{em} : 553 nm). A kinetic study was performed using 10 µM Bim +- Fe and culture cells (5.10^5 cells/ml) or the plasma membrane preparation (0.01 mg protein/ml).

EPR Measurement : 50 ml of cell suspension were centrifuged, and the cell pellet was washed twice with 30 ml of NaCl (9 g/l). The cells were collected by centrifugation and resuspended in 20 ml of the same isotonic buffer containing 20 µg/ml 5-doxylstearic acid. This spin label partitions into cellular membranes and is oriented with the carboxyl group adjacent to the phospholipid head group and the acyl chain oriented perpendicular to the bilayer (20). The motion of the 5-doxylstearic acid probe reports on fluidity near the interior of the bilayer (Fig. 1). After 8 min incubation at 20°C, the cells were collected, washed 3 times to avoid contamination by free spin label then resuspended in 10 ml buffer NaCl (9 g/l). Under these conditions, the signal of free 5-doxylstearic acid was negligible compared to that of 5-doxylstearic acid bound to cells and did not interfere with the spectral measurements. Exclusion of trypan blue was observed in more than 90 % of the cells. The appropriate amount of buffer or Bim or Bim-Fe complex was added to adjust the concentration at 10 µM, the drug- containing cell suspension was drawn into a flat quartz cell (still at ambient temperature). Total time of exposure of the cells to Bim or Bim-Fe complex did not exceed 30 min. The quartz cell was then placed in the cavity of a Varian E 109 X-band spectrometer with a E 238 cavity operating in the TM mode . Measurements were made at a 1.0 G modulation amplitude, 0.30 s time constant, 1 min time scan, 10 mW microwave power on a scan range of 100 G. The order parameter S was calculated according to (21):

$$S = \frac{a_{//} - a_{\perp}}{a_{zz} - 1/2(a_{xx} + a_{yy})} \cdot \frac{1/3(a_{xx} + a_{yy} + a_{zz})}{1/3(a_{//} + 2a_{\perp})}$$

The inner and outer hyperfine splittings, 2a and $2a_{//}$ were measured directly form the EPR spectrum (Fig. 1B) and the principal components of the hyperfine tensor

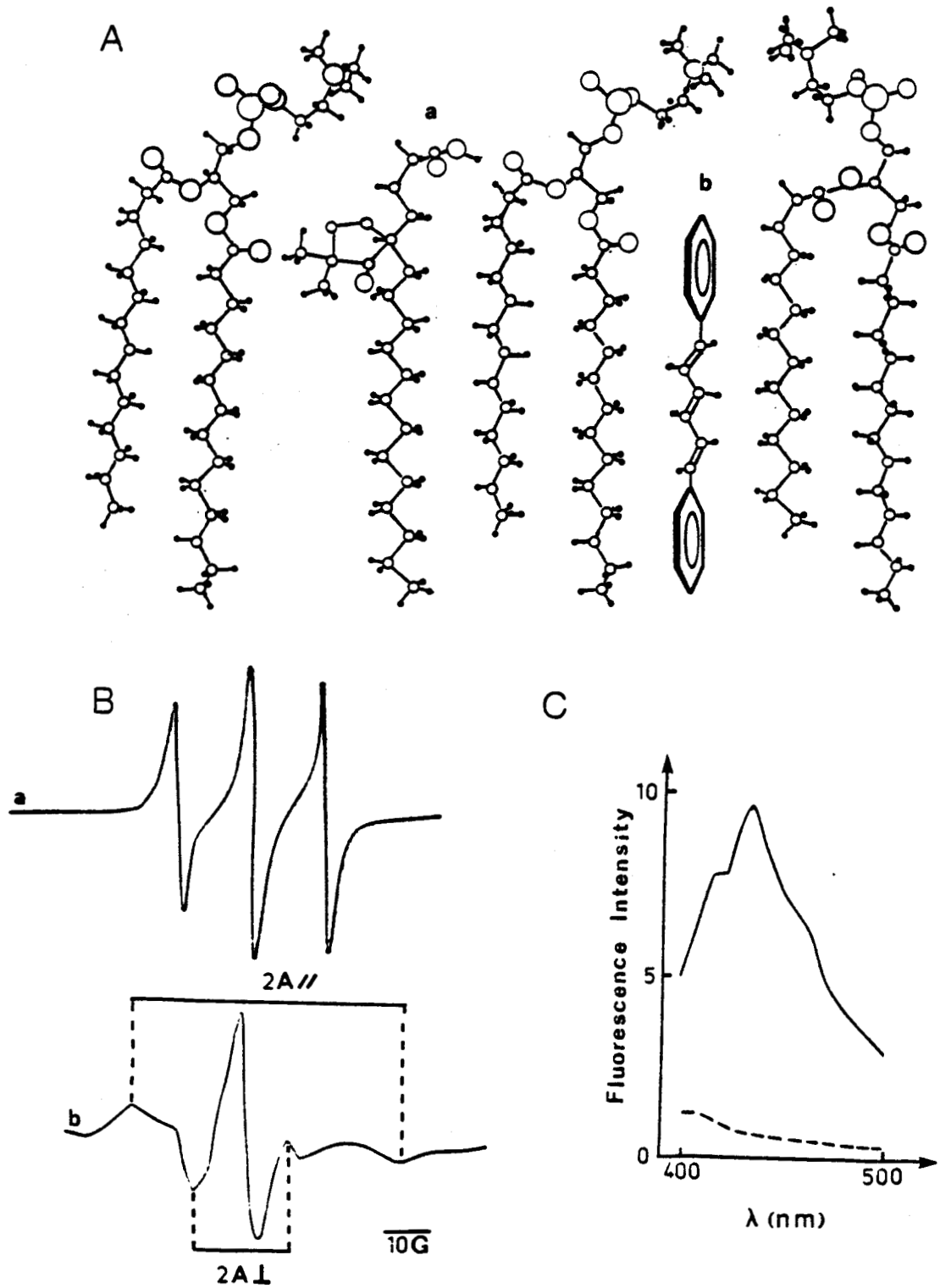

Fig.1 : A- Molecular arrangements of the spin-probe (5-doxylstearic acid, a) and the fluorescent probe (DPH, b) in lipid layer.

B- Representative EPR spectra of free (a) and membrane-bound (b) spin label 5-doxylstearic acid. The appropriate outer and inner extrema used to determine the order parameter (S) are indicated.

C- Typical fluorescence emission spectrum of DPH-labeled KB cells after 30 min incubation at 37°C. The scatter of unlabeled KB cells under identical conditions (---) is shown for comparison. Fluorescence intensity is given in arbitrary unit.

(a_{xx}, a_{yy}, a_{zz}, measured from a spin label oriented in a crystalline lattice) are respectively : 6.3, 5.8, and 33.6 (22).
The EPR spectra obtained were indicative of anisotropic motion resulting from rotational and segmental movements within the bilayer. The data are presented as order parameters which are related to the time-averaged angle that the nitroxide axis of the probe makes with the bilayer surface and are thus a measure of the flexibility of the probe. The order parameter is assigned a value of 0 to 1, with higher values representing more ordered or less flexible environments. Any factors which alter probe motion will result in a change in the order parameter for the receptor molecule.

DPH Fluorescence Microphotography : This technique was applied to demonstrate the specificity of DPH as a plasma membrane marker in intact cells and to investigate the labeling evolution with KB cells. In EPR and FP experiments, the cell suspension was incubated with 1 µM DPH at 37°C but for microphotography a higher probe concentration (5 µM) was necessary to overcome the rapid bleaching of the probe due to photoisomerization of the DPH under strong UV illumination (23). The fluorescence of DPH-labeled KB cells was studied with a Leitz Orthoplan microscope using an excitation filter at 340-380 nm.

Fluorescence studies : 10 ml of cell suspension were washed at least 3 times and resuspended in buffer (9 g/l NaCl, pH7). An aliquot (3µl) of stock solution of DPH was added to 3 ml of this suspension while gently vortexing and introduced into 1 cm quartz fluorescence cells. The final concentration of the DPH in the cell suspension was 1 µM. The kinetics of the DPH binding to whole KB cells was assessed by the measurement of the fluorescence emission intensity at 418 nm (excitation at 355 nm, 10 nm excitation and emission band pass) (Fig. 1C) on a Jobin-Yvon J-Y-3 spectrophotofluorometer equipped with an X-Y recorder. The viability of the cell preparation was always >93 % as estimated by trypan blue exclusion. The cell concentration was determined accurately by turbidity measurements : 0.10 +- 0.01 absorbance unit at 355 nm corresponded to (1.8 +- 0.05). 10^5 cells/ml.

Steady-state fluorescence polarization analysis : Lipid fluidity was assessed by steady-state fluorescence polarization of DPH according to the method described by Shinitzky and Barenholz (24). The degree of fluorescence polarization of the DPH-labeled KB cell population was determined at 37°C, after 20 min of a labeling period, the required time for almost complete incorporation of the probe at 37°C (Fig. 1), with a SLM 4048 spectrofluopolarimeter. The samples were excited at 355 nm and the fluorescence light was detected in two dependent cross-polarized channels, equiped

with polarizers, after passing a cut-off filter for wavelengths below 408 nm to reduce the contribution from scattered light.

Fluorescence measurements were obtained by simultaneous determination of the two channels, where I//, and $I_{\perp}$ are the fluorescence intensities polarized parallel and perpendicular to the direction of polarization of the excitation beam, respectively. These values relate to the degree of fluorescence polarization, P, by the following equation :

$$P = (I// - I_{\perp}) / (I// + I_{\perp})$$

where high P values represent low lipid fluidity, whereas low P values represent high lipid fluidity. Measurements were made in quadruplicate . The reproducibility of the measurements was +- 0.005 P units. Strict control of temperature (37°C) was monitored with circulating water from a Haake unit set. The steady-state fluorescence anisotropy (rs) was calculated from the relation $r_S=2P/(3-P)$. The limiting fluorescence anisotropy (r) and the lipid structural order parameter (S_{DPH}) were calculated according to Van Blitterswijk (25) :

$$r = 4/3\, r_S - 0.10 \qquad \text{(where } 0.13 < r_S < 0.28\text{)}$$

$$S_{DPH} = (r\ /r_0)^{1/2} \qquad \text{(where } r_0 = 0.362\text{) (24)}$$

S is the same orientational order parameter as measured by EPR.

RESULTS

Membrane preparation. The isolation of cytoplasmic membranes from KB cells was carried out after disruption of the cells by homogeneization and differential centrifugation. The so obtained membrane fraction was not contamined by nuclei or mitochondria as assessed by electron microscopy (Fig. 2). This preparation was morphologically homogeneous and consisted mainly of large and small membranous structures, but was not completely devoid of contamination with endoplasmic membranes, free ribosomes and rare lysosomes. Nevertheless these elements were found present in a very weak proportion. Glucose 6-phosphatase assay (Table I) moreover confirmed the weak contamination with endoplasmic membranes.

Lipid peroxidation. The effects of Blm-metal free or Blm-Fe complex on lipid peroxidation were examined using intacts cells and isolated plasma membranes. As

TABLE 1	Marker enzyme specific activities (µmol/min/mg protein)	
	plasma membrane	homogenate
5'-nucleotidase	25.3+-2.1	267+-9.6
glucose-6-phosphatase	41.6+-3.6	6.8+-2.0
catalase	0.6+-0.1	6.6+-1.4

Table 1 : Marker enzyme specific activities in homogenate and membrane fractions. Plasma membranes were isolated as described in "Materials and Methods". Enzyme specific activity is shown as the mean +- S. E. of values from four separate preparations.

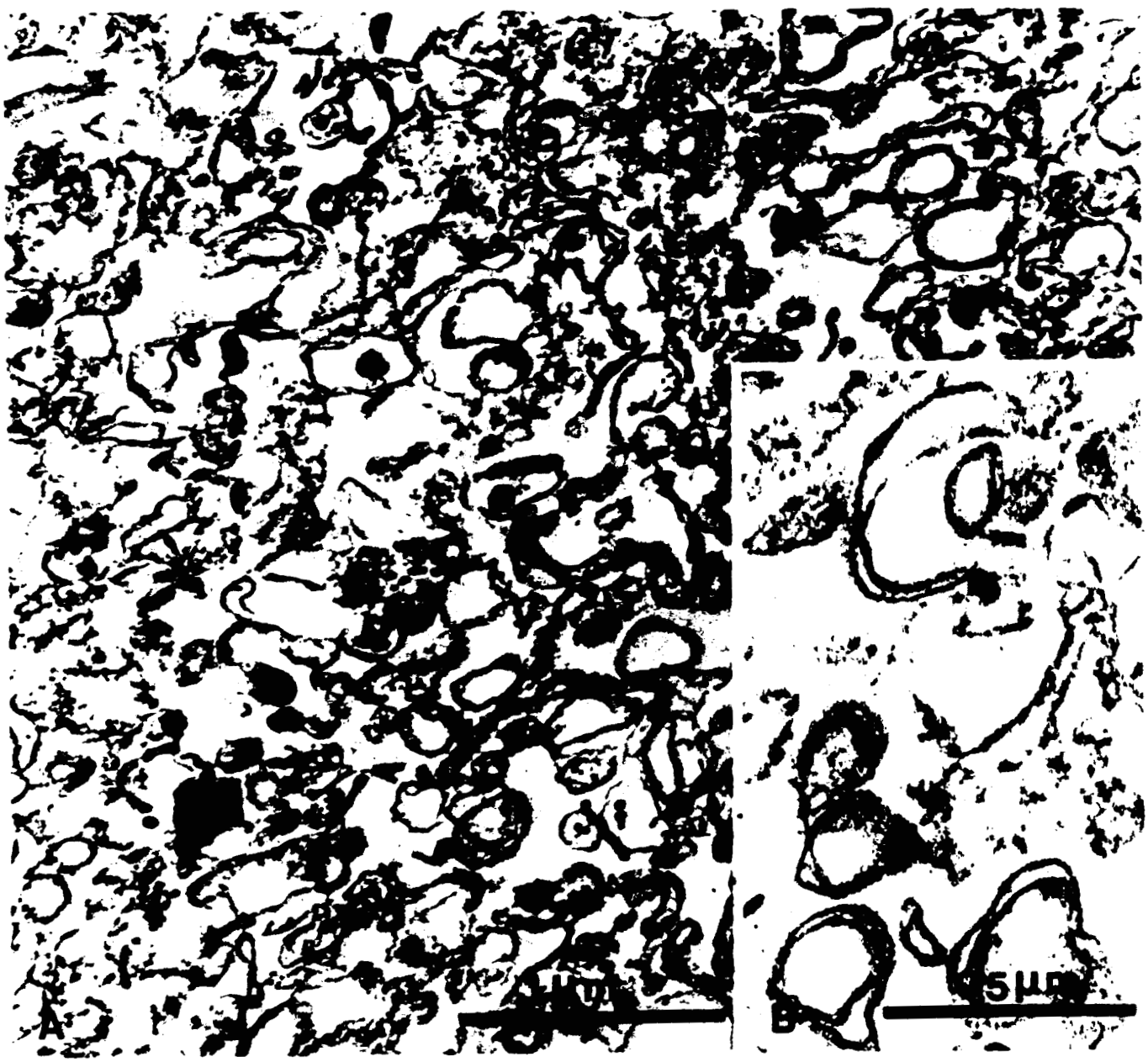

Fig.2 : A- Electron micrograph showing that majority of elements are plasma membranes. Ribosomes are sometimes visible indicating that ergastoplasmic membranes are present. Occasionally some lysosomes are observable.

B- Higher magnification of an other part of pellet showing cytoplasmic membranes.

shown in Fig. 3, the presence of Fe markedly enhanced the lipid peroxidation. Results obtained with plasma membranes are nearly similar to those reported by Ekimoto et al. using arachidonic acid (26). A rapid increase of peroxidation occurred during the first min., followed by a stabilization to a high level of peroxidation. The phenomenon was not observed in intact cells. The rate of malondialdehyde formation in intact cells was biphasic and characterized by an initial rapid phase (as observed with membranes or lipids) limited to about 30 sec, decreasing thereafter to 55-60 % of the maximum value during the following 5 min and reaching a plateau level for the further incubation period.

Spin-Label EPR Measurements. The effect of increasing incubation times from 0 to 30 min at 20°C of 10 µM Blm and Blm-Fe(II) complex on the order parameter (S) determined from spin-labeled KB cells, is shown in Fig. 4B. The data were obtained from three independent experiments performed on different days and correspond to S values obtained by others (27,28) for cultured cells at 20°C using 5-doxylstearic acid as the spin label probe. No significant rate difference in the order parameter occurred between untreated and Blm-metal free treated cells. Over the same range of incubation times, the Blm-Fe(II) complex briefly induced a consistent decrease of the S value for the incorporated fatty acid spin probe (Fig. 4), thus indicating an increase in bilayer fluidity. In these experiments the accuracy of the reported order parameter is about +- 0.01 unit.

Fluorescence Micrographs. Representative micrographs of DPH staining KB cells at various incubation times are shown in Fig. 5. In spite of a strong photobleaching of DPH, the following features have been observed on the pictures ; the probe appeared to be located in the peripheral region of the cells from 0 to approximately 40 min. Over 40 min the evolution of the staining is well shown, the labeled border line is markedly enlarged and at upper time the staining is extended to the whole cell except the nucleus. After a labeling period of 20 min we studied the interaction of Blm +- Fe with the cell for a period that did not exceed 30 min. The change in membrane fluidity occurs during the first 15 min, i.e. after 35 min of DPH labeling. As the DPH probe is essentially located in the periphery of the cell during the first 30 minutes, the fluorescence polarization data give reliable informations about lipid fluidity of the plasma membranes essentially, without any significative contribution of the other internal membrane structures.

The kinetics of the penetration of the DPH was also monitored by fluorescence spectroscopy (Fig. 6). The DPH fluorescence at 418 nm only appears when it was incorporated into organized structure, no signals come from the free probe. The

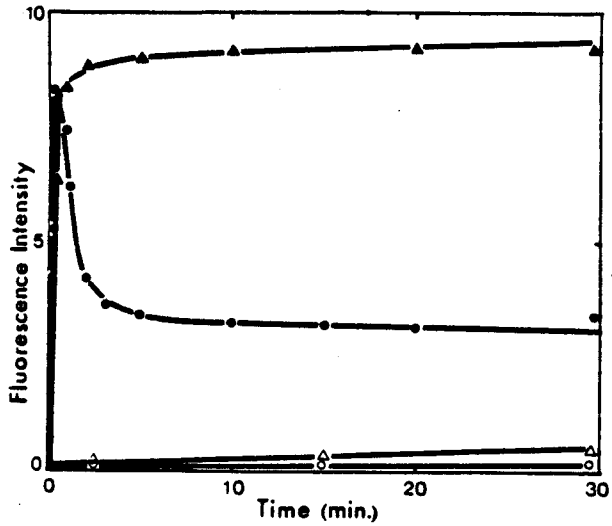

Fig. 3 : Kinetic study of the effect of 10 µM Blm (△,○) and 10 µM Blm-Fe(II) complex (▲ ,●) on lipid peroxidation. Peroxidation was assessed by fluorescence detection of malondialdehyde adducts (exc : 515 nm, em : 553 nm) in whole KB cells (●, ○) or isolated plasma membranes (▲,△). Fluorescence intensity is given in arbitrary units. Mean values of four separate determinations are shown.

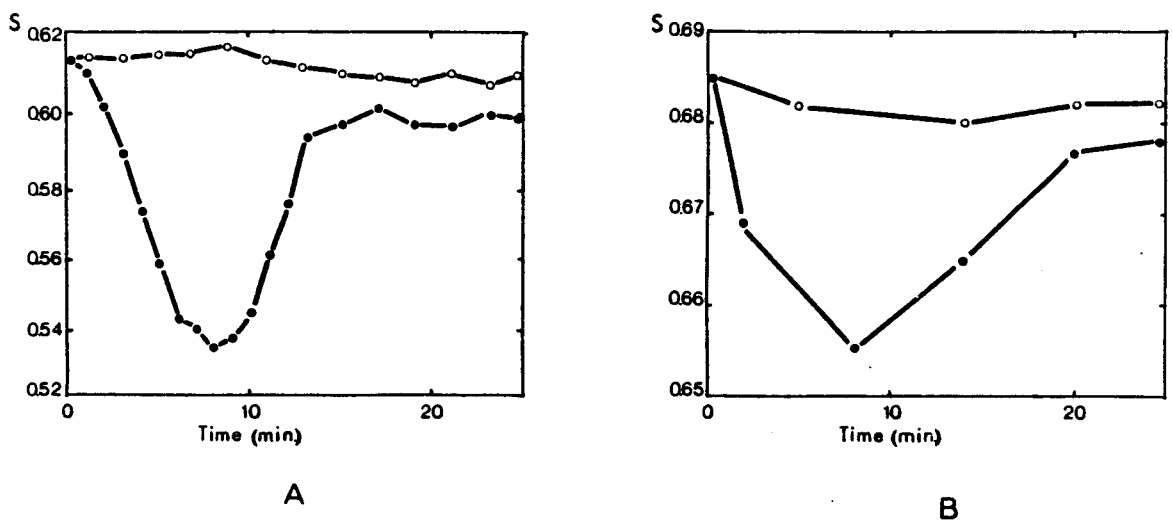

Fig.4 : Kinetic study of the effect of 10 µM Blm (○) and 10 µM Blm-Fe(II) complex (●) on the order parameter (S) measured by (A) PF with the DPH probe at 37°C and (B) EPR with the 5-doxylstearic acid spin-probe at 20°C. The S values are the mean of determinations on four separate experiments. S was measured as described in "Materials and Methods".

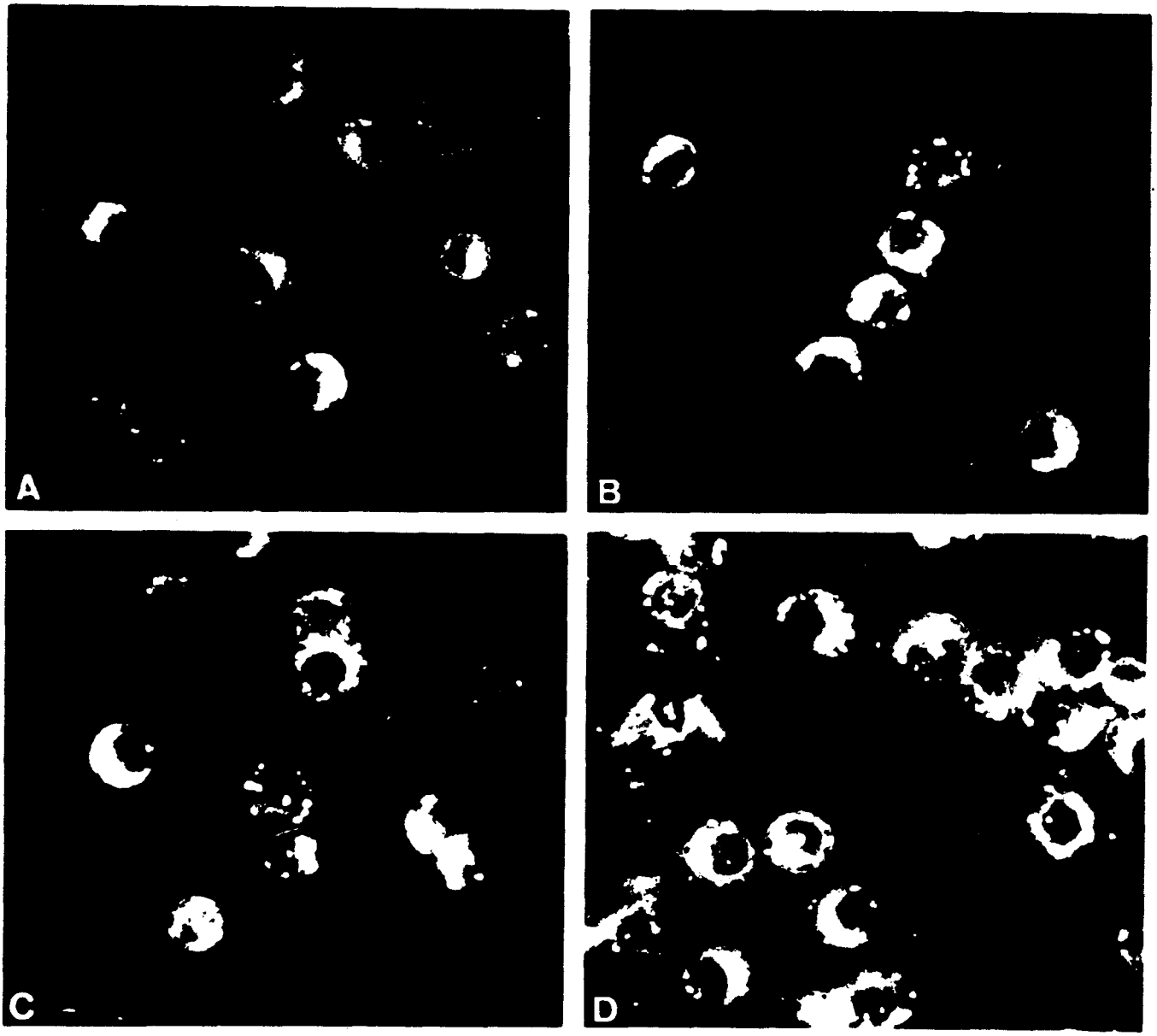

Fig.5 : Fluorescence microphotographies of DPH-labeled KB cells after 20 min (A), 30 min (B), 40 min (C), and 50 min (D) incubation. The original magnification was 40 x. In A, B, the fluorescence is observable at the periphery of the cells. In C, the great majority is still outside and in D a great part of the fluorescence is visible in the cytoplasm.

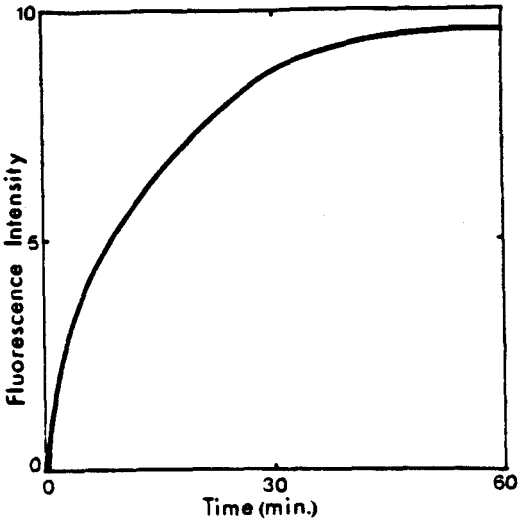

Fig.6 : Kinetics of incorporation of DPH (1 μM) in KB cells at 37°C, monitored by fluorescence intensity (λ_{exc} : 355 nm). Fluorescence intensity is given in arbitrary units. Values are the mean of three experiments.

measurement of the fluorescence gives account of the penetration of the probe into the cell without giving information on the exact localization of the probe in the different compartments of the cell. After 20 min of labeling, more than 70 % of the DPH is located in the periphery of the cell-membrane giving precise and intense informations about the interaction of the Blm-Fe complex with membrane.

Fluorescence Polarization Measurements. Fig. 4A shows the results of kinetic studies of the effect of Blm and Blm-Fe(II) complex on the KB cell membrane fluidity measured with DPH. Blm-Fe(II) complex induced a transient fluidization of the membrane. This effect reached a maximum within 10 min incubation and return to the initial value after 15 min. A similar time dependent decrease in polarization was obtained for each set of experiments. No change in fluorescence polarization occurred in KB cells incubated in the same conditions but treated with metal-free Blm, or with Fe alone. Thus, the two spectroscopic techniques (FP and EPR) reported the same results but with different intensities. S values obtained by FP experiments performed at 37°C are lower than S values measured by EPR at ambient temperature where no strict control temperature could be made. These results are in good agreement since the order parameter S is know as increasing significantly with decreasing temperature (25).

DISCUSSION

The "fluidity", characteristic of the various parts of the membrane at the molecular or submolecular level is usually determined by several spectroscopic techniques. In evaluating such studies, it is helpful to remember that these techniques may measure primarily either average orientational order or average rate of motion and that the definition of fluidity at the molecular level must include both of these concepts. Although orientational order (usually expressed as the order parameter, S) and rate of motion (usually expressed as a relaxation or correlation time) are normally inversely related, a simple inverse relationship between two parameters may not always exist. For example, changes in the temperature, fatty acid composition and cholesterol content of biological membranes generally affect order and motion in opposite ways (29).

In this work, the factors cited above which are of great importance have not to be taken into consideration since conclusions have been given only by comparison of the membrane fluidity in the absence or in the presence of Blm.

However when critically evaluating EPR and FP spectroscopies for measurements of lipid fluidity in biological membranes, the question arises whether intrinsic probes (Fig. 1A), nitroxide fatty acid in the case of EPR and DPH in the case of

FP spectroscopy, can seriouly perturb the local organization of membrane or not. The disadvantage of the EPR and FP techniques lies in the fact that a probe molecule must be added to the membrane system, thereafter necessitating to be extremely cautious in the interpretation of results.

It is unlikely that the effects of Bim on the mobility of the spin label were the result of direct Bim-probe interactions involving the hydrogen bonding establishment between the oxy radical and hydrogen donor groups of Bim for example. Since such interactions are not possible with diphenylhexatriene used in fluorescence polarization studies, the results of EPR and FP experiments can be taken as surely reflecting a change in membrane fluidity without any reference to some lipid-drug interaction. Hence, this fluidity refers only to the local environment of each probe and does not directly indicate the motional properties of native membrane constituents. Moreover, these motional parameters do not provide us with lateral diffusion coefficients for endogenous lipids or proteins.

However, knowledge of the location of the probes is necessary for conclusions of viscosity to be meaningful. With DPH, for example, a distribution of sites within the membranes was described (24,30,31). When experiments are carried out with intact cells, an estimation of the distribution pattern of the probe molecules between the various cellular membranes is essential for proper interpretation of the fluorescence polarization data. DPH, like most other hydrophobic solutes, can passively migrate from one outer membrane to endomembrane and lipid material inside intact cells by either partitioning through the aqueous media or by direct contact (32,33).

High resolution fluorescence microscopy provides a reliable tool for estimation of the fluorescence generated from the interior of the cell. Unfortunately DPH-labeled cells tend to bleach rapidly (21) and up to date photographic recordings of the fluorescing cells have only partially been successful (31,34). In our hands, with a high concentration in DPH (5 μM) microphotographic pictures (Fig. 5) appeared clear enough to follow the distribution of the fluorescent probe and to assure that DPH was well located in the cell membrane all over the experiments.

For the initiation of a lipid oxidation chain, the appearance of a free radical in the membrane lipid phase is essential (35). The main candidate for lipid oxidation initiation in the living cell is, undoubtedly, hydroxyl radical which is formed from hydrogen peroxide (36). It is well known that in the presence of the system Bim-Fe(II)-O2, the superoxide radical generation and consequently the hydroxyl radical production take place (37,39) leading to the degradation of DNA (40) and also to lipid peroxidation when they are produced in the vicinity of unsaturated fatty acids (Fig. 3). If the respective levels of lipid peroxidation observed with intact cells or isolated plasma membrane cannot be directly compared, the kinetics of production are

different, this being logically explained. It is likely that the decrease of production of lipid peroxides observed with intact cells in one minute incubation is due to the stimulation of metabolic processes which could not occur with isolated membranes because a complex system involving activators (iron-reducing system : NADH, ascorbate...) and inhibitors (such as superoxide dismutase-catalase, glutathion reductase-thiols...) regulates lipid peroxidation intensity in living cells (35). In unliving systems, such as membranes, no control occurs and the peroxidation process increases up to inactivation of the oxidizing source or up to complete elimination of polyunsaturated fatty acid residues leading to saturated fatty acids unable to undergo peroxidation.

This lipid peroxidation process modifies numerous physicochemical properties of membrane components including phospholipids. The microviscosity of the bilayer is enhanced : so, the mobility of fatty acid chains decreases as shown in various cases by FP (41,42) or EPR (43,45) in particular at the level of C_{10}-C_{12} carbon atoms (44). The increase in the viscosity of lipid bilayer can easily be explained by the elimination of polyunsaturated fatty acid residues and the enrichment of the lipid phase with satured fatty caids unable to undergo peroxidation.

Other changes in membrane elements are connected with oxidation of protein thiol groups with the formation of disulfide bridges and sulfonic groups and consequently protein aggregation. In our testing, it appears that the earliest changes in membrane properties are in favor of an increase in the molecular mobility of lipids. Such a phenomenon was previously observed by Rosen et al. (40) who studied human erythrocyte membrane fluidity by EPR spectroscopy. They clearly indicate that treatment of spin-labeled ghosts with superoxide anions was followed by an increase in membrane fluidity. However, after exposure of these membranes to anions superoxide, the nitroxide spectrum returned to a S value indicating a reduction of membrane fluidity. It was undoubtedly demonstrated that this decrease was due to the presence of hydroxyl radicals inducing a lipid peroxidation, a polymerization of the lipid components leading to decreased fluidity and protein mobility.

Our own results (Fig. 4) are in perfect agreement with these findings. In a first time, superoxide anions produced by Bim-Fe complex (37-40) induced a reduction of membrane fluidity as shown by both EPR and FP studies. The tendancy was reversed after 8 minutes corresponding to the formation of hydroxyl radicals responsible for the peroxidation of lipids.

Similar results were obtained by Deliconstantinos et al. (46) with the antineoplastic agent doxorubicin which was found to be able to increase the bilayer fluidity of dog brain synaptosomal plasma membranes labeled with DPH and also to induce lipid peroxidation. These authors concluded that the increase in lipid fluidity

was "an early key event in brain cytotoxicity induced by doxorubicin" without making any relation to superoxide production although oxygenated free radicals were considered as responsable for the toxicity of the drug (47).

In conclusion, the results of the present work obtained by two different methods using extrinsic probes clearly indicate that interaction of Blm with KB cell membranes finds expression in an increase fluidity as a primary event followed in a few minutes by a reverse phenomenon. Anion superoxides and hydroxyl radicals would be responsible for the two steps respectively. Thus, these toxic oxygenated species able to cleave DNA (40) and responsible for the cytotoxic properties of Blm (3,4,14) are also able to have a perturbing action at the membrane level. The significance of this effect with regard to its therapeutic action remains unclear. However, since transformed cells in general have altered membrane fluidity (48) modulation of this parameter may be expected to contribute to the action of antineoplastic drugs including Blm. The membrane-related properties of Blm could explain the side effects of the drug on pulmonary tissue (49,50) and may also contribute to the entering and cytotoxicity of coadministered agents leading to a potentialization of the antitumor effects (51).

REFERENCES

1. Hickman, J.A., Scanlon, K.J., Tritton, T.R. Membrane targets in cancer chemotherapy. TIPS Review, 5 : 15-17, 1984.
2. Tritton, T.R., Yee, G. The anticancer agent Adriamycin can be actively cytotoxic without entering cells. Science, 217 : 248-250, 1982.
3. Carter, S.K. The current role of bleomycin in cancer therapy. In:S.K. Carter, S.T. Crooke, and H. Umezawa (eds), Bleomycin:current status and new developments, pp. 9-14. New York : Academic Press, Inc., 1978.
4. Carter, S.K. Bleomycin : more than a decade later. In:B.I. Sikic, M. Rozencweig, and S.K. Carter (eds), Bleomycin chemotherapy, pp. 3-35. New York : Academic Press, Inc., 1985.
5. Hénichart, J.P., Bernier, J.L., Helbecque, N., Houssin, R. Is the bithiazole moiety of bleomycin a classical intercalator ? Nucl. Acids Res., 13 : 6703-67, 1985.
6. Barranco, S.C., Bolton, W.E., Novak, J.K. Time-dependent changes in drug sensitivity expressed by mammalian cells after exposure to trypsin. J. Natl. Cancer Inst. 64 : 913-916, 1980.
7. Uehera, Y., Hori, M., Umezawa, H. Specificity of transport of bleomycin and cobalt-bleomycin in LS178Y cells. Biochem. Biophys. Res. Commun., 104 : 416-421, 1982.
8. Terashima, T., Takabe, Y., Katsumata, T., Watanabe, M., Umezawa, H. Effect of bleomycin on mammalian cell survival. J. Natl. Cancer Inst., 49 :1093-1100, 1972.
9. Urano, M., Fukura, N., Joike, S. The effect of bleomycin on survival and tumor growth in a C3H mouse mammary carcinoma. Cancer Res., 33 : 2849-2855, 1973.
10. Lee, A.G. Spectroscopy in the study of drug-membrane interactions. TIPS, 3 : 145-147, 1982.
11. Stubbs, C.D., Smith, A.D. The modification of mammalian membrane polyunsaturated fatty acid composition in relation to membrane fluidity and function. Biochem. Biophys. Acta, 779 : 89-137, 1984.
12. Chapman, D. Biomembrane fluidity:the concept and its development. In R.C. Aloia, (ed). Membrane fluidity in biology, vol. 2, pp. 5-42. New York : Academic Press, Inc., 1983.

13. Sugiura, Y., Suzuki, T., Kuwahara, J., Tanaka, H. On the mechanism of hydrogen peroxide-, superoxide-, and ultraviolet light-induced DNA cleavages of inactive bleomycin. iron (III) complex. Biochem. Biophys. Res. Commun., 105 : 1511-1518, 1982.

14. Dabrowiak, J.C. Metal binding to antitumor antibiotics. In:H. Sigel (ed) Metal ions in biological systems, vol. 11, metal complexes as anticancer agents, pp. 306-336. New York : M. Dekker, Inc., 1980.

15. Ishizuka, M., Takayama, H., Takeuchi, T., Umezawa, H. Activity and toxicity of bleomycin J. Antibiotics, Ser. A, 20 : 15-24, 1967.

16. Maeda, T., Balakrishnan, K., Medhi, S.Q. A simple and rapid method for the preparation of plasma membranes. Biochim. Biophys. Acta, 731 : 115-120, 1983.

17. Aronson, N.N., Touster, O. Isolation of rat liver plasma membrane fragments in isotonic sucrose. Methods Enzymol., 31A : 90-102, 1974.

18. Higgins, C.P., Baehner, R.L., Mc Callister, J., Boxer, L.A. Polymorphonuclear leukocyte species differences in the disposal of hydrogen peroxide. Proc. Soc. Exp. Biol. Med., 158 : 478-481, 1978.

19. Ohkawa, H., Ohismi, N., Yagi, K. Assay for lipid peroxides in animal tissues by thiobarbituric acid reaction. Anal. Biochem., 95 : 351-358, 1979.

20. Hubbel, W.L., Mc Connel, H.M. Molecular motion in spin-labeled phospholipids and membranes. J. Am. Chem. Soc., 93 : 314-326, 1971.

21. Brogger, C., Azzi, A. Applications of spin-labels to biological systems. In : A. Azzi, U. Brodbeck, and P. Zahler (eds), Membrane proteins, pp. 177-193. Berlin : Springer-Verlag, 1981.

22. Berliner, L.J. Principal values of the g and hyperfine tensors for several nitroxides reported to date. In : L.J. Berliner (ed), Spin labeling : Theory and applications, pp. 564-565. Academic Press : New York, 1976.

23. Duportail, G., Weinreb, A. Photochemical changes of fluorescent probes in membranes and their effect on the observed fluorescence anisotropy values. Biochim. Biophys. Acta, 736 : 171-177, 1983.

24. Shinitzky, M., Barenholz, Y. Fluidity parameters of lipid regions determined by fluorescence polarization. Biochim. Biophys. Acta, 515 : 367-394, 1978.

25. Van Blitterswijk, W.J., Van Hoeven, R.P., Van Der Meer, B.W. Lipid structural order parameters in biomembranes derived from steady-state fluorescence polarization measurements. Biochem. Biophys. Acta, 644 : 323-332, 1981.

26. Ekimoto, H., Takahashi, K., Matsuda, A., Takita, T., Umezawa, H. Lipid peroxidation by bleomycin-iron complexes in vitro. J. Antibiotics, 38 : 1077-1082, 1985.

27. Ramu, A., Glaubiger, D., Magrath, I.T., Joshi, A. Plasma membrane lipid structural order in doxorubicin-sensitive and -resistant P 388 cells. Cancer Res., 43 : 5533-5537, 1983.

28. Burns, C.P., Lutteneger, D.G., Dudley, D.T., Buettner, G.R., Spector, A.A. Effect of modification of plasma membrane fatty acid composition on fluidity and methotrexate transport in L 1210 murine leukemia cells. Cancer Res., 39 : 1726-1732, 1979.

29. Mc Elhaney, R.N. Membrane lipid fluidity, phase state, and membrane function in prokariotic microorganisms. In : R.C. Aloia, and J.M. Boggs (eds), Membrane fluidity in biology, vol. 4,pp. 147-208. New York : Academic Press, Inc., 1985.

30. Kutchai, H., Huxley, V.H., Chandler, L.H. Determination of fluorescence polarization of membrane probes in intact erythrocytes. Possible scattering artifacts. Biophys. J., 39 : 229-236, 1982.

31. Collard, J.G., De Wildt, A. Localisation of the lipid probe 1,6-diphenyl-1,3,5-hexatriene (DPH) in intact cells by fluorescence microscopy. Exp. Cell. Res., 116 : 447-450, 1978.

32. Stubbs, G.W., Litman, B.J., Barenholz, Y. Microviscosity of the hydrocarbon region of the bovine retinal rod outer segment disk membrane determined by fluorescent probe measurements. Biochemistry, 15 : 2766-2772, 1979.

33. Lentz, B.R., Barenholz, Y., Thompson, T.E. Fluorescence depolarization studies of phase transitions and fluidity in phospholipid bilayer. 2. Two-component phosphatidylcholine liposomes. Biochemistry, 15 : 4529-4537, 1976.

34. De Laat, S.W. Van Der Saag, P.T., Shinitzky, M. Microviscosity modulation during cell cycle of neuroblastoma cells. Proc. Natl. Acad. Sci. USA, 74 : 4458-4461, 1978.

35. Vladimirov, Y.A. Free radical lipid peroxidation in biomembranes : mechanism, regulation, and biological consequences. In : Jr J.E. Johnson, R. Walford, D. Harman, and J. Miquel (eds), Free radicals, aging, and degenerative diseases, vol. 8, pp. 141-195. New York : A.R. Liss, Inc, 1986.

36. Vladimirov, Y.A., Olenev, V.I., Suslova, T.B., Cheremisina, Z.P. Lipid peroxidation in mitochondrial membrane. Adv. Lipids Res., 17 : 173-249, 1980.

37. Otsuka, M., Yoshida, M., Kobayashi, S., Ohno, M., Sugiura, Y., Takita, T., Umezawa, H. Transition-metal binding site of bleomycin. A synthetic analogue capable of binding Fe(II) to yield an oxygen-sensitive complex. J. Am. Chem. Soc., 103 : 6986-6988, 1981.

38. Hénichart, J-P., Bernier, J-L., Houssin, R., Lohez, M., Kenani, A., Catteau, J-P. Copper(II)- and Iron(II)-complexes of methyl 2-(2-amino-ethyl)-aminomethyl-

pyridine-6carboxyl-histidinate (Amphis), a peptide mimicking the metal chelating moiety of bleomycin. Biochem. Biophys. Res. Commun. 126 : 1036-1041, 1985.

39. Kénani, A., Bailly, C., Helbecque, N., Catteau, J-P., Houssin, R., Bernier, J-L., Hénichart, J-P. The role of the gulose-mannose part of bleomycin in activation of iron-molecular oxygen complexes. Biochem. J., 253 : 497-504, 1988.
40. Lown, J.W., Sim, S. The mechanism of bleomycin-induced cleavage of DNA. Biochem. Biophys. Res. Commun., 77 : 1150-1157, 1977.
41. Eichenberger, K., Bohni, P., Winterhalter, K.H., Kawato, S., Richter, C. Microsomal lipid peroxidation causes an increase in the order of the membrane lipid domain. FEBS Lett., 142 : 59-62, 1982.
42. Rice-Evans, C., Mockstein, P. Alteration in the erythrocyte membrane fluidity by phenylhydrazine-induced peroxidation of lipids. Biochem. Biophys. Res. Commun. 100 : 1537-1543, 1981.
43. Rosen, G.M., Barber, M.J., Rauckman, E.J. Disruption of erythrocyte membranal organization by superoxide. J. Biol. Chem. 258 : 2225-2228, 1983.
44. Brush, R.C., Thayer, W.S. Differential effect of lipid peroxidation on membrane fluidity as determined by electron spin resonance probes. Biochim. Biophys. Acta, 733 : 216-222, 1983.
45. Curtis, M.T., Gilfor, D., Farber, J.L. Lipid peroxidation increases the molecular order of microsomal membranes. Arch. Biochem. Biophys., 235 : 644-649, 1984.
46. Deliconstantinos, G., Kopeikina-Tsiboukidou, L., Villiotou, V. Evaluation of membrane fluidity effects and enzyme activities alterations in adriamycin neurotoxicity. Biochem. Pharmacol., 36 : 1153-1161, 1987.
47. Lown, J.W. Ethidium binding assay for reactive oxygen species generated from reductively activated adriamycin. Methods Enzymol., 105 : 532-539, 1984.
48. Van Blitterswijk, W.J., De Veer, G., Krol, J.H., Emmelot, P. Comparative lipid analysis of purified plasma membranes and shed extracellular membrane vesicles from normal murine thymocytes and leukemic GRSL cells. Biochim. Biophys. Acta, 688 : 495-504, 1982.
49. Muggia, F.M., Louie, A.C., Sikic, B.I. Pulmonary toxicity of antitumor agents. Cancer Treat. Rev., 10 : 221-243, 1983.
50. Copper, Jr J.A.D., White, D.A., Matthay, R.A. Drug-induced pulmonary disease. Am. Rev. Respir. Dis., 133 : 321-340, 1986.
51. Bajetta, E., Rovej, R., Buzzoni, R., Vaglini, M., Bonadonna, G. Treatment of advanced malignant melanoma with vinblastine, bleomycin, and cisplatin. Cancer Treat. Rep., 66 : 1299-1307, 1982.

Les modifications de la structure et/ou de la fonction de la membrane plasmique des cellules ne constituent certainement pas la cause principale de l'activité antitumorale de la Blm. Par contre ces effets sont probablement responsables de certains effets toxiques de la Blm, en particulier de sa toxicité pulmonaire.

c) La cible protéine.

La Blm perturbe l'action de diverses protéines enzymatiques comme :

- les ligases, DNA polymérases et DNases (MULLER & ZAHN,1977; YAMAKI et al., 1971).
- la tyrosinase (BERND et al., 1986).
- la prolyl hydroxylase (TAKEDA et al., 1979).
- les enzymes à activité antioxydante : glutathion peroxydase, glutathion réductase, catalase, superoxyde dismutase (GIRI et al., 1983).
- l'ATPase (NA^+-K^+ dépendante) (VYSKOCIL et al., 1983)
- la collagénase (HIRAIWA et al., 1983).

La Blm modifie également le taux de collagène (GIRI et al., 1983) et la synthèse protéique, à forte concentration, par action sur l'ARNt (HAIDLE & STEPHEN, 1980).

Ainsi la bléomycine affecte en plus de l'ADN un grand nombre de composés cellulaires. Tous ces effets influent à des degrés divers sur les propriétés biologiques de la Blm.

5°)Activité biologique de la Blm.

La Blm est un puissant inhibiteur de la multiplication des bactéries (ONISHI et al., 1973; SUZUKI et al., 1968), des virus (TAKESHITA et al., 1974), des champignons (IQBAL et al., 1976) et surtout des cellules en culture (SUZUKI et al., 1968, SAITO & ANDOH, 1973; RAO et al., 1980; MIYAMOTO & TERASIMA, 1986). Les cellules en mitose, notamment en phase G2, sont plus sensibles à la Blm (TWENTYMAN, 1984).

La Blm inhibe plus spécifiquement la croissance des cellules cancéreuses que celle des cellules saines (CHEN et al., 1977). Cette cytosélectivité serait due à la teneur plus faible des cellules tumorales en Blm hydrolase (UMEZAWA, 1974b), une enzyme capable de dégrader la Blm (NISHIMURA et al., 1987; SEBTI & LAZO, 1987). Cette hypothèse reste néanmoins à vérifier.

Les carcinomes cutanés, testiculaires et de la sphère bucco-pharyngée ainsi que les lymphomes de Hodgkin sont les cancers où les régressions les plus nettes sont obtenues avec la Blm (BLUM et al., 1973). Les effets secondaires sont faibles (alopécie, anorexie, nausées, vomissements, fièvre) de sorte que son utilisation est généralisée à presque tous les cancers (hormis les tumeurs pulmonaires).

L'absence de toxicité sanguine, immunosuppressive ou mutagène vaut à la Blm d'être associée à de très nombreux protocoles de polychimiothérapie (SIKIC et al., 1985). Par exemple :

_ Pour le traitement de la maladie de Hodgkin (caractérisée cliniquement par la tuméfaction des ganglions en de nombreux points de l'organisme), l'association Doxorubicine-Bléomycine-Vinblastine-Décarbazine (ABVD) est efficace dans 92% des cas (taux de rémission complète à 5 ans : 84%) (BONADONNA & SANTORO, 1982).

_ Pour le traitement de lymphomes diffus, la Blm ajoutée à la combinaison Cyclophosphamide-Doxorubicine-Vincristine-Prednisone (CHOP) donne de très bons résultats (NEWCOMER et al., 1982).

La Blm peut complémenter de nombreux médicaments anticancéreux sans résistance croisée. Par exemple une culture de cellules tumorales résistantes à la vinblastine et la doxorubicine est généralement sensible à la Blm.

Cependant la Blm n'est pas dénuée de toute toxicité. Dix à quinze pour cent des patients traités par la Blm développent des pneumonies interstitielles. Heureusement , celles-ci n'évoluent que rarement (1% des cas) en fibroses interstitielles diffuses fatales (COOPER & HONG, 1981; MUGGIA et al., 1983; COOPER et al., 1986).

Remarque : cette propriété est utilisée pour l'induction de fibroses expérimentales chez l'animal.

Deux éléments à l'origine de cette toxicité pulmonaire sont avancés :

1_ La forte concentration en oxygène du poumon qui potentialise les effets toxiques de la Blm (TOLEDO et al., 1982; HAY et al., 1987)

2_ La faible teneur en Blm hydrolase du tissu pulmonaire (LAZO & HUMPHREYS, 1983).

Enfin la Blm est couramment utilisée en dermatologie pour le traitement du psoriasis ou des verrues (usage externe).

II Les modèles synthétiques

1°) Les analogues de la Blm.

L'utilisation clinique de la Blm à une très large échelle est essentiellement due à son efficacité, son absence de toxicité sanguine (facteur limitant dans l'utilisation des autres médicaments anticancéreux) et à sa cytosélectivité pour les cellules cancéreuses. Cependant elle est toujours administrée à faible dose du fait de sa toxicité pulmonaire. A ce titre, la conception de composés structuralement analogues à la Blm s'avère intéressante. Le but serait bien sûr d'élaborer une substance "Blm-like" non toxique sur le plan pulmonaire, tout en conservant l'extrême aptitude de la Blm à dégrader l'ADN.

Si ce principe est séduisant, il n'en reste pas moins complexe à appliquer du fait de la structure même de la Blm. La synthèse de dérivés de poids moléculaire "élevé"(1000 à 1500) est difficile, inapplicable à grande échelle et non rentable économiquement, si bien que très peu d'équipes se sont engagées sur cette voie.

SUGIURA et al., ont conçu en 1982 un modèle (PYML-1) mimant la partie complexante de la Blm (Figure 20) (SUGIURA et al., 1982). Des améliorations successives de ce modèle ont abouti à l'élaboration d'un "homologue supérieur" (PYML-6, Figure 20) également apte à complexer les métaux mais aussi à dégrader l'ADN grace aux radicaux oxygénés produits in situ (SUGIURA et al., 1983; UMEZAWA et al., 1984; SUGANO et al., 1986; OTSUKA et al., 1986a, 1986b). Dans cette série, les pharmacomodulations concernent exclusivement la partie complexante de la Blm, et ont permis de "décortiquer" cette fraction sur le plan moléculaire afin d'établir très précisément le rôle de chacun des atomes dans la coordination des complexes métalliques.

Parallèlement, au laboratoire, une modélisation de la partie complexante de la Blm avait été engagée. Un analogue nommé AMPHIS (Figure 20,HENICHART et al., 1982a) a été synthétisé; son aptitude à complexer le cuivre et à produire des radicaux libres a été vérifiée (HENICHART et al., 1985a). Mais rapidement la conception d'"analogues complets" de la Blm a été envisagée.

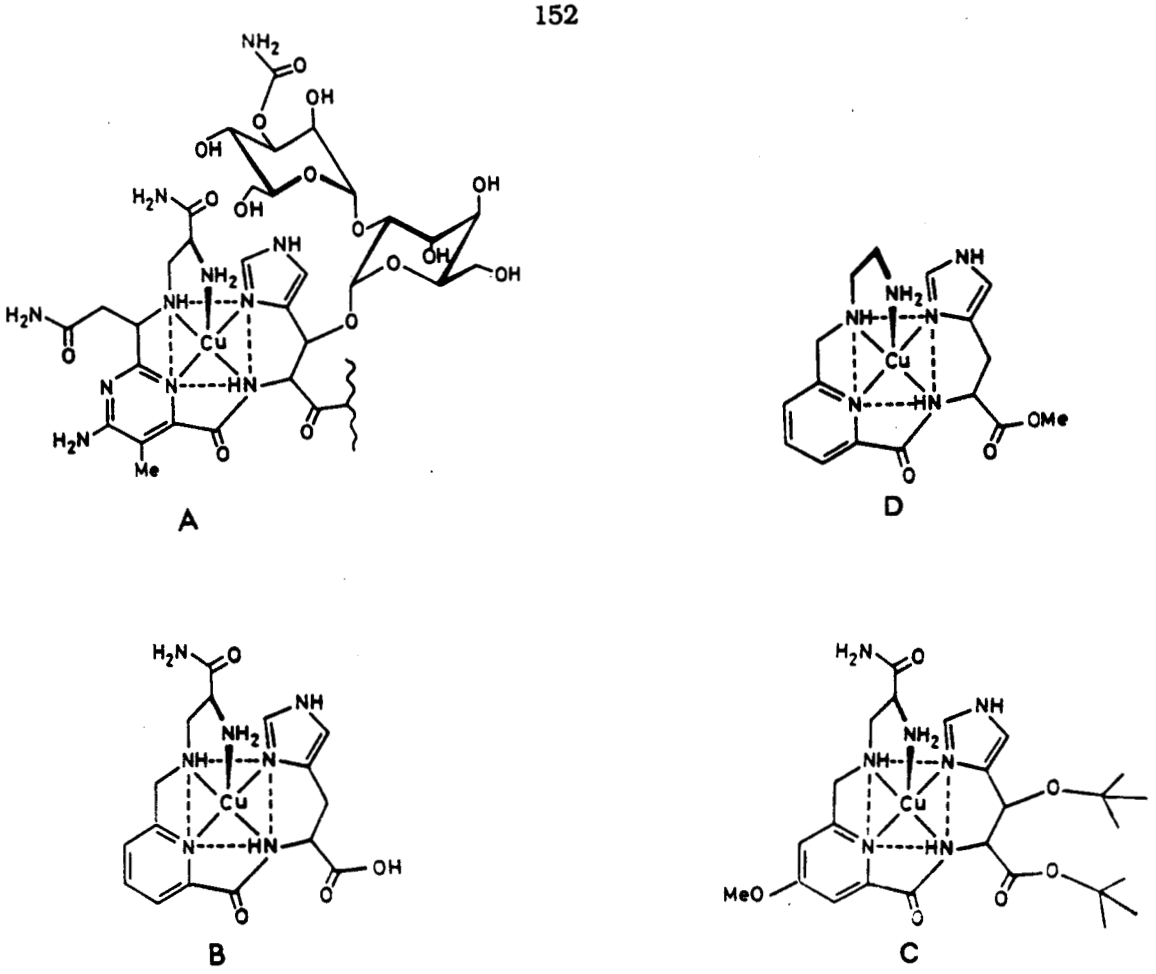

Figure 20 : Structure de la fraction complexante de la bléomycine (A) et de ses analogues synthétiques PYML-1 (B), PYML-6 (C) et AMPHIS (D).

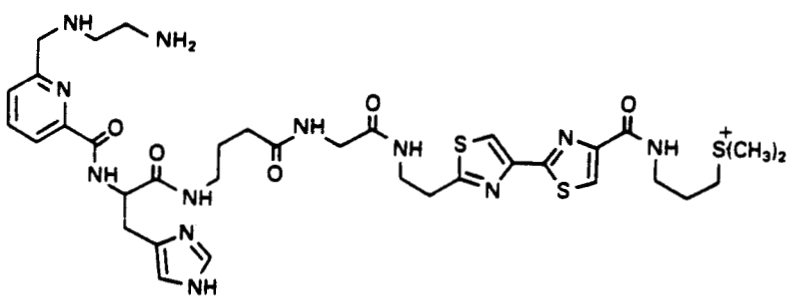

Figure 21 : Stucture de AMBI A_2.

AMPHIS ne dégrade pas l'ADN car les radicaux oxygénés produits par le complexe ferreux ne sont pas générés directement au contact du désoxyribose. Il fut donc envisagé de lier de manière covalente cette fraction complexante AMPHIS au noyau bithiazolique par un bras espaceur de même longueur que celui de la Blm. Le modèle nommé AMBI-A_2 (Figure 21) ainsi conçu s'avérait apte à dégrader l'ADN mais à des concentrations nettement supérieures à celles de la Blm dans les mêmes conditions (KENANI et al., 1987). Il apparaissait dès lors indispensable de regrouper sur une même molécule non seulement la partie complexante et la partie liant l'ADN, mais aussi une fraction glycannique.

En effet, le disaccharide de la Blm, s'il n'est pas absolument indispensable à la complexation du cuivre ou du fer et à la production de radicaux oxygénés, intervient dans la stabilisation du complexe ternaire Blm-Fe(II)-O_2.

Ce disaccharide gulose-mannose permettrait la formation d'une poche sous le complexe dans laquelle l'oxygène serait protégé et stabilisé. Ces constatations ressortent d'une étude comparative de la Blm et de la déglyco-Blm pour leur aptitude à complexer les métaux et à produire des radicaux libres (KENANI et al., 1988a).

Tenant compte de cette hypothèse, le modèle AMBI-A_2 a été perfectionné par l'adjonction d'une fraction monosaccharidique. Un résidu de glucosamine a été greffé par sa fonction amine libre à l'extrémité γ-acide d'un résidu glutamyle. Le modèle synthétique appelé AMBIGLU a été élaboré. La synthèse, l'étude de la complexation, de la liaison à l'ADN et de la dégradation de l'ADN ont fait l'objet de la publication suivante :

article n°6 :

Metal-complexing, DNA-binding and DNA-cleaving properties
of a synthetic molecule AMBIGLU, a simplified model
for the study of bleomycin.

KENANI A., BAILLY C., HELBECQUE N., HOUSSIN R.,
BERNIER J-L., HENICHART J-P.

European Journal of Medicinal Chemistry 1989 (sous presse).

Metal-complexing, DNA-binding and DNA-cleaving properties of a synthetic molecule AMBIGLU, a simplified model for the study of bleomycin.

ABDERRAOUF KENANI[1] , CHRISTIAN BAILLY[1] , NICOLE HELBECQUE[1] , RAYMOND HOUSSIN[2] , JEAN-LUC BERNIER[1] and JEAN-PIERRE HENICHART[1].

[1]INSERM U16, [2]Institut de Chimie Pharmaceutique, Université de Lille II, 59045 LILLE, France.

SUMMARY

On the basis of the previous studies on simple synthetic molecules structurally related to the anti-tumor drug bleomycin-A_2 (BLM-A_2), the roles of the main parts of the parent compound, a metal-chelating peptide, a DNA-binding heterocycle and a protecting activating sugar residue, were delineated. A new synthetic compound, AMBIGLU was designed taking into account these results. The synthesis, the copper-chelating properties, the radicals production, the DNA-binding and DNA-cleaving ability are described here and compared to those of BLM-A_2.

KEY WORDS

Bleomycin-like antitumor drug - Synthesis - Metal-chelating properties - Radical production - DNA-binding - DNA-cleaving ability.

INTRODUCTION

Recent advances in cancer cell biology and in molecular biology allow the identification of new appropriate targets for chemotherapeutics in the treatment of cancer. On the other hand, the discovery of natural toxins with a very high cytotoxicity may reveal compounds with biological effects pertinent to severe human diseases such as cancer. Thus, the rational design of new synthetic drugs with precise action on specific targets can find inspiration from natural products. If the mechanism of action of the parent natural drug is known, by adequate chemical modifications of the initial structure, it is possible to optimize the desired effect and to minimize adverse effects. This approach has been used here starting from the anti-tumor drug bleomycin.

Bleomycin (fig. 1) is an anti-tumor antibiotic drug isolated from Streptomyces Verticillus and employed for the treatment of lymphomas, squamous cell carcinomas and testicular carcinomas (1-3). In fact it is the generic name of closely related natural glycopeptides with a common structure, bleomycinic acid, and which differ only in the substituent on their heterocyclic unit, bithiazole.

The biological activity of bleomycin involves two well defined parts of the molecule. A metal ion-chelating fraction is able to form a copper(II) complex which has two biological roles : the resistance to the inactivation enzyme and the protection against manifestation of the biological activity (4). The same part is able to form with iron(II) and molecular oxygen an active complex which generates free radicals responsible for the cleavage of DNA (5,6). On the other hand, a bithiazole containing moiety contributes to the binding of bleomycin to DNA (7). DNA-binding and DNA-cleaving are believed to be the two essential steps of the cytotoxic process.

By the design of synthetic model molecules (8,9), we have delineated the exact role of the heterocyclic bithiazole ring of bleomycin in the binding to DNA (10). The complexing properties of the pseudopeptide chain have also been studied using a synthetic simplified molecule, AMPHIS (11) (fig. 1). This compound was found to form a copper(II) complex exhibiting ESR parameters substantially similar to those of the copper(II)-bleomycin complex and to produce $OH^{\cdot}$ radicals in the presence of iron(II) and oxygen in the same conditions as bleomycin does (12). Similar results were obtained with a simple synthetic molecule named AMBI-A_2, related to BLM-A_2 and possessing in its structure both simplified complexing and binding parts of BLM-A_2 (13) (fig. 1). This compound has been shown to mimic the chelating and binding properties of the parent drug BLM-A_2 but to cleave DNA at higher concentration. At least, to explain the role of the carbohydrate part of bleomycin we have compared the

properties of deglycobleomycin (14) and of bleomycin. It can be stated that the gulose-mannose part undoubtedly plays a role both in the stabilization of iron(II)-oxygen-bleomycin complex and in its activation to produce oxygenated free radicals (15).

On the basis of these results, a model was designed. Taking into account the previous observations, this molecule named AMBIGLU was built by connecting the simplified chelating part AMPHIS, the DNA-binding part bithiazole and a glucosamine residue to a short spacer, glutamic acid (fig. 1). We report here the synthesis, the metal-complexing and DNA-binding properties of the synthetic molecule together with the DNA-cleaving ability compared to those of the parent drug bleomycin.

CHEMISTRY

AMBIGLU was synthesized by a multi-step strategy (scheme 1). The simplified complexing part of BLM (AMPHIS, 8) (11) was here linked to the bithiazole ring 11 (9) via a glycopeptidic spacer : N-glutamidoglucosamine. This linker part was prepared starting from glucosamine hydrochloride (1). N-protection of the amine function with di-tertio-butyldicarbonate led to the terbutyloxycarbonyl derivative (2), acetylation of hydroxyl groups with acetic anhydride gave the fully protected sugar 3. Cleavage of the BOC group with dry hydrogen chloride in acetic acid gave the desired compound 4 with a 86 % yield. Coupling of the primary amine 4 with the α-protected glutamic acid derivative 5, in the presence of dicyclohexylcarbodiimide (DCC) and 1H-hydroxybenzotriazole (HOBt), afforded the amine 6 after column chromatography. After cleavage of the BOC-protecting group in trifluoroacetic medium, the amino-glucidic unit 7 was coupled to compound 8 using the mixed anhydride method. The resulting benzyl ester 9 was converted into the acid 10 by saponification. This reaction conducted in MeOH and aqueous sodium hydroxyde during two days furnished the deacetylated acid 10 in a 53 % yield. This free acid was coupled to the bithiazole moiety 11 using a classical DCC-HOBt procedure. Pure 12 was isolated by careful flash-chromatography.

The last step consisted in removal of the protecting groups by hydrobromic acid in acetic acid medium. The final compound was dissolved in water. After extraction with ethyl acetate, the aqueous layer was lyophilized to give AMBIGLU as a white powder.

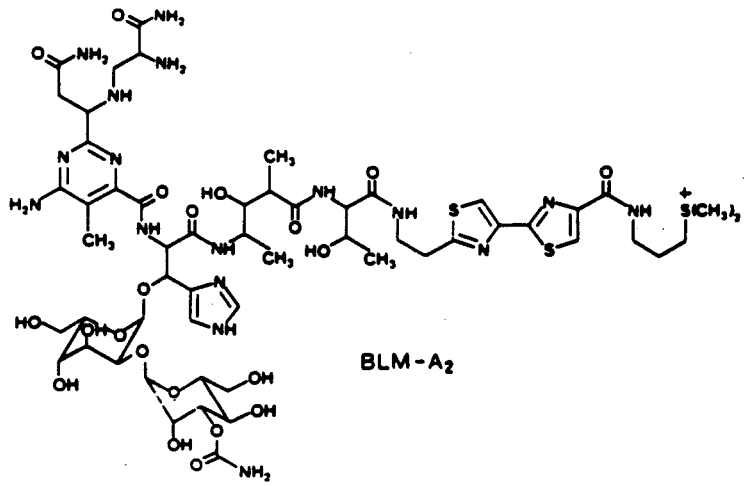

BLM-A_2

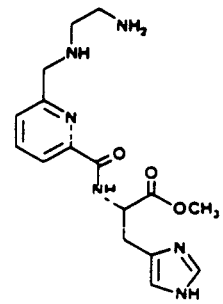

AMPHIS

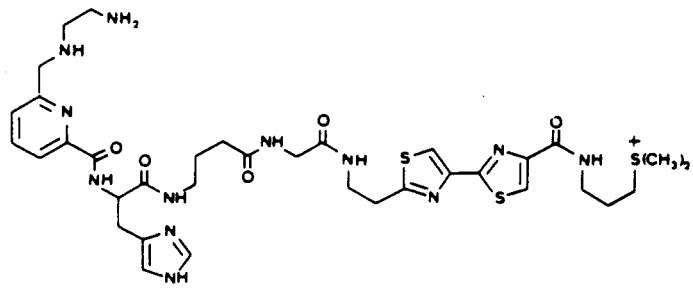

AMBI-A_2

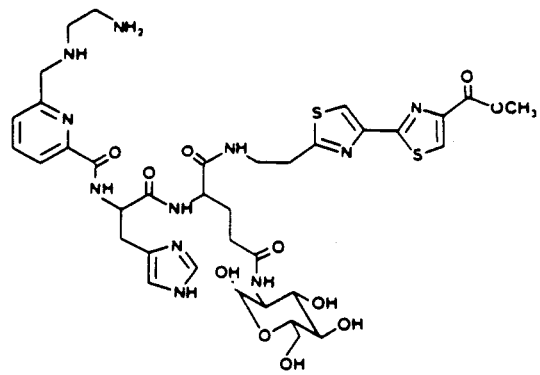

AMBIGLU

Figure 1 : Structure of BLM-A_2, AMPHIS, AMBI-A_2 and AMBIGLU.

Scheme 1 : Synthesis of AMBIGLU.

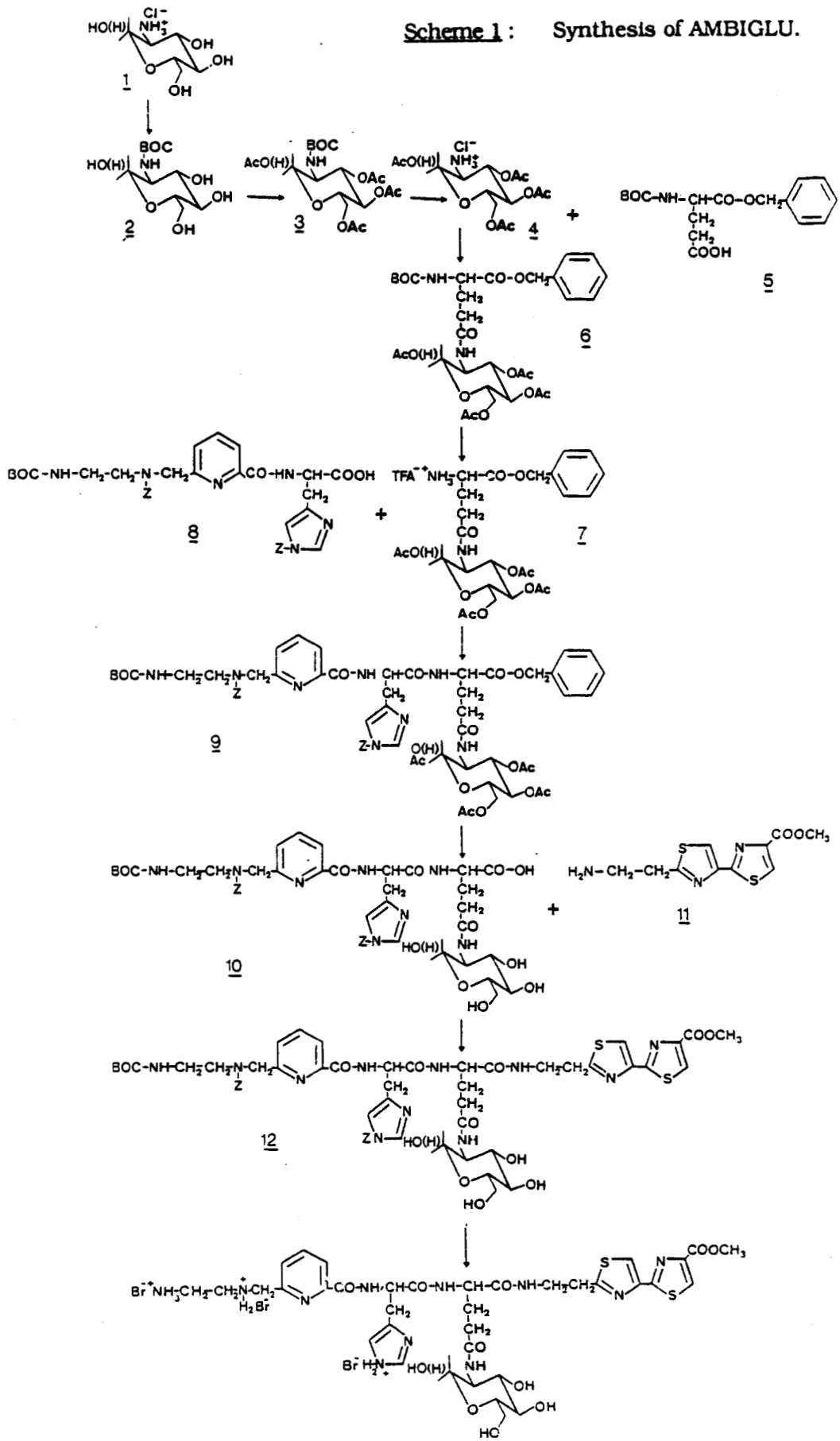

AMBIGLU

RESULTS

Cu(II) Complexes : The ESR spectrum of AMBIGLU-Cu(II) looks like the one exhibited by BLM-A_2-Cu(II). Parameters values ($g_{//}$:2.20, $g_{\perp}$:2.05, $A_{//}$:177G) are quite similar to those of BLM-A_2-Cu(II) and AMPHIS-Cu(II).

Spin-trapping : The air oxidation of AMBIGLU-Fe(II) gives rise to the formation of an OH· radical adduct with PBN spin-trap, well characterized by the corresponding ESR spectrum : triplet of doublet with a g factor of 2.006 and a_N =15.3 G. These values are identical to those found by Harbour et al (22).

Free radical production in the presence of (i) BLM-Fe(II)-O_2 (5,23), (ii) AMPHIS-Fe(II)-O_2 (12) and (iii) AMBI-A_2 -Fe(II)-O_2 (13) has been observed in similar conditions. The present results indicate that the spin density is significantly higher for radicals produced in the presence of AMBIGLU compared to the order analogues. Nevertheless, it is lower than those produced by BLM-A_2 (fig.2).

DNA unwinding : The effect of AMBIGLU on the superhelicity of a modified pBR 322 plasmid has been followed by viscometry experiments. It yields the characteristic rise-and-fall response, reflecting removal and reversal of the supercoiling. However, reversal of the supercoiling produced by AMBIGLU is not so pronounced as in the case of ethidium bromide. This can be due to the fact that AMBIGLU binds DNA by different mechanisms including intercalation. Measurement of the length increase of the DNA helix can help in elucidating these mechanisms. At the maximum of the curve (fig. 3), when the DNA was completely relaxed, which is hydrodynamically equivalent to nicked circular DNA, the reduced viscosity indicates an apparent unwinding angle of 12.7°. This value is quite similar to those obtained for BLM-A_2 and AMBI-A_2 (13) and can be thought to reflect a similar DNA binding mode.

Helix extension : The change in contour length (from L_0 to L) has been related to the change in intrinsic viscosities (from $[\eta_0]$ to $[\eta]$) of the free and complexed DNA (24). The data are directly transformed from flow times to values for the relative contour length using the expression $L/L_0 = (t_C-t_0/t_D-t_0)^{1/3}$ where L is the contour length in the presence of drug, L_0 is the contour length of free DNA, t_C is the flow time for the complex, t_D is the flow time for pure DNA, and t_0 is the flow time for buffer at a given total volume.

On the opposite to BLM-A_2 and AMBI-A_2, which decrease the DNA contour length (10, 13), AMBIGLU induces a linear increase in DNA length (0.82 Å).

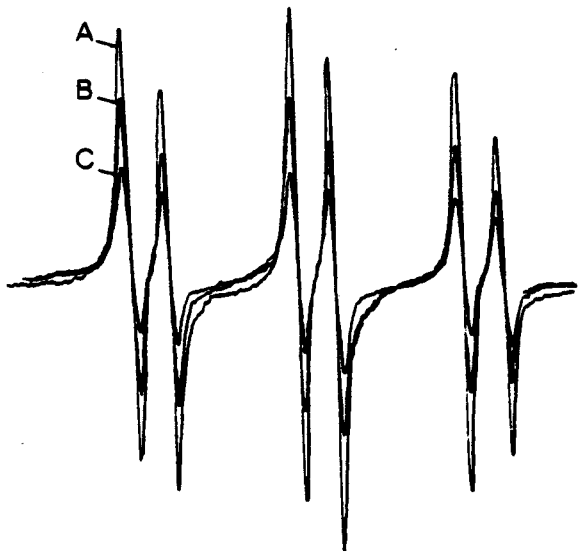

Figure 2 : ESR spin-trapping by phenyl-N-t-butyl-nitrone in the presence of BLM-A_2-Fe(II)-O_2 (A), AMBIGLU-Fe(II)-O_2 (B) and AMBI-A_2-Fe(II)-O_2 (C) complexes at 10 mM concentration. ESR spectra consist of triplet of doublet with a g factor of 2.006 and a_N : 15.3 G.

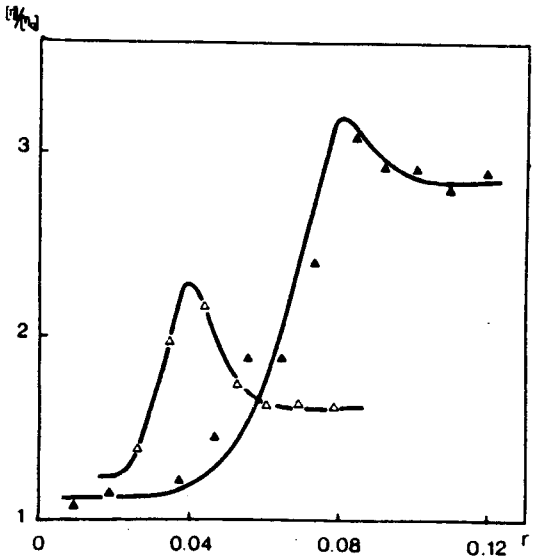

Figure 3 : DNA unwinding produced by AMBIGLU (▲), compared to the one observed for ethidium bromide (△). (DNA : 150 µM, 0.01 SHE buffer).

DNA cleavage : The extent of mono- and double-strand degradation of pBR 322, induced by BLM-A_2, AMBI-A_2 and AMBIGLU was visualized by agarose gel electrophoresis. As illustrated in fig.4a, incubation with BLM-A_2 produces much more double-strand degradation of the plasmid than AMBIGLU does.

The DNA break production (forms II and III) was analysed by densitometry of the gel electrophoretic pattern shown in Fig.4a and of five other experiments (Fig. 4b). The densitometric scanning result shows that with 0.1 μM Blm-Fe(II), about 85 % of the covalently closed supercoiled (form I) pBR 322 DNA was converted to form II. Then, with increasing concentration of Blm-Fe(II) 1 to 5 μM, linear double strand DNA (form III) became the major form, leading to a complete degradation of the DNA with 5 μM (fig. 4a, lane C). In contrast, both synthetic models AMBI-A_2 and AMBIGLU caused DNA degradation basically by single-strand breakage (fig. 4a, lane E-F). As shown in fig. 4b, gradual shift appeared in the production of form II to reach a maximum near 2 μM. The higher DNA cleaving capacity of AMBIGLU compared to AMBI-A_2 was clearly demonstrated when we compared the production of form III. At 10 μM, only 10 % form III DNA was obtained with AMBI-A_2-Fe(II), in contrast to AMBIGLU-Fe(II) for which 10 μM produced about 45 % form III DNA.

DISCUSSION

On the basis of ESR data, the synthetic model AMBIGLU was found to chelate cupric ions in the same conditions as bleomycin does. The ESR parameters similar to those exhibited by the spectra of AMPHIS-Cu(II), AMBI-A_2-Cu(II) and BLM-Cu(II) complexes are in favour of a square-pyramidal coordination geometry (fig. 5).

The copper ligands are undoubtedly the N^{π} and N^{α} of the histidyl residue, the heterocyclic N atom of the pyridine ring, the N atom of the secondary amine, these four atoms forming a square plane, and the primary amine N of the side chain as an apical ligand.

The major structural difference between AMBIGLU and AMBI-A_2 is the presence of a glucosamine residue in the structure of the former. It was reasonable to expect slight differences in the ESR parameters between AMBIGLU-Cu(II) and AMBI-A_2-Cu(II)-complexes spectra as observed between ESR parameters of BLM-A_2 and deglyco-BLM-A_2 (15). In the case of the parent drug and its aglycon, these differences were analyzed in terms of a Jahn-Teller effect : in the absence of the sugar part, a modification of the Cu(II) complex structure occurs with a displacement of the Cu(II) center out of the plane towards the fifth ligand. Such a modification of the geometry of copper complex was not observed by comparison between AMBIGLU and AMBI-A_2. It

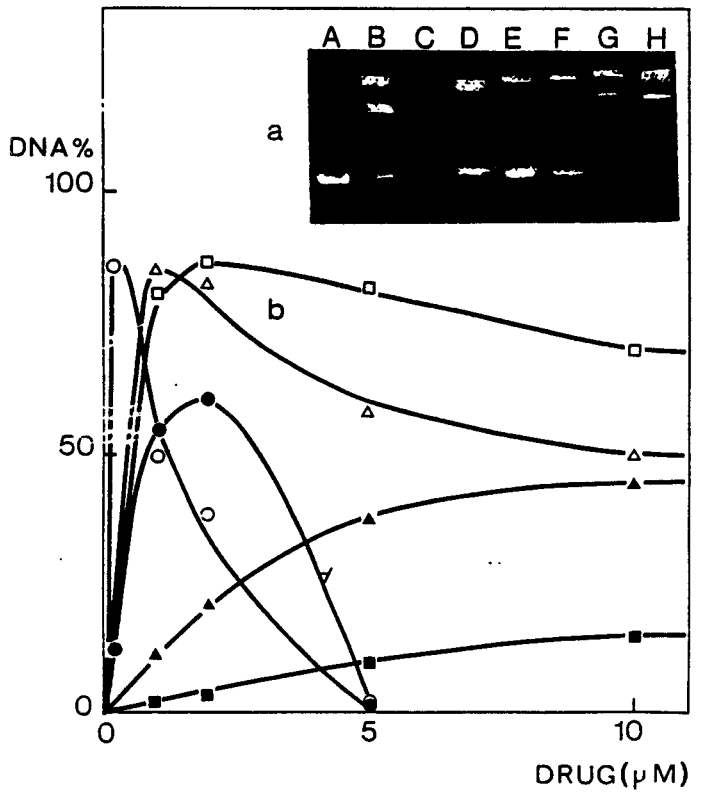

Figure 4 : a) Agarose (1%) gel electrophoretic patterns of ethidium bromide-stained pBR 322 DNA after treatment with AMBI-A_2-Fe(II) complex (lanes D-E), AMBIGLU-Fe(II) complex (lane F-H) and control (lanes A-C). DNA migrated from top to bottom in order of decreasing distance of form I, form III and form II DNAs. Lane A : untreated DNA. Lanes B,C : 0.1, 5 μM Blm-Fe(II). Lanes D,E : 10, 1 μM AMBI-A_2-Fe(II). Lanes F,G,H : 1, 5, 10 μM AMBIGLU-Fe(II).

b) Percentage distribution of DNA conformational isomers after treatment with increasing concentrations of Blm (○,●) AMBI-A_2 (□,■) and AMBIGLU (△,▲). Open and filled symbols represent respectively the forms II and III DNAs. Control experiments with Fe(II) only have been made and are not reported here.

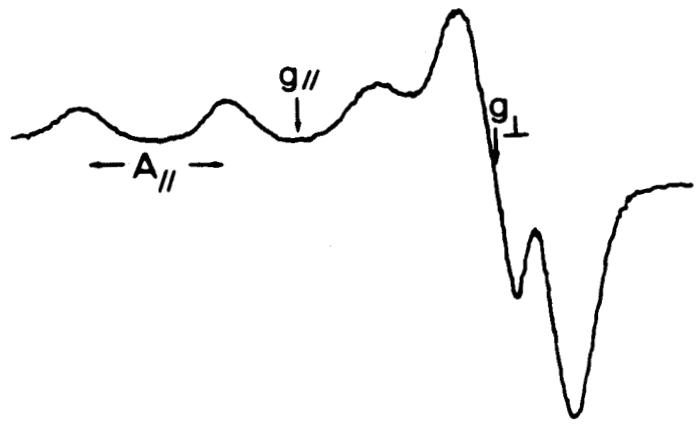

Figure 5 : ESR spectrum and structure of AMBIGLU-Cu(II) complex.

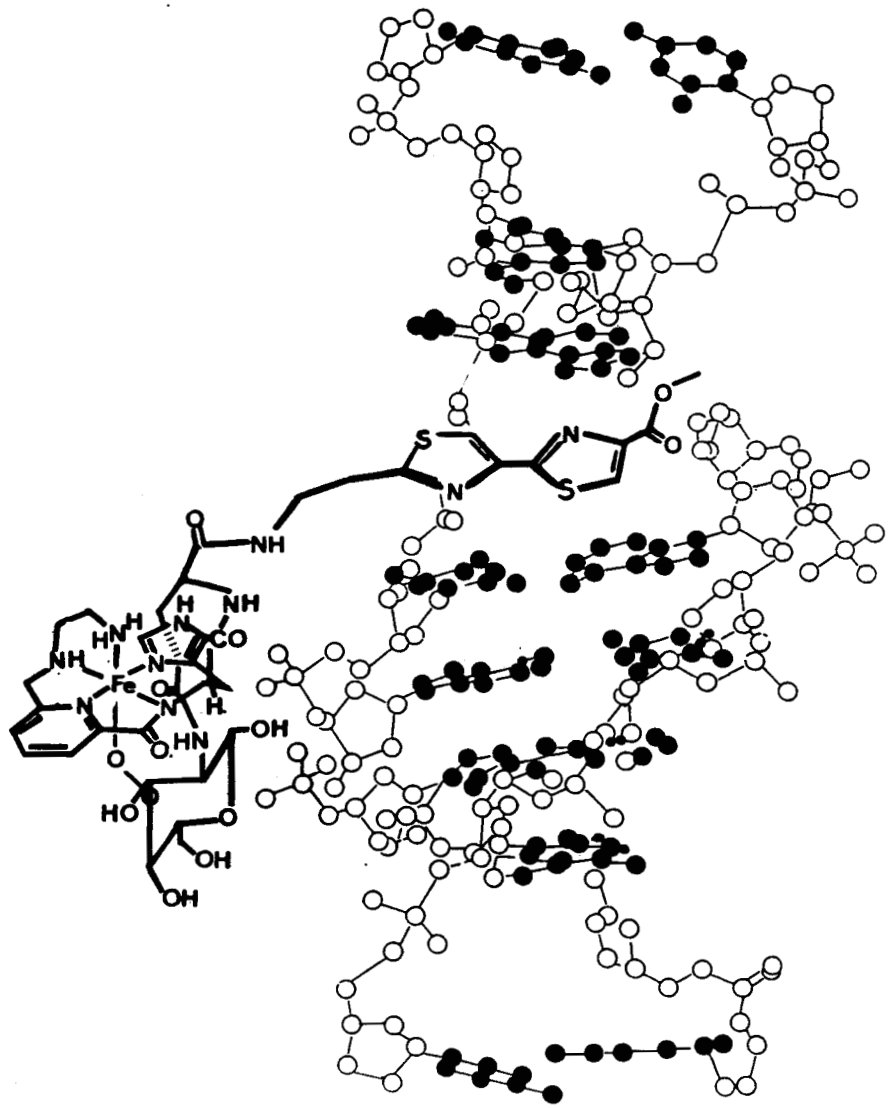

Figure 6 : A proposal for AMBIGLU-DNA interaction.

can be envisaged that in the parent drug the sugar part gulose-mannose plays a role much more important due to the bulky character of the disaccharide.

However, the glucosaminyl group has been demonstrated to be a key element in the stabilization of the ternary complex AMBIGLU-Fe(II)-O_2 and consequently in the activation of the molecular oxygen. The glucosaminyl residue could form a protecting pocket in the surrounding of the oxygen molecule. The presence on the sugar structure of several hydroxyl groups could explain the establishment of hydrogen bondings with oxygen and its activation. The enhanced production of free radicals by AMBIGLU compared to their formation in the presence of AMBI-A_2 is demonstrative on this point.

Moreover, the DNA strands breakage induced by AMBIGLU was found more effective than by AMBI-A_2. This result confirms the role that the glucosamine residue plays in the stabilization of the complex and in the activation of molecular oxygen.

Concerning the mode of binding of AMBIGLU, a partial intercalation of the bithiazole moiety between the base pairs of DNA can be advanced on the basis of viscometry data (fig. 6).

These results demonstrate the importance of the terminal amine in the BLM-DNA binding and confirm previous studies indicating that the interaction of BLM-A_2, and probably of AMBI-A_2, with DNA involved primarily the cationic terminus of the drug. AMBIGLU, which lacks the terminal amine cannot establish ionic bonds with the phosphate backbone of the nucleic acid.

Thus, AMBIGLU which possesses in its structure the main parts necessary to a BLM-like activity, i.e. a pseudopeptide chelating part and a heterocyclic DNA-binding part, appears to be an acceptable model for the design of further medicinal drugs. This study confirms previous results (13) leading to the conclusion that to have a DNA-cleavage activity comparable to that of BLM, both binding and complexing parts are required on the same molecule. In addition, the presence of a glucosamine residue in AMBIGLU enhances its DNA breakage ability relative to other models which do not contain an osidic part. Therefore the role of the sugar part in the activation of oxygen and production of free radicals can be proposed confirming the hypotheses previously advanced by the comparative study of BLM and deglycoBLM (15).

EXPERIMENTAL SECTION

SYNTHESIS

- General : The IR spectra were obtained on a Perkin-Elmer 177 spectro photometer, using KBr pellets. ^{1}H-NMR spectra were recorded on a Brucker WP 80 SY or on a Brucker AM 400 WB spectrophotometers. Chemical shifts are reported in ppm from tetramethylsilane as an internal standard and are given in δ units. EI mass spectra were recorded on a Ribermag R10.10 (combined with Riber 400 data system) mass spectrophotometer at 70 eV by using direct insertion. FAB mass spectra were determined on a Kratos MS-50 RF mass spectrometer arranged in an EBE geometry. The sample was bombarded using a beam of xenon with a kinetic energy of 7 keV. The mass spectrometer was operated at 8 KV accelerating voltage with a mass resolution of 3000. Thin layer chromatography (TLC) was carried out using silica gel 60F-254 Merck (0,25 mm thick) precoated UV-sensitive plates, generally in solvent system A ($CHCl_3$-MeOH, 80 : 20 (v/v) in a satured NH_3 atmosphere). Spots were visualized by inspection under U.V. light at 254 nm and after exposure to vaporized I_2 and/or ninhydrin. Kieselgel 60 (230-400 mesh) of Merck was used for chromatography.

2-deoxy-2[[(1,1-dimethylethoxy)carbonyl]amino]-D-glucopyranose (2)

A solution of glucosamine hydrochloride 1 (6 g, 27.8 mmol, Aldrich) in 1,4 dioxane-H_2O (2/1, v:v, 200 ml), adjusted to pH 9 with dilute NaOH, was treated with di-tert-butyldicarbonate (5.73 g, 27.8 mmol) for 4 h. After removal of dioxane and acidification to pH 3 with dilute HCl, the N-protected sugar 2 precipitated as a white powder with a 87 % yield. mp: 186°C, litt. 191°C (16) ; Rf(pyridine/ethyl acetate/acetic acid/H_2O, 5/5/1/3, v:v:v:v) : 0.82 ; IR ν 1690 (BOC) cm^{-1} ; ^{1}H-NMR 80 MHz(Me_2SO-d_6) δ 1.45 (s, 9H, $(CH_3)_3$), 3.15-3.45 (m, H_2, H_4, H_5, H_6), 4.30 (m, H_3), 4.95 (d, 1H, H_1), 6.0 (m, 1H, NH) ; $[\alpha]_D^{18}$: +20.3°(c 0.1, CH_3OH), litt. $[\alpha]_D^{20}$: +65.5 (c 1, CH_3OH) (16) ; MS-m/e 279 (M^+) ; Anal. Calcd for $C_{14}H_{21}NO_7$: C, 47.3 ; H, 7.5 ; N 5.0 ; Found : C, 46.5 ; H, 7.5 ; N, 4.5.

1,3,4,6-tetra-O-acetyl-2-deoxy-2[[(1,1-dimethylethoxy)carbonyl]amino]-D-glucopyranose (3)

50 ml of acetic anhydride were slowly added to a solution of 2 (6.8 g, 24 mmol) in dry pyridine (50 ml). After stirring for 18 h at room temperature, the solution was evaporated in vacuo, the slurry residue was then dissolved in ethyl acetate and the starting material was extracted with water. The organic layer was dried, and evaporated. Compound 3 was obtained as a white powder with a 97 % yield. mp : 59°C ;

Rf (A) : 0.87 ; IR ν 2990 (NH), 1760 (CO), 1700 (O-CO), 1240 (acetyl CH_3) cm^{-1} ; ^{1}H-NMR 80 MHz(Me_2SO-d_6) δ 1.36 (s, 9H, $(CH_3)_3$), 1.93, 1.98, 2.02, 2.14 (4s, 12H, 4CO-CH_3), 3.95 (m, 2H, H_2-H_5), 4.05 (m, 2H,H_6), 5.05 (m, 2H, H_3-H_4), 5.98 (d, 1H, H_1, J : 5.45 Hz), 6.95 (d, 1H, J : 9.1 Hz) ; $[\alpha]_D^{17.5}$: +18.1° (c O.1, CH_3OH) ; MS-m/e 447 (M^+) ; Anal. Calcd for $C_{19}H_{29}NO_{11}$: C, 51.0 ; H, 6.5 ; N, 3.1 ; Found : C, 51.0 ; H, 6.6 ; N, 2.9.

2-amino-2-deoxy-1,3,4,6-tetra-O-acetylα-D-glucopyranose-hydrochloride (4)

A solution of 3 in 1,4 dioxane was flushed with dry HCl. After 30 min stirring, removal of the solvent left the crude amine 4. This compound was recrystallized from ethanol to give a white powder ; mp : 170°C ; 86% yield ; Rf (A) : 0.66 ; IR ν 2800-3000 (broad, NH_3^+), 1740-1770 (CO), 1240 (acetyl CH_3) cm^{-1} ; ^{1}H-NMR 80 MHz(Me_2SO-d_6) δ 1.94, 1.97, 2.04, 2.19 (4s, 12H, 4CO-CH_3), 3.77 (m, 2H, H_2-H_5), 4.08 (m, 2H, H_6), 5.19 (m, 2H, H_3-H_4), 6.29 (d, 1H, H_1, J : 5.45 Hz), 8.94 (m, 3H, NH_3^+) ; $[\alpha]_D^{17.5}$: +10.1° (c O. 1, CH_3OH), litt. $[\alpha]_D^{21}$: 29.7° (water) (17) ; MS-m/e 347 (M^+) ; Anal. Calcd for $C_{14}H_{22}NO_9Cl$: C, 43.8 ; H, 5.7 ; H, 3.6 ; Found : C, 44.1 ; H, 5.7 ; H, 3.

1,3,4,6-tetra-O-acetyl-2-deoxy-2[(N-tert-butyloxycarbonyl)glutamido α-benzylester]-D-glucopyranose (6)

A solution of α-benzyl tert-butyloxycarbonylglutamate 5 (2.72 g, 8.06 mmol, Serva) in anhydrous CH_2Cl_2 (100 ml) was cooled to 0°C and dicyclohexylcarbodiimide (1.82 g, 8.87 mmol) and 1H-hydroxy-1, 2, 3-benzotriazole hemihydrate (1.35 g, 8.87 mmol) in 10 ml of CH_2Cl_2 were added. After 1 h 30, a cooled (O°C) solution of 4 (3.09 g, 8.06 mmol) in 30 ml of CH_2Cl_2 containing triethylamine (1.12 ml, 8.06 mmol) was added. The mixture was stirred at O°C for 2 h and allowed to rise to room temperature ; stirring was continued for 10 h. The precipitated dicyclohexylurea was collected and the CH_2Cl_2 solution was washed successively with 30 ml of 1N HCl, H_2O and 1M $NaHCO_3$. After drying over Na_2SO_4, the solvent was removed in vacuo. The remaining dicyclohexylurea was discarded by precipitation with acetone. The residue obtained after evaporation of the solvent was thoroughly triturated with diethylether. The yield of crude, chromatographically pure product obtained as a white powder was 3.65 g (68 % yield). mp : 184°C ; Rf (A) : 0.91 ; IR ν 2980 (NH), 1740 (CO), 1690 (OCO), 1670 (CONH), 1220 (acetyl CH_3) cm^{-1} ; ^{1}H-NMR 400MHz(Me_2SO-d_6) δ 1.38 (s, 9H, $(CH_3)_3$), 1.91, 1.97, 2.01, 2.15 (4s, 12H, 4CO-CH_3), 3.95 (m, 2H, H_5-H_2), 4.16 (m, 2H, H_6), 4.25 (m, 1H, aCH), 4.98 (m, 1H, H_3), 5.12 (m, 2H, CH_2Bzl), 5.15 (m, 1H, H_4), 5.93 (d, 1H, H_1), 7.25 (1H, NH-CO), 7.34 (s, 5H, aromatic), 7.98 (m, 1H, NHCO), $[\alpha]_D^{17.8}$: +4.4 (c O.1, $CHCl_3$) ; Anal. Calcd for $C_{31}H_{42}N_2O_{14}$: C, 55.8 ; H, 6.3 ; N, 4.2 ; Found : C, 55.0 ; H, 6.5 ; H, 4.5.

1,3,4,6-tetra-O-acetyl-2-deoxy-2(glutamamido α-benzyl ester)-D-gluco pyranose (7)

The t-BOC protected amine 6 (1 g, 1.5 mmol) was deprotected with pure TFA (10 ml) to give the corresponding free amine 7 in a good yield (> 85 %). After 1 h stirring, the excess of TFA was evaporated and the residue was diluted with absolute ethanol (30 ml) before evaporation of the solvent. This procedure was repeated three times and resulted in the complete elimination of TFA. After thorough drying is necessary to eliminate the retained ethanol - the resulting 7 (hygroscopic powder, 0.95 g, 92 %) is quite suitable for the next reaction. mp : 53°C ; Rf(A) : 0.82 ; IR ν 3200-3600 (broad, NH), 1750 (CO), 1660 (CONH), 1220 (CH_3) cm^{-1} ; FAB-MS : 567 (M^++1) ; Anal. Calcd for $C_{28}H_{35}N_2O_{14}F_3$: C, 49.4 ; H, 5.2 ; N, 4.1 ; Found : C, 48.2 ; H, 5.4 ; H, 4.1.

2-[N-[2-(tert-butyloxycarbonylamino)-ethyl]-N-(benzyloxycarbonyl)-aminomethyl]-pyridine-6-carboxyl-N-π-(benzyloxycarbonyl)-histidyl-γ-[(tetra-O-acetyl)-glucosaminyl]-glutamic acid α-benzyl ester (9)

To 0.44 g (0.55 mmol) of 8 (N-BOC, N-Z, N-AMPHIS see ref. 11) dissolved in 10 ml of dimethylformamide at -15°C were added 73 ml of isobutylchloroformate (0.55 mM) and 61 µl of N-methylmorpholine (0.55 mM). The solution was vigorously stirred for 30 min at -15°C before adding 374 mg (0.55 mM) of 7 and 61 µl of N-methylmorpholine (0.55 mM) in 10 ml of dimethylformamide. The solution was stirred for 15 min at -15°C and overnight at room temperature. Solvent was then evaporated in vacuo (below 50°C). The residue was dissolved in CH_2Cl_2(100 ml) and the solution washed successively with 1N HCl, H_2O, 1M $NaHCO_3$ and saturated aqueous NaCl and dried over Na_2SO_4. The solvent was then evaporated to dryness and the desired product obtained as a grey powder. 67 % yield, Rf(A) : 0.95 ; IR ν 2980 (NH), 1760 (CO), 1680 (OCO), 1220-1250 (CH_3 acetyl) cm^{-1} ; FAB-MS : 1108 (M^+-Z).

2-[N-[-2(tert-butyloxycarbonylamino)-ethyl]-N-(benzyloxycarbonyl)-aminomethyl]-pyridine-6-carboxyl-N-π-(benzyloxycarbonyl)-histidyl-γ-[(tetra-O-acetyl)-glucosaminyl]-glutamic acid (10)

The benzyl ester 9 (0.2 g, 0.16 mmol) was saponified in the presence of aqueous sodium hydroxide in methanol for 48 h at room temperature. After acidification, evaporation of the solvent, trituration in hot absolute ethanol, elimination of sodium chloride by filtration and evaporation of the solvent, the resulting residue was identified as the deacetylated acid 10 : 53 % yield, Rf (A) : 0 ; ^{1}H-NMR (Me_2SO-d_6) δ 1.4 (CH_3), 2.9-4.1 (m, CH_2), 4.25-5.3 (m, aCH, CH-carbohydrate), 6.5 (m, CH_2-histidyl), 7.2

(m, NH), 7.35 (s, CH-benzyl), 7.5-8.4 (m, CH-pyridyl, CH-imidazol, NH); FAB-MS : 991 (M^++1, FAB^+), 989 (M^+-1, FAB^-).

Methyl 2'-[2-[N-[2-(tert-butyloxycarbonylamino)-ethyl]-N-(benzyloxy-carbonyl)-aminomethyl]-pyridine-6-carboxyl-N-π-(benzyloxycarbonyl)-histidyl-(glucosaminyl)-glutamyl-(2-aminoethyl)]-2,4'-bithiazole-4-carboxylate (12)

The acid 10 (50 mg, 0.05 mmol) was coupled to methyl 2'-aminoethyl-2-4'-bithiazole-4-carboxylate 11 (18 mg, 0.05 mmol, see ref 9) using DCC and HOBt as described for 6. The protected compound 12 was purified by flash-chromatography in the system solvent CH_2Cl_2/methanol, 95:5 (v/v). White powder, 46 % yield, Rf(A) : 0.71; FAB-MS : 1242 (M^++1).

Methyl [2'-[2-(2-aminoethyl)-aminomethyl]-pyridine-6-carboxyl-histidyl-γ-(glucosaminyl)-glutamyl-2-(aminoethyl)]-2,4'-bithiazole-4-carboxylate trihydrobromide (AMBIGLU)

A solution of 12 (30 mg, 0.024 mmol) in acetic acid (5 ml) saturated by bromhydric acid was stirred for 15 min and evaporated to dryness. The crude residue is dissolved several times in ethanol and evaporated to assume complete elimination of the HBr. The final product was then dissolved in water, extracted twice with ethyl acetate and CH_2Cl_2. Final lyophilisation of the aqueous layer afforded AMBIGLU as a white powder. 73 % yield, Rf(A) : 0; ^{1}H-NMR (Me_2SO-d_6) δ 2.85-4.1 (m, CH_2), 4.24-5.5 (m, aCH, CH-carbohydrate), 6.5 (m, CH_2-histidyl), 7.2-8.8 (m, CH-pyridyl, CH-imidazol, NH) ; FAB-MS : (M^++1).

ESR measurements

ESR measurements were recorded on a Varian E-109 X-band spectrometer with a dual cavity operating in the TE 104 mode. A 100 kHz high frequency modulation with a maximum amplitude of 8 gauss was used with a 10 mW microwave power and g values were determined from α-α'-diphenyl-β- picrylhydrazyl (g = 2.0036). For the spin trapping experiments, we used a cavity operating in the TM 110 mode with a maximum modulation amplitude of one gauss.

- Cu(II) complexes

Bleomycin-A_2-Cu(II) and AMBIGLU-Cu(II) complexes were prepared by adding cupric perchlorate 10^{-3} M to a pH 6.9 phosphate buffer containing the drugs in a 1:1 ratio, or by adding NaOH to aqueous solutions of the drugs and the cupric ion. The

samples were disposed into a 3 millimeters diameter cylindrical quartz tube. ESR analyses were conducted at 77K on glycerol glasses.

-Spin-trapping technique

The technique of spin-trapping makes use of diamagnetic spin traps which react with free radicals giving rise to relatively more stable ESR-observable free radicals. Phenyl N-t-butyl-nitrone (PBN) (18) was used to detect the production of OH· radicals. The reaction mixture for spin-trapping experiments consisted of 1:1 bleomycin-A_2-Fe(II), or 1:1 AMBIGLU-Fe(II) complexes (10 mM in aqueous solution) and PBN (80 mM ethanolic solution) in buffered solution at pH 6.9 Oxygen was bubbled through the mixture ; an aliquot for the sample solution was rapidly transferred to the quartz flat cell and the spectrum recorded.

Control experiments were made to be sure that ESR spectra neither resulted from nitrone spin trap alone, nor from the separate addition of Fe(II) or drugs.

Viscometry

-Unwinding studies using closed-circular DNA (plasmid pBR 322 containing fragments of adenovirus) were performed essentially as previously described (19,20) using a Ubbelohde semi micro dilution viscometer. Temperature was maintained at 25+-0.01°C in a thermostatically controlled water bath. Flow times were electronically measured to an accuracy of 0.1 s (Schott ABS/G type detector). The viscometer contained 2.0 ml of a 150 µM solution of DNA. AMBIGLU was added in increments of 5-10 µl from a stock solution (c = 150 µM). Ethidium bromide was used as reference, inducing an unwinding angle of 26° (21).

- For the helical lengthening measurements, calf thymus DNA was reduced to rod-like species with a French press and experiments were done in 0.01 SHE buffer (9.4 mM NaCl/2mM HEPES/10mM EDTA buffer, pH 7.0). Solutions were filtered through 0.45 µm Millipore filters before measurements. The viscometer contained 2.0 ml of a 500 µM solution of DNA. AMBIGLU was added in increments of 5-10 µl from a stock solution (c : 3mM).

DNA degradation

Single-strand and/or double-strand DNA breaks were visualized by the use of supercoiled DNA (form I). The appearence of relaxed circular DNA (form II) and open

linear DNA (form III), with either BLM-A_2, AMBI-A_2 or AMBIGLU was observed on a 1 % agarose gel, containing 0.5 µg/ml of ethidium bromide.

Plasmid pBR 322 was incubated in 50 mM Tris-HCl, pH 8.0 buffer containing 10 mM 2-mercaptoethanol. $Fe(NH_4)_2(SO_4)_2$, $6H_2O$ was added in the same final concentration as the product. After 20 min at room temperature, the reaction was terminated with the addition of EDTA 2.5 mM ; 5 µl of 0.01 % bromophenol blue were added to the reaction mixture (50 µl). Agarose electrophoresis was performed in TBE buffer at 5V/cm for 6 hours and examined under a 254 nm UV light. The negative films of gels were used for densitometric scannings.

ACKNOWLEDGMENTS

The authors are indebted to the Fédération Nationale des Centres de Lutte contre le Cancer and the Insitut National de la Santé et de la Recherche Médicale for financial support.

References

1 - Crooke S.T. (1978) in : Bleomycin : Current Status and NewV Developments (Carter S.K. , Crooke S.T. & Umezawa H., eds.), Academic Press, New-York, pp 1-8.

2 - Carter S.K. (1978) in : Bleomycin : Current Status and New Developments (Carter S.K., Crooke S.T. & Umezawa H., eds.) Academic Press, New-York, pp 9-14.

3 - Umezawa H. (1979) in : Bleomycin : Chemical, Biochemical and Biological Aspects (Hecht S.M., ed.), Springer-Verlag, New-York, pp 24-36.

4 - Sugiura Y., Muraoka Y., Fujii A., Takita T. & Umezawa H. (1979) J. Antibiot. 32, 756-758.

5 - Oberley L.W. & Buettner G.R. (1979) FEBS Lett. 97, 47-49.

6 - Burger R.M., Peisach J. & Horwitz S.B. (1981) J. Biol. Chem. 256, 11636-11644.

7 - Chien M., Grollman A.P. & Horwitz S.B. (1977) Biochemistry 16, 3641- 3647.

8 - Houssin R., Bernier J-L. & Hénichart J-P. (1984) J. Heterocyclic Chem. 21, 465-469.

9 - Houssin R., Bernier J-L. & Hénichart J-P. (1984) J. Heterocyclic Chem. 21, 681-683.

10 - Hénichart J-P., Bernier J-L., Helbecque N. & Houssin R. (1985) Nucl. Acids Res. 13, 6703-6717.

11 - Hénichart J-P., Houssin R., Bernier J-L. & Catteau J-P. (1982) J. Chem. Soc., Chem. Commun., 1295-1297.

12 - Hénichart J-P., Bernier J-L., Houssin R., Lohez M., Kenani A. & Catteau J-P. (1985) Biochem. Biophys. Res. Commun. 126, 1036-1041.

13 - Kenani A., Lohez M., Houssin R., Helbecque N., Bernier J-L., Lemay P. & Hénichart J-P. (1987) Anti-Cancer Drug Design 2, 47-59.

14 - Kenani A., Lamblin G. & Hénichart J-P. (1988) Carbohydr. Res. 177, 81-89.

15 - Kenani A., Bailly C., Helbecque N., Catteau J-P., Houssin R., Bernier J-L. & Hénichart J-P. (1988) Biochem. J. 253, 497-504.

16 - Pozbnev V.F. (1980) Khimia Prirod. Soedin. 3, 408-409.

17 - Bergmann M. & Zervas L. (1931) Ber. 64B, 975-980.

18 - Janzen E.G. & Blackburn B.J. (1968) J. Am. Chem. Soc. 90, 5909-5910.

19 - Saucier J.M., Festy B. & Le Pecq J.B. (1971) Biochimie 53, 973-980.

20 - Revet B.M.J., Schmid M. & Vinograd J. (1971) Nature New Biology 229, 10-13.

21 - Wang J.C. (1974) J. Mol. Biol. 89, 783-801.

22 - Harbour J.R., Chow V. & Bolton J.R. (1974) Can. J. Chem. 52, 3549-3561.

23 - Sugiura Y. & Kikuchi T. (1978) J. Antibiot. 31, 1310-1315.

24 - Cohen G. & Eisenberg H. (1966) Biopolymers 4, 429-440.

Avec ce modèle AMBIGLU, le but physicochimique que nous nous étions fixé, à savoir mimer le mode d'action de la Blm, était atteint. Mais l'activité pharmacologique est restée discrète. Une statégie nouvelle fut alors envisagée.

2°) Les modèles hybrides : bléomycine-anilinoamino-9 acridine.

En 1975, Bearden et Haidle démontraient que la dégradation de l'ADN induite par la Blm était potentialisée par la présence d'intercalants comme le bromure d'ethidium, l'actinomycine ou un dérivé de l'acridine : la proflavine. Il fut par la suite mis en évidence que les changements de conformation de l'ADN induits par l'intercalation permettent une meilleure liaison de la Blm à sa cible. (AGOSTINO et al., 1984).

L'amplification est observée avec des composés cationiques polyaromatiques intercalants (GRIGG et al., 1984) mais également avec des non intercalants. Strekowski et al., ont montré qu'il existait une relation étroite entre l'aptitude de ces composés à modifier la structure tertiaire de l'ADN et leur capacité à potentialiser la coupure d'ADN induite par la Blm. En général, plus la structure de l'ADN est perturbée, plus l'amplification est importante (STREKOWSKI et al., 1986, 1987, 1988a).

L'association covalente Blm-intercalant, se révélait ainsi parfaitement justifiée. En ce qui concerne l'intercalant, le chromophore anilinoacridine a été logiquement choisi compte tenu d'une part de la bonne connaissance de son mécanisme de liaison à l'ADN (HENICHART et al., 1982b) et d'autre part d'une étude menée également au laboratoire démontrant le rôle catalytique exercé par la Blm sur l'oxydation de l'amsacrine (le dérivé actif de l'anilinoamino-9 acridine)(BERNIER et al., 1986b).

La fraction complexante AMPHIS n'a pas été changée car elle répondait parfaitement aux hypothèses posées initialement, d'autant plus que ce modèle synthétique avait été repris avec succès par l'équipe de S. Hecht aux Etats-Unis (KILKUSKIE et al., 1985).

AMPHIS a été greffé au fragment intercalant anilinoamino-9 acridine. Dans un premier temps, des bras espaceurs linéaires du type γ-amino-butyrylglycyle (ou Gaba-Gly) ou ramifiés du type (N-morpholino-3 propylamino)-γ glutamylglycyle ont servi de lien entre les deux fragments complexant et intercalant.

Les deux composés **AGGA** (pour **A**mphis-**G**aba-**G**ly-**A**nilinoaminoacridine) et **AGAMGA** (pour **A**mphis-**G**lu(**A**minopropyl-**M**orpholine)-**G**ly-**A**nilinoaminoacridine) ont été étudiés. Ce travail a été publié :

article n°7 :

Design of two metal-chelating, DNA-binding models : molecular combinations of bleomycin and amsacrine antitumour drugs.

BAILLY C., BERNIER J-L., HOUSSIN R., HELBECQUE N., HENICHART J-P.

Anti-Cancer Drug Design 1987, 1, 303-312.

Anti-Cancer Drug Design (1987), **1**, 303–312

Design of two metal-chelating, DNA-binding models: molecular combinations of bleomycin and amsacrine anti-tumour drugs

C. Bailly[1], J.L. Bernier[1], R. Houssin[2], N. Helbecque[1] & J.P. Hénichart[1]

[1]*INSERM U16, Département de Biochimie, place de Verdun, 59045 Lille, and* [2]*Institut de Chimie Pharmaceutique, Faculté de Pharmacie, rue Laguesse, 59045 Lille, France*

Summary: In the course of studies on bleomycin, we recently showed that the bithiazole ring is a poor intercalator into DNA. Therefore we have designed new models, replacing this heterocyclic moiety by an anilinoacridine ring in order to increase the affinity for DNA. This work presents results obtained for two model compounds showing (i) that the anilinoacridine nucleus leads to a good stabilization of the DNA helix, and (ii) that the presence of a bulky group near the complexing part of bleomycin is essential to the activation of molecular oxygen.

The bleomycins are a group of glycopeptide anti-tumour drugs used in the treatment of Hodgkin's lymphoma, carcinomas of the skin, head, neck, and tumours of the testis (Carter, 1978, 1985; Crooke, 1978). Many studies have been devoted to the mode of action of bleomycin. A pseudo-peptidic part of the molecule is able to combine with iron(II) and molecular oxygen to form an active complex responsible for the cleavage of DNA (Sausville *et al.*, 1978; Oppenheimer *et al.*, 1979; Burger *et al.*, 1981; Giloni *et al.*, 1981). A bithiazole-containing moiety contributes to the binding of bleomycin to DNA (Chien *et al.*, 1977; Povirk *et al.*, 1979; Chen *et al.*, 1980).

On account of the coplanarity of the bithiazole rings, model studies (Miller *et al.*, 1985) and spectroscopic measurements (Chien *et al.*, 1977; Lin & Grollman, 1981) are in favour of an intercalative binding process. We have recently proposed a binding model involving a partial insertion of one thiazole ring which wedges in between DNA base pairs. This non-intercalative binding mode has been established on the basis of thermal denaturation data and viscometry experiments (Hénichart *et al.*, 1985).

Moreover, in order to improve the full stacking interaction with the bases, we have replaced the bithiazole ring with a condensed heterocycle, namely, a triazolothiazolylthiazole, with the intention of inducing a more extended electronic π-cloud. The binding of this compound to DNA is characterized by helix extension and DNA unwinding in accordance with the properties of a classical intercalator (Houssin *et al.*, 1986).

We report here the design, synthesis, DNA binding and chelating properties of new model compounds including a simplified complexing part of bleomycin named AMPHIS (methyl 2-(2-aminoethyl)-aminomethyl-pyridine-6-carboxylhistidinate, Hénichart *et al.*, 1982a) and a more potent intercalative moiety involving the 9-anilinoacridine ring linked by a peptide chain structurally related to the aliphatic chain of bleomycin. The first product synthesized in this series possesses a GABA (γ-aminobutyric acid)-Gly aliphatic chain and will be abbreviated as AGGA, i.e. [[(amino-2-ethyl)-2-aminomethyl]-2-pyridine-6-carboxylhistidyl-amino-4-butyryl-glycylamino]-4-phenyl-1-amino-9-acridine

Correspondence: J.P. Hénichart
Received 17 *October* 1986; *accepted* 2 *January* 1987

(Figure 1). The other derivative which will be reported here, AGAMGA (Figure 2), has a hydrophilic (*N*-morpholino-3-propylamino)-γ-glutamylglycyl linking chain. The choice of 9-anilinoacridine in replacement of the bithiazole ring of bleomycin is due to the fact that anilinoacridines have been reported to exhibit a high experimental anti-tumour activity (Cain & Atwell, 1974) and one of the derivatives of the series, *m*-AMSA (amsacrine), has been found to be an active anti-leukaemia drug (Arlin *et al.*, 1980; Baguley, 1984). Anilinoacridine binds to DNA by intercalation of the acridine moiety (Waring, 1976) and location of the anilino group in the minor groove of the DNA double helix (Wilson *et al.*, 1981). Attempting to take advantage of the proven specificity of peptides for DNA, we have incorporated oligopeptides into the

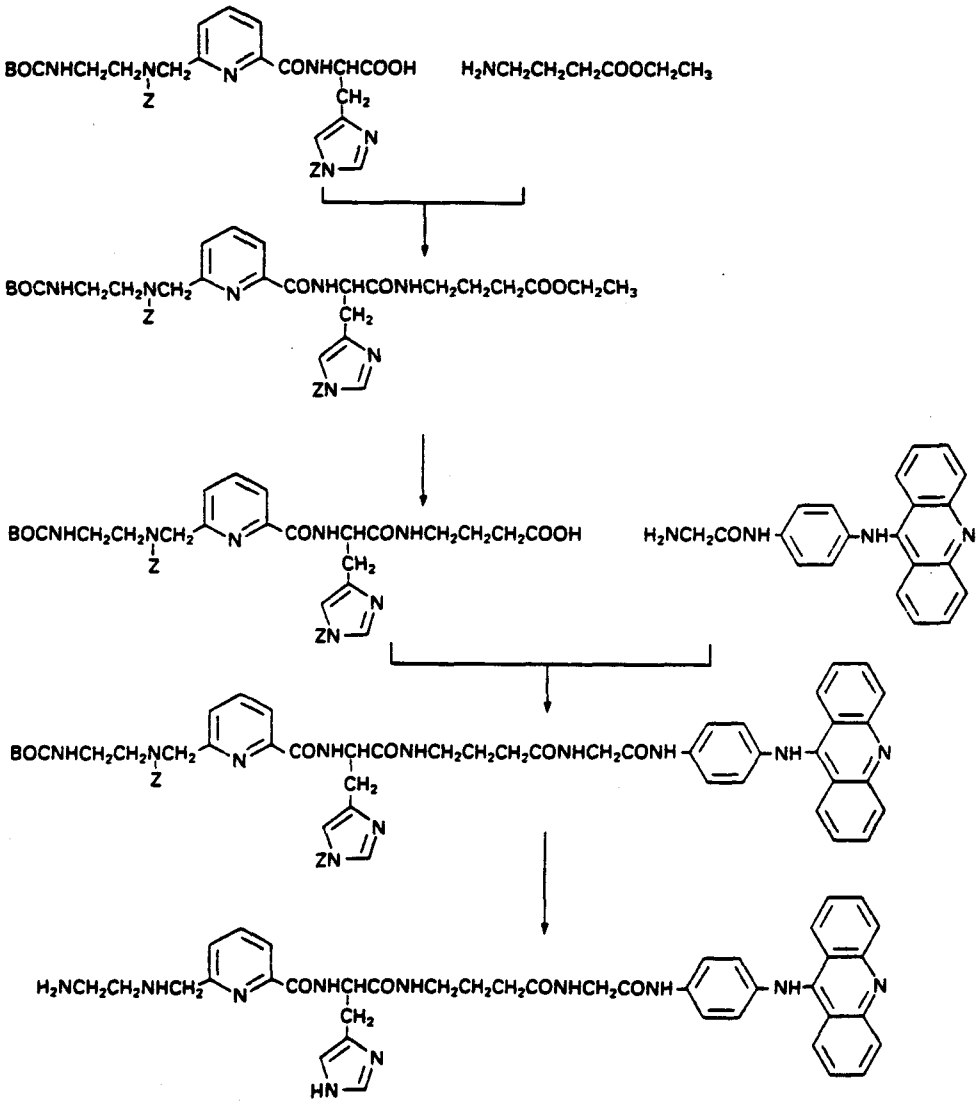

Figure 1 Synthesis of AGGA. BOC = *t*-butyloxycarbonyl; Z = benzyloxycarbonyl

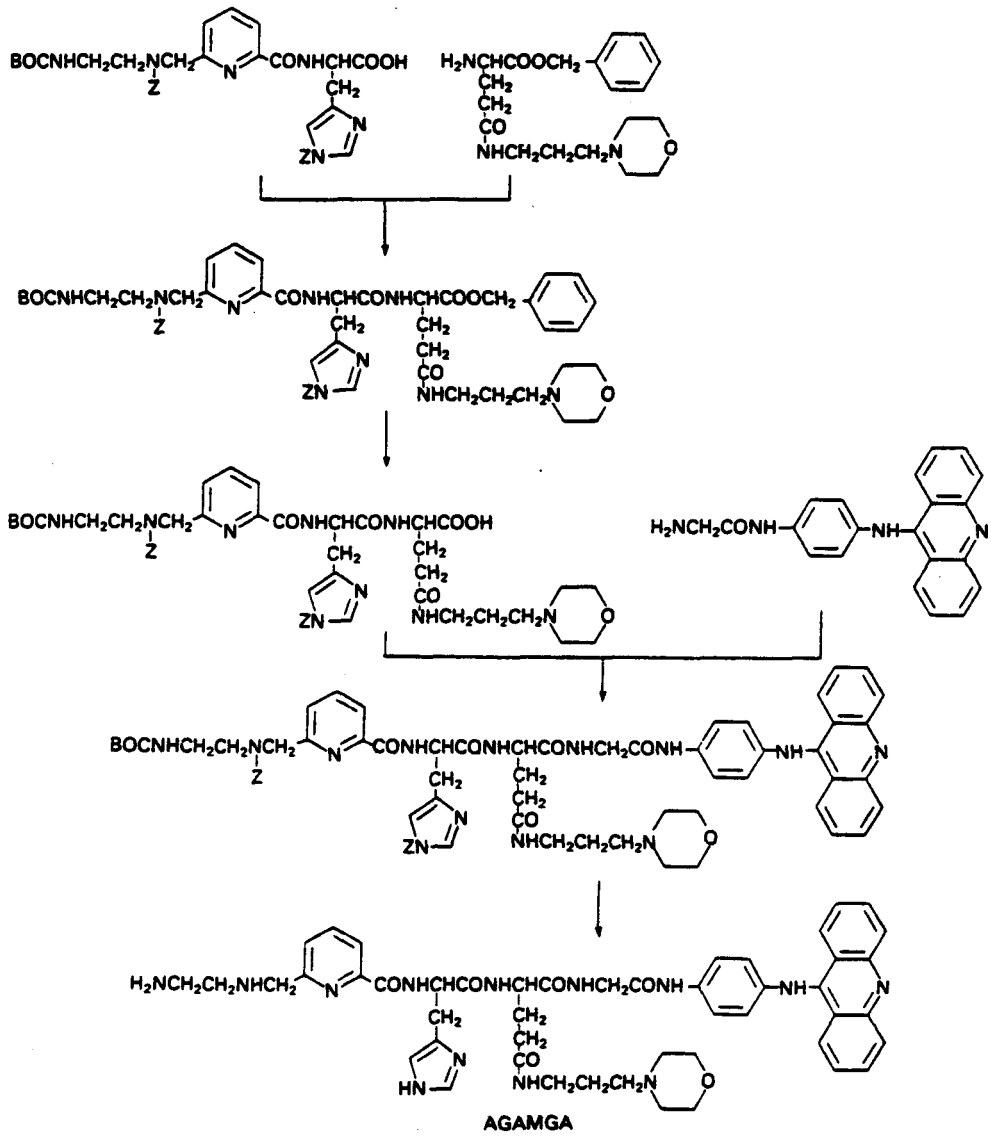

Figure 2 Synthesis of AGAMGA. BOC = *t*-butyloxycarbonyl; Z = benzyloxycarbonyl

side chain of 9-anilinoacridine with the intention of enhancing affinity for DNA (Hénichart *et al.*, 1982b).

Although intercalation of *m*-AMSA was found to be one of the primary steps of the biological activity, it has been claimed that the anti-neoplastic activity of the drug involves an oxidative pathway: *m*-AMSA is oxidized in the presence of Cu(II) ions and molecular oxygen with simultaneous production of superoxide ions inducing DNA strand scission (Wong *et al.*, 1984a, b). The presence of a methoxy group at the *meta* position on the phenyl ring of *m*-AMSA seems to be crucial in this mechanism. Indeed, 4'-(9-acridinylamino)methanesulphon-*ortho*-aniside (*o*-AMSA), on which the methoxy group is located at the *ortho* position, intercalates into DNA leading to the same unwinding angle as *m*-AMSA (Waring, 1976) but is ineffective in inducing DNA strand breaks (Wong *et al.*, 1984a, b)

and protein-associated DNA breakage (Zwelling *et al.*, 1981). Furthermore, *o*-AMSA does not interact with Cu(II) ions in a redox reaction (Wong *et al.*, 1984a, b) and is essentially inactive in killing L1210 leukaemia cells. Thus it is conceivable that the anti-tumour activity of *m*-AMSA may be dependent on its ability to form coordinate complexes with a transition metal ion involving the oxygen atom of the *meta*-methoxy group. The DNA breakage, or the protein-associated DNA breakage, can be induced by the redox reaction of a metal close to a site where damage to DNA may readily occur and by the formation of a quinonimine (Shoemaker *et al.*, 1984) reacting as an electrophile able to bind covalently on the nucleic bases or on the associated proteins. Such a mechanism has been postulated for other anti-tumour drugs such as adriamycin (Someya & Tanaka, 1979) or mitomycin C (Iyengar *et al.*, 1986). These observations prompted us to investigate the association of the simplified complexing part of bleomycin with the anilinoacridine part of *m*-AMSA on the same molecule. This model appears interesting on two accounts. On the one hand, the former part brings a metallic ion into the proximity of the intercalative aminoacridine moiety. Thus, unwinding and cutting of the double helix can be induced either by a redox mechanism or by a covalent binding to nucleic bases or their associated proteins. On the other hand, such a model can be considered as a bleomycin-like molecule with enhanced intercalative properties.

Materials and methods

Synthesis of AGGA

The simplified model of the complexing part of bleomycin, AMPHIS, was prepared according to a previously published procedure (Hénichart *et al.*, 1982a), purified using flash chromatography (Still *et al.*, 1978) on silica gel eluted with 9:1 dichloromethane–methanol and then analyzed by mass spectrometry (laser desorption: 347 (M + H), 260, 219, 201, 183; SIMS-ionization: 368 (M − H + Na), 239, 218, 125, 91). After saponification of protected AMPHIS at room temperature in the presence of NaOH, the corresponding free acid was submitted to a coupling reaction with ethyl γ-aminobutyrate, in the presence of dicyclohexylcarbodiimide (DCCI) and hydroxybenzotriazole in dichloromethane at 0°C for 2 h, then at room temperature for 12 h. After filtration of dicyclohexylurea, purification by successive washings with 1 N hydrochloric acid, 1 M sodium bicarbonate and water, and drying over sodium sulphate, the solvent was evaporated under reduced pressure and the residue crystallized in diethyl ether. Free acid was obtained by saponification at room temperature.

The above acid was coupled with 4-(9-acridinylamino)-*N*-glycylaniline (Hénichart *et al.*, 1982b) in the presence of isobutyl chloroformate and *N*-methylmorpholine at −20°C to give protected AGGA after classical purifications. Protecting *t*-butyloxycarbonyl- (BOC) and benzyloxycarbonyl- (Z) groups were both removed by hydrobromic acid in acetic acid medium and AGGA was purified by flash chromatography (n.m.r., δ[$(CD_3)_2SO$] 9.10, 8.40, 8.15, 7.17, 7.0 (s, NH); 8.10–7.40 (m, aromatic and heterocyclic protons); 4.70–3.65 (m, CH_2)).

Synthesis of AGAMGA

The strategy for the synthesis of AGAMGA is similar to that used for AGGA. The 3-morpholinopropylamino-γ-glutamyl residue was introduced in the synthetic sequence in place of GABA, in similar conditions. This amide was prepared by coupling 3-morpholinopropylamine with α-benzyl *N*-α-BOC-glutamate in the presence of DCCI and hydroxybenzotriazole. Partial deprotection by cleaving of the BOC substituent in trifluoroacetic acid medium allowed coupling with AMPHIS. After subsequent saponification of the benzyl ester, coupling with 4-(9-acridinylamino)-*N*-glycylaniline was carried out in the above conditions. Protecting BOC- and Z-groups were removed by hydrobromic acid in acetic acid and pure AGAMGA was obtained after flash chromatography (n.m.r.,

δ[$(CD_3)_2SO$] 8.20, 7.45, 7.27, 7.17, 7.0 (s, NH); 8.05–7.40 (m, aromatic and heterocyclic protons); 4.0, 3.60 (t, morpholine CH_2); 3.15–2.90 (m, CH_2)).

Melting temperature studies

Calf thymus DNA (type I, highly polymerized, sodium salt, Sigma Chemical Co.) was dissolved in 0.1 SSC buffer (0.15 M NaCl, 0.015 M sodium citrate, pH 7.0). The concentration expressed in terms of the nucleotide as a unit of DNA was determined spectrophotometrically at 260 nm by using a molar absorption coefficient of 6600 M cm^{-1}. Melting curves were measured using a Uvikon Kontron 810/820 spectrophotometer coupled to a Uvikon Recorder 21 and a Uvikon Thermoprinter 48. Samples were placed in a thermostatically controlled cell-holder (10-mm pathlength). The cuvette was heated by circulating water from a Haake unit set. The temperature inside the cuvette was monitored using a thermocouple in contact with the solution. The absorbance at 260 nm was measured over the range 20–95°C with a heating rate of 1°C/min. The 'melting' temperature (T_m) was taken to be the mid-point of the hyperchromic transition.

Viscometry

Unwinding studies using closed-circular DNA (plasmid pBR322 containing fragments of adenovirus) were performed essentially as previously described (Saucier *et al.*, 1971; Revet *et al.*, 1971) using a Ubbelohde semimicro dilution viscometer. Temperature was maintained at 25 ± 0.01°C in a thermostatically controlled water bath. Flow times were electronically measured to an accuracy of 0.1 s (Schott ABS/G type detector). The viscometer contained 2.0 ml of a 150-μM solution of DNA. Drugs were added in increments of 5–10 μl from a stock solution (c = 150 μM). Flow times were measured with an accuracy of 0.1 s. Ethidium bromide was used as reference, inducing an unwinding angle of 26° (Wang, 1974).

E.s.r. measurements

E.s.r. measurements were recorded on a Bruker ESP 300 X-band spectrometer with a TE 102 cavity. A 100 kHz frequency modulation was used with a 50 mW microwave power and g values were determined from α,α'-diphenyl-β-picrylhydrazyl (g = 2.0036). The simple solutions were disposed into a flat quartz cell.

Cu(II) complexes

Bleomycin-A_2–Cu(II), AGGA–Cu(II) and AGAMGA–Cu(II) complexes were prepared by adding cupric perchlorate 10^{-3} M to a pH 6.9 phosphate buffer containing the drugs in a 1:1 ratio, or by adding NaOH to aqueous solutions of the drugs and the cupric ion. E.s.r. analyses were conducted at 77K on glycerol glasses.

Spin-trapping technique

Bleomycin-A_2–Fe(II), AGGA–Fe(II) and AGAMGA–Fe(II) complexes were prepared by the addition of stoichiometric amounts of ammonium Fe(II) sulphate hexahydrate to the drugs. Complexes are air-sensitive and readily oxidized to Fe(III) complexes with the production of radicals.

The technique of spin-trapping makes use of diamagnetic spin traps which react with free radicals giving rise to relatively more stable e.s.r.-observable free radicals. Phenyl *N*-*t*-butyl-nitrone (PBN) (Janzen & Blackburn, 1968) was used to detect the production of $OH^{\cdot}$ radicals. The reaction mixture for spin-trapping experiments consisted of 1:1 bleomycin-A_2–Fe(II), 1:1 AGGA–Fe(II) and 1:1 AGAMGA–Fe(II) complexes (10 mM in aqueous solution) and PBN (80 mM ethanolic solution) in buffered solution at pH 6.9. Oxygen was bubbled through the mixture; an aliquot of the sample solution was rapidly transferred to the quartz flat cell and the spectrum recorded.

Control experiments were made to be sure that e.s.r. spectra neither resulted from nitrone spin trap alone, nor from the separate addition of Fe(II) or drugs.

Results

Cu(II) complexes

Bleomycin, AGGA and AGAMGA provide, in the presence of Cu(II) ions, stable complexes well characterized by e.s.r. (Figure 3). E.s.r. constants have been easily measured from corresponding spectra: $g_{\parallel} = 2.204$, $g_{\perp} = 2.050$, $A_{\parallel} = 177.5$ G. These values allow the determination of the nature of the Cu(II) ligands. The N_{π} and the deprotonated N_{α} of histidine, the heterocyclic N of the pyridine ring and the secondary amino group occupy the square basal positions of a square-pyramidal structure where the primary amino group represents the fifth ligand.

Spin-trapping

The radicals generated by AGGA and AGAMGA in the presence of Fe(II) ions and oxygen give rise to the formation of $OH^{\cdot}$ radical adducts with PBN as spin trap, characterized by the corresponding e.s.r. spectrum: triplet of doublet with $g = 2.006$ and $A_N = 15.3$ G. These values are identical to those found by Harbour *et al.* (1974) who could detect a PBN adduct from an Fe(II)–H_2O_2 system and assigned unambiguously this adduct to PBN–OH produced by $OH^{\cdot}$ radical trapping. Control experiments were made on PBN, ammonium Fe(II) sulphate and drugs used separately, and are essential if one is to draw meaningful conclusions based on the spin-trapping of $OH^{\cdot}$ radicals, which did not produce the same e.s.r. signals.

Figure 4 clearly shows that the spin density of radicals produced by AGGA–Fe(II)–O_2 and AGAMGA–Fe(II)–O_2 are significantly different.

Melting temperature studies

The T_m of calf thymus DNA was 68.7 ± 0.2°C. $T_m$values obtained after interaction of bleomycin, AGGA and AGAMGA are reported in Table I.

The ΔT_m value found for AGGA is of the same order of magnitude as those obtained for 9-aminoacridine or 9-anilinoacridine, whereas AGAMGA does not produce the same stabilization; the ΔT_m value found for this compound is of the same order of magnitude as that for bleomycin.

Unwinding

The change in the superhelicity of circular DNA, a necessary consequence of intercala-

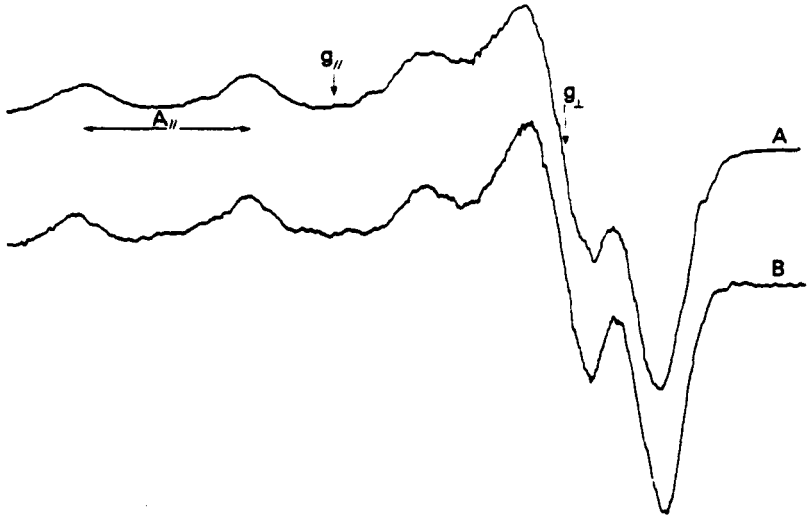

Figure 3 Electron spin resonance spectra of AGGA–Cu(II) (A) and AGAMGA–Cu(II) (B) complexes at pH 9

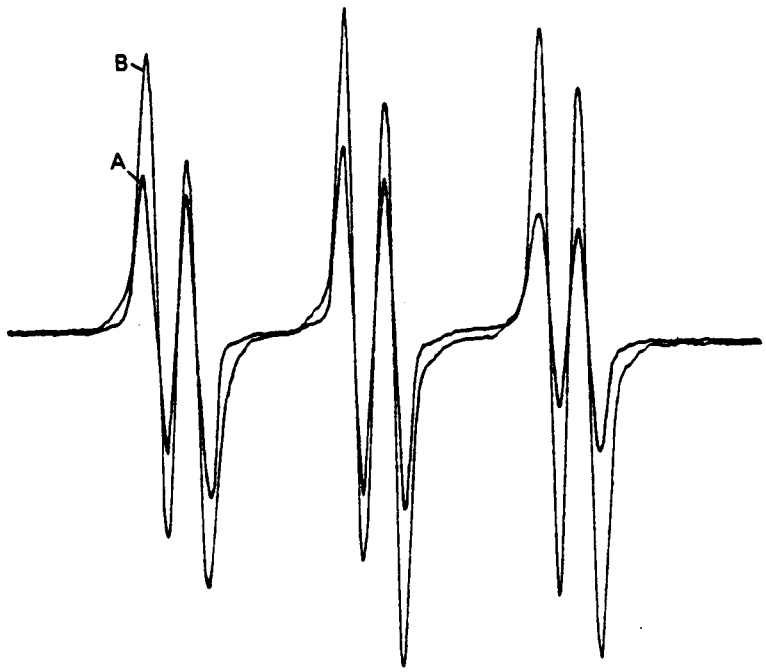

Figure 4 Electron spin resonance spin-trapping by phenyl *N*-*t*-butyl-nitrone in the presence of AGGA–Fe(II)–O_2 (A) and AGAMGA–Fe(II)–O_2 (B) complexes

Table I. Effect of bleomycin, amsacrine (*m*-AMSA), AGGA and AGAMGA on the T_m of the helix-coil transition of calf thymus DNA (10^{-4} M) in 0.1 SSC buffer, pH 7.0. The ΔT_m values are the expression of four measurements made for each drug

	Bleomycin A_2	m-*AMSA*	*AGGA*	*AGAMGA*
ΔT_m	+2.5	+7	+8	+1.5

tion, was followed by viscosity of the complexes AGGA–DNA and AGAMGA–DNA as increasing amounts of dye were added. The degree of angular unwinding measured by the reversal of negative supercoiling in a covalently closed-circular double-stranded DNA, is conventionally calculated relative to the 26° value for ethidium (Wang, 1974). By addition of AGGA, the right-handed superhelical turns were removed until the DNA was completely relaxed. No such effect was observed for AGAMGA. If more AGGA was added, a necessary reversal of the supercoiling, indicative of intercalation, occurred with the formation of a left-handed superhelical structure. If AGAMGA did not produce any effect on supercoiling, AGGA caused an unwinding angle of 7°, a value which is similar to the total amount of unwinding observed with classical intercalators such as daunomycin (Jain *et al.*, 1977) or some derivatives of 9-aminoacridine (Braithwaite & Baguley, 1980).

Discussion

AGGA and AGAMGA exhibit a common structural feature which constitutes the minimum structural requirement necessary for metal binding. This feature permits one to determine unambiguously the nature of the ligands for Cu(II) or Fe(II) in the metal complexes of bleomycin. The secondary amine *N*, the *N* atoms of the heterocyclic nuclei pyrimidine and imidazole and the N_α

of histidine form a square plane centred on the metal ion. The *N* atom of the terminal primary amine group constitutes the apical ligand of the metal ion. It is therefore demonstrated that the bithiazole ring, which may be a metal ligand (Sheridan & Gupta, 1981), and the carbohydrate moiety, are not involved in the metal complexation (Hénichart *et al.*, 1982a).

Both models are able to produce oxygenated free radicals in the presence of Fe(II) and molecular oxygen but AGGA and AGAMGA do not activate molecular oxygen at the same level. The spin density was found to be significantly lower for radicals produced by AGGA than for radicals produced by AGAMGA. This could be explained in terms of stabilization of the AGAMGA–Fe(II)–O_2 complex by the morpholinopropyl chain of AGAMGA. The bulky morpholine group could form a binding site pocket around the molecular oxygen potentially stabilized by hydrogen bondings with the peptidic moiety. A similar stabilization has been observed for the haemoglobin–Fe(II)–O_2 complex in which histidine and adjacent peptide bonds are able to establish hydrogen bondings with oxygen (Shaanan, 1982). The detection of free radicals using spin traps in aerobic Fe(II)–AGGA or Fe(II)–AGAMGA solutions has been carried out with a view to demonstrating that both synthetic models were able to produce hydroxyl radicals in a manner similar to mixtures containing bleomycin–Fe(II) and spin-trapping reagents (Sugiura & Kikuchi, 1978; Oberley & Buettner, 1979). Nevertheless, it is clear that production of diffusible $OH^{\cdot}$ radicals is low compared to drug concentrations. This feature was observed for bleomycin and it has been established that the DNA-nicking reaction involves an activated bleomycin complex containing iron-bound oxygen (Burger *et al.*, 1981).

This activated bleomycin, responsible for hydrogen atom abstraction from the C-4′ position and subsequent rupture of the (C-3′)–(C-4′) bond of deoxyribose (Giloni *et al.*, 1981) was found to display an e.s.r. spectrum typical of a low-spin ferric species (Burger *et al.*, 1981). Under our conditions, such a spectrum was not observed and this could be explained by the presence of an anilinoacridine group in the vicinity of the complexing part of the molecules. The anilinoacridine ring is oxidized to a quinonimine (Bernier *et al.*, 1986) and consequently the oxidative forms of iron complexes are not stable.

The results of thermal denaturation and unwinding studies indicate that meanwhile AGGA is able to stabilize the DNA helix by the same mechanism as *m*-AMSA or anilinoacridine derivatives; AGAMGA does not intercalate its aminoacridine residue between DNA base pairs. The introduction of a morpholinopropyl side chain useful for stabilization of the Fe(II)–O_2 complex, as shown above, induces a steric constraint for the accessibility of the anilinoacridine group to the intercalative site. In addition, the basicity of the morpholino group facilitates the establishment of electrostatic bonds with a phosphate group of the DNA helix. When these bonds are established, the bulky morpholinopropyl group prevents the aromatic residue from intercalating in DNA.

In conclusion, the results provide evidence that the anilinoacridine nucleus is a good candidate for DNA binding, inducing a better stabilization of the helix than the bithiazole ring which was found to be a poor intercalator (Hénichart *et al.*, 1985). The second important result of the present work is that a bulky group in the surrounding of the complexing part is necessary to facilitate the activation of molecular oxygen. The presence of proton donors on this moiety is favourable but strong basic groups must be avoided. The disaccharide moiety of bleomycin seems to meet these requirements apart from its putative capacity to recognize some part of the cell membrane. The design and synthesis of simplified adequate molecules taking into account these considerations are in progress in our laboratory.

Acknowledgements

The authors are grateful to Michèle Lohez for help with the experimental work.

This work was supported by grants from the Institut de la Santé et de la Recherche Médicale and from the Fédération Nationale des Centres de Lutte contre le Cancer.

References

ARLIN, Z.A., SKLARUFF, R.B., GEE, T.S. & 4 others (1980). Phase I and II trial of 4'-(9-acridinylamino)methanesulfon-*m*-anisidide in patients with acute leukemia. *Cancer Research*, **40**, 3304.

BAGULEY, B.C. (1984). Amsacrine: a new anti-leukemia agent. *Drugs Today*, **20**, 237.

BERNIER, J.L., KENANI, A., HOUSSIN, R. & 4 others (1986). Molecular interaction between bleomycin and amsacrine in the presence of cupric ions. *Journal of Inorganic Biochemistry*, **27**, 271.

BRAITHWAITE, A.W. & BAGULEY, B.C. (1980). Existence of an extended series of antitumor compounds which bind to deoxyribonucleic acid by non intercalative means. *Biochemistry*, **19**, 1101.

BURGER, R.M., PEISACH, J. & HORWITZ, S. (1981). Activated bleomycin. A transient complex of drug iron and oxygen that degrades DNA. *Journal of Biological Chemistry*, **256**, 11636.

CAIN, B.F. & ATWELL, G.J. (1974). The experimental anti-tumour properties of three congeners in the acridinyl-methanesulphon-anilide (AMSA) series. *European Journal of Cancer*, **10**, 539.

CARTER, S.K. (1978). The current role of bleomycin in cancer therapy. In *Bleomycin: Current Status and New Developments*. Carter, S.K., Crooke, S.T. & Umezawa, H. (eds), p. 9, Academic Press: New York.

CARTER, S.K. (1985). Bleomycin: more than a decade later. In *Bleomycin Chemotherapy*. Sikic, B.I., Rozencweig, M. & Carter, S.K. (eds), p. 3, Academic Press: New York.

CHEN, D.M., SAKAI, T.T., GLICKSON, J.D. & PATEL, D.J. (1980). Bleomycin-A_2 complexes with poly (dA-dT): a proton nuclear magnetic resonance study of the non-exchangeable hydrogens. *Biochemical and Biophysical Research Communications*, **92**, 197.

CHIEN, M., GROLLMAN, A.P. & HORWITZ, S.B. (1977). Bleomycin–DNA interactions: fluorescence and proton magnetic resonance studies. *Biochemistry*, **16**, 3641.

CROOKE, S.T. (1978). Bleomycin: a brief review. In *Bleomycin: Current Status and New Developments*. Carter, S.K., Crooke, S.T. & Umezawa, H. (eds), p. 1, Academic Press: New York.

GILONI, L., TAKESHITA, M., JOHNSON, F., IDEN, C. & GROLLMAN, A.P. (1981). Bleomycin-induced strand-scission of DNA. Mechanism of deoxyribose cleavage. *Journal of Biological Chemistry*, **256**, 8608.

HARBOUR, J.R., CHOW, V. & BOLTON, J.R. (1974). An electron spin resonance study of the spin adducts of OH and HO_2 radicals with nitrones in the ultraviolet photolysis of aqueous hydrogen peroxide solutions. *Canadian Journal of Chemistry*, **52**, 3549.

HENICHART, J.P., HOUSSIN, R., BERNIER, J.L. & CATTEAU, J.P. (1982a). Synthetic model of a bleomycin metal complex. *Journal of Chemical Society Chemical Communications*, 1295.

HENICHART, J.P., BERNIER, J.L. & CATTEAU, J.P. (1982b). Interaction of 4-(9-acridinylamino)-aniline and derivatives with DNA. Influence of a lysylglycyl side chain on the binding parameters. *Hoppe-Seyler's Zeitschrift für Physiologische Chemie*, **363**, 835.

HENICHART, J.P., BERNIER, J.L., HELBECQUE, N. & HOUSSIN, R. (1985). Is the bithiazole moiety of bleomycin a classical intercalator? *Nucleic Acids Research*, **13**, 6703.

HOUSSIN, R., HELBECQUE, N., BERNIER, J.L. & HENICHART, J.P. (1986). A new bithiazole derivative with intercalative properties. *Journal of Biomolecular Structure and Dynamics*, **4**, 219.

IYENGAR, B.S., SAMI, S.M., TAKAHASHI, T., SIKORSKI, E.E., REMERS, W.A. & BRADNER, W.T. (1986). Mitomycin C analogues with increased metal complexing ability. *Journal of Medicinal Chemistry*, **29**, 1760.

JAIN, S.C., TSAI, C. & SOBELL, H.M. (1977). Visualization of drug–nucleic acid interactions at atomic resolution. II. Structure of an ethidium–dinucleoside monophosphate crystalline complex, ethidium:5-iodocytidylyl(3'–5')-guanosine. *Journal of Molecular Biology*, **114**, 317.

JANZEN, E.G. & BLACKBURN, B.J. (1968). Detection and identification of short-lived free radicals by electron spin resonance trapping technique. *Journal of American Chemical Society*, **90**, 5909.

LIN, S.Y. & GROLLMAN, A.P. (1981). Interactions of a fragment of bleomycin with deoxyribodinucleotides: nuclear magnetic resonance studies. *Biochemistry*, **20**, 7589.

MILLER, K.J., LAUER, M. & CALOCCIA, W. (1985). Interactions of molecules with nucleic acids. Theoretical model for the interaction of a fragment of bleomycin with DNA. *Biopolymers*, **24**, 913.

OBERLEY, L.W. & BUETTNER, G.R. (1979). The production of hydroxyl radical by bleomycin and iron (II). *FEBS Letters*, **97**, 47.

OPPENHEIMER, N.J., RODRIGUEZ, L.O. & HECHT, S.M. (1979). Structural studies of 'active complex' of bleomycin: assignment of ligands to the ferrous ion in a ferrous–bleomycin–carbon monoxide complex. *Proceedings of the National Academy of Sciences of the USA*, **76**, 5616.

POVIRK, L.H., HOGAN, M. & DATTAGUPTA, N. (1979). Binding of bleomycin to DNA: intercalation of the bithiazole rings. *Biochemistry*, **18**, 96.

REVET, B., SCHMIR, M. & VINOGRAD, J. (1971). Direct determination of the superhelix density of closed circular DNA by viscometric titration. *Nature New Biology*, **229**, 10.

SAUCIER, J.M., FESTY, B. & LE PECQ, J.B. (1971). The change of the torsion of DNA helix caused by intercalation. *Biochimie*, **53**, 973.

SAUSVILLE, E.A., PEISACH, J. & HORWITZ, S.B. (1978). Effect of chelating agents and metal ions on the degradation of DNA by bleomycin. *Biochemistry*, **17**, 2740.

SHAANAN, B. (1982). The iron–oxygen bond in human oxyhaemoglobin. *Nature*, **296**, 683.

SHERIDAN, R.P. & GUPTA, R.K. (1981). A ^1H nuclear relaxation study of the Mn^{2+}–bleomycin complex. *Journal of Biological Chemistry*, **256**, 1242.

SHOEMAKER, D.D., CYSYK, R.L., GORMLEY, P.E., DESOUZA, J.J.V. & MALSPEIS, L. (1984). Metabolism of 4'-(9-acridinylamino)-methanesulfon-*m*-anisidide by rat liver microsomes. *Cancer Research*, **44**, 1939.

SOMEYA, A. & TANAKA, N. (1979). DNA strand scission induced by adriamycin and aclacinomycin A. *Journal of Antibiotics*, **32**, 839.

STILL, W.C., KAHN, M. & MITRA, A. (1978). Rapid chromatographic technique for preparative separations with moderate resolution. *Journal of Organic Chemistry*, **43**, 2923.

SUGIURA, Y. & KIKUCHI, T. (1978). Formation of superoxide and hydroxy radicals in iron (II)–bleomycin–oxygen system: electron spin resonance detection by spin trapping. *Journal of Antibiotics*, **31**, 1310.

WANG, J.C. (1974). The degree of unwinding of the DNA helix by ethidium. *Journal of Molecular Biology*, **89**, 783.

WARING, M.J. (1976). DNA-binding characteristics of acridinyl methanesulphonanilide drugs: comparison with antitumour properties. *European Journal of Cancer*, **12**, 995.

WILSON, W.R., BAGULEY, B.C., WAKELIN, L.P.G. & WARING, M.J. (1981). Interaction of the antitumor drug 4'-(9-acridinylamino)-methanesulfon-*m*-anisidide and related acridines with nucleic acids. *Molecular Pharmacology*, **20**, 404.

WONG, A., HUANG, C.H. & CROOKE, S.T. (1984a). Deoxyribonucleic acid breaks produced by 4'-(9-acridinylamino)methanesulfon-*m*-anisidide and copper. *Biochemistry*, **23**, 2939.

WONG, A., HUANG, C.H. & CROOKE, S.T. (1984b). Mechanism of deoxyribonucleic acid breakage induced by 4'-(9-acridinylamino)-methanesulfon-*m*-anisidide and copper: role for cuprous ions and oxygen free radicals. *Biochemistry*, **23**, 2946.

ZWELLING, L.A., MICHAELS, S., ERICKSON, L.C., UNGERLEIDER, R.S., NICHOLS, M. & KOHN, K.W. (1981). Protein-associated deoxyribonucleic acid strand breaks in L1210 cells treated with the deoxyribonucleic acid intercalating agents 4'-(9-acridinylamino)-methanesulfon-*m*-anisidide and adriamycin. *Biochemistry*, **20**, 6553.

Conclusion :

Le composé AGAMGA émet donc proportionnellement plus de radicaux libres que son homologue AGGA, l'intervention du bras morpholino-propyle ne peut en être que la cause. Ceci conforte l'hypothèse d'une stabilisation du complexe Blm-Fe(II)-O_2. Cependant ce dérivé ne se fixe pas à l'ADN par intercalation, ne dégrade pas l'ADN comme AGGA du reste et est de plus biologiquement inactif.

Par contre AGGA, sans être idéal, est plus performant sur le plan biologique. Sa capacité à inhiber la synthèse d'ADN in vitro et à inhiber la prolifération de cellules cancéreuses est notable comme en réfère la publication suivante :

article n° 8 :

DNA-synthesis and tumor growth inhibitions by AGGA,
a bleomycin-amsacrine hybrid derivative.

BAILLY C., POMMERY N., HENICHART J-P.

Cancer Letters 1988, **38**, 321-328.

Cancer Letters, 38 (1988) 321 – 328
Elsevier Scientific Publishers Ireland Ltd.

DNA-SYNTHESIS AND TUMOR GROWTH INHIBITIONS BY AGGA, A BLEOMYCIN-AMSACRINE HYBRID DERIVATIVE

C. BAILLY[a], N. POMMERY[b] and J.P. HENICHART[b]

[a]*INSERM U-16, Place de Verdun and* [b]*Faculty of Pharmacy, rue du Professeur Laguesse, 59045 Lille (France)*

(Received 6 August 1987)
(Accepted 29 September 1987)

SUMMARY

AGGA, [[(amino-2-ethyl)-2-aminomethyl]-2-pyridine-6-carboxylhistidyl-amino-4-butyrylglycylamino]-4-phenyl-1-amino-9-acridine is a synthetic model gathering the simplified metal-chelating part of bleomycin and the intercalating moiety of amsacrine. This molecule was found to possess the metal-complexing and intercalative properties of both antitumor parent drugs. On the basis of results obtained on L1210 and HeLa S_3 cells growth inhibition studies and labeled thymidine assay, AGGA clearly indicates a cytostatic activity. On the other hand, the oxygenated free radicals produced in the presence of iron and oxygen do not seem to be able to cleave DNA as BLM does. This lack of cytotoxicity is analyzed in terms of fundamental differences between BLM and AGGA-DNA complexes.

INTRODUCTION

Bleomycin (BLM) is the generic name of a group of antitumor drugs used in the treatment of squamous cell carcinomas and malignant lymphomas [1,2]. The mode of action of BLM, able to inhibit the growth of tranformed cells in vitro and in vivo, involves two defined parts of the molecule: a DNA-binding part and a metal-chelating-DNA-cleaving part. On the basis of spectroscopic results obtained with a synthetic simplified model (AMPHIS) of the complexing part of BLM [3], we have delineated the exact metal-ligands of BLM and the mechanism of production of free radicals [4]. But we have demonstrated that this complexing part was not able to cleave DNA deoxyriboses in the absence of the DNA-binding part [5]. This part, consisting of a bithiazole ring which binds to DNA bases by a stacking process when linked to the complexing part, is able to get it into position for selective cleavage near the deoxyriboses.

We have proposed a binding mode involving a partial insertion of a thiazole

0304-3835/88/$03.50

322

ring which wedges in between the bases at a bending point of DNA [6]. This position is due in part to the geometry of the bithiazole ring exhibiting a small aromatic surface which does not allow a full overlap with a base pair.

Consequently, we decided the design of a new model including the simplified complexing part of BLM, AMPHIS, linked by a dipeptide chain to a 9-

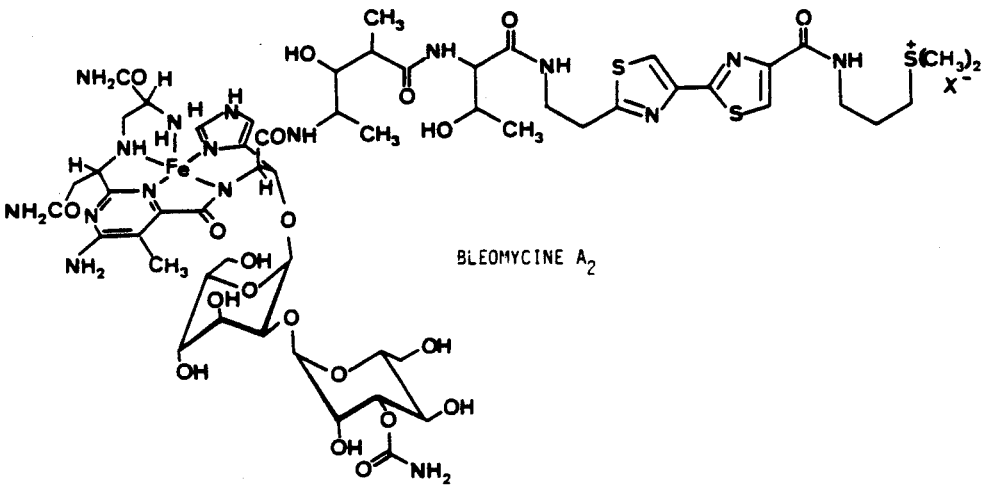

BLEOMYCINE A_2

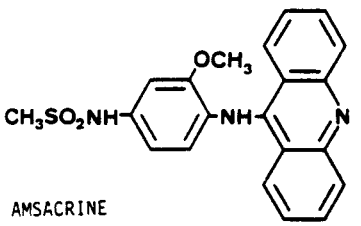

AMSACRINE

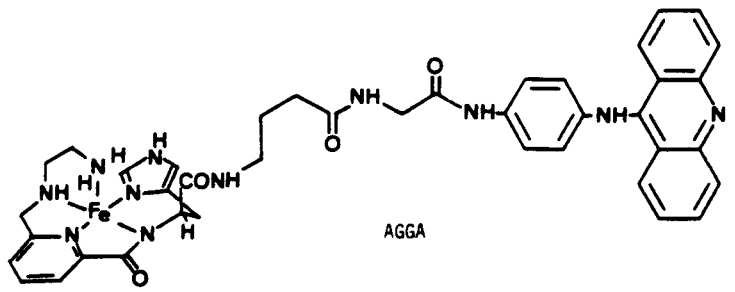

AGGA

AMPHIS

Fig. 1. Structures of bleomycin A_2, amsacrine and AGGA.

anilinoacridine ring. This heterocycle has been choiced in replacement of the bithiazole ring of BLM because some anilinoacridines exhibit a high experimental antitumor activity [7] and one of the derivatives of the series, amsacrine, has been found to have a major activity in acute leukemia [8]. Moreover, we have shown that a peptidic derivative of anilinoacridine was able to bind to DNA by intercalation with a higher affinity than amsacrine [9] and to possess an interesting antitumor activity against L1210 and EMT6 cells with an accumulation of cells in the S phase followed by a cycle arrest in the G_2 phase, characteristic of intercalating drugs [10].

The synthesis [11] and the metal-chelating properties [12] of the new model, AGGA (Fig. 1), were previously reported and the purpose of the present paper is to define (i) the DNA-cleavage, (ii) the inhibition of incorporation of labeled thymidine into KB cells DNA in culture, correlated with (iii) the growth inhibition and decrease viability of two different cancer cells culture: L1210 mouse leukemia and HeLa S_3 (derived from solid tumor), when AGGA is directed against them. The possible mechanism of action of this potential anti-cancer agent is discussed (Table 1).

MATERIALS AND METHODS

Preparation of AGGA and amsacrine

Full details of the synthesis of AGGA together with complete spectral and analytical characterization were previously given [11].

Amsacrine was obtained by a modification of the initial procedure of Cain et al. [3,7]. Bleomycin was a generous gift of Roger Bellon Laboratories: it contains approximately 60% Blm-A_2, 30% BLM-B_2 and 10% other BLMs.

Cell cultures

KB cells were grown as a suspension culture in a Joklik modified Eagle's Medium (Seromed, Munich, F.R.G.) supplemented with 5% heat inactivated colt serum at a 4×10^5 cells/ml concentration.

Human transformed cells (HeLa S_3) in monolayer culture in SMEM medium (GIBCO BRL, France) supplemented by foetal calf serum (5%) GIBCO were used for the tests. Suspensions of these cells were performed in the same medium added to 16 mM Hepes and BTP buffers (*N*-2-hydroxyethylpiperazine *N'*-2-ethanesulfonic acid and 1,3-bis-[tris(hydroxymethyl)methylamino]propane). Final concentration varied from 5×10^5 to 10^6 cells/ml [13].

L1210 mouse leukemia cells were grown in RPMI 1640 medium (GIBCO) containing foetal calf serum (10%) and the assays were performed in the same medium.

Cultures utilized to assess drug effects were in exponential growth phase with a doubling time of 13–15 h.

Growth and viability assays

Cell suspensions containing either 6×10^5 HeLa S_3 cells/ml or 10^6 L1210

cells/ml were incubated with AGGA at various concentrations: 10^{-6}, 10^{-5}, 10^{-4}, 10^{-3} M for 24 h.

Cell growth and viability were estimated by counting the cells after dilution by trypan blue solution at 0 h and after 24 h. Results were expressed as a percentage of control growth and viability.

Measurements of DNA synthesis

KB cells in exponential growth were incubated for 1 h at 37 °C in growth medium containing various doses of AGGA (1–100 μM). The cells were incubated for 15 h at 37 °C in growth medium containing 10 μCi/ml [^{3}H]thymidine (43 Ci/mM, CEA). The radioactive medium was removed, the cells washed twice in saline buffer and allowed to swell for 10 min in ice in 1 ml of hypotonic buffer (TNE: 0.01 M Tris–HCl (pH 8.1); 0.05 M NaCl; 0.001 M EDTA). The cells were then disrupted by congelation-decongelation (3 times), digested by proteinase K (100 μg/ml, 4 h at 37 °C). The TCA precipitable radioactivity was collected on filters and counted in a liquid scintillation counter.

Single strand and double strand DNA breakage

This can be visualized by the use of supercoiled DNA (form I). The products of plasmid reaction (form II: relaxed circular DNA, form III: open linear DNA) with either BLM-A_2, AMPHIS or AGGA were separated on a 1.2% agarose gel, containing 0.5 μg/ml of ethidium bromide.

Plasmid pVM 216 was incubated with BLM, AMPHIS or AGGA in 50 mM Tris–HCl, (pH 8.0) buffer containing 10 mM 2-mercaptoethanol. $Fe(NH_4)_2(SO_4)_2, 6H_2O$ was added in the same final concentration as the product.

After 30 min at room temperature, the reaction was terminated with the addition of EDTA 2.5 mM. Five microliters of 0.01% bromophenol blue were added to the reaction mixture (50 μl). Agarose electrophoresis was performed in TBE buffer at 3 V/cm for 20 h and examined under a 254 nm UV light.

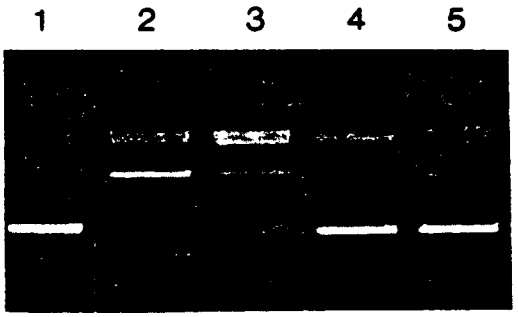

Fig. 2. Supercoil DNA cleavage by bleomycin analogues. Reaction mixtures contain 4.5 μg pVM 216 in 50 mM Tris–HCl (pH 8.0) (lane 1); plus Fe(II)-BLM-A_2, 10^{-4} M (lane 2); 2×10^{-7} M (lane 3); Fe(II)AGGA, 10^{-4} M; Fe(II)-AMPHIS, 10^{-4} M (lane 5). Electrophoresis is at 60 V for 20 h on a 1.2% agarose gel.

RESULTS

DNA cleavage: Though both antineoplastic drugs BLM [5] and amsacrine [14] have been shown to induce cleavage of DNA, the very sensitive method using plasmid indicates that the synthetic hybrid model AGGA does not produce DNA degradation in spite of its ability to induce formation of free radicals (Fig. 2).

Cell growth inhibition: The effects on growth of L1210 and HeLa S_3 cells grown with 10^{-3}, 10^{-4}, 10^{-5} and 10^{-6} M AGGA are shown in Fig. 3. Only the 1 mM concentration has a small effect on cell viability. AGGA is a poor cytotoxic agent and shows a good cytostatic activity. A 5-μM concentration permits to inhibit HeLa cell growth by 50% (IC_{50} HeLa S_3 = 5 μM). For L1210 leukemia cell, a greater concentration (IC_{50} L1210 = 45 μM) is needed to observe this 50% growth inhibition.

Effect on DNA synthesis: Amsacrine inhibits incorporation of labeled thymidine into DNA of L1210 cells in vivo or in culture [15].

Incorporation of [*methyl*-^{3}H]thymidine into cells during a 16-h assay period is inhibited by AGGA (Fig. 4) in a manner reflecting its antiproliferative potential. A cell count with trypan blue at the end of the 16-h period of treatment with the IC_{50} concentration shows that the number of non-viable cells present is always less than 3% of the total cell population. This observation

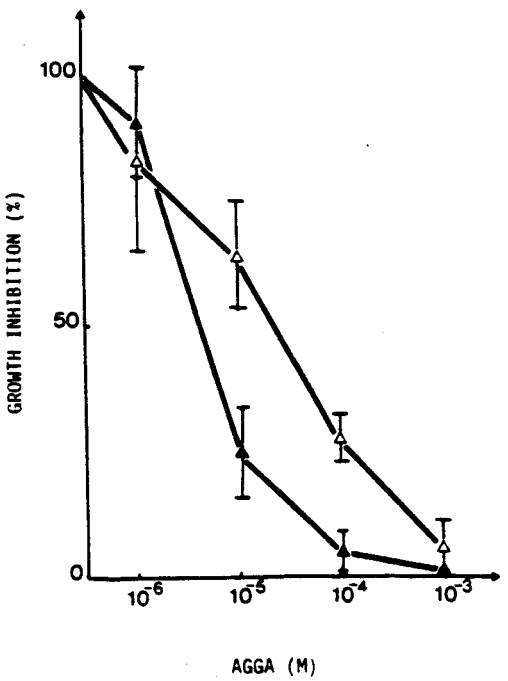

Fig. 3. Effects of increasing AGGA dose on the growth of L1210 (△) and HeLa S_3 (▲) cells. The results are expressed as a percentage of control growth. Vertical bars indicate S.E.M.

326

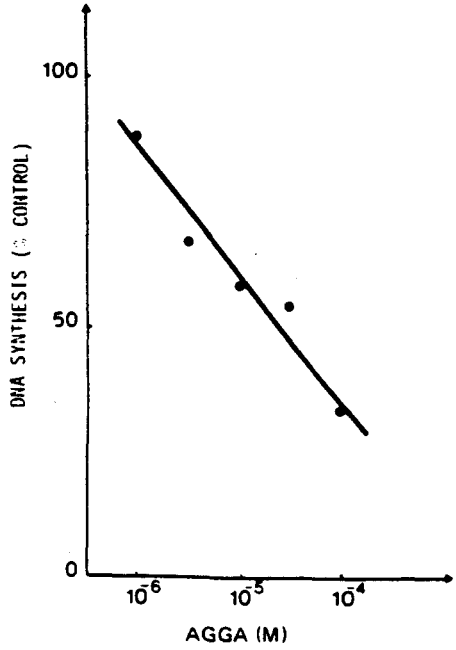

Fig. 4. Effects of increasing AGGA dose on the rate of DNA synthesis in KB cells. The rate of DNA synthesis is expressed as a percentage of untreated control cells. Each point represents the mean of 6 experiments.

would suggest that loss of viable cells, unrelated to DNA synthesis inhibition, is not a major cause for the antineoplastic activity of AGGA.

Results from these experiments therefore indicate that impairment of DNA template function might well represent an essential feature in the mechanism of action of the investigated hybrid model AGGA.

DISCUSSION

On the basis of the results obtained on growth of L1210 and HeLa S_3 cells, AGGA is found as a cytostatic agent. Moreover, it seems to be more active

TABLE 1

EFFECTS OF INCREASING AGGA DOSE ON THE VIABILITY OF L1210 AND HeLa S_3 CELLS

The results are expressed as a percentage of control cells. Each reported value represents the mean of triplicate measurements.

	10^{-4} M	10^{-5} M	10^{-6} M	10^{-7} M
L1210	92	91	87	70
HeLa S_3	97	92	94	63

against cancer cell derived from solid tumor (HeLa S_3, IC_{50} = 5 μM) than against leukemia cell (L1210, IC_{50} = 45 μM). The cytostatic effect was confirmed by the incorporation of labeled thymidine assay which clearly indicated the inhibition of DNA synthesis by AGGA.

The lack of cytotoxicity is more unexpected. AGGA was found to be a good metal-chelating agent [12] and to produce oxygenated free radicals in the same conditions as BLM does [11]. On the other hand, the intercalative power of the acridine part of AGGA [11] induces to this model a higher affinity to DNA than bithiazole derivatives. Thus it was reasonable to think that AGGA could be a good candidate for efficient DNA-cleavage. The experiments made on supercoiled DNA undoubtedly prove the opposite. The differences between BLM and AGGA behaviors could be explained by structural considerations. In the case of BLM, the bithiazole moiety is located in a kink of DNA [6] and free radicals are produced in the vicinity of the deoxyribose moiety, being responsible for strand breakage of the double helix.

In the case of AGGA, strong binding and complexing parts are borne by the same structure but it is reasonable to think that after intercalation of the acridine moiety, the chelating part is not readily positioned at a short distance of the desoxyribose target. Then hydroxyl radicals are produced not immediately in the vicinity of the cleaving site. For this reason, no strand break could be detected with AGGA. The geometry of anilinoacridine derivatives in interaction with DNA is well known [16]. The acridine moiety binds to DNA by intercalation and the anilino group is located in the minor groove of the DNA helix in a perpendicular plane. In these conditions, the complexing part AMPHIS linked to the aniline part in para position is pushed back far from the deoxyriboses. Moreover, when the anilinoacridine moiety is intercalated, the double helix is submitted to an unwinding and to a lengthening but no folding occurs, whereas DNA adopts a bended conformation when BLM is attached to it. For these reasons, the move of the chelating part responsible for $OH^{\cdot}$ production closer to the cleaving site would not be favored in the AGGA-DNA complex.

Nevertheless, the high reactive species produced in the DNA environment could alter some nuclear components such as DNA-binding proteins which are necessary for the DNA replication. Especially, the topoisomerase could be one of these potential targets becaue this enzyme is implied in the mode of action of amsacrine [16].

In conclusion, the results provide evidence that AGGA is undoubtedly a cytostatic compound without any cytotoxic effect. The mode of action of this drug remains unclear but the association on the same molecule of the chelating part of BLM and of the intercalating part of amsacrine constitutes an interesting model for the design of acridine derivatives useful for the treatment of solid tumors. Such an association had been previously proposed on the basis of studies on molecular interaction between BLM and amsacrine leading to a potentialisation of the effects of both drugs [17].

328

ACKNOWLEDGEMENTS

This research was supported by grants from the Institut National de la Santé et de la Recherche Médicale and the Ligue Nationale contre le Cancer. We thank Dr. P. Lemay for his assistance and his valuable discussions and C. Fréart for typing the manuscript.

REFERENCES

1 Carter, S.K. (1978) The current role of bleomycin in cancer therapy. In: Bleomycin, Current Status and New Developments, pp. 9–14. Editors: S.K. Carter, S.T. Crooke and H. Umezawa. Academic Press, New York.
2 Carter, S.K. (1985) Bleomycin: more than a decade later. In: Bleomycin Chemotherapy, pp. 3–35. Editors: B.I. Sikic, M. Rosencweig and S.K. Carter, Academic Press, New York.
3 Hénichart, J.P., Houssin, R., Bernier, J.L. and Catteau, J.P. (1982) Synthetic model of a bleomycin metal complex. J. Chem. Soc. Chem. Commun., 1295–1297.
4 Hénichart, J.P., Bernier, J.L., Houssin, R., Lohez, M., Kenani, A. and Catteau, J.P. (1985) Copper(II)- and Iron(II)-complexes of methyl 2-(2-aminoethyl)-aminomethyl-pyridine-6-carboxyl-histidinate (AMPHIS), a peptide mimicking the metal-chelating moiety of bleomycin. An ESR investigation. Biochem. Biophys. Res. Commun., 126, 1036–1041.
5 Kenani, A., Lohez, M., Houssin, R., Helbecque, N., Lemay, P. and Hénichart, J.P. (1987) Chelating, DNA-binding and DNA-cleaving properties of a bleomycin synthetic model. Anti-Cancer Drug Design, in press.
6 Hénichart, J.P., Bernier, J.L., Helbecque, N. and Houssin, R. (1985) is the bithiazole moiety of bleomycin a classical intercalator? Nucleic Acids. Res., 13, 6703–6717.
7 Cain, B.F. and Atwell, G.J. (1974) The experimental antitumor properties of three congeners in the acridinyl-methanesulphonanilide (AMSA) series. Eur. J. Cancer, 10, 539–549.
8 Cassileth, P.A. and Gale, R.P. (1986) Amsacrine: a review. Leukemia Res., 10, 1257–1265.
9 Hénichart, J.P., Bernier, J.L. and Catteau, J.P. (1982) Interaction of 4-(9-acridinylamino)aniline and derivatives with DNA. Influence of a lysylglycyl side chain on the binding parameters. Hoppe-Seyler's Z. Physiol. Chem., 363, 835–841.
10 Collyn-d'Hooghe, M., Bernier, J.L. and Hénichart, J.P. (1987) Cytotoxic action and cell cycle effects of ALGA, a peptidic derivative of the antileukemic drug amsacrine. Cancer Biochem. Biophys., in press.
11 Bailly, C., Bernier, J.L., Houssin, R., Helbecque, N. and Hénichart, J.P. (1987) Design of two metal-chelating, DNA-binding models: molecular combination of bleomycin and amsacrine anti-tumor drugs. Anti-Cancer Drug Design, 1, 303–312.
12 Bailly, C., Catteau, J.P., Helbecque, N., Bernier, J.L., Houssin, R., Denis, C. and Hénichart, J.P. (1987) Complexation of copper(II) by a peptide hybrid of bleomycin and amsacrine. Circular dichroism and electron spin resonance studies. J. Inorg. Biochem., in press.
13 Fauris, C., Danglot, C. and Vilagines, R. (1985) Rapidity of RNA synthesis in human cells: a highly sensitive parameter for water cytotoxicity evaluation. Water Res., 19, 677–684.
14 Wong, A., Huang, C.-H. and Crooke, S.T. (1984) Deoxyribonucleic acid breaks produced by 4'-(9-acridinylamino)methanesulfon-m-anisidide and copper. Biochemistry, 23, 2939–2945.
15 Burr Furlong, N., Sato, J., Brown, T., Chavez, F. and Hurlbert, R.B. (1978) Induction of limited DNA damage by the antitumor agent Cain's acridine. Cancer Res., 38, 1329–1335.
16 Pommier, Y., Schwartz, R.E., Kohn, K.W. and Zwelling, L.A. (1984) Formation and rejoining of deoxyribonucleic acid double-strand breaks induced in isolated cell nuclei by antineoplastic intercalating agents. Biochemistry, 23, 3194–3201.
17 Bernier, J.L., Kenani, A., Houssin, R., Helbecque, N., Lohez, M., Hecquet, B. and Hénichart, J.P. (1986) Molecular interaction between bleomycin and amsacrine in the presence of cupric ions. J. Inorg. Biochem., 27, 271–285.

Sur le plan physicochimique, l'étude plus approfondie de la complexation du cuivre par ce dérivé hybride, par les techniques de RPE et dichroïsme circulaire, nous a amené à constater que la géométrie du complexe était largement perturbée par le reste acridinyle :

article n° 9 :

Complexation of copper(II) by a peptide hybrid of bleomycin and amsacrine. Circular dichroism and electron spin resonance studies.

BAILLY C., CATTEAU J-P., HELBECQUE N., BERNIER J-L.
HOUSSIN R., DENIS C., HENICHART J-P.

Journal of Inorganic Biochemistry 1987, **31**, 211-220.

Complexation of Copper(II) by a Peptide Hybrid of Bleomycin and Amsacrine. Circular Dichroism and Electron Spin Resonance Studies

Christian Bailly, Jean-Pierre Catteau, Nicole Helbecque, Jean-Luc Bernier, Raymond Houssin, Claude Denis and Jean-Pierre Hénichart

CB, NH, J-LB, J-PH. *U-16 INSERM, Lille.*—J-PC. *Laboratoire de Chimie Organique Physique, USTL.*—RH. *Laboratoire de Chimie de Synthèse des Médicaments, Faculté de Pharmacie, Lille.*—CD. *U-124 INSERM, Lille*

ABSTRACT

A model incorporating the metal chelating moiety of bleomycin and an anilinoacridine ring able to intercalate in DNA has been synthesized. The copper(II) complex of that molecule has been studied using circular dichroism and electron spin resonance by comparison with bleomycin. The introduction of the anilinoacridine ring involves a modification in the geometry of the complex. A distortion of the square-pyramidal form (type II complex) gives rise to a type I complex in which the metallic atom is drawn out of the plane of the four square-planar ligands and displaced slightly towards the fifth ligand.

INTRODUCTION

Bleomycin (BLM) is an antitumor antibiotic used clinically in the treatment of squamous cell carcinoma, malignant lymphoma, and testicular tumours [1]. BLM gives an in situ complex with cupric ions, Cu(II)–BLM (Figure 1A), the activation of which involves initial conversion to Cu(I)–BLM [2]. This latter complex is subsequently converted to an Fe(II) complex [1], Fe(II)–BLM, which is able to bind molecular oxygen, producing an active complex responsible for DNA breaks [3–5]. On the other hand, a synthetic intercalating drug, amsacrine, or *m*-AMSA ((4′-(9-

Address reprint requests to Dr. J. P. Hénichart, Unité INSERM 16, Place de Verdun, 59045 Lille Cedex, France.

Journal of Inorganic Biochemistry 31, 211-220 (1987) 211
 0162-0134/87/$3.50

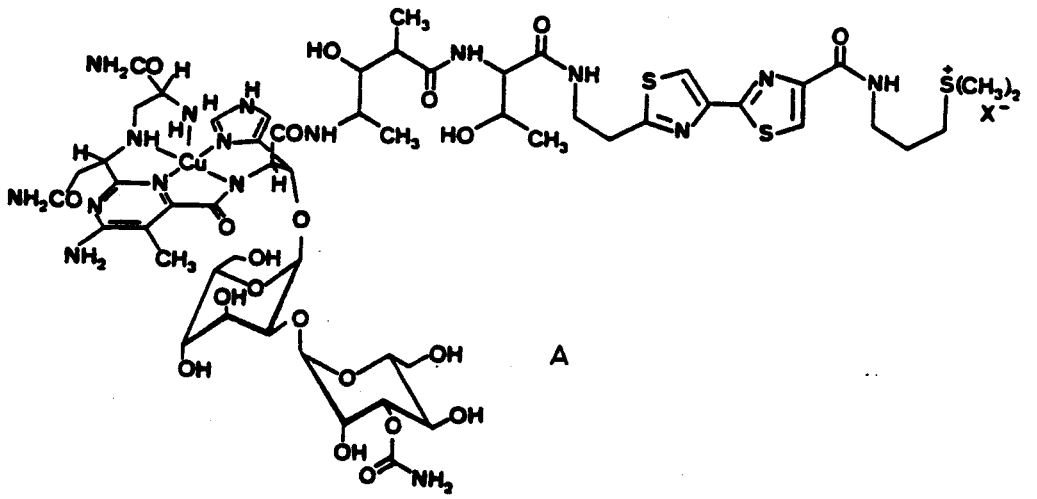

A

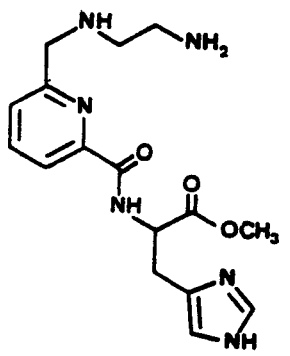

B

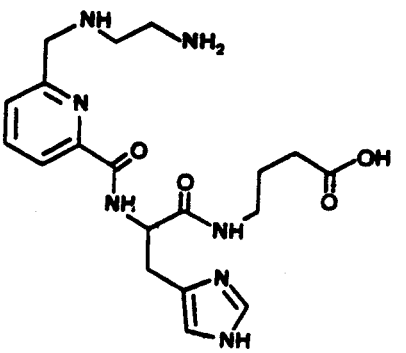

C

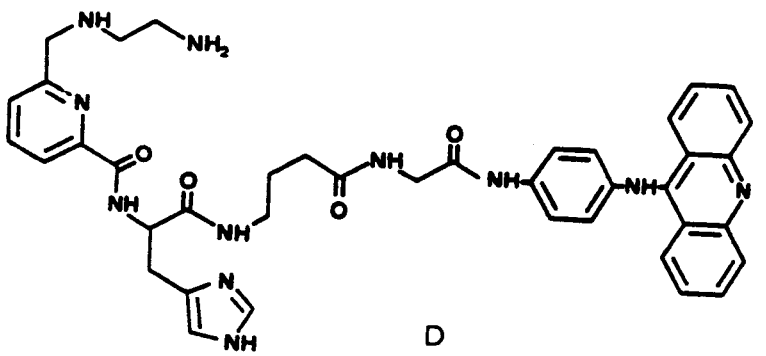

D

FIGURE 1. Structures of BLM-A_2-Cu(II) (A), AMPHIS (B), AMPHIS-GABA (C), and AGGA (D).

acridinylamino)-methansulfon-*m*-anisidide)), was shown to possess a good antileukemic activity [6]. It has been proposed [7] that first a ternary complex involving DNA, *m*-AMSA and, CU(II) is formed. A redox reaction subsequently occurs, leading to the new complex DNA-*m*-AQDI-Cu(I) (*m*-AQDI: *N*-methylsulfonyl-*N'*-(9-acridinyl)-3-methoxy-2,5-cyclohexadiene-1,4-diimide), which is able to reduce molecular oxygen and to generate radicals responsible for the DNA breaks. It has recently been demonstrated that the rate of oxidation is greatly increased by addition of BLM [8].

Thus, in the course of studies on simplified models of bleomycin, it seemed interesting to us to associate in the same molecule the anilino-acridine ring able to strongly bind to DNA [9] with the complexing part of BLM (or, more precisely, AMPHIS (methyl 2-(2-aminoethyl)-aminomethyl-pyridine-6-carboxylhistidinate) (Figure 1B), a peptide mimicking the metal-chelating moiety of BLM [10]). This hybrid drug, AGGA ([[(amino-2-ethyl)-2-aminomethyl]2-pyridine-6-carboxylhistidylamino-4-butyrylglycylamino]4-phenyl-1-amino-9-acridine) (Figure 1D), a bleomycinlike molecule with enhanced intercalative properties, has the advantage of bringing a cupric ion (chelated by AMPHIS) into the proximity of the anilinoacridine moiety, thus inducing a redox process responsible for the DNA cleaving activity.

We report here the results of CD and ESR studies in order to identify the ligands involved in the Cu(II)–AGGA complex.

EXPERIMENTAL

Materials

AMPHIS was prepared according to a previously published procedure [10]. AMPHIS–GABA (Figure 1C) was obtained by coupling the free acid of *N*-protected AMPHIS [10] with ethyl γ-aminobutyrate in the presence of DCCI and hydroxybenzotriazole in dichloromethane at 0°C for 2 h, and then at room temperature for 12 h. After classic purifications, the free acid was obtained by saponification at room temperature. Cleavage of *N*-protecting groups by hydrobromic acid in acetic acid and purification using flash chromatography on silica gel (elution with 9:1 dichloromethane-methanol) yield AMPHIS–GABA.

AGGA was obtained by coupling *N*-protected AMPHIS–GABA with 4-(9-acridinylamino)-*N*-glycylaniline [9] in the presence of isobutyl chloroformate and *N*-methylmorpholine at −20°C. After classic purifications and deprotection by hydrobromic acid in acetic acid, AGGA was purified by flash chromatography (n.m.r., δ[$(CD_3)_2SO$] 9.10, 8.40, 8.15, 7.17, 7.00 (s, NH); 8.10–7.40 (*m*, aromatic and heterocyclic protons); 4.70–3.65 (*m*, CH_2)).

Spectroscopic Measurements

Absorption spectra were recorded on a Cary 118 spectrophotometer. The circular dichroism spectra were recorded with a Jobin-Yvon dichrograph R-J Mark III in quartz cells of appropriate pathlengths in order to achieve an absorbance of less than 1.5. The ellipticity was expressed in degrees/cm^2/$dmole^{-1}$. AMPHIS–GABA and AGGA were dissolved in water containing less than 1% methanol. The pH was adjusted by adding either HCl or NaOH.

ESR measurements were recorded on a Varian E 109 X-band ESR spectrometer,

with a dual cavity operating in the TE 104 mode. A 100 kHz high frequency modulation with a maximum amplitude of 8 gauss was used with 10 mW microwave power.

The sample solutions were prepared in quartz tubes by mixing a 10^{-2} *M* solution of $Cu(ClO_4)_2$ with a small excess of a 10^{-2} *M* solution of the complexing molecule. NaOH and glycerol were then added at 77°K to obtain a good glass.

The *g*-factor measurements were carried out by reference to the VARIAN "strong pitch".

RESULTS

CD Data

Since the geometry of the AMPHIS–Cu(II) complex has already been determined by ESR [10], we decided to successively study the complexation of cupric ions, either by AMPHIS–GABA or by AGGA using circular dichroism.

Whereas AMPHIS–GABA does not exhibit any dichroism by itself, its Cu(II) complex at pH 5.25 (Fig. 2) is characterized by a positive band at 282 nm ($n \rightarrow \pi^*$ pyridine) and a negative one at 252 nm (charge transfer for Cu(II)); the Cu(II) transitions give a negative band at 625 nm and a small positive one at 545 nm. This spectrum is very similar to the one obtained for bleomycin–Cu(II) at pH 2.6, and reflects the existence of a square-planar complex involving the pyridine nitrogen, the peptide bond NH, and presumably the imidazole nitrogen and one NH of the 2-aminoethyl moiety. The very small values of ellipticies favor an unconstrained complex. The same complex was expected to occur at basic pH, but no conclusion can be drawn from the CD spectrum since it is dominated in the UV region by the charge transfer Cu(II) $\rightarrow d_{x^2-y^2}$ band.

FIGURE 2. CD spectra of AMPHIS–GABA–Cu(II) [1:1 complex] at pH 5.25.

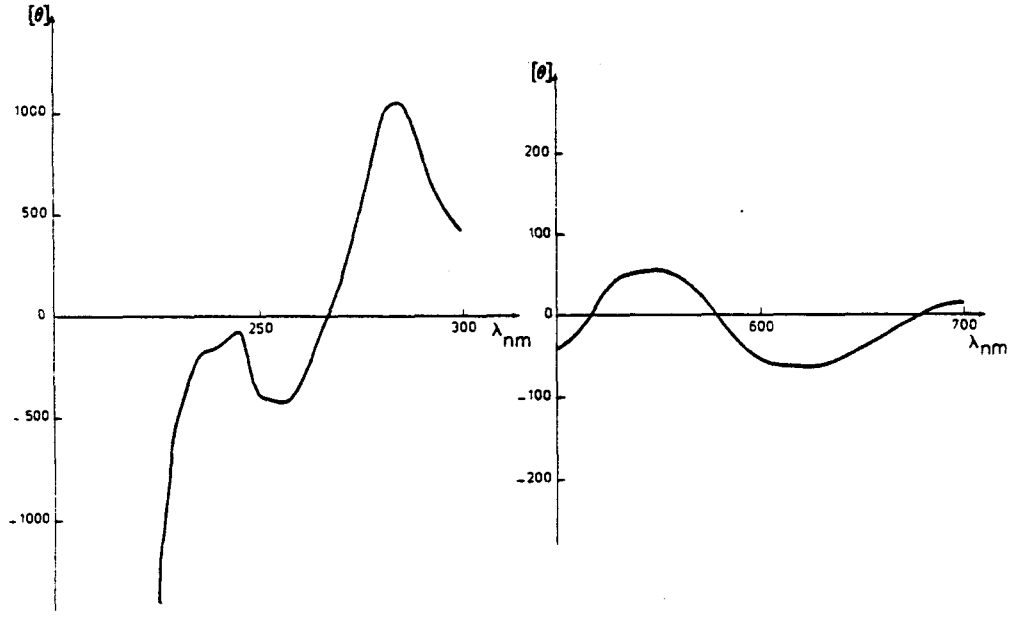

A thorough study of the complex formed between AGGA and Cu(II) as a function of pH was undertaken in order to investigate the role played by the acridine nucleus in the complex. At acidic or neutral pH, AGGA alone exhibits only a broad negative band centered near 250 nm ($[\theta] = -700$ degrees/cm^2/dmole^{-1}), whereas at pH 8.2 two positive bands can be seen, one located at 272 nm ($[\theta] = +800$ degrees/cm^2/dmole^{-1}, $n \rightarrow \pi^*$ pyridine), and the other at 237 nm ($[\theta] = +450$ degrees/cm^2/dmole^{-1}; $\pi \rightarrow \pi^*$ imidazole) (Fig. 3). Adding copper induces a small dichroic effect in the acridine absorption region, whatever the pH (broad band between 370 and 440 nm; $[\theta]_{390} = -300$ degrees/cm^2/dmole^{-1} at pH 2.9; $[\theta]_{400} = -370$ degrees/cm^2/dmole^{-1} at pH 5.9 and 8.0) and a higher one in the Cu(II) region (Table 1 and Fig. 4)). Important changes can simultaneously be detected in the UV region. At pH 5.95, two well-resolved positive bands can be seen ($\lambda = 280$ nm: $n \rightarrow \pi^*$ pyridine; $\lambda = 235$ nm: charge transfer for Cu(II)), and a small negative one is seen at 310 nm (amide $\rightarrow$ Cu(II) transfer). At pH 8.0, this latter band becomes more intense and a broadening of the positive bands is observed (Fig. 4).

The addition of Cu(II) to AGGA induces changes in the dichroic spectrum which are located at the same wavelengths as for AMPHIS-GABA-Cu(II) except for the $d_{xy} \rightarrow d_{x^2-y^2}$ transition at neutral pH or for the d_{xz}, $d_{yz} \rightarrow d_{x^2-y^2}$ transition at basic pH. Moreover the ellipticities are higher in the case of AGGA except for the $d_{xy} \rightarrow d_{x^2-y^2}$ transition (625-655 nm region) where they are of the same order of magnitude.

FIGURE 3. CD spectra of AGGA at pHs 3.22 (——), 5.30 (— — —), and 8.20 (· · · · ·).

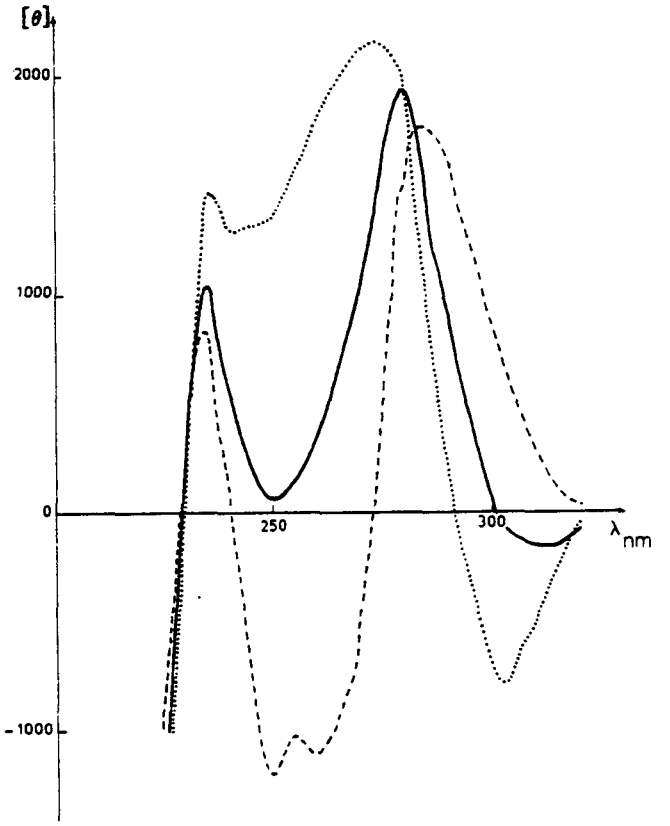

TABLE 1. Circular Dichroism Spectra Characteristics for Cu(II) Complexes of PYML-1, PEML, P-3A, BLM, AMPHIS-GABA, and AGGA

Complex	λ_{max}	CD extrema
PYML-1-Cu(II)[a]	597	545 (+2,900) 655 (−330)
PEML-Cu(II)[a]	588	No CD signals
P-3A-Cu(II)[a]	625	580 (+1,850) 700 (+690)
BLM-Cu(II)[a]	595	555 (+3,990) 665 (−1,980)
AMPHIS-GABA-Cu(II)		
pH 5.25	646	252 (−420); 282 (+1,050); 545 (+55); 625 (−75)
pH 11.70	612	252-275 (broad band, +1,100); 570 (+30); 655 (−40)
AGGA-Cu(II)		
pH 2.90	615	235 (+840); 250 (−1,200); 260 (−1,100); 285 (+1,750) 390 (−300); 530 (+525); 640 (−115)
pH 5.95	600	235 (+1,050); 280 (+1,960); 400 (−370); 540 (+505); 650 (−85)
pH 8.00	596	235 (+1,480); 275 (+2,200); 400 (−370); 540 (+440); 655 (−80)

[a] From [18]; pH. 7.20.

Noteworthy also is the induction of a dichroism around 400 nm, indicative of the fact that acridine lies in a asymmetric environment. In the light of these observations, it can be concluded that there are no changes in the planar ligands involved in the Cu(II) complexes of AGGA, AMPHIS-GABA and BLM as the wavelengths corresponding to the different transitions are closely related (Table 1). However discrepancies in the intensity of the ellipticities of AGGA-Cu(II), if compared to those of AMPHIS-GABA-Cu(II), can be considered as a reflection of steric constraints inducing an asymmetry in the geometry of this complex since circular dichroism is known to be very sensitive to such effects.

The contribution of acridine to the asymmetry is substantiated by the appearance of a dichroic effect in the wavelength range associated with this group. Thus, while BLM-Cu(II) as well as AMPHIS-GABA-Cu(II) exhibit CD spectra representative of a classical square-pyramidal structure, referred to as type II complexes, one might reasonably assume that the AGGA-Cu(II) complex is distorted about the cupric ion.

ESR Results

At basic pH, the ESR spectrum of AMPHIS-GABA-Cu(II) is very similar to the AMPHIS-Cu(II) already described [10] (Table 2). In the same conditions the ESR spectrum of AGGA-Cu(II) is more complicated. A careful analysis exhibits four characteristic additional peaks in the spectrum, which are shown in Figure 5. Other small peaks in the $g_\perp$ region may be attributed to $[Cu(OH)_4]^{2-}$, as shown by comparison with the ESR spectrum of a basic solution of $Cu(ClO_4)_2$.

The existence of the four additional bands favors the formation of a Cu(II) type I complex, as previously described [11, 12]. According to Peisach and Blumberg [11], those Cu(II) type I complexes have $g_\parallel$ values between 2.20 and 2.30 and A in the range 4–9 mK (1 mK = 10^{-3} cm^{-1}). A, an important quantitative parameter representative of the interaction energy, is expressed in millikaisers [11] and is directly related to the nuclear splitting ΔH, expressed in gauss by the relationship $A = 0.046686\ g\Delta H$. The

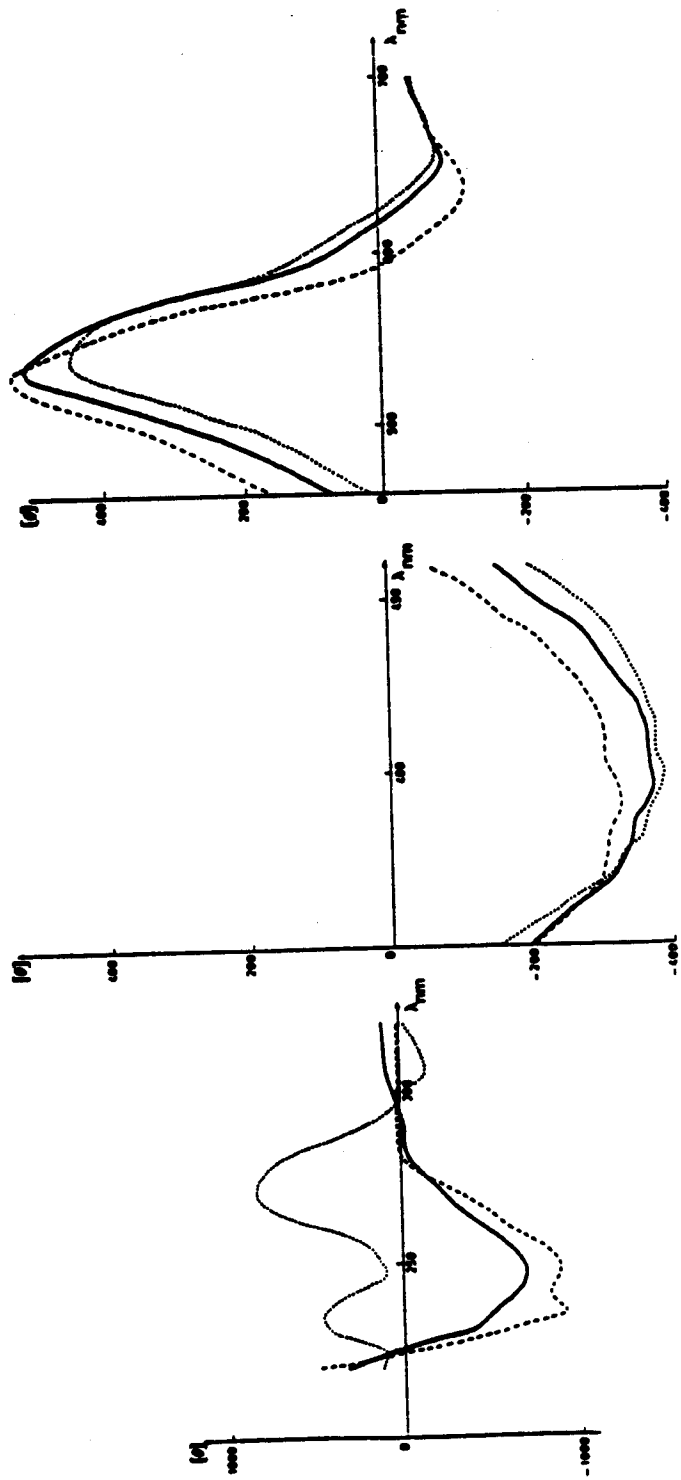

FIGURE 4. CD spectra of AGGA–Cu(II) [1:1 complex] at pHs 2.9 (– – –), 5.95 (——), and 8.0 (· · · · ·).

TABLE 2. ESR Parameters for AMPHIS–Cu(II), AMPHIS–GABA–Cu(II), and AGGA–Cu(II)

Complex	$A_{\parallel}$ (gauss)	$g_{\parallel}$
AMPHIS–Cu(II)	177.5	2.2040
AMPHIS–GABA–Cu(II)	178.5	2.2036
AGGA–Cu(II)	180	2.2042
	85	2.2172

ESR spectrum of AGGA–Cu(II) is at least constituted of a superposition of two complexes, one of type II similar to the AMPHIS–Cu(II) complex and a new one of type I. Similar cases have already been described [13].

The presently accepted view of the unusual magnetic properties of the type I Cu(II) complex is primarily related to the symmetry of the site. The geometry of the Cu(II) site has been computed on the basis of crystal field theory in a number of studies [14–16]. The small $A_{\parallel}$ values are consistent with a nearly tetrahedral coordination for Cu(II).

The tetrahedral distortion of the Cu(II) site leading to a type I complex may be attributed to the presence of the acridinyl substituent and to the extension of the molecular chain which involves steric constraints on the ligand environment [17].

DISCUSSION

Optical and paramagnetic spectroscopies are in accordance with the suggestion that the introduction of an acridine ring gives rise to some differences in the observed spectra. A distortion in the coordination geometry is apparent from the CD, while two isomers appear through ESR, corresponding to type I and type II complexes. Both spectroscopies yield little information about the apical ligand (which is at a greater

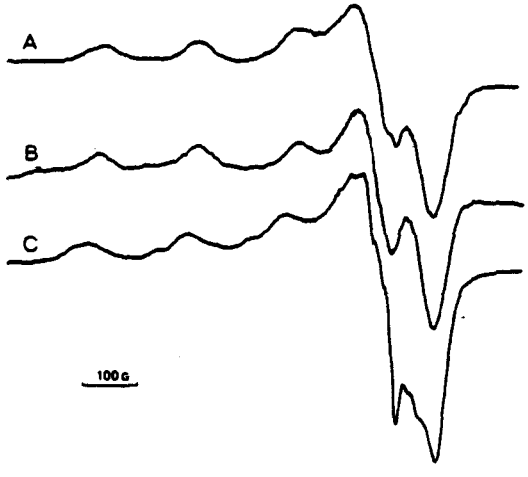

FIGURE 5. ESR spectra of AMPHIS–Cu(II) (A), AMPHIS–GABA–Cu(II) (B), and AGGA–Cu(II) (C) complexes at pH 9.0.

distance than the four inplane ligands), but the x-ray structure determination of the BLM–Cu(II) fragment, P-3A (showing cupric ion in a square-pyramidal coordination with an axial terminal amine [19]), can be taken into account in our discussion. Thus, it can be assessed that complexes with BLM and AMPHIS–GABA have the same square-pyramidal geometry, referred to as a type II complex, while a type I complex is suggested for AGGA, corresponding to a distortion of the geometry in which the cupric ion is out of plane with regard to the four coplanar ligands.

That the metal is forced out of plane and displaced slightly towards the fifth ligand can be explained in terms of steric hindrance or electronic effects of the acridine nucleus on the apical ligand, or by the introduction of the basic nitrogen of the acridine as a new ligand.

CONCLUSION

The introduction of an acridine ring in place of the bithiazole moiety in AGGA involves changes in the coordination geometry of the cupric complex. This modification has noticeable implication on the optical and magnetic properties of the molecule, and may play a dramatic role in its biological properties.

This work was supported by grants from the Institut National de la Santé et de la Recherche Médicale and the Fédération des Centres de Lutte contre le Cancer. The authors with to thank Mrs. C. Masson for typing the manuscript.

REFERENCES

1. H. Umezawa, in Hecht, Ed., *Bleomycin: Chemical, Biochemical, Biological Aspects*, Springer-Verlag, New York: 1979, pp. 1-36.
2. K. Takahashi, O. Yoshioka, A. Matsuda, and H. Umezawa, *J. Antibiot.* **30**, 861 (1977).
3. N. J. Oppenheimer, L. O. Rodriguez, and S. M. Hecht, *Proc. Natl. Acad. Sci. USA*, **76**, 5616 (1979).
4. R. M. Burger, A. R. Berkowitz, J. Peisach, and S. B. Horwitz, *J. Biol. Chem.* **255**, 11832 (1980).
5. J. H. Freedman, S. B. Horwitz, and J. Peisach, *Biochemistry* **21**, 2203 (1982).
6. B. F. Cain and G. J. Atwell, *Eur. J. Cancer* **10**, 539 (1974).
7. A. Wong, C. H. Huang, and S. T. Crooke, *Biochemistry* **23**, 2939, 2946 (1984).
8. J. L. Bernier, A. Kenani, R. Houssin, N. Helbecque, M. Lohez, B. Hecquet, and J. P. Hénichart, *J. Inorg. Biochem.* **27**, 271 (1986).
9. J. P. Hénichart, J. L. Bernier, and J. P. Catteau, *Hoppe-Seyler's Z. Physiol. Chem.*, **363** (1982).
10. J. P. Hénichart, J. L. Bernier, R. Houssin, M. Lohez, A. Kenani, and J. P. Catteau, *Biochem. Biophys. Res. Commun.* **126**, 1036 (1985).
11. J. Peisach and W. E. Blumberg, *Arch. Biochem. Biophys.* **165**, 691 (1974).
12. B. G. Malström, B. Reinhammar, and T. Vänngard, *Biochim. Biophys. Acta* **156**, 67 (1968).
13. B. G. Malström, B. Reinhammar, and T. Vänngard, *Biochim. Biophys. Acta* **205**, 48 (1970).
14. A. S. Brill and G. F. Bryce, *J. Chem. Phys.* **48**, 4398 (1968).

15. D. C. Gould and A. Ehrenberg, *Eur. J. Biochem.* **5**, 451 (1968).
16. D. Forster and V. W. Weiss, *J. Phys. Chem.* **72**, 2669 (1968).
17. T. E. Jones, D. B. Rorabacher, and L. A. Ochrymowycz, *J. Am. Chem. Soc.* **97**, 7485 (1975).
18. Y. Sugiura, T. Suzuki, M. Otsuka, S. Kobayashi, M. Ohno, T. Takita, and H. Umezawa, *J. Biol. Chem.* **258**, 1328 (1983).
19. Y. Iitaka, N. Nakamura, T. Nakatani, Y. Muraoka, A. Fujii, T. Takita, and H. Umezawa, *J. Antibiot.* **31**, 1070 (1978).

Received March 18, 1987; accepted June 16, 1987

Conclusion :

Il est à noter que le complexe de type I relaté dans l'article ci-dessus n'est observé qu'en l'absence d'ADN. En RPE, le complexe classique AGGA-Cu en présence d'ADN donne un signal correspondant à un complexe de structure pyramidale à base carrée dont le métal occupe le centre du plan. La fraction acridinique de AGGA s'intercale normalement et ne peut donc plus perturber la géométrie du complexe.

Les résultats obtenus avec les deux modèles AGGA et AGAMGA se résument de la façon suivante :

_ La liaison à l'ADN par intercalation de l'acridine ne devrait pas être perturbée par le voisinage du complexe métallique mais est rendue impossible par la proximité de résidus fortement basiques.
_ La complexation s'accompagne d'une production de radicaux libres, production d'autant plus intense que l'oxygène moléculaire est stabilisé et activé.
_ Des coupures mono- ou double-brin de l'ADN n'ont pas lieu ; il faut accroître la production de radicaux libres oxygénés produits (en particulier les radicaux OH·).

Prenant en compte ces informations et les résultats obtenus avec les analogues de la Blm, AMBI-A_2 et AMBIGLU, il apparaissait dès lors très probable que le remplacement du bras protecteur de type morpholinopropyle par le chaînon glutamyl-glucosamine conduirait à un dérivé très performant . Encore fallait-il vérifier cette hypothèse : la publication suivante la vérifie.

article n° 10 :

DNA-binding and DNA-cleaving properties of a synthetic model AGAGLU related to the antitumor drugs AMSA and Bleomycin.

BAILLY C., KENANI A., HELBECQUE N., BERNIER J-L.,
HOUSSIN R., HENICHART J-P.

Biochemical and Biophysical Research Communications 1988, **152**, 695-702.

Vol. 152, No. 2, 1988 BIOCHEMICAL AND BIOPHYSICAL RESEARCH COMMUNICATIONS
April 29, 1988 Pages 695-702

DNA-BINDING AND DNA-CLEAVING PROPERTIES OF A SYNTHETIC MODEL AGAGLU RELATED TO THE ANTITUMOUR DRUGS AMSA AND BLEOMYCIN

Christian Bailly[1], Abderraouf Kenani[1], Nicole Helbecque[1], Jean-Luc Bernier[1], Raymond Houssin[2], and Jean-Pierre Hénichart[1]

[1]INSERM U-16, Place de Verdun, 59045 Lille, (France)

[2]Laboratoire de Chimie de Synthèse de Médicaments, Faculté de Pharmacie, rue Laguesse, 59045 Lille, (France)

Received February 19, 1988

We have previously described two synthetic models gathering a simplified model of the complexing part of Bleomycin (Blm) and the intercalating moiety of m-AMSA. These molecules, namely AGGA and AGAMGA, do not seem able to cleave DNA as Blm does. The present work is devoted to the study of a new derivative, AGAGLU, which includes in its structure a judiciously chosen connector between the two parts of the molecule. This compound, the chelating and DNA-binding properties of which are described here, has been shown to induce single-strand breakage of duplex DNA in a high level.

m-AMSA, 4'-(9-acridinylamino)-methanesulfon-m-anisidide is active against a wide spectrum of transplantable tumors (1-3) including L1210 and P388 leukemia, B16 melanoma, Lewis lung carcinoma, C3H mammary adenocarcinoma and mammary tumor in $CD8F_1$ mice and is currently in clinical use. The antineoplastic activity of the drug is believed to be due to DNA strand scissions involving an oxidative process (4,5) and/or a modification of DNA topoisomerases II function (6,7). It has been demonstrated that the primary step of the mode of action is a recognition of the DNA target by intercalation of the acridine ring (8). A lot of chemical modifications of this key structure have been reported by different laboratories in order to improve the affinity of the molecule to the binding sites. In particular, we have introduced at the 4-position of the phenyl ring a dipeptide Lys-Gly and the obtained compound ALGA was found to bind DNA with a high affinity, to show a high cytotoxic activity and a cell cycle effect (9,10). Another important modification consisted in replacing the dipeptide chain by a more sophisticated peptide including the simplified complexing part of Bleomycin (Blm), an antitumor drug used in the treatment of squamous cell carcinomas and malignant lymphomas (11,12). The DNA-binding, the metal-chelating and cytotoxic properties of this interesting molecule AGGA were

0006-291X/88 $1.50

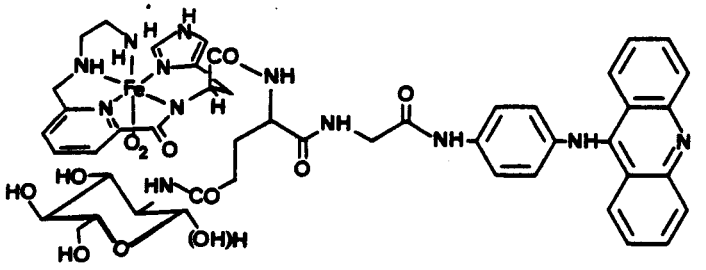

Fig. 1- Structure of the AGAGLU-Fe(II)-O_2 complex.

established (13,14). In addition, it was postulated that the DNA-cleaving properties of the molecule could be improved by the introduction of a bulky hydrophilic group in the surrounding of the complexing part to facilitate the activation of molecular oxygen in the iron(II)-drug-O_2 complex. This hypothesis was confirmed by the comparative studies on Blm and deglycoBlm (15,16) and their synthetic models (17,18), which clearly demonstrated that both binding and complexing parts are required in the same molecule in order to obtain strand scission by hydroxyl radicals produced in the immediate vicinity of the deoxyribose. Moreover, it can be stated that the disaccharide part of Blm plays a role in the stabilization of the iron-oxygen complex and in the activation of molecular oxygen to generate free radicals.

On the basis of these observations, a new synthetic model AGAGLU is here proposed (Fig. 1). Taking into account previous studies, AGAGLU was built by connecting the simplified chelating part of Blm, namely AMPHIS, to the anilinoacridine ring via a short peptidic spacer Glu-Gly on which a glucosamine residue was linked. The glucosamine can play the role of a protecting pocket as the gulose-mannose carbohydrate part of Bleomycin-iron-O_2 complex and the Glu-(glcNH$_2$)-Gly glycopeptide could facilitate the location of the peptide part of AGAGLU in the minor groove by the establishment of hydrogen bonds with DNA bases.

MATERIALS AND METHODS

Materials

* Blm A_2 hydrochloride was supplied by the Nippon Kayaku Company.
* AGAGLU was prepared by coupling 4-(9-acridinylamino)-N-glycylaniline (9) with [[(amino-2-ethyl)-2-aminomethyl]-2-pyridine-6-carboxylhistidinyl-6-(2-amino-2-deoxy-D-glucosyl)-glutamic acid (16) in the presence of isobutyl chloroformate and N-methylmorpholine at -20°C to give protected AGAGLU which was purified by flash chromatography (19) in the system solvent : ethylacetate-acetone (1/1, v/v), (Rf : 0.51). The protecting groups were removed by hydrobromic acid in acetic medium to give pure AGAGLU ([[(amino-2-ethyl)-2-aminomethyl]-2-pyridine-6-carboxylhistidyl-6-(2-amino-2-deoxy-D-glucosyl)glutamylglycylamino]-4-phenyl-1-aminoacridine) : NMR-^{1}H, DMSO-d_6,δ ppm : 8.10-7.20 (m,aromatic and heterocyclic protons), 5.25-4.05 (m,carbohydrate CH and α-CH), 3.70-2.90 (m, CH_2) ; MS-FAB : 947 (M^++1).

Methods

* Spectroscopic Measurements

Absorption spectra were recorded on a Cary 118 spectrophotometer. The circular dichroism (C.D.) spectra were recorded with a Jobin-Yvon dichrograph R-J Mark III in quartz cells of appropriate pathlengths in order to achieve an absorbance of less than 1.5. The ellipticity was expressed in degrees.cm^2. $dmole^{-1}$. AGAGLU was dissolved in water and the pH was adjusted by adding either HCl or NaOH.

Fluorescence spectra were recorded at 20°C on a Jobin-Yvon J-Y-3 spectrofluorometer equipped with an X-Y recorder. All measurements were made in a 4 ml, 10 mm pathlength quartz cuvettes. AGAGLU and calf thymus DNA were dissolved in 0.1 SSC buffer (pH 7.0). The excitation wavelength was set at 400 nm. Uncorrected fluorescence spectra were reported.

E.s.r. measurements were recorded on a Brüker ESP 300 X-band spectrometer with a TE 102 cavity. A 100 kHz frequency modulation was used with a 50 mw microwave power and g values were determined from α,α'-diphenyl-β-picrylhydrazyl (g=2.0036). The sample solutions were disposed into a flat quartz cell.

* Spin-trapping technique and melting temperature studies were made as previously described (13, 20).

* Viscometry

Viscometric measurements were made by using a Ubbelohde semi-micro dilution viscometer. Temperature was maintained at 25 ± 0.01°C in a thermostatically controlled water bath. Flow times were electronically measured to an accuracy of 0.1 s (Schott ABS/G type detector). Experiments were done in 0.01 SHE buffer [9.4mM NaCl/2mM HEPES(N-(2-hydroxyethyl)piperazine-N'-2 ethanesulfonic acid)/10 μM EDTA (ethylenediaminetetraacetic acid) buffer, pH 7.0]. Low (sonicated) and high molecular weight DNA are from calf thymus. Solutions were filtered through 0.45 μm Millipore filters before measurements.

Unwinding studies using closed circular DNA (plasmid pII 1A) were performed essentially as described by Saucier (21) and Revet (22) on the apparatus described above. The viscometer contained 2.0 ml of a 150 μM solution of DNA. Drugs were added in increments of 5-10 μl from a stock solution (c = 150 μM). Flow times were measured with an accuracy of 0.1 s. Ethidium bromide was used as reference inducing an unwinding angle of 26°, according to Wang (23).

* Single strand and double strand DNA breakage

This can be visualized by the use of supercoiled DNA (form I). The products of plasmid reaction (form II : relaxed circular DNA, form III : open linear DNA) with either Blm-A_2 or AGAGLU were separated on a 0.8 % agarose gel, containing 0.5 μg/ml of ethidium bromide.

Plasmid pBR 322 was incubated with Blm or AGAGLU in 50 mM Tris-HCl, pH 8.0 buffer containing 10 mM 2-mercaptoethanol. $Fe(NH_4)_2(SO_4)_2,6H_2O$ was added in the same final concentration as the product. After 20 min at room temperature, the reaction was terminated with the addition of EDTA 2.5 mM, 5μl of 0.01 % bromophenol blue were added to the reaction mixture (50 μl). Agarose electrophoresis was performed in TBE buffer at 8V/cm for 3 hours and examined under a 254 nm UV light. The negative films of gels were used for densitometric scannings.

RESULTS

Complexation studies : In order to study the ability of AGAGLU to complex Cu (II) in the same way as AGGA and Blm-A_2, circular dichroism experiments were conducted at different pHs. (Fig. 2). Complexation of Cu(II) by AGAGLU is accompanied by a change in the conformation of the local site, which should in turn lead to a change in the contribution of that site to the overall AGAGLU C.D. spectrum. Whatever the pH, AGAGLU alone (Fig 2a) exhibits a positive band at 278 nm ($n \rightarrow \pi^*$ pyridine) while the $\pi \rightarrow \pi^*$ imidazole transition is

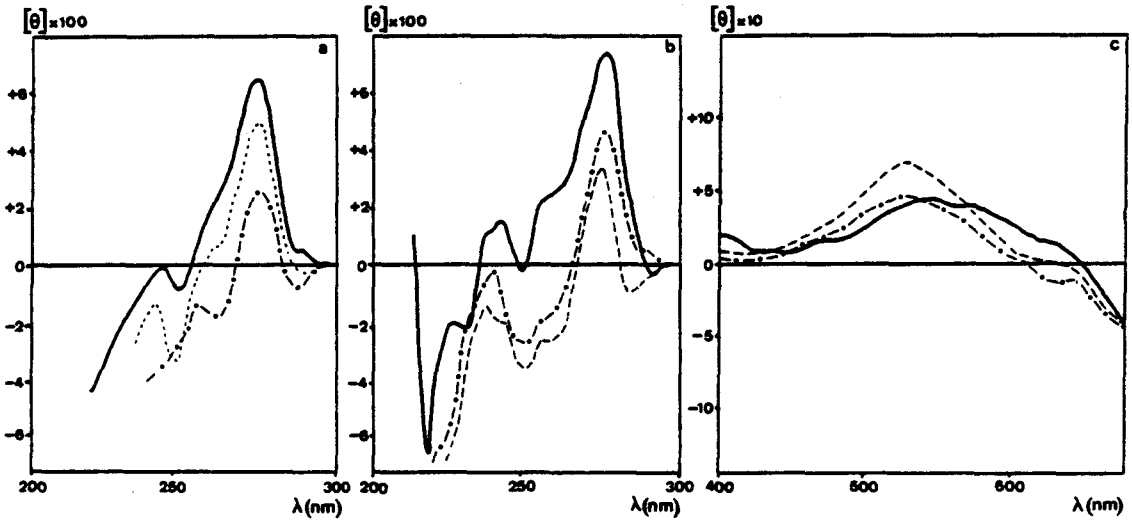

Fig. 2-(a) CD spectra of AGAGLU at pHs 11.4 (—), 10.7 (·····) and 5.5, 4.2, 2.05, 1.5 (— · —). (b,c) CD spectra of AGAGLU-Cu(II) [1:1 complex] at pHs 11.2 (-), 6.5 (---) and 4.4, 3.3, 2.5 (-·-·).

characterized by a band located at 265 nm, either positive at basic pH ([θ]=+ 200 degrees.cm^2.dmole^{-1}), or negative at acidic pH ([θ]=-180 degrees.cm^2. dmole^{-1}). It has to be noted that the anilinoacridine moiety of the molecule does not exhibit any dichroism, such as m-AMSA itself. By adding Cu(II) (Fig. 2b), a change in the 240-260 nm region immediately occurs characterizing transitions attributable to $\pi \rightarrow \pi^*$ imidazole, and N → Cu charge transfer. Two bands can be seen in the Cu(II) absorption region, one positive at 530 nm and a small negative one near 680 nm, while no dichroism was generated in the 400-450 nm region (acridine).The major differences observed in the spectra when adding Cu(II) are those characteristically observed for a complexation process. The spectrum obtained for AGAGLU-Cu(II) is reminiscent of the one exhibited by AMPHIS-GABA-Cu(II) at similar pH (24).

Moreover, it has to be noted that small values of ellipticity were observed, but this fact was not surprising since C.D. is known to be very sensitive to steric constrainsts. This results are in favour of a chelating process which requires the same ligands for Cu(II) (and Fe(II)) in the square planar complexes of AGAGLU and AMPHIS-GABA.

DNA interaction : An interaction with DNA has been demonstrated on the basis of results obtained by fluorescense quenching, melting temperature studies and viscometry measurements.

The fluorescence spectra of AGAGLU in the presence of increasing amounts of calf thymus DNA are shown in Fig. 3. A bathochromic shift of 8 nm and a decrease of approximately 50 % of the maximum of fluorescence were observed.

The ΔTm value found for AGAGLU is 9°C, in the same order of magnitude as those

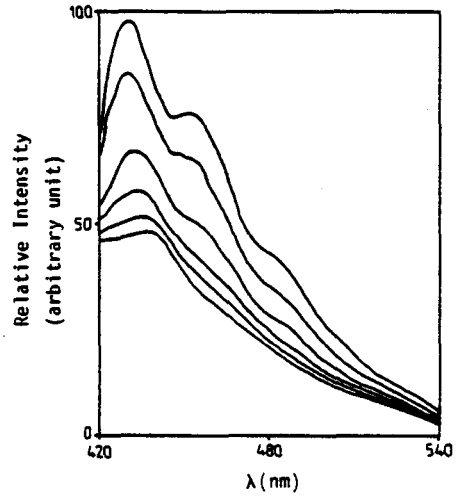

Fig. 3- Fluorescence quenching of AGAGLU by calf thymus DNA ; with 250 µM AGAGLU in 0.01 M SSC buffer pH 8.0 ; concentrations of DNA are : 50, 100, 150, 200 and 250 µM. Fluorescence spectra were recorded after 5 min. of incubation at room temperature.

obtained for 9-anilinoacridine derivatives (m-AMSA,7°C(10);AGGA,8°C(13); ALGA,10°C(10)). The slightly higher ΔTm observed for AGAGLU than for m-AMSA could be attributed to supplementary hydrogen bondings between the hydroxyl residues of the $GlcNH_2$ moiety and heteroatoms of DNA.

The effect of AGAGLU, under standard conditions, on the variation of the supercoiling of pII 1A DNA was studied by viscometry. It yields the characteristic rise-and-fall response reflecting removal and reversal of the supercoiling, attributable to drug-induced unwinding of the DNA helix usually observed in the case of intercalative drugs. The reduced viscosity at the maximum of the curve indicates an unwinding angle of 9°, a value which is similar to the total amount of unwinding observed with classical intercalators such as daunomycin or some derivatives of 9-aminoacridine.

Surprisingly a decrease in viscosity was observed when adding AGAGLU either to high or to low molecular weight DNA. Such a result was previously obtained when studying the interaction of small peptides having an aromatic side chain with DNA(25) and in the case of BLM-DNA complexes (26) and reflects a decrease in DNA length (distance between two base pairs : 2.99Å for DNA-AGAGLU, 3.4Å for DNA).

Free radicals production : In addition, the spin trapping experiment of the AGAGLU-Fe(II)-O_2 gave the E.s.r. absorptions (triplet of doublet, g = 2.0057, and a^N = 15.3 G) due to the hydroxyl spin adduct of α-phenyl N-t-butyl-nitrone (spectrum not reported).

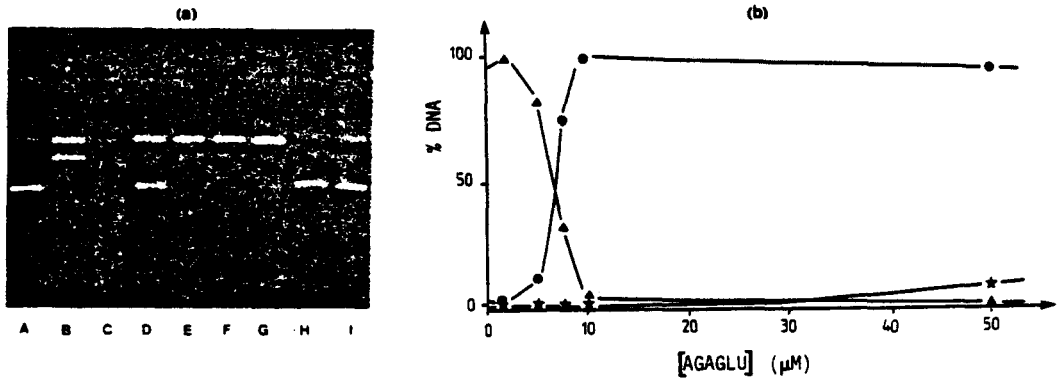

Fig. 4-(a) Agarose (0.8 %) gel electrophoretic patterns of ethidium bromide-stained pBR322 DNA after treatment with AGAGLU-Fe(II) complex (lanes E-I) and controls (lanes A-D). DNA migrated from top to bottom in the order of decreasing distance of form I, form III and form II DNAs. Lane A : untreated DNA. Lane B,C : 1,50 μM Blm-Fe(II). Lane D : 30μM m-AMSA-Cu(II). Lanes E-I : 100,50,10,5,1 μM AGAGLU-Fe(II). Reaction mixtures were in 50 mM Tris-HCl, pH 8.0, incubated at room temperature for 20 min. (b) Percentage distribution of DNA conformational isomers after treatment with AGAGLU and Fe(II). Data were obtained from the gel pattern shown in (a), lanes A and E-I and three others. DNA was treated with increasing concentrations of AGAGLU and Fe (II). Key : (▲) form I DNA ; (●) form II DNA and (★) form III DNA.

DNA-cleavage : When the reaction mixture containing 0.5 μg DNA, 50 mM Tris-HCl buffer (pH 8.0), and AGAGLU-Fe(II) complex was incubated at 37°C for 20 min., the typical agarose (0.8%) gel electrophoretic pattern of the covalently closed supercoiled (form I) pBR 322 DNA clearly demonstrated that this ferrous complex significantly induced single-strand breaks of DNA to form nicked (form II) DNAs (see Fig. 4a). There was an apparent gradual shift in the production of form II (single strand breaks). Iron(II) or AGAGLU (100 μM), when used alone, produced only a small amount of single-strand breakage.

The DNA break production was analysed by densitometry and revealed that the untreated pBR 322 DNA contained approximately 95 % form I DNA and 5 % form II DNA. Fig. 4b shows the densitometric scanning results of lanes A and E-I of Fig. 4a. In the presence of Fe(II), DNA breakage increased rapidly with AGAGLU concentration (1 to 10 μM). At 10 μM, the total amount of form I DNA was converted to form II. This result clearly indicates that AGAGLU caused DNA degradation basically by single strand breakage. At 50-100 μM, only 10 to 15 % form III DNA was obtained, contrarily to Blm for which 1μM Blm produced approximately 50 % form III DNA. (Fig. 4a, lane B).

DISCUSSION

The first purpose of this work was to design a new compound with a simple structure, able to chelate metals, to produce free radicals and to induce DNA-strand breakage as Blm does and in addition to have a higher affinity for

the target. The result of fluorescence quenching and thermal denàturation indicate that AGAGLU is able to bind DNA with a high affinity. Though the results of unwinding studies are in favour of an intercalative process of binding, the observed decrease in length leads us to propose a binding process similar to the one found for Phe-containing oligopeptide amides (25) or for Blm (26). This consists in a partial insertion of anilinoacridine between base pairs of DNA accompanied by a bending of the double helix. AGAGLU which possesses the minimum structural requirements for metal chelating (17) was found to complex copper and iron in the same conditions as Blm or AGGA.

Moreover, a significant advance of this report is the demonstration of the role of the sugar part. The bulky glucosaminyl group in the surrounding of the complexing part seems to play a key role in the activation of the molecular oxygen. The stabilization of the ternary complex AGAGLU-Fe(II)-O_2 and its activation were visualized by the increased production of free radicals. This bulky group could form a binding site pocket around the molecular oxygen potentially stabilized by hydrogen bonding with the peptidic moiety. A similar stabilization has been observed for the haemoglobin-Fe(II)-O_2 complex in which histidine and adjacent peptide bonds are able to establish hydrogen bondings with oxygen. The disaccharide moiety of Blm seems to meet these requirements apart from its putative capacity to recognize some part of the cell membrane. The glucosaminyl moiety which stabilizes the ternary complex is linked to a short spacer (the glutaminyl residue) which gets the chelating part into ideal position at a short distance from the deoxyribose target. If hydroxyl radicals are regarded as responsible for the degradation of DNA as previously reported (28-30), they are produced in the immediate vicinity of the deoxyribose.

The other aim of this work comes within the scope of the establishment of coherent structure-activity relationships in view to design new synthetic cytotoxic anti-cancer drugs. The conception of drugs able to cleave DNA requires on the same molecule a strong DNA-binding part and a free radicals producing part. But previous works and the present report clearly demonstrate that this condition is necessary but not sufficient. Another important consideration is the relative position of the cleaving site with respect to the binding part and consequently the choice of the connector is of a crucial importance. The nature of the linking chain and the presence of hydrophilic groups may play a role in the pharmacological activity.

Nevertheless, such rationally developped rules are not always so precise enough to design highly active compounds. Adequate chemical modifications, even if they could lead to the design of very active compounds in vitro, must take into account critical factors : (i) the susceptibility of these compounds to inactivation by enzymatic or non-enzymatic metabolisms (ii) the possible interaction with transport systems or membrane components which might affect

rates of penetration into different types of cells. These factors are to be considered for the design of more efficient medicinal drugs.

ACKNOWLEDGEMENTS

This research was supported by grants from the "Institut National de la Santé et de la Recherche Médicale" and the "Fédération Nationale des Centres de Lutte contre le Cancer". We thank Pascale DOOLAEGHE for typing the manuscript.

REFERENCES

1. Corbett, T.H., Griswold Jr, D.P., Roberts, B.J., Peckham, J.C., Schabel Jr, F.M. (1977) Cancer 40, 2660-2680.
2. Louie, A.C., Issell, B.F. (1985) J. Clin. Oncol. 3, 562-570.
3. Cassileth, P.A., Gale, R.P. (1986) Leukemia Res. 10, 1257-1265.
4. Wong, A., Huang, C.H., Crooke, S.T. (1984 a) Biochemistry 23, 2939-2945.
5. Wong, A., Huang, C.H., Crooke, S.T. (1984 b) Biochemistry 23, 2946-2952.
6. Pommier, Y., Minford, J.K., Schwartz, R.E., Zwelling, L.A., Kohn, K.W. (1985a) Biochemistry 24, 6406-6410.
7. Pommier, Y., Minford, J.K., Schwartz, R.E., Zwelling, L.A., Kohn, K.W. (1985 b) Biochemistry 24, 6410-6416.
8. Waring, M.J. (1976) Eur. J. Cancer 12, 995-1001.
9. Hénichart, J.P., Bernier, J.L., Catteau, J.P. (1982) Hoppe-Seyler's Z. Physiol. Chem. 363, 835-841.
10. Collyn-d'Hooghe, M., Bernier, J.L., Hénichart, J.P. (1987) Cancer Biochem. Biophys. 9, 257-264.
11. Carter, S.K. (1985). In Bleomycin Chemotherapy. Sikic, B.I., Rozencweig, M., Carter, S.K. (eds), pp. 3-43, Academic Press : New-York.
12. Crooke, S.T. (1978) In Bleomycin : Current Status and New Developments. Carter, S.K., Crooke, S.T., Umezawa, H. (eds), pp 9-14, Academic Press : New-York.
13. Bailly, C., Bernier, J.L., Houssin, R., Helbecque, N., Hénichart, J.P. (1987) Anti-Cancer Drug Design 1, 303-312.
14. Bailly, C., Pommery, N., Hénichart, J.P. (1987) Cancer Lett. in press.
15. Kenani, A., Lamblin, G., Hénichart, J.P. Carbohyd. Res. in press.
16. Kenani, A. (1987) Ph. D. Thesis (Lille).
17. Hénichart, J.P., Bernier, J.L., Houssin, R., Lohez, M., Kenani, A., Catteau, J.P. (1985) Biochem. Biophys. Res. Commun. 126, 1036-1041.
18. Kenani, A., Lohez, M., Houssin, R., Helbecque, N., Bernier, J.L., Lemay, P., Hénichart, J.P. (1987) Anti-Cancer Drug Design 2, 47-59.
19. Still, W.C., Kahn, M., Mitra, A. (1978) J. Org. Chem. 43, 2923-2925.
20. Janzen, E.G., Blackburn, B. J. (1968) J. Am. Chem. Soc. 90, 5909-5910.
21. Saucier, J.M., Festy, B., Le Pecq, J.B. (1971) Biochimie 53, 973-980.
22. Revet, B., Schmir, M., Vinograd, J. (1971) Nature New Biol. 229, 10-13.
23. Wang, J.C. (1974) J. Mol. Biol. 89, 783-801.
24. Bailly, C., Catteau, J.P., Helbecque, N., Bernier, J.L., Houssin, R., Denis, C., Hénichart, J.P. (1987) J. Inorg. Biochem. 31, 211-220.
25. Gabbay, E.J., Adawadkar, P.D., Wilson, W.D. (1976) Biochemistry 15, 146-151; ibid. 152-157.
26. Hénichart, J.P., Bernier, J.L., Helbecque, N., Houssin, R. (1985) Nucl. Acids Res. 13, 6703-6717.
27. Shaanan, B. (1982) Nature 296, 683-684.
28. Sugiura, Y., Kikuchi, T. (1978) J. Antibiot. 31, 1310-1312.
29. Lown, J.W. (1979). In Bleomycin : Chemical, Biochemical and Biological Aspects. Hecht, S.M. (ed) pp. 184-194, Springer-Verlag : New-York.
30. Oberley, L.W., Buettner, G.R. (1979) FEBS Lett. 97, 47-49.

Conclusion :

Le dérivé AGAGLU répond donc parfaitement à nos prévisions en ce qui concerne la complexation et la dégradation de l'ADN et démontre ainsi la cohérence des relations structure-activité fondées initialement.

La série chimique AMPHIS, AMBI-A_2, AMBIGLU, AGGA, AGAMGA et AGAGLU nous a apporté des résultats précis et directement extrapolables pour une meilleure compréhension du mécanisme d'action de la Blm, l'enseignement principal étant d'avoir montré le rôle de la fraction glycannique de la Blm non seulement par une étude directe sur la substance naturelle (KENANI, 1988; KENANI et al., 1988b) mais également par modélisation. La pharmacomodulation entreprise est incontestablement concluante.

Tenter de reproduire un mécanisme d'action aussi complexe que celui de la Blm a représenté un travail très lourd particulièrement sur le plan de la chimie de synthèse. Le but principal n'était pas de rechercher une activité pharmacologique supérieure à celle de la Blm mais d'en démontrer le mode d'action. Néanmoins la conception de substances nouvelles au cours de cette étude aurait pu nous amener à l'élaboration de molécules structuralement simples et biologiquement actives.

A ce sujet, les deux composés les plus performants sur le plan de la fixation à la cible, AMBIGLU et AGAGLU, se sont révélés inactifs. Par contre, AGGA, sans dégrader l'ADN s'imposait comme un composé relativement actif.

La conception de tels composés n'est donc pas dénuée d'espérance thérapeutique à long terme. D'ailleurs cet avis est, au vue de la richesse bibliographique sur ce sujet, partagé par d'autres équipes qui ont elles-aussi retenu le concept " Peptide Chélateur-Intercalant " par une approche chimique différente.

3°) Le concept Peptide Chélateur-Intercalant : les analogues fonctionnels de la Blm.

a) Introduction.

La Blm se compose très schématiquement de deux fragments : une fraction complexante et une fraction se liant à l'ADN.

Il est à noter que, si parmi les substances naturelles répondant à ce concept, la Blm apparaît comme l'archétype, de nombreux autres composés anticancéreux isolés d'organismes bactériens ou fongiques sont à inclure dans cette catégorie. C'est le cas notamment de :

-La daunomycine et l'adriamycine
-La chromomycine, l'olivomycine et la mithramycine
-La streptomycine
-La néocarzinostatine
-La mitomycine

Le mode d'action de ces composés est toujours métal-dépendant (le fer est très souvent impliqué) et DNA-dépendant (l'intercalation n'est pas toujours observée) (DABROWIAK J.C., 1980a).

Tenant compte de cette seule définition, de nombreuses approches chimiques ont été envisagées pour répondre à ce concept.
Parmi les analogues synthétiques, on peut citer entre autres :

Domaine "metal-binding"	Domaine "DNA-binding" (intercalants uniquement)
Porphyrine	acridine (LOWN et al., 1982, 1986c)
	acodazole " " "
	dipyridoimidazole (HASHIMOTO et al., 1986)
EDTA	méthidium (HERTZBERG & DERVAN, 1982, 1984)

Pour notre part, le modèle complexant choisi est le tripeptide Gly-His-Lys

b) Les modèles Gly-His-Lys—Intercalant.

Gly-His-Lys est un peptide isolé du plasma sanguin sous forme de complexe cuivrique à la concentration importante de 200 ng/ml (PICKART & THALER, 1973). Ce peptide constitue un facteur de croissance pour différentes cellules : hépatocytes, lymphocytes, fibroblastes et certaines cellules tumorales (KB, HeLa) (PICKART & LOVEJOY, 1987). Il est donc biologiquement stable sous forme complexée.

La liaison d'un tel peptide à une fraction intercalante présente divers avantages :

1- Faciliter la pénétration cellulaire de l'intercalant.
2- Amener à proximité de l'ADN un système chélateur et producteur de radicaux libres.
3- Intensifier la liaison à l'ADN par l'intermédiaire du résidu lysyle susceptible d'engager une liaison saline avec un groupement phosphate de l'ADN (KARUP et al., 1988).
4- Potentialiser l'action antitumorale de l'intercalant.

Ce dernier point est basé sur les travaux de Kimoto et al. montrant que le tripeptide Gly-Gly-His (la fraction complexante de la sérum albumine humaine, LAU et al., 1974) amplifie l'activité antitumorale de l'ascorbate (KIMOTO et al., 1983). L'analogie avec le tripeptide Gly-His-Lys est possible, compte tenu de la similitude des complexes : tous deux ont une structure plane tétracoordinée (CAMERMAN et al., 1976; LAUSSAC et al., 1983; FREEDMAN et al., 1982b) .

Les peptides Gly-His-Lys et Gly-His complexent le cuivre de la même façon. Le résidu lysyle n'est pas impliqué dans la complexation mais est essentiel à l'activité biologique de Gly-His-Lys-Cu(II) (PICKART et al., 1979; PICKART & THALER, 1979). La lysine serait impliquée dans la reconnaissance d'un récepteur membranaire.

Ce peptide a été greffé sur deux intercalants :

a- l'anilinoamino-9 acridine : fraction purement intercalante de l'amsacrine (composé 1). Un résidu glycyle sert de pontage entre l'acridine et le tripeptide; deux raisons nous ont conduit à ce choix :

1. Faciliter la synthèse de l'intercalant (HENICHART et al., 1982b).
2. Obtenir le produit Gly-His-Lys-Gly-anilinoamino-9 acridine, au sein duquel on retrouve l'enchaînement Lys-Gly-anilinoamino-9 acridine (ou ALGA) pourvu de propriétés antitumorales importantes (COLLYN-d'HOOGHE et al., 1987).

b- le bithiazole : fraction pseudo-intercalante de la Blm (composé 2).

L'étude de la liaison à l'ADN et de l'activité biologique de ces deux modèles du type "Complexant-Intercalant" est présentée dans l'article suivant :

article n° 11 :

Synthesis, biological activity and DNA interaction of anilinoacridine and bithiazole peptide derivatives related to AMSA and bleomycin antitumor drug.

MORIER-TEISSIER E., BAILLY C., BERNIER J-L., HOUSSIN R., HELBECQUE N., CATTEAU J-P., COLSON P., HOUSSIER C., HENICHART J-P.

Accepté pour publication dans Anti-Cancer Drug Design.

Synthesis, biological activity and DNA interaction of anilinoacridine and bithiazole peptide derivatives related to AMSA and bleomycin antitumor drug.

E. MORIER-TEISSIER[+], C. BAILLY[+], J-L. BERNIER[+], R. HOUSSIN[++], N. HELBECQUE[+], J-P. CATTEAU[*], P. COLSON[**], C. HOUSSIER[**] and J-P. HENICHART[+]

[+]INSERM U.16, Place de Verdun 59045 Lille, France, [++]Institut de Chimie Pharmaceutique, Faculté de Pharmacie, Rue Laguesse 59045 Lille, France,
[*]Laboratoire de Chimie Organique Physique , USTL, 59655 Villeneuve d'Ascq, France,
[**]Laboratoire de Chimie Macromoléculaire et Chimie Physique, Université de Liège, Sart-Tilman, 4000 Liège, Belgique.

Summary : The synthesis of two depsipeptides including a peptide metal chelating moiety (Gly-His-Lys) and a moiety with DNA affinity namely either glycyl-anilino-9-aminoacridine 1 or 2'-(2aminoethyl)-4-methoxycarbonyl-2'-4'-bithiazole 2, has been carried out. The goal was to introduce separately on the same molecule the two factors contributing to the biological activity of most of antitumoral drugs. The interaction of both drugs with DNA has been studied and the acridine ring of 1 was found to intercalate in the double helix. The production of free radicals has been evidenced by spin-trapping for 1 although both compounds revealed to be good copper chelating agents. In vitro cytostatic activity and inhibition of [^{3}H]-thymidine incorporation was obtained for 1 while 2 exhibited no activity in both tests. In view of these results, it can be pointed out that the antitumor properties of such drugs were relied (i) on their ability to reach and to bind DNA and (i,i) on redox mechanisms involving interactions between the drugs, metals and molecular oxygen. The latter phenomenon leads to the formation of active radical species, able to degrade the DNA.

Introduction :

Intercalating drugs have been shown to possess high antitumor activity and have proved their usefulness in clinical medicine (Neidle and Waring, 1983). Although intercalation of these agents in the double helix of DNA was found to be the primary step in their activity, it has been established that other processes are involved, particularly redox reactions leading to DNA damages (Favaudon, 1982). Such is the case for bleomycin, a glycopeptide antibiotic (Umezawa et al., 1966), widely used in the treatment of malignant tumors (Umezawa, 1979). The mechanism of action of this drug has been well studied and involves two well-defined parts of the molecule : a metal ion-chelating moiety responsible for the cleavage of DNA (Burger et al., 1981) associated with a bithiazole containing moiety which contributes to the binding of the drug to DNA (Povirk et al., 1979 ; Hénichart et al., 1985a). Another intercalating drug with antileukaemic activity, m-AMSA N-[4-(9-acridinylamino)-3-methoxyphenyl] methanesulfonamide was shown to be bioactivated by oxidation in the presence of cupric ions to a quinonimine form, m-AQDI N^1-(9-acridinyl)-N^4-(methanesulfonyl)-2-methoxy-2,5-cyclohexadien-1,4-diimine (Jurlina et al., 1987).

In the course of a program aimed at providing new antineoplastic drugs, we have designed synthetic models of bleomycin in order to define the role of the different parts of the drug (Hénichart et al., 1982a, 1984, 1985a and b ; Houssin et al., 1984a and b ; Kenani et al., 1987, and have investigated the 9-anilinoacridines series (Hénichart et al., 1982b ; Lemay et al., 1983 ; Helbecque et al., 1985). Since, in our opinion, the bithiazole part of bleomycin was not proved to be a classical intercalating agent (Hénichart et al., 1985a) we thought to improve the antitumor activity by synthesizing a hybrid model incorporating the metal chelating moiety of bleomycin (AMPHIS) and a 9-anilinoacridine moiety able to intercalate in DNA. The design of such models (Bailly et al., 1987a and b) leads to the concept of metal-chelating-intercalating drug. The present paper reports the use of a simpler peptidic metal-chelating part in association with either a bithiazole moiety or an anilino-acridine ring, in place of the bleomycin-type chelating moiety (AMPHIS). The choice of the tripeptide glycyl-L-histidyl-L-lysine was dictated by its ability to complex copper and iron, such as illustrated by its co-isolation with albumin and α-globulin fractions from human plasma (Pickart and Thaler, 1973). It has been proposed that the peptide acts synergistically with these transition metals to alter the growth and the metabolism of cultured hepatoma cells and hepatocytes. Furthermore, the results also showed that the tripeptide was able to compete with albumin for Cu(II) at

physiological pH and to facilitate copper uptake into cells. The introduction of such a peptide on a molecule with anti-tumor properties, presented some potential advantages : it confers to the molecule (i) metal chelating properties, (i,i) a specificity towards some tumor cells since this tripeptide has been found to be a growth factor for human KB and Hela cells (Pickart and Lovejoy, 1987) and (i,i,i,) it facilitates penetration into the cell and access of the drug to the nucleus. Thus, the syntheses of two depsipeptides including this peptide and a moiety with DNA affinity have been carried out : peptide chelator-glycyl-anilino-9-aminoacridine and peptide chelator-bithiazole. The synthesis of the latter molecule was planned in order to evaluate the importance of the intercalation and redox mechanisms in the biological activity, since contrarily to the 9-aminoacridine ring, the bithiazole is not a classical intercalating agent (Hénichart et al., 1985a) and is not involved in redox reactions.

1

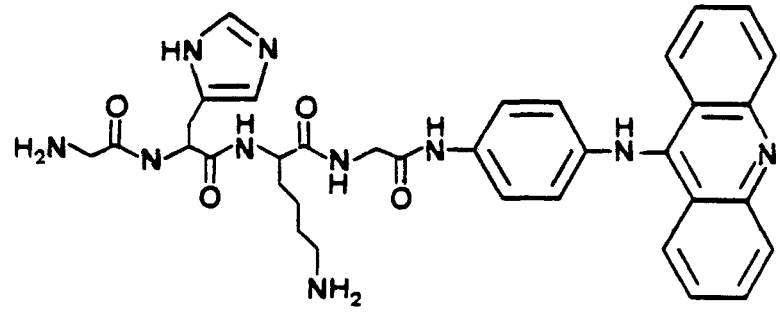

2

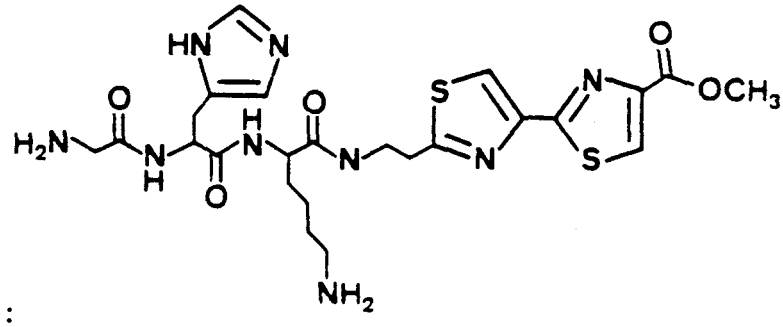

Materials and methods :

The purity of all compounds has been assessed by TLC, ^{1}H NMR and FAB mass spectroscopy.

Melting points were determined in capillary tubes and are uncorrected. The IR spectra were obtained on a Perkin-Elmer 177 spectrophotometer in KBr pellets. ^{1}H-NMR spectra were recorded on a Brucker WP 80 SY or on a Brucker AM 400 WB spectrophotometers. Chemical shifts are reported in ppm from tetramethylsilane as an internal standart and are given in δ units. EI mass spectra were recorded on a Ribermag R10.10 mass spectrometer (combined with Riber 400 data system) at 70 eV by using direct insertion. FAB mass spectra were determined on a Kratos MS-50 RF mass spectrometer arranged in an EBE geometry. The sample was bombarded using a beam

of xenon with a kinetic energy of 7 keV. The mass spectrometer was operated at 8 KV accelerating voltage with a mass resolution of 3,000. Thin layer chromatography (TLC) was carried out using silica gel 60F-254 Merck (0.25 mm thick) precoated UV-sensitive plates, generally in solvent system A ($CHCl_3$-MeOH, 80:20 (v/v) in a saturated NH_3 atmosphere). Spots were visualized by inspection under U.V. light at 254 nm and after exposure to vaporized I_2 and/or ninhydrin. Kieselgel 60 (230-400 mesh) of Merck was used for flash-chromatography according to the procedure of Still (Still et al., 1978).

*Abbreviations : BOC = t-butyloxycarbonyl, Z = benzyloxycarbonyl, AAA = anilino-9-aminoacridine, Gly-AAA = glycyl-AAA.

BOC-L-histidyl-N ε-Z-L-lysine benzyl ester (3)

To a solution of BOC-L-histidine (1.4 g, 5.5 mmole), N-hydroxybenzotriazole (HOBt) (0.92 g, 6 mmole) and N-N' dicyclohexylcarbodiimide (DCC) (1.24 g, 6 mmole) in 30 ml of dry dimethylformamide (DMF) stirred at 0°C for 1 h, was added a solution of Nε-Z-L-lysine benzyl ester hydrochloride (2.23 g, 5.5 mmole) and triethylamine (0.8 ml, 5.5 mmole) in DMF (20 ml). The reaction mixture was stirred at 0°C for 1 h and then at room temperature overnight. N-N' dicyclohexylurea (DCU) was removed by filtration and the solvent evaporated to dryness in vacuo. The crude product was separated from the remaining DCU by dissolution in acetone, then dissolved in methylene chloride ; this solution was washed successively with 1 M HCl, water and 1 M $NaHCO_3$ and then dried over anhydrous Na_2SO_4. The organic solvent was evaporated to dryness to give a white powder (2 g ; 60 % yield); mp 186-194 °C ; Rf = 0.76 ; IR : ν = 1750 (CO ester) ; 1700 (CO urethane) ; 1665 cm^{-1} (CO amide). ^{1}H-NMR (Me_2SO-d_6) : δ = 1.30 (s, 9H, CH_3 BOC), 1.30-1.70 (m, 6H, β,γ, δ CH_2 Lys), 2.80 (m,2H, β CH_2 His), 2.90 (m, 2H, CH_2 Lys), 4.20 (m, 1H, αCH Lys), 4.25 (m, 1H, αCH His), 5.00 (s, 2H, CH_2 benzyl), 5.05 (s, 2H, CH_2 benzyl), 6.75 (s,1H, C^2H His), 7.10 (d, 1H, NH BOC) , 7.40 (2 s, 2 x 5H, aromatic protons), 7.50 (s, 1H, C^4H His), 7.50 (m, 1hH, NH Lys), 8.10 (d, 1H, NH Lys).

L-Histidyl-N-εZ-L-lysine benzyl ester (4)

The BOC protecting group of (3) (2 g, 3.3 mmole) was removed by treatment with 15 ml of trifluoroacetic acid (TFA) at room temperature for 1 h. The trifluoroacetic solution was evaporated in vacuo to give an oil; ethanol was added to the oil and evaporated. The dipeptide trifluoroacetate was dissolved in water, washed with ethyl acetate (AcOEt) ; addition of 1M $NaHCO_3$ and extraction by ethyl acetate gave, after evaporation of the organic phase, 1.40 g (90 % yield) of white powder; mp = 116-126°C

Rf = 0.45 ; IR : disparition of the CO urethane band at 1700 cm^{-1}. ^{1}H-NMR (Me_2SO-d_6) : δ = 1.4 ppm (m, 8H, CH_2), other peaks as above.

Nα-BOC-glycyl-L-histidyl-Nε-Z-L-lysine benzyl ester (5)

To a solution of Nα-BOC-glycine (1.4 g, 3 mmole), HOBt (0.5 g, 3.3 mmole) and DCC (0.7 g, 3.3 mmole) in dry DMF (25 ml) stirred at 0°C for 1 h was added a solution of (4) (1.4 g, 3 mmole) in 50 ml of methylene chloride. The tripeptide was treated and purified as described above. White powder (1.7 g, 85 % yield); mp 160-168°C; Rf = 0.68; IR : ν = 1760 (CO ester) ; 1700 (CO urethane) ; 1630-1680 cm^{-1} (CO amide). ^{1}H-NMR (Me_2SO-d_6) : δ = 1.30 (s, 9H, BOC CH_3), 1.40-1.70 (m, 6H, β, γ, δ CH_2 Lys), 2.80 (m, 2H, β CH_2 His), 2.90 (m, CH_2 Lys), 3.50 (d, 2H, CH_2 Gly), 4.20 (m, 1H, α CH Lys), 4.50 (m, 1H, α CH His), 5.0 and 5.10 (2s, 4H, $2CH_2$ benzyl), 6.75 (s, 1H, C^2H His), 7.20 (m, 1H, NH BOC), 7.40 (s, 10H, aromatic protons), 7.40 (m, 1H, NH Lys), 7.50 (s, 1H, C^4H His), 8.0 (d, 1H, NH His), 8.20 (d, 1H, NH Lys).

Nα-BOC-glycyl-L-histidyl-Nε-Z-L-lysine (6)

1.7 g (2.5 mmole) of (5) in 100 ml MeOH and 0.4 g (10 mmole) NaOH in 10 ml water were left at room temperature for 2 days. After TLC control, the solution was acidified to pH = 3-4 by addition of HCl M and evaporated to dryness. The residue was dissolved in MeOH to separate the insoluble NaCl, dried and used without further purification. Hygroscopic white powder (1.5 g); mp = 135-139°C; Rf = 0; IR : no more band at 1750 cm^{-1} (CO ester). ^{1}H-NMR : disparition of the peaks corresponding to OCH_2 at 5.2 ppm and of 5 aromatic hydrogens, other peaks as above.

Purification of 4-(9-acridinylamino)-N-glycylaniline (7)

The corresponding trifluoroacetate (Hénichart et al., 1982b) is dissolved in water and washed with AcOEt to eliminate the fluorescent side-product acridinone. The aqueous layer is made alkaline by 1M $NaHCO_3$ and the pure free base extracted with AcOEt. A side-product is left in the aqueous layer. The AcOEt layer is dried over Na_2SO_4 and evaporated to dryness to give a brick-red powder homogeneous in TLC. Rf = 0.60 (acridinone : 0.88, side-product in $NaHCO_3$: 0.41).

4-(9-acridinylamino)-N-[Nα-BOC-glycyl-L-histidyl-Nε-ZL-lysyl-glycyllaniline (8)

To a solution of (6) (600mg, 1 mmole) HOBt (168 mg, 1.1 mmole) and DCC (227 mg, 1.1 mmole) in dry DMF (50 ml) stirred at 0°C for 1 h was added 342 mg (1 mmole) of (7). The reaction mixture was treated and purified as described previously for the di- and tripeptide. The yellow compound is then submitted to a flash chromatography on silica gel with CH_2Cl_2MeOH (80:20, v/v) as eluent. Yellow powder (200 mg, 22 % yield);

^{1}H-NMR (Me_2SO-d_6) : apparition of peaks in the aromatic region (7-8 ppm) corresponding to the anilino-9-acridinylamino moiety. FAB : M^++1 = 899; Rf = 0.45 (chloroform/methanol, 9:1 v/v).

4-(9-acridinylamino)-N-(glycyl-L-histidyl-L-lysyl-glycyl)aniline, hydrobromide (1)

A solution of (8) (100 mg, 0.11 mmole) in 5 ml of AcOH saturated in HBr was stirred for 15 min and evaporated to dryness. The residue is dissolved several times in ethanol and evaporated to dryness, then dissolved in water (10 ml), washed with AcOEt (2 x 10 ml) and lyophilized. Yellow powder (50 mg, 50 % yield); Rf = 0; UV : λmax = 255, 410 and 438 nm. FAB : M^++1=665; ^{1}H-NMR (Me_2SO-d_6) : δ = 1.40-1.70 (m, 6H, β, γ, δ CH_2 Lys), 2.80 (m, 2H, β CH2 His), 2.90 (m, 2H, CH_2Lys), 3.60 (m, 2H, CH_2 Gly), 4.0 (m, 1H,CHα Lys), 4.20 (m, 2H, CH_2 N-terminal Gly), 4.80 (m, 1H, CHα His), 7.20-8.20 (m, aromatic protons, NH Gly, ε-NH_3^+ Lys), 8.60, 9.00 (2d, NH Lys, NH His), 10.20 (s, NH_2 aniline), 11.40 (s, NH aniline), 14.00 (m, NH^+ acridinium).

BOC-glycyl-L-histidyl-N-εZ-L-Z-lysyl-(4"-methoxycarbonyl-2"-4-bithiazole-2'-yl)ethylamine (9)

A solution of 135 mg of DCC (0.66 mmole) and a suspension of 101 mg of HOBt (0.66 mmole) in dichloromethane (30 ml) at 0°C were added to a solution of 400 mg (0.6 mmole) of (6) in CH_2Cl_2 (15 ml). The mixture was stirred at 0°C for 1 h. A solution of methyl-2'(2"-aminoethyl)-2,4'-bithiazole-4-carboxylate, hydrobromide (Houssin et al., 1984b) (210 mg, 0.6 mmole) and triethylamine (83 µl, 0.6 mmole) in dichloromethane (10 ml) was added. The procedure was strictly identical to that described for 1. The crude product (395 mg, 80 % yield) was chromatographed on silica gel with a mixture of chloroform-methanol (9:1, v/v) as eluent . White powder. (336mg, 68% yield). Rf(A) : 0.91; Rf($CHCl_3$/MeOH, 9:1, v/v) : 0.52; IR ν : 1735 ($COOCH_3$), 1720 (benzyl), 1700 (BOC), 1680, 1650 (CONH) cm^{-1}. FAB : M^++1 = 826. ^{1}H-NMR ($CDCl_3$) : δ= 1.30 (s, 9H, BOC CH_3), 1.50 (m, 2H, γ CH_2 Lys), 1.65 (m, 2H, β CH_2 Lys), 1.85 (m, 2H, δ CH_2 Lys), 3.0 (m, 2H, CH_2 Lys), 3.15 (m, 2H, β CH_2 His), 3.20 (m, 2H, 2'-CH_2 (thiazole)), 3.60 (m, 4H, CH_2-NH (thiazole), and CH_2 Gly), 3.95 (s, 3H, OCH_3), 4.20, 4.40 (2m, 2H, CHα, His, Lys), 5.0 (s, 2H, CH_2 benzyl), 7.0 (d, 1H, NH BOC), 7.20 (d, 1H, NH urethane), 7.30 C^4H (s, 5H, aromatic CH), 7.30 (s, 1H, C^2H His), 7.90 (s, 1H, C^4H His), 7.90, 8.10 (2s, 2H, CH thiazoles), 7.90, 8.10 (2d, 2H, NH His, Lys).

N-(glycyl-L-histidyl-L-lysyl)-2-(4"-methoxycarbonyl-2",4'-bithiazol-2'-yl) ethylamine (2)

The N-protected depsipeptide (9) (200 mg, 0.24 mmole) was treated by dry HBr in AcOH (20 ml) and stirred for 45 min at room temperature. After evaporation to

dryness in vacuo and washing with absolute ethanol (4 x 30 ml), the residue was dissolved in a minimum of acetone (2 ml) and precipitated with diethyl ether giving 155 mg (77 % yield) of a white cristal. Rf(A) : 0; Rf(AcOH-CH_2Cl_2-H_2O, 30:20:6:24) : 0.62; FAB : M^++1 = 591; ^1H NMR (D_2O) : δ = 1.50-1.90 (α, β, δ CH_2 Lys), 2.85 (m, 2H, β CH_2 His), 3.0 (m, 2H, CH_2 Lys), 3.10 (m, 2H, 2'-CH_2 thiazole), 3.20 (s, 2H, CH_2 Gly), 3.65 (m, 2H, CH_2 thiazole), 3.90 (s, 3H, OCH_3), 4.15, 4.60 (2m, 2H, α CH His, Lys), 7.15 (s, 1H, C^2H His), 7.30 (s, 1H, C^4H His), 8.30, 8.50 (2s, 2H, 2CH thiazole).

DNA solutions

Calf thymus DNA (type I, highly polymerized Mw : 400,000 ; Sigma Chemical Co.) was used throughout the experiments. U.V. and fluorescence measurements were conducted in phosphate buffer, (0.05 M, pH 6.9), whereas viscometry experiments were done in 0.01 SHE buffer, (9.4 mM NaCl/2 mM HEPES (N-(2-hydroxyethyl)piperazine-N'-2-ethanesulfonic acid) /10 mM EDTA (ethylenediaminetetraacetic acid) buffer, pH 7.0) as described by Wakelin and Waring (1976).

For EPR determinations, DNA (20 mg) was dissolved in 100 ml of 0.1 SSC buffer (0.15 M NaCl/0.015M sodium citrate, pH 7.0).

The molar concentration expressed in terms of mononocleotide residues of DNA was determined spectrophotometrically at 260 nm, using a molar extinction coefficient of 6600 M^{-1} .cm^{-1} (Malher et al., 1964);

Absorption coefficients and "melting" curves were measured by using a Uvikon Kontron 810/820 spectrophotometer coupled to a Uvikon Recorder 21 and a Uvikon Thermoprinter 48. Samples were placed in a thermostatically controlled cell-holder (10 mm pathlength). The cuvette was heated by circulating water from a Haake unit set. The temperature inside the cuvette was monitored by using a thermocouple in contact with the solution. The absorbance at 260 nm was measured over the range 20-95°C with a heating rate of 1°C/min. The "melting" temperature Tm was taken to be the mid-point of the hyperchromic transition.

Fluorescence spectra were recorded at 20°C on a Jobin-Yvon J-Y-3 spectrophoto fluorometer equipped with an X-Y recorder. All measurements were made in a 1 cm lightpath cuvette in a 0.1 SSC buffer, pH 7.0.

Helical lengthening measurements were made by using a Ubbelohde semi-micro dilutionviscometer. Temperature was maintened at 28 +- 0.01°c in a thermostatically controlled water bath. Flow times were electronically measured to an accuracy of 0.1 s (Schott ABS/G type detector). Calf thymus DNA was sonicated as

described by Wakelin and Waring (1976). Solutions were filtered through 0.45 µm Millipore filters before measurements.

EPR measurements were recorded on a Varian E-109 X-band spectrometer with an E-238 cavity operating in the TM_{110} mode. A 100 KHz high-frequency modulation was used with a 20 mW microwave power. The sample solution were dispensed into a flat quartz cell in the presence of spin-trapper (PBN : phenyl N-tert-butylnitrone) to evidence the formation of free radicals. The cupric complexes were studied by preparating sample solutions in quartz tubes by mixing a 10^{-3} M solution of $Cu(ClO_4)_2$ with a small excess of 10^{-3} M solution of the complexing molecule. Glycerol was then added to obtain a good glass at 77°K. The g-factor measurements were carried out by reference to the Varian 'strong pitch".

Linear dichroism

The electric dichroism measurements were performed with a computerized instrumentation described elsewhere (Houssier and O'Konski, 1981) using the procedures previously outlined (Houssier and O'Konski, 1981 ; Fredericq and Houssier, 1973). The optical set-up of a high sensitivity T-jump instrumentation equipped with a Glan polarizer was used under following conditions : bandwidth : 3 nm ; sensitivity limit 0.001 in $\Delta A/A$; response time 3 ms. The rectangular electric pulses applied to the vertical platinum electrodes (1.5 mm separation) were delivered by a Cober 606 P generator (0-2,500 V, 12.5 A; Cober Electronics, Stamford, Conn. 06902). The field strength range covered is from 1 to 14 kV/cm; the pulse duration was around 50 to 100 µs, decreasing with field increase and adjusted to reach the steady-state of the signals. The dichroism results will be expressed in terms of the reduced dichroism $\Delta A/A = (A_{//} - A_{\perp})/A$ (ΔA is obtained from the measurements of $\Delta A_{//} = A_{//} - A$ using the relation $\Delta A = 1.5 (A_{//} - A)$ where A is the absorbance in the absence of field, measured under the same pathlength (10 mm) with a Perkin-Helmer Lambda 5 spectrophotometer.

Cell cultures

* KB cells were grown as a suspension culture in a Joklik modified Eagle's Medium (Seromed, Munich, GFR) supplemented with 5 % heat inactivited Colt serum at a 4×10^5 cells/ml concentration.

* L1210 mouse leukaemia cells were grown in RPMI 1640 medium (Gibco) containing foetal calf serum (10 %) and the assays were performed in the same medium.

* Cultures utilized to assess drug effects were in exponential growth phase with a doubling time of 13-15 hours.

Growth and viability assays

Cell suspensions containing 10^6 L1210 cells/ml were incubated with 1 or 2 at various concentrations : 10^{-6}, 10^{-5}, 10^{-4}, 10^{-3} M for 24 h.

Cell growth and viability were estimated by counting the cells after dilution by trypan blue solution at 0 h and after 24 h. Results were expressed as a percentrage of control growth and viability.

Measurements of DNA synthetis

L1210 cells in exponential growth were incubated for 1 h at 37°C in growth medium containing various doses of 1 and 2 (0.1-100 µM). Cells were incubated for 15 h at 37°C in growth medium containing 10 µCi/ml [^{3}H] thymidine (43 Ci/mM, CEA). The radioactive medium was removed, the cells washed twice in saline buffer and allowed to swell for 10 min in ice in 1 ml of hypotonic buffer (TNE : 0.01 M Tris-HCl, pH 8.1 ; 0.05 M NaCl ; 0.001 M EDTA). The cells were then disrupted by congelation-decongelation (3 times), digested by proteinase K (100 µg/ml, 4 h at 37°C). The TCA precipitable radioactivity was collected on filter and counted in a liquid scintillation conter.

Results and discussion :

Chemistry

Previous preparations of Gly-His-Lys were reported either by solid-phase synthesis (Pickart et al., 1973) or in solution (Freedman et al., 1982). In the latter technique, histidine was totally protected and a mixed anhydride procedure was used. We employed a simplified procedure, coupling Nα-BOC-L-histidine with N-ε(Z)-L-lysine-benzylester using dicyclohexylcarbodiimide (DCC) and N-hydroxybenzo triazole (HOBt). N-deprotection with trifluoroacetic acid produced the dipeptide which was then coupled by the same method with BOC-glycine. Saponification of the fully protected tripeptide by NaOH-MeOH yielded the free acid.

The 4-(9-acridinylamino)-N-glycylaniline was obtained by neutralization of the corresponding trifluoroacetate (Hénichart et al., 1982b) with $NaHCO_3$ and then coupled with the tripeptide acid with DCC and HOBt. The protected compound was purified by liquid chromatography and treated with HBr-acetic acid (AcOH) to give compound 1.

The bithiazole moiety, 2'-(2-aminoethyl)-4-methoxycarbonyl-2,4'-bithiazole hydrobromide was prepared as previously described (Houssin et al., 1984b) and

coupled with the tripeptide BOC-Gly-His-Lys(Z)-OH to give, after complete deprotection, compound 2.

Interaction with DNA

The intercalative binding to DNA of compounds 1 and 2 was studied by four experimental techniques :

(1) fluorescence quenching in the presence of DNA.

(2) thermal denaturation of DNA.

(3) linear electric dichroism.

(4) viscometry.

Interaction of 1 and 2 with DNA could not be studied by UV spectroscopy since 2 absorbed in the same region as DNA with a major peak at 288 nm (ε = 10,000 $M^{-1}.cm^{-1}$). On the other hand, 1 presented an absorption in the visible region with a major peak at 431.6 nm but, due to a relatively low extinction coefficient (3,700 $M^{-1}.cm^{-1}$ at 431 nm), high concentrations of 1 (0.25 x 10^{-4} M, D.O. < 0.1) had to be employed. In these conditions of concentration, in 0.1 SSC buffer (pH 7), 1 caused precipitation of DNA in yellow filaments which impeded any absorption measurement.

Fluorescence studies

The fluorescence spectra of 1 and 2 in the presence of calf thymus DNA at different concentrations have been recorded. For 1 at pH 7.0, excitation and emission maxima lie at 380 and 410 nm respectively, while for 2, they were found at 280 and 375 nm. For both drugs, no noticeable quenching was observed in the presence of various concentrations of DNA.

The effect of the drugs on ethidium-DNA fluorescence has been studied : it is noteworthy that the fluorescence of ethidium is markedly enhanced when bound to DNA. For example, with poly[d(A-T).d(A-T)] and ethidium, employing an excitation wavelength of 525 nm and monotoring emission at 595 nm, there is a 50-fold increase of fluorescence. Addition of a second DNA binding ligand with comparable or higher affinity to such DNA-ethidium complexes provides a reduction of fluorescence caused by displacement of ethidium from DNA. The curves obtained by using DNA (20 µM in nucleotides) in the presence of ethidium bromide (2 µM) with various concentrations of 1 and 2 are presented in figure 1.

The percentage of fluorescence decrease seen with added drugs and an initial ethidium binding ratio D/P (molar dye concentration over molar mononucleotide concentration) of 0.1 are designed as quenching values Q. Q 50 % were obtained from

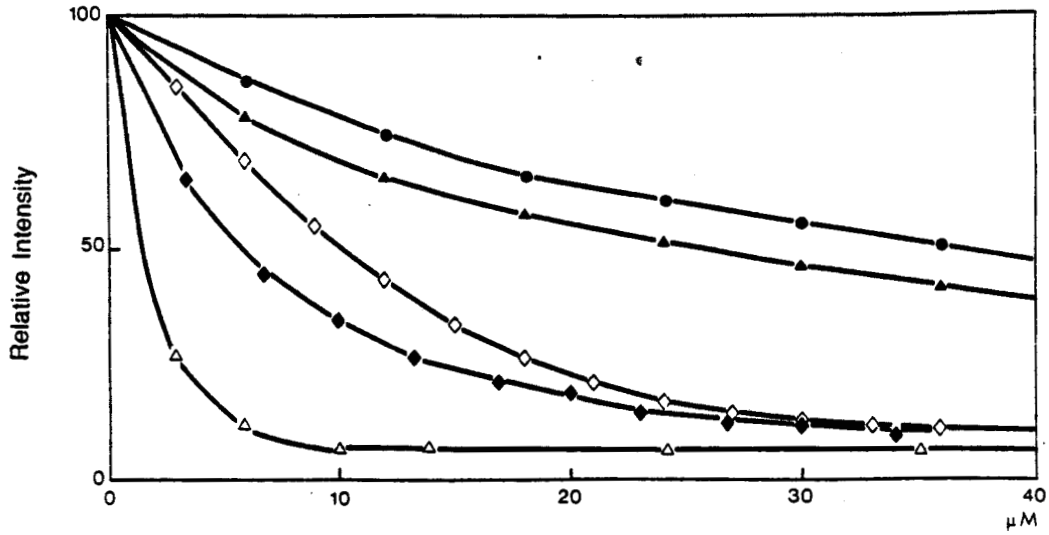

Figure 1 : Reduction of the fluorescence intensity of ethidium-DNA complexes by addition of different anilino-9-aminoacridine (AAA). The calf thymus DNA and ethidium were at concentrations of 20 mM (in base pairs) and 2 mM respectively, in 0.1 SSC buffer. (◇) 1, (●) 2, (▲) m-AMSA, (◆) anilino-9-aminoacridine : AAA, (△) glycyl-AAA.

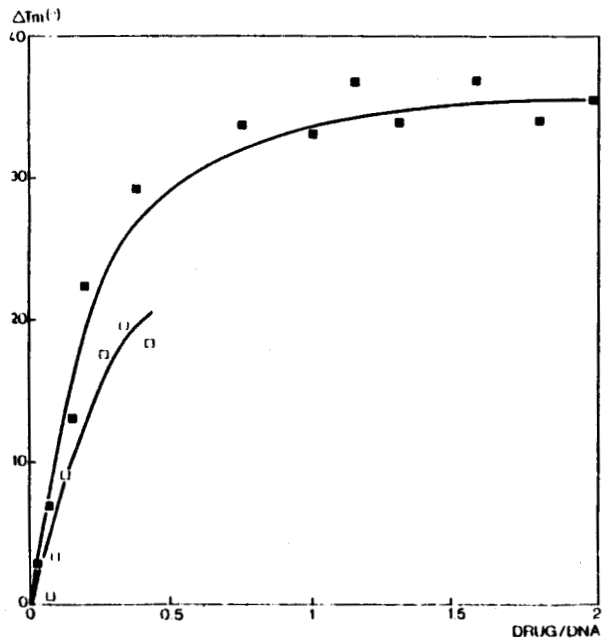

Figure 2 : Effects of 1 on the Dtm of the helix coil transition of calf thymus DNA (10^{-4}M expressed in base pairs) (□) and poly[d(A-T).d(A-T)] 10^{-4}M (■), in phosphate buffer 0.01 M ionic strength (pH 6.9).

the curves and compared with other 9-anilino-acridines such as m-AMSA. Compound 2 gave a slight quenching of fluorescence. A neat decrease was observed for 1 with a Q 50 % obtained for a 10 µM concentration, higher than the one of the antitumor drug m-AMSA (25 µM) and lower than the one of the parent molecules (AAA and Gly-AAA, figure 1). These results led to the conclusion that 1 and other 9-anilinoacridines competed with ethidium bromide and could be considered as intercalating ligands, while 2 apparently had no particular affinity for the binding sites of ethidium bromide.

Thermal denaturation

The Δtm technique may provide also information about the interaction of the drugs with the double helix. It has been shown that a typical effect of DNA-intercalating drugs was to stabilize double-helical DNA against heat denaturation. Thus, thermal denaturation of calf thymus DNA and poly[d-(A-T).d(A-T)] has been evaluated in the absence (67.5°C and 46°C respectively) and in the presence of 1 and 2. While 2 gave even for high concentrations (DNA/drug ratio = 1) slight Δtm of 4°C identical to those observed for bleomycin and related compounds (Hénichart et al., 1985a), 1 caused dramatic Δtm (figure 2) with a maximum of 24°C for calf thymus DNA and 32°C for poly[d(A-T).(A-T)]. These high values for 1 are representative of a strong interaction involving an intercalative process, likely strengthened by the establishement of electrostatic bonds between the basic peptide and the phosphates of the double helix.

Viscometry

Viscometry is a classical technique to appreciate helical lengthening and DNA unwinding and therefore to study the intercalative properties of drugs. Experiments designed to measure the helix extension produced by binding of compounds 1 and 2 were performed essentially by the method of Cohen and Eisenberg (Cohen and Eisenberg, 1966, 1969). The data were transformed directly from flow times to values for the relative contour length using the expression : $L/L_0 = [(t_C-t_0)/(t_D-t_0)]^{1/3}$ where L is the contour length in the presence of drug, L_0 is the contour length of free DNA, t_C is the flow time for the complex, t_D is the flow time for pure DNA, and t_0 is the flow time for the same volume of buffer solution. This expression derives directly from the theory of Cohen and Eisenberg with the added assumption that the intrinsic viscosity approximates to the reduced viscosity of the complexes. Results obtained with 1 and 2 showed a small length decrease on adding each of these drugs to sonicated DNA at pH 7.0 (figure 3 and 4). After reaching a total concentration ratio (drug/DNA) of 0.1, length is stabilized for compound 2 while an increase of length corresponding to a

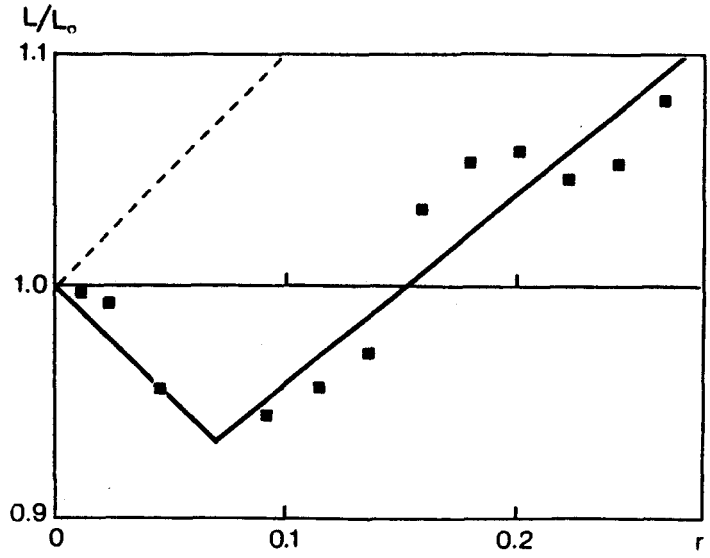

Figure 3 : Alteration of DNA viscosity upon addition of 1. Low molecular weight DNA from calf thymus (C = 7 x 12 mM) is used in this experiment. 1 is added in 5 ml increments from a stock solution (C = 3 mM).

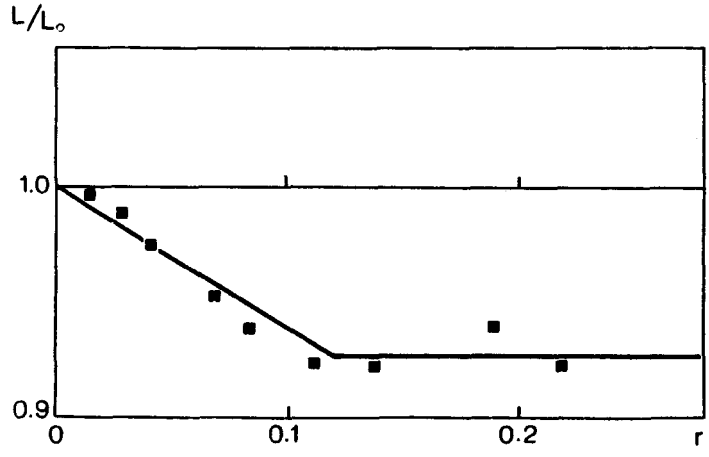

Figure 4 : Alteration of DNA viscosity upon addition of 2. Low molecular weight DNA from calf thymus (C = 592 mM) is used in this experiment. 2 is added in 5 ml increments from a stock solution (C = 3 mM).

monointercalative process is observed for compound 1. These curves probably reflect a complex mechanism of interaction with DNA due to

-for 1 : the ability to interact electrostatically for the basic peptide and to intercalate for the acridine moiety.

-for 2 : the electrostatic interaction of the basic peptide and perhaps a partial intercalation of one thiazole as for bleomycin compounds (Hénichart et al., 1985b).

In order to verify the intercalation of 1 in DNA, linear electric dichroism studies have been undertaken.

Linear electric dichroism

The interaction of calf thymus DNA (Mw = 400,000) with two anilino-9-aminoacridine derivatives in which peptide chains of variable lengths (Gly-AAA : one amino-acid, 1 : four amino-acids) are attached to the amino group of the heterocyclic moiety, has been investigated by electric dichroism in the long-wavelength visible absorption band of the dye (440 nm). For the two compounds, a negative dichroism of amplitude close to that of the purine and pyrimidine base was observed (figure 5). Such results indicate that the dye transition moment is parallel to the base planes. To confirm this, the ratios of the reduced dichroism values at a given field (12.4 KV/cm) for the basess and for 1 or Gly-AAA at E = 12.3 KV/cm in their respective absorption bands were calculated. They are respectively of 1.0 (1, D/P = 0.166) and 1.2 (Gly-AAA, D/P = 0.133). Such values, ranging from 0.9 to 1.1, are of the same order of magniture as those observed for some well-know intercalators such as proflavine (1.09) or acridine orange (1.09) (Houssier et al., 1977 ; Houssier, 1981). Considered together, these results can be seen as a strong argument in favour of intercalation and support evidence that the peptide side chains do not play a major role in the interaction with DNA. On the other hand, a study of the variation of the reduced dichroism with the total concentration ratios D/P has been made to fully characterize the binding process.

At low D/P ratios, the slightly lower dichroism values measured for both ligands are due to the higher DNA concentration required to reach D/P values of 0.02 to 0.1, namely 3 to 15 times larger than the DNA concentration used for the measurements in the 260 nm band, whereas at high D/P ratios the dichroism decrease is probably due to the presence of free dye and externally bound dye molecules which do not contribute to the measured dichroism.

The curves shown in figure 6 are reminiscent of the ones obtained for intercalating dyes bound to DNA (Houssier, 1981). Another fact to be noted is a more pronounced decrease in the reduced dichroism with increasing D/P ratios in the case

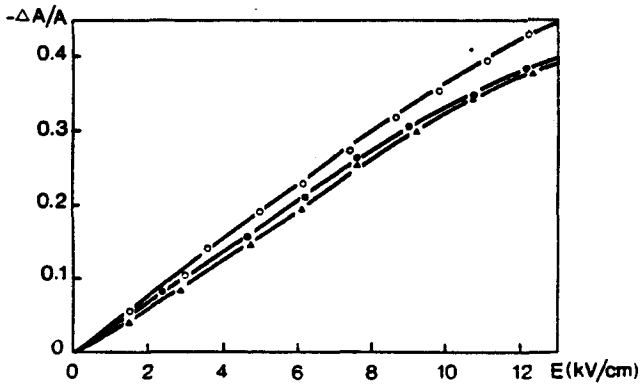

Figure 5 : Field strength dependence of the reduced electric dichroism for DNA alone (▲l = 260 nm) and Gly-AAA (○), 1 (●)-DNA complexes at 440 nm respective P/D of 7.5 and P/D = 6 in 1 mM Tris-HCl buffer.

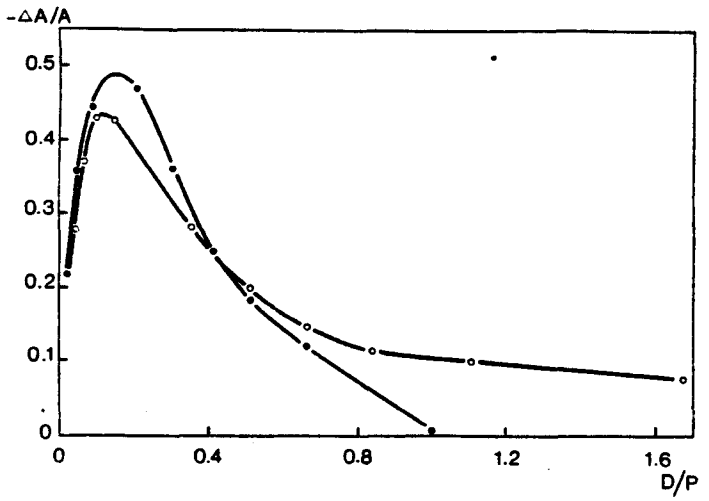

Figure 6 : Dependence of the reduced electric dichroism on the binding ratio, for Gly-AAA (○) and 1 (●)-DNA complexes. E = 12.3 kV/cm, 1 mM Tris-HCl buffer ; l= 440 nm.

of 1 when compared to Gly-AAA. This suggests a higher affinity of Gly-AAA for DNA or a non-zero contribution of the externally-bound dye molecules, for Gly-AAA.

Cu(II) complexation and free radicals production

The structure of the Gly-His-Lys-copper(II) complex has been well studied in solution and in the solid state (Freedman et al., 1982 ; Laussac et al., 1983 : Pickart et al., 1980). E.P.R. parameters and X-ray analysis fit well with the contention that Cu(II) is ligated to Gly-His-Lys throught one oxygen atom and three nitrogen atoms in a square-planar configuration. Thus E.P.R. studies of the Cu(II) complexes of 1 or 2 have been performed in order to verify whether they were different from those of the parent peptide.

As shown in table 1, E.P.R. parameters of the Cu(II) complexes of 1 and 2 were almost identical to those of the Gly-His-Lys-Cu(II) complexes. Although superhyperfine structure of the $g_{\perp}$ position was poorly resolved at pH 7.0, seven superhyperfine lines with an approximately 15 G splitting can be observed. Furthermore, $g_{//}$ values around 2.20 with an interaction energy $A_{//}$ of 20 mK suggested a square planar complex with N_3O equatorial ligation (Peisach and Blumerg, 1974) as previously described for the tripeptide Gly-His-Lys. Thus it can be concluded that the mode of complexation of 1 or 2 with copper was identical with the one of the Gly-His-Lys tripeptide.

Table 1 : EPR parameters for copper(II) complexes in solution.

Complex	pH	$g_{//}$	$H_{//}$	$A_{//}$	$g_{\perp}$	H(hyperfine)
Gly-His-Lys	7.0	2.22	195 G	20.21 mK	2.06	13.75 G
	9.0	2.20	197 G	20.23 mK	2.06	15 G
1	7.0	2.20	195 G	20.02 mK	2.06	15 G
	9.0	2.18	200 G	20.35 mK	2.06	17.5 G
2	7.0	2.23	190 G	19.78 mK	2.06	13 G
	9.0	2.22	192.5 G	19.95 mK	2.06	15 G

The production of free radicals by the complex 1 has been evaluated by E.P.R. using phenyl N-tert-butylnitrone as spin-trap. Cupric complex of 1 unambiguously triggered up the formation of radicals in the presence of molecular oxygen dissolved in the solution. Reaction of the spin-trap with the activated oxygen produced a characteristic spin-trapped adduct consisting of a triplet of doublets. Integration of the six peaks allowed direct relative measurements of the production of radicals. A regular production of radicals was observed in the first twenty minutes, followed by a gradual decrease and a levelling-off after three hours (figure 7).

Oxidation of 1

m-AMSA has been shown to be oxidized to a quinone imine form, m-AQDI, in the presence of copper (Wong et al., 1984a and b). This oxidation was found to be responsible for DNA strand breaks and seemed to be correlated with the biologacal activity. The oxidation rate can be evaluated by absorption spectroscopy : m-AMSA exhibits a visible absorption spectrum below 600 nm, with a major peak at 435 nm and a shoulder around 420 nm. The addition of Cu(II) ions in borate buffer (0.05 M pH 9.0) resulted in a decrease in the absorption above 400 nm ans a simultaneous increase below 400 nm. An isosbestic point at approximatively 395 nm was observed and two new absorption peaks were found at 356 and 377 nm. As shown in figure 8, 1 in the presence of copper evolves slowly, with a decrease of the major peak at 415.5 nm and a simultaneous increase at 357 nm. The rate of oxidation is low when compared with the one of m-AMSA (Wong et al., 1984a and b) and points out the importance of the methoxy group in meta position on the aniline in the redox properties of the drug.

In vitro cytostatic activity

Inhibition of growth of cultured L1210 and KB cells has been tested for the two depsipeptides 1 and 2. Compound 1 was found to be active ($ID_{50} = 5 \times 10^{-6}M$ in both systems) whereas 2 was about 30-fold less potent. The effects of these compounds on [^{3}H]-thymidine incorporation in L1210 and KB cells were also performed and gave the same results. No sigificant DNA synthesis inhibition was obtained with 2, while 1, at $12 \times 10^{-6}M$, induced 50 % inhibition of DNA synthesis.

Conclusion :

The concept of an antitumor drug consisting of an intercalative moiety associated with a metal chelating peptide deserves attention since it brings some

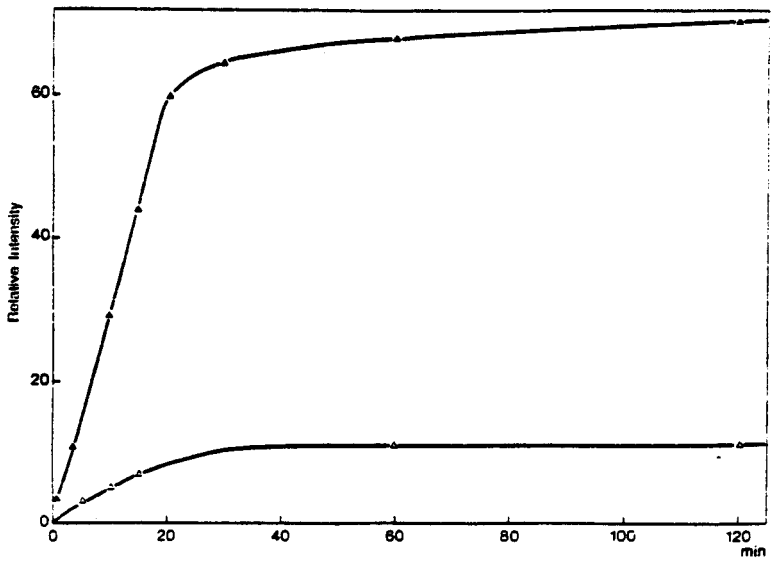

Figure 7 : Evolution with time of the production of radicals estimated by the formation of spin-trapped adducts of PBN (in 0.09 M ethanolic solution). Integration of the arae of the six peaks observed in e.s.r. allowes relative measurement. (Δ) PBN = 200 ml, NaOH N = 50 ml, Cu(II) 10^{-3} M = 200 ml, water = 200 ml. (▲) PBN = 200 ml, NaOH N = 50 ml, Cu(II) 10^{-3} M = 200 ml, 1 10^{-3} M = 200 ml.

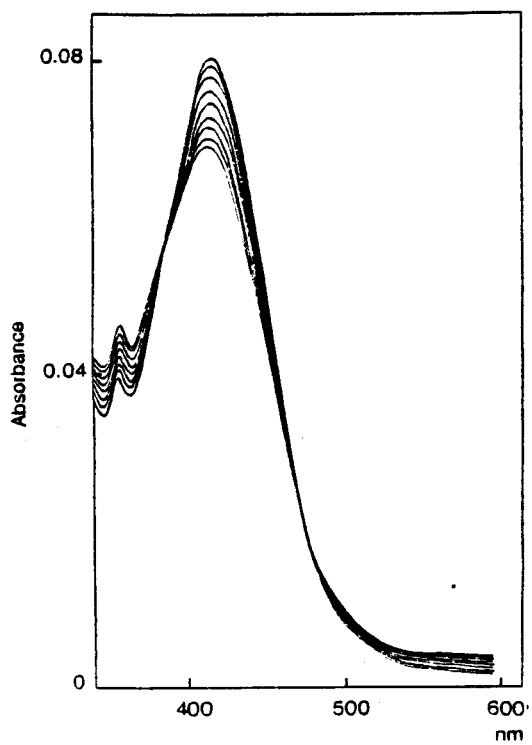

Figure 8 : Effects of Cu(II) on the absorption spectrum of 1. 1 (50 ml, 10^{-3} M) was incubated at 25°C with Cu(II) (50 ml, 10^{-3} M) in borate buffer 0.05 M (2.90 ml, pH 9.0). Absorption spectra were recorded at intervals of 15 min.

information on the mechanism of activity and points out some interesting structure-activity relationships. Compound 2 exhibited a poor DNA affinity and was not able to induce a redox system with the cupric ion since the bithiazole moiety cannot be oxidized. Consequently, no cytotoxic activity was found on tumor cells in vitro. Compound 1 was shown to interact tightly with DNA likely by a complex process involving on one hand the intercalation of the 9-anilinoacridine ring, as evidence by linear dichroism and the quenching of ethidium fluorescence , and on the other hand, by electrostatic interaction of the peptide poiety.

The latter assumption lies on the high values of ΔTm observed and the observation in those experiments of a higher affinity for the poly[d(A-T).d(A-T). Indeed, while 9-anilinoacridines are know to have a greater specificity towards G-C nucleotide sequences, A-T nucleotide sequence specificity is more characteristic of minor groove binders such as netropsin or distamycin (Van Dyke and Dervan, 1983). Thus, it can be speculated that, besides intercalation of the acridine ring, the basic peptide may bind in the minor groove. Results obtained by viscometry and the observation that, in the presence of high concentrations of 1, the dissolved calf thymus DNA precipitated, were also in favor of electrostatic interactions leading to an aggregation of DNA as observed for histone-DNA interaction. Therefore, although affinity for DNA has been enhanced by the introduction of a basic peptide, the biological activity of 1 remains discrete when compared with m-AMSA. Despite its proven efficacy, the molecule can still be improved : the hydrophilic character of the peptide is perhaps not favorable to membrane transport, m-AMSA ia a more lipophilic molecule; furthemore by comparison with m-AMSA the oxidation rate of the 9-anilinoacridine mioety has been found to be small and the formation of electrophilic and/or radical species was weak, which lowered DNA damages. This emphasizes the role of redox reactions in the bioactivation of most of intercalating drugs.

In conclusion, the results of this investigation are sufficiently encouraging to warrant further studies in this family of compounds with a view towards optimization of the cell penetration by (i) introducing hydrophobic residues in the chelating peptide sequence and (ii) improving the redox properties by replacement of the 9-anilinoacridine moiety by an activated aromatic system exhibiting stronger redox properties.

Acknowledgements

This research was supported by grants from the "Institut National de la Santé et de la Recherche Médicale" and the "Fédération Nationale des Centres de Lutte contre le Cancer".

References :

BAILLY, C., BERNIER, J-L., HOUSSIN, R., HELBECQUE, N. and HENICHART, J-P. (1987a). Anti-Cancer Drug Design, 1, 303.

BAILLY, C., CATTEAU, J-P., HELBECQUE, N., BERNIER, J-L., HOUSSIN, R., DENIS, C. and HENICHART, J-P. (1987b). Journal of Inorganic Biochemistry, 31, 211.

BURGER, R.M., PEISACH, J. and HORWITZ, S.B. (1981). Journal of Biological Chemistry, 256, 11636.

COHEN, G. and EISENBERG, H. (1966). Biopolymers, 4, 429.

COHEN, G. and EISENBERG, H. (1969). Biopolymers, 8, 45.

FAVAUDON, V. (1982). Biochimie, 64, 457.

FREDERICQ, E. and HOUSSIER, C. (1973). In Electric Dichroism and Electric Birefringence, Clarendon Press, Oxford.

FREEDMAN, J.H., PICKART, L., WEINSTEIN, B., MIMS, W.B. and PEISACH, J. (1982). Biochemistry, 21, 4540.

HELBECQUE, N., BERNIER, J-L. and HENICHART, J-P. (1985). Biochemical Journal, 225, 829.

HENICHART, J-P., HOUSSIN, R., BERNIER, J-L. and CATTEAU, J-P. (1982a). Journal of the Chemical Society, Chemical Communications, 1295.

HENICHART, J-P., BERNIER, J-L. and CATTEAU, J-P. (1982b). Hoppe-Zeyler's Zeitschrift fur Physiologische Chemie, 363, 835.

HENICHART, J-P., BERNIER, J-L., LEMAY, P., HOUSSIN, R. and CATTEAU, J-P. (1984). Cancer Biochemistry and Biophysics, 7, 239.

HENICHART, J-P., BERNIER, J-L., HELBECQUE, N. and HOUSSIN, R. (1985a). Nucleics Acids Research, 13, 6703.

HENICHART, J-P., BERNIER, J-L., HOUSSIN, R., LOHEZ, M., KENANI, A. and CATTEAU, J-P. (1985b). Biochemical and Biological Research Communications, 126, 1036.

HOUSSIER, C., BONTEMPS, J., EMONDS, A. and FREDERICQ, E. (1977). Annals of the New York Academy of Sciences, 303, pp. 170-189.

HOUSSIER, C. (1981). In Molecular electro-optics, Krause S., Ed. Series B64 Nato Advanced Study Institute, pp. 363-378.

HOUSSIER, C. and O'KONSKI, C.T. (1981). In Molecular electro-optics, Krause S., Ed. Series B64 Nato Advanced Study Institute, pp. 309-339.

HOUSSIN, R., BERNIER, J-L. and HENICHART, J-P. (1984b). Journal of Heterocyclic Chemistry, 21, 681.

JURLINA, J.L., LINDSAY, A., PACKER, J.E., BAGULEY, B.C. and DENNY, W.A. (1987). Journal of Medicinal Chemistry, 30, 473.

KENANI, A., LOHEZ, M., HOUSSIN, R., HELBECQUE, N., BERNIER, J-L., LEMAY, P. and HENICHART, J-P. (1987). Anti-Cancer Drug Design, 2, 47.

LAUSSAC, J.P., HARAN, R. and SARKAR, B. (1983). Biochemical Journal, 209, 533.

LEMAY, P., BERNIER, J-L. HENICHART, J-P., and CATTEAU, J-P. (1983). Biochemical and Biological Research Communications, 111, 1074.

MAHLER, H.R., KLINE, B. and MEHROTRA, B.D. (1964). Journal of Molecular Biology, 9, 801.

NEIDLE, S. and WARING, M.J. (1983). In Molecular Aspects of Anti-Cancer Drug Action, Verlag Chemie, Basel.

PEISACH, L. and BLUMBERG, W.E. (1974). Archives of Biochemistry and Biophysics, 165, 691.

PICKART, L. and THALER, M.M. (1973). Nature (London) New Biol., 243, 85.

PICKART, L., THALER, L. and THALER, M.M. (1973). Biochemical and Biological Research Communications, 54, 562.

PICKART, L., FREEDMAN, J.M., LOKER, W.J., PEISACH, J., PERKINS, C.M., STENKAMP, R.E. and WEINSTEIN, B. (1980). Nature (London), 288, 715.

PICKART, L. and LOVEJOY, S. (1987). Methods in Enzymology, 147, 314.

POVIRK, L.F., HOGAN, M. and DATTAGUPTA, N. (1979). Biochemistry, 18, 96.

STILL, W.C., KAHN, M. and MITRA, A. (1978). Journal of Organic Chemistry, 43, 2923.

UMEZAWA, H., MAEDA, K., TAKEUCHI, T. and OKAMI, Y. (1966). Journal of Antibiotics, 19, 200.

UMEZAWA, H. (1979). In Bleomycin : Chemical, Biochemical and Biological Aspects. Hecht, S.M. (ed.), Springer Verlag, New York, pp. 1-36.

VAN DYKE, M.W. and DERVAN, P.B. (1983). Nucleic Acids Research, 11, 5555.

WAKELIN, L.P.G. and WARING, M.J. (1976). Biochemical Journal, 157, 721.

WONG, A., HUANG, C.H. and CROOKE, S.T. (1984a). Biochemistry, 23, 2939.

WONG, A., HUANG, C.H. and CROOKE, S.T. (1984b). Biochemistry, 23, 2946.

Conclusion :

L'inactivité du composé 2 est due à sa faible affinité pour l'ADN et à l'abscence de propriétés redox comme le démontre la publication précédente mais également, selon toute vraisemblance, à sa faible aptitude à pénétrer dans les cellules. Ceci avait été constaté en RPE avec des analogues bithiazoliques greffés à un marqueur de spin, par exemple SL-NETBI ou même le dérivé suivant (HENICHART et al., 1984):

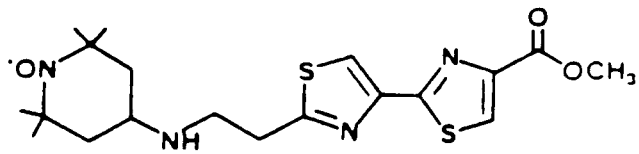

Pour le dérivé 2 tout au moins, il est probable que Gly-His-Lys ne facilite pas le transport membranaire.

Le composé 1 répond mieux à nos espérances. Concernant la fixation du tétrapeptide Gly-His-Lys-Gly dans le petit sillon, il faut souligner qu'en plus des arguments physicochimiques évoqués dans l'article, l'intercalation de l'acridine impose le positionnement de l'aniline également dans le petit sillon (DENNY et al., 1983), facilitant ainsi la même orientation du peptide. L'intercalation du chromo phore et l'insertion du tétrapeptide dans le petit sillon s'apparentent au mode de liaison à l'ADN de l'actinomycine : antibiotique antitumoral composé d'un chromophore aromatique phénoxazone, capable de s'intercaler entre deux plateaux G-C, couplé à deux pentapeptides cycliques (forme lactone) identiques qui s'insèrent dans le petit sillon de part et d'autre du site d'intercalation (GALE et al, 1981).

Ce dérivé se lie à l'ADN par un processus intercalatif rigoureusement défini par dichroisme linéaire et, de plus, produit des radicaux libres oxygénés. Mais aucune coupure d'ADN n'a été décelée quelles que soient les conditions utilisées (avec ou sans réducteur, avec ou sans eau oxygénée, pH neutre ou alcalin, temps d'incubation variable). Ce résultat est à première vue contradictoire avec ceux rapportés pour le tripeptide analogue Gly-Gly-His apte à cliver l'ADN (CHIOU, 1983; MACK et al., 1988). Mais une étude beaucoup plus détaillée de la coupure d'ADN par ce type de dérivé a permis d'élucider ce problème (voir chapitre III).

Les propriétés antitumorales du composé 1 sont satisfaisantes (ID_{50}= 5 µM sur cellules L1210 et KB3) et semblent correspondre à la capacité de ce dérivé à inhiber la synthèse d'ADN in vitro. Les relations Liaison à l'ADN - Activité Biologique sont dans ce cas parfaitement cohérentes : le composé 1 se lie fortement à l'ADN et est actif in vitro, le composé 2 se lie mal à l'ADN et est inactif.

La première approche du concept "Peptide Chélateur-Intercalant" abordée par le tripeptide Gly-His-Lys est positive. Des pharmacomodulations autour du composé 1 sont envisagées pour potentialiser son action. Notamment le maintien du groupement méthoxy en méta sur l'aniline est prévu dans un premier temps. Ce substituant permet de rétablir les propriétés oxydatives de l'amsacrine (BERNIER et al., 1986b). La coupure de l'ADN en est facilitée(WONG et al., 1984). De plus, le groupe méthoxy joue un rôle déterminant dans le transport de l'amsacrine in vivo (DARKIN & RALPH, 1985).

Les substances naturelles nétropsine et distamycine, d'une part, et bléomycine, d'autre part, nous ont conduit respectivement aux concepts de "Peptide à liaison spécifique-Intercalant" et "Peptide Chélateur-Intercalant". Dans les deux cas, la stratégie mise en oeuvre pour la conception de modèles synthétiques s'est avérée concluante.

Chacune des fractions moléculaires que ce soit le complexant, le peptide à liaison spécifique ou l'intercalant semble potentialiser l'action du fragment voisin. Aussi pour mener à terme cette étude et aller encore plus loin dans le raisonnement chimique mis en place, nous avons regroupé au sein d'un même modèle chacune de ces trois fractions.

CHAPITRE III

LE CONCEPT PEPTIDE CHELATEUR - PEPTIDE

A LIAISON SPECIFIQUE - INTERCALANT

Dans la première série de pharmacomodulations effectuées autour de la nétropsine et de la distamycine, le modèle NETGA qui regroupe un fragment bis-pyrrolique et le fragment anilinoamino-9 acridine s'est révélé être extrêmement performant. Sa structure a donc été préservée. Mais les informations acquises avec les modèles analogues de la bléomycine ont également été prises en compte. La partie complexante Gly-His-Lys a été retenue.

Un composé nommé Gly-His-Lys-NETGA a été élaboré.

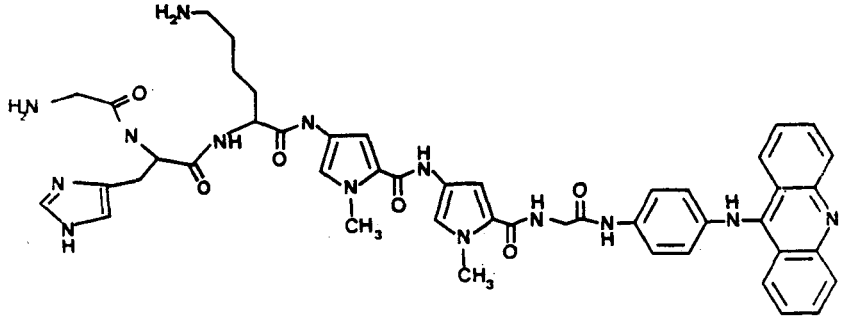

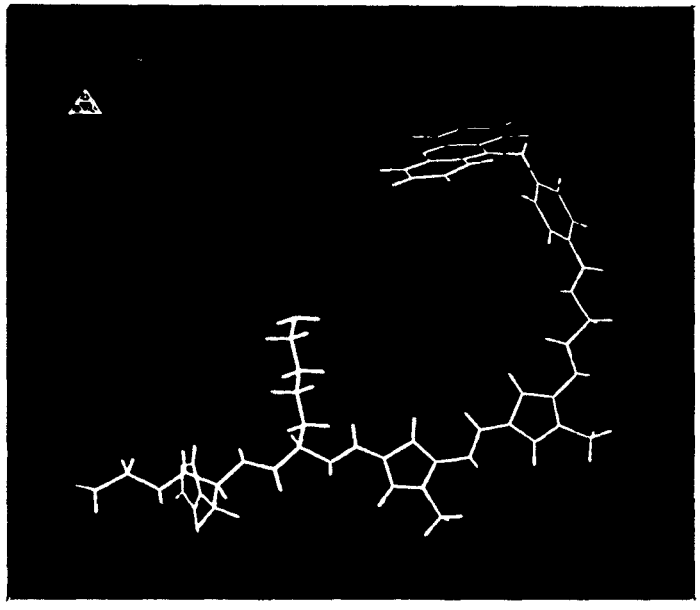

Figure 22 : Structure de Gly-His-Lys-NETGA

Les buts recherchés par l'intermédiaire de ce composé sont multiples :

1 - Se fixer à l'ADN avec une forte affinité et si possible avec une haute spécificité de liaison

2 - Couper l'ADN au niveau du site de fixation

3 - Elaborer un composé possédant une forte activité anticancéreuse.

Suite à la synthèse de ce dérivé, sa capacité à se fixer et à dégrader l'ADN et son activité antitumorale ont été étudiées.

a) Liaison à l'ADN

1-Intensité de la liaison

Dans un premier temps l'existence d'une interaction avec l'ADN a été vérifiée. Le spectre d'absorption UV-Visible de Gly-His-Lys-NETGA est modifié de façon importante en présence d'ADN (Figure 23). Un effet hypochrome à 440 nm (zone d'absorption de l'acridine) et à 265 nm (zone d'absorption de l'aniline) est observé. De plus un shift de 8 nm vers le rouge apparaît dans la zone de l'acridine (λ_{max} = 432 nm — λ_{max} = 440 nm); ceci traduit une délocalisation des électrons π du chromophore en présence d'ADN. L'intercalation de l'acridine est donc envisageable.

Une analyse de type Scatchard (Figure 24) a été effectuée pour quantifier cette interaction. La pente de la droite obtenue indique que Gly-His-Lys-NETGA se fixe à l'ADN avec une constante apparente d'affinité de $6x10^6$ M^{-1} (K_a) soit avec une intensité dix fois plus forte que celle mesurée pour le composé NETGA ($K_a = 6.3x10^5$ M^{-1}) dans les mêmes conditions.

L'accroissement de l'intensité de la liaison à l'ADN est due à la présence de la partie complexante peptidique Gly-His-Lys, seule fraction différenciant les deux modèles NETGA et Gly-His-Lys-NETGA. Le tripeptide stabilise donc la liaison à l'ADN; l'intervention de liaisons salines entre les résidus phosphate de l'ADN et les groupements amine terminaux du peptide (αNH_2 de Gly et εNH_2 de Lys) est certainement à considérer comme elle l'avait été lors de l'étude de l'interaction Gly-His-Lys-anilinoamino-9 acridine-ADN (article n°11).

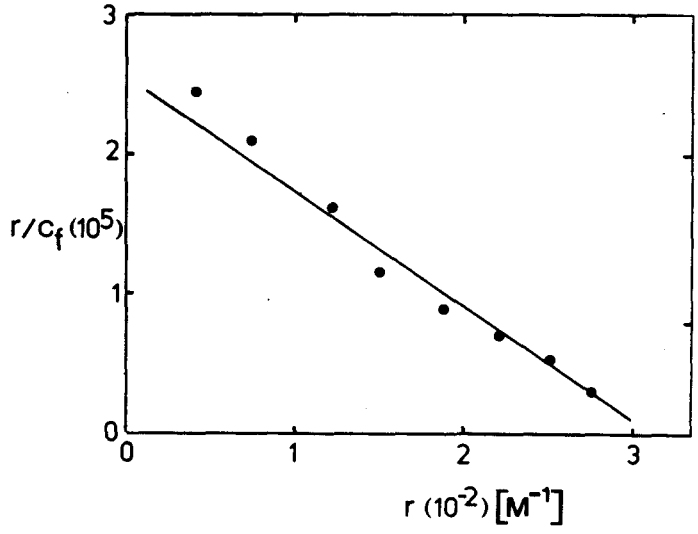

Analyse de type Scatchard (r/cf en fonction de r) pour l'évaluation de la constante apparente d'affinité (K_a) de Gly-His-Lys-NETGA pour l'ADN de thymus de veau (tampon Tris-HCl 1 mM, pH 7.0).

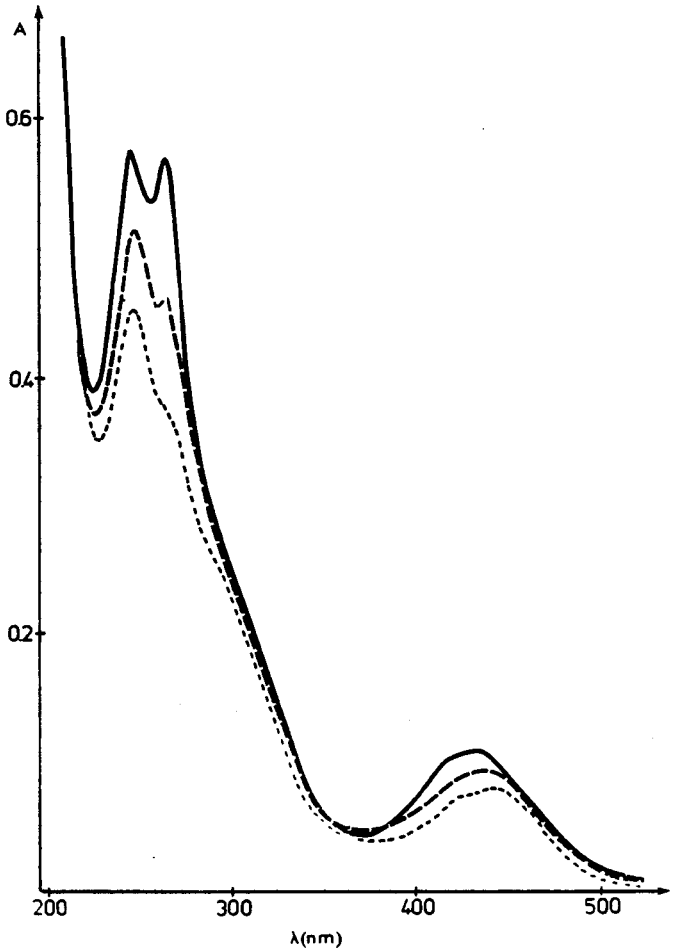

Figure 23 : Spectre d'absorption UV-Visible de Gly-His-Lys-NETGA (10 µM) (—) et du complexe Gly-His-Lys-NETGA-ADN aux rapports ligand/ADN de 0.5 (- -) et 0.2 (···). Les cellules de mesure et de référence contiennent la même concentration en ADN de thymus de veau, respectivement 20 µM (- -) et 50 µM (···) dans un tampon Tris-HCl 1 mM pH 7.0.

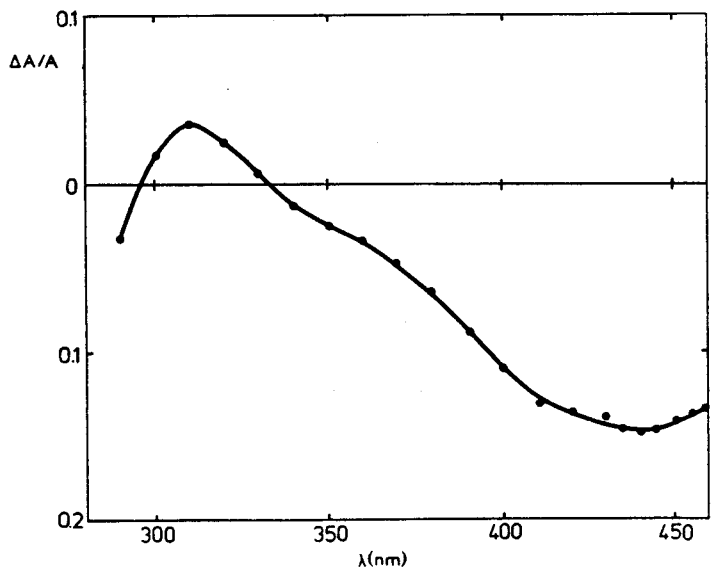

Figure 25 : Spectre de dichroïsme linéaire électrique du complexe Gly-His-Lys-NETGA-ADN (ligand/ADN = 0.1, Λ = 2 mS, tampon Tris-HCl 1 mM, pH 7.0).

2 - Mode de liaison

Le mode de liaison à l'ADN a été étudié par la technique de dichroïsme linéaire électrique, particulièrement bien adaptée pour ces dérivés. Les résultats obtenus sont représentés Figure 25. L'interaction Gly-His-Lys-NETGA-ADN (fragment de 400 paires de bases environ) se traduit en dichroïsme électrique par :

-un dichroïsme négatif intense dans la zone 340-460 nm avec un minimum à 440 nm, ce qui traduit l'intercalation de l'acridine
-un dichroïsme positif dans la région 300-340 nm avec un maximum à 310 nm correspondant à la position de la fraction bis-pyrrolique en périphérie de l'ADN

Remarque : le dichroïsme négatif enregistré en dessous de 300 nm est dû à l'ADN dont la concentration est 10 fois supérieure à celle du ligand.

Au vu de ces résultats, l'intervention de deux mécanismes de liaison distincts, à savoir l'intercalation de l'acridine et la fixation du chaînon bis-pyrrole dans le petit sillon, peut être logiquement postulée. Le mode de liaison à l'ADN est schématisé sur la figure 26.

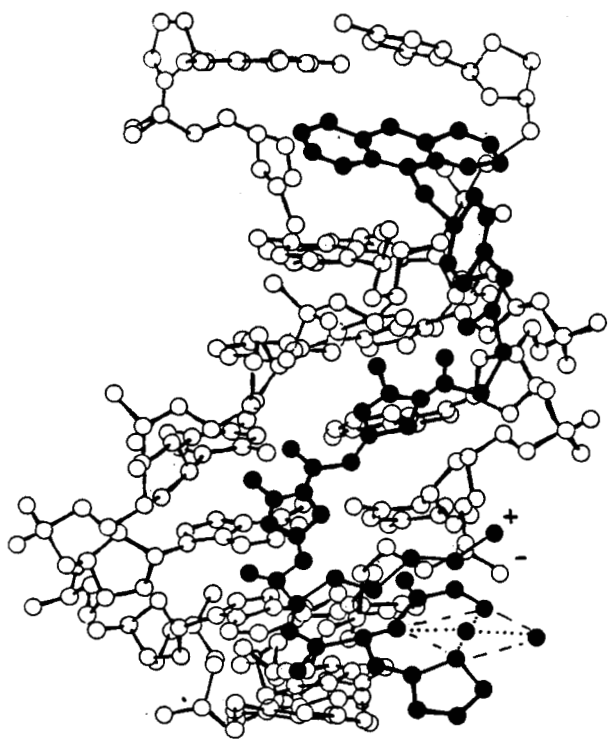

Figure 26 : Complexe Gly-His-Lys-NETGA-ADN (structure proposée).

b) Complexation

La complexation des métaux (en particulier Cu et Fe) est indispensable à la production de radicaux libres et à la coupure d'ADN qui en résulte. L'aptitude de Gly-His-Lys-NETGA à complexer le cuivre a été vérifiée par RPE. Le spectre de RPE de Gly-His-Lys-NETGA-Cu(II) est comparable à celui de Gly-His-Lys-Cu(II); la géométrie des complexes serait donc identique et impliquerait quatre atomes (trois atomes d'azote et un atome d'oxygène) comme en témoigne la présence de 9 pics correspondant à des couplages superhyperfins.

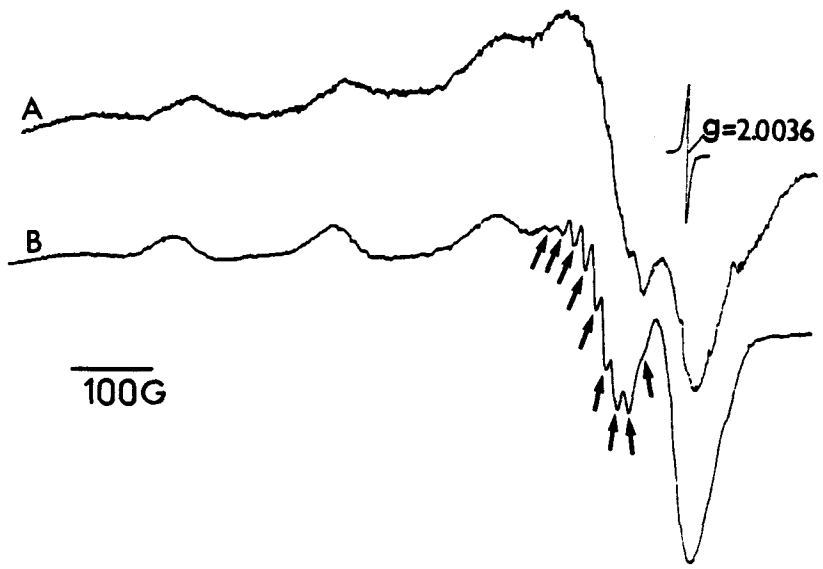

Spectre de RPE des complexes Gly-His-Lys-NETGA-Cu(II) (A) et Gly-His-Lys-Cu(II) (B). (→) couplage superhyperfin.

c) Dégradation de l'ADN

La méthode choisie est celle qui utilise comme cible l'ADN plasmidique superenroulé (pBR 322). L'examen du gel d'agarose à 254 nm montre que Gly-His-Lys-NETGA ou le tripeptide Gly-His-Lys pris séparément, en présence de cuivre (ou de fer) ou d'eau oxygénée ou en présence d'un réducteur, sont totalement inaptes à dégrader l'ADN.

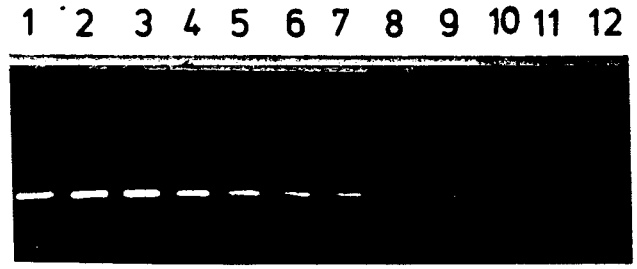

Figure 27 : Gel d'agarose (0.8%) du plasmide pBR 322 révélé au bromure d'éthidium et traité par Gly-His-Lys-NETGA ou Gly-His-Lys.

1 : plasmide pBR 322.

2-3 : plasmide + Cu(II) - Gly-His-Lys-NETGA (1/1, 10 µM-5 µM).

4-5 : plasmide + Cu(II) (10 µM-5 µM) + H_2O_2 + ascorbate de sodium (10 µM).

6-7 : plasmide + Cu(II) - Gly-His-Lys-NETGA (1/1, 10 µM-5 µM)+ H_2O_2 + ascorbate de sodium (10 µM).

8-9 : plasmide + Cu(II) - Gly-His-Lys (1/1, 10 µM-5 µM).

10-11 : plasmide + Cu(II) - Gly-His-Lys (1/1, 10 µM-5 µM)(1/1, 10 µM-5 µM)+ H_2O_2 + ascorbate de sodium (10 µM).

12 : plasmide pBR 322.

De même, la présence simultanée du modèle complexant, de cuivre, d'eau oxygénée et d'un réducteur comme le β-mercaptoéthanol est aussi inefficace. Les coupures n'ont été observées qu'en présence d'ascorbate de sodium comme agent réducteur. Ceci confirme les travaux de Chiou avec le tripeptide Gly-Gly-His (CHIOU, 1983).

Le composé Gly-His-Lys-NETGA potentialise l'action du système H_2O_2/Cu(II)/ascorbate. Mais cette amplification est, d'une part, faible comparée au système bléomycine/Fe(II)/O_2 et, d'autre part, très difficile à observer; plusieurs raisons à cela :

-. le système H_2O_2/Cu(II)/ascorbate, à des concentrations supérieures ou égales à 50 µM dégrade totalement l'ADN. Aucune amplification ne peut donc être observée à ces concentrations. La plus forte concentration en H_2O_2/Cu(II) utilisable sans induire de coupure est de 10 µM dans nos conditions.

- le complexe Gly-His-Lys-NETGA-Cu(II)-ADN précipite à des concentrations supérieures ou égales à 50 µM. Ce phénomène avait été observé également avec le composé Gly-His-Lys-Gly-anilinoamino-9 acridine (article n° 11).

L'effet recherché doit donc nécessiter de très faibles concentrations en produit testé. C'est à la concentration de 10 µM que des différences significatives d'intensité de coupure de l'ADN entre le système Cu(II)/H_2O_2/ascorbate (le témoin) et le système Gly-His-Lys-NETGA/Cu(II)/H_2O_2/ascorbate ont été notées. A des concentrations inférieures les coupures sont trop faibles pour être considérées (Figure 27).

L'activité amplificatrice de la coupure d'ADN par Gly-His-Lys-NETGA est légèrement supérieure à celle du tripeptide Gly-His-Lys (Cell Growth Factor, Serva).

La technique utilisée confirme que le dérivé étudié accroît la coupure de l'ADN.Toutefois il nous reste à savoir si la coupure est base-spécifique ou non. La technique employée s'apparente directement à celle du foot-printing (voir article n°3). Cette étude, en cours de réalisation en collaboration avec le Pr J.W. LOWN, nous indiquera les sites préférentiels de liaisons. De plus cette technique permet de s'affranchir des faibles concentrations en Cu, H_2O_2 et ascorbate. De fortes concentrations en H_2O_2-ascorbate (1 mM) peuvent être utilisées, car dans ces conditions la destruction de l'ADN par l'eau oxygénée est non spécifique et ne perturbe donc pas l'analyse des sites de coupure spécifiques (MACK et al., 1988).

Concernant la liaison spécifique à l'ADN, les premiers éléments d'information, récoltés par l'étude en dénaturation thermique d'ADN de différentes compositions semblent révéler une fixation plus importante de Gly-His-Lys-NETGA sur les ADN riches en paires de bases AT. Le ΔTm (variation de la température de demi-transition de l'ADN) est de 22°C avec le poly[d(AT).d(AT)] contre 15°C avec l'ADN de thymus de veau (48 % de GC) pour un même rapport ligand/ADN de 1/1. Il est probable que Gly-His-Lys-NETGA présente la même spécificité de liaison à l'ADN de type AAAT que son homologue NETGA (article n° 3).

d) Activité biologique

Le modèle Gly-His-Lys-NETGA inhibe la prolifération de cellules leucémiques L1210 avec une efficacité légèrement inférieure à celle de son homologue NETGA. Le pouvoir cytostatique reste toutefois important. Le phénomène d'hyperplasie cellulaire est observé aux concentrations de 10 µM et 50 µM. Par contre ce dérivé n'est pas cytotoxique (à 100 µM, le pourcentage de viabilité cellulaire est de 59 %).

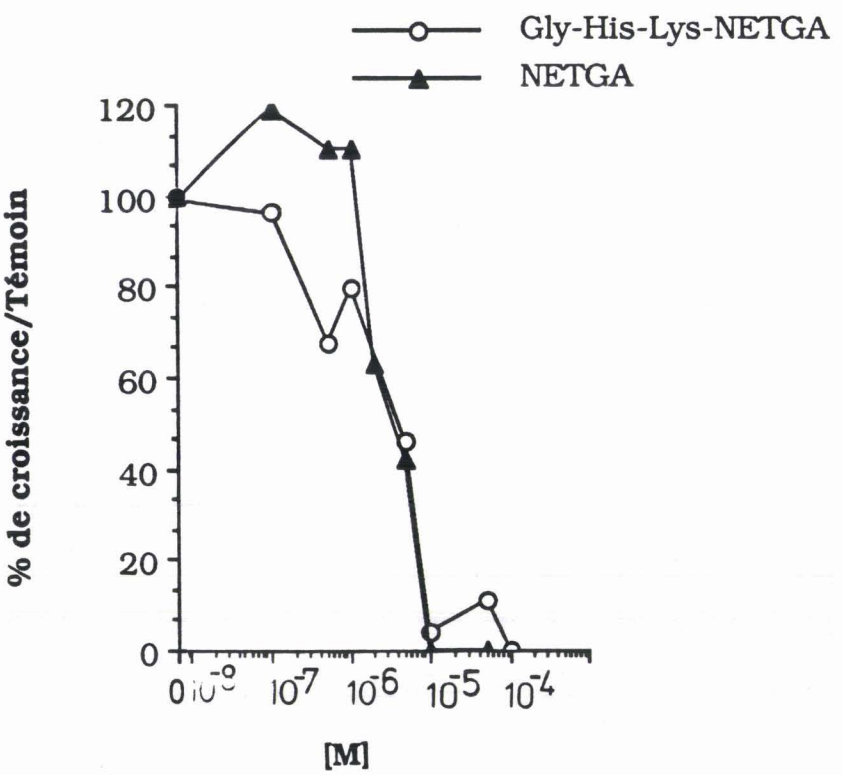

Cette activité a été mesurée avec le produit seul. D'autres essais seront effectués en associant ce produit avec du cuivre et de l'ascorbate de sodium. Le couple cuivre-ascorbate est à lui seul doué de propriétés antitumorales (BRAM et al., 1980). L'addition d'un peptide complexant du cuivre au système Cu(II)-ascorbate accroît de façon significative les potentialités anticancéreuses de ce système (KIMOTO et al., 1983) alors que le peptide seul est inactif.

Ainsi le modèle Gly-His-Lys-NETGA déjà actif sous forme libre non complexée devrait s'avérer encore plus efficace en présence de cuivre et d'ascorbate. Cependant si cette hypothèse est encourageante, l'addition de cuivre à une culture cellulaire est toujours délicate du fait de la toxicité du cuivre libre non complexé.

Le mécanisme d'action de ce modèle s'apparente à celui des endonucléases. Au sein de ces enzymes, deux domaines sont souvent juxtaposés : un site de reconnaissance de l'ADN et un site catalytique. Gly-His-Lys-NETGA peut être considéré comme l'union d'un site catalytique (Gly-His-Lys) et d'une unité de reconnaissance de l'ADN (NETGA).

En perfectionnant ce modèle,on peut espérer aboutir à la conception d'enzymes artificiels. La conversion de système reconnaissant spécifiquement l'ADN en système dégradant l'ADN a déjà été réalisé avec des protéines notamment :

- le répresseur du gène du Trp auquel la phénanthroline qui coupe l'ADN, a été fixée (CHEN & SIGMAN, 1987).
- un fragment de 52 acides aminés de la recombinase Hin. Ce fragment peptidique responsable de la reconnaissance de l'ADN par la protéine Hin a été couplé à l'EDTA (SLUKA et al., 1987) ou au tripeptide Gly-His-Lys (MACK et al., 1988) afin d'obtenir un système capable de dégrader l'ADN.

Si ces deux modèles protéiques sont de bons outils pour la biologie moléculaire, ils sont toutefois dépourvus d'activité biologique du fait de leur sensibilité aux protéases.

Pour notre part, suite aux résultats encourageants obtenus avec le modèle Gly-His-Lys-NETGA, un programme pour la conception de composés analogues a été élaboré en collaboration avec Monsieur le Docteur J-P BEHR (CNRS UA 422,

Strasbourg). Un premier composé qui associe un résidu de type Dst-A se liant à l'ADN, un complexant du cobalt capable d'hydrolyser les liaisons phosphodiester de l'ADN (CHIN & ZOU, 1988) et un intercalant, est en cours de synthèse.

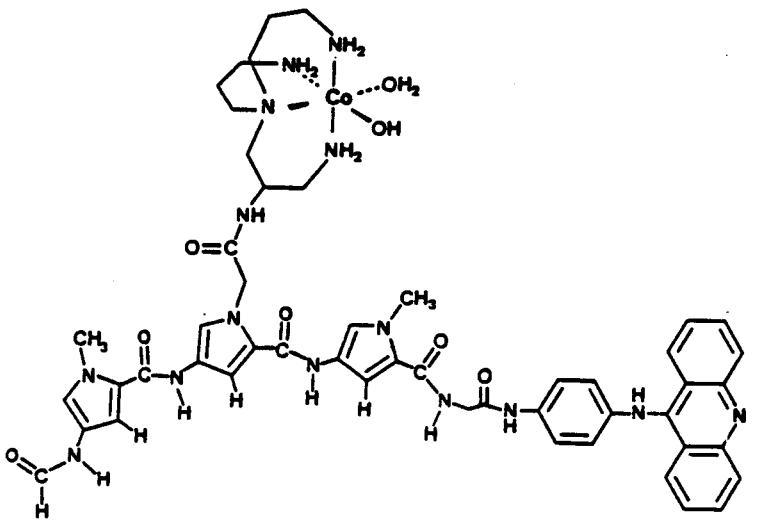

De tels dérivés, résistant aux protéases, devraient nous permettre dans un proche avenir d'élaborer des composés antitumoraux structuralement simples.

La conception d'enzymes artificiels telles qu'elle est envisagée devrait déboucher sur des composés anticancéreux, antibactériens, antiviraux ...

CONCLUSION

A partir de la connaissance du mécanisme d'action de substances naturelles, divers concepts ont été avancés puis appliqués par la synthèse de nombreux modèles.

L'élaboration de chaque modèle repose sur l'existence de relations Structure-Activité élucidées de proche en proche. Cette démarche logique qui fait appel aussi bien à la chimie et à la physicochimie qu'à la biochimie et à la biologie, a débouché sur des composés actifs.

Cette étude montre entre autres qu'il est désormais possible de concevoir des composés susceptibles de se lier à l'ADN par un mécanisme choisi à l'avance.

Il est probable que dans un très proche avenir il sera également possible de prédéterminer le site préférentiel de liaison d'une substance sur l'ADN.

Le but d'un grand nombre d'équipes est de créer des modèles capables d'inhiber sélectivement l'expression de certains oncogènes. Beaucoup d'éléments sont encore à découvrir pour maîtriser l'expression des gènes du cancer. Notre étude s'inscrit dans ce programme et contribuera peut-être à sa réalisation.

Un autre point, également abordé dans ce travail concerne l'étude des interactions substances anticancéreuses-membranes. Il apparait de plus en plus distinctement que les transits cellulaires et membranaires sont des paramètres à considérer au même titre que la liaison à l'ADN pour la conception de substances antitumorales.

Si jusqu'à présent très peu de médicaments anticancéreux, à part le Fluoro-5 Uracile et l'amsacrine, ont été conçus à partir d'une approche chimique rationnelle, la rigueur de cette démarche devrait aboutir à la création de composés utilisables en clinique.

APPENDICE TECHNIQUE

SYNTHESE CHIMIQUE

Les synthèses ont nécessité l'optimisation d'un grand nombre d'étapes dont il serait fastidieux de détailler point par point les conditions opératoires. Bon nombre d'entre-elles ont été largement explicitées dans nos publications incluses dans le texte. Ces synthèses seront donc décrites brièvement et les caractérisations des produits de réaction ou de leurs intermédiaires seront souvent proposées sous forme de données spectrales.

1°) Synthèse des analogues thiazoliques de la nétropsine et de la distamycine

a) Dérivés thiazoliques :

Ces synthèses peuvent être schématiquement scindées en 3 étapes :

1- conception d'un motif commun : le (t-butyloxyaminométhyl)-2 thiazole-4 carboxylate d'éthyle.

2- di- et trimérisation de ce motif par des réactions de couplage peptidique en présence de dicyclohexylcarbodiimide (DCC) et d'hydroxybenzotriazole (HOBt).

3- synthèse de la chaîne latérale aminopropionamidine et fixation à l'extrémité C-terminale du pseudopeptide.

Cette synthèse a fait l'objet de la publication suivante :

article n° 12 :

DEPSIPEPTIDE ANALOGS OF THE ANTITUMOR DRUG DISTAMYCIN CONTAINING THIAZOLE AMINO ACIDS RESIDUES.

BAILLY C., HOUSSIN R., BERNIER J-L., HENICHART J-P.

Tetrahedron 1988, **44**, 5833-5843.

Tetrahedron Vol. 44. No. 18. pp. 5833 to 5843. 1988
Printed in Great Britain.

0040–4020/88 $3.00+.00

DEPSIPEPTIDE ANALOGS OF THE ANTITUMOR DRUG DISTAMYCIN CONTAINING THIAZOLE AMINO ACIDS RESIDUES

Christian BAILLY[+], Raymond HOUSSIN[++], Jean-Luc BERNIER[+] and Jean-Pierre HENICHART[+*]

[+]INSERM U.16 Place de Verdun 59045 Lille, France

[++]Institut de Chimie Pharmaceutique, Faculté de Pharmacie, Rue Laguesse 59045 Lille, France

(*Received in Belgium* 20 *June* 1988)

ABSTRACT

Three compounds structurally related to the natural antiviral antitumor drugs netropsin and distamycin have been synthetized. They have been designed starting from 2-((aminomethyl)-thiazole-4 carboxylic acid, gly (Thz), a key element in the structure of highly cytotoxic natural peptides. In the structure of the three new compounds, this unit replaces N-methyl pyrrole carboxylic acid which seems to play a crucial role in DNA base sequence recognition by the parent natural agents.

Distamycin-A (Dst) (Fig. 1), a compound possessing antibacterial, antiviral and antitumor activities, has attracted considerable attention of many research groups (for a review see ref. 1) since its isolation[2] and its total synthesis[3]. Physico-chemical studies indicates that Dst, like the other pyrrole amidine antibiotic netropsin (Nt) (Fig. 1), is able to block the template function of DNA by binding to specific nucleotide sequences in the minor groove of double strand DNA[1]. The molecular recognition site was found to be a AT rich segment as revealed by foot-printing or DNA-affinity cleaving [4-6] techniques. In order to understand the conformational and chemical basis of DNA binding and to delineate the role of the heterocyclic moiety in the base specificity, structural modifications of the parent molecules Dst and Nt, have been rationally carried out. Peptide analogs of Dst and Nt synthesised hitherto can be regrouped in three classes. First, those on which the pyrrole ring is replaced by phenyl[7], pyridine[8,9], thiophene[9], imidazole[10,11] groups. In the second class, the pyrrole carboxamide unit and the side chains (formyl and amidine) were present but the number of pyrrole units is different[12] or the linking chains between the heterocyclic rings is more extended[13]. In the last class, the modifications are centered on the side chain without modification of the two (Nt) or three (Dst) pyrrole units[14].

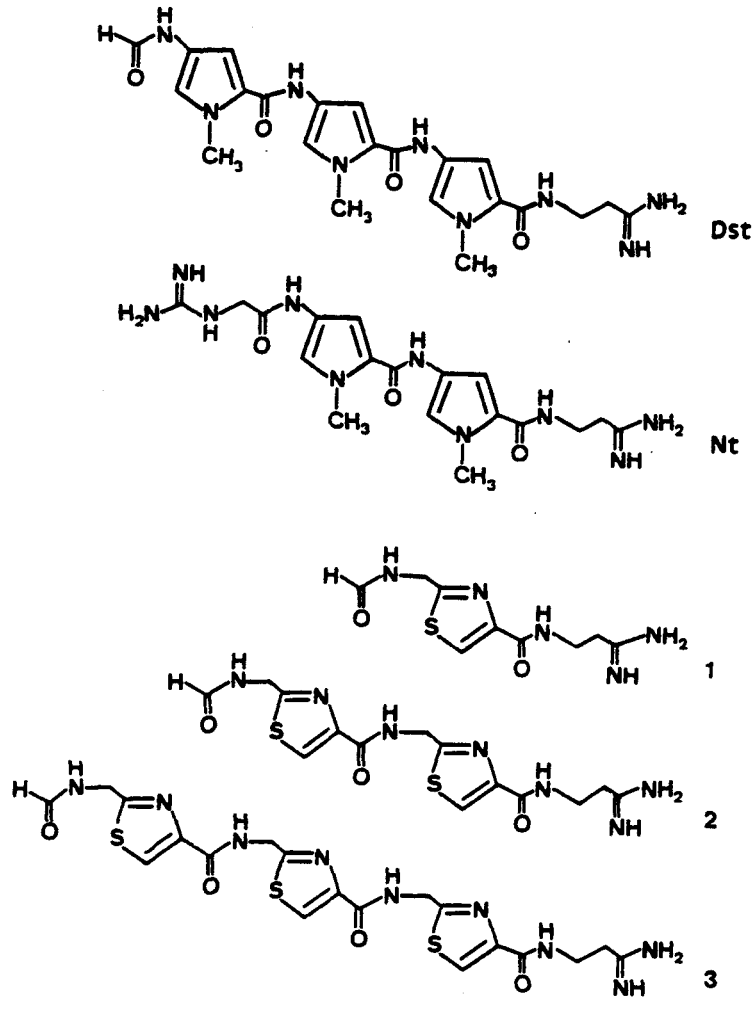

Figure 1. Structure of the oligopeptide antibiotics, Distamycin A (Dst), Netropsin (Nt) and related synthetic compound formyl-gly(Thz)-aminopropionamidine (1), formyl-gly(Thz)$_2$-aminopropionamidine (2), formyl-gly(Thz)$_3$-aminopropionamidine (3).

Taking into account these previous works, rational conformational structure-DNA binding relationships have been developed. In order to design non-intercalative DNA-binding compounds with a modified DNA specificity and enhanced biological activities compared to Dst, we report here the synthesis of three new compounds related to the Dst antibiotic (Fig. 1). The distinctive features of these three compounds is the introduction of 2-(aminomethyl) thiazole-4-carboxylic acid unit in place of the N-methyl-pyrrole unit of Dst (Fig. 1). The peptides, reported in this paper, contain the common synthon 2-aminomethylthiazole carboxylic acid. This ring has several advantages :

i) First the heterocyclic N atom is a hydrogen accepting site for the NH_2 of guanine as it has been demonstrated in similar cases[10,11].

ii) The additional methylene group undoubtedly disrupts the extensive π-electron delocalization which occurs in the parent drug structure and which has been regarded as responsible for the stabilization of the drug-DNA complex[13]. However, since the base sequence information can be read out by Van der Waals contacts[15], the supplementary CH_2 group is able to induce a modified binding specificity to DNA sequence.

iii) Are also present in the structure of the new models the formyl and amidine groups able to form electrostatic bonds with DNA phosphates and the amide bonds necessary for a relative rigid conformation and the establishment of hydrogen bonds with a heteroatom of purines and pyrimidines as found for Dst.

iv) The 2-(aminoalkyl)-thiazole-4 carboxylic acid seems to be important for the biological activity of highly cytotoxic cyclopeptides isolated from marine animals (dolastatin [16], ulicyclamide, ulithiacyclamide [17] and patellamides [18-21] from tunicates) and the thiazole ring seems to play a crucial role in the action of other naturally occurring peptides of pharmacological interest such as thiostrepton [22,23], botromycin [24], dysidenin [25] or isodysidenin [26].

Synthetic strategy

The three new compounds formyl-gly(Thz)-aminopropionamidine[27] 1, formyl gly(Thz)$_2$-aminopropionamidine 2 and formyl-gly(Thz)$_3$-aminopropionamidine 3 have been synthesized according to schemes I and III.

Reaction of aminoacetonitrile hydrochloride with di-t-butyldicarbonate anhydride ((BOC)$_2$O) in the presence of triethylamine afforded the BOC protected aminoacetonitrile 4 in high yield. Thionation of the nitrile 4 was accomplished with H_2S under pressure. Ethyl BOC-aminomethylthiazole carboxylate was then prepared from the thioamide 5 and ethyl bromopyruvate by an improvement of the classical Hantzsch condensation using a procedure which has previously been exploited by our group [28,29]. The resulting unstable air sensitive ester 6 was immediately converted into the stable amine 7 : cleavage of the BOC group with dry hydrogen bromide, in acetic acid, gave the desired synthon 7 in 95 % yield. N-formylation of 7 was carried out with formic acid by a classical procedure using dicyclohexylcarbodiimide (DCC) and 1H-hydroxy-1,2,3-benzotriazole as coupling agent. This procedure provided the N-formyl product 8 in 63 % yield. This approach was preferred to that which uses other reagents like formic anhydride [30] or formamide and ethyl formate [31]. Such formyl derivatives 8, 12 and 20 were more hydrophilic than their corresponding BOC protected amines and extreme precautions must be taken with all the washing procedures with aqueous media. For this reason, we decided for the Thz-Dst derivative 3 to introduce the formyl side chain in the last step of the synthetic strategy, just before the amidine moiety.

Alkaline hydrolysis of 8 afforded the formyl-gly(Thz) carboxylic acid 9, after acidification, in a 98 % yield. Coupling of the primary amine 7 with 9 in the presence of DCC-HOBt, gave the amide 12 *in excellent yield and saponification of 12 with sodium hydroxide afforded the desired acid 13.* With the formyl-gly(Thz) carboxylic acid 9 and the formyl-gly(Thz)$_2$ carboxylic acid 13, we now turned to the attachment of the aminopropionamidine end group. The literature[32] method of coupling, first with aminopropionitrile followed by addition of ammonia to the nitrile group via an intermediate iminoester, was in this case unsatisfactory because of the very low yield caused by the degradation of the thiazole system. Therefore an alternative procedure was examined. The direct coupling of β-aminopropionamidine dihydrobromide[33] (scheme II) with succinimidyl esters of 9 and 13 suggested an alternative method[30]. Best results were obtained by using one equivalent of the succinimidyl esters, 10, 14 (isolated as pure compound by recrystallisation from 2-propanol), 1.2 equiv. of 11d and 1.2 equiv of $NaHCO_3$. The two compounds 1 and 2 were finally obtained as pure white needles by two successive recrystallisations from 2-propanol. The method of purification used here avoided chromatography which is not suitable for such polar products because of contamination of the final compounds with inorganic salts eluted from the adsorbent.

The synthesis of 3 was carried out as depicted in scheme III. This thiazole-containing Dst analogue was prepared using the BOC-protected aminoacid 15 as starting material. Two different ways could be envisaged in the synthesis of 15. First saponification of the easily obtained synthon 6 with sodium hydroxide seemed to be the more appropriate procedure. However by this method, the yield of purified 15 did not exceed 10 % and this experiment was not easily reproducible. In an alternative method, the acid 15 was obtained in a high yield by direct condensation of thioamide 5 with bromopyruvic acid[34]. This reaction, conducted in ethyl acetate, needed one equivalent of triethylamine to neutralize HBr formed in situ which could cleave the BOC group. Careful examination of the crude reaction mixture revealed the presence of unreacted 5 ($\simeq$ 1 %), and pure compound 15 was obtained by flash chromatography[35].

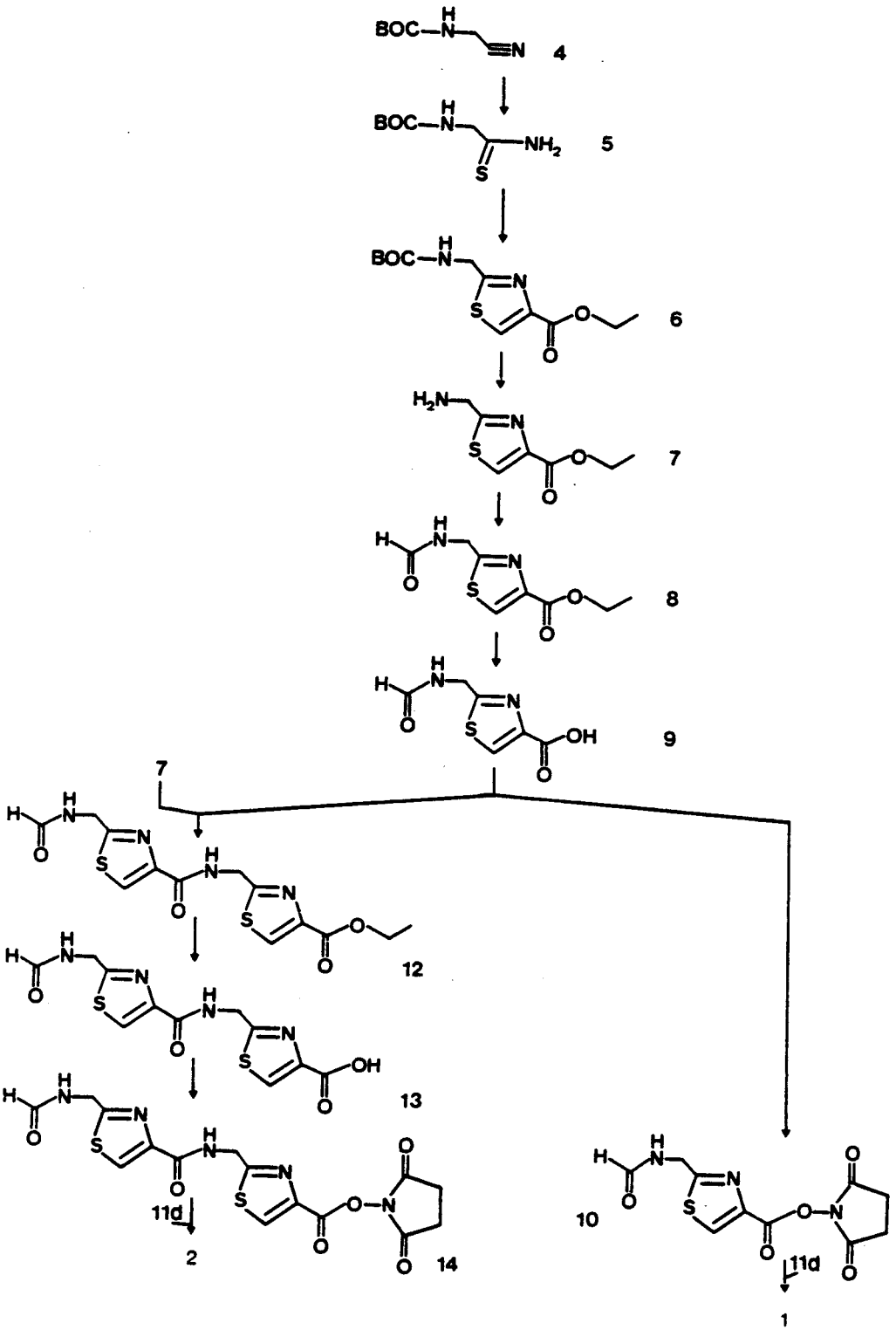

Scheme I

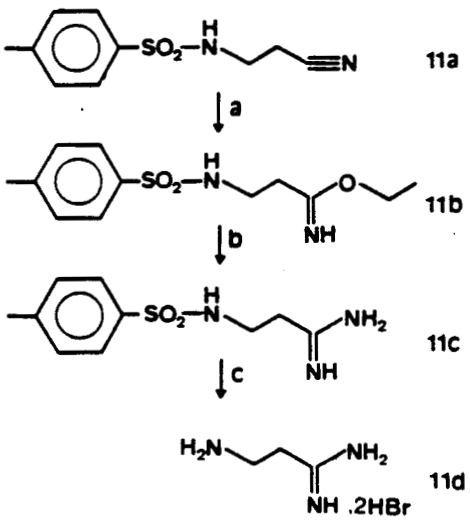

Scheme II[a] Reaction conditions : (a) HCl in dry EtOH, (b) dry NH_3 in ETOH, (c) phenol, HBr and acetic acid.

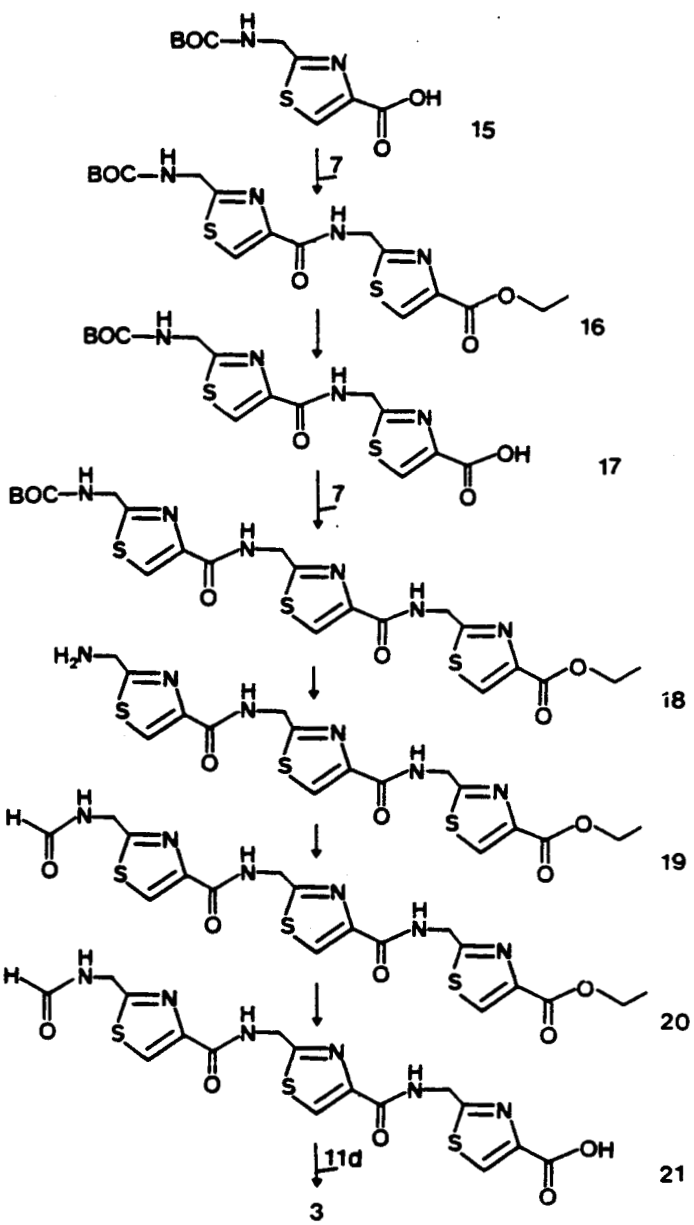

Scheme III

The condensation of 15 with amine 7 using DCC-HOBt furnished the protected dimer in a reasonable yield. After alkaline hydrolysis of the ester group, this procedure was repeated to give protected trimer 18. The BOC protecting group in 18 was conveniently removed, according to a standard procedure, with trifluoroacetic acid at room temperature. The N-formylated compound 20 was obtained from the amine 19, using the method of formylation described above for the conversion of 7 to 8.

The final incorporation of the amidine side chain in the molecule constituted a crucial step in the synthesis of 3. When the succinimidyl active ester of 21 (prepared as described for 10) was isolated, the yield was very poor and degradation of this active ester occurred readily. When DCC was used without N-hydroxysuccinimide as coupling agent, only minor amounts of 3 were produced and it was severely contaminated with several other substances. This obstacle was finally overcome by using N-hydroxysuccinimide in presence of DCC without isolation of the intermediate active ester.

Thus, the yield in the last step was unsatisfactory and was due to the difficulty in eliminating the unreacted amidine 11d without chromatographic methods unsuitable for such polar compounds. Generally two or three successive recrystallisations are necessary to obtain highly pure final products 1, 2, and 3.

Experimental section

General

- Melting points were determined in capillary tubes and are uncorrected. The IR spectra were obtained on a Perkin-Elmer 177 spectrophotometer, using KBr pellets. ^{1}H-NMR spectra were recorded on a Brucker WP 80 SY or on a Brucker AM 400 WB spectrophometers. Chemical shifts are reported in ppm from tetramethylsilane as an internal standard and are given in δ units. EI mass spectra were recorded on a Ribermag R10.10 (combined with Riber 400 data system) mass spectrophotometer at 70 eV by using direct insertion. FAB mass spectra were determined on a Kratos MS-50 RF mass spectrometer arranged in an EBE geometry. The sample was bombarded using a beam of xenon with a kinetic energy of 7 keV. The mass spectrometer was operated at 8 KV accelerating voltage with a mass resolution of 3000. Thin layer chromatography (TLC) was carried out using silica gel 60F-254 Merck (0,25 mm thick) precoated UV-sensitive plates, generally in solvent system A ($CHCl_3$-MeOH, 80 : 20 (v/v) in a satured NH_3 atmosphere). Spots were visualized by inspection under U.V. light at 254 nm and after exposure to vaporized I_2 and/or ninhydrin. Kieselgel 60 (230-400 mesh) of Merck was used for flash-chromatography according to the procedure of Still[35].

t-Butoxyaminoacetonitrile (4). To a solution of 9.25 g (0.1 mol) of 2-aminoacetonitrile hydrochloride (Aldrich) in CH_2Cl_2 (300 mL), TEA (27.7 mL, 0.2 mol) and di-t-butyldicarbonate (21.82 g, 0.1 mol) in CH_2Cl_2 (100 mL) were added. The stirred mixture was refluxed for 12 hours. Triethylamine salt was extracted twice by 30 mL of water, and the organic phase was evaporated in vacuo to yield 14.3 g (92 % yield) of an oil which solidified by trituration in petroleum ether, mp<35°C ; Rf(A) : 0.8 ; IR 3380 (NH), 2220 (C N), 1700 (O-CO) cm^{-1} ; ^{1}H-NMR ($CDCl_3$) δ 1.5 (s,9H, $(CH_3)_3$), 4.1 (d, 2H, J=6Hz, CH_2), 6.1 (m, 1H, NH). Anal. Calcd for $C_7H_{12}N_2O_2$: C,53.83 ; H, 7.69 ; N, 17.94. Found : C, 53.61 ; H, 7.65 ; N, 17.80.

t-Butoxyaminothioacetamide (5). A solution of 4 (14 g, 89.7 mmol) in dimethylformamide (50 mL) and diethylamine (20 mL) was poured in a stainless steel bomb and allowed to react with hydrogen sulfide under 2 atmospheres pressure for 12 hours at 20°C. The solvent was evaporated and the residual solid recrystallized twice from water, giving 14.45 g (85 % yield) of white crystals : mp:125°C ; Rf(A):0.8 ; IR 3420 (NH_2 thioamide), 3300 (NH-BOC) 1685 (O-CO), 1610 (C=S) cm^{-1} ; ^{1}H-NMR ($Me_2SO.d_6$) δ 1.4 (s, 9H, $(CH_3)_3$), 3.8 (d, 2H, J = 0.55Hz, CH_2), 6.9 (m, 1H, NH), 8.9 (m, 1H, NH_2-C=S), 9.6 (m, 1H, NH_2-C=S) ; MS, m/e (rel intensity) 190 (17, M^+). Anal. Calcd for $C_7H_{14}N_2O_2S$: C, 44.21 ; H, 7.36 ; N, 14.73. Found : C, 44.08 ; H, 7.47 ; N, 14.57.

Ethyl 2-(t-butoxyaminomethyl)-thiazole-4-carboxylate (6). A mixture of 5 g (26.3 mmol) of 5 and 3.29 mL (26.3 mmol) of ethyl bromopyruvate (Aldrich) in 250 mL of dry ether was stirred at room temperature for 2 h. Filtration of the precipitate afforded 6.96 g (92.5 % yield) of white unstable crystalline 6 immediately used for preparation of 7 and 15. mp:133°C ; Rf(A):0.68 ; IR 1760 ($COOCH_2$), 1705 (OCO) cm^{-1} ; ^{1}H-NMR (Me_2SO-d_6) δ 1.3 (t, 3H, CH_3-CH_2), 1.4 (s,9H, $(CH_3)_3$), 4.3 (q, 2H, CH_2-CH_3), 4.4 (d, 2H, CH_2-NH), 6.0 (m, 1H,NH-CH_2) 8.35 (s, 1H, CH), MS, m/e (rel intensity) 286 (24, M^+).

Ethyl 2-(aminomethyl) thiazole -4-carboxylate hydrobromide (7). A solution of 6.8 g (23.8 mmol) of 6 in 200 mL of glacial acetic acid was treated with dry HBr gas. After saturation, the reaction mixture was set aside at room temperature for 2 h after which time a solid precipitated. The white solid (5.97 g, 94 % yield) was collected, washed with large quantities of diethyl ether and dried under reduced pressure. An authentic specimen was recrystallised from absolute ethanol : mp:190°C, Rf(A):0.40 ; IR 3000 (NH_3), 1740 ($COOCH_2$) cm^{-1} ; ^{1}H-NMR (Me_2SO-d_6) δ 1.3 (t, 3H, J=6.4Hz, CH_3-CH_2), 4.3 (q, 2H,J=6.4Hz,CH_2-CH_3), 4.5 (m, 2H, CH_2-C), 7.35 (m, 1H, NH_3-CH_2), 8.6 (s, 1H, CH). MS, m/e (rel intensity) 186 (12, M^+), 158 (9.9), 112 (46), 82 (100). Anal. Calcd for $C_7H_{11}N_2O_2SBr$: C, 31.46 ; H, 4.12 ; N, 10.48. Found : C, 31.39 ; H, 4.20 ; N, 10.32.

Ethyl 2-(formamidomethyl)thiazole-4-carboxylate (8). Formic acid (0.36 mL, 9.36 mmol) in cold dry CH_2Cl_2 was stirred with dicyclohexylcarbodiimide (2.12 g, 10.3 mmol) and 1H-hydroxy-1,2,3-benzotriazole (1.58 g, 10.3 mmol) for 1 h ; a cold solution of 7 (2.5 g, 9.36 mmol) and TEA (1.3 mL, 9.36 mmol) in CH_2Cl_2 (30 mL) was added. Stirring was continued for 2 h at 0°C and 15 h at 20 °C. The dicyclohexylurea was discarded by precipitation with acetone and the CH_2Cl_2 solution was concentrated and washed with a minimum volume (5 mL) of 1N HCl and 1M $NaHCO_3$. After drying over Na_2SO_4, the solvent was removed in vacuo and compound 8 was obtained in 1.26 g (63 % yield) as a white pure powder as ascertained by TLC. mp:84-86°C, Rf(A):0.68 ; IR 1735 (COOEt), 1685 (CHO) cm^{-1} ; ^{1}H-NMR (Me_2SO-d_6) δ 1.3 (t, 3H, CH_3-CH_2), 4.3 (q, 2H, CH_2-CH_3), 4.6 (d, 2H, CH_2-NH), 8.15 (s, 1H, CHO), 8.35 (s, 1H, CH), 8.83 (m, 1H, NH) ; MS,m/e (rel intensity) 214 (71.3, M^+), 185 (18.3), 168 (27.8), 139 (61.0), 112 (100). Anal. Calcd. for $C_8H_{10}N_2O_3S$: C, 44.86 ; H, 4.67 ; N, 13.08 ; Found. C, 44.55 ; H, 4.77 ; N, 12.85.

2-(Formamidomethyl) thiazole-4-carboxylic acid (9). A solution of 1.2 g (5.6 mmol) of 8 in MeOH and 0.9 g (22.4 mmol) of sodium hydroxide in water (2 mL) was stirred at room temperature. The progress of the reaction was monitored by TLC and was thereby judged to be complete after 20 h . The resulting solution was cautiously acidified to pH 3.0 with a few drops of dilute HCl. Evaporation of the solvent, trituration in absolute ethanol, elimination of sodium chloride by filtration, and evaporation of ethanol, yielded 1.02 g of a white solid suitable for further synthesis (98% yield). An analytical pure sample was obtained by recrystallisation from 95 % ethanol. mp:246°C, Rf(A):0 ; IR 1730 (COOH), 1710 (CHO) cm^{-1} ; ^{1}H-NMR (Me_2SO-d_6) δ 4.0 (m, 1H, COOH) ; 4.65 (d, 2H, CH_2), 8.2 (s, 1H, CHO), 8.35 (s, 1H, CH), 8.7 (m,1H, NH) ; MS, m/e (rel intensity) 186 (30.2, M^+), 168 (77.7), 157 (24.8), 139 (100). Anal. Calcd for $C_6H_6N_2O_3S$: C, 38.71 ; H, 3.22 ; N, 15.05 ; Found : C, 38.69 ; H, 3.28 ; N, 15.16.

Succinimidyl 2-(formamidomethyl) thiazole-4-carboxylate (10). A mixture of 9 (0.5 g, 2.69 mmol) and N-hydroxysuccinimide (0.34 g, 2.95 mmol) dissolved in dry DMF (20 mL), was cooled in an ice bath. To this well-stirred solution was added solid dicyclohexylcarbodiimide (0.61 g, 2.95 mmol) and stirring was continued for an additional 1h at 0°C and then at 20°C overnight. After evaporation, the dicyclohexylurea formed was collected and washed with small portions of cold acetone. The combined yellowish filtrate and washings were evaporated to dryness under reduced pressure (temperature below 40°C). This semi-solid residue was purified by dissolution in a small quantity of acetone, and precipitation with cold ether. This material, obtained as a white powder, was finally recrystallized from 2-propanol to give a white microcrystalline solid. (0.29 g, 38 % yield) ; mp:144-146°C ; Rf(A):0.56 ; IR 1800; 1745 (COON), 1680 (CHO) cm^{-1} ; ^{1}H-NMR (Me_2SO-d_6) δ

3.15 (m, 4H, $2CH_2CO$), 4.7 (d, 2H, CH_2NH), 8.2 (s, 1H, CHO), 8.7 (m, 1H, NH), 8.8 (s, 1H, CH). Anal. Calcd for $C_{10}H_9N_3O_5S$: C, 42.40 ; H, 3.18 ; N, 14.84 ; Found : C, 42.45; H, 3.27 ; N, 14.71.

3-Aminopropionamidine dihydrobromide (11d). The title compound was prepared as previously described by Hilgetag et al[33]. Only the physico-chemical characteristics of intermediate and final products are reported here.

3-(p-Toluenesulfonylamino)-propionitrile (11a). mp>250°C ; Rf(A) : 0.68 ; IR 2240 (C N), 1340 (SO_2) cm^{-1} ; ^{1}H-NMR (Me_2SO-d_6) δ 2.4 (s, 3H, CH_3), 2.6 (m, 2H, CH_2-NH),, 3.0 (t, 2H, CH_2-C N), 6.8 (m, 1H, $NHSO_2$), 7.5 (m, 4H, CH) ; MS, m/e (rel intensity) 224 (8.2 M^+), 184 (20.5), 155 (42.0), 91 (100).

Ethyl 3-(p-toluenesulfonylamino)-propionimidate hydrochloride (11b). mp:126°C ; Rf(A):0.93 ; IR 1340 (SO_2), 1730 (CNHOEt) cm^{-1} ; ^{1}H-NMR (Me_2SO-d_6) δ 1.15 (t, 3H, CH_3-CH_2), 2.4 (s, 3H, CH_3-C), 3.0 (m, 4H, CH_2-CH_2), 4.0 (q, 2H, CH_2-CH_3), 6.7 (m, 1H, NH-SO_2), 7.6 (m, 4H, CH), 7.95 (m, 1H, HN = C,) ; MS, m/e (rel intensity) 271 (0.2 M^+), 226 (11.8), 184 (35.6), 155 (89.5), 116 (94.4), 91 (100).

3-(p-Toluenesulfonylamino)-propionamidine (11c). Rf(A):0, Rf (H_2O/MeOH /HCOOH, 9/3/0.1, v:v):0.57 ; IR 1680 (amidine), 1335 (SO_2) cm^{-1} ; ^{1}H-NMR (Me_2SO-d_6) δ 2.4 (s,3H,CH_3), 3.0 (m, 2H, CH_2), 3.4 (m, 2H, CH_2), 6.5 (m, 1H, $NHSO_2$), 6.6 (m, NH), 7.5 (m, 4H, CH). No molecular ion peak was present in the 70-eV mass spectrum ; same fragmentation as observed for 11b.

3-Aminopropionamidine dihydrobromide (11d). mp:159°C ; Rf(A):0, Rf(H_2O/MeOH/ HCOOH, 9/3/0.1, v:v):0.72 ; IR 3340 (NH_2-C), 1690 (amidine) cm^{-1} ; ^{1}H-NMR (Me_2SO-d_6) δ 2.9 (m, 2H, CH_2), 3.2 (m, 2H, CH_2), 8.5 (m, NH) ; no molecular ion peak was present in the 70-eV mass spectrum (parent peak, m/e 80). Anal. Calcd for $C_3H_{11}N_3Br_2$: C, 14.45 ; H 4.41 ; N, 16.86. Found : C, 14.39 ; H, 4.48 ; N, 16.64.

[2-Formamidomethyl)thiazole-4carboxamido]propionamidine hydrobromide (1). To a well stirred solution of β-aminopropionamidine 11d (210 mg, 0.84 mmol) and $NaHCO_3$ (70.6 mg, 0.84 mmol) in dioxane - water 1 : 2 (v:v, 15 mL) was added a fresh solution of 10 (200 mg, 0.7 mmol) in dioxane (5mL). The solution was stirred for 48 h at room temperature and then evaporated ; after filtration of the solution obtained by dissolution in water (4 mL), the lyophilizated material was dissolved in hot absolute ethanol to remove NaBr and the starting amidine 11d. The alcoholic filtrate was evaporated to dryness and the residual powder recrystallised twice in 1-butanol giving 53 mg (15 % yield) of hygroscopic compound 1 pure as indicated by usual analytical criteria . Rf(A):0, Rf(H_2O/MeOH/HCOOH, 9/3/0.1, v:v):0.62 ; ^{1}H-NMR (Me_2SO-d_6) δ 2.85 (m, 2H, CH_2), 3.8 (m,2H, CH_2),4.8 (d, 2H, CH_2 - NH), 8.25 (s, 1H, CHO), 8.35 (s, 1H, CH), 8.7 (m, 1H, NH). Non analysable by MS (EI). Anal. Calcd. for $C_9H_{14}N_5O_2SBr$: C, 32.14 ; H, 4.17 ; N, 20.83. Found : C, 32.26 ; H, 4.19 ; N, 20.74

Ethyl2-[2'-(formamidomethyl)thiazole - 4'-carboxamidomethyl]thiazole-4-carboxylate (12). A solution of compound 9 (1.5 g, 8.06 mmol) in anhydrous CH_2Cl_2 (100 mL) was cooled to 0°C and dicyclohexylcarbodiimide (1.82 g, 8.87 mmol) and 1H-hydroxy-1,2,3-benzotriazole hydrate (1.35 g, 8.87 mmol) in 10 mL of CH_2Cl_2 were added. After 1 h 30, a solution of 7 (2.15 g, 8.06 mmol) in 30 mL CH_2Cl_2 and TEA (1.12 mL, 8.06 mmol) cooled to 0°C was added. The mixture was stirred at 0°C for 2 h and allowed to rise to ambient temperature, stirring was continued for 10 h. The precipitated dicyclohexylurea was collected and the CH_2Cl_2 solution was washed successively with 30 mL of 1N HCl, , H_2O and 1M $NaHCO_3$. After drying over Na_2SO_4 the solvent was removed in vacuo. The remaining dicyclohexylurea was discarded by classically precipitation with acetone. The resulting residue obtained after evaporation of the solvent was thoroughly triturated with diethylether. The yield of crude, chromatographically pure product obtained as a white powder was 3.24 g (68 % yield). mp:134-135°C, Rf(A):0.78, IR 1720 (COOEt), 1665 (CHO), 1635 (CONH)cm^{-1}, ^{1}H-NMR (Me_2SO-d_6) δ 1.3 (t, 3H, CH_3CH_2),

4.3 (q, 2H, CH_2CH_3), 4.6 (d, 2H, CH_2), 4.8 (d, 2H, CH_2), 8.2 (s, 1H, CHO), 8.35 (2s, 2H, 2CH), 8.7 (m, 1H, NH,), 9.05 (m, 1H, NH). MS-FAB 355 (75, M^++1). Anal. Calcd for $C_{13}H_{14}N_4O_4S_2$: C, 44.07 ; H, 3.95 ; N, 15.82 ; Found : C, 44.35 ; H, 4.08 ; N, 15.74.

2-[2'-(Formamidomethyl)thiazole-4'-carboxamidomethyl]thiazole-4-carboxylic acid (13). This compound was prepared using the same conditions as described for 9. Recrystallisation from absolute ethanol provided 1.64 g of 13 (94 % yield). mp:128°C, Rf(A):0, IR 1730 (COOH), 1710 (CHO), 1640 (CONH) ; ^{1}H-NMR (Me_2SO-d_6) δ 4.7 (d, 2H, CH_2), 4.8 (d, 2H, CH_2), 8.2 (s, 1H, CH), 8.3 (s, 1H, CH), 8.35 (s, 1H, CHO), 8.8 (m, 1H, NH), 9.0 (m, 1H, NH). MS, m/e (rel intensity) 326 (0.3, M^+), 320 (1.1), 305 (5.4) 223 (10.2), 141 (21.6), 113 (39.9), 98 (100). Anal. Calcd. for $C_{11}H_{10}N_4O_4S_2$: C, 40.49 ; H, 3.07 ; N, 17.18 ; Found : C,40.41 ; H, 3.15 ; N, 16.97.

Succinimidyl 2-[2'-formamidomethyl)thiazole-4'-carboxamidomethyl]thiazole-4-carboxylate (14). This succinimidyl ester was prepared according to the previously established procedure for 10. 0.26 g of needles from isopropanol. (40 % yield) ; Rf(A) : 0.45 ; IR 1745 (COON), 1680 (CHO), 1660 (CONH) ; ^{1}H-NMR (Me_2SO-d_6) δ 3.20 (m, 4H, $2CH_2CO$), 4.75 (d, 2H, CH_2), 4.8 (d, 2H, CH_2), 8.2 (s, 1H, CH), 8.3 (s, 1H, CH), 8.35 (s, 1H, CHO), 8.8 (m, 1H, NH), 9.1 (m, 1H, CH). Anal. Calcd. for $C_{15}H_{13}N_5O_6S_2$: C, 42.55 ; H, 3.07 ; N,16.55. Found : C, 42.66; H, 3.02 ; N, 16.40.

[2[2'-(Formamidomethyl)thiazole-4'-carboxamidomethyl]thiazole-4-carboxamido]propionamidine hydrobromide (2). 38 mg (17% yield) of amidine 2 were obtained according to the procedure described 1. mp:76°C ; Rf(A):0, Rf(H_2O/MeOH/HCOOH, 9/3/0.1, v:v):0.58 ; ^{1}H-NMR (Me_2SO-d_6) δ 2.5 (m, 2H, CH_2-CH_2) ; 3.6 (m, 2H, CH_2-CH_2) ; 4.7 (d, 2H, CH_2NH), 4.85 (d, 2H, CH_2-NH), 8.1 (s, 1H, CHO), 8.2 (s, 1H, CH), 8.25 (s, 1H, CH), 8.9 (m, 1H, NH), 9.1 (m, 1H, NH). FAB-MS 396 (M^++1). Anal. Calcd. for $C_{14}H_{18}N_7O_3S_2Br$: C, 35.29 ; H, 3.78 ; N, 20.59. Found C, 35.03; H, 3.71 ; N, 20.46.

2-(t-Butoxyaminomethyl)thiazole-4-carboxylic acid (15). (a) saponification of ester 6. 6 (1 g, 3.5 mmol) was dissolved in 50 mL of MeOH and a sodium hydroxide solution (0.15 g, 3.85 mmol in a minimum of water) was added. The mixture was stirred at room temperature for 30 min and then evaporated. The resulting residue was rapidly acidified with 30 mL of 1N HCl ; trituration of the gummy product gave 80 mg of the desired acid 15 in a poor yield (less than 10 %) but as a white powder essentially pure by TLC.

(b) Cyclisation using bromopyruvic acid. In an alternative procedure, 2.64 g of bromopyruvic acid (15.8 mmol, Aldrich) was added to a solution of 3 g of 5 (15.8 mmol) and 2.4 mL of TEA (17.36 mmol) in 100 mL of ethyl acetate. The mixture was stirred for 2 h at ambient temperature, the precipitate was collected and the solvent evaporated in vacuo. Trituration of a gummy product with ether gave a crude yellow crystalline substance which was collected : 2.89 g (71 % yield). Remaining traces amounts of 5 could be removed by flash chromatography (ethyl acetate : acetone (1 : 1 by volume) as eluent, followed by MeOH) to collect 15. An analytical sample could be obtained by dissolution of the chromatographed material in a minimum volume of acetone followed by addition of sufficient cold dry ether under rapid stirring. The precipitated white powder was then collected and dried. mp:184°C ; Rf(A):0.1 ; IR 1780 (COOH), 1710 (OCONH) cm^{-1} ; ^{1}H-NMR (Me_2SO-d_6) δ 1.45 (s, 9H, $(CH_3)_3$), 4.4 (m, 2H, CH_2), 7.1 (m, 1H, COOH), 8.35 (s. 1H, CH). MS, m/e (rel intensity) 258 (3.3, M^+), 241 (2.6), 226 (1.8), 214 (1.9), 202 (14.5), 198 (1.5), 185 (9.4), 158 (20.4) 100 (100). Anal. Calcd. for $C_{10}H_{14}N_2O_4S$: C, 46.51 ; H, 5.42 ; N, 10.85. Found : C, 46.62 ; H, 5.55 ; N, 10.79.

Ethyl 2-[2'-(t-butoxyaminomethyl)thiazole-4'- carboxamidomethyl]thiazole-4-carboxylate (16). Fresh, thoroughly dried acid 15 (2.6 g, 11.2 mmol) was coupled to the amine 7 (3 g, 11.2 mmol) using dicyclohexylcarbodiimide (2.5 g, 12.4 mmol), 1H-hydroxy-1,2,3-benzotriazole (1.9 g, 12.4 mmol) and TEA (1.55 mL, 11.2 mmol) in a mixture of CH_2Cl_2/DMF (9/1, v:v) according to the procedure described for 12. White powder, 3.24 g ; 68 % yield ; mp:118°C ; Rf(A):0.85 ; IR 1720 (COOEt), 1685 (OCONH), 1660 (CONH) cm^{-1} ; ^{1}H-NMR (Me_2SO-d_6) δ 1.25 (t, 3H, CH_3-CH_2), 1.4 (s, 9H, $(CH_3)_3$), 4.25 (q, 2H,

CH_2-CH_3), 4.45 (d, 2H, CH_2), 4.75 (d, 2H, CH_2), 7.7 (m, 1H, NH-BOC), 8.2 (s, 1H, CH), 8.35 (s, 1H, CH), 9.15 (m, 1H, NH-CO). Anal. Calcd for $C_{17}H_{22}N_4O_5S_2$: C, 47.88 ; H, 5.16 ; N, 13.14. Found : C, 48.01 ; H, 5.07; N, 13.02.

2-[2'(t-Butoxyaminomethyl) thiazole-4'- carboxamidomethyl]thiazole-4-carboxylic acid (17). The crude ethyl ester 16 (3 g, 7.04 mmol) was totally converted after 35 h to the corresponding acid 17, according to the method of preparation for 9. The material used for the further reaction was conveniently recovered after the following purification into a sinter glass charged with silica gel. The deposited mixture was first eluted with $CHCl_3$ to remove impurities, then with MeOH which afforded the neat 17 (2. 13 g, 76 % yield). mp:173-175°C, Rf(A):0 ; IR 1780 (COOH), 1680 (OCONH), 1665 (CONH)cm^{-1} ; ^{1}H-NMR (Me_2SO-d_6) δ 1.4 (s, 9H, $(CH_3)_3$), 4.45 (d, 2H, CH_2), 4.75 (d, 2H, CH_2), 7.68 (m, 1H, NH-BOC), 8.2 (s, 1H, CH), 8.3 (s, 1H, CH), 9.4 (m, 1H, NH-CO). Anal. Calcd for $C_{15}H_{18}N_4O_5S_2$: C, 45.22 ; H, 4.52 : N, 14.07. Found : C, 45.34 ; H, 4.55 ; N, 13.93.

Ethyl 2-[2'-[[2"-(t-butoxyaminomethyl)thiazole]-4"carboxamidomethyl]thiazole-4'-carboxamidomethyl]-thiazole-4-carboxylate (18). The procedure adopted for the preparation of the tristhiazole 18 is strictly identical to that described for 12. 64 % yield, mp:123°C, Rf(A):0.85 ; IR 1720 (COOEt), 1690 (O-CO), 1665 (CONH) cm^{-1} ; ^{1}H-NMR (Me_2SO-d_6) δ 1.4 (s, 9H, $(CH_3)_3$), 4.45 (d, 2H, CH_2), 4.7 (d, 2H, CH_2), 8.25 (s, 1H, CH), 8.3 (s, 1H, CH), 9.15 (m, 2H, 2NH) ; MS-FAB 567 (55, M^++1). Anal. Calcd. for $C_{22}H_{26}N_6O_6S_3$: C, 46.64 ; H, 4.59 ; N, 14.84 ; Found : C, 46.50 ; H,4.71 ; N, 14.69.

Ethyl 2-[2'-[[2"-(aminomethyl)thiazole]-4"carboxamidomethyl]thiazole-4'-carbo xamidomethyl]thiazole--4-carboxylate (19). The t-BOC protected amine 18 (1 g, 1.77 mmol) was deprotected with pure TFA (10mL) to give the corresponding free amine 19 in a good yield (>85%). After 1 h stirring, the excess of TFA was evaporated and the residue was diluted with absolute ethanol (30 mL) before evaporation of the solvent. This procedure was repeated three times and resulted in the complete elimination of TFA. A thorough drying is necessary to eliminate the retained ethanol and the resulting 19 is quite suitable for the next reaction. Hygroscopic powder ; 0.95 g ; 93 % yield ; no distinct melting point ; Rf(A):0.6 ; IR 1720 (NH_3^+ TFA^-)cm^{-1} ; ^{1}H-NMR (Me_2SO-d_6) δ 1.2 (t, 3H, CH_3-CH_2), 4.25 (q, 2H, CH_2-CH_3), 4.8 (m, 6H, $3CH_2$), 8.15 (s, 1H, CH), 8.3 (s, 1H, CH), 8.4 (s, 1H, CH), 9 (m, 3H, NH_3^+ TFA^-). MS - FAB 467 (80, M^++1).

Ethyl 2-[2'-[[2"-(formamidomethyl)thiazole]-4"carboxamidomethyl]thiazole-4'-carboxamidomethyl]thiazole-4-carboxylate (20). The formamido derivative 20 is prepared according to the procedure adopted for compound 8. Extreme care should be observed during the washing procedure due to the extreme solubility of 20 in the aqueous media. The crude residue was purified by flash chromatography (acetone : $CHCl_3$ (7 : 3)). 54 % yield, Rf(A):0.64 ; IR 1720 (COOEt), 1670 (CHO), 1660 (CONH) cm^{-1}, ^{1}H-NMR ($CDCl_3$) 1.35 (t, 3H, CH_3-CH_2), 4.35 (q, 2H, CH_2-CH_3), 4.8 (m, 6H, $3CH_2$), 7.5 (m, 1H, NH),8.0 (s, 1H, CH) ; 8.05 (s, 1H, CH), 8.1 (s, 1H, CH), 8.3 (s, 1H, CHO), 8.4 (m, 2H, 2NH) ; MS-FAB 495 (15, M^++1). Anal. Calcd for $C_{18}H_{18}O_5N_6S_3$: C, 4 3.72 ; H, 3.64 ; N,17.00. Found : C, 43.57 ; H, 3.63 ; N, 16.81.

2-[2'-[[2"-(Formamidomethyl)thiazole]-4"carboxamidomethyl]thiazole-4'-carboxamidomethyl]thiazole--4-carboxylic acid (21). The crude ethyl ester 20 was totally converted to the corresponding acid within 30 h, according to the method of preparation of 17. 69 % yield ; Rf(A):0 ; IR 1780 (COOH), 1680 (CHO), 1660 (CONH) cm^{-1} ; ^{1}H-NMR ($CDCl_3$) δ 4.8 (m, 6H, $3CH_2$), 7.5 (m, 1H NH), 8.0, 8.05, 8.10 (3s, 3H, 3CH), 8.3 (s, 1H, CHO), 8.4 (m, 2H, 2NH) ; MS-FAB 467 (45, M^++1). Anal. Calcd. for $C_{16}H_{14}O_5N_6S_3$: C, 41.20 ; H, 3.00 N, 18.03 ; Found : C, 41.16 ; H, 2.87 ; N, 17.91.

[2-[2'-[[2"-(Formamidomethyl)thiazole]-4"carboxamidomethyl]thiazole-4'-carboxamidomethyl]thiazole-4 carboxamido]propionamidine hydrobromide (3). The amidine 3 was obtained by initial in situ preparation of the corresponding succinimidyl ester and then condensation with the amino derivative 11d.

The procedures referred respectively to the preparation of structures 10 and 1. The final product is recrystallized from absolute ethanol. 15 mg ; 11 % yield, mp:188°C, Rf(A):0, Rf(H_2O/MeOH/HCOOH, 9/3/0.1, v:v):0.4 ; ^{1}H-NMR (400MHz) (D_2O) δ 3.5 (m, 2H, CH_2-C), 3.6 (m, 2H, $NHCH_2$), 4.9 (m, 6H, CH_2-NH), 8.09 (s, 1H, CH), 8.15 (s, 1H, CH), 8.155 (s, 1H, CH), 8.12 (s, 1H, CHO). FAB-MS 536 (23, M^{+2} - Br) Anal. Calcd for $C_{19}H_{22}N_9O_4S_3$ Br : C, 37.01 ; H, 3.57 ; N, 20.45 ; Found : C, 37.19 ; H, 3.60 ; N, 20.36.

REFERENCES

1- C. Zimmer, and U. Wahnert, Prog. Biophys. Mol. Biol., 1986, 47, 31.
2- F. Arcamone, F. Bizioli, G. Canevazzi, and A. Grein, German Pat. 1958, 1, 027,667.
3- S. Penco, S. Redaelli, and F. Arcamone, Gazz. Chim. Ital., 1967, 97, 1110.
4- B. Ward, R. Rehfuss, and J.C. Dabrowiak, J. Biomol. Struct. Dyn., 1987, 4, 685.
5- M.W. Van Dyke, and P.B. Dervan, Nucl. Acids Res., 1983, 11, 5555.
6- J.S. Taylor, P.G. Schultz, and P.B. Dervan, Tetrahedron, 1984, 40, 457.
7- D. Dasgupta, M. Rajagopalan, and V. Sasisekharan, Biochem. Biophys Res. Comm. 1986, 140, 626.
8- W.S. Wade, and P.B. Dervan, J. Am. Chem. Soc., 1987, 109, 1574.
9- D.H. Jones, and R.H. Wooldridge, J. Chem. Soc., 1968, 550.
10- J.W. Lown, K. Krowicki, U.G. Bhat, A. Skorobogaty, B. Ward, and J.C. Dabrowiak, Biochemistry, 1986, 25, 7408.
11- K. Kissinger, K. Krowicki, J.C. Dabrowiak, and J.W. Lown, Biochemistry, 1987, 26, 5590.
12- R.S. Youngquist, and P.B Dervan, Proc. Natl. Acad. Sci. USA, 1985, 82, 2565.
13- D. Dasgupta, P. Parrack, and V. Sasisekharan, Biochemistry, 1987, 26, 6381.
14- J.W. Lown, personal communication.
15- M.L. Kopka, C. Yoon, D. Goodsell, P. Pjura, and R.E. Dickerson, Proc. Natl. Acad. Sci. USA, 1985, 82, 1376.
16- G.R. Pettit, Y. Kamano, P. Brown, D. Gust, M. Inoue, and C.L. Herald, J. Am. Chem. Soc., 1982, 104, 905.
17- C.M. Ireland, and P.J. Sheuer, J. Am. Chem. Soc., 1980, 102, 5688.
18- C.M. Ireland, A.R. Durso, Jr. R.A. Newman, and M.P. Hacker, J. Org. Chem. 1982, 47, 1807.
19- J.E. Biskupiak, and C.M. Ireland, J. Org. Chem. 1983, 48, 2302.
20- Y. Hamamoto, M. Endo, M. Nakagawa, T. Nakanishi, and K. Mizukawa, J. Chem. Soc., Chem. Commun., 1983, 323.
21- J.M. Wasylyk, J.E. Biskupiak, C.E. Costello, and C.M. Ireland, J. Org. Chem., 1983, 48, 4445.
22- M. Bodanszky, J. Fried, J.T. Sheehan, N.J. Williams, J. Alicino, Cohen, A.I. B.T. Keller, and C.A. Birkhimer, J. Am. Chem. Soc., 1964, 86, 2478.
23- B. Anderson, D.C. Hodgkin, and M.A. Viswamitra, Nature (London), 1970, 225, 233.
24- J.M. Waisvicz, M.G. van der Hoeven, and B. te Nijenhuis, J. Am. Chem. Soc., 1957, 79, 4524.
25- R. Kazlauskas, R.O. Lidgard, R.J. Walls, and W. Vetter, Tetrahedron Lett., 1977, 3183.
26- C. Charles, J.C. Brackman, D. Daloze, B. Tursch, and R. Karlsson, Tetrahedron Lett., 1978, 1519.
27- The abbreviation gly(Thz) for 2-(1-aminomethyl)thiazole-4-carboxylic acid corresponds to the Pettit's proposal[16].
28- R. Houssin, M. Lohez, J.L. Bernier, and J.P. Hénichart, J. Org. Chem., 1985, 50, 2787.
29- J.L. Bernier, R. Houssin, and J.P. Hénichart, Tetrahedron, 1986, 42, 2695.
30- L. Grehn, and U. Ragnarsson, J. Org. Chem., 1981, 46, 3492.
31- F. Arcamone, V. Nicolella, S. Penco, and S. Redaelli, Gazz. Chim. Ital., 1969, 99, 632.
32- J.W. Lown, and K. Krowicki, J. Org. Chem., 1985, 50, 3774.
33- G. Hilgetag, H. Paul, J. Gunther, and M. Witt, Chem. Ber., 1964, 97, 704.
34- R.C. Kelly, I. Gebhard, and N. Wicnienski, J. Org. Chem., 1986, 51, 4590.
35- W.C. Still, M. Kahn, and A. Mitra, J. Org. Chem.. 1978, 43, 2923.

b) Le modèle Thia-Net.

Cette synthèse est détaillée dans l'article n°1.

2°) Synthèse des modèles hybrides nétropsine-intercalant.

A) Les dérivés nétropsine-anilinoamino-9 acridine.

La stratégie a consisté à élaborer séparément l'intercalant et le motif poly(amino-4 méthyl-1 pyrrole-2 carboxylate) puis de les coupler lors de l'étape ultime. Le motif intercalant (glycyl-anilinoamino-9 acridine) a été réalisé selon un procédé mis au point au laboratoire (HENICHART et al., 1982b). Le motif de type nétropsine ou distamycine a été conçu selon une stratégie détaillée dans l'article n°2.

Dans cette série, le composé NETGA (ou II) a été pris comme référence pour les expérimentations physicochimiques et pharmacologiques. Pour cette raison, sa synthèse sera prise comme exemple. Celle-ci est présentée sur les planches suivantes ainsi que les spectres de RMN-^{1}H et les spectres de masse.

-L'acide N-méthyl pyrrole-2 carboxylique est estérifié par l'iodure de méthyle dans un milieu acétone/carbonate de sodium. Une estérification par HCl sec /méthanol est impossible car dans ces conditions le pyrrole est complètement dégradé.

La nitration du N-méthyl pyrrole-2 carboxylate de méthyle s'effectue en milieu acide nitrique 65 %/anhydride acétique et conduit aux deux isomères nitro-4 et nitro-5 ainsi qu'au dérivé dinitro-4,5 (3-4 %). Après une séparation chromatographique de ces produits, chacun des deux isomères est caractérisé en RMN-^{1}H :

. nitro-4 méthyl-1 pyrrole-2 carboxylate de méthyle : les protons du pyrrole apparaissent sous forme de doublet (J = 4.5 Hz). La faible constante de couplage traduit le couplage β-α' des deux protons. Ces deux protons subissent de la même façon l'influence du groupement NO_2.

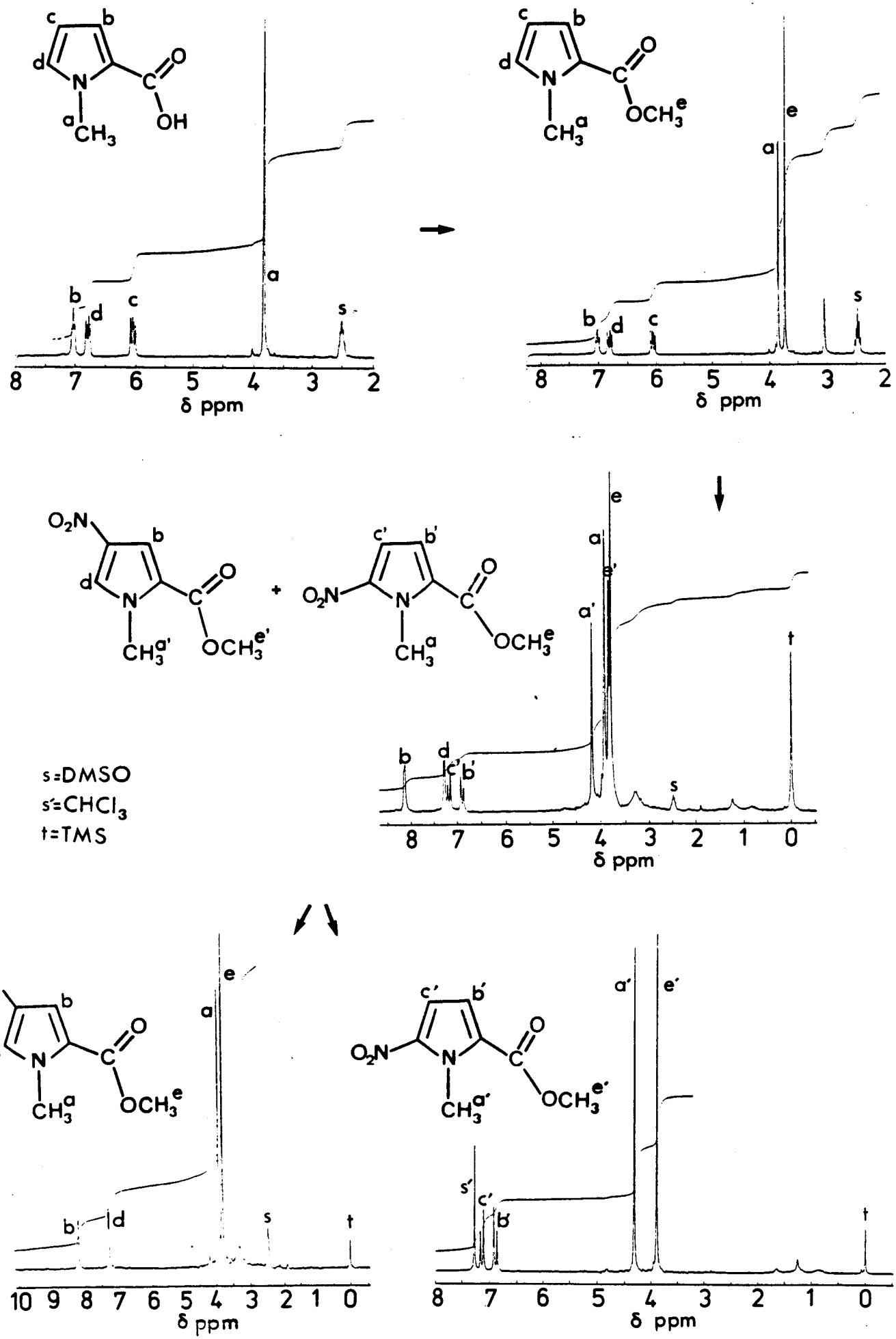

Synthèse de NETGA : spectres de RMN-^{1}H (80 MHz)

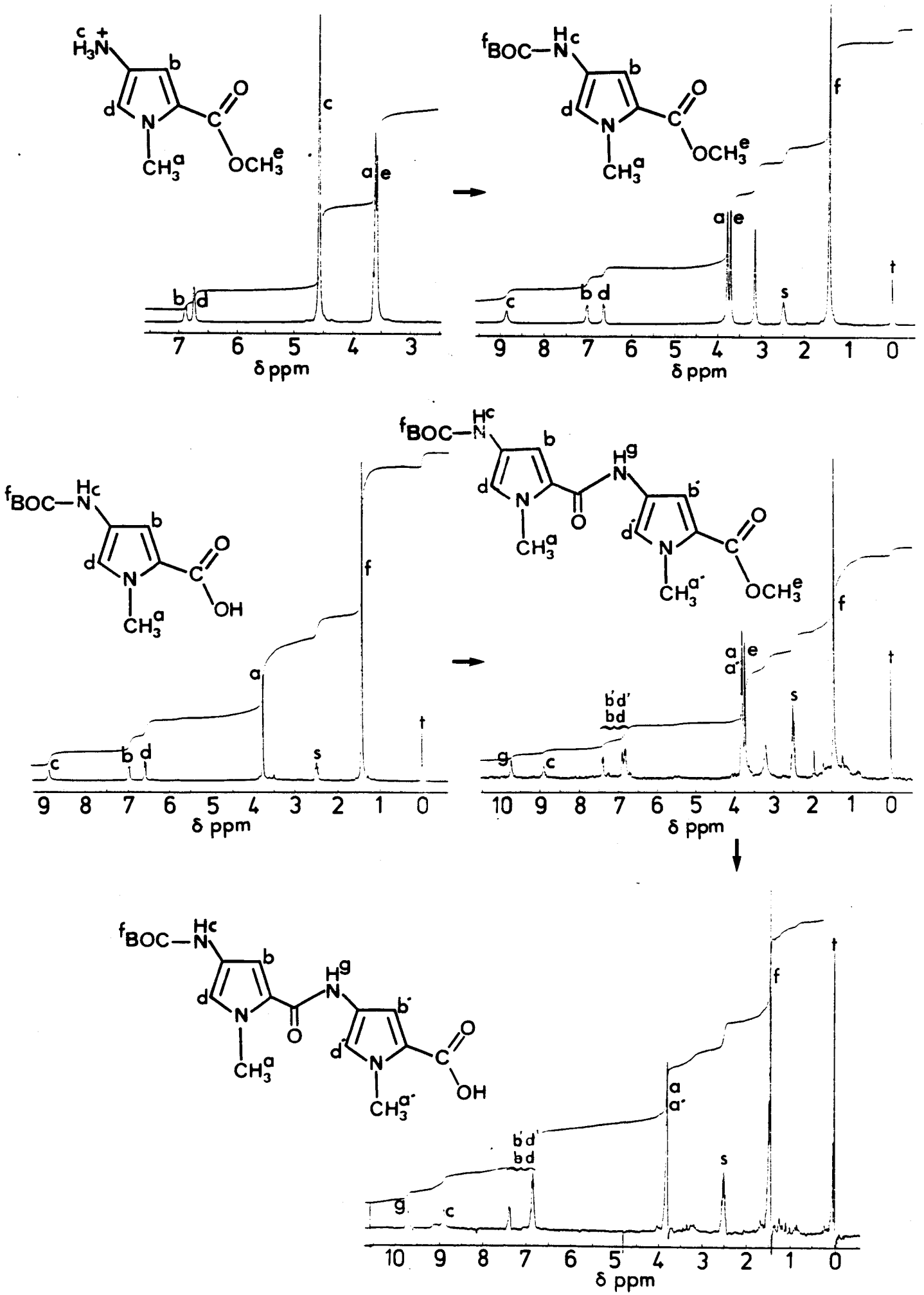

Synthèse de NETGA : spectres de RMN-^{1}H (80 MHz)

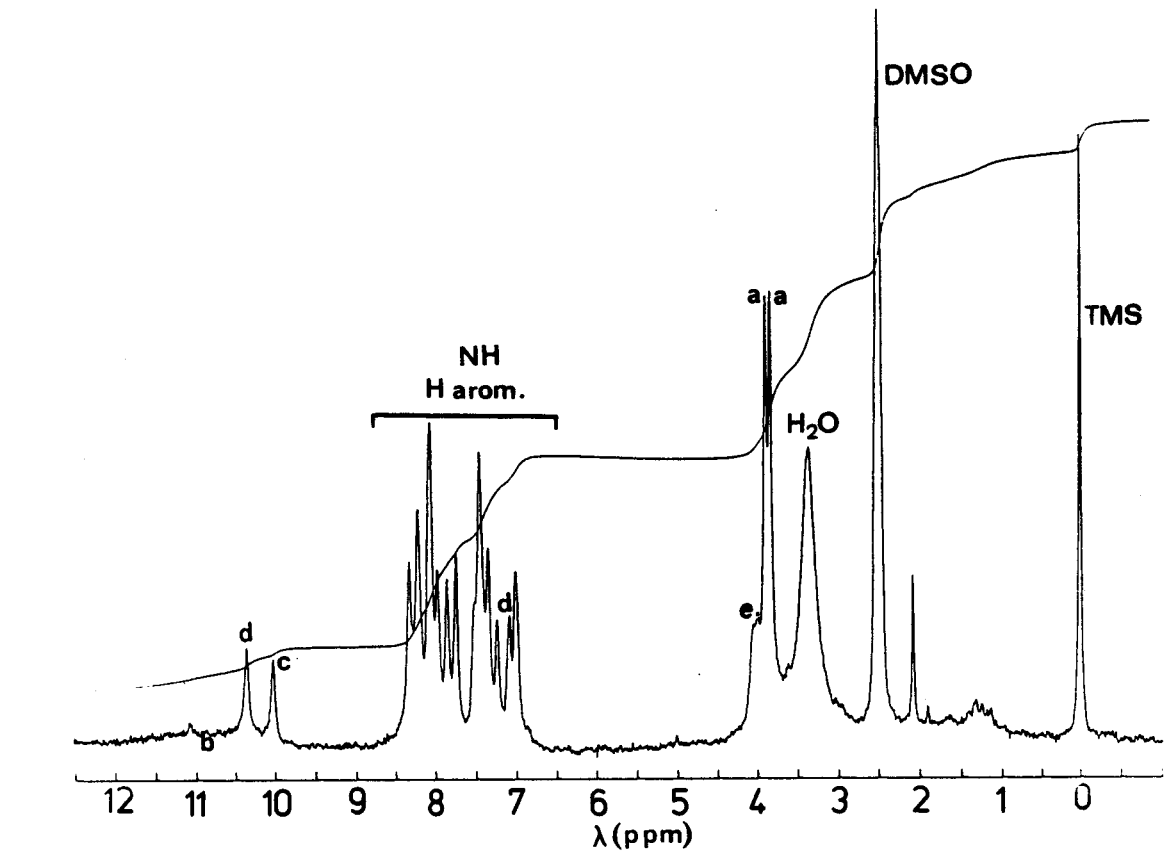

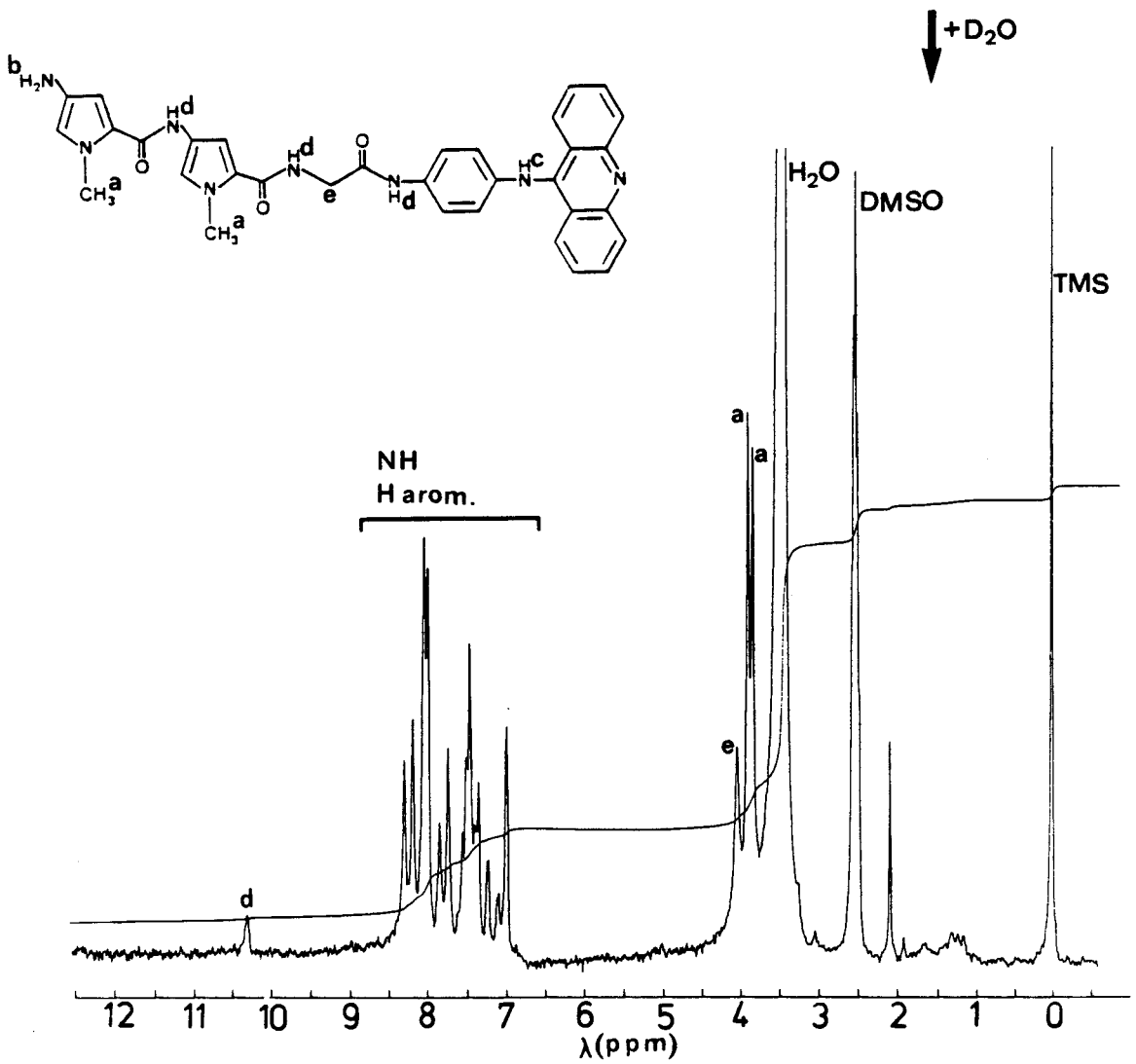

Synthèse de NETGA : spectres de RMN-^{1}H (80 MHz)

. nitro-5 méthyl-1 pyrrole-2 carboxylate de méthyle : la constante de couplage des protons du pyrrole est plus grande (J= 4.7 Hz) du fait du couplage β-β'. Le proton en β' subit directement l'influence du NO_2 voisin et apparaît donc plus déblindé que le proton en β.

-L'isomère nitro-4 est ensuite réduit (H_2, Ni Raney, 50°C, 50 kg, 12 h). Le passage du NO_2 (attracteur d'électrons) au NH_2 (donneur d'électrons) se traduit pour les protons du pyrrole par un glissement vers les hauts champs mais sans modification de l'ordre de résonance de ces protons.

-Après N-protection par un groupement t-butyloxycarbonyle (BOC) (groupement tertiobutyle à 1,45 ppm) puis saponification (disparition du pic ester), l'acide (tertiobutyloxycarbonylamino)-4 méthyl-1 pyrrole-2 carboxylique est couplé avec l'amino-4 méthyl-1 pyrrole-2 carboxylate de méthyle en présence de DCC/HOBt. En RMN-^{1}H, la liaison peptidique créée se traduit par la présence d'un pic NH à 9.7 ppm.

-La saponification du dimère (disparition du pic ester) puis le couplage de l'acide avec le (glycylamino-4 phényl)-1 amino-9 acridine conduit au composé final N-protégé (BOC-NETGA).

-Dans une dernière étape NETGA est purifié après élimination en milieu acide du groupement protecteur. Le spectre de RMN-^{1}H de ce produit se décompose de la façon suivante :

1- deux pics N-méthyle à 3.8 et 3.9 ppm.

2- un doublet à 4.0 ppm (J= 7.7 Hz) correspondant au CH_2 glycyle. Ce doublet devient singulet après addition de D_2O.

3- un massif de 6.8 à 8.5 ppm comprenant 18 protons dont 16 CH et 12 NH.

4- deux pics NH à 10.0 et 10.4 ppm correspondant respectivement à un NH mobile (rapide échange avec l'eau lourde) et à un NH peptidique

5- un massif très étalé (10-11 ppm), peu visible correspondant au NH_3^+ terminal (échange total avec l'eau lourde).

Remarque : les valeurs des glissements chimiques indiquées ici sont parfois légèrement différentes de celles répertoriées dans l'article n°2 (pour un même solvant : le DMSO). La présence d'eau résiduelle dans des proportions variables selon les essais est certainement à l'origine de ces variations.

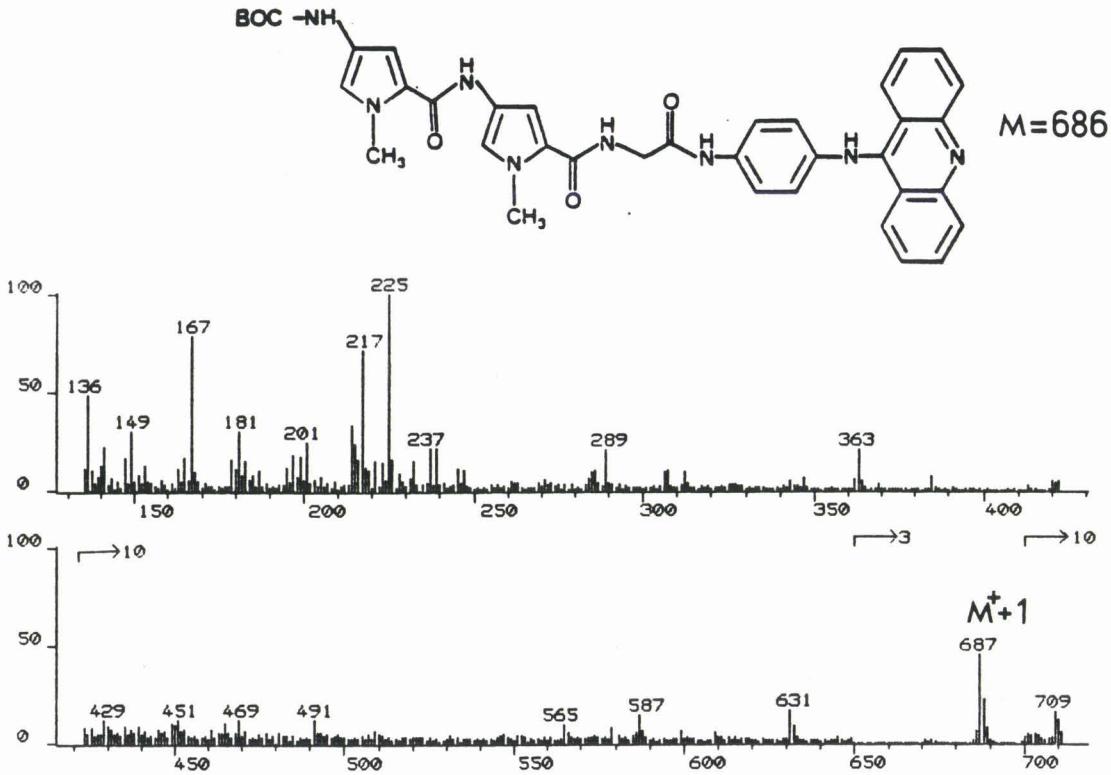

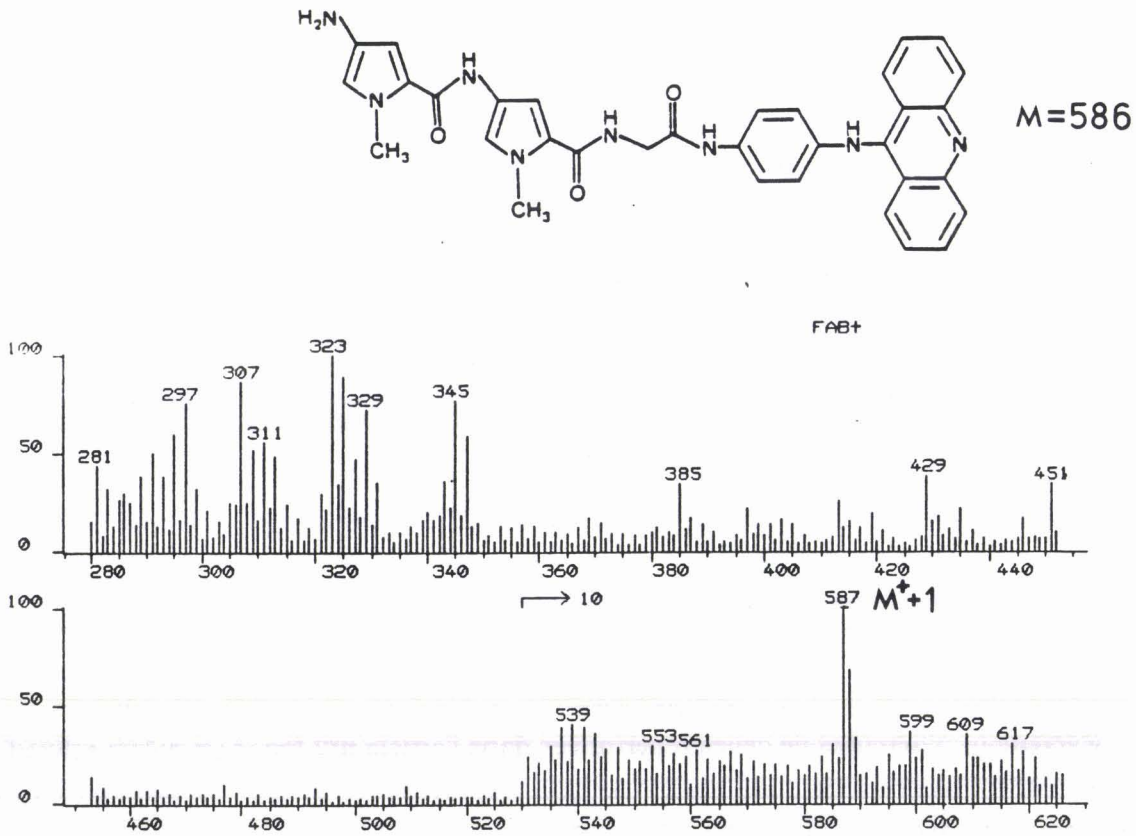

Synthèse de NETGA : spectres de masse FAB (matrice = thioglycérol ; solvant = DMSO)

Les spectres de masse du produit final protégé (M = 687) ou non (M = 587) sont témoins de l'identité de ces produits.

En ce qui concerne les autres composés du type nétropsine(ou distamycine)-acridine, la stratégie chimique adoptée est identique : synthèse de la fraction poly(N-méthylpyrrole carboxamide) avant couplage final avec l'acridine.

Néanmoins pour le composé IV (distamycine-acridine), une approche légèrement différente a dû être adoptée en raison de la fragilité du groupement formyle N-terminal en milieu alcalin (déformylation au cours des saponifications de l'ester méthylique). Le passage par un ester benzylique (hydrogéno-labile) a été réalisé. Les spectres de RMN ^{13}C des esters benzyliques du mono- et bispyrrole sont présentés ainsi que ceux des deux isomères de position du dérivé nitropyrrole.

a) spectre RMN ^{13}C des nitro-4 et nitro-5 pyrroles

Les carbones $C_1(N\text{-}CH_3)$, $C_6(CO)$ et $C_7(OCH_3)$ ont des glissements identiques pour les deux isomères, respectivement 35, 160 et 52 ppm. Les carbones C_2 (porteur de la fonction ester) et C_3 (en a du C_2) subissent faiblement l'influence du groupement nitro en position 4 ou 5. Dans les deux cas l'ordre des glissements est identique : C_2 vers 125-130 ppm et C_3 vers 110-115 ppm.

Par contre les modifications concernent logiquement les C_4 et C_5. Le carbone porteur du groupement nitro (le C_4 pour l'isomère nitro-4 et le C_5 pour l'isomère nitro-5) subit l'effet attracteur du NO_2 (déblindage) et résonne donc à bas champ (135-140 ppm). Le carbone a du groupement nitro sort à plus haut champ (110-115 ppm).

b) spectre RMN ^{13}C des esters benzyliques

1. "Monopyrrole" (t-butyloxycarbonylamino-4 méthyl-1 pyrrole)-2 carboxylate de benzyle. Le spectre présenté est un spectre non découplé (utilisé pour mesurer les constantes de couplage $^1J_{C\text{-}H}$). Le glissement chimique de chaque carbone est figuré sur le spectre.

2. "Bis-pyrrole" (((t-butyloxycarbonylamino-4 méthyl-1 pyrrolyl)-2 carboxamido)-4 méthyl-1 pyrrole)-2 carboxylate de benzyle. Le spectre présenté ne permet pas de différencier les carbones de chacun des deux hétérocycles pyrrole. Cependant les glissements chimiques des couples $C_2\text{-}C_2'$, $C_3\text{-}C_3'$, $C_4\text{-}C_4'$ et $C_5\text{-}C_5'$ ont été attribués sur le spectre.

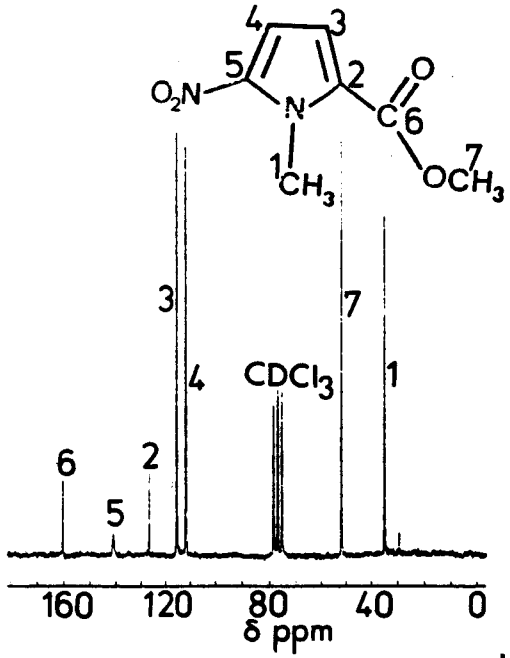
O2N
CH3
OCH3
CDCl3
160 120 80 40 0
δ ppm

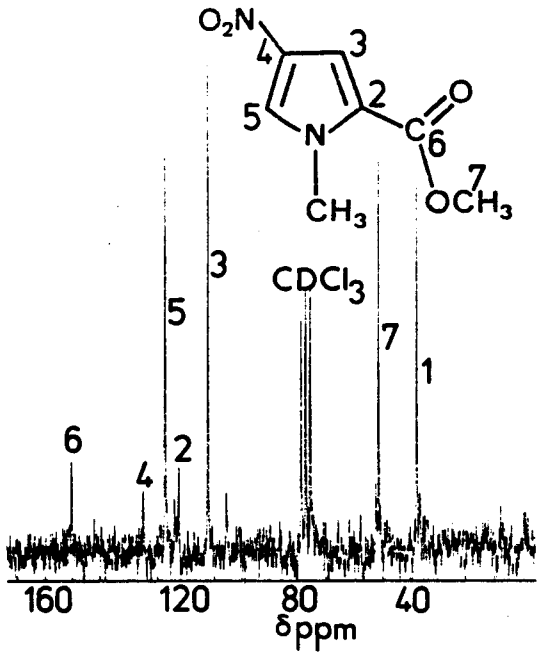
O2N
CH3
OCH3
CDCl3
160 120 80 40
δ ppm

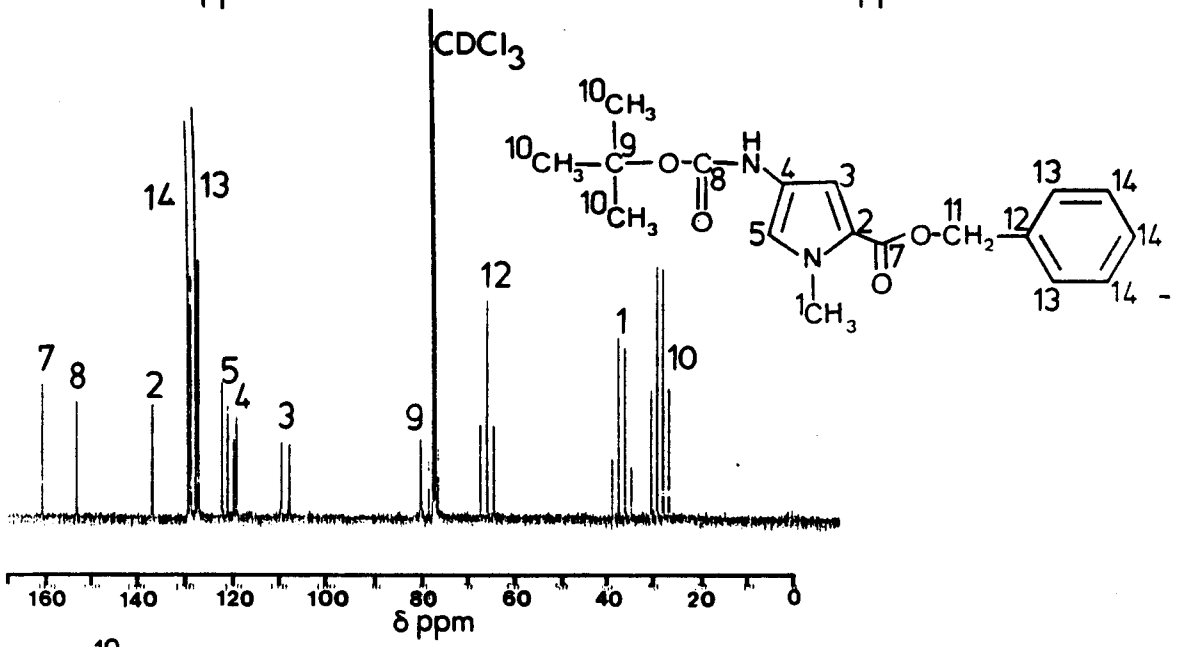
CDCl3
160 140 120 100 80 60 40 20 0
δ ppm

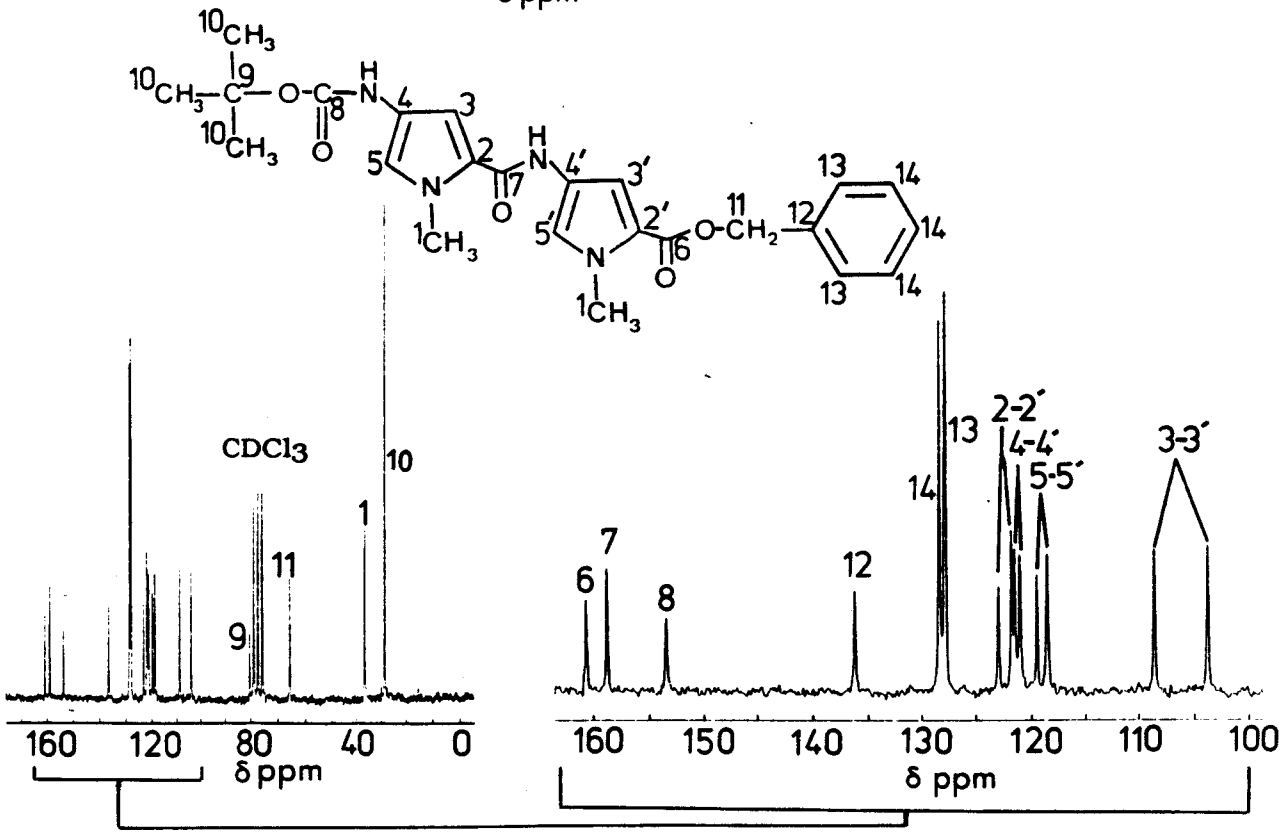
CDCl3
160 120 80 40 0
δ ppm
2-2'
4-4'
5-5'
3-3'
160 150 140 130 120 110 100
δ ppm

B) Le dérivé nétropsine-bithiazole (NETBI)

Chacune des composantes de ce modèle a déjà été répertoriée : fraction nétropsine (voir précédemment), fraction bithiazolique (HOUSSIN et al., 1984b).

Le couplage de ces deux unités amène aux composés N-protégé (BOC-NETBI), puis, final dont les spectres de masse et de RMN-^{1}H sont présentés à la page suivante. Le spectre 2D des protons pyrroliques de NETBI permet de différencier chacun d'entre eux :

- les protons se répartissent en 2 couples de singulets (6.5-6.9 et 6.7-7.0 ppm) correspondant à chacun des 2 hétérocycles.
- le couple 6.7-7.0 correspond aux protons de l'hétérocycle terminal (A) porteur du NH_2 libre.
- le couple 6.5-6.9 correspond aux protons de l'hétérocycle B disubstitué en 2 et 4 par des liaisons peptidiques.

3°) Synthèse des analogues de la Blm.

a) Modèle AMBIGLU

Schématiquement, trois fractions sont regroupées dans ce modèle.

. la fraction complexante (AMPHIS) dont la synthèse a été mise au point précédemment (HENICHART et al., 1982a)

. la fraction intercalante bithiazolique (HOUSSIN et al., 1984b)

. la fraction glucosaminylglutaminyle dont la synthèse est complètement décrite dans l'article n°6.

b) Modèle hybrides complexant-acridine : AGGA, AGAMGA et AGAGLU

La synthèse de ces modèles fait appel uniquement à des synthèses déjà décrites comme celles de :

. la fraction intercalante glycylanilinoamino-9 acridine (HENICHART et al., 1982b).

. la fraction glucosaminylglutaminyle (cf article n° 6).

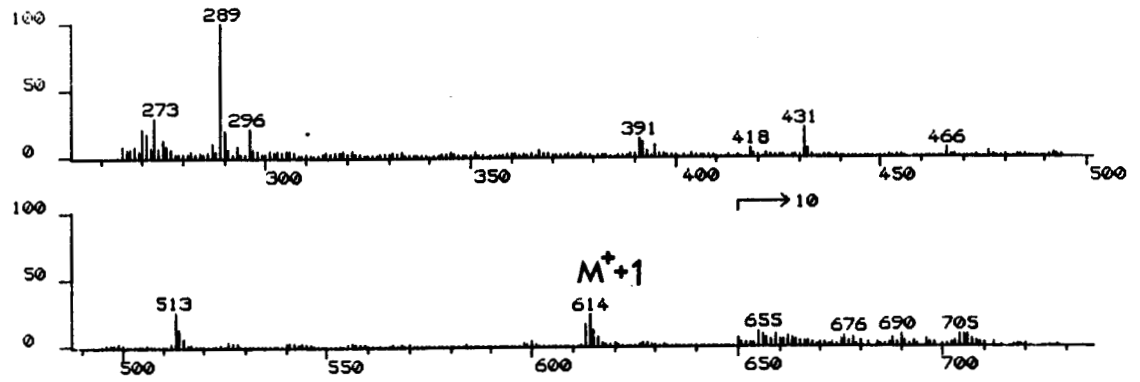

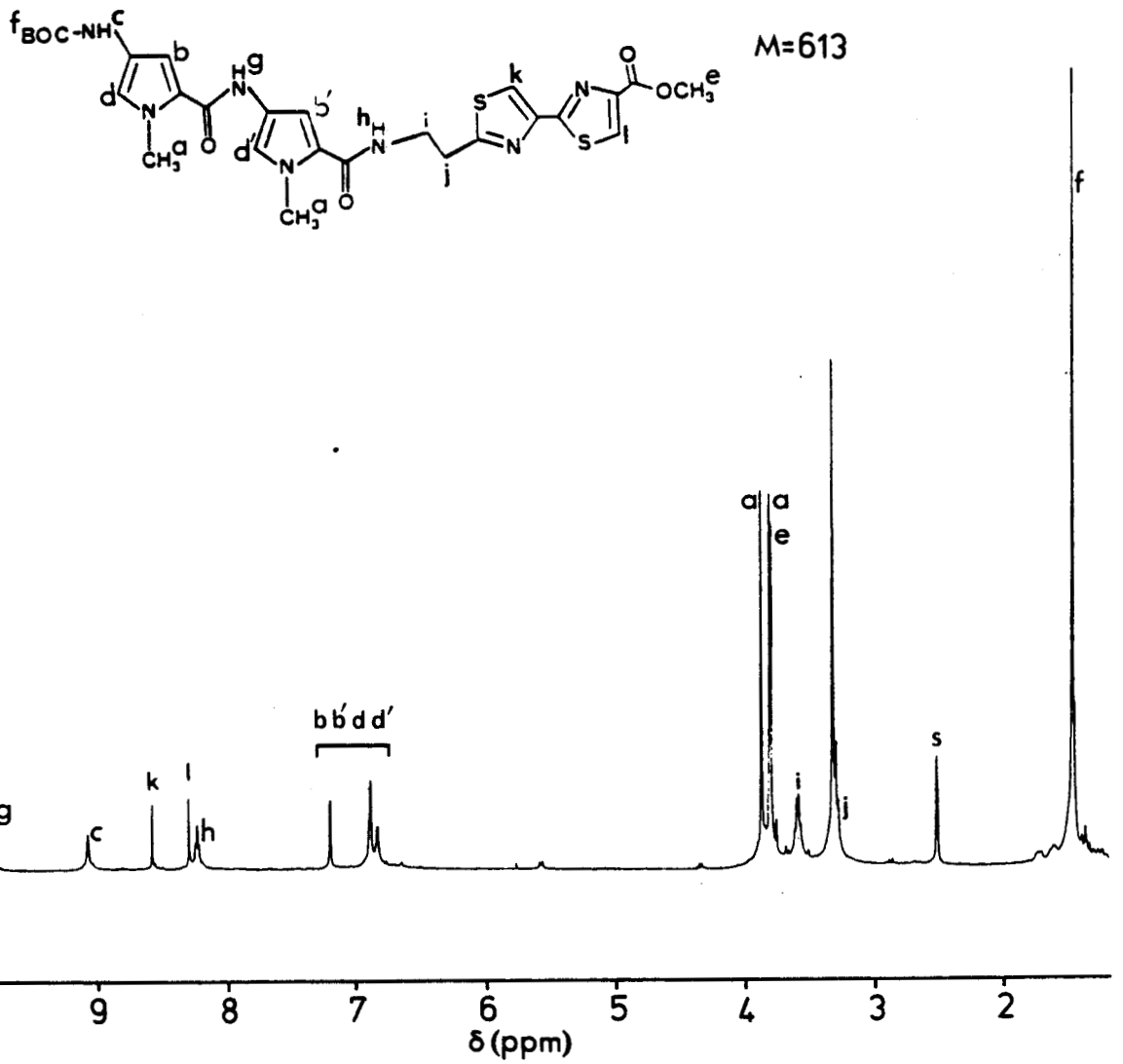

Synthèse de NETBI : spectres de masse FAB (matrice = thioglycérol ; solvant = DMSO)
spectre de RMN-^{1}H (400 MHz)

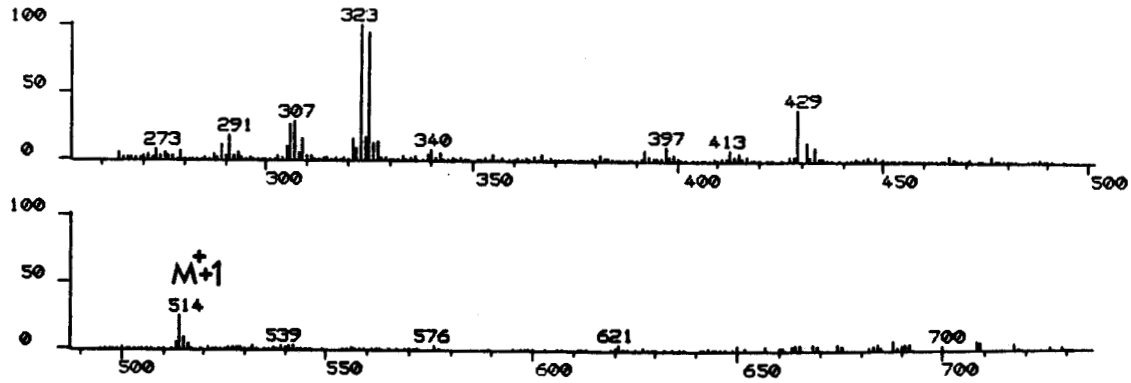

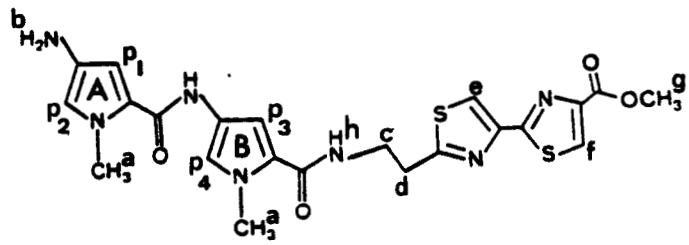

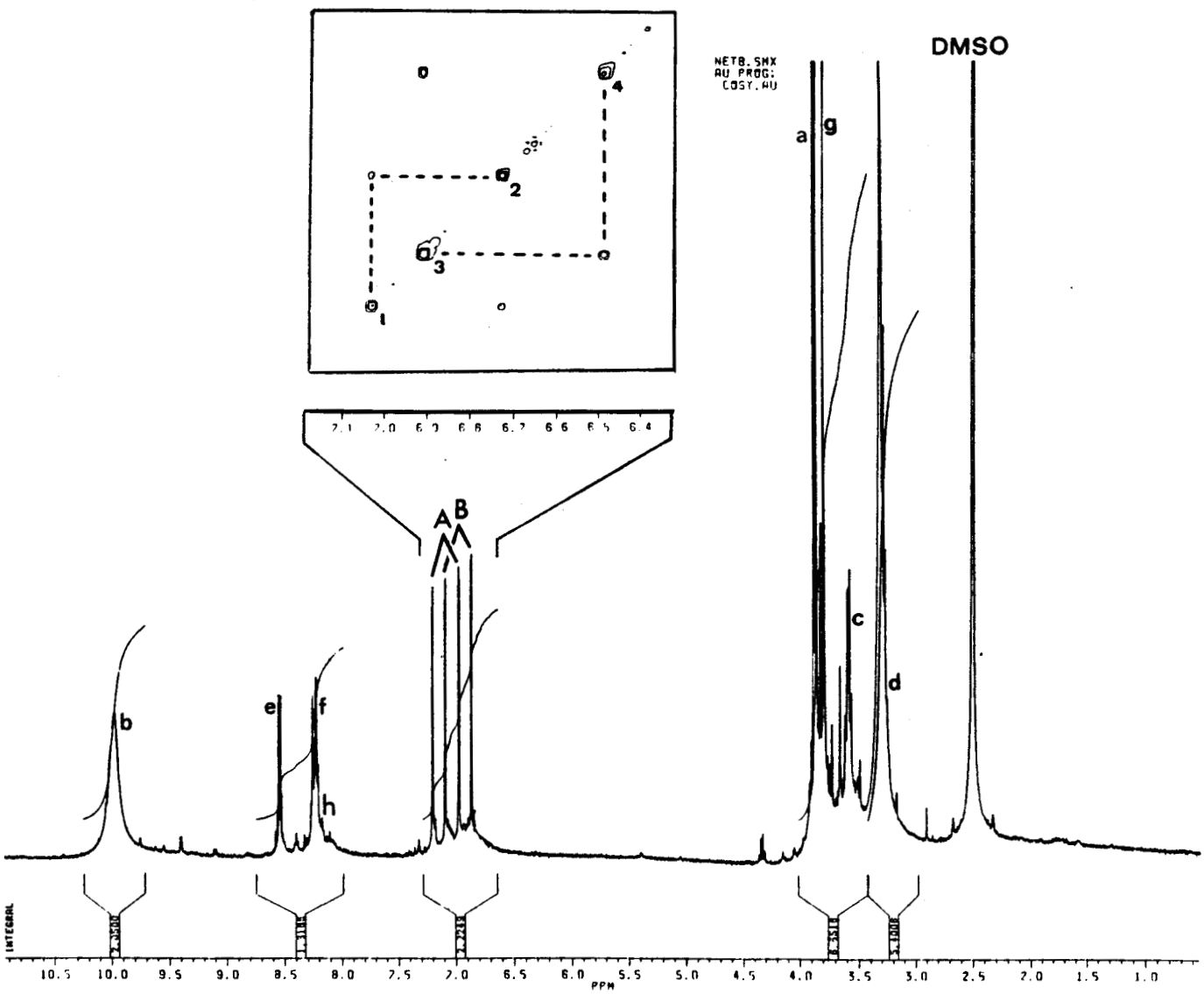

Synthèse de NETBI : spectres de masse FAB (matrice = thioglycérol ; solvant = DMSO) spectre de RMN-^{1}H (400 MHz) et spectre de RMN-1H 2D (Cosy, protons pyrroliques).

. la fraction complexante :

- de type BLM (AMPHIS) (HENICHART et al., 1982a).
- de type Gly-His-Lys : la synthèse de ce tripeptide est décrite dans l'article n°11 et correspond à une synthèse peptidique classique sans difficultés majeures.

4°) Synthèse du modèle Gly-His-Lys-NETGA

La stratégie adoptée pour cette synthèse a consisté à élaborer séparément le tripeptide Gly-His-Lys (article n°11), la portion bis-pyrrolique de type nétropsine (article n°2) et la fraction glycylanilino amino-9 acridine (HENICHART et al., 1982b). Le couplage de ces différentes unités est suivi par les spectres de masse des différents composés intermédiaires de synthèse de ce composé Gly-His-Lys-NETGA (pages suivantes).

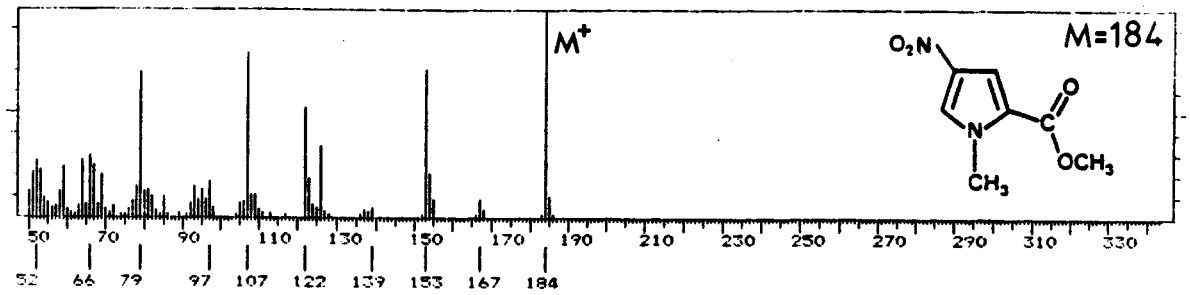

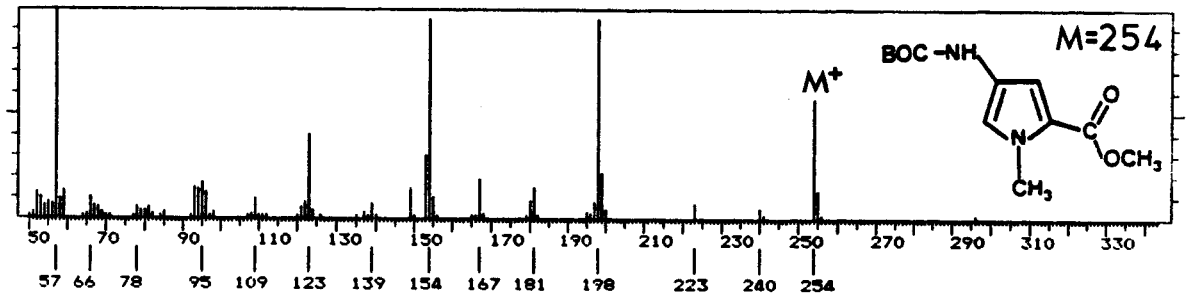

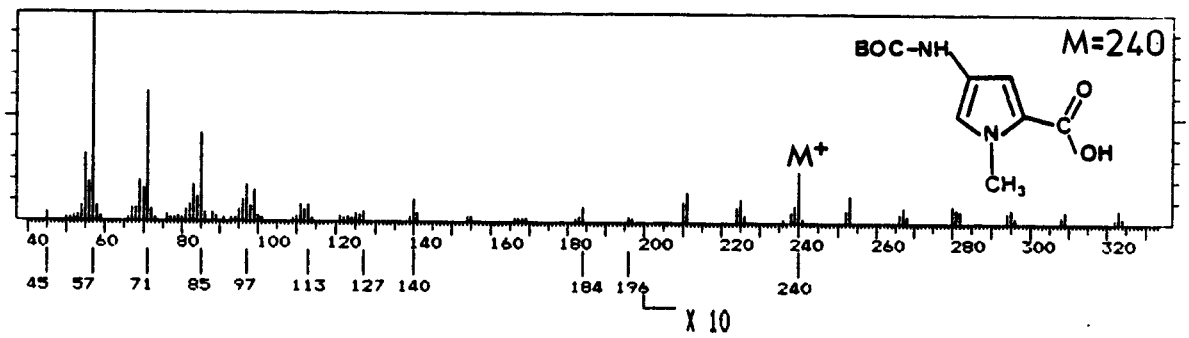

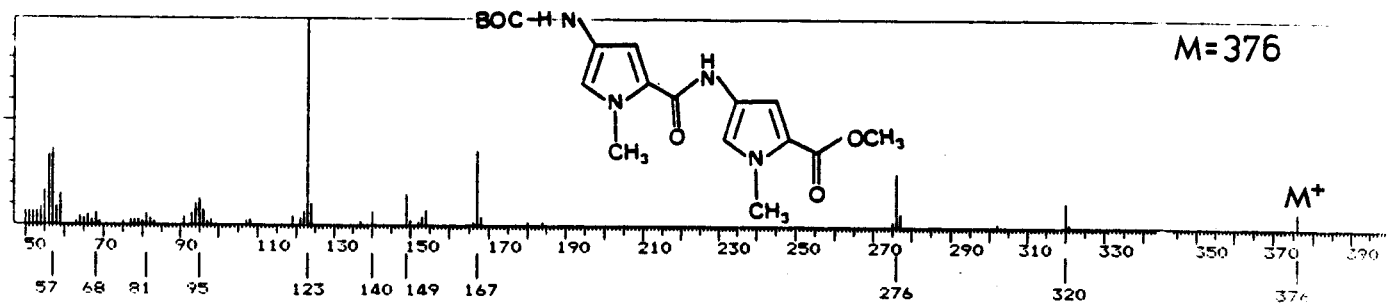

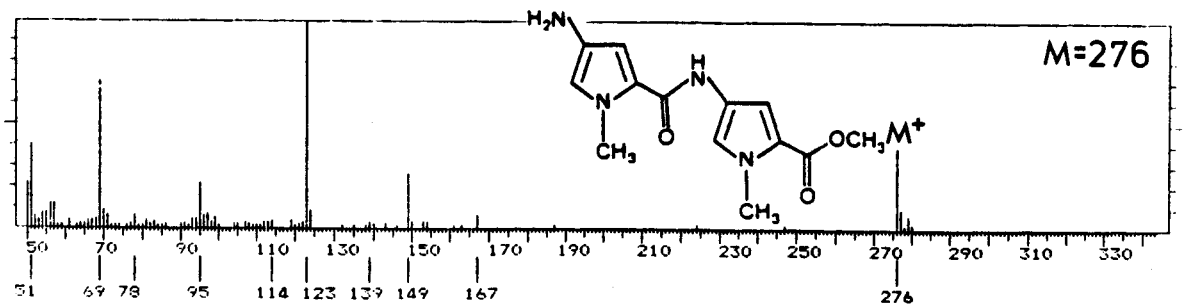

Synthèse de Gly-His-Lys-NETGA : spectres de masse (IE)

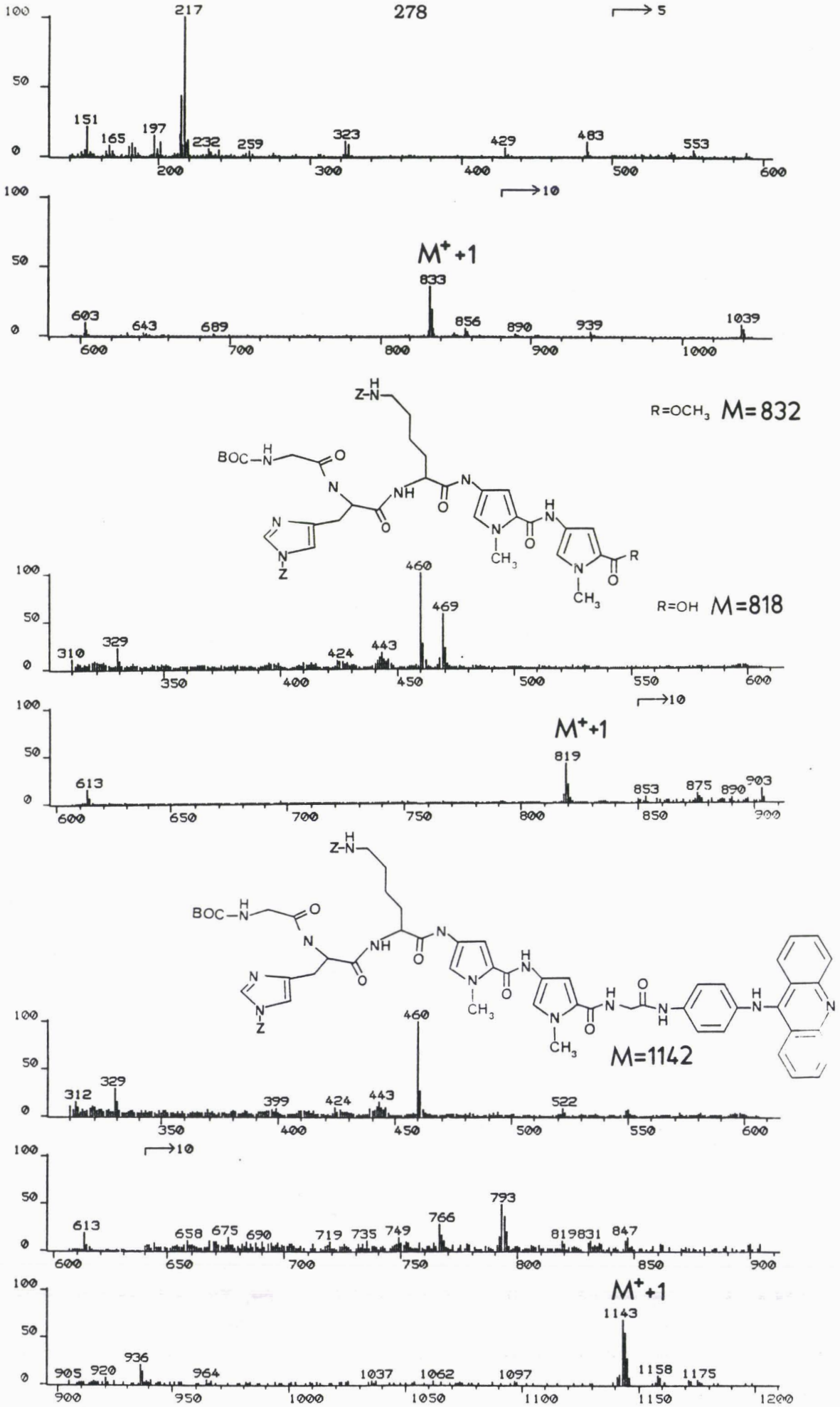

Synthèse de Gly-His-Lys-NETGA : spectres de masse (FAB)

(matrice = thioglycérol ; solvant = DMSO)

METHODES ANALYTIQUES

Au cours de ce travail, les techniques mises en oeuvre ont été les suivantes :

- spectroscopie U.V.
  - . analyse de type "Scatchard"
  - . dénaturation thermique
- fluorescence
- polarisation de fluorescence
- résonance paramagnétique électronique (RPE)
  - . complexation du cuivre
  - . production de radicaux libres
- dichroïsme circulaire
- dichroïsme linéaire électrique
- viscosimétrie
  - . élongation de l'ADN
  - . détorsion de l'ADN
- coupure d'ADN (mono-brin et double-brin)
- résonance magnétique nucléaire (RMN)
- spectrométrie de masse
  - . impact électronique
  - . FAB
- foot-printing

Les appareils ainsi que les protocoles expérimentaux utilisés pour la mise en oeuvre de ces techniques sont bien détaillés dans les diverses publications présentées.

METHODES BIOLOGIQUES

1°) Mesure de la synthèse endocellulaire d'ADN

Les cellules en culture sont exposées à la thymidine tritiée (43 Ci/mM, CEA) pendant la durée d'un cycle cellulaire au minimum, en présence ou non du produit à tester. Après la période de marquage, l'incorporation du précurseur dans l'ADN est mesurée par comptage radioactif.

Compte tenu de sa spécificité pour l'ADN, la thymidine constitue un précurseur idéal. La thymidine exogène doit être phosphorylée en thymidine triphosphate (TTP) et entrer dans le pool de TTP qui est essentiellement dérivé de la synthèse de novo. La concentration en thymidine dans le milieu est fixée à 3 µM de façon à constituer un pool endogène de TTP suffisant et permettre une mesure satisfaisante de la synthèse d'ADN.

La concentration endogène en thymidine ne doit pas excéder 10 mM car des concentrations supérieures inhibent toute synthèse d'ADN par rétroinhibition de la ribonucléotide réductase (CLEAVER, 1967).

Le protocole expérimental utilisé est détaillé dans les articles n°s 2 et 8.

2°) Mesure de l'activité antitumorale

a) Sur cellules L 1210

Les cellules leucémiques L 1210 sont maintenues en phase exponentielle de croissance dans un milieu RPMI-1640 (GIBCO) additionné de 10 % de sérum de veau foetal. Les cellules sont incubées par fraction de 10 ml à 37°C en présence de concentration variable de produit à tester.

Après une période d'incubation de 24 h (la durée d'au moins un cycle cellulaire), les cellules sont colorées au bleu trypan pour différencier les cellules vivantes (perméables au colorant) des cellules mortes (imperméables au colorant), puis numérées. Deux paramètres sont mesurés:

- le taux de croissance par rapport au témoin
- le taux de viabilité cellulaire

b) Sur cellules MCF7

1- Courbe de croissance

2 ml de suspension cellulaire (5 10^4 cellules / ml) dans un milieu DULBECCO (MEM) additionné de 10 % de sérum de veau foetal, sont incubés en présence de concentrations variables du produit à tester. Tous les jours, pendant 8 jours, les cellules sont décollées à la trypsine, puis numérées à l'aide d'un compteur électronique. Avant la numération cellulaire, le milieu de culture est enlevé et le tapis cellulaire lavé de façon à éliminer les cellules mortes non adhérentes au support. Seules les cellules vivantes sont donc numérées.

2- Courbe de survie

Les cellules sont ensemencées dans un milieu DULBECCO (plus 10 % de sérum de veau foetal) pendant 48 h à 37°C. Les cellules, en phase exponentielle de croissance, sont décollées du support par la trypsine (SEROMED, 1 g/l), numérées (au moyen d'une nageotte) puis ensemencées dans des boîtes FALCON de 25 cm^2 à diverses concentrations en cellules (de 2000 à 100 000 cellules/boîte) et en produit à tester (de 0.5 à 20 µM). Ces cellules sont maintenues à 37°C (+ 10 % CO_2) pendant au minimum 15 jours sans les déplacer. Le temps d'incubation est variable (15-20 jours) et correspond au temps nécessaire pour qu'une cellule donne naissance à au moins 50 cellules filles soit un clone. Les clones sont colorés au violet cristal (2 g dans 100 ml de formol à 30 % et 900 ml de méthanol à 80 %) et numérés.

Les résultats sont exprimés en terme d'efficacité de clonage (%) par rapport au témoin. L'indice de clonage du témoin (platting efficiency) est d'environ 3-4 % pour les cellules MCF7. Les résultats sont pondérés par rapport à cet indice témoin et reportés sur un graphique en coordonnées semi logarithmiques de manière à obtenir la courbe de survie. La dose létale à 50 % (LD_{50}), déterminée sur la courbe de survie, correspond à la concentration en produit testé nécessaire pour tuer 50 % de la population cellulaire.

Ce critère permet de comparer l'efficacité des différents produits testés les uns par rapport aux autres.

REFERENCES BIBLIOGRAPHIQUES.

AGOSTINO M.J., BERNACKI R.J., BEERMAN T.A. (1984). Synergistic interactions of ethidium bromide and bleomycin on cellular DNA and growth inhibition. Biochem. Biophys. Res. Commun. **120**,156-163.

AJMERA S., WU J.C., WORTH L. Jr, RABOW L.E., STUBBE J., KOZARICH J.W. (1986). DNA degradation by bleomycin : evidence for 2'R-proton abstraction and for C-O bond cleavage accompanying base propenal formation. Biochemistry **25**,6586-6592.

AKKERMAN M.A.J., HAASNOOT C.A.G., HILBERS C.W. (1988). Studies of the solution structure of the bleomycin A_2-Zinc complex by means of two-dimensional NMR spectroscopy and distance geometry calculations. Eur. J. Biochem. **173**,211-225.

ALBERTINI J.P. (1984). Rôle des ions de métaux de transition dans l'activité antitumorale de la bléomycine : étude spectroscopique. Thèse de doctorat ès-Sciences (Paris).

ALBERTINI J.P., GARNIER-SUILLEROT A. (1984). Iron-bleomycin-deoxyribonucleic acid system. Evidence of deoxyribonucleic acid interaction with the α-amino group of the β-aminoalanine moiety. Biochemistry **23**,47-53.

ANDERSON J.E., PTASHNE M., HARRISON S.C. (1985). A phage repressor-operator complex at 7 Å resolution. Nature **316**,596-601.

ARCAMONE F., PENCO S., OREZZI P., NICOLELLA V., PIRELLI A. (1964). Structure and synthesis of distamycin A. Nature **203**, 1064-1065.

ARCAMONE F. & PENCO S. (1986). Chemical derivatives of anticancer antibiotics with different DNA binding properties. In " Molecular mechanism of carcinogenic and antitumor activity " , CHAGAS C., PULLMAN B., eds, Adenine Press, pp. 226.

BAGULEY B.C. (1982). Non intercalative DNA-binding antitumour compounds. Mol. Cell. Biochem. **43**, 167-181.

BARRANCO S.C., BOLTON W.E., NOVAK J.K. (1980). Time-dependent changes in drug sensitivity expressed by mammalian cells after exposure to trypsin. J. Natl. Cancer Inst. **64**,913-916.

BEARDEN Jr J. & HAIDLE C.W. (1975). Stimulation of bleomycin-induced fragmentation of DNA by intercalating agents. Biochem. Biophys. Res. Commun. **65**,371-377.

BECKER Y.,ASCHER Y., ZAKAY-RONES Z. (1972).In "Antimicrobial agents and chemotherapy " (F.L. HORBY, ed) 1,p.483.

BEREMAN R.D. & WINKLER M.E. (1980). A spectral investigation of the copper(II) complex of the antitumor compound bleomycin. J. Inorg. Biochem. **13**,95-104.

BERND A., ALTMETER P., SCHAFER G., MARSCH W.C., HOLZMANN H. (1986). Bleomycin enhances the tyrosinase activity of human malignant melanoma cells in culture. Pharmacol. Res. Commun. **18**,1075-1091.

BERNIER J-L., HENICHART J-P., CATTEAU J-P. (1981). Design, synthesis and DNA-binding capacity of a new peptidic bifunctional intercalating agent. Biochem. J. **199**, 479-484.

BERNIER J-L., HOUSSIN R., HENICHART J-P. (1986a). Analog of dolastatin 3. Synthesis, ^1H NMR studies and spatial conformation. Tetrahedron **42**,2695-2702.

BERNIER J-L., KENANI A., HOUSSIN R., LOHEZ M., HECQUET B., HENICHART J-P. (1986b). Molecular interaction between bleomycin and amsacrine in the presence of cupric ions. J. Inorg. Biochem. **27**,271-285.

BERRY D.E., KILKUSKIE R.E., HECHT S.M. (1985). DNA damage induced by bleomycin in the presence of dubicaine is not predictive of cell growth inhibition. Biochemistry **24**,3214-3219.

BIALER M., YAGEN B., MECHOULAM R. (1975). A total synthesis of distamycin A, an antiviral antibiotic. Tetrahedron **34**,2389-2391.

BIALER M., YAGEN B., MECHOULAM R., BECKER Y. (1980a). Structure-activity relationships of pyrrole amidine antiviral antibiotics III. Preparation of distamycin and congocidine derivatives based on 2,5-disubstituted pyrroles. J. Pharm. Sci. **69**,1334-1338.

BIALER M., YAGEN B., MECHOULAM R. (1980b). Structure-activity relationships of pyrrole amidine antiviral antibiotics II. Preparation of mono- and tripyrrole derivatives of congocidine. J. Med. Chem. **23**,1144-1148.

BLUM R.H., CARTER S.K., AGRE K.A. (1973). A clinical review of bleomycin: a new antineoplastic agent. Cancer **31**, 903-914.

BOBST A.M. (1979). Applications of spin labeling to nucleic acids. In " Spin labeling. Theory and applications " (BERLINER L.J., ed) Academic Press, p.313.

BONADONNA G. & SANTORO A. (1982). ABVD chemotherapy in the treatment of Hodgkin's disease. Cancer Treat. Rev. **9**,21-35.

BOOTH T.E., SAKAI T.T., GLICKSON J.D., (1983). Interaction of bleomycin A_2 with poly(deoxyadenylylthymidilic acid). A proton nuclear magnetic resonance study of the influence of temperature, pH and ionic strength. Biochemistry **22**,4211-4217.

BRAM S., FROUSSARD P., GUICHARD M., JASMIN C., AUGERY Y., SINOUSSI-BARRE F., WRAY W. (1980). Vitamin C preferential toxicity for malignant melanoma cells. Nature **284**,629-631.

BRUZIK J.P., AUBLE D.T., DE HASETH P.L. (1987). Specific activation of transcription initiation by the sequence-specific DNA-binding agents distamycin A and netropsin. Biochemistry **26**,950-956.

BURCKARDT G., VOTAVOVA H., SPONAR G., LUCK G., ZIMMER C. (1985). Two binding modes of netropsin are involved in the complex formation with poly(dA-dT) : poly(dA-dT) and other alternating DNA duplex polymers. J. Biomolec. Struct. and Dyn. **2**,721-736.

BURGER R.M., HORWITZ S.B., PEISACH J., WITTENBERG J.B. (1979). Oxygenated iron bleomycin. J. Biol. Chem. **254**,12299-12302.

BURGER R.M., BERKOWITZ A.R., PEISACH J., HORWITZ S.B., (1980). Origin of malondialdehyde from DNA degraded by Fe(II)-bleomycin. J. Biol. Chem. **255**,11832-11838.

BURGER R.M., PEISACH J., HORWITZ S.B., (1981). Activated bleomycin : a transient complex of drug, iron and oxygen that degrades DNA. J. Biol. Chem. **256**,11636-11644.

BURGER R.M., PEISACH J., HORWITZ S.B. (1982). Stoichiometry of DNA strand scission and aldehyde formation by bleomycin. J. Biol. Chem. **257**,8612-8614.

BURGER R.M., FREEDMAN J.H., HORWITZ S.B., PEISACH J. (1984). DNA degradation by manganese(II)-bleomycin plus peroxide. Biochemistry 24,81-92.

BURGER R.M., BLANCHARD J.S., HORWITZ S.B., PEISACH J. (1985). The redox state of activated bleomycin. J. Biol. Chem. **260**,15406-15409.

BURGER R.M., PROJAN S.J., HORWITZ S.B., PEISACH J. (1986). The DNA cleavage mechanism of iron-bleomycin: kinetic resolution of strand scission from base propenal release.J. Biol. Chem. **261**,15955-15959.

CALLADINE C.R. (1982). Mechanisms of sequence-dependent stacking of bases in B DNA. J. Mol. Biol. **161**,343-352.

CAMERMAN N., CAMERMAN A., SARKAR B. (1976). Molecular design to mimic the copper(II) transport site of human albumin. The crystal and molecular structure of copper(II)-glycyl-glycyl-L-histidine-N-methyl amide monoaquo complex. Can. J. Chem. **54**,1309-1316.

CHANDRA P., GOTZ A., WACKLER A., VERINI M.A., CASAZZA A.M., FIORETTI A., ARCAMONE F., GHIONE M. (1971). Some structural requirements for the antibiotic action of distamycins. FEBS Lett. **16**,249-252.

CHANDRA P., ZUNINO F., GOTZ A., WACKER A., GERICKE D., DIMARCO A., CASAZZA A.M., GIULIANI F. (1972). Template specific inhibition of DNA polymerase from DNA tumor viruses distamycin A and its structural analogs. FEBS Lett. **21**,154-158.

CHANG C.H., MEARES C.F. (1982). Light-induced nicking of deoxyribonucleic acid by cobalt(II)-bleomycin. Biochemistry **21**,6332-6334.

CHANG C.H., MEARES C.F. (1984). Cobalt-bleomycins and deoxyribonucleic acid: sequence-dependent interactions, action spectrum for nicking, and indifference to oxygen. Biochemistry **23**,2268-2274.

CHEN D.M., HAWKINS B.L., GLICKSON J.D. (1977). Proton nuclear magnetic resonance study of bleomycin in aqueous solution. Assignment of resonances. Biochemistry **16**,2731-2738.

CHEN D.M., SAKAI T.T., GLICKSON J.D., PATEL D.J. (1980). Bleomycin-A_2 complexes with poly(dA-dT) : a proton nuclear magnetic resonance study of the nonexchangeable hydrogens. Biochem. Biophys. Res. Commun. **92**,197-205.

CHEN C-H.B. & SIGMAN D.S. (1987). Chemical conversion of a DNA-binding protein into a site-specific nuclease. Science **237**,1197-1201.

CHIEN M., GROLLMAN A.P., HORWITZ S.B. (1977). Bleomycin-DNA interaction: fluorescence and proton magnetic resonance studies. Biochemistry **16**, 3641-3647.

CHIN J. & ZOU X. (1988). Cobalt(III) complex promoted hydrolysis of phosphate diesters : change in rate-determining step with change in phosphate diester reactivity. J. Am. Chem. Soc. **110**,223-225.

CHIOU S-H. (1983). DNA- and protein-scission activities of ascorbate in the presence of copper ion and a copper-peptide complex. J. Biochem. **94**,1259-1267.

CLEAVER J.E. (1967). Thymidine metabolism and cell kinetics. North Holland Publishing Co, Amsterdam, pp. 1-259.

COLL M., FREDERICK C.A., WANG A.H-J., RICH A. (1987). A bifurcated hydrogen-bonded conformation in the d(A.T) base pairs of the DNA dodecamer d(CGCAAATTTGCG) and its complex with distamycin. Proc. Natl. Acad. Sci. USA **84**,8385-8389.

COLLYN-d'HOOGHE M., BERNIER J-L., HENICHART J-P. (1987). Cytotoxic action and cell cycle effects of ALGA, a peptidic derivative of the antileukemic drug amsacrine. Cancer Biochem. Biophys. **9**,257-264.

COOPER K.R., HONG W.K., (1981). Prospective study of the pulmonary toxicity of continuously infused bleomycin. Cancer Treat. Rep. **65**, 419-425.

COOPER Jr J.A.D., WHITE D.A., MATTHAY R.A. (1986). Drug-induced pulmonary disease. Am. Rev. Respir. Dis. **133**,321-340.

COSAR C., NINET L., PINNET-SINDICO S., PREUD'HOMME J. (1952).Activité trypanocide d'un antibiotique produit par un Streptomyces. C.R. Acad. Sci. **234**,1498-1499.

DABROWIAK J.C., GREENAWAY F.T., GRULICH R. (1978a). Transition-metal binding site of bleomycin A_2. A carbon 13 nuclear magnetic resonance study of the zinc(II) and copper(II) derivatives. Biochemistry **17**,4090-4096.

DABROWIAK J.C., GREENAWAY F.T., LONGO W.E., VAN HUSEN M., CROOKE S.T. (1978b). A spectroscopic investigation of the metal binding site of bleomycin A_2. The copper(II) and zinc(II) derivatives. Biochem. Biophys.Acta **517**,517-526.

DABROWIAK J.C., GREENAWAY F.T., SANTILLO F.S. (1979a). The metallo bleomycins. In : " Bleomycin : chemical, biochemical and biological aspects " . Hecht S.M. (Eds), Springer-Verlag, pp.137-155.

DABROWIAK J.C., GREENAWAY F.T., SANTILLO F.S., CROOKE S.T. (1979b). The iron complexes of bleomycin and tallysomycin. Biochem. Biophys. Res. Commun. **91**,721-729.

DABROWIAK J.C. (1980a). Metal binding to antitumor antibiotics. In " Metal ions in biological system ", vol.11 : metal complexes as anticancer agents (SIGEL H., ed) Dekker, pp.305-336.

DABROWIAK J.C. (1980b). The coordination chemistry of bleomycin : a review. J. Inorg. Biochem. **13**,317-337.

D'ANDREA A.D. & HASELTINE W.A. (1978). Sequence-specific cleavage of DNA by the antitumor antibiotics neocarzinostatin and bleomycin. Proc. Natl. Acad. Sci. USA **74**,3608-3612.

DARKIN S. & RALPH R.K. (1985). Transport of AMSA drug into cells. FEBS Lett. **190**,349-353.

DASGUPTA D., PARRACK P., SASISEKHARAN V. (1987). Interaction of synthetic analogues of distamycin with poly(dA-dT) : role of the conjugated N-methylpyrrole system. Biochemistry **26**, 6381-6386.

DENNY W.A., ATWELL G.J., BAGULEY B.C. (1983). Potential antitumor agents. 39. Anilino ring geometry of amsacrine and derivatives : relationship to DNA binding and antitumor activity. J. Med. Chem. **26**,1625-1630.

DERVAN P.B. (1986). Design of sequence-specific DNA-binding molecules. Science **232**,464-471.

DICKERSON R.E. (1983). The DNA helix and how it is read. Sci. Am. **249**,3-15.

DIMARCO A., SOLDATI M., FIORETTI A. (1964). Antimitotic activity of distamycin A. Acta Univ. Intern. Contra. Cancrum **20**,423-426.

DREW H.R. & TRAVERS A.A. (1985). Structural junctions in DNA : the influence of flanking sequence on nuclease digestion specificities. Nucl. Acids Res. **13**,4445-4467.

EHRENFELD G.M., RODRIGUEZ L.O., HECHT S.M. (1985). Copper(I)-Bleomycin : structurally unique complex that mediates oxidative DNA strand scission. Biochemistry **24**,81-92.

EHRENFELD G.M., SHIPLEY J.B., HEIMBROOK D.C., SUGIYAMA H., LONG E.C., VAN BOOM J.H., VAN DER MAREL G.A., OPPENHEIMER N.J., HECHT S.M. (1987). Copper-dependent cleavage of DNA by bleomycin. Biochemistry **26**,931-942.

EKIMOTO H., TAKAHASHI K., MATSUDA A., TAKITA T., UMEZAWA H. (1985). Lipid peroxidation by bleomycin-iron complexes in vitro. J. Antibiotics **38**,1077-1082.

FEIGON J., DENNY W.A., LEUPIN W., KEARNS D.R. (1984). Interactions of antitumor drugs with natural DNA : ^{1}H NMR study of binding mode and kinetics. J. Med. Chem. **27**,450-465.

FENTON H.J.H. (1894). Oxidation of tartaric acid in presence of iron. J. Chem. Soc. **01**,899-910.

FINLAY A.C., HOCHSTEIN F.A., SOBIN B.A., MIRPHY F.X. (1951). Netropsin, a new antibiotic produced by a Streptomyces. J. Am. Chem. Soc. **73**,341-343.

FISHER L.M., KURODA R., SAKAI T.T. (1985). Interaction of bleomycin A_2 with deoxyribonucleic acid : DNA unwinding and inhibition of bleomycin-induced DNA breakage by cationic thiazole amides related to bleomycin A_2. Biochemistry **24**,3199-3207.

FLOYD R.A. (1981). DNA-ferrous iron catalyzed hydroxyl free radical formation from hydrogen peroxyde. Biochem. Biophys. Res. Commun. **99**,1209-1215.

FOURNEL J., GANTER P., KOENIG F., DE RATULD Y., WERNER G.H. (1965). Antiviral activity of distamycin A. In " Antimicrobial Agents Chemotherapy " HOBBY G.L. (ed.) pp.599-604.

FOX K.R., GRIGG G.W., WARING M.J. (1987). Sequence-selective binding of phleomycin to DNA. Biochem. J. **243**,847-851.

FREDERICK C.A., GRABLE J., MELIA M., SAMUDZI C., JEN-JACOBSON L., WANG B-C., GREENE P., BOYER H.W., ROSENBERG J.M. (1984). Kinked DNA in crystalline complex with Eco RI endonuclease. Nature **309**,327-331.

FREEDMAN J.H., HORWITZ S.B., PEISACH J. (1982a). Reduction of copper(II)-bleomycin : a model for in vivo drug activity. Biochemistry **21**,2203-2210.

FREEDMAN J.H., PICKART L., WEINSTEIN B., MIMS W.B., PEISACH J. (1982b). Structure of the glycyl-L-histidyl-L-lysine—copper(II) complex in solution. Biochemistry **21**,4540-4544.

FUJIMOTO J. (1974). Radioautographic studies on the intracellular distribution of bleomycin ^{14}C in mouse tumor cells. Cancer Res. **34**,2969-2974.

GABBAY E.J., ADAWADKAN P.D., WILSON W.D. (1976a). Stereospecific binding of diastereomeric peptides to salmon sperm DNA. Biochemistry **15**,146-151.

GABBAY E.J., ADAWADKAN P.D., KAPICAK L., PEARCE S., WILSON W.D. (1976b). The interaction specificity of peptides with DNA. Evidence for peptide beta-sheet-DNA binding. Biochemistry **15**,152-157.

GALE E.F., CUNDLIFFE E., REYNOLDS P.E., RICHMOND M.H., WARING M.J. (1981). In " The molecular basis of antibiotic action. " Wiley, second edition, pp.314-333.

GENDLER P.L. & RAPOPORT H. (1981). Permethyl analogue of the pyrrolic antibiotic distamycin A. J. Med. Chem. **24**,33-38.

GILONI L., TAKESHITA M., JOHNSON F., IDEN C., GROLLMAN A.P. (1981). Bleomycin-induced strand scission of DNA. J. Biol. Chem. **256**, 8608-8615.

GIRI S.N., CHEN Z-L., YOUNKER W.R., SCHIEDT M.J. (1983). Effects of intratracheal administration of bleomycin on GSH-shuttle enzymes, catalase, lipid peroxidation, and collagen content in the lungs of hamsters. Toxicol. Applied Pharm. **71**,132-141.

GLICKSON J.D., PILLAI R.P., SAKAI T.T. (1981). Proton NMR studies of the Zn(II)-bleomycin A_2-poly(dA-dT) ternary complex. Proc. Natl. Acad. Sci. USA **78**,2967-2971.

GREHN L. & RAGNARSSON U. (1981). Novel efficient total synthesis of antiviral antibiotic distamycin A. J. Org. Chem. **46**,3492-3497.

GRIGG G.W., GERO A.M., SASSE W.H., SLEIGH M.J. (1984). Inhibition and enhancement of phleomycin-induced DNA breakdown by aromatic tricyclic compounds. Nucl. Acids Res. **12**,9083-9093.

GROKHOVSKY S.L., ZHUZE A.L., GOTTIKH B.P. (1975). DNA base pair specific ligands. I. Synthesis of distamycin A and its analogs with different number of N-methyl and N-propylpyrrole residues. Bioorgan. Khim. **1**,1616-1623.

GROLLMAN A.P., TAKESHITA M., PILLAI D.M.R., JOHNSON F. (1985). Origin and cytotoxic properties of base propenals derived from DNA. Cancer Res. **45**,1127-1131.

HABER F. & WEISS J. (1934). The catalytic decomposition of hydrogen peroxide by iron salts. Proc. Roy. Soc. Lond. (A) **147**,332-335.

HAHN F.E. (1977). Distamycin and netropsin as inhibitors of RNA and DNA polymerases. Pharmac. Ther. A (Pergamon Press) **1**,475-485.

HAIDLE C.W. (1971). Fragmentation of deoxyribonucleic acid by bleomycin. Mol. Pharmacol. **7**,645-652.

HAIDLE C.W. & BEARDEN J. Jr (1975). Effect of bleomycin on an RNA-DNA hybrid. Biochem. Biophys. Res. Commun. **65**,815-821.

HAIDLE C.W. & STEPHEN L.R. (1980). Action of bleomycin on DNA. In "Bleomycin : Current status and new developments", S.K. CARTER, S.T. CROOKE, H. UMEZAWA eds, Academic Press **4**,21-23.

HASHIMOTO Y., ILJIMA H., NOZAKI Y., SHUDO K. (1986). Functional analogues of bleomycin : DNA cleavage by bleomycin and hemin-intercalators. Biochemistry **25**,5103-5110.

HAUPT I., THRUM H. (1971). Effect of netropsin on the growth and nucleic acid and protein biosynthesis of E. coli. Z. Allg. Mikrobiol. **11**,457-460.

HAY J.G., HASLAM P.L., DEWAR A., ADDIS B., TURNER-WARWICK M., LAURENT G.J. (1987). Development of acute lung injury after the combination of intravenous bleomycin and exposure to hyperoxia in rats. Thorax **42**,383-391.

HELBECQUE N., BERNIER J-L., HENICHART J-P.(1985). Design of a new DNA-polyintercalating drug, a bisacridinyl peptidic analogue of Triostin A. Biochem. J. **225**,829-832.

HELENE C. & THUONG N.T. (1986). Oligodeoxynucleotides covalently linked to intercalating agents and to nucleic acid-cleaving reagents. New families of gene regulatory substances. In " Molecular mechanisms of carcinogenic and antitumor activity. " , CHAGAS C., PULLMAN B., Eds, Adenine Press, pp.205-222.

HENICHART J-P., HOUSSIN R., BERNIER J-L., CATTEAU J-P. (1982a). Synthetic model of a bleomycin metal complex. J. Chem. Soc., Chem. Commun. 1295-1297.

HENICHART J-P., BERNIER J-L., CATTEAU J-P. (1982b). Interaction of 4-(9-acridinylamino)-aniline and derivatives with DNA. Hoppe-Seyler's Z. Physiol Chem. **363**,835-841.

HENICHART J-P., BERNIER J-L., LEMAY P., HOUSSIN R., CATTEAU J-P. (1984). Subcellular distribution of spin-labelled bithiazoles and bleomycin in living KB cells: an ESR study. Cancer Biochem. Biophys. **7**,239-244.

HENICHART J-P., BERNIER J-L., HOUSSIN R., LOHEZ M., KENANI A., CATTEAU J-P. (1985a). Copper(II)- and iron(II)-complexes of methyl 2-(2-aminoethyl)-aminomethyl-pyridine-6-carboxyl-histidinate (AMPHIS), a peptide mimicking the metal chelating moiety of bleomycin. An ESR investigation. Biochem. Biophys. Res. Commun. **126**,1036-1041.

HENICHART J-P., BERNIER J-L., HELBECQUE N., HOUSSIN R. (1985b). Is the bithiazole moiety of bleomycin a classical intercalator ? Nucl. Acids Res. **13**,6703-6717.

HERTZBERG R.P. & DERVAN P.B. (1982). Cleavage of double helical DNA by (methidiumpropyl-EDTA)-ironII. J. Am. Chem. Soc. **104**,313-315.

HERTZBERG R.P. & DERVAN P.B. (1984). Cleavage of DNA with methidiumpropyl-EDTA-iron(II) : reaction conditions and product analyses. Biochemistry **23**,3934-3945.

HERTZBERG R.P., CARANFA M.J., HECHT S.M. (1985). DNA methylation diminishes bleomycin-mediated strand scission. Biochemistry **24**,5285-5289.

HIRAIWA K., OKA T., YAGI K. (1983). Effect of bleomycin on lipid peroxides, glutathione peroxidase and collagenase in cultured lung fibroblasts. J. Biochem. **93**,1203-1210.

HOSSAIN M.B., VAN DER HELM D., OLSEN R.K., JONES P.G., SHELDRICK G.M., EGERT E., KENNARD O., WARING M.J., VISWAMITRA M. A. (1982). Crystal and molecular structure of the quinoxaline antibiotic analogue TANDEM (Des-N-tetramethyl triostin A). J. Am. Chem. Soc. **104**,3401-3408.

HOUSSIN R., BERNIER J-L. HENICHART J-P. (1984a). Synthesis of spin-labelled bithiazoles, useful probes for studying bleomycin-DNA binding. J. Heterocyclic. Chem. **21**,465-469.

HOUSSIN R., BERNIER J-L., HENICHART J-P. (1984b). Aminoalkyl derivatives of 2,4'-bithiazole-4-carboxylic acid, the intercalating part of bleomycin. J. Heterocyclic Chem. **21**,681-683.

HOUSSIN R., LOHEZ M., BERNIER J-L., HENICHART J-P. (1985a). A convenient method for the preparation of 2-(1-aminoalkyl)thiazole-4-carboxylic acids, key intermediates in the total synthesis of naturally occurring antitumor cyclopeptides. J. Org. Chem. **50**,2787-2788.

HOUSSIN R., BERNIER J-L., HENICHART J-P. (1985b). Synthesis of 2-isopropylidenehydrazinylthiazole and its subsequent annelation to the corresponding thiazolo[2,3-c]-s-triazole. J. Heterocyclic Chem. **22**,1185-1187.

HOUSSIN R., HELBECQUE N., BERNIER J-L., HENICHART J-P. (1986). A new bithiazole derivative with intercalative properties. J. Biomolec. Struct. and Dyn. **4**,219-229.

HUANG C-H., MIRABELLI C.K., JAN Y., CROOKE S.T. (1981). Single strand and double strand deoxyribonucleic acid breaks produced by several bleomycin analogues. Biochemistry **20**,233-238.

IITAKA Y., NAKAMURA H., NAKATANI T., MURAOKA Y., FUJII A., TAKITA T., UMEZAWA H. (1978). Chemistry of bleomycin. XX. The X-Ray structure determination of P-3A - Cu(II) complex, a biosynthetic intermediate of bleomycin. J. Antibiotics **31**,1070-1072.

IQBAL Z.M., KOHN K.W., EWIG R.A.G., FORNACE A.J. (1976). Single strand scission and repair of DNA in mammalian cells by bleomycin. Cancer Res. **36**,3834-3838.

JULIA M., PREAU-JOSEPH N. (1967). Amidines et guanidines apparentées à la congocidine. I. Structure de la congocidine. Bull. Soc. Chim. Fr. **11**, 4348-4356.

KANAO M., TOMITA S., ISHIDA S., MURAKAMI A., OKADA H. (1973). Chelation of bleomycin with copper in vivo. Chemotherapy **21**,1305-1310.

KANOFSKY J.R. (1986). Singlet oxygen production by bleomycin. A comparison with heme-containing compounds. J. Biol. Chem. **261**,13546-13550.

KAPPUS H., MULIAWAN H., SCHEULEN S. (1982). Liver microsome lipid peroxidation by bleomycin-ferrous-oxygen complex. In " Microsomes, drug oxidations, and drug toxicity ". SATO R., KATO R., eds , Japan Scientific Societies Press, Tokyo, New York, pp.555-556.

KARUP G., MELDAL M., NIELSEN P.E., BUCHARDT O. (1988). 9-acridinylpeptides and 9-acridinyl-4-nitrophenylsulfonylpeptides. Int. J. Peptide Protein Res. **32**,331-343.

KASAI H., NAGANAWA H., TAKITA T., UMEZAWA H. (1978). Interaction of bleomycin with nucleic acids, preferential binding to guanine base and electrostatic effect of the terminal amine. J. Antibiotics **31**,1316-1320.

KENANI A., LOHEZ M., HOUSSIN R., HELBECQUE N., BERNIER J-L., LEMAY P., HENICHART J-P. (1987). Chelating, DNA-binding and DNA-cleaving properties of a synthetic model for bleomycin. Anti-Cancer Drug Design **2**,47-59.

KENANI A., BAILLY C., HELBECQUE N., CATTEAU J-P., HOUSSIN R., BERNIER J-L., HENICHART J-P. (1988a). The role of the gulose-mannose part of bleomycin in activation of iron-molecular oxygen complexes. Biochem. J. **253**,497-504.

KENANI A., LAMBLIN G., HENICHART J-P. (1988b). A convenient method for the cleavage of the D-mannosyl-L-gulose disaccharide from bleomycin-A_2. Carbohydrate Res. **177**,81-89.

KENANI A. (1988). Rôle des parties bithiazolique, peptidique et glycannique de la bléomycine dans son action sur l' ADN. Thèse de doctorat d' Université (Lille).

KILKUSKIE R.E., SUGUNA H., YELLIN B., MURUGESAN N., HECHT S.M. (1985). Oxygen transfer by bleomycin analogues dysfunctionnal in DNA cleavage. J. Am. Chem. Soc. **107**,261-262.

KIMOTO E., TANAKA H., GYOTOKU J., MORISHIGE F., PAULING L. (1983). Enhancement of antitumor activity of ascorbate against Ehrlich ascites tumor cells by the copper : glycylglycylhistidine complex. Cancer Res. **43**,824-828.

KISSINGER K. , KROWICKI K. , DABROWIAK J.C. , LOWN J.W. (1987). Molecular recognition between oligopeptides and nucleic acids : monocationic lexitropsins that display enhanced GC sequence dependent DNA binding. Biochemistry **26**,5590-5595.

KLEVIT R.E., WEMMER D.E., REID B.R. (1986). ^{1}H NMR studies on the interaction between distamycin A and a symmetrical DNA dodecamer. Biochemistry **25**,3296-3303.

KOPKA M.L., YOON C., GOODSELL D., PJURA P., DICKERSON R.E. (1985a). The molecular origin of DNA-drug specificity in netropsin and distamycin. Proc. Natl. Acad. Sci. USA **82**,1376-1380.

KOPKA M.L. , YOON C. , GOODSELL D. , PJURA P. , DICKERSON E. (1985b). Binding of an antitumor drug to DNA : Netropsin and CGCGAATT^{Br}CGCG. J. Mol. Biol. **183**,553-563.

KOYAMA G., NAKAMURA H., MUROAKA Y., TAKITA T., MAEDA K., UMEZAWA H., ITAKA Y. (1968). Chemistry of bleomycin. II. The molecular and crystal structure of a sulfur-containing chromophoric amino acid. Tetrahedron Lett. 4635-4638.

KRIVTSORA M.A., MOROSHKINA E.B., GLIBIN E. (1984). DNA interaction with low molecular weight ligands with different structures. III. Complexes of DNA with distactins . Mol. Biol. **18**,950-956.

KROSS J., HENNER W.D., HASELTINE W.A., RODRIGUEZ L., LEVIN M.D., HECHT S.M. (1982). Structural basis of the deoxyribonucleic acid affinity of bleomycins. Biochemistry 21,3711-3721.

KRUEGER W.C., PSCHIGODA L.M., REUSSER F. (1973). Circular dichroism study of the bleomycin-DNA complex. J. Antibiotics **26**,424-428.

KRYLOV A.S., GROKHOVSKY S.L., ZASEDATELEV A.S., ZHUZE A.L., GURSKY G.V., GOTTIKH B.P. (1979). Quantitative estimation of the contribution of pyrrolecarboxamide groups of the antibiotic distamycin A into specificity of its binding to DNA AT pairs. Nucl. Acids Res. **6**,289-304.

KUO M.T., AUGER L.T., SAUNDERS G.F., HAIDLE C.W. (1977). Effect of bleomycin on the synthesis and function of RNA. Cancer Res. **37**,1345-1348.

KURAMOCHI H., TAKAHASHI K., TAKITA T., UMEZAWA H. (1981). An active intermediate formed in the reaction of bleomycin-Fe(II) complex with oxygen. J. Antibiotics **34**,576-582.

KUROYEDOV A.A., GROKHOVSKY S.L., ZHUZE A.L., NOSIKOV V.V., POLYANOVSKY O.L. (1977). Distamycin A and its analogs as agents for blocking of endo R Eco RI activity. Gene **1**,389-395.

KUWAHARA J., SUZUKI T., SUGIURA Y. (1985). Effective DNA cleavage by bleomycin-vanadium(IV) complex plus hydrogen peroxide. Biochem. Biophys. Res. Commun. **129**,368-374.

LAU S-J., KRUCK T.P.A., STARKER B. (1974). A peptide molecule mimicking the copper(II) transport site of human serum albumin. J. Biol. Chem. **249**,5878-5884.

LAUSSAC J-P., HARAN R., SARKAR B. (1983). N.M.R. and E.P.R. investigation of the interaction of copper(II) and glycyl-L-histidyl-L-lysine, a growth-modulating tripeptide from plasma. Biochem. J. **209**,533-539.

LAZO J.S. & HUMPHREYS C.J. (1983). Lack of metabolism as the biochemical basis of bleomycin-induced pulmonary toxicity. Proc. Natl. Acad. Sci. USA **80**,3064-3068.

LEE M., CHANG D-K., HARTLEY J.A., PON R.T., KROWICKI K., LOWN J.W. (1988a). Structural and dynamic aspects of binding of a prototype lexitropsin to the decadeoxyribonucleotide d(CGCAATTGCG)$_2$ deduced from high resolution ^{1}H NMR studies. Biochemistry **27**,445-455.

LEE M., HARTLEY J.A., PON R.T., KROWICKI K., LOWN J.W. (1988b). Sequence specific molecular recognition by a monocationic lexitropsin of the decadeoxyribonucleotide d(CATGGCCATG)$_2$: structural and dynamic aspects deduced from high field ^{1}H-NMR studies . Nucl. Acids Res. **16**,665-684 .

LEE M., KROWICKI K., HARTLEY J.A., PON R.T., LOWN J.W. (1988c). Molecular recognition between oligopeptides and nucleic acids : influence of Van der Waals contacts in determining the 3'-terminus of DNA sequences read by monocationic lexitropsins. J. Am. Chem. Soc. **110**, 3641-3649.

LEMAY P., BERNIER J-L., HENICHART J-P. CATTEAU J-P. (1983). Subcellular distribution of nitroxide spin-labelled 9-aminoacridine in living KB cells. Biochem. Biophys. Res. Commun. **111**,1074-1081.

LERMAN L.S. (1961). Structural considerations in the interaction of DNA and acridines. J. Mol. Biol. **3**,18-30.

LEVY M.J. & HECHT S.M. (1988). Copper(II) facilitates bleomycin-mediated unwinding of plasmid DNA. Biochemistry **27**,2647-2650.

LIM L.O. & NEIMS A.H. (1987). Mitochondrial DNA damage by bleomycin. Biochem. Pharmacol. **36**,2769-2774.

LIN S.Y. & GROLLMAN A.P. (1981). Interaction of a fragment of bleomycin with deoxyribodinucleotides : nuclear magnetic resonance studies. Biochemistry **20**,7589-7598.

LOW C.M.L., DREW H.R., WARING M.J. (1984a). Sequence-specific binding of echinomycin to DNA : evidence for conformational changes affecting flanking sequences. Nucl. Acids Res. **12**,4865-4879.

LOW C.M.L., OLSEN R.K., WARING M.J. (1984b). Sequence preferences in the binding to DNA of triostin A and TANDEM as reported by DNase I footprinting. FEBS Lett. **176**,414-420.

LOWN J.W. & SIM S.K. (1977). The mechanism of bleomycin-induced cleavage of DNA. Biochem. Biophys. Res. Commun. **77**,1150-1157.

LOWN J.W. & JOSHUA A.V. (1982). Bleomycin models. Haemin-acridines which bind to DNA and cause oxygen-dependent scission. J. Chem. Soc., Chem. Commun. 1298-1300.

LOWN J.W. (1985). Molecular mechanism of action of anticancer agents involving free radical intermediates. In " Free Radical Biol. Med. " Vol.1, W.A. PRYOR ed., New York, Academic Press, 225-264.

LOWN J.W., KROWICKI K. (1985). Efficient total synthesis of the oligopeptide antibiotics netropsin and distamycin. J. Org. Chem. **50**,3774-3779.

LOWN J.W., KROWICKI K., BALZARINI J., DE CLERCQ E. (1986a). Structure activity relationship of novel oligopeptide antiviral and antitumor agents related to netropsin and distamycin. J. Med. Chem. **29**,1210-1214.

LOWN J.W. , KROWICKI K. , BHAT U.G. , SKOROBOGATY A. , WARD B. , DABROWIAK J.C. (1986b). Molecular recognition between oligopeptides and nucleic acids : novel

imidazole-containing oligopeptides related to netropsin that exhibit altered DNA sequence specificity. Biochemistry **25**,7408-7416.

LOWN J.W., SONDHI S.M., ONG C-W. (1986c). Deoxyribonucleic acid cleavage specificity of a series of acridine- and acodazole-iron porphyrins as functional bleomycin models. Biochemistry **25**,5111-5117.

LOWN J.W. (1988). Lexitropsins: rational design of DNA sequence reading agents as novel anti-cancer agents and potential cellular probes. Anti-Cancer Drug Design **3**,25-40.

LUCK G. & ZIMMER C. (1973). Interaction of netropsin with DNA in the course of the B-A transition. Studia Biophys. **40**,9-12.

LUCK G., TRIEBEL H., WARING M.J., ZIMMER C. (1974). Conformational dependent binding of netropsin and distamycin to DNA and DNA model polymers. Nucl. Acids Res. **1**,503-530.

LUCK G. , ZIMMER C., REINERT K-E., ARCAMONE F. (1977). Specific interaction of distamycin A and its analogs with (A-T) rich and (G-C) rich duplex regions of DNA and deoxypolynucleotides. Nucl. Acids Res. **4**,2655-2670.

LYMAN S., TAYLOR P., BEERY L., PETERING D.H. (1986). Is metal-binding required for bleomycin to inhibit cell proliferation ? Fed.Proc. **45**,1723.

MACK D.P., IVERSON B.L., DERVAN P.B. (1988). Design and chemical synthesis of sequence-specific DNA-cleaving protein. J. Am. Chem. Soc. **110**,7572-7574.

MAHMUTOGLU I., SCHEULEN M.E., KAPPUS H. (1987). Oxygen radical formation and DNA damage due to enzymatic reduction of bleomycin-Fe(III). Arch. Toxicol. 60,150-153.

MANNING M.C. & WOODY R.W. (1986). Molecular orbital calculations on the oligopeptides netropsin, distamycin and related compounds. Biopolymers **25**,2065-2082.

MARKY L.A., BLUMENFELD K.S., BRESLAUER K.J. (1983). Calorimetric and spectroscopic investigation of drug-DNA interactions. I. The binding of netropsin to polyd(AT). Nucl. Acids Res. **11**,2857-2870.

MARTIN J.C., WARTELL R.M., O'SHEA D.C. (1978). Conformational features of distamycin-DNA and netropsin-DNA complexes by Raman spectroscopy. Proc. Natl. Acad. Sci. USA **75**,5483-5487.

MATTHEWS H.R., PEARSON M.D., MACLEAN N. (1980). Cat satellite DNA. Isolation using netropsin with CsCl gradients. Biochem. Biophys. Acta 606,228-235.

MAZZA G., GALIZZI A., MINGHETTI A., SICCRADI A. (1973). Interaction between DNA and distamycin A studied by transformation in Bacillus subtilis. Antimicrob. Ag. Chemother. **3**,384-391.

MELNIKOVA A.F., ZAZEDATELEV A.S., KOLCHINSKY A.M., GURSKY G.V., ZHUZI A.L., GROKHOVSKY S.L., MIRZABEKOV A.D. (1975). Accessibility of the minor groove of DNA in chromatin to the binding of antibiotics netropsin and distamycin A. Molec. Biol. Rep. **2**,135-142.

MELNYK D.L., HORWITZ S.B., PEISACH J. (1981). Redox potential of iron-bleomycin. Biochemistry **20**,5327-5331.

MICHENKOVA L. & ZIMMER C. (1980). Reversion of the B to A transition of DNA induced by specific interaction with the oligopeptide distamycin A. Biopolymers **19**,823-831.

MILLER K.J., LAUER M., CALOCCIA W. (1985). Interactions of molecules with nucleic acids. Theoretical model for the interaction of a fragment of bleomycin with DNA. Biopolymers **24**,913-934.

MIRABELLI C.K., HUANG C-H., CROOKE S.T. (1983). Role of deoxyribonucleic acid topology in altering the site/sequence specificity of cleavage of deoxyribonucleic acid by bleomycin and talisomycin. Biochemistry **22**,300-306.

MIYAMOTO T. & TERASIMA T. (1986). Effects of bleomycin on burkitt lymphoma cells grown in vitro and in vivo. Gann. **77**,674-681.

MIYOKA M., ONO T., HORI S., UMEZAWA H. (1975). Binding of bleomycin to DNA in bleomycin-sensitive and resistant rat-ascites hepatoma cells. Cancer Res. **35**,2015-2019.

MOORE C.W. (1988). Internucleosomal cleavage and chromosomal degradation by bleomycin and phleomycin in yeast. Cancer Res. **48**,6837-6843.

MUGGIA F.M., LOUIE A.C., SIKIC B.I. (1983). Pulmonary toxicity of antitumor agents. Cancer Treat. Rev. **10**,221-243.

MULLER W. & GAUTIER F. (1975). Interactions of heterochromatic compounds with nucleic acids. AT-specific non intercalating DNA ligands. Eur. J. Biochem. **54**,385-394.

MULLER W.E.G. & ZAHN R.K. (1977). Bleomycin, an antibiotic that removes thymine from double-stranded DNA. Prog. Nucleic Acids Res. Mol. Biol. **40**,21-57.

MURAKAMI H., MORI H., TAIRA S. (1976). Molecular embrace of bleomycin with helical DNA. J. Theor. Biol. **59**,1-23.

MURRAY V. & MARTIN R.F. (1985). Comparison of the sequence-specificity of bleomycin cleavage in two slightly different DNA sequences. Nucl. Acids Res. **13**,1467-1481.

MURRAY V., TAN L., MATTHEWS J., MARTIN R.F. (1988). The sequence specificity of bleomycin damage in three cloned DNA sequences that differ by a small number of base substitutions. J. Biol. Chem. **263**,12854-12859.

NAKAMURA S., YONEHARA H., UMEZAWA H. (1964). On the structure of netropsin. J. Antibiotics Ser. A **17**,220-221.

NAKAMURA M. & PEISACH J. (1988). Self-inactivation of Fe(II)-bleomycin. J. Antibiotics. **41**,638-647.

NEIDLE S., PEARL L.H., SKELLY J.V. (1987). DNA structure and perturbation by drug binding. Biochem. J. **243**,1-13.

NEWCOMER L.N., CADMAN E.C., NERENBERG M.I., CHEN M., BERTINO J.R., FARBER L.R., PROSNITZ L.R. (1982). Randomized study comparing doxorubicin, cyclophosphamide, vincristine, methotrexate with leuvovorin rescue, and cytarabine (ACOMLA) with cyclophosphamide, doxorubicin, vincristine, prednisone and bleomycin (CHOP-B) in the treatment of diffuse histiocytic lymphoma. Cancer Treat. Rep. **66**,1279-1284.

NISHIMURA C., TANAKA N., SUZUKI H. (1987). Purification of bleomycin hydrolase with a monoclonal antibody and its characterization. Biochemistry **26**,1574-1578.

NORSKOV-LAURITSEN N., DEMANT E.J.F., EBRESEN P. (1987). Mobilization of ferritin-iron by the anticancer agent bleomycin. Biochem. Pharmacol. **36**,2685-2686.

OBERLEY L.W. & BUETTNER G.R. (1979). The production of hydroxyl radical by bleomycin and iron(II). FEBS Lett. **97**,47-49.

OCHI H., WATANABE S., YAMAMOTO H. (1988). New heritable fragile site on chromosome 8 induced by distamycin A. Gann **79**,145-147.

OHLENDORF D.H., ANDERSON W.F., FISHER R.G., TAKEDA Y., MATTHEWS B.W. (1982). The molecular basis of DNA-protein recognition inferred from the structure of cro repressor. Nature **298**,718-723.

OLLIS D.L. & WHITE S.W. (1987). Structural basis of protein-nucleic acid interactions. Chem. Rev. **87**,981-995.

ONISHI T., SHIMADA K., TAKAGI Y. (1973). Effects of bleomycin on E. Coli strains with various sensitivities to radiations. Biochim. Biophys. Acta **312**,248-258.

ORTNER M.J., TUREK N., CHIGNELL C.F. (1981). Spectroscopic studies of rat mast cells, mouse mastocytoma cells, and compound 48/80-I. A spin-label study of membranes fluidities and the effect of 48/80. Biochem. Pharmacol. **30**,277-282.

OTSUKA M., KITTAKA A., OTSUKA M., OHNO M., SUGIURA Y., UMEZAWA H. (1986a). Transition-metal binding site of bleomycin. A synthetic analogue equivalent to bleomycin in activating molecular oxygen. Tetrahedron Lett. **27**,3635-3638.

OTSUKA M., KITTAKA A., OHNO M., SUZUKI T., KUWAHARA J., SUGIURA Y. (1986b). Synthetic study towards man-designed bleomycins. Synthesis of a DNA cleaving molecule based on bleomycin. Tetrahedron Lett. **27**,3639-3642.

PARDI A., MORDEN K.M., PATEL D.J., TINOCO I. (1983). Kinetics for exchange of the imino protons of the d(CGCGAATTCGCG) double helix in complexes with the antibiotics netropsin and/or actinomycin. Biochemistry **22**,1107-1113.

PATEL D.J. (1979). Netropsin-dGdGdAdAdTdTdCdC complex. A. antibiotic binding at adenine thymine base pairs in the minor groove of self-complementary octanucleotide duplex. Eur. J. Biochem. **99**,369-378.

PATEL D.J. (1981). Mutual interaction between adjacent dG.dC actinomycin binding sites and dA.dT netropsin binding sites on the self-complementary d(CGCGAATTCGCG) duplex in solution. Proc. Natl. Acad Sci. USA **78**,7281-7284.

PATEL D.J. (1982). Antibiotic DNA interaction : intermolecular Overhauser effects in the netropsin-d(CGCGAATTCGCG) complex in solution. Proc. Natl. Acad. Sci. USA **79**,6424-6428.

PATEL D.J., KOZLWSKI S.A., PARDI A., BHATT R., IKUDA S., ITAKURA K. (1983). Sequence dependence of DNA conformation, dynamics and interactions in solution. In " Specificity and biological interactions ", Int. Symp. at the Pontificial Academy of Sciences, vol.55, CHAGAS C., PULLMAN B., eds, Vatican Press, pp.133-173.

PELTON J.G. & WEMMER D.E. (1988). Structural modeling of the distamycin A-d(CGCGAATTCGCG)$_2$ complex using 2D NMR and molecular mechanics. Biochemistry **27**,8088-8096.

PENCO S., REDAELLI S., ARCAMONE F. (1967). Distamycin A. II. Total synthesis. Gazz. Chim. Ital. **97**,1110-1115.

PICKART L. & THALER M.M. (1973). Tripeptide in human serum which prolongs survival on normal cells and stimulates growth in neoplastic liver. Nature (London) New Biol. **243**,85-87.

PICKART L. & THALER M.M. (1979). Growth-modulating human plasma tripeptide : relationship between molecular structure and DNA synthesis in hepatoma cells. FEBS Lett. **104**,119-122.

PICKART L., THALER M.M., MILLARD M. (1979). Effect of transition metals on recovery from plasma of the growth-modulating tripeptide glycylhistidyllysine. J. Chromatogr. **175**,65-73.

PICKART L. & LOVEJOY S. (1987). Biological activity of human plasma copper-binding growth factor glycyl-L-histidyl-L-lysine. Methods in enzymology **147**,314-328.

POVIRK L.F., HOGAN M., DATTAGUPTA N. (1979). Binding of bleomycin to DNA : intercalation of the bithiazole rings. Biochemistry **18**,96-101.

PUSCHENDORF B. (1969). Effect of distamycin A on the template activity of DNA in a DNA polymerase system. FEBS Lett. **4**,355-357.

PUSCHENDORF B. (1971). Effect of distamycin A on the DNA dependent RNA polymerase system. Biochem. Biophys. Res. Commun. **43**,617-624.

PUSCHENDORF B., BECHER H., BOHLANDT D., GRUNICKE H. (1974). Effect of distamycin A on T_4-DNA-directed RNA synthesis. Eur. J. Biochem. **49**,531-537.

RAISFELD I.H. (1981). Role of the terminal substituents in the pulmonary toxicity of bleomycins. Tox. Appl. Pharmacol. **57**,355-366.

RAO E.A., SARYAN L.A., ANTHOLINE W.E., PETERING D.H. (1980). Cytotoxic and antitumour properties of bleomycin and several of its metal complexes. J. Med. Chem. **23**,1310-1318.

RASKER J.J., VAN DE POLL M.A.P.C., BEEKHUIS H., WOLDRING M.G., NIEWEG H.O. (1975). Some experience with ^{57}Co-labelled bleomycin as a tumour-seeking agent. J. Nucl. Med. **16**,1058-1069.

REINERT K.E. & THRUM H. (1970). Conformational changes of DNA by interactions with oligopeptide antibiotics as studied by viscometric investigations. Studia Biophys. **24/25**,319-325.

REINERT K.E., STUTTER E., SCHWEISS H. (1979). Aspects of specific protein-DNA interaction : multimode binding of the oligopeptide antibiotic netropsin to (AT)-rich DNA segments. Nucl. Acids Res. **7**,1375-1391.

REINERT K.E., SARFERT E., THRUM H. (1980). Counterion dependent variation of DNA secondary structure in (A-T) clusters : evidence by use of netropsin as a structural probe. Nucl. Acids Res. **8**,5519-5531.

REINERT K.E., GELLER D., STUTTER E. (1981). Temperature mediated variation of DNA secondary structure in (A-T) clusters : evidence of the oligopeptide antibiotic netropsin as astructural probe. Nucl. Acids Res. **9**,2335-2349.

ROY S.N. & HORWITZ S.B. (1984). Characterization of the association of radiolabeled bleomycin A_2 with HeLa cells. Cancer Res. **44**,1541-1546.

RUBIN J. & SUNDARALINGAM M. (1984). An unexpected major groove binding of netropsin and distamycin A to t-RNA^{phe}. J. Biomolec. Struct. and Dyn. 2,165-174.

SAITO M. & ANDOH T. (1973). Breakage of a DNA-protein complex induced by bleomycin and their repair in cultured mouse fibroblasts. Cancer Res. **33**,1696-1700.

SAKAI T.T., RIORDAN J.M., GLICKSON J.D. (1982). Models of bleomycin interactions with poly(deoxyadenylylthymidilic acid). Fluorescence and proton nuclear magnetic resonance studies of cationic thiazole amides related to bleomycin A_2. Biochemistry **21**,805-816.

SAKAI T.T., RIORDAN J.M., GLICKSON J.D. (1983). Bleomycin interactions with DNA. Studies on the role of the C-terminal cationic group of bleomycin A_2 in association with and degradation of DNA. Biochem. Biophys. Acta. **758**,176-180.

SAUSVILLE E.A., PEISACH J., HORWITZ S.B. (1978a). Effect of chelating agents and metal ions on the degradation of DNA by bleomycin. Biochemistry **17**,2740-2746.

SAUSVILLE E.A., STEIN R.W., PEISACH J., HORWITZ S.B. (1978b). Properties and products of the degradation of DNA by bleomycin and iron(II). Biochemistry **17**,2746-2754.

SAWYER D.T. & VALENTINE J.S. (1981). How super is superoxide ? Acc. Chem. Res. **14**,393-400.

SCHABEL F.M., LASTER Jr W.R., BROCKMAN Jr R.W., SKIPPER H.E.E. (1953). Antiviral activity of netropsin . Proc. Soc. Exptl. Biol. Med. **83**,1-3.

SCHEVITZ R.W., OTWINOWSKI Z., JOACHIMIAK A., LAWSON C.L., SIGLER P.B. (1985). The three-dimensional structure of trp repressor. Nature **317**,782-788.

SCHMID M., KLETT C., NEIDERHOFER A. (1980). Demonstration of a heritable fragile site in human chromosome 16 with distamycin A. Cytogenet. Cell Genet. **28**,87-94.

SEBTI S.M. & LAZO J.S. (1987). Separation of pulmonary bleomycin hydrolase from pulmonary aminopeptidases. Biochemistry **26**,432-437.

SEBTI S.M. & LAZO J.S. (1988). Metabolic inactivation of bleomycin analogs by bleomycin hydrolase. Pharmac. Ther. **38**,321-329.

SHERIDAN R.P. & GUPTA R.K. (1981). A ^1H nuclear relaxation study of the Mn^{2+}-bleomycin complex. J. Biol. Chem. **256**,1242-1247.

SICCARDI A.G., LANZA E., NIELSON E., GALLIZZI A., MAZZA G. (1975). Genetic and physiological studies on the site of action of distamycin A. Antimicrob. Ag. Chemother. **8**,370-376.

SIKIC B.I., ROZENCWEIG M., CARTER S.K. (1985). In" Bleomycin chemotherapy" , SIKIC B.I., ROZENCWEIG M., CARTER S.K., Eds , Academic Press, N.Y.

SLUKA J.P., HORVATH S.J., BRUIST M.F., SIMON M.I., DERVAN P.B. (1987). Synthesis of a sequence-specific DNA-cleaving peptide. Science **238** ,1129-1132.

SMITH P.J. (1987). Ferrous iron-mediated enhancement of DNA damage and recovery potential in bleomycin-treated human cells. Biochem. Pharmacol. **36**,475-480.

STONE T.J., BUCKMAN T., NORDIO P.L., McCONNEL (1965). Spin-labeled biomolecules. Proc. Natl. Acad. Sci. **54**,1010-1017.

STREKOWSKI L., CHANDRASEKARAN S., WANG Y-H., EDWARDS W.D., WILSON W.D. (1986). Molecular basis for anticancer drug amplification : interaction of phleomycin amplifiers with DNA. J. Med. Chem. **29**,1311-1315.

STREKOWSKI L., STREKOWSKA A., WATSON R.A., TANIOUS F.A., NGUYEN L.T., WILSON W.D. (1987). Amplification of bleomycin-mediated degradation of DNA. J. Med. Chem. **30**,1415-1420.

STREKOWSKI L., MOKROSZ J.L., TANIOUS F.A., WATSON R.A., HARDEN D., MOKROSZ M., EDWARDS W.D., WILSON W.D. (1988a). Molecular basis for bleomycin amplification : conformational and stereoelectronic effects in unfused amplifiers. J. Med. Chem. **31**,1231-1240.

STREKOWSKI L., MOKROSZ J.L., WILSON W.D. (1988b). A biphasic nature of the bleomycin-mediated degradation of DNA. FEBS Lett. 241,24-28.

STUBBE J., KOZARICH J.W. (1987). Mechanisms of bleomycin-induced DNA degradation. Chem. Rev. **87**,1107-1136.

SUGANO Y., KITTAKA A., OTSUKA M., OHNO M., SUGIURA Y., UMEZAWA H. (1986). Transition-metal binding site of bleomycin. A synthetic analogue equivalent to bleomycin in activating molecular oxygen. Tetrahedron Lett. **27**,3635-3638.

SUGIURA Y., KIKUCHI T. (1978). Formation of superoxyde and hydroxy radicals in iron(II)-bleomycin-oxygen system: electron spin resonance detection by spin trapping. J. Antibiotics **31**,1310-1312.

SUGIURA Y., MURAOKA Y., FUJII A., TAKITA T., UMEZAWA H. (1979). Chemistry of bleomycin. XXIV. Deamido bleomycin from viewpoint of metal coordination and oxygen activation. J. Antibiotics **32**,756-758.

SUGIURA Y., SUZUKI T., TANAKA H. (1982). Some properties, oxygen activation, and DNA cleavage of iron complexes of bleomycin and its synthetic analogs. Oxygenases and oxygen metabolism. 511-519.

SUGIURA Y. & SUZUKI T. (1982). Nucleotide sequence specificity of DNA cleavage by iron-bleomycin. J. Biol. Chem. **257**,10544-10546.

SUGIURA Y., SUZUKI T., OTSUKA M., KOBAYASHI S., OHNO M., TAKITA T., UMEZAWA H. (1983). Synthetic analogues and biosynthetic intermediates of bleomycin. J. Biol. Chem. **258**, 1328-1336.

SUGIYAMA H., KILKUSKIE R.E., CHANG L.H., MA L.T., HECHT S.M., VAN DER MAREL G., VAN BOOM J.H. (1986). DNA strand scission by bleomycin: catalytic cleavage and strand selectivity. J. Am. Chem. Soc. **108**,3852-3854.

SUKUMAR S. & BARBACID M. (1986). The role of ras oncogenes in chemically-induced tumors. In " Molecular mechanisms of carcinogenic and antitumor activity ", CHAGAS C., PULLMAN B., eds, Adenine Press, pp.36-53.

SUN I.L. & CRANE F.L. (1985). Bleomycin control of transplasma membrane redox activity and proton movement in HeLa cells. Biochem. Pharmacol. **34**,617-622.

SUZUKI H., NAGAI K., YAMAKI H., TANAKA N., UMEZAWA H. (1968). Mechanism of action of bleomycin. Studies with growing cultures of bacterial and tumor cells. J. Antibiotics **21**,379-386.

SUZUKI T., KUWAHARA J., SUGIURA Y. (1985). Copper-bleomycin has no significant DNA cleavage activity. Biochemistry 24,4719-4721.

TAKAHASHI K., TOSKIOKA O., MATSUDA A., UMEZAWA H. (1977). Intracellular reduction of the cupric ion of bleomycin copper complex and transfer of the cuprous ion to a cellular protein. J. Antibiotics **30**,861-869.

TAKAHASHI K., TAKITA T., UMEZAWA H. (1987). The nature of thiol-compounds which trap cuprous ion reductively liberated from bleomycin-Cu(II) in cells. J. Antibiotics **40**,348-353.

TAKEDA K., KATO F., KAWAI S., KONNO K. (1979). The effect of bleomycin on prolyl hydroxylase and DNA chain breakage : structure-activity relationship. J. Antibiotics **32**,43-47.

TAKEDA Y. , OHLENDORF D. H. , ANDERSON W. F. , MATTHEWS B. W. (1983). DNA-binding proteins. Science **221**,1020-1026.

TAKESHITA M., HORWITZ S.B., GROLLMAN A.P. (1974). Bleomycin, an inhibitor of vaccinia virus replication. Virology **60**,455-465.

TAKESHITA M., GROLLMAN A.P., OHTSUBO E., OHTSUBO H. (1978). Interaction of bleomycin with DNA. Proc. Natl. Acad. Sci. USA **75**,5983-5987.

TATTI K.M., HUDSPETH E.S., JOHNSON P.H., GROSSMAN L.J. (1978). Enhancement of buoyant separations between DNAs in preparative Cs Cl gradients containing distamycin A or netropsin. Anal. Biochem. **89**,561-571.

TOLEDO C.H., ROSS W.E., HOOD C.I., BLOCK E.R. (1982). Potentiation of bleomycin toxicity by oxygen. Cancer Treat. Rep. **66**,359-362.

TWENTYMAN P.R. (1984). Bleomycin-mode of action with particular reference to the cell cycle. Pharmacol. Ther. **23**,417-441.

UEHARA Y., HORI M., UMEZAWA H. (1982). Specificity of transport of bleomycin and cobalt-bleomycin in L5178Y cells. Biochem. Biophys. Res. Commun. **104**,416-421.

UMEZAWA H. (1974a). Chemistry and mechanism of action of bleomycin. Fed. Proc. **33**,2296-2302.

UMEZAWA H. (1974b). A bleomycin-inactivating enzyme in mouse liver. J. Antibiotics **27**,419-424.

UMEZAWA H. (1979). Advances in bleomycin studies. In " Bleomycin, chemical, biochemical and biological aspects ", Hecht S.M. ed, Springer-Verlag, N.Y., pp.24-36.

UMEZAWA H., TAKITA T., SUGIURA Y., OTSUKA M., KOBAYASHI S., OHNO M. (1984). DNA-bleomycin interaction. Nucleotide sequence-specific binding and cleavage of DNA by bleomycin. Tetrahedron. **40**,501-509.

VAN TAMELEN E.E., WHITE D.M., KOGON C., POWELL A.D.G. (1956). Structural studies on the antibiotic netropsin. J. Am. Chem. Soc. **78**,2157-2159.

VERINI M.A. & GHIONE M. (1965). Activity of distamycin A on vaccinia virus infection of cell cultures. Chemotherapia **9**,145-160.

VISWAMITRA M.A., KENNARD O., CRUSE W.B.T., EGERT E., SHELDRICK G.M., JONES P.G., WARING M.J., WAKELIN L.P.G., OLSEN R.K. (1981). Structure of TANDEM and its implication for bifunctional intercalation into DNA. Nature **289**,817-819.

VYSKOCIL F., PILAR J., ZEMKOVA H., SVOBODA P., VITEK V., TEISINGER J. (1983). Bleomycin stimulates both membranes (Na^+-K^+)ATPase and electrogenic (Na^+-K^+) pump and partially removes the inhibition by vanadium ions. Biochem. Biophys. Res. Commun. **116**,783-790.

WALLER C.W., WOLF C.F., STEIN W.J., HUTCHINGS B.L. (1957).The structure of antibiotic T 1384. J. Am. Chem. Soc. **79**,1265-1266.

WANG A.H.J., UGHETTO G., QUIGLEY G.J., HAKOSHIMA T., VAN DER MAREL G.A., VAN BOOM J.H., RICH A. (1984). The molecular structure of a DNA-Triostin A complex. Science **225**,1115-1121.

WARING M.J. (1976). DNA-binding characteristics of acridinyl methanesulphoanolide drugs : comparison with antitumour properties. Eur. J. Cancer **12**,995-999.

WARING M.J. (1986). Recognition of DNA by quinoxaline antibiotics. In " Molecular mechanisms of carcinogenic and antitumor activity " (Chagas C., Pullman B. eds) Adenine Press, pp.317-337.

WARTELL R.M., LARSON J.E., WELLS R.D. (1974). Netropsin : a specific probe for A-T regions of duplex deoxyribonucleic acid. J. Biol. Chem. **249**,6719-6731.

WARTELL R.M., LARSON J.E., WELLS R.D. (1975). The compatibility of netropsin and actinomycin binding to natural deoxyribonucleic acid. J. Biol. Chem. **250**,2698-2702.

WATANABE K. (1956). Sinanomycin produced by Streptomyces. J. Antibiotics Ser. A **9**,102-107.

WEINER P.K., LANGRIDGE R., BLANEY J.M., SCHAEFER R., KOLLMAN P.A. (1982). Electrostatic potential molecular surfaces. Proc. Natl. Acad. Sci. USA **79**,3754-3758.

WEISS M.J., WEBB J.B., SMITH Jr J.M. (1957). The structure of antibiotic T 1385. Synthesis of the degradation fragments. J. Am. Chem. Soc. **79**,1266.

WERNER G.H., GANTER P., DE RATULD Y. (1965). The antiviral activity of distamycin A. Chemotherapia **9**,65-79.

WHITE R.E. & COON M.J. (1980). Oxygen activation by cytochrome P 450. Ann. Rev. Biochem. **49**,315-356.

WILSON W.R., BAGULEY B.C., WAKELIN L.P.G., WARING M.J. (1981). Interaction of antitumor drug 4'-(9-acridinylamino)-methanesulfon-m-anisidide and related acridines with nucleic acids. Mol. Pharmacol. **20**,404-414.

WILKINS R.J. (1982). Selective binding of actinomycin D and distamycin A to DNA. Nucl. Acids Res. **10**,7273-7282.

WONG A., HUANG C-H., CROOKE S.T. (1984). Deoxyribonucleic acid breaks produced by 4'-(9-acridinylamino)methanesulfon-m-anisidide and copper. Biochemistry **23**,2939-2945.

WU J.C., KOZARICH J.W., STUBBE J. (1983). The mechanism of free base formation from DNA by bleomycin. J. Biol. Chem. **258**,4694-4697.

WU J.C. & KOZARICH J.W. (1985). Mechanism of bleomycin : evidence for a rate-determining 4'-hydrogen abstraction from poly(dA-dU) associated with the formation of both free base and base propenal. Biochemistry **24**,7562-7568.

YAMAKI H., SUZUKI H., NAGAI K., TANAKA N., UMEZAWA H. (1971). Effect of bleomycin A_2 on deoxyribonucleases, DNA polymerase and ligase reaction. J. Antibiotics **24**,178-184.

YOUNGQUIST R.S. & DERVAN P.B. (1985). Sequence specific recognition of B-DNA by oligo(N-methylpyrrole carboxamides). Proc. Natl. Acad. Sci. USA **82**,2565-2569.

ZAKRZEWSKA K. & PULLMAN B. (1985). Theoretical exploration of netropsin binding to t-RNA^{phe}. J. Biomolec. Struct. Dyn. **2**,737-743.

ZASEDATELEV A.S., ZHUZE A.L., ZIMMER C., GROKHOVSKY S.L., TUMANYAN V.G., GURSKY G.V., GOTTIKH B.P. (1978). A stereochemical model for molecular mechanism of AT pair recognition exhibited by binding of distamycin A and netropsin to DNA . Studia Biophys. **67**,47-48.

ZIMMER C., LUCK G., THRUM H., PITRA C. (1972). Binding of analogues of the antibiotics distamycin A and netropsin to native DNA. Effect of chromophore systems and basic residues of the oligopeptides on thermal stability, conformation and template activity of the DNA complexes. Eur. J. Biochem. **26**,81-89.

ZIMMER C. (1975). Effects of the antibiotics netropsin and distamycin A on the structure and function of nucleic acids. Prog. Nucleic Acid Res. Molec. Biol. **15**,285-318.

ZIMMER C., MARCK C.H., SCHEIDER C.H., GUSCHLBAUER W. (1979). Influence of nucleotide sequence on dA-dT-specific binding of netropsin to double stranded DNA. Nucl. Acids Res. **6**,2831-2837.

ZIMMER C., KAKIUCHI N., GUSCHLBAUER W. (1982). Differential stabilization by netropsin of inductible B-like conformations in deoxyribo-, nitro- and 2'-deoxy-2'-fluoribo-adenosine containing duplexes of $(dA)_n$-$(dT)_n$ and $(dA)_n$-$(dU)_n$. Nucl. Acids Res. **10**,1721-1732.

ZIMMER C., MARCK C.H., GUSCHLBAUER W. (1983). Z-DNA and other non B-DNA structures are reversed to B-DNA by interaction with netropsin. FEBS Lett. **154**,156-160.

ZYGMUNT W.A. (1961). Reversal of netropsin inhibition of growth in E. coli. Biochem. Biophys. Res. Commun. **6**,324-327.

RESUME

La distamycine et la bléomycine sont deux anbiotiques antitumoraux capables de se lier à l'ADN respectivement par fixation dans le petit sillon et par intercalation.

Des modèles synthétiques analogues de ces deux substances naturelles ont été conçus afin d'étudier en détail leur mode de liaison à l'ADN. D'autres composés hybrides entre, d'une part la bléomycine ou la distamycine, et d'autre part, l'anilinoamino acridine ont été élaborés dans le but d'obtenir des substances capables de se lier à l'ADN avec une grande affinité et une spécificité de liaison pour des sites nucléiques définis. Ces composés répondent aux concepts Peptide Chélateur-Intercalant et Peptide à liaison Spécifique-Intercalant. Le mode de liaison à l'ADN de ces dérivés a été clairement défini par la convergence de nombreuses techniques physicochimiques (spectroscopie d'absorption UV; fluorescence et polarisation de fluorescence; dichroïsme circulaire et linéaire; RMN; RPE) et biochimiques (foot-printing). L'activité biologique (coupure d'ADN) et l'activité pharmacologique (propriétés antitumorales in vitro) ont été également étudiées.

Depuis la conception jusqu'à la réalisation de composés synthétiques potentiellement anticancéreux, une démarche logique de pharmacomodulation est présentée. Cette étude débouche sur la réalisation d'un modèle complexe du type Peptide Chélateur - Peptide à liaison Spécifique - Intercalant, point de départ pour l'élaboration de composés capables d'exciser des séquences nucléiques définies au sein d'oncogènes inducteurs du mécanisme d'initiation du cancer (conception d'enzymes artificielles).

MOTS-CLES :

NETROPSINE (Nt)	DISTAMYCINE (Dst)
BLEOMYCINE (Blm)	ACRIDINE
LIAISON A L'ADN	MODELISATION
INTERCALATION	FIXATION DANS LE PETIT SILLON
COMPLEXATION	ACTIVITE ANTITUMORALE